Syracuse University

SURFACE at Syracuse University

Dissertations - ALL

SURFACE at Syracuse University

12-8-2022

The Design, Synthesis, and Investigation into Small Molecule Modulators of the Src Homology 2 Domain-Containing Inositol 5’-Phosphatase (SHIP)

Shea Thomas Meyer

Follow this and additional works at: https://surface.syr.edu/etd

Part of the Organic Chemistry Commons

Recommended Citation

Meyer, Shea Thomas, "The Design, Synthesis, and Investigation into Small Molecule Modulators of the Src Homology 2 Domain-Containing Inositol 5’-Phosphatase (SHIP)" (2022). *Dissertations - ALL*. 1588.
https://surface.syr.edu/etd/1588

This Dissertation is brought to you for free and open access by the SURFACE at Syracuse University at SURFACE at Syracuse University. It has been accepted for inclusion in Dissertations - ALL by an authorized administrator of SURFACE at Syracuse University. For more information, please contact surface@syr.edu.

Abstract

The PI3K pathway is a major cell signaling pathway that influences survival and longevity in eukaryotic cells. Abnormal signaling of this pathway has been implicated in a number of disorders, including Alzheimer's disease and cancer. The PI3K pathway utilizes the inositolphospholipid PI(3,4,5)P_3 as a key secondary messenger in the transmission of signals from outside the cell to the nucleus. The SRC Homology 2 containing Inositol 5'-Phosphatase (SHIP) also plays a key role in the PI3K pathway, mediating hydrolysis of the inositol phospholipid PI(3,4,5)P_3 to PI(3,4)P_2. Early testing has shown modulation of SHIP activity through the use of small molecule modulators is effective at treating certain types of cancer and inflammatory diseases in cell-based assays and in murine xenografts.

This report details the investigation into tryptamine-based pan-SHIP1/2 inhibitors, as well as studies into a newly discovered sulfonamide-based SHIP1 selective agonist. Attempts to modulate SHIP activity by means of small molecules led us to develop and synthesize various small molecule tryptamine inhibitors in hopes of increasing the selectivity and potency, as well as probe the structure-activity relationships. The recently uncovered bis-sulfonamide SHIP1 agonist was synthesized for preliminary testing and investigation. Additionally, studies were undertaken to design and synthesis new sulfonamide-based SHIP1 agonists allowing for the development of more potent agonists that are less likely to biodegrade when exposed to CYP enzymes.

The Design, Synthesis, and Investigation into Small Molecule Modulators of the Src Homology 2 Domain-Containing Inositol 5'-Phosphatase (SHIP)

by

Shea Thomas Meyer

B.S., The Pennsylvania State University, 2017
M.Phil., Syracuse University, 2019

Dissertation
Submitted in partial fulfillment of the requirements for the degree of
Doctor of Philosophy in Chemistry.

Syracuse University
December 2022

Copyright © Shea Thomas Meyer
2022
All Rights Reserved

Acknowledgements

Pursuing this degree at Syracuse University has been a long and difficult journey filled with a myriad of failures and successes along the way. There are many who helped and inspired me along this journey and I want to take a moment to thank them.

First, I would like to thank my research advisor, Dr. John Chisholm. Over the past 5 years your mentorship, guidance, and patience have helped mold me into the chemist I am today. Thank you for all your help and advice over the years, as I know this wouldn't have been possible without it. I would also like to thank my committee members, Dr. Davoud Mozhdehi, Dr. Michael Sponsler, Dr. Nancy Totah, Dr. Rachel Steinhardt, and Dr. James Henderson who is serving as my committee chair. Thank you all for serving on my defense committee as my time as a Syracuse graduate student comes to an end.

To my friends and labmates I've made along the way, Dr. Otto Dungan, Dr. Rowan Meador, Dr. Nilamber Mate, Katelyn Leets, Jacob Moose, Shawn Dormann, Angela Pacherille, Rob Anderson, Christos Nixarlidis, and Alexandra Millimaci. Thank you for making the lab a fun and enjoyable experience with many memories. From countless walks to Marshall Street, to always hunting down a free meal, to the never-ending jokes and laughter, it was always a welcomed improvement to the day. Thank you all for the help, advice, and insight in lab with the various projects I've worked on. I wish you all success in your future career paths and endeavors, and I look forward to watching all of your accomplishments!

I would also like to thank the rest of my friends who have supported me throughout this journey. Nick Quagliani, Brock McCullough, Steve Spirk, Aly Kulp, and Ian Tinsley. The visits, countless conversations and continued friendship were essential for finishing this degree and I could not have accomplished it without all of you. Thank you to Olivia Kuzio, my "Pal in Pain." Your check-ins, conversations, and frequent get togethers were greatly appreciated and needed as we both pursued our own graduate degrees. I wish you the best of luck as you complete the final stages of obtaining your own Ph.D.

Last, but certainly not least, I would like to thank my family. Without all of your support none of this would have been possible. To my parents, Wes and Shelli, thank you for all the love and support as I pursued this degree. I could not have accomplished this without you believing in me and always challenging me to achieve my dreams. To my sister, Sierra, thank you for all the love and laughter you've provided over the years. You always knew when I needed a little laughter to pick me up. Thank you to my grandparents, Joe and Sue, for your never-ending love and belief in me. And thank you to my Aunt DeeDee, for the inspiration you've provided through your strength and courage in your continued fight.

Table of Contents

Abstract i
Acknowledgements iv
Table of Contents vi
List of Figures viii
List of Schemes viii
List of Tables ix
List of Abbreviations/Symbols x

Chapter 1: Therapeutic Potential of SHIP Modulation with Small-Molecules

1.1 The PI3K Cell Signaling Pathway 1
1.2 Modulation of SHIP for Therapeutic Effect 4
1.3 SHIP Modulation as a Target for Alzheimer's Disease 6
1.4 SHIP Modulation for Targeting Cancer 8
1.5 SHIP Modulation for Targeting Inflammatory Diseases 12
1.6 SHIP Modulation for Targeting Diabetes and Obesity 13
1.7 SHIP Modulation by Inhibitors/Antagonists 15
1.8 SHIP Agonists 21
1.9 Conclusion 25
1.10 References 27

Chapter 2: The Design and Synthesis of Small Molecule SHIP Inhibitors

Abstract 43
2.1 Introduction & Background 43
2.2 Objectives 49
2.3 Results & Discussion 50
2.4 Conclusion 66
2.5 Experimental 67
2.6 References 94

Chapter 3: The Design, Synthesis and SAR of Bis-Sulfonamide SHIP1 Agonists

Abstract 101
3.1 Introduction & Background 101
3.2 Objectives 106
3.3 Results & Discussion 107

3.4 Conclusion & Future Work 129

3.5 Experimental 131

3.6 References 180

Appendix: Biological Testing Procedures 184
Appendix: Spectroscopic Data 187

Vitae 315

List of Figures

Figure 1.1.1: Phosphoinositides in the PI3K Pathway 2
Figure 1.1.2: Cellular Signaling induced by SHIP Regulation 3
Figure 1.3.1: SHIP2 Inhibitors Targeting Alzheimer's Disease 7
Figure 1.4.1: 3AC, a Selective SHIP1 inhibitor 10
Figure 1.6.1 SHIP Inhibitors for Diabetic Relief 15
Figure 1.7.1: PI(3,4,5)P_3 mutated SHIP inhibitors 16
Figure 1.7.2: Phosphorylated Polyphenol SHIP2 Selective Inhibitors 17
Figure 1.7.3: Crystal Structure of the SHIP2 Phosphatase Domain Bound to **1.12** 18
Figure 1.7.4: Astellas Pharmaceutical SHIP2 Inhibitors 19
Figure 1.7.5: Aminosteroid SHIP Inhibitors 20
Figure 1.7.6: Kerr Group Discovered SHIP Inhibitors 21
Figure 1.8.1: Terpenoid Containing SHIP Agonists 22
Figure 1.8.2: Water Soluble SHIP Agonists 23
Figure 1.8.3: SHIP1 Agonist AQX-1125 24
Figure 1.8.4: Natural Product SHIP1 Agonists 24
Figure 1.8.5: Newly Discovered Bis-sulfonamide Selective SHIP1 agonist 25
Figure 2.1.1: Tryptamine Small Molecule Pan-SHIP1/2 Inhibitors 47
Figure 2.1.2: Binding Modes of Tryptamines to SHIP 48
Figure 2.1.3: AS1949490, a Selective SHIP2 Inhibitor 49
Figure 2.2.1: Base Tryptamine Core and Numbering System...50
Figure 2.2.2: SHIP2 Inhibitor AS1949490...50
Figure 2.3.1: Tryptamine Derivative **2.11** 52
Figure 2.3.2: Tryptamine-based SHIP Inhibitors vs. leukemia, multiple myeloma and breast cancer cell lines 62
Figure 3.1.1: Aquinox Pharmaceutical SHIP1 Agonists 102
Figure 3.1.2: SHIP1 Agonists Identified Via Virtual Screening 104
Figure 3.1.3: SHIP1 Agonists vs. LPS-stimulated BV2 cell TNF-α and IL-6 Production 105
Figure 3.2.1: Sections of Bis-sulfonamide 3.7 to be Modified in SAR studies 107
Figure 3.3.1: Sulfoxide and Sulfone Analogs 108
Figure 3.3.2: Design and Development of Bis-sulfonamide **3.7** Analogs 109
Figure 3.3.3: Bis-Sulfonamide **3.7** Amino Acid Analogs 119
Figure 3.3.4: Functionalized Aromatic Core Analogs 123
Figure 3.3.5: Bis-sulfonamide **3.7** iNOS Expression Study 125
Figure 3.3.6: Evaluation of Bis-Sulfonamides in the iNOS Expression Assay 126

List of Schemes

Scheme 2.3.1: Synthesis of Tryptamine Salt **2.2**, a selective SHIP2 Inhibitor 51
Scheme 2.3.2: Synthetic Route for tryptamine derivative **2.18** 54
Scheme 2.3.3: Synthetic Route for tryptamine derivative **2.20** 54
Scheme 2.3.4: Synthetic Route for Acetamide **2.21** 54
Scheme 2.3.5: Synthetic Route for Tryptamine Derivative **2.22** 55
Scheme 2.3.6: Synthesis of 5-Substituted Tryptamine Analogs 56
Scheme 2.3.7: Synthesis of Unfunctionalized Tryptamine Analog **2.45** 57
Scheme 2.3.8: Synthesis of 2-Bromo-N-Phthaloyltryptamine Derivative 63

Scheme 2.3.9: Synthetic Plan for the Synthesis of 2-Aryltryptamines and 2-Vinyltryptamines 64
Scheme 2.3.10: Synthesis of 5-Bromo-N-phthaloyltryptamine Derivative 65
Scheme 2.3.11: Synthesis of AS1949490 (**2.3**) 65
Scheme 3.3.1: Synthetic Route for the SHIP1 Agonist **3.7** 108
Scheme 3.3.2: Aromatic Core Amide Linker Derivative 123
Scheme 3.3.3: Hybrid Analog Synthesis 128

List of Tables

Table 2.3.1: Methylthio Tryptamine Analogs 53
Table 2.3.2: Malachite Green Assay Results for N-Alkyl Tryptamine Analogs 58
Table 2.3.3: Malachite Green Assay Results for Tryptamine Analogs with Substitution on the α-Amine 59
Table 2.3.4: Malachite Green Assay Results for 5-Substituted Tryptamine Analogs 60
Table 3.3.1: Quadrant D Sulfonamide formation via *N*-sulfonylation of **3.10** 110
Table 3.3.2: Nitro Reduction of Quadrant D Analogs 111
Table 3.3.3: Coupling and Deprotection of Quadrant D Analogs 112
Table 3.3.4: *N*-Sulfonylation Reactions of Quadrant D Analogs 113
Table 3.3.5: Malachite Green Assay Results for Sulfonamide Quadrant D 115
Table 3.3.6: Aryl Sulfonyl Quadrant A Derivatives 116
Table 3.3.7: Malachite Green Assay Results for Aryl Sulfonyl Quadrant A 118
Table 3.3.8: Malachite Green Assay Results for Amino Acid Quadrant B 120
Table 3.3.9: Quadrant C Aromatic Core Analogs 122
Table 3.3.10: Malachite Green Assay Results for Aromatic Core Quadrant C 124
Table 3.3.11: Malachite Green Assay Results for Hybrid Analog 129

List of Abbreviations/Symbols

˚C	degrees Celsius
$^{13}C\{^{1}H\}$NMR	carbon nuclear magnetic resonance
^{1}HNMR	proton nuclear magnetic resonance
3AC	3α-aminocholestane
Ac_2O	acetic anhydride
AD	Alzheimer's Disease
AI	artificial intelligence
AKT	protein kinase
anal. calcd	combustion elemental analysis
aq	aqueous
ATR	attenuated total reflection
BDNF	brain-derived neurotrophic factor
Bn	benzyl
Boc	tert-butoxycarbonyl
br	broad (spectral)
Bu	butyl
Bz	benzoyl
calcd	calculated
CD	Crohn's Disease
ClogP	calculating the partition coefficient
cm^{-1}	wavenumber(s)
DCM	dichloromethane
dec	decomposed
DIPEA	N,N-Diisopropylethylamine
DMAP	4-(N,N-dimethylamino)pyridine
DMF	dimethylformamide
DMSO-d_6	deuterated dimethyl sulfoxide
DMSO	dimethyl sulfoxide
EA	ethyl acetate
EC_{50}	half maximal effective concentration
EDCI	1-ethyl-3-(3-dimethylaminopropyl)carbodiimide
EGFR	epidermal growth factor receptors
equiv	equivalent
Et	ethyl
FDA	Food and Drug Administration
g	gram(s)
G-CSF	granulocyte colony-stimulating factor
GvHD	graft versus host disease
h	hour(s)
HATU	hexafluorophosphate azabenzotriazole tetramethyl uronium
IBD	inflammatory bowel disease
IC_{50}	half maximal inhibitor concentration
IL-6	Interleukin 6
INPP5D	inositol polyphosphate-5-phosphatase D

iNOS	inducible nitrite synthase
IR	infrared spectroscopy
LPS	lipopolysaccharide
m	multiplet (spectral)
Me	methyl
MHz	megahertz
MHz	megahertz
min	minute(s)
MLOGP	Moriguchi octanol-water partition coefficient
mM	millimolar
mol	mole(s)
mp	melting point
Ms	methylsulfonyl (mesyl)
mTOR	mammalian target of rapamycin
MW	molecular weight
nm	nanometer(s)
NMR	nuclear magnetic resonance
OBOC	one-bead-one-compound
p	pentet
PH	pleckstrin homology
$PI(3,4,5)P_3$	phosphatidylinositol-3,4,5-trisphosphate
$PI(3,4)P_2$	phosphatidylinositol-3,4-bisphosphate
$PI(4,5)P_2$	phosphatidylinositol-4,5-bisphosphate
PI3K	phosphoinositide 3-kinase
ppm	part(s) per million
PTEN	phosphatase and tensin homolog protein
P4IM	P4-interactive motif
q	quartet (spectral)
R_f	retention factor
rt	room temperature
s	singlet (spectral)
SAR	structure-activity relationship
SHIP	SH2-containing inositol-5’-phosphatase
SNP	single-nucleotide polymorphism
t	triplet (spectral)
TEA	triethylamine
TFA	trifluoroacetic acid
THF	tetrahydrofuran
TLC	thin-layer chromatography
TNFα	tumor necrosis factor alpha
TREM	triggering receptors expressed on myeloid cells
δ	chemical shift in parts per million

Chapter 1: Therapeutic Potential of SHIP Modulation with Small-Molecules

1.1 The PI3K Cell Signaling Pathway

To react to changes in their environment eukaryotic cells have the ability to transfer information about their surroundings to the cell nucleus. These signals influence a number of important cellular events, including control over proliferation and apoptosis. The intracellular plasma lipid bilayer serves a key role in these receptor-based signaling cascades, being the residence of inositol phospholipids. These phospholipids serve as secondary messengers in cell signaling pathways, responsible for the transfer of information between the exterior of the cell and the nucleus.[1–4] Two important classes of enzymes, inositol kinases and inositol phosphatases, control the phosphorylation pattern on these inositol phospholipids.[1–7] Their role in signaling is dependent on the phosphorylation patterns, as different patterns recognize and activate other enzymes, usually protein kinases, which pass the signals on deeper into the cell.[6] The phosphorylation and dephosphorylation of these inositol phospholipids are tightly regulated by the previously mentioned inositol kinases and phosphatases to avoid incorrect signaling, which can lead to a number of disease states. Perhaps the most important phosphatidylinositol second messenger is [PI(3,4,5)P_3], which is formed in very low concentration at the inside of the phospholipid membrane. [PI(3,4,5)P_3] rapidly recruits and activates protein kinases like protein kinase B (AKT), which then amplifies the signal by activating a larger number of protein kinases in the cytoplasm, passing the signal to the nucleus. One key inositol kinase, phosphoinositide 3-kinase (PI3K), is responsible for the conversion of phosphatidylinositol (4,5)-bisphosphate [PI(4,5)P_2] to phosphatidylinositol (3,4,5)-trisphosphate [PI(3,4,5)P_3] (**Figure 1.1.1**).[1–4,6,7]

Figure 1.1.1: Phosphoinositides in the PI3K Pathway[4]

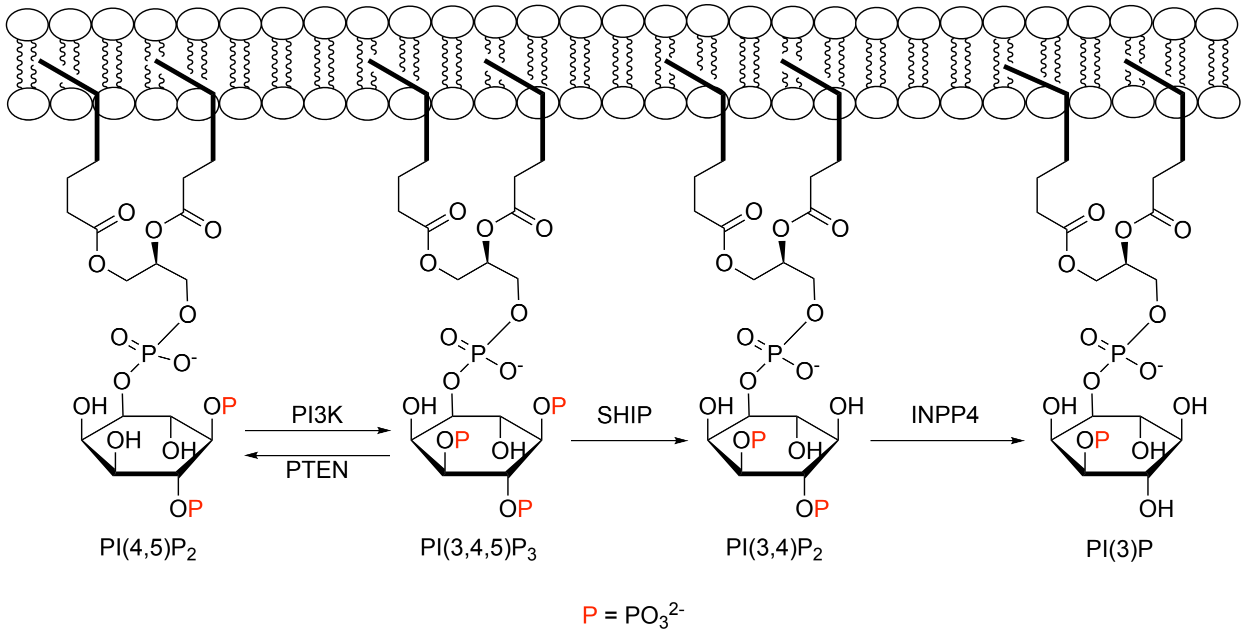

Once signaling has been accomplished, PI(3,4,5)P_3 must be metabolized back to a less signaling active inositol phospholipid. This is typically accomplished with the help of inositol phosphatase. The 5'-phosphate can be cleaved by the SH2-containing inositol-5’-phosphatase (SHIP) resulting in the formation of PI(3,4)P_2, or the 3'-phosphate can be cleaved by the phosphatase and tensin homolog protein (PTEN).[1,2,4,6,8,9] A balance of both PI(3,4,5)P_3 and PI(4,5)P_2 is required in order to fully activate many downstream signaling enzymes,[2,8–10] including the key signaling kinase AKT (**Figure 1.1.2**). AKT contains a Pleckstrin homology domain (PH domain) that can recognize both PI(3,4,5)P_3 and PI(3,4)P_2, and this recognition plays a vital role in PI3K signaling. The AKT controlled phosphorylation cascade relays signals to the nucleus, influencing cellular processes responsible for cellular proliferation and survival.[2,8,9]

Figure 1.1.2: Cellular Signaling induced by SHIP Regulation[11]

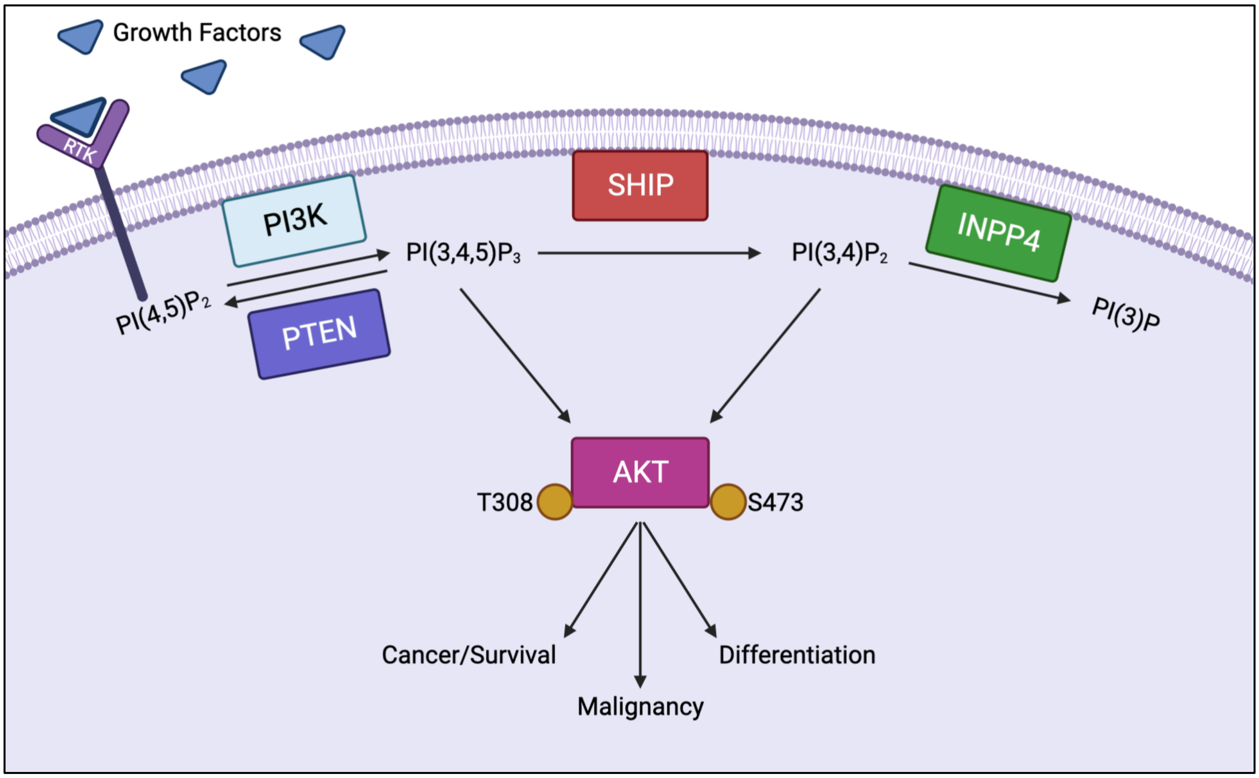

Overactivation of the PI3K pathway has been implicated in the development of numerous human diseases, including cancer, obesity, autoimmune diseases and neurological disorders.[1,3,5,7,8,12] Attempts at regulating cell signaling via direct inhibition of PI3K has led to some clinical success with regard to cancer treatment.[2,4,13] Resistance to PI3K inhibitors is now being observed in some circumstances, however.[14,15] Therefore, modulation of the PI3K signaling pathway through other enzyme targets is now being explored. One prime target for these efforts is the SHIP enzyme. SHIP modulation has been shown to play a vital role in the cellular functioning of endothelial, hematopoietic, and stem cells, including the enhancement of chemoresistance, changes in cell migration and cell invasion, and increased blood cell production.[1,4,7,12,16,17] One complication in targeting SHIP is the presence of two distinct isoforms within the body. SHIP1 is found in cells with a myeloid lineage such as blood and bone marrow cells, as well as microglia in the brain, while SHIP2 is found in endothelial and muscle cells throughout the body.[7,16,17] The two enzymes share a very similar amino acid sequence, having a 43% overlap between the two isoforms. Furthermore, both isoforms also share a similar SH2 and catalytic domain, containing a 54% and 64% identity in the primary structure, respectively.[18,19] Despite these similarities, SHIP1 and SHIP2 differ greatly in their fundamental expression and modes of action. As stated previously, SHIP1 is expressed almost exclusively in hematopoietic cells, while SHIP2 can be found in endothelial cells, or better put virtually in all cell types. Due to this, SHIP1 is preferentially recruited to the plasma membrane of hematopoietic cells, while SHIP2 is the preferred isoform recruited by most other cells. Additionally, the SHIP2 SH2 domain was found to undergo protein association/disassociation at a very slow rate when tested against a one-bead-one-compound (OBOC) pY peptide library, while SHIP1's SH2 domain was able to fully associate or disassociate in only a matter of minutes.[20] Interest in the modulation of SHIP activity and the potential therapeutic effects has led to the investigation of both isoform selective and pan-SHIP inhibitors (molecules that inhibit SHIP1 and SHIP2 at the same time), as well as selective SHIP1 agonists.

1.2 Modulation of SHIP for Therapeutic Effect

$PI(3,4,5)P_3$ is known to play a vital role in cell signaling and the induced downstream cellular responses. Finding a way to regulate the levels of $PI(3,4,5)P_3$ at the cell membrane has been pursed in the hopes of offering relief for the numerous human diseases and disorders attributed to misregulation of the PI3K pathway. $PI(3,4,5)P_3$ is naturally regulated by three enzymes: PI3K, PTEN, and SHIP. PI3K is responsible for producing $PI(3,4,5)P_3$ by phosphorylating $PI(4,5)P_2$. Inhibition of PI3K has been heavily explored, with multiple small molecule PI3K inhibitors being taken to preclinical and clinal trials.[21,22] It is known that different isoforms of PI3K play critical roles in particular types of tumors, leading to the desire for isoform-selective inhibitors.[21–24] Pharmaceutical companies such as Novartis, Takeda, and GlaxoSmithKline have all successfully synthesized various isoform-selective PI3K inhibitors, many of which have proceeded to clinical trials. However, despite the high toxicity of these isoform selective inhibitors, little success has been seen from monotherapy trials, most commonly attributed to poor drug efficacy. As a result, combination therapies are currently being employed using kinase inhibitors that act upon two different signaling pathways for therapeutic relief.[21] This has resulted in PI3K inhibitors being divided into three distinct classifications: inhibitors that target one isoform, those that target two isoforms and pan-PI3K inhibitors, which strongly bind to all PI3K isoforms.[24] Additionally, new approaches are being tested that focus on combining small molecule inhibitors in unison with non-targeted therapies such as biotherapies, chemotherapies, hormonal therapies or immunotherapies. However, one common problem PI3K inhibitors face is systemic toxicity issues. It has been found that the optimal drug efficacy is achieved when about 90% of cell signaling has been inhibited within the tumor. However, this often is only achievable at high doses, typically leading to adverse and unwanted side effects.[24] The need for such high inhibition to achieve therapeutic relief is attributed to the fact that gain of function mutations in the PI3K pathway do not appear to be the leading factor in cancer growth.

PTEN, responsible for the dephosphorylation of $PI(3,4,5)P_3$ to $PI(4,5)P_2$, has not widely been evaluated for modulation due to its natural role as a tumor suppressor. More recent findings believe both inhibition and agonism of PTEN could provide increased tumor suppressor activity, as well as provide possible treatments for various forms of autism and cancer predisposition syndromes.[25] However, PTEN activation has proven challenging as initial strategies such as direct protein delivery, the use of synthesized variants of PTEN with enhanced phosphatase activity and targeting PTEN miRNAs have led to problems associated with poor membrane permeability and poor pharmacodynamics.[25] Alternatively, SHIP can lower levels of PI(3,4,5)P_3 by catalyzing the hydrolysis to PI(3,4)P_2, offering a more direct target. A SHIP agonist could therefore decrease PI(3,4,5)P_3 levels. Alternatively, a SHIP inhibitor could lower the levels of PI(4,5)P_2, which has also been shown to be necessary to fully activate AKT. The regulation and modification of SHIP activity may also provide more targeted and direct treatments, as the SHIP1 paralog is expressed in hematopoietic cells, while the SHIP2 paralog can be found in most other cells. The research and development of SHIP modulators could provide possible therapeutic agents to combat the overactivation of PI3K signaling.

1.3 SHIP Modulation as a Target for Alzheimer's Disease

Recent studies have shown an underlying link between SHIP2 activity and the development and progression of Alzheimer's Disease (AD). SHIP2 is known to be expressed in endothelial cells, which are abundant in the brain.[25,26] SHIP2 has also been shown to have a significant impact on insulin signaling, which is believed to play a role in AD. Previous AD studies found that patients exhibiting insulin resistance could be attributed to SHIP2 insulin signaling, rather than a diabetic response. These patients had little to no response to traditional diabetic insulin treatment, supporting the notion the insulin resistance was caused by the development of AD.[27] Furthermore, studies have shown heightened SHIP2 expression may be correlated with β-amyloid plaque growth and the associated cognitive decline.[28] Inhibition of SHIP2 has been shown to reduce tau hyperphosphorylation and reverse memory impairment, which has been attributed to β-amyloid plaque caused by AD.[29] With the role of SHIP2 firmly established, interest in SHIP2 inhibitors with the potential to cross the blood-brain barrier has increased. One such inhibitor, AS1919490

(**1.1**, **Figure 1.3.1**), was found to improve memory retention, as well as increase synaptic plasticity when studied in db/db mice.[30] A second selective SHIP2 inhibitor, AS191940 has also been shown to increase brain derived neurotropic factor (BDNF), which is a protein responsible for the survival of neurons by influencing the growth and development of these cells.[31] Another SHIP2 inhibitor found to have a profound influence on AD, aminopyrimidine **1.2**, was derived from crizotinib, a FDA approved anticancer drug discovered through the use of a high-throughput screen targeting SHIP2. This inhibitor was found to easily pass through the blood-brain barrier, as well as inhibit SHIP2 activity and PI(3,4,)P_2 production in HT22 neuron cells.[29] The discovery of these early inhibitors and the ongoing research and development into additional SHIP2 inhibitors could someday provide a potential treatment for Alzheimer's disease.

Figure 1.3.1: SHIP2 Inhibitors Targeting Alzheimer's Disease

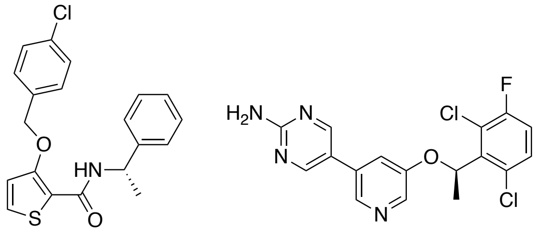

1.1

1.2

SHIP1 has also been found to play a role in the development and progression of AD. SHIP1 is found in the brain due to the presence of myeloid derived microglial cells. SHIP1 has been shown to limit TREM2 signaling which promotes microglial activity responsible for cellular responses such as proliferation and metabolism.[32–34] However, one single-nucleotide polymorphism (SNP) found in TREM2, R47H, has been shown to have a direct correlation to AD. This specific SNP, when activated, decreases TREM2 signaling leading to a response from cell receptor Dectin1 to compensate for the decreased signaling. This finding supports the belief that SHIP1 inhibition could provide potential relief for AD patients by ultimately preventing the

Dectin1 response that leads to increased cellular survival and proliferation tied to the decrease in TREM2 function. With the new findings regarding SHIP inhibition, and the continued need for new Alzheimer's Disease therapeutics, the research and development of SHIP inhibitors that are able to cross the blood brain barrier provides an innovative strategy to the continued attempts at treating Alzheimer’s Disease.

1.4 SHIP Modulation for Targeting Cancer

The modulation of SHIP has become a major focus in the prevention and treatment of cancer. SHIP1 and SHIP2 have been linked to cancer development in numerous ways, most notably by SHIP’s conversion of $PI(3,4,5)P_3$ to $PI(3,4)P_2$ leading to AKT activation and cell survival, their involvement in cellular apoptosis, SHIP1’s role in immune response, and SHIP2’s role in cellular migration and metastasis.[5]

As has already been established, SHIP is responsible for the dephosphorylation of $PI(3,4,5)P_3$ to $PI(3,4)P_2$. The presence of both inositol phospholipids is necessary for complete AKT activation. Overactivation of AKT may lead to an AKT induced override of fundamental cell death mechanisms.[10,38] Therefore while loss of SHIP activity may lead to too much $PI(3,4,5)P_3$, overactivation of SHIP may lead to too much $PI(3,4)P_2$ which can also increase AKT signaling to undesired levels. This belief was further supported by finding amplified $PI(3,4)P_2$ levels in leukemia cells.[39] Furthermore, it has been found that increased levels of $PI(3,4)P_2$ caused by mutations in INPP4A/B, which hydrolyses $PI(3,4)P_2$ to PI(3)P, promoted the transformation and development of breast tumors and embryonic fibroblasts in mice.[40–42] Previous studies have confirmed the link between $PI(3,4)P_2$ induced AKT activation and increased cell survival in numerous cancer cell types. The delivery of $PI(3,4)P_2$ to these identified cell lines leads to a resistance to apoptosis, providing the potential for SHIP inhibition to regulate $PI(3,4)P_2$ levels present in the plasma membrane.[3,7] The possibility for $PI(3,4)P_2$ regulation via SHIP inhibition could be especially effective for epithelial cancers known to utilize epidermal growth factor receptors (EGFR). Studies have shown EGFR recruitment of SHIP2 leads to the promotion of several signaling pathways responsible for AKT activation, cell migration, CXCR4 expression and ultimately cancer formation.[43] Overactivation of EGFR is known to lead to an increase in cancer cell survival, however; in the absence of SHIP2 EGFR degrades and is unable to initiate any further cell signaling cascades.[44,45] Additionally, $PI(3,4)P_2$ is known to promote mTORC1 signaling, an important serine/threonine kinase, while also inhibiting activity when found in nutrient-poor lysosomal cells.[46,47] Due to these findings SHIP2 provides a second possible method of treating cancer cells, in addition to the previously explored $PI(3,4)P_2$ regulation offered by SHIP inhibition.

A major factor leading to tumor growth and development is the increased AKT signaling that causes reduced cell death and an overriding of fundamental cell death mechanisms. Furthermore, CD95/Fas, a FAS gene protein responsible for programmed cell death, provides a secondary way of controlling cancer cell growth due to the T cell involvement initiating Fas/FasL expression. In-vitro studies have shown SHIP1 activity could lead to increased resistance to programmed cell death in T cells by eliminating CD95/Fas glycosylation.[48] SHIP1 has also been shown to recruit CD95/Fas to reduce the activity Caspase requires for the activation of Caspase 8, a caspase protein involved in programmed cell-death.[49] The SHIP dependency observed in this pathway was further confirmed through testing, utilizing the selective SHIP1 inhibitor 3α-aminocholestane, 3AC (**1.3, Figure 1.4.1**).

Figure 1.4.1: 3AC, a Selective SHIP1 inhibitor

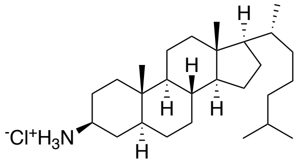

1.3

Use of this inhibitor, and the subsequent decrease in SHIP1 activity, led to an increase in the level of Caspase 8 activity and cell death when tested in both murine T and B and human T and B lymphoma cells.[49,50] This activity has also been found to be crucial for the longevity and survival of T cells, specifically located in the lungs and intestine. Studies performed on SHIP1 knockout mice (SHIP1$^{-/-}$) utilizing a Caspase 8 inhibitor showed an increase in lung and intestine T cell survival rates. This increase in T cell survival rate was further marked by a decrease in myeloid-mediated lung and gut inflammation typically seen in SHIP1$^{-/-}$ mice.[49,51] These results support the notion that inhibition of SHIP1 may serve as a possible therapeutic target for hematopoietic cancers that develop as a result of overactivity leading to disruption of the Fas-Caspase 8 cell death pathway.

SHIP1's role in immune responses also provides an opportunity for SHIP modulated immunotherapy that could be useful in cancer treatment. The role of SHIP1 regulation in both adaptive and innate immune response has been well established. The SHIP1 enzyme acts as a negative regulator in a variety of signaling pathways in various cell types, most notably in B cells, T cells, and mast cells.[52,53] Induced SHIP1 deficiencies in mice were found to lead to an increase in regulatory T cells and Myeloid-derived suppressor cells, while also leading to an overall decrease in natural killer cell function. These findings go against previous reports which utilized SHIP inhibitors to foster tumor immunity and control.[54–58] Additional studies performed on mice treated with the SHIP1-selective inhibitor 3AC (**1.3**) reproduced these results, showing an increase in regulatory T and Myeloid-derived suppressor cells, while again showing decreased activity of natural killer cells.[59,60] This was proposed to be from a prolonged SHIP1 deficiency, caused by genetic defects or by pathway inactivation, which led to a hyperactivation of tumor-responsive T and natural killer cells causing them to become disabled. This was further confirmed by altering the SHIP1 inhibitor dosing schedule, moving from a daily application to a more staggered plan allowing for recovery of immune responses and control.[61] This change in the dosing schedule also saw marked increases in natural killer cell function, as well as tumor-responsive T cell receptors. These results substantiate that SHIP inhibition is dependent upon both proper natural killer cell and T cell function.[55,61,62] Furthermore, these studies support the belief that SHIP activity could be inhibited in order to regulate T-cell response, allowing for new immunosuppressive strategies to be developed in the fight against cancer.

Modulation of SHIP2 also provides useful opportunities for cancer therapeutics. SHIP2 is known to be found in endothelial cells, whereas SHIP1 is mainly found in myeloid lineage cells. Due to this fact, overexpression of SHIP2, rather than SHIP1, has been found to be implicated in numerous types of cancer, most notably colon and breast cancer.[63–65] These endothelial-derived tumors lack the traditional SHIP1 isoform, however; the presence of an active cancer stem cell promotor indicates the s-SHIP isoform of SHIP1 may be present and actively contributes to tumor stem cell survival.[66–69] Typically, epithelial cancer caused by overexpression of SHIP2 is associated with an increase in cellular migration and increased development of invadopodia, actin-rich assemblies capable of crossing an extracellular membrane, leading to an increase in metastatic capacity.[65,70–72] SHIP2 has also been reported to normalize focal adhesion and reduce the motility seen in PI(4,5)P_2 active PTEN-deficient glioblastoma.[73] However, inhibition of SHIP2 at this site has shown a reduction in the fibronectin involved cell migration of glioblastoma.[74,75] Additionally, SHIP2 has been detected in nuclear speckles, interchromatin granule masses enhanced in pre-mRNA splicing factors, when phosphorylation of SHIP2's serine 132 occurs.[76,77] Therefore, the entry of SHIP2 into the nucleus may help to regulate the inositol phospholipid composition leading to a remodeling of the chromatin and changes in transcriptional regulation that have been associated with epithelial to mesenchymal transition.[78,79] Additionally, $PI(4,5)P_2$ was also found in speckles of nuclear proteins and is believed to play an important role in the regulation of pre-mRNA splicing.[80,81] SHIP2 has also been linked to podosome and invadopodia formation through its production of $PI(3,4)P_2$.[82] It has been found that $PI(3,4)P_2$ accumulation, the direct product of SHIP2 activity, in the tyrosine kinase Tks5 of breast carcinoma leads to invadopodia maturation.[72] This finding further supports the claim that increased levels of $PI(3,4)P_2$ resulting in overactivation of the AKT pathway may be responsible for the decrease in apoptosis. Studies have also shown mice with little SHIP activity, either caused by a deficiency or treatment with a SHIP1 selective inhibitor, to have reduced levels of SDF-1/CXCL12, a chemokine protein used by metastatic and cancer stem cells to spread and metastasize.[59,83] These findings open the door for potential therapeutic strategies through SHIP modulation in numerous types of aggressive cancer, including colon and breast cancer.

1.5 SHIP Modulation for Targeting Inflammatory Diseases

Recent studies have shown a link between the PI3K pathway and inflammatory diseases such as IBD and Crohn's Disease (CD). Studies have shown a significant group of CD patients have significantly lower SHIP1 protein levels, and more specifically the SHIP1 deficiency has been associated with a significant reduction in the T cell CD4. Unsurprisingly, SHIP1 knockout mice were found to develop severe intestinal inflammation, similar that that experienced by

Crohn's Disease patients.[4,84,85] The notion that SHIP1 deficiency contributed to this inflammation was further supported by a lack of T cells found within the mice's intestines.[85] These findings indicate SHIP1 plays a vital role in T cell homeostasis in both humans and mice, leading to the potential for possible SHIP1 agonist based therapeutics. A SHIP1 agonist may allow for upregulation of SHIP1 activity to increase AKT signaling, ultimately leading to an increase in T cell production and a decrease in the inflammation. With these findings, investigations into SHIP1 agonists have been undertaken in the hopes of utilizing a second mechanism of the PI3K pathway to control the levels of PI(3,4,5)$P_{3.}$

1.6 SHIP Modulation for Targeting Diabetes and Obesity

SHIP2 has also been shown to play a prominent role in regulation of the body's insulin-signaling pathway. The PI3K enzyme is activated upon insulin's binding to an insulin receptor substrate (IRS) on the cell surface, initiating phosphorylation of PI(3,4)P_2 to PI(3,4,5)P_3 leading to complete activation of protein kinase B.[86,87] However, it is known that SHIP2 is responsible for dephosphorylation of PI(3,4,5)P_3 at the 5'-postion producing PI(3,4)P_2, which in turn would suppress the insulin-signaling cascade and reduce glucose uptake. This has led to the acceptance that SHIP2 serves as a negative regulator along the insulin-signaling pathway, although to exactly what extent SHIP2 serves remains debated.

Studies involving SHIP2 knockout mice have provided data that further support the claims of SHIP2's role in the insulin-signaling pathway. In one study performed by Schurmans and co-workers, SHIP2 knockout mice displayed an increased insulin sensitivity, which was marked by higher rates of hypoglycemia, a decreased gene expression of genes involved in gluconeogenesis and death.[62] They also found that adult mice who were bred heterozygous for the SHIP2 mutation possessed an increased glucose tolerance and insulin sensitivity. Related studies performed by Sleeman reported SHIP2 knockout mice exhibited a lowered body weight when eating a traditional 24-hour food intake, and exhibited a normal body weight when food intake was increased.[88] Additionally, when these mice were fed a 45% higher fat diet over a 6-week period they showed little weight gain, gaining only 10% body weight when compared to the 45% body weight for the wild type SHIP2 mice. The SHIP2 knockout mice also showed no signs of obesity, having not developed hyperglycemia or increased insulin levels typically seen in the wild type SHIP2 mice. The fat resistance of the knockout mice was attributed to an insulin induced increase of AKT activation in the liver and muscle. Also, p70S6 kinase, a PIP3 serine/threonine kinase regulated by AKT activity, also saw increased activity.[88] These results appear to indicate that SHIP2 does indeed play a vital role in the insulin-signaling pathway and provides the possibility for SHIP2 inhibition as a possible diabetes therapeutic.

Early studies into the role of SHIP inhibition in diabetes has provided some promising results. The use of selective SHIP2 inhibitors **1.4** and **1.5** (**Figure 1.6.1**) on in vitro cultured myotubes has shown a significant SHIP2 inhibition leading to a dose-dependent AKT response. This response was notably marked by an increase in the levels of glucose transporter 4 within the cell and improved glucose uptake.[89] Additionally, in-vivo studies have been performed utilizing diabetic db/db mice and the previously discussed SHIP2 inhibitor AS1919490 (**1.1**), which also showed promising results. The SHIP2 inhibitor treated mice were found to possess lower blood glucose levels and improved glucose uptake when compared to the vehicle mice. These results were again attributed to the inhibition of SHIP leading to a desired AKT response.[90] Studies were also performed utilizing a pan-SHIP1/2 inhibitor for possible therapeutic benefits. These in vivo studies, performed on diet-induced obese mice treated with the pan-SHIP inhibitor **1.6** (**Figure

1.6.1), showed a decrease in body fat, as well as an improvement in blood glucose levels and insulin response.[91] These promising early results, and the continued development of diabetes as a major worldwide health problem, make SHIP inhibition and the modification of the insulin-signaling pathway a promising target for the development of future therapeutics.

Figure 1.6.1 SHIP Inhibitors for Diabetic Relief

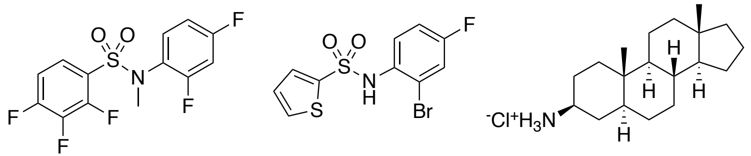

1.4 **1.5** **1.6**

1.7 SHIP Modulation by Inhibitors/Antagonists

With the unique role of SHIP1 and SHIP2 established in many disease states such as cancer, Alzheimer's Disease, diabetes and obesity, several studies have described small molecules with the potential to modulate the phosphatase activity of SHIP1 and/or SHIP2.[26,62,88] However, the identification and development of such inhibitors has proved challenging. Often times possible inhibitors are found through the use of compound screening campaigns which can be problematic due to the significant homology of the 5'-inositol phosphatases causing problems with enzyme selectivity.[92] The multiple SHIP isoforms present, SHIP1 and SHIP2, mean there is a need for selective inhibitors in order to curtail possible side effects, however; a pan-inhibitor may also prove to be useful in instances when cells are able to substitute the active paralog for the inhibited one. Although challenging, there has been a number of successfully synthesized SHIP1, SHIP2, and pan-SHIP1/2 inhibitors to date. The use of these early inhibitors will allow for improvements as we gain a greater understanding of the biological activities undertaken by SHIP.

The earliest SHIP inhibitors were established by the Prestwich group, acting as probes to gain a better understanding of the role these lipids play within the cellular composition These inhibitors were practically identical to PI(3,4,5)P_3, however the phosphates in **1.7** and the phosphate at the 5’ position in **1.8** was substituted out for a phosphorthioate or a methylenephosphonate (**1.9**) in order to inhibit hydrolysis.[4,93] (**Figure 1.7.1**)

Figure 1.7.1: PI(3,4,5)P_3 mutated SHIP inhibitors

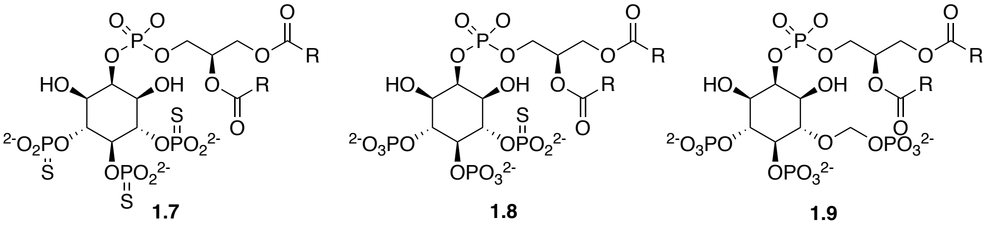

1.7 **1.8** **1.9**

R = C_7H_{15}

Testing of these early inhibitors versus SHIP1 and SHIP2 showed a roughly 50% inhibition of SHIP1, while also showing mild SHIP2 inhibition.[4] This difference in rate of inhibition proved that the two SHIP enzymes could potentially be inhibited selectively of each other. However; the ability to inhibit SHIP1 while also weakly inhibiting SHIP2 also emphasizes the similarity of the inositol binding pockets of the two isoforms.

Building off these initial SHIP inhibitors, molecular modeling was utilized to develop inhibitors that closely resemble PI(3,4,5)P_2. This modeling led to the discovery of phosphorylated polyphenols **1.10**, **1.11** and **1.12**, all of which were found to inhibit SHIP2 at the micromolar level (**Figure 1.7.2**). Bz(1,2,3,4)P_4 (**1.10**) was found to possess an IC_{50} vs SHIP2 of 19.6 μM, Bz(1,2,4,5)P_4 (**1.11**) possessed an IC_{50} of 11.2 μM, and Biphenyl(2,3′,4,5′,6)P_5 (**1.12**) possessed an IC_{50} of 1.8 μM.[4,94]

Figure 1.7.2: Phosphorylated Polyphenol SHIP2 Selective Inhibitors

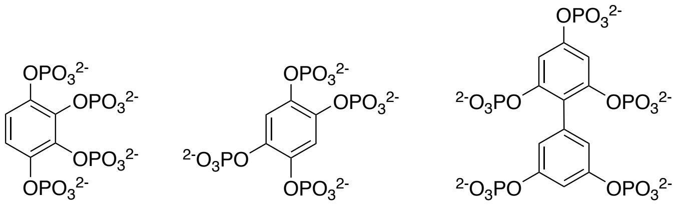
1.10 **1.11** **1.12**

Although these compounds all showed moderate SHIP2 inhibition, their highly polar nature makes them unable to cross cellular membranes rendering them useless as possible therapeutic treatment. However, the Potter lab was able to successfully use polyphenol **1.12** with a crystal of the SHIP2 phosphatase domain to obtain an x-ray structure of **1.12** bound in the active site.[95] The crystal structure provided valuable information regarding how these small molecule inhibitors interaction within the active site. A P4-interactive motif, P4IM, (below in blue) was found to be present that serves as a "door" for the key aspartic acid in the SHIP active site (in red), folding over and covering bound molecules to assist in binding interactions.[4] (**Figure 1.7.3**) The construction of a SHIP2 crystal structure containing the active site provided invaluable information and set forth ideas and designs for future SHIP inhibitors.

Figure 1.7.3: Crystal Structure of the SHIP2 Phosphatase Domain Bound to **1.12**[95]

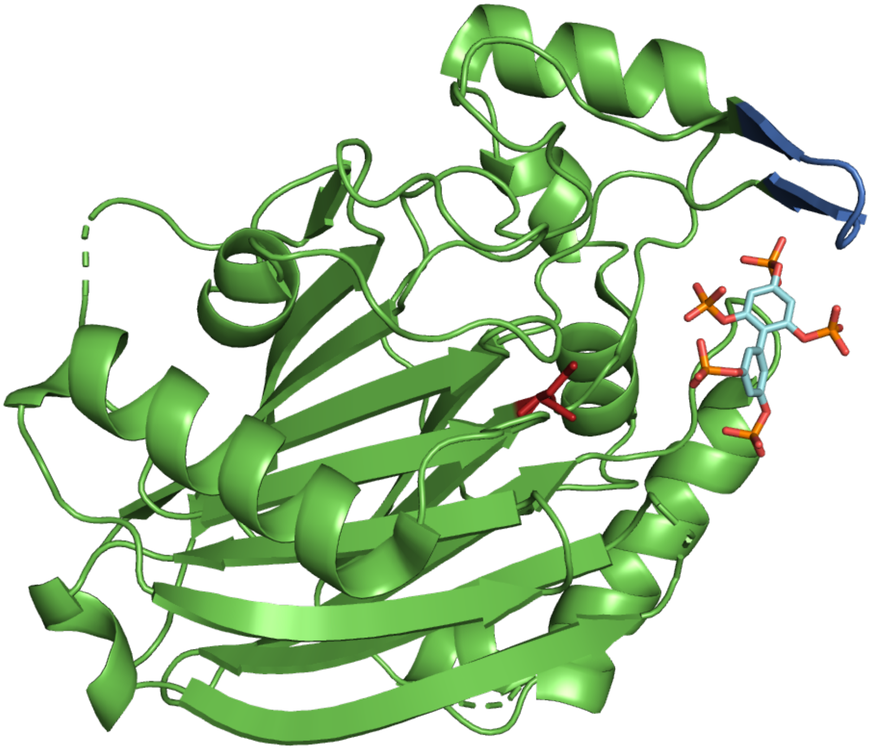

One of the most well-known SHIP inhibitors is that of AS1949490 (**1.1**), a selective SHIP2 inhibitor produced by Astellas Pharmaceuticals. AS1949490 (**1.1**) was found to inhibit SHIP2 at an IC_{50} of 0.62 μM, while also weakly inhibiting SHIP1 with an IC_{50} of 13 μM.[90] Kinetic analysis proved the inhibition was a result of AS1949490 binding to the SHIP active site, a process known as competitive binding inhibition. When treating L6 myotubes with AS1949490 (**1.1**) an increase in glucose usage and gluconeogenesis in hepatocyte FAO cells was seen. Additional studies in db/db mice showed AS1949490 (**1.1**) was able to reduce blood glucose levels without causing significant changes to insulin levels, food consumption or overall body mass. Using AS1949490 (**1.1**) as a template, Astellas Pharmaceuticals was able to produce a second viable SHIP inhibitor, AS193890 (**1.13**), which possessed similar characteristics. AS193890 (**1.13**) was found to be a selective SHIP2 inhibitor, with a greater selectivity for SHIP2 but a similar potency to AS1949490

(**1.1**).[90,96] While these inhibitors possess strong inhibitory potential, they tend to suffer poor pharmacodynamic properties.[5] However, metformin, a commercially available drug used to treat type 2 diabetes, recently has been identified as a SHIP2 inhibitor. Previously metformin's method of action had been unclear and poorly defined, however new studies suggest it acts as a SHIP2 inhibitor resulting in the bodies increased glucose uptake.[97,98] Polianskyte-Prause and coworkers demonstrated that metformin binds to recombinant SHIP2 resulting in a reduction of the catalytic activity of the SHIP2 phosphatase domain when tested in-vitro.[98] Furthermore, they also determined metformin inhibits SHIP2 in cultured cells, as well as skeletal and kidney muscle of db/db mice, confirming the belief that SHIP2 inhibition may lead to therapeutic relief.

Figure 1.7.4: Astellas Pharmaceutical SHIP2 Inhibitors

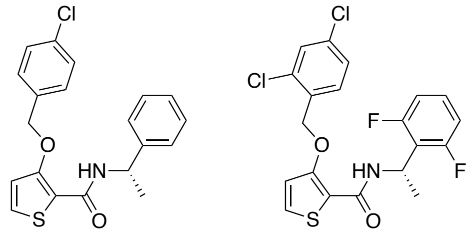

1.1 **1.13**

The Kerr group at SUNY Upstate Medical University was also able to identify a group of SHIP inhibitors using a high-throughput screening approach. One of the first inhibitors pulled from the screen was 3AC (**1.3**), a steroid derivative possessing an IC_{50} of 10 μM vs SHIP1 and no inhibition of SHIP2.[4] 3AC (**1.3**) was found to decrease the growth and survival of the leukemia cell lines KG-1 and C1498, as well as multiple myeloma cell lines like OPM2 cells.[5] Additional studies proved 3AC hindered tumor growth when tested on immunosuppressed mice compared to mice with OPM2 cells. However, several mice showed signs of significant tumor growth as a result of increased SHIP2 expression to compensate for the SHIP1 inhibition.[3,4] One other major drawback of 3AC (**1.3**) was its lack of water solubility, making dosing protocols challenging to establish. This led to the development of 3AC analogs **1.6, 1.14,** and **1.15** in order to improve solubility. All three analogs were found to be pan-SHIP inhibitors, rather than a selective SHIP1 inhibitor like the 3AC (**1.3**) parent. This change in inhibition shows the importance of the substituent at the C17 position, as well as gives further information to how these molecules may be interacting within the active site.[99]

Figure 1.7.5: Aminosteroid SHIP Inhibitors

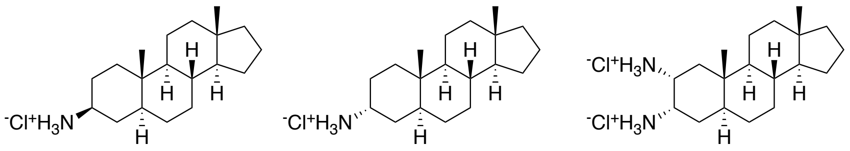

1.6 **1.14** **1.15**

The screening completed by the Kerr lab also produced hits for a number of other possible SHIP inhibitors containing various functionality vastly different from the established aminosteroid line. These new inhibitors, two of which contained a quinoline core and another two which contained a tryptamine core, were all found to be pan-SHIP1/2 inhibitors. The quinoline molecules, **1.16** and **1.17** (**Figure 1.7.6**), were initially developed by a program at the Walter Reed Medical Center in the hopes of developing new antimalarial drugs.[100] When tested against OPM2 cell lines, both quinoline inhibitors were found to induce apoptosis, as well as displayed a cytotoxicity versus SHIP2 in breast cancer cell lines MCF-7 and MDA-MD-231.[5] The third group of inhibitors, tryptamines **1.18** and **1.19** (**Figure 1.7.6**), were both found to be potent pan-SHIP1/2 inhibitors, and like the quinolines induced apoptosis when tested against myeloma and breast cancer cell lines.[3,5]

Figure 1.7.6: Kerr Group Discovered SHIP Inhibitors

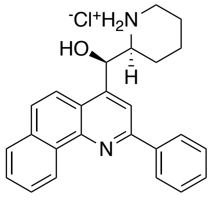

1.16

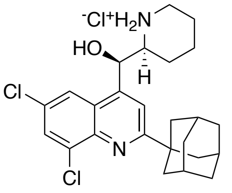

1.17

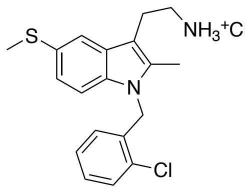

1.18

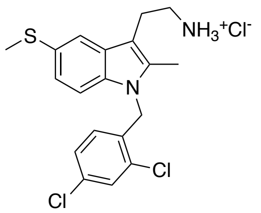

1.19

Tryptamine **1.18** was found to possess an IC_{50} of 4-5 μM against SHIP1 and 9-10 μM against SHIP2, however; it was later discovered it had toxic side effects and induced psychotropic effects in mice. After further testing, the tryptamine analog **1.19** was found to induce a similar, although less potent, response in tumor models without the psychotropic side effects. **1.19** was found to possess an IC_{50} of 20-30 μM against SHIP1 and an IC_{50} of 30 μM against SHIP2.[4] These results show SHIP inhibition may be a way forward in providing therapeutic strategies for a number of cancer types. The continued development of these inhibitors, as well as an increased understanding of their interactions within the SHIP active site will prove vital as we look to advance SHIP modulation, specifically through the use of small-molecule inhibitors.

1.8 SHIP Agonists

SHIP has been shown to be an allosterically controlled enzyme, meaning inhibition or activation can be achieved through the use of a small molecule binding at a site other than the active site.[101] This is due to the activation of the enzyme by the enzyme product, PI(3,4)P_2, which is known to bind to SHIP and accelerate the phosphatase activity. The binding site of PI(3,4)P_2 may also be occupied by a small molecule, which can then also accelerate the phosphate hydrolysis. The exact mechanism by which binding of PI(3,4)P_2 accelerates the enzyme activity is not known, however molecular dynamics studies appear to implicate a number of conformational changes to the enzyme that lead to a more active conformation.[102]

One of the first SHIP agonists known, pelorol (**1.20**, **Figure 1.8.1**), was originally isolated in 1999, but its SHIP activity was not discovered until a crude marine invertebrate screening was performed in 2004 by the Anderson group looking possible SHIP1 agonists.[103,104] Pelorol (**1.20**), isolated from the Great Barrier Reef marine sponge *Dacylospongia elegans*, was found to possess a 2-fold activation of SHIP when tested at a concentration of 5 μg/mL.[103,104] However, due to minimal amounts of pelorol available from natural products a synthetic route was developed along with several pelorol analogs possessing SHIP activity. Two of the analogs synthesized, AQX-016A (**1.21**) and AQX-MN100 (**1.22**), exhibited higher levels of SHIP activity (**Figure 1.8.1**). AQX-016A (**1.21**), a catechol containing pelorol derivative, exhibited a 6-fold activation of SHIP1 at 5 μg/mL.[103] In addition to the higher activity, AQX-016A (**1.21**) also showed selectivity for SHIP1 over SHIP2 by a factor of 5.[101]

Figure 1.8.1: Terpenoid Containing SHIP Agonists

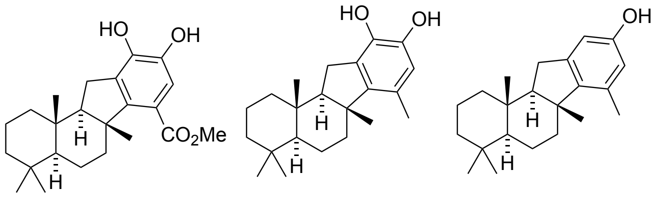

1.20 **1.21** **1.22**

However, one of the major drawbacks of AQX-016A (**1.21**) is the catechol functionality, which is known to cause undesirable side effects due to unwanted metal binding interactions. Catechols are known to bind to metals and readily oxidized to orthoquinones, which allow for protein modifications via Michael reactions.[101] In order to mitigate these possible side-effects AQX-MN100 (**1.22**), the monophenolic version of AQX-016A (**1.21**) was synthesized. AQX-MN100 (**1.22**) possessed the same 6-fold activation of SHIP1, as well as maintaining the SHIP1 selectivity exhibited by that of AQX-016A (**1.21**).[101] The removal of the catechol in AQX-MN100

(**1.22**) eliminated concerns of possible toxicity effects, without lessening the potency and effectiveness of the analog.

One major issue all three potential agonists suffered from was poor water solubility due to their high carbon concentration and minimal heteroatom incorporation. In order to try to achieve better solubility new analogs were developed with a greater heteroatom incorporation yielding AQX-435 (**1.23**) and ZPR-151 (**1.24) (Figure 1.8.2**). Both of these compounds were found to have slightly improved solubility and bioavailability, while AQX-435 (**1.23**) was also found to be a strong tumor suppressor when tested in murine model mice.[105]

Figure 1.8.2: Water Soluble SHIP Agonists

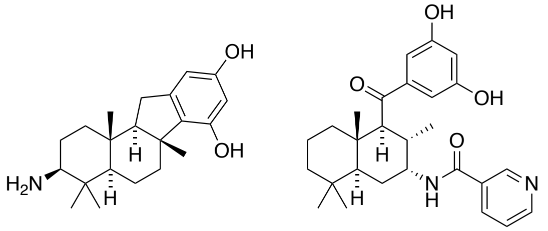

1.23 **1.24**

Additional screening led to the discovery of AQX-1125 (**1.25**), a steroid derived indane that showed strong anti-inflammatory effects and a 20% increase in SHIP1 activation at concentrations of 300 μM.[106,107] (**Figure 1.8.3**) These promising results gave way to AQX-1125 (**1.25**) being recognized as one of the first compounds to target SHIP1 to advance to clinical trials. Aquinox Pharmaceuticals went on to take AQX-1125 (**1.25**) to clinical trials where it unfortunately showed little efficacy, providing no reason to continue development as a therapeutic.[106,107] Recent studies from the Mui and Chisholm groups have shown that AQX-1125 (**1.25**) is actually not a very potent SHIP1 agonist, which may explain its poor showing in the clinic.[108,109]

Figure 1.8.3: SHIP1 Agonist AQX-1125

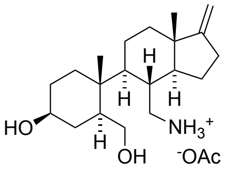

1.25

Another SHIP agonist, Australin E (**1.26**), was isolated from the soft marine coral *Cladiella sp.* from the island of Pohnpei by Anderson and researchers (**Figure 1.8.4**).[110] Australin E (**1.26**) is derived from the eunicellin diterpenoids family, a class of compounds known to show in-vitro toxicity against numerous cancer cell lines, and possesses a roughly 12% increase in the activation of SHIP1 at 100 µm concentrations.[110] Australin E (**1.26**) is the first from this class of compounds to exhibit SHIP1 agonist activity.

Figure 1.8.4: Natural Product SHIP1 Agonists

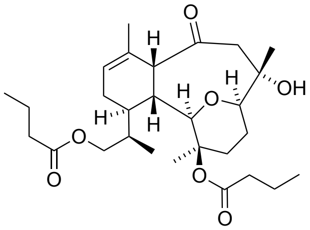

1.26

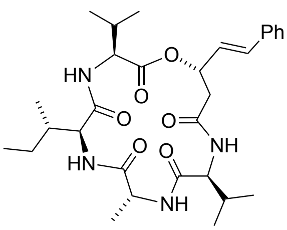

1.27

Similarly, cyclic depsipeptides, such as turnagainolide B (**1.27**), have shown potential to activate SHIP1. Turnagainolide B (**1.27**) was isolated from the marine bacterium *Bacillus sp.* and has been shown to exhibit strong SHIP activation similar to that of AQX-MN100. Turnagainolide B (**1.27**) was found to increase SHIP1 activity by 12% when tested at a concentration of 10 µm.[111]

The Kerr group in collaboration with Atomwise performed a high-throughput virtual screening on the SHIP1 active site, aided by the use of an artificial intelligence-based algorithm. One of the predicted hit compounds, bis-sulfonamide **1.28** (**Figure 1.8.5**) was shown to significantly increase SHIP1 activity, while also binding to SHIP1 at a new allosteric regulation site.

Figure 1.8.5: Newly Discovered Bis-sulfonamide Selective SHIP1 agonist

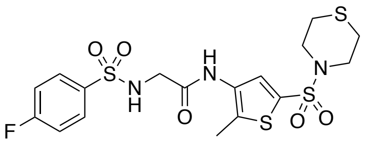

1.28

SHIP agonist **1.28**, often referred to as K306, was found to agonize SHIP1 at an EC_{50} of 0.2051 μM, while the previously known SHIP1 selective agonist, AQX-MN100 (**1.22**), only agonizes SHIP1 at an EC_{50} of 0.5896 μM. Additionally, it was also found to possess an EC_{50} of 0.1192 μM against SHIP1 compared to an EC_{50} of 1.169 μM against SHIP2 in a slightly different assay, marking a 10-fold preference for SHIP1 agonism over SHIP2.[112] **1.28** has also been found to show biological activity in cell-based assays, specifically in its suppression of inflammatory cytokines in both macrophages and BV2 microglial cells. It was also shown to suppress LPS-induced TNF-α production leading to the belief it may possess therapeutic potential for anti-inflammatory diseases.[112]

1.9 Conclusion

The development of SHIP modulators for the treatment of a number of diseases and disorders has proven difficult, while also providing valuable information on how these enzymes are involved in many biological processes. One of the many challenges when targeting SHIP is the multiple isoforms present, as well as the fact it can have both upregulating and downregulating cell signaling affects. However, recent discoveries have led to viable SHIP modulators that demonstrated anti-inflammatory and/or tumor suppressant characteristics. Due to the vital role the PI3K signaling pathway plays in many disease states, continued development of new and improved small molecule modulators selective for SHIP1 and SHIP2 seems certain, with a heavy focus on improving the pharmacodynamics and pharmacokinetics of any future modulators.

1.10 References

(1) Hoekstra, E.; Das, A. M.; Willemsen, M.; Swets, M.; Kuppen, P. J. K.; van der Woude, C. J.; Bruno, M. J.; Shah, J. P.; Ten Hagen, T. L. M.; Chisholm, J. D.; et al. Lipid Phosphatase SHIP2 Functions as Oncogene in Colorectal Cancer by Regulating PKB Activation. *Oncotarget* **2016**, *7* (45), 1–16.

(2) Majerus, P. W.; Kisseleva, M. V.; Anderson Norris, F. The Role of Phosphatases in Inositol Signaling Reactions. *J. Biol. Chem.* **1999**, *274* (16), 10669–10672.

(3) Fuhler, G.; Brooks, R. Therapeutic Potential of SH2 Domain-Containing Inositol-5′-Phosphatase 1 (SHIP1) and SHIP2 Inhibition in Cancer. *Mol. Med.* **2012**, *18* (1), 1.

(4) Viernes, D. R.; Choi, L. B.; Kerr, W. G.; Chisholm, J. D. Discovery and Development of Small Molecule SHIP Phosphatase Modulators. *Med. Res. Rev.* **2014**, *34* (4), 795–824.

(5) Pedicone, C.; Meyer, S. T.; Chisholm, J. D.; Kerr, W. G. Targeting SHIP1 and SHIP2 in Cancer. *Cancers (Basel).* **2021**, *13* (4), 1–24.

(6) Gericke, A.; Leslie, N. R.; Lösche, M.; Ross, A. H. PtdIns(4,5)P2-Mediated Cell Signaling: Emerging Principles and PTEN as a Paradigm for Regulatory Mechanism. In *Lipid-mediated Protein Signaling*; Capelluto, D. G. S., Ed.; Springer Netherlands: Dordrecht, 2013; pp 85–104.

(7) Brooks, R.; Fuhler, G. M.; Iyer, S.; Smith, M. J.; Park, M.-Y.; Paraiso, K. H. T.; Engelman, R. W.; Kerr, W. G. SHIP1 Inhibition Increases Immunoregulatory Capacity and Triggers Apoptosis of Hematopoietic Cancer Cells. *J. Immunol.* **2010**, *184* (7), 3582–3589.

(8) Balch, A.; Kerr, W. A Novel Therapeutic Approach in Breast and Hematopoietic Cancers : Inhibition of SH2-Domain Containing Inositol 5 ’ Phosphatase (SHIP), 2013.

(9) Zhang, X.; Majerus, P. W. Phosphatidylinositol Signalling. *Cell* **1998**, *9*, 153–160.

(10) Scheid, M. P.; Huber, M.; Damen, J. E.; Hughes, M.; Kang, V.; Neilsen, P.; Prestwich, G. D.; Krystal, G.; Duronio, V. Phosphatidylinositol (3,4,5)P3 Is Essential but Not Sufficient for Protein Kinase B (PKB) Activation; Phosphatidylinositol (3,4)P2 Is Required for PKB Phosphorylation at Ser-473. Studies Using Cells from SH2-Containing Inositol-5-Phosphatase Knockout Mice. *J. Biol. Chem.* **2002**, *277* (11), 9027–9035.

(11) Fernandes, S.; Iyer, S.; Kerr, W. G. Role of SHIP1 in Cancer and Mucosal Inflammation. *Ann. N. Y. Acad. Sci.* **2013**, *1280* (1), 6–10.

(12) Hamilton, M. J.; Ho, V. W.; Kuroda, E.; Ruschmann, J.; Antignano, F.; Lam, V.; Krystal, G. Role of SHIP in Cancer. *Experimental Hematology*. ISEH - Society for Hematology and Stem Cells 2011, pp 2–13.

(13) P.Y., W.; E.Q., L.; D.A., R.; K.L., L.; W.K., A. Y. Current Clinical Development of PI3K Pathway Inhibitors in Glioblastoma. *Neuro. Oncol.* **2012**, *14* (7), 819–829.

(14) Park, S.; Kim, Y. S.; Kim, D. Y.; So, I.; Jeon, J.-H. PI3K Pathway in Prostate Cancer: All Resistant Roads Lead to PI3K. *Biochim. Biophys. Acta - Rev. Cancer* **2018**, *1870* (2), 198–206.

(15) Brown, K. K.; Toker, A. The Phosphoinositide 3-Kinase Pathway and Therapy Resistance in Cancer. *F1000Prime Rep.* **2015**, *7*.

(16) Tu, Z.; Ninos, J. M.; Ma, Z.; Wang, J.; Lemos, M. P.; Desponts, C.; Ghansah, T.; Howson, J. M.; Kerr, W. G. Plenary Paper Embryonic and Hematopoietic Stem Cells Express a Novel SH2 – Containing Inositol 5 J -Phosphatase Isoform That Partners with the Grb2 Adapter Protein. *Blood* **2016**, *98* (7), 2028–2039.

(17) Erzenberg, L. E. A. H. Analysis of Lipopolysaccharide-Response Genes in B-Lineage

Cells Demonstrates That They Can Have Differentiation Stage-Restricted Expression and Contain SH2 Domains. *Genetics* **1996**, *93* (April), 3947–3952.

(18) Erneux, C.; Govaerts, C.; Communi, D.; Pesesse, X. The Diversity and Possible Functions of the Inositol Polyphosphate 5-Phosphatases. *Biochim. Biophys. Acta - Mol. Cell Biol. Lipids* **1998**, *1436* (1–2), 185–199.

(19) Pesesse, X.; Deleu, S.; De Smedt, F.; Drayer, L.; Erneux, C. Identification of a Second SH2-Domain-Containing Protein Closely Related to the Phosphatidylinositol Polyphosphate 5-Phosphatase SHIP. *Biochem. Biophys. Res. Commun.* **1997**, *239* (3), 697–700.

(20) Zhang, Y.; Wavreille, A.-S.; Kunys, A. R.; Pei, D. The SH2 Domains of Inositol Polyphosphate 5-Phosphatases SHIP1 and SHIP2 Have Similar Ligand Specificity but Different Binding Kinetics. *Biochemistry* **2009**, *48* (46), 11075–11083.

(21) Alzahrani, A. S. PI3K/Akt/MTOR Inhibitors in Cancer: At the Bench and Bedside. *Semin. Cancer Biol.* **2019**, *59*, 125–132.

(22) Yang, J.; Nie, J.; Ma, X.; Wei, Y.; Peng, Y.; Wei, X. Targeting PI3K in Cancer: Mechanisms and Advances in Clinical Trials. *Mol. Cancer* **2019**, *18* (1), 26.

(23) Thorpe, L. M.; Yuzugullu, H.; Zhao, J. J. PI3K in Cancer: Divergent Roles of Isoforms, Modes of Activation and Therapeutic Targeting. *Nat. Rev. Cancer* **2015**, *15* (1), 7–24.

(24) Hillmann, P.; Fabbro, D. PI3K/MTOR Pathway Inhibition: Opportunities in Oncology and Rare Genetic Diseases. *Int. J. Mol. Sci.* **2019**, *20* (22), 5792.

(25) McLoughlin, N. M.; Mueller, C.; Grossmann, T. N. The Therapeutic Potential of PTEN Modulation: Targeting Strategies from Gene to Protein. *Cell Chem. Biol.* **2018**, *25* (1), 19–29.

(26) Kerr, W. G.; Pedicone, C.; Dormann, S.; Pacherille, A.; Chisholm, J. D. Small Molecule Targeting of SHIP1 and SHIP2. *Biochem. Soc. Trans.* **2020**, *48* (1), 291–300.

(27) Talbot, K.; Wang, H.-Y.; Kazi, H.; Han, L.-Y.; Bakshi, K. P.; Stucky, A.; Fuino, R. L.; Kawaguchi, K. R.; Samoyedny, A. J.; Wilson, R. S.; et al. Demonstrated Brain Insulin Resistance in Alzheimer's Disease Patients Is Associated with IGF-1 Resistance, IRS-1 Dysregulation, and Cognitive Decline. *J. Clin. Invest.* **2012**, *122* (4), 1316–1338.

(28) Mostafavi, S.; Gaiteri, C.; Sullivan, S. E.; White, C. C.; Tasaki, S.; Xu, J.; Taga, M.; Klein, H.-U.; Patrick, E.; Komashko, V.; et al. A Molecular Network of the Aging Human Brain Provides Insights into the Pathology and Cognitive Decline of Alzheimer's Disease. *Nat. Neurosci.* **2018**, *21* (6), 811–819.

(29) Lim, J. W.; Kim, S. K.; Choi, S. Y.; Kim, D. H.; Gadhe, C. G.; Lee, H. N.; Kim, H.-J.; Kim, J.; Cho, S. J.; Hwang, H.; et al. Identification of Crizotinib Derivatives as Potent SHIP2 Inhibitors for the Treatment of Alzheimer's Disease. *Eur. J. Med. Chem.* **2018**, *157*, 405–422.

(30) Soeda, Y.; Tsuneki, H.; Muranaka, H.; Mori, N.; Hosoh, S.; Ichihara, Y.; Kagawa, S.; Wang, X.; Toyooka, N.; Takamura, Y.; et al. The Inositol Phosphatase SHIP2 Negatively Regulates Insulin/IGF-I Actions Implicated in Neuroprotection and Memory Function in Mouse Brain. *Mol. Endocrinol.* **2010**, *24* (10), 1965–1977.

(31) Miranda, M.; Morici, J. F.; Zanoni, M. B.; Bekinschtein, P. Brain-Derived Neurotrophic Factor: A Key Molecule for Memory in the Healthy and the Pathological Brain. *Front. Cell. Neurosci.* **2019**, *13*.

(32) Peng, Q.; Malhotra, S.; Torchia, J. A.; Kerr, W. G.; Coggeshall, K. M.; Humphrey, M. B. TREM2- and DAP12-Dependent Activation of PI3K Requires DAP10 and Is Inhibited by

SHIP1. *Sci. Signal.* **2010**, *3* (122).

(33) Jay, T. R.; Hirsch, A. M.; Broihier, M. L.; Miller, C. M.; Neilson, L. E.; Ransohoff, R. M.; Lamb, B. T.; Landreth, G. E. Disease Progression-Dependent Effects of TREM2 Deficiency in a Mouse Model of Alzheimer's Disease. *J. Neurosci.* **2017**, *37* (3), 637–647.

(34) Ulland, T. K.; Song, W. M.; Huang, S. C.-C.; Ulrich, J. D.; Sergushichev, A.; Beatty, W. L.; Loboda, A. A.; Zhou, Y.; Cairns, N. J.; Kambal, A.; et al. TREM2 Maintains Microglial Metabolic Fitness in Alzheimer's Disease. *Cell* **2017**, *170* (4), 649-663.e13.

(35) Blanco-Menéndez, N.; del Fresno, C.; Fernandes, S.; Calvo, E.; Conde-Garrosa, R.; Kerr, W. G.; Sancho, D. SHIP-1 Couples to the Dectin-1 HemITAM and Selectively Modulates Reactive Oxygen Species Production in Dendritic Cells in Response to Candida Albicans. *J. Immunol.* **2015**, *195* (9), 4466–4478.

(36) Malik, M.; Simpson, J. F.; Parikh, I.; Wilfred, B. R.; Fardo, D. W.; Nelson, P. T.; Estus, S. CD33 Alzheimer's Risk-Altering Polymorphism, CD33 Expression, and Exon 2 Splicing. *J. Neurosci.* **2013**, *33* (33), 13320–13325.

(37) Griciuc, A.; Serrano-Pozo, A.; Parrado, A. R.; Lesinski, A. N.; Asselin, C. N.; Mullin, K.; Hooli, B.; Choi, S. H.; Hyman, B. T.; Tanzi, R. E. Alzheimer's Disease Risk Gene CD33 Inhibits Microglial Uptake of Amyloid Beta. *Neuron* **2013**, *78* (4), 631–643.

(38) Rodgers, S. J.; Ferguson, D. T.; Mitchell, C. A.; Ooms, L. M. Regulation of PI3K Effector Signalling in Cancer by the Phosphoinositide Phosphatases. *Biosci. Rep.* **2017**, *37* (1).

(39) Jain, S.; Susa, M.; Keeler, M.; Carlesso, N.; Druker, B.; Varticovski, L. PI 3-Kinase Activation in BCR/Abl-Transformed Hematopoietic Cells Does Not Require Interaction of P85 SH2 Domains with P210 BCR/Abl. *Blood* **1996**, *88* (5), 1542–1550.

(40) Fedele, C. G.; Ooms, L. M.; Ho, M.; Vieusseux, J.; O'Toole, S. A.; Millar, E. K.; Lopez-

Knowles, E.; Sriratana, A.; Gurung, R.; Baglietto, L.; et al. Inositol Polyphosphate 4-Phosphatase II Regulates PI3K/Akt Signaling and Is Lost in Human Basal-like Breast Cancers. *Proc. Natl. Acad. Sci.* **2010**, *107* (51), 22231–22236.

(41) Gewinner, C.; Wang, Z. C.; Richardson, A.; Teruya-Feldstein, J.; Etemadmoghadam, D.; Bowtell, D.; Barretina, J.; Lin, W. M.; Rameh, L.; Salmena, L.; et al. Evidence That Inositol Polyphosphate 4-Phosphatase Type II Is a Tumor Suppressor That Inhibits PI3K Signaling. *Cancer Cell* **2009**, *16* (2), 115–125.

(42) Ivetac, I.; Gurung, R.; Hakim, S.; Horan, K. A.; Sheffield, D. A.; Binge, L. C.; Majerus, P. W.; Tiganis, T.; Mitchell, C. A. Regulation of PI(3)K/Akt Signalling and Cellular Transformation by Inositol Polyphosphate 4-phosphatase-1. *EMBO Rep.* **2009**, *10* (5), 487–493.

(43) Prasad, N. K.; Decker, S. J. SH2-Containing 5′-Inositol Phosphatase, SHIP2, Regulates Cytoskeleton Organization and Ligand-Dependent Down-Regulation of the Epidermal Growth Factor Receptor. *J. Biol. Chem.* **2005**, *280* (13), 13129–13136.

(44) Xie, J.; Erneux, C.; Pirson, I. How Does SHIP1/2 Balance PtdIns(3,4)P 2 and Does It Signal Independently of Its Phosphatase Activity? *BioEssays* **2013**, *35* (8), 733–743.

(45) Prasad, N. K. SHIP2 Phosphoinositol Phosphatase Positively Regulates EGFR-Akt Pathway, CXCR4 Expression, and Cell Migration in MDA-MB-231 Breast Cancer Cells. *Int. J. Oncol.* **2009**, *34* (1), 97–105.

(46) Ben-Sahra, I.; Manning, B. D. MTORC1 Signaling and the Metabolic Control of Cell Growth. *Curr. Opin. Cell Biol.* **2017**, *45*, 72–82.

(47) Marat, A. L.; Wallroth, A.; Lo, W.-T.; Müller, R.; Norata, G. D.; Falasca, M.; Schultz, C.; Haucke, V. MTORC1 Activity Repression by Late Endosomal Phosphatidylinositol 3,4-

Bisphosphate. *Science (80-.).* **2017**, *356* (6341), 968–972.

(48) Charlier, E.; Condé, C.; Zhang, J.; Deneubourg, L.; Di Valentin, E.; Rahmouni, S.; Chariot, A.; Agostinis, P.; Pang, P.-C.; Haslam, S. M.; et al. SHIP-1 Inhibits CD95/APO-1/Fas-Induced Apoptosis in Primary T Lymphocytes and T Leukemic Cells by Promoting CD95 Glycosylation Independently of Its Phosphatase Activity. *Leukemia* **2010**, *24* (4), 821–832.

(49) Park, M. Y.; Srivastava, N.; Sudan, R.; Viernes, D. R.; Chisholm, J. D.; Engelman, R. W.; Kerr, W. G. Impaired T-Cell Survival Promotes Mucosal Inflammatory Disease in SHIP1-Deficient Mice. *Mucosal Immunol.* **2014**, *7* (6), 1429–1439.

(50) Tummers, B.; Green, D. R. Caspase-8: Regulating Life and Death. *Immunol. Rev.* **2017**, *277* (1), 76–89.

(51) Maxwell, M. J.; Duan, M.; Armes, J. E.; Anderson, G. P.; Tarlinton, D. M.; Hibbs, M. L. Genetic Segregation of Inflammatory Lung Disease and Autoimmune Disease Severity in SHIP-1 −/− Mice. *J. Immunol.* **2011**, *186* (12), 7164–7175.

(52) Kerr, W. G. Inhibitor and Activator: Dual Functions for SHIP in Immunity and Cancer. *Ann. N. Y. Acad. Sci.* **2011**, *1217* (1), 1–17.

(53) Roongapinun, S.; Oh, S.-Y.; Wu, F.; Panthong, A.; Zheng, T.; Zhu, Z. Role of SHIP-1 in the Adaptive Immune Responses to Aeroallergen in the Airway. *PLoS One* **2010**, *5* (11), e14174.

(54) Wang, J.-W.; Howson, J. M.; Ghansah, T.; Desponts, C.; Ninos, J. M.; May, S. L.; Nguyen, K. H. T.; Toyama-Sorimachi, N.; Kerr, W. G. Influence of SHIP on the NK Repertoire and Allogeneic Bone Marrow Transplantation. *Science (80-.).* **2002**, *295* (5562), 2094–2097.

(55) Ghansah, T.; Paraiso, K. H. T.; Highfill, S.; Desponts, C.; May, S.; McIntosh, J. K.; Wang, J.-W.; Ninos, J.; Brayer, J.; Cheng, F.; et al. Expansion of Myeloid Suppressor Cells in SHIP-Deficient Mice Represses Allogeneic T Cell Responses. *J. Immunol.* **2004**, *173* (12), 7324–7330.

(56) Paraiso, K. H. T.; Ghansah, T.; Costello, A.; Engelman, R. W.; Kerr, W. G. Induced SHIP Deficiency Expands Myeloid Regulatory Cells and Abrogates Graft-versus-Host Disease. *J. Immunol.* **2007**, *178* (5), 2893–2900.

(57) Collazo, M. M.; Wood, D.; Paraiso, K. H. T.; Lund, E.; Engelman, R. W.; Le, C.-T.; Stauch, D.; Kotsch, K.; Kerr, W. G. SHIP Limits Immunoregulatory Capacity in the T-Cell Compartment. *Blood* **2009**, *113* (13), 2934–2944.

(58) Wahle, J. A.; Paraiso, K. H. T.; Costello, A. L.; Goll, E. L.; Sentman, C. L.; Kerr, W. G. Cutting Edge: Dominance by an MHC-Independent Inhibitory Receptor Compromises NK Killing of Complex Targets. *J. Immunol.* **2006**, *176* (12), 7165–7169.

(59) Fernandes, S.; Brooks, R.; Gumbleton, M.; Park, M.-Y.; Russo, C. M.; Howard, K. T.; Chisholm, J. D.; Kerr, W. G. SHIPi Enhances Autologous and Allogeneic Hematopoietic Stem Cell Transplantation. *EBioMedicine* **2015**, *2* (3), 205–213.

(60) Malek, M.; Kielkowska, A.; Chessa, T.; Anderson, K. E.; Barneda, D.; Pir, P.; Nakanishi, H.; Eguchi, S.; Koizumi, A.; Sasaki, J.; et al. PTEN Regulates PI(3,4)P2 Signaling Downstream of Class I PI3K. *Mol. Cell* **2017**, *68* (3), 566-580.e10.

(61) Gumbleton, M.; Sudan, R.; Fernandes, S.; Engelman, R. W.; Russo, C. M.; Chisholm, J. D.; Kerr, W. G. Dual Enhancement of T and NK Cell Function by Pulsatile Inhibition of SHIP1 Improves Antitumor Immunity and Survival. *Sci. Signal.* **2017**, *10* (500).

(62) Clément, S.; Krause, U.; Desmedt, F.; Tanti, J.-F.; Behrends, J.; Pesesse, X.; Sasaki, T.;

Penninger, J.; Doherty, M.; Malaisse, W.; et al. The Lipid Phosphatase SHIP2 Controls Insulin Sensitivity. *Nature* **2001**, *409* (6816), 92–97.

(63) Hoekstra, E.; Das, A. M.; Willemsen, M.; Swets, M.; Kuppen, P. J. K.; van der Woude, C. J.; Bruno, M. J.; Shah, J. P.; Hagen, T. L. M. ten; Chisholm, J. D.; et al. Lipid Phosphatase SHIP2 Functions as Oncogene in Colorectal Cancer by Regulating PKB Activation. *Oncotarget* **2016**, *7* (45), 73525–73540.

(64) Prasad, N. K.; Tandon, M.; Handa, A.; Moore, G. E.; Babbs, C. F.; Snyder, P. W.; Bose, S. High Expression of Obesity-Linked Phosphatase SHIP2 in Invasive Breast Cancer Correlates with Reduced Disease-Free Survival. *Tumor Biol.* **2008**, *29* (5), 330–341.

(65) Fu, M.; Fan, W.; Pu, X.; Ni, H.; Zhang, W.; Chang, F.; Gong, L.; Xiong, L.; Wang, J.; Gu, X. Elevated Expression of SHIP2 Correlates with Poor Prognosis in Non-Small Cell Lung Cancer. *Int. J. Clin. Exp. Pathol.* **2013**, *6* (10), 2185–2191.

(66) Tu, Z.; Ninos, J. M.; Ma, Z.; Wang, J.-W.; Lemos, M. P.; Desponts, C.; Ghansah, T.; Howson, J. M.; Kerr, W. G. Embryonic and Hematopoietic Stem Cells Express a Novel SH2–Containing Inositol 5′-Phosphatase Isoform That Partners with the Grb2 Adapter Protein. *Blood* **2001**, *98* (7), 2028–2038.

(67) Bai, L.; Rohrschneider, L. R. S-SHIP Promoter Expression Marks Activated Stem Cells in Developing Mouse Mammary Tissue. *Genes Dev.* **2010**, *24* (17), 1882–1892.

(68) Tian, L.; Truong, M.-J.; Lagadec, C.; Adriaenssens, E.; Bouchaert, E.; Bauderlique-Le Roy, H.; Figeac, M.; Le Bourhis, X.; Bourette, R. P. S-SHIP Promoter Expression Identifies Mouse Mammary Cancer Stem Cells. *Stem Cell Reports* **2019**, *13* (1), 10–20.

(69) Brocqueville, G.; Chmelar, R. S.; Bauderlique-Le Roy, H.; Deruy, E.; Tian, L.; Vessella, R. L.; Greenberg, N. M.; Rohrschneider, L. R.; Bourette, R. P. S-SHIP Expression

Identifies a Subset of Murine Basal Prostate Cells as Neonatal Stem Cells. *Oncotarget* **2016**, *7* (20), 29228–29244.

(70) Augoff, K.; Hryniewicz-Jankowska, A.; Tabola, R. Invadopodia: Clearing the Way for Cancer Cell Invasion. *Ann. Transl. Med.* **2020**, *8* (14), 902–902.

(71) Sánchez-Sendra, B.; Serna, E.; Navarro, L.; González-Muñoz, J. F.; Portero, J.; Ramos, A.; Murgui, A.; Monteagudo, C. Transcriptomic Identification of MiR-205 Target Genes Potentially Involved in Metastasis and Survival of Cutaneous Malignant Melanoma. *Sci. Rep.* **2020**, *10* (1), 4771.

(72) Sharma, V. P.; Eddy, R.; Entenberg, D.; Kai, M.; Gertler, F. B.; Condeelis, J. Tks5 and SHIP2 Regulate Invadopodium Maturation, but Not Initiation, in Breast Carcinoma Cells. *Curr. Biol.* **2013**, *23* (21), 2079–2089.

(73) Edimo, W. E.; Ghosh, S.; Derua, R.; Janssens, V.; Waelkens, E.; Vanderwinden, J.-M.; Robe, P.; Erneux, C. SHIP2 Controls Plasma Membrane PI(4,5)P2 Thereby Participating in the Control of Cell Migration in 1321 N1 Glioblastoma. *J. Cell Sci.* **2016**.

(74) Ramos, A. R.; Ghosh, S.; Dedobbeleer, M.; Robe, P. A.; Rogister, B.; Erneux, C. Lipid Phosphatases SKIP and SHIP2 Regulate Fibronectin-Dependent Cell Migration in Glioblastoma. *FEBS J.* **2019**, *286* (6), 1120–1135.

(75) Ghosh, S.; Scozzaro, S.; Ramos, A. R.; Delcambre, S.; Chevalier, C.; Krejci, P.; Erneux, C. Inhibition of SHIP2 Activity Inhibits Cell Migration and Could Prevent Metastasis in Breast Cancer Cells. *J. Cell Sci.* **2018**.

(76) Spector, D. L.; Lamond, A. I. Nuclear Speckles. *Cold Spring Harb. Perspect. Biol.* **2011**, *3* (2), a000646–a000646.

(77) Elong Edimo, W.; Derua, R.; Janssens, V.; Nakamura, T.; Vanderwinden, J.-M.;

Waelkens, E.; Erneux, C. Evidence of SHIP2 Ser132 Phosphorylation, Its Nuclear Localization and Stability. *Biochem. J.* **2011**, *439* (3), 391–404.

(78) Bunce, M. W.; Bergendahl, K.; Anderson, R. A. Nuclear PI(4,5)P2: A New Place for an Old Signal. *Biochim. Biophys. Acta - Mol. Cell Biol. Lipids* **2006**, *1761* (5–6), 560–569.

(79) Sun, Y.; Thapa, N.; Hedman, A. C.; Anderson, R. A. Phosphatidylinositol 4,5-Bisphosphate: Targeted Production and Signaling. *BioEssays* **2013**, *35* (6), 513–522.

(80) Osborne, S. L.; Thomas, C. L.; Gschmeissner, S.; Schiavo, G. Nuclear PtdIns(4,5)P2 Assembles in a Mitotically Regulated Particle Involved in Pre-MRNA Splicing. *J. Cell Sci.* **2001**, *114* (13), 2501–2511.

(81) Blind, R. D.; Suzawa, M.; Ingraham, H. A. Direct Modification and Activation of a Nuclear Receptor–PIP 2 Complex by the Inositol Lipid Kinase IPMK. *Sci. Signal.* **2012**, *5* (229).

(82) Blouw, B.; Patel, M.; Iizuka, S.; Abdullah, C.; You, W. K.; Huang, X.; Li, J.-L.; Diaz, B.; Stallcup, W. B.; Courtneidge, S. A. The Invadopodia Scaffold Protein Tks5 Is Required for the Growth of Human Breast Cancer Cells In Vitro and In Vivo. *PLoS One* **2015**, *10* (3), e0121003.

(83) Brauweiler, A.; Merrell, K.; Gauld, S. B.; Cambier, J. C. Cutting Edge: Acute and Chronic Exposure of Immature B Cells to Antigen Leads to Impaired Homing and SHIP1-Dependent Reduction in Stromal Cell-Derived Factor-1 Responsiveness. *J. Immunol.* **2007**, *178* (6), 3353–3357.

(84) Somasundaram, R.; Fernandes, S.; Deuring, J. J.; de Haar, C.; Kuipers, E. J.; Vogelaar, L.; Middleton, F. A.; van der Woude, C. J.; Peppelenbosch, M. P.; Kerr, W. G.; et al. Analysis of SHIP1 Expression and Activity in Crohn's Disease Patients. *PLoS One* **2017**,

12 (8), e0182308.

(85) Fernandes, S.; Srivastava, N.; Sudan, R.; Middleton, F. A.; Shergill, A. K.; Ryan, J. C.; Kerr, W. G. SHIP1 Deficiency in Inflammatory Bowel Disease Is Associated With Severe Crohn's Disease and Peripheral T Cell Reduction. *Front. Immunol.* **2018**, *9*.

(86) Lehtonen, S. SHIPping out Diabetes—Metformin, an Old Friend among New SHIP2 Inhibitors. *Acta Physiol.* **2020**, *228* (1).

(87) Baumgartener, J. W. SHIP2: An Emerging Target for the Treatment of Type 2 Diabetes Mellitus. *Curr. Drug Targets - Immune, Endocr. Metab. Disord.* **2003**, *3* (4), 291–298.

(88) Sleeman, M. W.; Wortley, K. E.; Lai, K.-M. V; Gowen, L. C.; Kintner, J.; Kline, W. O.; Garcia, K.; Stitt, T. N.; Yancopoulos, G. D.; Wiegand, S. J.; et al. Absence of the Lipid Phosphatase SHIP2 Confers Resistance to Dietary Obesity. *Nat. Med.* **2005**, *11* (2), 199–205.

(89) Berg, M. E. A.; Naams, J.-B.; Hautala, L. C.; Tolvanen, T. A.; Ahonen, J. P.; Lehtonen, S.; Wähälä, K. Novel Sulfonanilide Inhibitors of SHIP2 Enhance Glucose Uptake into Cultured Myotubes. *ACS Omega* **2020**, *5* (3), 1430–1438.

(90) Suwa, A.; Yamamoto, T.; Sawada, A.; Minoura, K.; Hosogai, N.; Tahara, A.; Kurama, T.; Shimokawa, T.; Aramori, I. Discovery and Functional Characterization of a Novel Small Molecule Inhibitor of the Intracellular Phosphatase, SHIP2. *Br. J. Pharmacol.* **2009**, *158* (3), 879–887.

(91) Srivastava, N.; Iyer, S.; Sudan, R.; Youngs, C.; Engelman, R. W.; Howard, K. T.; Russo, C. M.; Chisholm, J. D.; Kerr, W. G. A Small-Molecule Inhibitor of SHIP1 Reverses Age- and Diet-Associated Obesity and Metabolic Syndrome. *JCI Insight* **2016**, *1* (11).

(92) Pirruccello, M.; Nandez, R.; Idevall-Hagren, O.; Alcazar-Roman, A.; Abriola, L.;

Berwick, S. A.; Lucast, L.; Morel, D.; De Camilli, P. Identification of Inhibitors of Inositol 5-Phosphatases through Multiple Screening Strategies. *ACS Chem. Biol.* **2014**, *9* (6), 1359–1368.

(93) Zhang, H.; He, J.; Kutateladze, T. G.; Sakai, T.; Sasaki, T.; Markadieu, N.; Erneux, C.; Prestwich, G. D. 5-Stabilized Phosphatidylinositol 3,4,5-Trisphosphate Analogues Bind Grp1 PH, Inhibit Phosphoinositide Phosphatases, and Block Neutrophil Migration. *Chembiochem* **2010**, *11* (3), 388–395.

(94) Vandeput, F.; Combettes, L.; Mills, S. J.; Backers, K.; Wohlkönig, A.; Parys, J. B.; De Smedt, H.; Missiaen, L.; Dupont, G.; Potter, B. V. L.; et al. Biphenyl 2,3′,4,5′,6-pentakisphosphate, a Novel Inositol Polyphosphate Surrogate, Modulates Ca 2+ Responses in Rat Hepatocytes. *FASEB J.* **2007**, *21* (7), 1481–1491.

(95) Mills, S. J.; Persson, C.; Cozier, G.; Thomas, M. P.; Trésaugues, L.; Erneux, C.; Riley, A. M.; Nordlund, P.; Potter, B. V. L. A Synthetic Polyphosphoinositide Headgroup Surrogate in Complex with SHIP2 Provides a Rationale for Drug Discovery. *ACS Chem. Biol.* **2012**, *7* (5), 822–828.

(96) Suwa, A.; Kurama, T.; Yamamoto, T.; Sawada, A.; Shimokawa, T.; Aramori, I. Glucose Metabolism Activation by SHIP2 Inhibitors via Up-Regulation of GLUT1 Gene in L6 Myotubes. *Eur. J. Pharmacol.* **2010**, *642* (1–3), 177–182.

(97) Rena, G.; Hardie, D. G.; Pearson, E. R. The Mechanisms of Action of Metformin. *Diabetologia* **2017**, *60* (9), 1577–1585.

(98) Pernicova, I.; Korbonits, M. Metformin—Mode of Action and Clinical Implications for Diabetes and Cancer. *Nat. Rev. Endocrinol.* **2014**, *10* (3), 143–156.

(99) Pedicone, C.; Fernandes, S.; Dungan, O. M.; Dormann, S. M.; Viernes, D. R.; Adhikari,

A. A.; Choi, L. B.; De Jong, E. P.; Chisholm, J. D.; Kerr, W. G. Pan-SHIP1/2 Inhibitors Promote Microglia Effector Functions Essential for CNS Homeostasis. *J. Cell Sci.* **2020**, *133* (5).

(100) Trenholme, G. M.; Williams, R. L.; Desjardins, R. E.; Frischer, H.; Carson, P. E.; Rieckmann, K. H.; Canfield, C. J. Mefloquine (WR 142,490) in the Treatment of Human Malaria. *Science (80-.).* **1975**, *190* (4216), 792–794.

(101) Ong, C. J.; Ming-Lum, A.; Nodwell, M.; Ghanipour, A.; Yang, L.; Williams, D. E.; Kim, J.; Demirjian, L.; Qasimi, P.; Ruschmann, J.; et al. Small-Molecule Agonists of SHIP1 Inhibit the Phosphoinositide 3-Kinase Pathway in Hematopoietic Cells. *Blood* **2007**, *110* (6), 1942–1949.

(102) Le Coq, J.; Camacho-Artacho, M.; Velázquez, J. V.; Santiveri, C. M.; Gallego, L. H.; Campos-Olivas, R.; Dölker, N.; Lietha, D. Structural Basis for Interdomain Communication in SHIP2 Providing High Phosphatase Activity. *Elife* **2017**, *6*.

(103) Yang, L.; Williams, D. E.; Mui, A.; Ong, C.; Krystal, G.; Van Soest, R.; Andersen, R. J. Synthesis of Pelorol and Analogues: Activators of the Inositol 5-Phosphatase SHIP. *Org. Lett.* **2005**, *7* (6), 1073–1076.

(104) Goclik, E.; König, G. M.; Wright, A. D.; Kaminsky, R. Pelorol from the Tropical Marine Sponge Dactylospongia Elegans. *J. Nat. Prod.* **2000**, *63* (8), 1150–1152.

(105) Lemm, E. A.; Valle-Argos, B.; Smith, L. D.; Richter, J.; Gebreselassie, Y.; Carter, M. J.; Karolova, J.; Svaton, M.; Helman, K.; Weston-Bell, N. J.; et al. Preclinical Evaluation of a Novel SHIP1 Phosphatase Activator for Inhibition of PI3K Signaling in Malignant B Cells. *Clin. Cancer Res.* **2020**, *26* (7), 1700–1711.

(106) Stenton, G. R.; MacKenzie, L. F.; Tam, P.; Harwig, C.; Raymond, J.; Toews, J.; Wu, J.;

Ogden, N.; MacRury, T.; Szabo, C. Characterization of AQX-1125, a Small-Molecule SHIP1 Activator Part 1. Effects on Inflammatory Cell Activation and Chemotaxis in Vitro and Pharmacokinetic Characterization in Vivo. *Br. J. Pharmacol.* **2013**, *168* (6), 1506–1518.

(107) Stenton, G. R.; Mackenzie, L. F.; Tam, P.; Cross, J. L.; Harwig, C.; Raymond, J.; Toews, J.; Chernoff, D.; MacRury, T.; Szabo, C. Characterization of AQX-1125, a Small-Molecule SHIP1 Activator. *Br. J. Pharmacol.* **2013**, *168* (6), 1519–1529.

(108) Chamberlain, T. C.; Cheung, S. T.; Yoon, J. S. J.; Ming-Lum, A.; Gardill, B. R.; Shakibakho, S.; Dzananovic, E.; Ban, F.; Samiea, A.; Jawanda, K.; et al. Interleukin-10 and Small Molecule SHIP1 Allosteric Regulators Trigger Anti-Inflammatory Effects through SHIP1/STAT3 Complexes. *iScience* **2020**, *23* (8), 101433.

(109) Dungan, O. M.; Dormann, S.; Fernandes, S.; Duffy, B. C.; Effiong, D. G.; Kerr, W. G.; Chisholm, J. D. Synthetic Studies on the Indane SHIP1 Agonist AQX-1125. *Org. Biomol. Chem.* **2022**, *20* (19), 4016–4020.

(110) Williams, D. E.; Amlani, A.; Dewi, A. S.; Patrick, B. O.; Van Ofwegen, L.; Mui, A. L. F.; Andersen, R. J. Australin e Isolated from the Soft Coral Cladiella Sp. Collected in Pohnpei Activates the Inositol 5-Phosphatase SHIP1. *Aust. J. Chem.* **2010**, *63* (6), 895–900.

(111) Li, D.; Carr, G.; Zhang, Y.; Williams, D. E.; Amlani, A.; Bottriell, H.; Mui, A. L. F.; Andersen, R. J. Turnagainolides A and B, Cyclic Depsipeptides Produced in Culture by a Bacillus Sp.: Isolation, Structure Elucidation, and Synthesis. *J. Nat. Prod.* **2011**, *74* (5), 1093–1099.

(112) Pedicone, C.; Fernandes, S.; Matera, A.; Meyer, S. T.; Loh, S.; Ha, J.-H.; Bernard, D.; Chisholm, J. D.; Paolicelli, R. C.; Kerr, W. G. Discovery of a Novel SHIP1 Agonist That

Promotes Degradation of Lipid-Laden Phagocytic Cargo by Microglia. *iScience* **2022**, *25* (4), 104170.

Chapter 2: The Design and Synthesis of Small Molecule SHIP Inhibitors

Abstract

SHIP is a key regulator along the PI3K signaling pathway, influencing the phosphorylation patterns of the inositol phospholipids intercalated along the cell membrane that serve as secondary messengers disseminating information throughout the cell. Abnormal signaling of this pathway, often from dysregulation of inositol phospholipid concentrations, has been implicated in a number of disorders, including Alzheimer's disease and cancer. Modulation of the P13K pathway, specifically changing the levels of the different phosphatidylinositols found in the cell membrane has become a focus in the treatment of numerous diseases, as controlling the amounts of these molecules may be used to eliminate undesired cellular functions. Inhibition of SHIP through the use of small molecule inhibitors has been shown to be an appealing approach to remedy abnormal signaling, while also leading to apoptosis in tumor cells. Pan-SHIP1/2 inhibitors, inhibitors that target both SHIP1 and SHIP2, are of particular interest in these areas since paralog compensation is prevented when both SHIP paralogs are inhibited. Attempts to modulate SHIP activity by means of small molecules has led us to develop and synthesize a series of tryptamine-based pan-SHIP1/2 inhibitors, as well as to explore key structure-activity relationships required to increase the potency and selectivity required for inhibition.

2.1 Introduction & Background

Inositol phospholipids play a significant role in the regulation of many essential cellular functions, such as cell division and cell survival. These lipids serve as secondary messengers in cell signaling pathways, responsible for the dissemination of information throughout the cell.[1–4] Their role as secondary messengers is dependent on the phosphorylation patterns on the inositol phospholipids which are intercalated on the interior of the cell membrane.[5] These phosphorylation patterns are recognized by serine/threonine kinases, notably AKT in the PI3K pathway, which are activated upon binding of the phospholipids. Following activation, a signaling cascade relays signals from the membrane to the cell nucleus. These downstream signaling effects influence key processes like DNA transcription and replication, cell proliferation, and apoptosis.[1–6]

The phosphorylation and dephosphorylation of inositol phospholipids are tightly regulated by inositol kinases and phosphatases, such as phosphoinositide 3-kinase (PI3K). PI3K is responsible for the conversion of phosphatidylinositol (4,5)-bisphosphate [PI(4,5)P_2] to phosphatidylinositol (3,4,5)-trisphosphate [PI(3,4,5)P_3].[1–6] Typically, PI(3,4,5)P_3 is maintained at a low concentration, however; upon activation by a nearby transmembrane receptor tyrosine kinase, PI3K rapidly synthesizes PI(3,4,5)P_3 from PI(4,5)P_2. Additionally, PI(3,4,5)P_3 levels can also be regulated through degradation by PTEN, which dephosphorylates the 3'-position. SHIP is also known to regulate the amount of PI(3,4,5)P_3 present at the cell membrane by dephosphorylating the 5’-position producing PI(3,4)P_2. Abnormal signaling of this pathway, often from dysregulation of inositol phospholipid concentrations, has been implicated in a number of disorders, including Alzheimer's disease and cancer. Modulation of the P13K pathway, specifically changing the levels of the different phosphatidylinositols found in the cell membrane has become a focus in the treatment of numerous diseases, as controlling the amounts of these molecules may be used to eliminate undesired cellular functions. Direct inhibition of PI3K has been one method examined for the regulation of the inositol phospholipids, with several PI3K inhibitors having been developed and taken to clinical trials.[7–9] However, resistance to PI3K inhibitors has been reported under select circumstances, leading to a desire for alternative approaches to influence PI3K signaling.[10–12] PTEN is a well-known tumor suppressor and because of this is rarely targeted, as modulation of PTEN has been linked to a variety of hereditary and non-hereditary cancers.[13–15] This has led to increased interest in the SHIP enzyme, as SHIP knockout mice are viable.[16] Modulation of SHIP may provide a new method to influence the PI3K pathway signaling. SHIP is often seen as opposing the activity of PI3K initiated signaling, working to reduce the concentration of the direct PI3K enzyme product.[17] However, the situation has been shown to be more complex, with evidence pointing to the SHIP enzyme being responsible for the survival of tumor cells.[3,6,14,18] The major differences between PTEN and SHIP can be found in their functions within the PI3K pathway. PTEN is responsible for hydrolyzing the 3' phosphate to generate PI(4,5)P_2 from PI(3,4,5)P_3, while SHIP is a 5' phosphatases, which converts PI(3,4,5)P_3 to PI(3,4)P_2. Consequently, SHIP and PTEN employ vastly different effects on downstream signaling. Additionally, AKT binds more tightly to the SHIP product PI(3,4)P_2, leading to a more potent activation of AKT than that observed when bound to PI(3,4,5)P_3, the product of PI3K.[19] Since both PI(3,4)P_2 and PI(3,4,5)P_3 are both signaling active, the presence of both inositols is believed to promote a malignant state, leading to excessive cell division and increased survival of neoplasms.[12,15] This occurrence has been labelled the "Two PIP Hypothesis," where both PI(3,4,5)P_3 and PI(3,4)P_2 are necessary to develop and perpetuate tumor growth.

Holding true with the "Two PIP Hypothesis", levels of PI(3,4)P_2 have been found to be elevated in leukemia cells, while increased levels of PI(3,4)P_2 have also been associated with the promotion of tumors in SHIP knockout mice.[20–22] Previously, the SHIP1 inhibitor 3α-aminocholestane (3AC) was shown to reduce AKT activation while also promoting apoptosis of human blood cell cancers that explicitly express SHIP1.[3,6] PI(3,4)P_2's function in cancer cell signaling was further validated by exhibiting that the presence of exogenous PI(3,4)P_2 in leukemia cells prevents apoptosis by SHIP1 inhibition following a dose-dependent fashion.[6] Additionally, studies have also indicated that agonism of SHIP1 leads to reductions in the growth and development of multiple myeloma cells when treating in vitro.[23] Recently, the Kerr lab at SUNY Upstate Medical University found that SHIP1 knock-out mice are able to accept mismatched bone marrow transplants without the rejection or development of Graft-versus-Host disease (GVHD).[6,24] Additionally, scientists at Purdue University confirmed that high levels of SHIP2 are present in breast cancer cell lines, supporting the notion SHIP2 plays a major role in cancer development. The study also showed inhibiting SHIP2 leads to a reduction of in vivo tumor growth and lung metastasis in a mouse model system.[15] These early studies show modulation of SHIP activity is effective at treating certain types of cancer when tested in cell-based assays, as well as demonstrates that both SHIP inhibitors and agonists are cytotoxic to cancer cell lines. These findings further emphasize the intricate balance of both PI(3,4,5)P_3 and PI(3,4)P_2 cancer cells must maintain to become and remain malignant. Due to this, SHIP modulators may be able to regulate inositol levels preventing a malignant state, promoting apoptosis of cancer cells.

In addition to selective inhibitors of each SHIP paralog, pan-SHIP1/2 inhibitors, inhibitors than inhibit both SHIP1 and SHIP2, provide new approaches in the treatment of several types of cancer. As stated previously, SHIP1 selective inhibitors exhibited cytotoxic effects on leukemia cells.[6] However, other cancers, those derived from endothelial cells rather than cells with a myeloid lineage, may be more responsive to SHIP2 inhibition. The inhibition of SHIP2 in breast cancer could prove useful, where SHIP2 expression is increased and has been shown to stimulate survival signals from EGFR in tumors.[15,25] Additional studies have shown pan-SHIP1/2 inhibitors have the potential to actually slow the growth of tumor cells.[1,3] Although the use of small molecule inhibitors allow for direct targeting of AKT and mTOR, the modulation of SHIP provides an alternative molecular mechanism allowing for PI3K signaling to be regulated by downstream modifications.[26] This alteration could prove beneficial in the treatment of tumors that are resistant to AKT and/or mTOR inhibitors, as they may still be receptive to SHIP inhibition. The ability to produce a pan inhibitor could prevent tumors from developing a resistance to the inhibition of one SHIP isoform, leading to the unwanted utilization of the alternative SHIP isoform. This paralog compensation has previously been observed in numerous tumor model systems.[3]

Due to the increased interest in SHIP inhibitors, a high-throughput screen of a small molecule library from the National Cancer Institute was performed utilizing a fluorescence polarization assay. The screen found a number of compounds with different structural classes that acted as SHIP inhibitors, including tryptamines and quinolines, which show biological activity versus multiple myeloma and blood cancer cell lines.[2–4,27–29] One of the hit compounds, tryptamine **2.1** (**Figure 2.1.1**), showed promising results as a pan-SHIP1/2 inhibitor and was found to have significant impact on killing breast cancer cells.[1,3,30] Although promising, it was later discovered **2.1** had significant side effects and induced psychotropic effects in mice. After further testing, the tryptamine analog **2.2** (**Figure 2.1.1)** was found to induce a similar, although less potent, response in tumor models with fewer psychotropic side effects.

Figure 2.1.1: Tryptamine Small Molecule Pan-SHIP1/2 Inhibitors

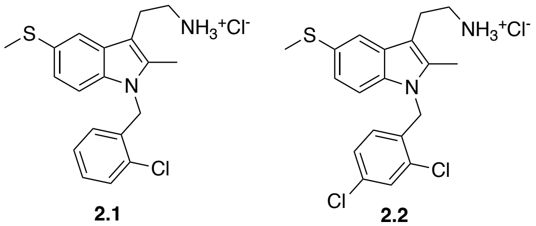

2.1

SHIP 1 IC_{50} = 4-5 µm
SHIP 2 IC_{50} = 9-10 µm

2.2

SHIP 1 IC_{50} = 20-30 µm
SHIP 2 IC_{50} = 30 µm

Using **2.2** as a platform, docking studies were performed with a model of the SHIP1 active site which provided several plausible binding modes for tryptamine inhibitors (**Figure 2.1.2**). These studies showed the amine residue appears to bind in the active site near the key aspartic acid residue, however the tryptamine inhibitors are too small to reach the P4-interacting motif (P4IM) loop region (the hydrophobic area where the lipids of PI(3,4,5)P_3 interact with the enzyme).[31] The P4IM region is more polar in SHIP2 than SHIP1, and this may explain the lack of selectivity of the tryptamine SHIP inhibitors. The docking also gave two possible poses for the orientation of the aromatic core. To attempt to determine which docking pose was most relevant, work began on synthesizing derivatives of tryptamine inhibitors with nonpolar groups at C2 and C5 of the indole to determine which pose was most relevant.

Figure 2.1.2: Binding Modes of Tryptamines to SHIP

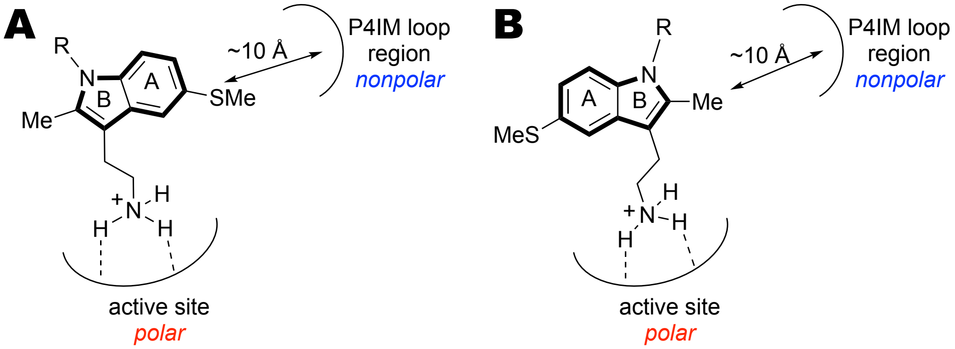

In order to gain further insight into the preferred orientation of the aromatic core, tryptamine analogs containing various sidechains at the 2 and 5-positions were synthesized. This allowed for the exploration of differing sidechain lengths that can span the P4IM loop distance. In addition to the structure activity relationship work, work was completed on the synthesis of tryptamine derivatives in an attempt to increase selectivity and potency. Inhibitors that have the ability to selectively inhibit SHIP1 or SHIP2, as well those that are able to inhibit both simultaneously (pan-SHIP inhibitors) are currently of great value and interest. Pan-SHIP inhibitors are of particular interest because they prevent tumors from becoming resistant to the inhibition of one SHIP isoform by exploiting the other isoform. These studies focused on various substituents at the 5-position, as well as looking at the different placements and substituents of the aryl halides.

In addition to the studies on tryptamine inhibitors, AS1949490 (**2.3, Figure 2.1.3**) was synthesized for comparison studies on the effects of pan-SHIP1/2 and SHIP2 selective inhibitors on numerous cancer cell lines.[32] AS1949490 (**2.3**) was found to be a selective SHIP2 inhibitor, discovered through the use of a high-throughput screening. This molecule has a reported IC_{50} of 0.62 uM when tested against the human SHIP2 paralog and an IC_{50} of 0.34 uM when tested on the mouse SHIP2 paralog. Additionally, kinetic studies showed that AS1949490 (**2.3**) was a competitive inhibitor with the PI(3,4,5)P3 substrate, with an inhibitory constant of 0.44 mM.[32] Along with studies in cancer model systems, a new study involving the use of SHIP inhibitors to treat Alzheimer's disease has been initiated using AS1949490 (**2.3**) and tryptamine-based SHIP inhibitors. This study will probe the use of SHIP inhibitors to influence the production of brain-derived neurotrophic factor (BDNF) through PI3K signaling.[33–35] BDNF is an essential factor required for maintaining proper brain functionality, such as cognition, memory, and learning. Since $PI(3,4,5)P_3$, plays a vital role in BDNF signaling and is produced in the PI3K pathway, SHIP inhibition has been explored as a targeted therapeutic strategy for neurological disorders, and the role of SHIP inhibitors on the production of BDNF will be explored.

Figure 2.1.3: AS1949490, a Selective SHIP2 Inhibitor

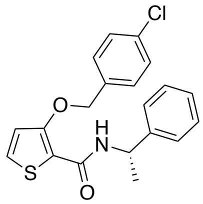

2.3

2.2 Objectives

The overall primary objective of this work was to develop and synthesize tryptamine analogs that displayed an increased potency and selectivity against SHIP. This goal was achieved by modifying individual sections of the tryptamine structure, mainly the 5-position, the primary amine, and the nitrogen at the 1-position, to find what functionality at each position provided the best inhibitory response. Additionally, tryptamine derivatives were derived that incorporate multiple sidechains at the 2 and 5 positions to flesh out information regarding the structure activity relationship.

Figure 2.2.1: Base Tryptamine Core and Numbering System

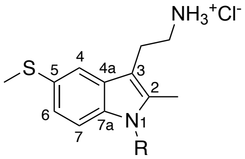

The second primary goal was to synthesize AS1949490 (**2.3**) for comparison studies on the effects of pan-SHIP1/2 and SHIP2 selective inhibitors on numerous cancer cell lines. The newly synthesized AS1949490 (**2.3**) was also involved in a new study initiated using tryptamine-based SHIP inhibitors to treat Alzheimer's disease.

Figure 2.2.2: SHIP2 Inhibitor AS1949490

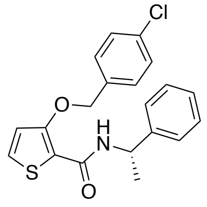

2.3

2.3 Results & Discussion

Initially, the synthesis of tryptamine **2.2** was pursued to provide more material to our Upstate Medical collaborators for use in ongoing testing. The synthesis of **2.2** began with the Gabriel amine synthesis of 5-chloro-2-pentanone (**2.4**) and phthalimide yielding ketone **2.5**. Phenylhydrazine derivative **2.7** was then prepared by forming the diazonium salt of 4-

(methylthio)aniline (**2.6**) using sodium nitrate and hydrochloric acid, which was then reduced with stannous chloride yielding hydrazine **2.7**. Protected tryptamine **2.8** was produced in a high yield of 86% via a Fischer-indole synthesis between intermediates **2.7** and **2.5**. Intermediate **2.9** was recovered via column chromatography after *N*-alkylation of the indole nitrogen utilizing cesium carbonate to promote the reaction, and 2,4-dichlorobenyzl chloride. The phthalimide protecting group was then removed by refluxing compound **2.9** in THF/MeOH in the present of hydrazine hydrate. The free amine was then stirred in a dilute HCl/ether mixture producing the tryptamine salt **2.2**.

Scheme 2.3.1: Synthesis of Tryptamine Salt **2.2**, a selective SHIP2 Inhibitor

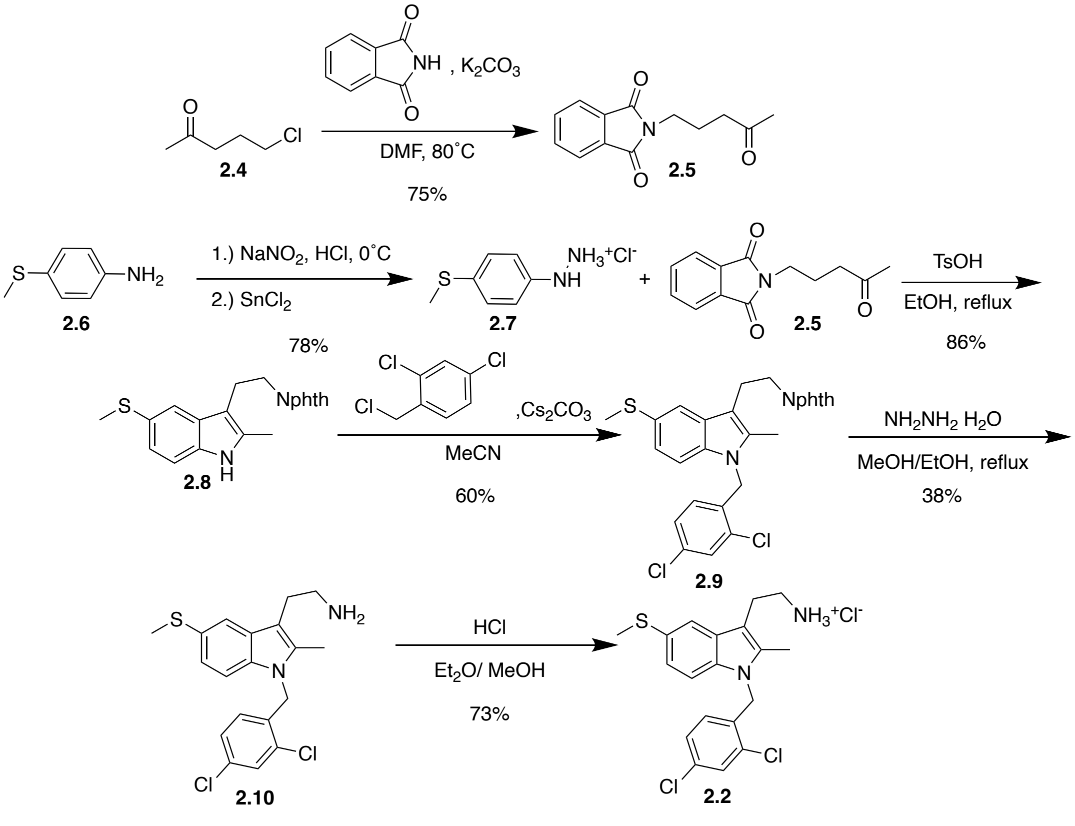

NH , K2CO3
DMF, 80˚C
75%
2.4
2.5
1.) NaNO2, HCl, 0˚C
2.) SnCl2
78%
2.6
2.7
NH3+Cl-
TsOH
EtOH, reflux
86%
2.8
Nphth
,Cs2CO3
MeCN
60%
2.9
NH2NH2 H2O
MeOH/EtOH, reflux
38%
2.10
HCl
Et2O/ MeOH
73%
2.2

Work then shifted to developing tryptamine analogs utilizing the **2.2** tryptamine core in the hopes of increasing the selectivity and activity of any future tryptamine inhibitors. The first analog prepared was tryptamine salt **2.11** in which the methylthio substrate at the 5 position, as well as the methyl group at the 2 position was maintained (**Figure 2.3.1**). This would allow for testing of the importance of the aromatic *N*-substitution to be explored.

Figure 2.3.1: Tryptamine Derivative **2.11**

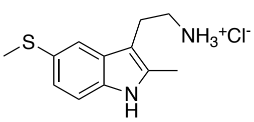

2.11

Work was then initiated on analogs with different substitution on the N-benzyl group. Starting with previously synthesized tryptamine core **2.8**, *N*-alkylation with the desired benzyl halide could be employed. The desired analogs contained a mix of halide functionality, swapping out the dichloro substitution of **2.2** for a mono chlorine at the ortho and para positions, an ortho/meta dichloro, and a para bromine as well as an unfunctionalized benzene ring. These changes allowed for the importance of the substitution pattern to be tested, as well as verifying the importance of the substituent itself. The same procedure that was utilized to synthesized **2.2** was used to synthesize the following tryptamine derivatives using different commercially available benzyl halides (**Table 2.3.1**).

Table 2.3.1: Methylthio Tryptamine Analogs

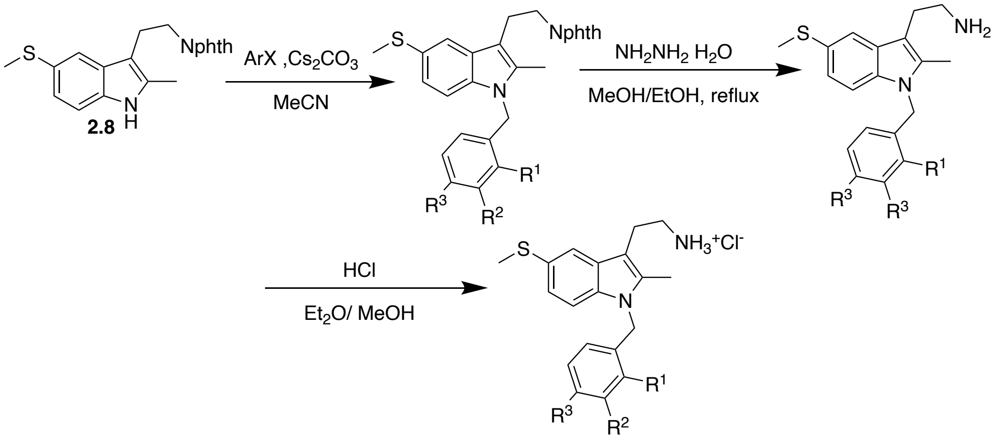

Entry	Compound	R¹	R²	R³	% Yield[a]
1	**2.1**	Cl	H	H	20%
2	**2.12**	H	H	Cl	15%
3	**2.13**	Cl	Cl	H	8%
4	**2.14**	H	H	Br	12%
5	**2.15**	H	H	H	23%

Notes: [a]Yield is over three steps

Additionally, analogs were synthesized focusing on manipulation of the primary amine. Using **2.1**, the initial tryptamine parent, the primary amine salt was turned into a methylamine salt, a dimethylamine salt, an acetamide, and a methanesulfonamide. Synthesis of the methylamine salt began by taking **2.1**, Boc anhydride and triethylamine and stirring them in a THF/MeOH solution, provided Boc carbamate **2.16**. Carbamate **2.16** was reduced with lithium aluminum hydride yielding methylamine **2.17**. The methylamine salt was then formed by stirring **2.17** in a HCl/ether solution producing **2.18**.

Scheme 2.3.2: Synthetic Route for tryptamine derivative **2.18**

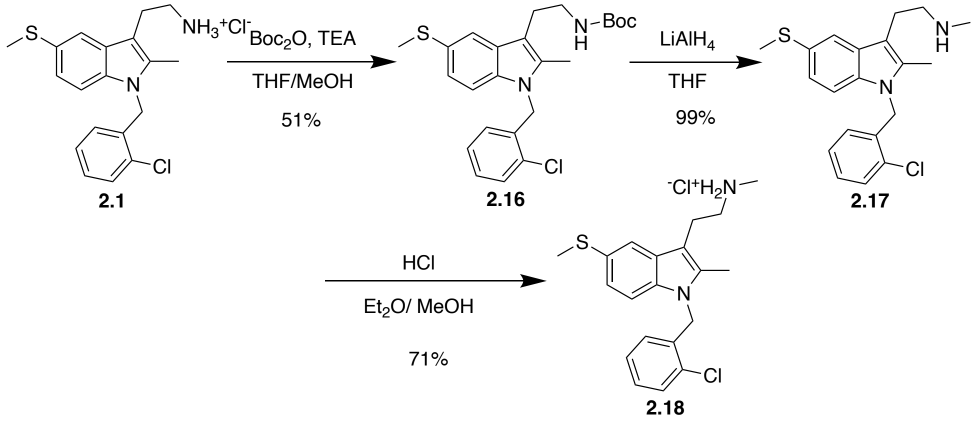
2.1
Boc₂O, TEA
THF/MeOH
51%
2.16
LiAlH₄
THF
99%
2.17
HCl
Et₂O/ MeOH
71%
2.18

Synthesis of the dimethylamine analog **2.20** again began with **2.1**. Utilizing formalin and sodium cyanoborohydride, **2.1** undergoes a reductive amination yielding dimethylamine **2.19**. The dimethylamine is then stirred in a HCl/ether mixture producing the dimethylamine salt **2.20**.

Scheme 2.3.3: Synthetic Route for tryptamine derivative **2.20**

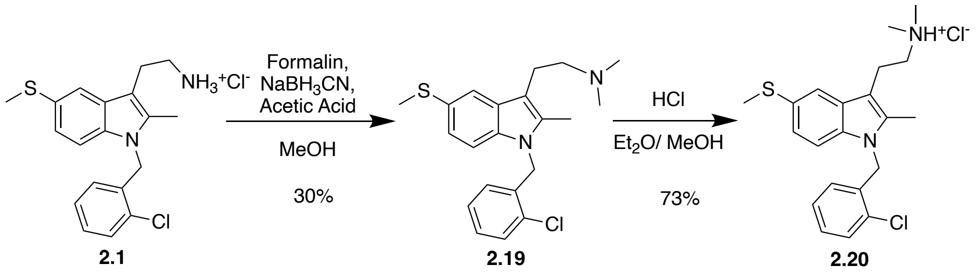
2.1
Formalin,
NaBH₃CN,
Acetic Acid
MeOH
30%
2.19
HCl
Et₂O/ MeOH
73%
2.20

The acetamide analog was formed by performing an acylation of the primary amine present in **2.1**, utilizing triethylamine to free base the salt, followed by acetic anhydride to perform the acylation yielding **2.21**.

Scheme 2.3.4: Synthetic Route for Acetamide **2.21**

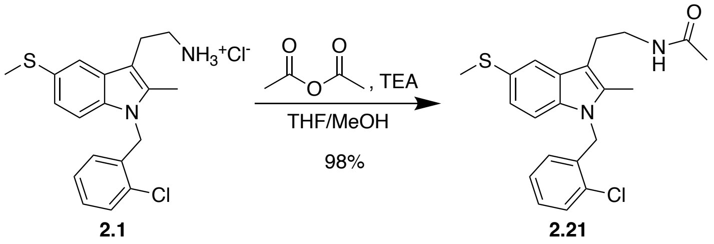
2.1
, TEA
THF/MeOH
98%
2.21

The methanesulfonamide derivative was formed by performing a mesyl protection of the **2.1** trypatmine primary amine using methanesulfonyl chloride and TEA in DCM. This reaction produced the desired sulfonamide **2.22**.

Scheme 2.3.5: Synthetic Route for Tryptamine Derivative **2.22**

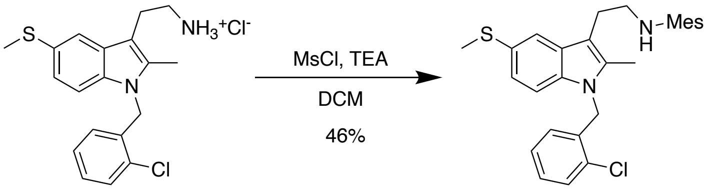

2.1 **2.22**

After preparation of the primary amine-based analogs, as well as alterations of the aryl halide on the N-benzyl group, attention was turned to altering the substituent at the indole 5-position. Up to this point, all analogs possessed a thiomethyl group at the 5-position, which could pose potential problems when it comes to viability in vivo. Thioethers are readily oxidized by cytochrome P450 in animals, which could potentially change the activity of the molecule and shorten the half-life. In order to test the importance of the thioester, as well as derive sulfur free analogs, alterations were made at this position, replacing the thioether with a bromine, chlorine, methoxy, and a hydrogen. Again, based on the known potency of tryptamine **2.1**, it was chosen to keep the 2-chlorobenzyl substitution pattern of the aromatic ring to facilitate comparisons. The desired tryptamines (**2.27-2.30**) were obtained by means of a Fischer indole synthesis between the previously synthesized ketone **2.5** and the desired phenyl hydrazine. Each tryptamine (**2.31**-**2.34**) then underwent *N*-alkylation with 2-chlorbenzyl chloride in the presence of Cs_2CO_3. The free amines (**2.35-2.38**) were then obtained by removal of the phthalimide protecting groups using hydrazine hydrate. Finally, the desired tryptamine salts (**2.39-2.42**) were obtained by stirring the free amines in a HCl/ether solution (**Scheme 2.3.6**).

Scheme 2.3.6: Synthesis of 5-Substituted Tryptamine Analogs

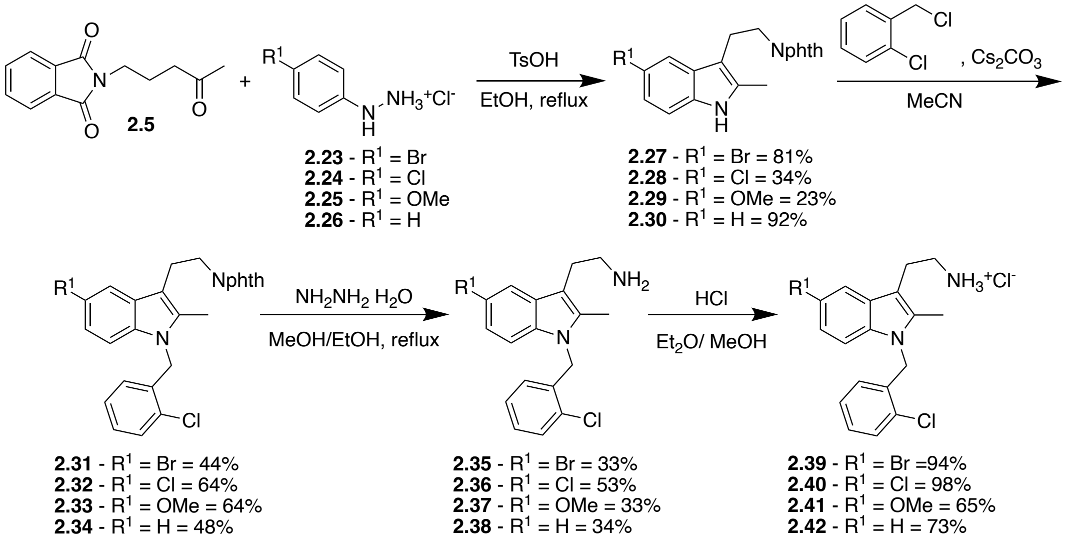
2.5
TsOH
EtOH, reflux
, Cs_2CO_3
MeCN
NH_2NH_2 H_2O
MeOH/EtOH, reflux
HCl
Et_2O/ MeOH
2.23 - R^1 = Br
2.24 - R^1 = Cl
2.25 - R^1 = OMe
2.26 - R^1 = H
2.27 - R^1 = Br = 81%
2.28 - R^1 = Cl = 34%
2.29 - R^1 = OMe = 23%
2.30 - R^1 = H = 92%
2.31 - R^1 = Br = 44%
2.32 - R^1 = Cl = 64%
2.33 - R^1 = OMe = 64%
2.34 - R^1 = H = 48%
2.35 - R^1 = Br = 33%
2.36 - R^1 = Cl = 53%
2.37 - R^1 = OMe = 33%
2.38 - R^1 = H = 34%
2.39 - R^1 = Br =94%
2.40 - R^1 = Cl = 98%
2.41 - R^1 = OMe = 65%
2.42 - R^1 = H = 73%

An additional analog was synthesized to further test the importance of the substitution at both the 5-position as well as the substitution on the benzyl ring. Analog **2.45** was formed from the previously mentioned tryptamine **2.30**. *N*-Alkylation was again used, this time using with 2-benzyl chloride. The use of tryptamine **2.30** and 2-chlorobenzyl chloride allows for minimal functionality to be incorporated into the tryptamine structure, allowing for activity testing of the bare-bones core. The primary amine **2.44** was then obtained by removal of the phthalimide protecting group using hydrazine hydrate. Finally, the desired tryptamine salt **2.45** was obtained by stirring the free amine in a HCl/ether solution (**Scheme 2.3.7**).

Scheme 2.3.7: Synthesis of Unfunctionalized Tryptamine Analog **2.45**

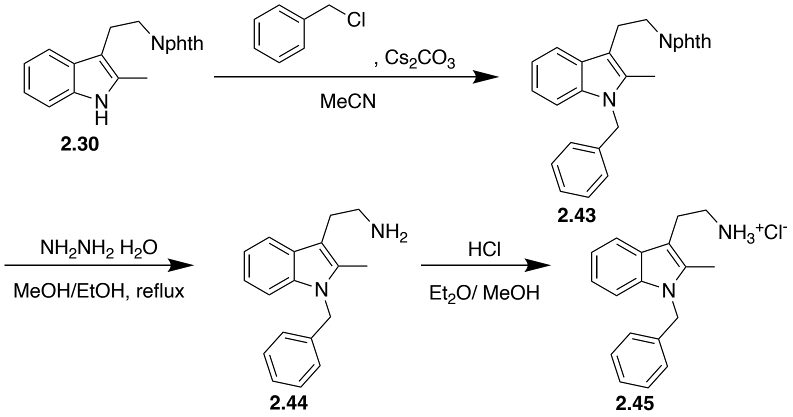
Nphth
N
H
2.30
Cl
, Cs_2CO_3
MeCN
Nphth
N
2.43
NH_2NH_2 H_2O
MeOH/EtOH, reflux
NH_2
N
2.44
HCl
Et_2O/ MeOH
$NH_3^+Cl^-$
N
2.45

These tryptamines were evaluated with the Malachite Green phosphatase assay by our collaborators at Upstate Medical. The Malachite Green assay evaluates the inhibition of SHIP based on the amount of free phosphate present. This assay is commonly used for measuring protein phosphatase activity as it is based on the ion association of phosphomolybdate and the charged malachite dye at highly acidic pHs. The absorbance of the green phosphomolybdic acid complex is then measured at 620 nm generating values correlating to the concentration of free phosphate present.[36,37] The results of these assays for the tryptamine analogs tested are shown in **Table 2.3.2**.

Table 2.3.2: Malachite Green Assay Results for N-Alkyl Tryptamine Analogs

Entry	Compound	% Inhibition						Selectivity Ratio SHIP1/2
		SHIP1 500 μM	SHIP1 250 μM	SHIP1 125 μM	SHIP2 500 μM	SHIP2 250 μM	SHIP2 125 μM	
1	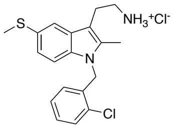 **2.1**	50%	8%	3%	59%	7%	3%	1:1
2	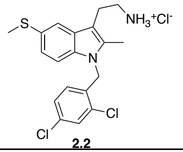 **2.2**	52%	31%	6%	58%	50%	17%	1:1
3	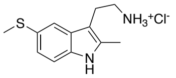 **2.11**	-35%	-41%	-41%	19%	2%	0%	N/A
4	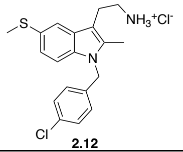 **2.12**	33%	-7%	-17%	49%	18%	-34%	1:1.5
5	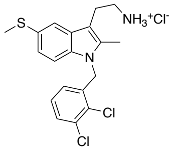 **2.13**	60%	50%	4%	--	--	--	N/A
6	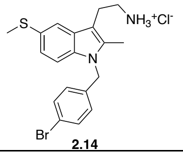 **2.14**	47%	4%	-16%	48%	48%	8%	1:1
7	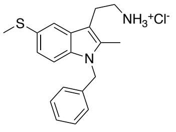 **2.15**	40%	0%	0%	39%	28%	9%	2:1

Analogs **2.2**, and **2.14** showed significant inhibition of both SHIP1 and SHIP2, matching the inhibitory potential seen for the tryptamine parent **2.1**, and could be classified as pan-SHIP inhibitors. All four derivatives contain halogen substituents on the *N*-benzyl ring. Additionally, analog **2.13**, a derivative containing an ortho/meta dichloro substitution, also showed strong inhibition versus SHIP1, however; has not been tested against SHIP2 yet. This is consistent with previous data which suggests having an ortho chlorine substitution, as seen in **2.1**, and **2.2**, could increase the inhibitory potential. The importance of the indole nitrogen *N*-substitution was further confirmed by the lack of inhibition of compound **2.11**, which appeared to be an agonist when tested against SHIP1 and a very weak inhibitor when tested on SHIP2. These results support the idea the benzyl ring plays a vital role in binding, most likely by helping to achieve the proper conformation needed for binding within the active site. Analogs **2.12** and **2.15** showed promising inhibition versus SHIP1 at high concentrations, but inhibition quickly plummets as the concentration decreases. Additionally, both of these inhibitors displayed moderate inhibition when tested against the SHIP2 paralog, maintaining a steady rate as the concentration was decreased.

Table 2.3.3: Malachite Green Assay Results for Tryptamine Analogs with Substitution on the α-Amine

Entry	Compound	% Inhibition						Selectivity Ratio SHIP1/2
		SHIP1 500 µM	SHIP1 250 µM	SHIP1 125 µM	SHIP2 500 µM	SHIP2 250 µM	SHIP2 125 µM	
1	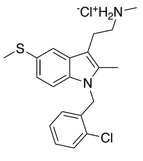 **2.18**	9%	-4%	-15%	39%	14%	0%	1:4
2	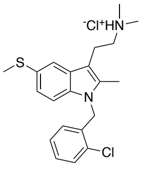 **2.20**	6%	-12%	-14%	6%	-18%	-28%	1:1
3	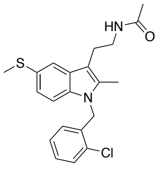 **2.21**	--	25%	16%	-34%	-15%	-11%	N/A
4	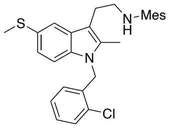 **2.22**	-27%	-22%	1%	--	--	--	N/A

Analogs **2.18**, **2.20**, **2.21**, and **2.22** all possessed modifications of the primary amine, which drastically altered the inhibitory response when compared to those with the primary amine present. Analog **2.18** showed no inhibition versus SHIP1 and only had weak inhibition when tested versus

SHIP2. The dimethylamine **2.20** showed no inhibitory response when tested versus SHIP1 or SHIP2. In contrast, the sulfonamide **2.22** actually appeared to be a weak SHIP1 agonist. The acetamide **2.21**, showed only weak SHIP1 inhibition and again appeared to have a response like a weak agonist. These results appear to indicate that the primary amine is vital for activity and binding within the active site.

Table 2.3.4: Malachite Green Assay Results for 5-Substituted Tryptamine Analogs

Entry	Compound	% Inhibition						Selectivity Ratio SHIP1/2
		SHIP1 500 µM	SHIP1 250 µM	SHIP1 125 µM	SHIP2 500 µM	SHIP2 250 µM	SHIP2 125 µM	
1	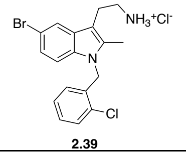 **2.39**	56%	35%	-8	--	--	--	N/A
2	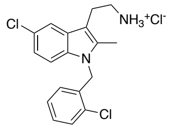 **2.40**	54%	45%	-6%	--	--	--	N/A
3	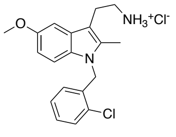 **2.41**	27%	-6%	--	--	--	--	N/A
4	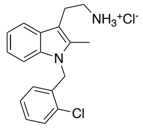 **2.42**	58%	29%	6%	50%	11%	0%	1:1
5	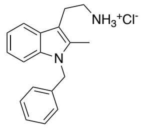 **2.45**	0%	0%	0%	10%	2%	0%	N/A

The final grouping of analogs, **2.39**, **2.40**, **2.41**, all have substitution at the 5'-position to gauge the importance of the thioether for activity, while **2.42** is unfunctionalized to further probe the importance of this position for activity. All four analogs have successfully been tested versus SHIP1 with SHIP2 testing ongoing. Derivatives **2.39** and **2.40** showed strong inhibitory effects, even at lower concentrations, while compound **2.41** showed weak inhibition at 500 µM, but was inactive at lower concentrations. Derivative **2.42** showed strong inhibition versus both SHIP1 and

SHIP2 at 500 μM and 250 μM concentrations. This data shows that alterations of the thioether are possible, without losing the inhibitory activity. While these analogs may provide a path forward to the development of selective SHIP inhibitors, these compounds are not presently useful in determining the effects of pan-SHIP inhibitors against tumors and tumor models.

Following the results of the malachite green assay, a number of the more active inhibitors (**2.1**, **2.2**, **2.12**, **2.15**), those closely matching the tryptamine parent **2.1** inhibitory potential, were evaluated for cytotoxicty on various cancer cell lines using the MTT assay looking at cell viability.[38] The four chosen tryptamines were tested on four different leukemia cell lines: NB4, HSB2, K562 and 697-Pre-B; as well the OPM-2 cell line of multiple myeloma cells. As previously stated, SHIP1 is solely expressed in endothelial cells such as blood and bone marrow cells. Therefore, all five of the chosen cell lines are known to express SHIP1 due to their myeloid lineage.[31] The breast cancer cell lines MBA-MD-231 and MCF-7 were also selected as SHIP2 is known to be overexpressed in breast cancer cells, and the inhibition of SHIP2 previously was shown to lead to cytotoxic affects when tested on cells.[1,3,25,39] Consistent with previous results, the parent tryptamine **2.1** showed strong activity across all cell lines, however; **2.2** displayed the greatest cytotoxicity against nearly all lines tested. These results are believed to be attributed to the increased hydrophobic nature of **2.2** when compared to **2.1**. This belief was further supported by calculating the partition coefficient (ClogP) of **2.2** and **2.1** using the MLOGP method with SwissADME.[40–42] The ClogP of **2.2** was calculated to be 4.6, while that of **2.1** was found to only be 4.11. The increase in activity when tested in the MTT assay can be attributed to the increased hydrophobic nature of **2.2**. This results in an increased association with the plasma membrane where SHIP activity is most important in signal transduction, leading to an increased effect on downfield signaling.

Figure 2.3.2: Tryptamine-based SHIP Inhibitors vs. leukemia, multiple myeloma and breast cancer cell lines

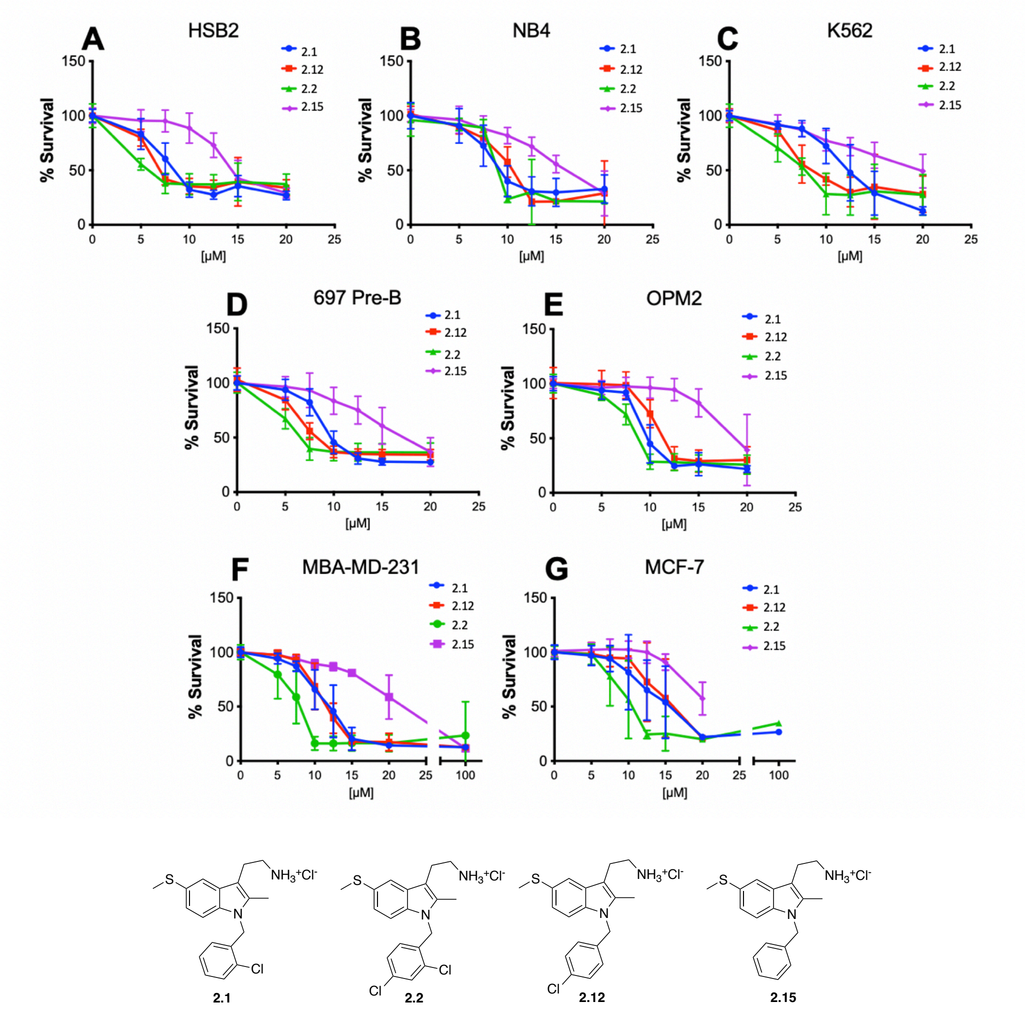

Figure 2.3.2: MTT cell viability assays performed on cancer cell lines. Cells were treated with various concentrations of compounds and analyzed 2 hours later for viable cells. The means of at least three independent experiments are shown. Error bars show standard deviations.

In addition to tryptamine analogs that explore the potential selectivity and potency, work has been completed on further understanding the structure-activity relationship between the analogs and the binding pocket. In order to achieve this, bromine substituents were added at the 2-position and the 5-position allowing for coupling conditions to be employed to add vinyl and aryl sidechains that may span the binding pocket. The synthesis of 2-bromo-*N*-phthaloyltryptamine (**2.49)** was undertaken to investigate the incorporation of lipophilic groups at C2 of the indole.

Protection of tryptamine (**2.46**) with phthalic anhydride gave phthalimide **2.47**, which was obtained in 57%. Bromination of **2.47** at the C2 position was accomplished with pyridinium tribromide in a DCM/THF mixture yielding **2.48** in 89% yield. Tryptamine **2.48** then underwent *N*-alkylation at the indole nitrogen utilizing 2,4-dichlorobenzyl chloride, tetrabutylammonium iodide, and sodium hydride producing the desired 2-bromo-N-phthaloyltryptamine (**2.49**).

Scheme 2.3.8: Synthesis of 2-Bromo-N-Phthaloyltryptamine Derivative

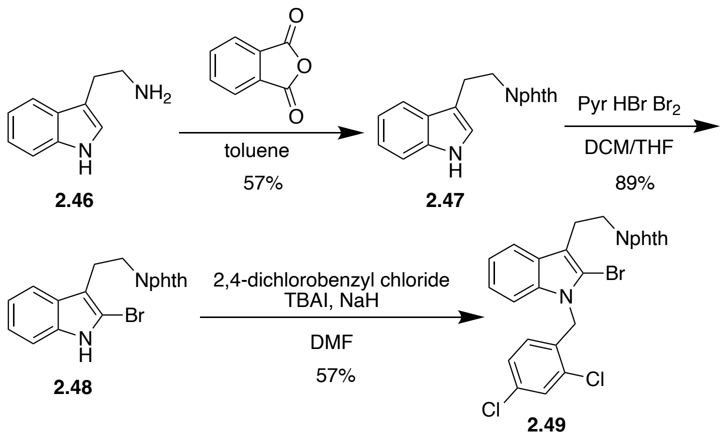
NH2
2.46
toluene
57%
Nphth
2.47
Pyr HBr Br2
DCM/THF
89%
Nphth
Br
2.48
2,4-dichlorobenzyl chloride
TBAI, NaH
DMF
57%
Nphth
Br
Cl
Cl
2.49

Suzuki couplings with 2-bromo-*N*-phthaloyltryptamine (**2.49**) were then explored (**Scheme 2.3.9**). Analog **2.50** was prepared in high yields utilizing phenylboronic acid, tris(dibenzylideneacetone)dipalladium(0), triphenylphosphine, and potassium carbonate, while **2.51** was prepared under the same conditions using *trans*-2-phenylvinylboronic acid.

Scheme 2.3.9: Synthetic Plan for the Synthesis of 2-Aryltryptamines and 2-Vinyltryptamines

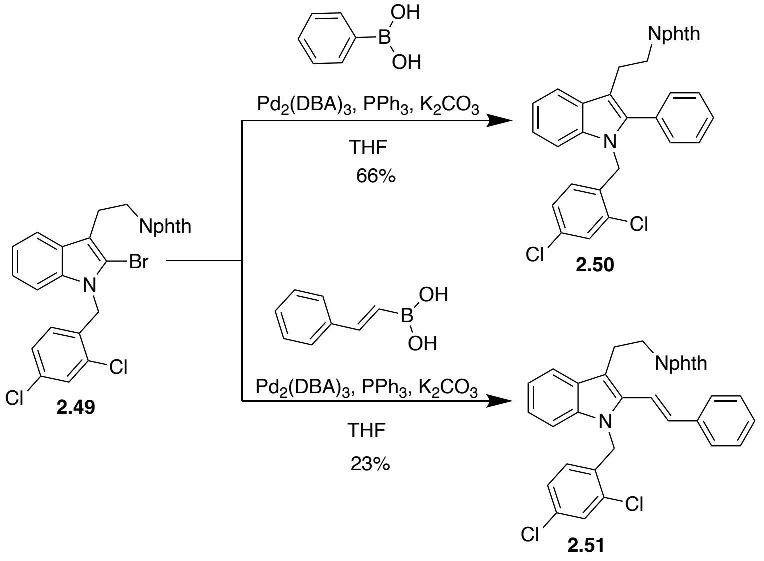

The successful synthesis of analogs **2.50** and **2.51** prove Suzuki coupling conditions can be used to attach the desired hydrophobic sidechains. Through continued exploitation of these reactions multiple sidechain derivatives can be synthesized to be used in future structure-activity relationship testing.

The synthesis of 5-bromo-N-phthaloyltryptamine derivative **2.52** began with the previously synthesized ketone **2.5**, which undergoes a Fischer indole synthesis with commercially available 4-bromophenylhydrazine hydrochloride (**2.23**) producing 5-bromotryptamine **2.27** at an 81% yield. *N*-Alkylation with 2,4-dichlorobenzyl chloride gives the desired analog **2.52**. From here the previously tested Suzuki and Sonagashira coupling reactions will be explored to add a lipophilic functionality at the indole C5 position. After removal of the phthalimide and formation of the HCl salt, testing of these analogs will be initiated with the goal of uncovering more information regarding the orientation of the tryptamine core within the SHIP binding site.

Scheme 2.3.10: Synthesis of 5-Bromo-N-phthaloyltryptamine Derivative

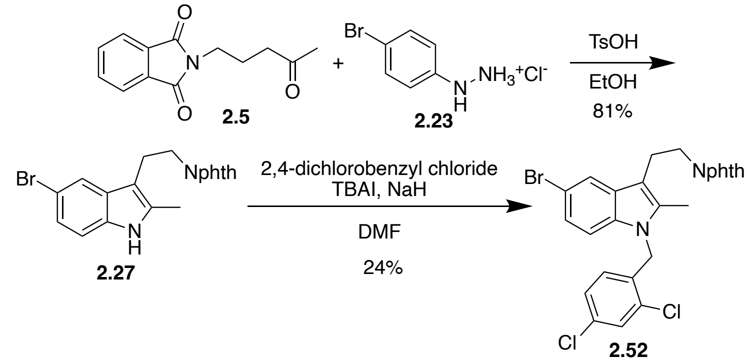
2.5
2.23
TsOH
EtOH
81%
Br
NH3+Cl-
Nphth
2.27
2,4-dichlorobenzyl chloride
TBAI, NaH
DMF
24%
Cl
2.52

Additionally, the selective SHIP2 inhibitor AS1949490 (**2.3**) was synthesized to be used as a control in new and ongoing biological studies, including new studies being done involving Alzheimer's Disease. The synthesis of AS1949490 (**2.3**) commenced with a Fiesselmann thiophene condensation between methyl thioglycolate (**2.53**) and methyl-2,3-dichloropropionate (**2.54**) yielding thiophene **2.55**. O-Alkylation of the alcohol present in **2.55** by 4-chlorobenzyl chloride yields thiophene derivative **2.56** in 52% yield. Hydrolysis of ester **2.56** with NaOH gave carboxylic acid **2.57** in 84% yield. Carboxylic acid **2.68** was then coupled with (S)-(-)-1-phenethlamine with N-(3-Dimethylaminopropyl)-N'-ethylcarbodiimide (EDCI) yielding AS1949490 (**2.3**).

Scheme 2.3.11: Synthesis of AS1949490 (**2.3**)

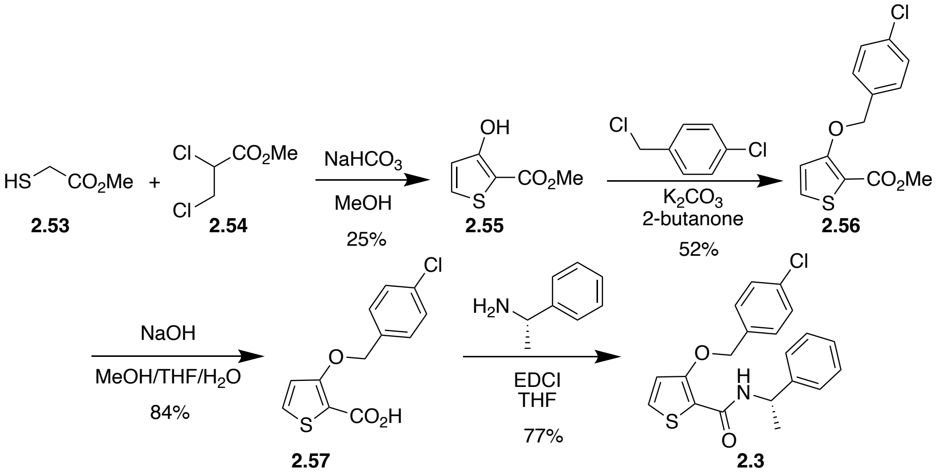
HS
CO2Me
2.53
Cl
CO2Me
2.54
NaHCO3
MeOH
25%
OH
2.55
K2CO3
2-butanone
52%
2.56
NaOH
MeOH/THF/H2O
84%
CO2H
2.57
H2N
EDCI
THF
77%
2.3

2.4 Conclusion

The synthesis of a number of small molecule tryptamine SHIP inhibitors, along with initial in-vitro testing has successfully been completed. The development and testing of this compounds have provided valuable binding data on the structure activity relationship of these small inhibitors and the SHIP enzyme, as well as offers clues as to what may be vital in order to achieve high levels of inhibition. Using these initial results, future work will be centered on the continued exploration of the SHIP active site through structure-activity relationship with the tryptamine scaffold. Additionally, future work will be focused on building a tryptamine inhibitor that maximizes the inhibitory potential, while eliminating any side effects.

2.5 Experimental

General Experimental Information: All anhydrous reactions were run under a positive pressure of argon. DCM (DCM) was dried by passage through an alumina column. Tetrahydrofuran (THF) was freshly distilled from Na/benzophenone still before use. Ethyl acetate (EA) and hexanes were purchased from commercial sources and used as received. Silica gel column chromatography was performed using 60 Å silica gel (230−400 mesh). Melting points are uncorrected. The 4-oxo-1-phthalimidopentane (**2.5**)[43] and the 4-(methylthio)phenylhydrazine hydrochloride (**2.7**) used in the indole synthesis were prepared as reported in the literature.[44]

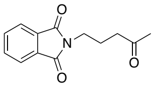

4-Oxo-1-phthalimidopentane (**2.5**)

To a solution of phthalimide (3.000 g, 20.00 mmol) dissolved in 20 mL of DMF was added K_2CO_3 (4.230 g, 30.60 mmol). After warming the mixture to 80˚C while stirring, 5-chloro-2-pentanone (4.69 mL, 40.80 mmol) was added and stirred for an additional 24 h. The reaction mixture was then poured into 100 mL of ice water and stirred in a 0˚C ice bath for 1 h. The stirred mixture was filtered resulting in a orangish-white solid. The solid was washed with cold water (3x) and dried under vacuum (5.890 g, 75.0%). TLC $R_f = 0.37$ (hexane: ethyl acetate, 50%:50%); ^{1}H NMR (400 MHz, $CDCl_3$) δ 7.83-7.86 (m, 2H), 7.71-7.73 (m, 2H), 3.71 (t, $J = 6.8$, 2H), 2.50 (t, $J = 7.2$, 2H), 2.14 (s, 3H), 1.96 (p, $J = 6.8$, 2H); ^{13}C NMR (100 MHz, $CDCl_3$) δ 207.4, 168.4, 134.0, 132.1, 123.2, 40.5, 37.2, 29.9, 22.7

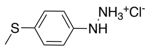

4-(Methylthio)phenylhydrazine hydrochloride (**2.7**)

4-(Methylthio)aniline (3.73 mL, 30.00 mmol) was suspended in 30 mL of 6M HCl. The mixture was heated to 60˚C while stirring until a solution was obtained, and then cooled to 0˚C forming a suspension. Sodium nitrate (2.480 g, 36.00 mmol) was dissolved in 20 mL of water and added slowly to the reaction mixture. After 30 min, tin (II) chloride, dissolved in 30 mL of 6M HCl, was added to the mixture and cooled to -25˚C. After stirring at -25˚C for 30 min, the reaction mixture was warmed to 0˚C and stirred for an additional 20 min. The mixture was filtered and washed with cold water (3x) and ethanol (3x) resulting in a tan paste (4.440 g, 77.6%). ^{1}H NMR (300 MHz, DMSO-*d$_6$*) δ 10.24 (s, 3H), 7.25 (d, *J* = 8.7, 2H), 6.96 (d, *J* = 8.7, 2H), 2.43 (s, 3H)

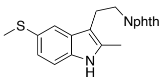

2-(2-(2-Methyl-5-(methylthio)-1H-indol-3-yl)ethyl)isoindoline-1,3-dione (**2.8**)

4-(Methylthio)phenylhydrazine hydrochloride **2.7** (1.96 g, 10.3 mmol) and 4-oxo-1-phthalimidopentane **2.5** (2.66 g, 11.5 mmol) were dissolved in ethanol (40 mL, 0.3 M). p-Toluenesulfonic acid monohydrate (3.51 g, 46.3 mmol) was added and the mixture was heated to reflux for 18 h. The mixture was then allowed to cool to room temperature and poured into 1M aq. NaOH solution. The mixture was then extracted with DCM, and the organic extracts were dried over anhydrous Na_2SO_4, filtered and concentrated. The residue was purified by precipitating the desired tryptamine with EA yielding a yellow solid (3.100 g, 86%). TLC R_f = 0.34 (20% EA/80% hexanes); IR (ATR) 3337, 1706, 1394, 717 cm^{-1}; ^{1}H NMR (400 MHz, DMSO-*d$_6$*) δ 10.79 (s, 1H), 7.79-7.84 (m, 4H), 7.37 (d, *J* = 1.8 Hz, 1H), 7.15 (d, *J* = 8.4 Hz, 1H), 6.94 (dd, *J* = 8.3, 1.8 Hz, 1H), 3.73 (t, *J* = 7.6 Hz, 2H), 2.94 (t, *J* = 7.3 Hz, 2H), 2.38 (s, 3H), 2.25 (s, 3H); ^{13}C{^{1}H} NMR

(100 MHz, DMSO-d_6) δ 168.3, 134.8, 134.3, 133.8, 132.0, 129.5, 126.1, 123.4, 121.9, 117.8, 111.6, 106.7, 38.5, 23.0, 18.3, 11.5. This compound has been previously reported.[45]

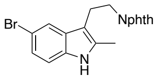

2-(2-(2-Methyl-5-(bromo)-1H-indol-3-yl)ethyl)isoindoline-1,3-dione (**2.27**)

4-(Bromo)phenylhydrazine hydrochloride (**2.23**) (1.35 g, 5.8 mmol) and 4-oxo-1-phthalimidopentane (**2.5**) (1.17 g, 5.2 mmol) were dissolved in ethanol (20 mL, 0.3 M). p-Toluenesulfonic acid monohydrate (4.47 g, 23.5 mmol) was added and the mixture was heated to reflux for 18 h. The mixture was then allowed to cool to room temperature and poured into 1M aq. NaOH solution. The mixture was then extracted with DCM, and the organic extracts were dried over anhydrous Na_2SO_4, filtered and concentrated. The residue was purified by precipitating the desired tryptamine with EA yielding a tan powder (1.61 g, 81%). TLC $R_f = 0.293$ (30% EA/70% hexanes); IR (ATR) 3172, 3063, 1705, 1124, 565 cm^{-1}; ^1H NMR (400 MHz, $CDCl_3$) δ 7.74 (m, 2H), 7.63 (m, 2H), 7.60 (s, 1H), 7.07 (dd, *J* = 1.6, 8.6 Hz, 1H), 7.02 (d, *J* = 8.6 Hz, 1H), 3.80 (t, *J* = 7.4, 2H), 2.94 (t, *J* = 7.4, 2H), 2.33 (s, 3H); $^{13}C\{^1H\}$ NMR (100 MHz, $CDCl_3$) δ 168.3, 133.9, 133.8, 132.1, 130.5, 128.8, 123.9, 123.9, 123.2, 120.5, 112.8, 111.6, 38.2, 23.2, 11.6

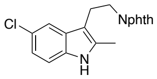

2-(2-(2-Methyl-5-(chloro)-1H-indol-3-yl)ethyl)isoindoline-1,3-dione (**2.28**)

4-(Chloro)phenylhydrazine hydrochloride (**2.24**) (1.15 g, 5.0 mmol) and 4-oxo-1-phthalimidopentane (**2.5**) (0.80 g, 4.4 mmol) were dissolved in ethanol (18 mL, 0.3 M). p-Toluenesulfonic acid monohydrate (3.79 g, 19.9 mmol) was added and the mixture was heated to reflux for 18 h. The mixture was then allowed to cool to room temperature and poured into 1M aq. NaOH solution. The mixture was then extracted with DCM, and the organic extracts were dried over anhydrous Na_2SO_4, filtered and concentrated. The residue was purified by precipitating the desired tryptamine with EA yielding a yellow-white powder (0.5057 g, 34%). TLC R_f = 0.268 (30% EA/70% hexanes); IR (ATR) 3366, 3063, 2943, 1703 cm^{-1}; ^1H NMR (400 MHz, $CDCl_3$) δ 7.82-7.85 (m, 2H), 7.82 (brs, 1H), 7.71-7.73 (m, 2H), 7.55 (s, 1H), 7.15 (d, *J* = 8.5, 1H), 7.03 (dd, *J* = 1.6, 8.5, 1H), 3.89 (t, *J* = 7.5, 2H), 3.04 (t, *J* = 7.7, 2H), 2.42 (s, 3H); $^{13}C\{^1H\}$ NMR (100 MHz, $CDCl_3$) δ 168.3, 133.8, 133.5, 133.5, 132.1, 129.8, 125.2, 123.1, 121.3, 117.4, 111.1, 108.0, 38.2, 23.2, 11.6

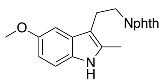

2-(2-(2-Methyl-5-(methoxy)-1H-indol-3-yl)ethyl)isoindoline-1,3-dione (**2.29**)

4-(Methyoxy)phenylhydrazine hydrochloride (**2.25**) (1.16 g, 5.0 mmol) and 4-oxo-1-phthalimidopentane (**2.5**) (0.78 g, 4.5 mmol) were dissolved in ethanol (18 mL, 0.3 M). p-Toluenesulfonic acid monohydrate (3.85 g, 20.2 mmol) was added and the mixture was heated to reflux for 18 h. The mixture was then allowed to cool to room temperature and poured into 1M aq. NaOH solution. The mixture was then extracted with DCM, and the organic extracts were dried over anhydrous Na_2SO_4, filtered and concentrated. The residue was purified by precipitating the desired tryptamine with EA yielding a as a tan-white powder (0.340 g, 23%). TLC R_f = 0.317 (30% EA/70% hexanes); IR (ATR) 3379, 2941, 2940, 1706 cm^{-1}; ^1H NMR (400 MHz, $CDCl_3$) δ 7.84-7.86 (m, 2H), 7.71-7.73 (m, 2H), 7.67 (brs, 1H) ,7.12-7.16 (m, 2H), 6.75 (dd, *J*= 2.4, 8.7, 1H), 3.91 (t, *J* = 7.9, 2H), 3.87 (s, 3H), 3.05 (t, *J* = 7.9, 2H), 2.43 (s, 3H); $^{13}C\{^{1}H\}$ NMR (100 MHz, $CDCl_3$) δ 168.3, 154.1, 133.8, 132.7, 132.2, 130.2, 129.1, 123.1, 111.0, 110.9, 107.9, 100.0, 55.9, 38.2, 23.5, 11.6

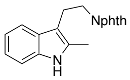

2-(2-(2-Methyl-1H-indol-3-yl)ethyl)isoindoline-1,3-dione (**2.30**)

Phenylhydrazine hydrochloride (**2.26**) (0.76 g, 7.72 mmol) and 4-oxo-1-phthalimidopentane (**2.5**) (2.00 g, 8.65 mmol) were dissolved in ethanol (3 mL, 0.3M). p-Toluenesulfonic acid monohydrate (6.61 g, 34.75 mmol) was added to the mixture and heated to reflux for 18 h. The mixture was then allowed to cool to room temperature and poured into 1M NaOH. The mixture was then extracted with DCM, and the combined organic extracts were dried over anhydrous Na_2SO_4, filtered and concentrated. The residue was purified by precipitating the desired tryptamine with EA yielding an orange powder (2.15 g, 92%). TLC $R_f = 0.36$ (30% EA/70% hexanes); IR (ATR) 3377, 3349, 2941, 1761, 1697, 1395, 711 cm^{-1}; ^{1}H NMR (400 MHz, DMSO-d_6) δ 10.72 (s, 1H), 7.80-7.85 (m, 4H), 7.42 (d, $J = 7.4$ Hz, 1H), 7.21 (d, $J = 7.8$ Hz, 1H), 6.96 (d, $J = 7.0$ Hz, 1H), 6.90 (d, $J = 7.6$ Hz, 1H), 3.74 (t, $J = 7.2$ Hz, 2H), 2.96 (t, $J = 7.3$ Hz, 2H), 2.27 (s, 3H); $^{13}C\{^{1}H\}$ NMR (100 MHz, DMSO) δ 168.2, 135.6, 134.8, 132.8, 132.1, 128.6, 123.4, 120.5, 118.7, 117.4, 110.9, 106.8, 38.5, 23.2, 11.5. This compound has been previously reported.[46]

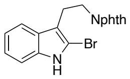

2-Bromo-N-phthalimidotryptamine (**2.48**)

To a solution of N-phthalimidotryptamine (1.760 g, 6.07 mmol) dissolved in 0.1M chloroform/tetrahydrofuran was added pyridinium tribromide (2.060g, 6.37 mmol). The mixture was stirred and cooled to -10˚C. After 1h the mixture was quenched with saturated thiosulfate and stirred for 30 min. The quenched solution was extracted with dichloromethane (3x), dried of $MgSO_4$, and concentrated. The dark oil was purified via trituration from dichloromethane and hexanes yielding a sand colored solid (2.00g, 89.3%). TLC R_f = 0.37 (hexane: ethyl acetate, 70%:30%); ^{1}H NMR (400 MHz, $CDCl_3$) δ 7.98 (s, 1H), 7.80-7.82 (m, 2H), 7.68-7.70 (m, 2H), 7.62 (d, *J* = 8, 1H), 7.28 (s, 1H), 7.06-7.16 (m, 2H), 3.95 (t, *J* = 7.6, 2H), 3.10 (t, *J* = 7.6, 2H) ; $^{13}C\{^1H\}$ NMR (100 MHz, $CDCl_3$) δ168.2, 136.0, 133.8, 127.7, 123.1, 122.4, 120.3, 118.1, 112.1, 110.4, 108.6, 37.5, 24.1

General Procedure for N-alkylation of indoles

The indole (1 equiv) was dissolved in acetonitrile (0.1 M). Cs_2CO_3 (6 equiv) and the benzyl halide (3 equiv) were added and the mixture was heated to 80˚C for 18 h. The mixture was cooled to rt, and then filtered to remove the remaining Cs_2CO_3 and other salts. The filtrate was poured into brine and extracted with DCM. The combined organic extracts were dried over anhydrous Na_2SO_4, filtered, and concentrated. Silica gel chromatography then provided the desired products.

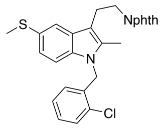

2-(2-(1-(2-Chlorobenzyl)-2-methyl-5-(methylthio)-1H-indol-3-yl)ethyl)isoindoline-1,3-dione **(2.1a)**

The crude oil was purified in 100% chloroform yielding a yellow powder (2.65 g, 65%). TLC R_f = 0.43 (100% $CHCl_3$); IR (ATR) 2936, 2929, 1707, 716 cm^{-1}; ^{1}H NMR (400 MHz, $CDCl_3$) δ 7.79-

7.82 (m, 2H), 7.67-7.69 (m, 2H), 7.64 (s, 1H), 7.39 (d, *J* = 8.0 Hz, 1H), 7.17 (t, *J* = 7.6 Hz, 1H), 7.07 (dd, *J* = 1.4, 8.4 Hz, 1H), 7.02 (t, *J* = 8.5 Hz, 2H), 6.19 (d, *J* = 8.5 Hz, 1H), 5.30 (s, 2H), 3.93 (t, *J* = 7.4 Hz, 2H), 3.12 (t, *J* = 7.4 Hz, 2H), 2.49 (s, 3H), 2.27 (s, 3H); $^{13}C\{^1H\}$ NMR (100 MHz, $CDCl_3$) δ 168.3, 135.1, 135.0, 134.3, 133.8, 132.1, 131.8, 129.3, 128.8, 128.5, 127.7, 127.4, 126.9, 123.1, 123.0, 118.5, 109.5, 108.0, 44.4, 38.4, 23.5, 18.6, 10.0; Anal. Calcd for $C_{27}H_{23}ClN_2O_2S$: C, 68.27; H, 4.88; N, 5.90. Found: C, 68.34; H, 4.51; N, 6.18.

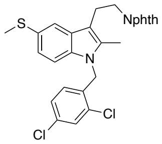

2-(2-(1-(2,4-Dichlorobenzyl)-2-methyl-5-(methylthio)-1H-indol-3-yl)ethyl)isoindoline-1,3-dione (**2.9**)

The crude oil was purified via silica gel column chromatography (80% hexanes: 20% EA) yielding a yellow solid (5.18 g, 60%). TLC R_f = 0.48 (80% hexanes: 20% EA), ^1H NMR (400 MHz, $CDCl_3$) δ 7.78-7.80 (m, 2H), 7.67-7.69 (m, 2H), 7.60 (d, *J* = 1.5 Hz, 1H), 7.40 (d, *J* = 2.0 Hz, 1H), 7.38 (d, *J* = 2.0 Hz, 1H), 7.02-7.09 (m, 2H), 6.10 (d, *J* = 8.4 Hz, 1H), 5.25 (s, 2H), 3.92 (t, *J* = 7.2 Hz, 2H), 3.12 (t, *J* = 7.3 Hz, 2H), 2.47 (s, 3H), 2.24 (s, 3H); $^{13}C\{^1H\}$ NMR (75 MHz, $CDCl_3$) δ 168.3, 134.9, 134.0, 133.9, 133.7, 133.6, 132.3, 132.1, 131.8, 129.1, 128.8, 128.0, 127.9, 127.7, 123.1, 118.5, 109.3, 108.4, 44.0, 38.4, 23.5, 18.5, 10.0.

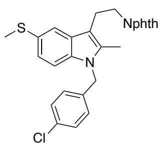

2-(2-(1-(4-Chlorobenzyl)-2-methyl-5-(methylthio)-1H-indol-3-yl)ethyl)isoindoline-1,3-dione (**2.12a**)

The crude oil was purified in 100% DCM yielding a yellow oil (0.470 g, 35%). TLC R_f = 0.63 (100% DCM); IR (ATR) 3038, 2920, 1702, 1027, 717 cm^{-1}; ^{1}H NMR (400 MHz, $CDCl_3$) δ 7.77-7.79 (m, 2H), 7.66-7.69 (m, 2H), 7.63 (s, 1H), 7.21 (d, *J* = 7.7 Hz, 2H), 7.08 (d, *J* = 8.4 Hz, 1H), 7.03 (d, *J* = 8.4 Hz, 1H), 6.83 (d, *J* = 8.1 Hz, 2H), 5.20 (s, 2H), 3.90 (t, *J* = 7.4 Hz, 2H), 3.10 (t, *J* = 7.4 Hz, 2H), 2.49 (s, 3H), 2.26 (s, 3H); $^{13}C\{^1H\}$ NMR (100 MHz, $CDCl_3$) δ 168.2, 136.2, 135.1, 134.2, 133.8, 133.1, 132.1, 128.9, 128.7, 127.7, 127.3, 123.1, 123.0, 118.6, 109.4, 108.0, 46.0, 38.4, 23.5, 18.7, 10.2.

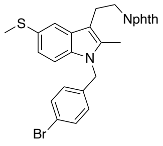

2-(2-(1-(4-Bromobenzyl)-2-methyl-5-(methylthio)-1H-indol-3-yl)ethyl)isoindoline-1,3-dione (**2.14a**)

The crude residue was purified in 30% EA: 70% hexanes yielding an orange oil (0.780 g, 53%). TLC R_f = 0.43 (30% EA: 70% hexanes); IR (ATR) 2919, 2857, 1705, 1010, 715 cm^{-1}; ^{1}H NMR (400 MHz, $CDCl_3$) δ 7.77-7.80 (m, 2H), 7.67-7.69 (m, 2H), 7.62 (s, 1H), 7.36 (d, *J* = 8.4 Hz, 2H), 7.08 (dd, *J* = 1.2, 8.4 Hz, 1H), 7.03 (d, *J* = 8.4 Hz, 1H), 6.76 (d, *J* = 8.3 Hz, 2H), 5.18 (s, 2H), 3.90 (t, *J* = 8.0 Hz, 2H), 3.10 (t, *J* = 8.0 Hz, 2H), 2.49 (s, 3H), 2.26 (s, 3H); $^{13}C\{^1H\}$ NMR (100 MHz, $CDCl_3$) δ 168.2, 136.7, 135.0, 134.2, 133.8, 132.1, 131.9, 128.7, 127.7, 127.7, 123.1, 123.0, 121.1, 118.6, 109.4, 108.0, 46.0, 38.4, 23.5, 18.7, 10.1.

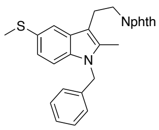

2-(2-(1-Benzyl-2-methyl-5-(methylthio)-1H-indol-3-yl)ethyl)isoindoline-1,3-dione (**2.15a**)

The crude oil was purified in 30% EA: 70% hexanes yielding a yellow oil (1.04 g, 83%). TLC R_f = 0.50 (30% EA: 70% hexanes); IR (ATR) 3028, 2917, 1703 cm^{-1}; ^{1}H NMR (400 MHz, $CDCl_3$) δ 7.97-8.00 (m, 2H), 7.84-7.86 (m, 2H), 7.83 (s, 1H), 7.37-7.45 (m, 4H), 7.26 (s, 1H), 7.09 (d, J = 7.0 Hz, 2H), 5.43 (s, 2H), 4.08 (t, J = 7.9 Hz, 2H), 3.28 (t, J = 7.9 Hz, 2H), 2.68 (s, 3H), 2.48 (s, 3H); $^{13}C\{^1H\}$ NMR (100 MHz, $CDCl_3$) δ 168.3, 137.7, 135.2, 134.4, 133.8, 132.1, 128.8, 128.7, 127.4, 127.3, 125.9, 123.1, 122.9, 118.6, 109.6, 107.7, 46.6, 38.4, 23.6, 18.7, 10.2. This compound has been reported previously.[45]

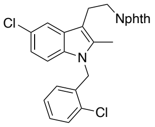

2-(2-{5-Chloro-1-[(2-chlorobenzyl)-2-methyl-1H-indol-3-yl)ethyl)isoindoline-1,3-dione (**2.32**)

The crude oil was purified in 30% EA: 70% hexanes yielding a yellow solid (0.440 g, 64%). TLC R_f = 0.55 (30% EA: 70% hexanes); IR (ATR) 3458, 2938, 1768, 1705, 1394, 1045, 718 cm^{-1}; ^{1}H NMR (400 MHz, $CDCl_3$) δ 7.78-7.81 (m, 2H), 7.67-7.71 (m, 2H), 7.58 (s, 1H), 7.39 (d, J = 7.9 Hz, 1H), 7.18 (t, J = 7.4 Hz, 1H), 7.05 (t, J = 7.6 Hz, 1H), 6.99 (s, 2H), 6.15 (d, J = 7.6 Hz, 1H), 5.29 (s, 2H), 3.92 (t, J = 7.3 Hz, 2H), 3.10 (t, J = 7.3 Hz, 2H), 2.26 (s, 3H); $^{13}C\{^1H\}$ NMR (100 MHz, $CDCl_3$) δ 168.3, 135.1, 134.8, 134.7, 133.9, 132.1, 131.8, 129.4, 129.0, 128.5, 127.4, 126.7, 125.4, 123.1, 121.4, 117.6, 109.9, 108.1, 44.5, 38.4, 23.5, 10.0.

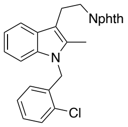

2-(2-(1-(2-Chlorobenzyl)-2-methyl-1H-indol-3-yl)ethyl)isoindoline-1,3-dione (**2.34**)

The crude oil was purified in 20% EA: 80% hexanes yielding a yellow solid (0.670 g, 48%). TLC R_f = 0.47 (20% EA: 80% hexanes); IR (ATR) 3300, 2918, 2860, 1704, 1042, 742 cm^{-1}; ^1H NMR (400 MHz, $CDCl_3$) δ 7.81-7.83 (m, 2H), 7.68-7.72 (m, 3H), 7.39 (d, *J* = 8.2 Hz, 1H), 7.16 (t, *J* = 7.7 Hz, 1H), 7.08-7.11 (m, 3H), 7.02 (t, *J* = 7.7 Hz, 1H), 6.21 (d, *J* = 7.7 Hz, 1H), 5.34 (s, 2H), 3.95 (t, *J* = 8.2 Hz, 2H), 3.16 (t, *J* = 7.7 Hz, 2H), 2.26 (s, 3H); $^{13}C\{^1H\}$ NMR (100 MHz, $CDCl_3$) δ 168.3, 136.3, 135.3, 133.8, 133.5, 132.2, 131.8, 129.3, 128.4, 128.0, 127.3, 126.9, 123.1, 121.2, 119.6, 118.1, 108.9, 108.2, 44.3, 38.5, 23.7, 9.9.

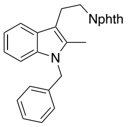

2-(2-(1-Benzyl-2-methyl-1H-indol-3-yl)ethyl)isoindoline-1,3-dione (**2.43**)

The crude oil was purified in 20% EA: 80% hexanes yielding a yellow-white solid (0.310 g, 24%). TLC R_f = 0.26 (20% EA: 80% hexanes); IR (ATR) 3028, 2920, 2854, 1704, 714, 695 cm^{-1}; ^1H NMR (400 MHz, $CDCl_3$) δ 7.81-7.83 (m, 2H), 7.68-7.70 (m, 3H), 7.16-7.25 (m, 4H), 7.08-7.10 (m, 2H), 6.93 (d, *J* = 7.0 Hz, 2H), 5.29 (s, 2H), 3.91 (t, *J* = 8.1 Hz, 2H), 3.12 (t, *J* = 8.1 Hz, 2H), 2.32 (s, 3H); $^{13}C\{^1H\}$ NMR (100 MHz, $CDCl_3$) δ 168.3, 137.9, 136.5, 133.8, 133.6, 132.2, 128.7, 127.9, 127.2, 125.9, 123.1, 121.0, 119.3, 118.0, 109.0, 107.9, 46.5, 38.5, 23.7, 10.1.

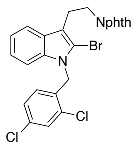

2-[2-(1-(2,4-Dichlorobenzyl)-2-bromo-1H-indol-3-yl)ethyl]-1H-isoindole-1,3(2H)-dione (**2.49**)

To a suspension of sodium hydride (60% dispersion, 0.054g, 1.354) in 2mL of N,N-dimethylformamide was added 2-bromo-N-phthalimidotryptamine (0.250 g, 0.677 mmol) dissolved in 3mL of N,N-dimethylformamide. The reaction was stirred for 30 min at r.t. and then cooled to 0˚C. To the cooled solution was added tetrabutylammonium iodide (0.415 g, 1.124 mmol) and 2,4-dichlorobenzyl chloride (0.103 mL, 0.75 mmol). The mixture was stirred for 4h (2h 0˚C, 2h r.t.), and then quenched with saturated ammonium chloride. The quenched solution was extracted with ethyl acetate, washed with water and brine, dried over $MgSO_4$, filtered, and concentrated. The residual oil was purified via silica gel column chromatography using an 80% hexanes:20% ethyl acetate eluent yielding a yellow solid (0.2050 g, 57.3%). TLC $R_f = 0.55$ (hexane: ethyl acetate, 80%:20%); ^{1}H NMR (400 MHz, $CDCl_3$) δ 7.76-7.78 (m, 2H), 7.62-7.68 (m, 3H), 7.38-7.46 (m, 2H) 7.05-7.14 (m, 4H) 6.21 (d, J = 8.4, 1H), 5.39 (s, 2H), 4.00 (t, J = 6.8, 2H), 3.19 (t, J= 6.8, 2H); ^{13}C NMR (100 MHz, $CDCl_3$) δ 168.3, 136.4, 133.8, 133.7, 133.2, 132.3, 132.1, 129.1, 128.1, 127.7, 127.5, 123.1, 122.6, 120.5, 118.3, 113.3, 112.4, 109.5, 45.5, 37.6, 24.5

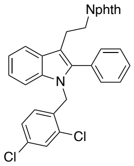

2-(2-(1-(2,4-Dichlorobenzyl)-2-phenyl-1H-indol-3-yl)ethyl)isoindoline-1,3-dione (**2.50**)

2-[2-(1-(2,4-dichlorobenzyl)-2-bromo-1H-indol-3-yl)ethyl]-1H-isoindole-1,3(2H)-dione (0.100 g, 0.189 mmol), phenylboronic acid (0.023g, 0.189 mmol), K_2CO_3 (0.078 g, 0.567 mmol), triphenyl phosphine (0.008 g, 0.030 mmol), and tris(dibenzylideneacetone)dipalladium(0) (0.007 g, 0.008 mmol) were added to a flame dried, argon purged Schlenk tube. 2mL of tetrahydrofuran was added and the tube was sealed and placed in a 100˚C oil bath. After 24h the reaction mixture was cooled to r.t. and diluted in diethyl ether. The mixture was filtered through a pad of Celite and washed with diethyl ether (3x). The filtrate was concentrated and purified via silica gel column chromatography using a 90% hexanes:10% ethyl acetate eluent yielding a yellow oil (0.0650 g, 65.7%). TLC R_f = 0.30 (hexane: ethyl acetate, 80%:20%); ^{1}H NMR (400 MHz, $CDCl_3$) δ 7.56-7.68 (m, 5H), 7.27 (d, *J* = 2.1, 1H), 7.18-7.24 (m, 3H), 7.13 (dd, *J* = 1.4, 5.9, 2H) 7.01-7.06 (m, 3H), 6.95 (dd, *J* = 1.9, 8.0, 1H), 6.36 (d, *J* = 8.4, 1H), 5.09 (s, 2H), 3.85 (t, *J* = 7.0, 2H), 3.07 (t, *J* = 7.0, 2H); ^{13}C NMR (100 MHz, $CDCl_3$) δ 168.1, 138.6, 136.4, 134.4, 133.7, 133.4, 132.2, 132.1, 130.8, 130.1, 129.1, 128.6, 128.4, 128.1, 127.5, 122.9, 122.4, 120.2, 119.0, 110.5, 109.9, 45.0, 38.8, 23.7

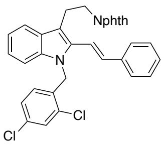

2-(2-(1-(2,4-Dichlorobenzyl)-(E)-2-phenylvinyl-1H-indol-3-yl)ethyl)isoindoline-1,3-dione **(2.51)**

2-[2-(1-(2,4-dichlorobenzyl)-2-bromo-1H-indol-3-yl)ethyl]-1H-isoindole-1,3(2H)-dione (0.100 g, 0.189 mmol), trans-2-phenyvinyllboronic acid (0.028g, 0.189 mmol), K_2CO_3 (0.078 g, 0.567 mmol), triphenyl phosphine (0.008 g, 0.030 mmol), and tris(dibenzylideneacetone)dipalladium(0) (0.007 g, 0.008 mmol) were added to a flame dried, argon purged Schlenk tube. 2mL of tetrahydrofuran was added and the tube was sealed and placed in a 100˚C oil bath. After stirring for 24h the reaction mixture was cooled to r.t. and diluted in diethyl ether. The mixture was filtered through a pad of Celite and washed with diethyl ether (3x). The filtrate was concentrated and purified via silica gel column chromatography using a 20% hexanes: 80% ethyl acetate eluent yielding a (0.024g, 23.1%). TLC R_f = 0.45(hexane: ethyl acetate, 20%:80%); ^{1}H NMR (400 MHz, $CDCl_3$) δ 7.68-7.72 (m, 3H), 7.48-7.63 (m, 4H), 7.34 (d, *J* = 2.0, 2H), 6.97-7.12 (m, 7H), 6.13 (d, *J* = 8.4, 1H), 5.32 (s, 2H), 3.93 (t, *J*= 7.0, 2H), 3.12 (t, *J* = 7.0, 2H)

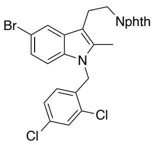

2-(2-(1-(2,4-Dichlorobenzyl)-2-methyl-5-(bromo)-1H-indol-3-yl)ethyl)isoindoline-1,3-dione **(2.52)**

The residual oil was purified via silica gel column chromatography using an 80% hexanes:20% ethyl acetate eluent yielding a yellow solid (0.0834 g, 23.6%). TLC R_f = 0.55 (hexane: ethyl acetate, 80%:20%); ^{1}H NMR (400 MHz, $CDCl_3$) δ 7.77-7.79 (m, 2H), 7.67-7.69 (m, 3H), 7.40 (d, *J* = 2.0, 1H), 7.11 (dd, *J* = 1.6, 8.4, 1H), 7.04 (dd, *J* = 2.0, 8.4, 1H) 6.90 (d, *J* = 8.4, 1H), 6.05 (d, *J* = 8.4, 1H) 5.23 (s, 2H), 3.91 (t, *J* = 7.6, 2H), 3.09 (t, *J* = 7.6, 2H), 2.23 (s, 3H); ^{13}C NMR (100 MHz, $CDCl_3$) δ 168.3, 134.8, 134.7, 133.9, 133.8, 133.4, 132.3, 132.0, 129.8, 129.2, 127.8, 124.1, 123.1, 120.7, 113.1, 110.2, 108.4, 44.1, 38.4, 23.4, 10.0

General method for deprotection of the phthalamide protecting group and hydrochloride salt formation.

To a solution of phthalimide protected tryptamine (1 equiv) dissolved in methanol (0.3 M) was added hydrazine hydrate (5 equiv). The reaction mixture was brought to reflux at 75˚C for 30 min. The mixture was then allowed to cool, filtered, and concentrated under vacuum. The residue was purified via silica gel column chromatography using an 95% DCM: 5% methanol: 1% conc. aq. NH_4OH. The resulting tryptamine was then dissolved in ethyl ether and added to a solution ethyl ether-hydrochloric acid (1M) and allowed to stir for 30 min. The mixture was concentrated under vacuum and purified via recrystallization from ether/methanol.

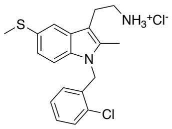

2-(1-(2-Chlorobenzyl)-2-methyl-5-(methylthio)-1H-indol-3-yl)ethanaminium chloride (**2.1**)

Recovered as an off-white solid (0.130 g, 74%). mp = 187-190 ˚C; IR (ATR) 2990, 2870, 2794, 1467, 1037, 752 cm^{-1}; ^{1}H NMR (400 MHz, CD_3OD) δ 7.60 (s, 1H), 7.46 (d, *J* = 8.0 Hz, 2H), 7.23 (t, *J* = 7.8 Hz, 1H), 7.14 (s, 1H), 7.07 (t, *J* = 7.5 Hz, 1H), 6.23 (d, *J* = 7.5 Hz, 1H), 5.44 (s, 2H), 3.11-3.16 (m, 4H), 2.49 (s, 3H), 2.31 (s, 3H); ^{13}C{^{1}H} NMR (100 MHz, CD_3OD) δ 135.5, 135.1

135.0, 131.6, 129.2, 128.5, 128.2, 128.2, 127.0, 126.5, 123.1, 118.1, 109.6, 105.7, 43.9, 39.8, 22.2, 17.4, 8.6; Anal. Calcd for $C_{19}H_{22}Cl_2N_2S$: C, 59.84; H, 5.81; N, 7.35. Found: C, 59.82; H, 5.71; N, 7.30.

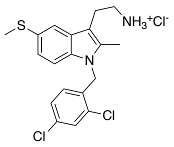

2-(1-(2,4-Dichlorobenzyl)-2-methyl-5-(methylthio)-1H-indol-3-yl)ethanaminium chloride (**2.2**)

Recovered as an off-white solid (0.403 g, 28%). IR (ATR) 2981, 2878, 2811, 1610, 1587, 1564, 1415 cm^{-1}; ^1H NMR (400 MHz, CD_3OD) δ 7.82 (s, 3H), 7.71 (d, *J* = 2.0 Hz , 1H), 7.57 (s, 1H), 7.24 - 7.28 (m, 2H), 7.05 (dd, *J* = 1.2, 8.2 Hz, 1H), 6.19 (d, *J* = 8.5 Hz, 1H), 5.41 (s, 2H), 2.94-3.01 (m, 4H), 2.49 (s, 3H), 2.25 (s, 3H); $^{13}C\{^1H\}$ NMR (100 MHz, CD_3OD) δ 135.4, 134.9, 134.2, 133.5, 132.4, 128.9, 128.4, 128.2, 127.8, 127.3, 123.2, 118.1, 109.6, 105.9, 43.6, 39.8, 22.2, 17.3, 8.6; Anal. Calcd for $C_{19}H_{22}Cl_2N_2S$: C, 59.84; H, 5.81; N, 7.35. Found: C, 59.82; H, 5.71; N, 7.30.

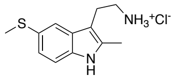

2-(2-Methyl-5-(methylthio)-1H-indol-3-yl)ethanaminium chloride (**2.11**)

Recovered as a brown plate-like solid (0.124 g, 66%). IR (ATR) 2980, 2915, 2162,1458, 1432, 1294, 797 cm^{-1}; ^1H NMR (400 MHz, CD_3OD) δ 7.52 (d, *J* = 1.6 Hz, 1H), 7.22 (d, *J* = 8.4 Hz, 1H), 7.04 (dd, *J* = 8.4, 1.6 Hz, 1H), 3.05-3.11 (m, 4H), 2.44 (s, 3H), 2.38 (s, 3H); $^{13}C\{^1H\}$ NMR (100 MHz, CD_3OD) δ 134.6, 133.9, 128.8, 126.8, 122.5, 117.9, 111.0, 104.4, 39.9, 21.9, 17.7, 10.2. This compound has been reported previously.[45]

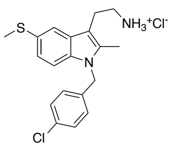

2-(1-(4-Chlorobenzyl)-2-methyl-5-(methylthio)-1H-indol-3-yl)ethanaminium chloride (**2.12**)

Recovered as an off-white solid (0.047 g, 15%). IR (ATR) 2911, 2137, 1608, 1577, 1489, 1012, 794 cm^{-1}; ^{1}H NMR (400 MHz, CD$_3$OD) δ 7.58 (s, 1H), 7.23-7.27 (m, 3H), 7.13 (d, *J* = 9.2 Hz, 1H), 6.94 (d, *J* = 7.4 Hz, 2H), 5.36 (s, 2H), 3.12 (bs, 4H), 2.48 (s, 3H), 2.34 (s, 3H); ^{13}C{^{1}H} NMR (100 MHz, CD$_3$OD) δ 136.9, 135.5, 135.0, 132.7, 128.4, 128.2, 127.9, 127.4, 123.0, 118.1, 109.7, 105.5, 45.4, 39.8, 22.2, 17.4, 8.8.

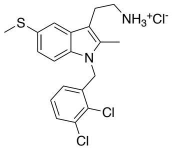

2-(1-(3,4-Dichlorobenzyl)-2-methyl-5-(methylthio)-1H-indol-3-yl)ethanamine chloride (**2.13**)

Recovered as an off-white solid (0.047 g, 86%). IR (ATR) 2911, 2137, 1608, 1577, 1489, 1012, 794 cm^{-1}; ^{1}H NMR (400 MHz, CD$_3$OD) δ 7.58 (s, 1H), 7.23-7.27 (m, 3H), 7.13 (d, *J* = 9.2 Hz, 1H), 6.94 (d, *J* = 7.4 Hz, 2H), 5.36 (s, 2H), 3.12 (m, 4H), 2.48 (s, 3H), 2.34 (s, 3H); ^{13}C NMR (100 MHz, CD$_3$OD) δ 136.9, 135.5, 135.0, 132.7, 128.4, 128.2, 127.9, 127.4, 123.0, 118.1, 109.7, 105.5, 45.4, 39.8, 22.2, 17.4, 8.8.

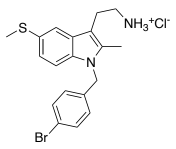

2-(1-(4-Bromobenzyl)-2-methyl-5-(methylthio)-1H-indol-3-yl)ethanaminium chloride (**2.14**)

Recovered as an off-white solid (0.0113 g, 40%). IR (ATR) 2964, 2914, 2854, 1606, 1577, 1469, 1009, 791 cm^{-1}; ^{1}H NMR (400 MHz, CD$_3$OD) δ 7.48 (d, *J* = 1.7 Hz, 1H), 7.30 (d, *J* = 8.4 Hz, 2H), 7.12 (d, *J* = 8.4 Hz, 1H), 7.03 (dd, *J* = 8.5, 1.8 Hz, 1H), 6.78 (d, *J* = 8.4 Hz, 2H), 5.24 (s, 2H), 2.97-3.06 (m, 4H), 2.38 (s, 3H), 2.23 (s, 3H); ^{13}C{^{1}H} NMR (100 MHz, CD$_3$OD) δ 137.4, 135.5, 135.0, 131.4, 128.2, 127.9, 127.8, 123.0, 120.6, 118.1, 109.7, 105.5, 45.5, 39.8, 22.2, 17.4, 8.9.

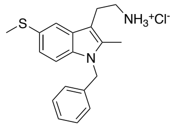

2-(1-Benzyl-2-methyl-5-(methylthio)-1H-indol-3-yl)ethanaminium chloride(**2.15**)

Recovered as an off-white solid (0.0443 g, 36%). IR (ATR) 2965, 2908, 1605, 1578, 1470, 1020, 717 cm^{-1}; ^{1}H NMR (400 MHz, CD$_3$OD) δ 7.57 (s, 1H), 7.21-7.28 (m, 4H), 7.14 (dd, *J* = 2.1, 8.5 Hz, 1H), 6.97 (d, *J* = 7.1 Hz, 2H), 5.38 (s, 2H), 3.107-3.16 (m, 4H), 2.48 (s, 3H), 2.34 (s, 3H); ^{13}C{^{1}H} NMR (100 MHz, CD$_3$OD) δ 138.0, 135.6, 135.1, 128.3, 128.1, 127.7, 126.9, 125.8, 123.0, 118.1, 109.8, 105.2, 46.0, 39.9, 22.2, 17.5, 8.8. This compound has been reported previously.[45]

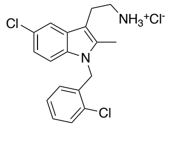

2-(2-{5-Chloro-1-[(2-chlorobenzyl)-2-methyl-1H-indol-3-yl)ethanaminium chloride (**2.40**)

Recovered as an off-white powder (0.18 g, 51%)%). IR (ATR) 3639, 3424, 2981, 2913, 2861, 1541, 1499, 1349, 1163, 941 cm^{-1}; ^{1}H NMR (400 MHz, CD$_3$OD) δ 7.61 (s, 1H), 7.48 (d, *J* = 7.9

Hz, 1H), 7.26 (t, $J = 7.4$ Hz, 1H), 7.19 (d, $J = 8.7$ Hz, 1H), 7.07-7.13 (m, 2H), 6.25 (d, $J = 7.4$ Hz, 1H), 5.48 (s, 2H), 3.10-3.18 (m, 4H), 2.34 (s, 3H); $^{13}C\{^1H\}$ NMR (100 MHz, CD_3OD) δ 136.0, 135.1, 134.9, 131.7, 129.2, 128.6, 128.6, 127.0, 126.5, 125.2, 121.2, 116.6, 110.2, 105.8, 44.0, 39.7, 22.1, 8.7.

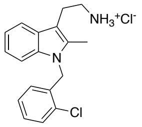

2-(1-(2-Chlorobenzyl)-2-methyl-5-1H-indol-3-yl)ethanaminium chloride (**2.42**)

Recovered as an off-white solid (0.130 g, 25%). IR (ATR) 2980, 2970, 1736, 1591, 1570, 1469, 743 cm^{-1}; ^1H NMR (400 MHz, CD_3OD) δ 7.58-7.60 (m, 1H), 7.45 (d, $J = 7.7$ Hz , 1H), 7.16-7.25 (m, 2H), 7.03-7.10 (m, 3H), 6.22 (d, $J = 7.2$ Hz, 1H), 5.45 (s, 2H), 3.17 (bs, 4H), 2.32 (s, 3H); $^{13}C\{^1H\}$ NMR (100 MHz, CD_3OD) δ 140.6, 139.2, 137.9, 135.6, 133.1, 132.3, 131.4, 130.9, 130.5, 125.1, 123.3, 121.1, 112.8, 109.8, 47.7, 43.8, 26.2, 12.5.

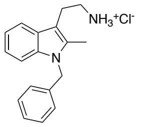

2-(1-Benzyl-2-methyl-1H-indol-3-yl) ethanaminium chloride (**2.45**)

Recovered as an off-white solid (0.1080 g, 46%). IR (ATR) 3026, 2913, 1604, 1568, 1467, 733 cm^{-1}; ^1H NMR (400 MHz, CD_3OD) δ 7.53 (d, $J = 6.8$ Hz, 1H), 7.20-7.30 (m, 4H), 7.04-7.12 (m, 2H), 6.97 (d, $J = 7.2$ Hz, 2H), 5.40 (s, 2H), 3.12-3.15 (m, 4H), 2.35 (s, 3H); $^{13}C\{^1H\}$ NMR (100 MHz, CD_3OD) δ 138.2, 136.8, 134.1, 128.3, 127.3, 126.8, 125.8, 120.9, 119.1, 116.9, 109.1, 105.4, 45.9, 39.9, 22.3, 8.8.

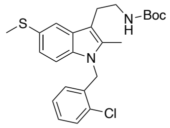

tert-Butyl-N-(2{1-[(2-chlorophenyl)methyl]-2-methyl-5-(methylsulfanyl)-1H-indol-3-yl}ethyl)carbamate (**2.16**).

Tryptamine **1** (0.200 g, 0.530 mmol) was dissolved in 3 mL of 2:1 methanol/THF. Triethylamine (0.081 mL, 0.53 mmol) and di-*tert*-butyl dicarbonate (0.108 g, 0.57 mmol) were added to the mixture. After 4 h at rt the solvent was removed via rotary evaporation and the residue was taken up in EA. The solution was washed with sat. $NaHCO_3$ (3 x 15 mL). The organic layer was collected, dried over anhydrous Na_2SO_4, filtered and concentrated. The residue was purified via silica gel chromatography using a 90% hexanes: 10% EA eluent yielding carbamate **12** as a foamy white solid (0.120 g, 51%). TLC $R_f = 0.25$ (10% EA: 90% hexanes); IR (ATR) 3350, 2975, 1692, 1162 cm^{-1}; ^1H NMR (400 MHz, $CDCl_3$) δ 7.57 (s, 1H), 7.40 (d, *J* = 8.0 Hz, 1H), 7.13-7.19 (m, 2H), 7.01-7.08 (m, 2H), 6.21 (d, *J* = 7.7 Hz, 1H), 5.33 (s, 2H), 4.56 (bs, 1H), 3.37 (bs, 2H), 2.94 (t, *J* = 6.5 Hz, 2H), 2.52 (s, 3H), 2.27 (s, 3H), 1.43 (s, 9H); $^{13}C\{^1H\}$ NMR (100 MHz, CD_3CN) δ 156.4, 136.2, 135.7, 135.5, 132.2, 129.9, 129.7, 129.3, 128.0, 127.9, 127.4, 122.8, 119.1, 110.2, 109.6, 78.5, 44.7, 41.5, 28.2, 25.2, 18.2, 9.9

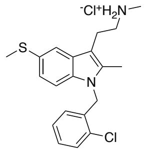

(2{1-[(2-Chlorophenyl)methyl]-2-methyl-5-(methylsulfanyl-1H-indol-3-yl}ethyl)methylaminium chloride (**2.18**).

Carbamate **12** (0.200 g, 0.450 mmol) was dissolved in dry THF (5 mL, 0.1M) and cooled to 0˚C. $LiAlH_4$ solution (1 M in THF, 1.92 mL, 1.92 mmol) was added slowly to the mixture at 0˚C. The reaction was allowed to warm to rt and then heated to reflux for 4h. After cooling the reaction to rt, the mixture was diluted with 10 mL of ethyl ether and quenched by the sequential addition of 80 μL of water, 240 μL of 15% aq. NaOH solution, and 80 μL of water. Approximately 1 g of anhydrous $MgSO_4$ was then added and, after stirring for 15 min, the mixture filtered through celite with ethyl ether and concentrated. The residue was purified via silica gel chromatography using a solvent gradient of 100% EA to 95% EA: 5% NH_4OH yielding the methylamine derivative. This was then added to a 1:1 ether-hydrochloric acid solution (1 mL, 2 M) and allowed to stir for 30 min. The mixture was concentrated under vacuum and purified via recrystallization from ether/methanol yielding **13** as a red solid (0.124 g, 70% from **12**). IR (ATR) 2917, 2696, 2431, 1466, 1441, 1038, 751 cm^{-1}; ^1H NMR (400 MHz, $CDCl_3$) δ 7.64 (s, 1H), 7.42 (d, *J* = 7.8 Hz, 1H), 7.19 (d, *J* = 7.8 Hz, 1H), 7.07 (s, 1H), 7.02 (t, *J* = 7.8 Hz, 1H), 6.20 (d, *J* = 7.4 Hz, 1H), 5.36 (s, 2H), 3.11-3.23 (m, 4H), 2.74 (s, 3H), 2.47 (s, 3H), 2.29 (s, 3H); $^{13}C\{^1H\}$ NMR (100 MHz, CD_3OD) δ 135.5, 135.1, 131.7, 129.2, 128.5, 128.2, 128.1, 127.0, 126.5, 123.1, 118.1, 111.4, 109.6, 105.3, 49.4, 43.9, 32.4, 21.1, 17.4, 8.6

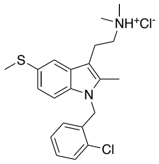

(2{1-[(2-Chlorophenyl)methyl]-2-methyl-5-(methylsulfanyl-1H-indol-3-yl}ethyl) dimethylaminium chloride (**2.20**).

Tryptamine **1** (0.175 g, 0.460 mmol) was dissolved in 0.60 mL of acetic acid. Sodium cyanoborohydride (0.289 g, 4.6 mmol) dissolved in 1 mL of methanol was added to the reaction followed by the addition of formalin (37%, 1.8 mL, 23 mmol). The mixture was stirred at rt for 18 h, followed by solvent removal in vacuo. The residue was dissolved in DCM and the mixture was washed using 2 M aq. NaOH solution (3 x 5 mL). The organic layer was then dried over anhydrous Na_2SO_4, filtered, and concentrated. The crude oil was purified via silica gel chromatography using a 90% DCM: 10% MeOH eluent yielding a clear oil that was then added to a 1:1 ether-hydrochloric acid solution (1 mL, 2M) and allowed to stir for 30 min. The mixture was concentrated under vacuum and purified via recrystallization from ether/methanol yielding **14** a red solid (0.040 g, 21% over 2 steps). IR (ATR) 2917, 2780, 2665, 2469, 1466, 1441, 1413, 1048, 750 cm^{-1}; ^1H NMR (400 MHz, $CDCl_3$) δ 12.94 (bs, 1H), 7.55 (s, 1H), 7.41 (d, *J* = 7.8 Hz, 1H), 7.15-7.21 (m, 2H), 7.01-7.09 (m, 2H), 6.17 (d, *J* = 7.5 Hz, 1H), 5.33 (s, 2H), 3.38-3.42 (m, 2H), 3.20 (m, 2H), 2.91 (s, 3H), 2.89 (s, 3H), 2.55 (s, 3H), 2.36 (s, 3H); $^{13}C\{^1H\}$ NMR (100 MHz, CD_3OD) δ 135.3, 135.2, 134.6, 131.9, 129.5, 128.7, 128.3, 127.8, 127.3, 126.6, 123.4, 118.2, 110.0, 105.3, 58.1, 44.5, 42.9, 20.2, 18.8, 10.3.

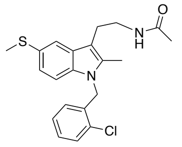

N-(2{1-[(2-Chlorophenyl)methyl]-2-methyl-5-(methylsulfanyl-1H-indol-3-yl}ethyl)acetamide **(2.21)**.

Tryptamine **1** (0.120 g, 0.314 mmol) was dissolved in 1.5 mL of 2:1 methanol/THF and cooled to 0˚C. Triethylamine (0.086 mL, 0.692 mmol) was added to the mixture and stirred 5 min. Acetic anhydride (0.033 mL, 0.346 mmol) was added and the reaction was brought to rt and stirred for 2 h. The mixture was then diluted in EA and washed with sat. aq. $NaHCO_3$ (3 x 15 mL). The organic layer was dried over anhydrous Na_2SO_4, filtered and concentrated. The residue was purified via silica gel chromatography (40% EA: 60% hexanes) yielding acetamide **16** as a red foamy solid (0.110 g, 98%). TLC R_f = 0.33 (40% EA: 60% hexanes); IR (ATR) 3249, 3067, 2919, 1630,

1468,1368, 752 cm^{-1}; ^{1}H NMR (400 MHz, CDCl$_3$) δ 7.57 (s, 1H), 7.40 (d, *J* = 8.0 Hz, 1H), 7.12-7.19 (m, 2H), 7.00-7.07 (m, 2H), 6.19 (d, *J* = 7.7 Hz, 1H), 5.79 (bs, 1H), 5.32 (s, 2H), 3.50 (q, *J* = 6.3 Hz, 2H), 2.96 (t, *J* = 6.8 Hz, 2H), 2.51 (s, 3H), 2.26 (s, 3H), 1.92 (s, 3H); ^{13}C{^{1}H} NMR (100 MHz, CDCl$_3$) δ 170.2, 135.3, 135.0, 134.5, 131.9, 129.5, 128.7, 128.6, 127.7, 127.3, 126.7, 123.2, 118.9, 109.7, 108.7, 44.5, 40.3, 24.5, 23.3, 18.8, 10.0.

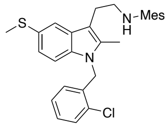

N-(2{1-[(2-Chlorophenyl)methyl]-2-methyl-5-(methylsulfanyl)-1H-indol-3-yl}ethyl)methanesulfonamide (**2.22**).

Tryptamine **1** (0.250 g, 0.530 mmol) was dissolved in 0.6 mL of DCM and cooled to -78˚C. Triethylamine (0.074 mL, 0.527 mmol) was added to the mixture and, after 5 min, methanesulfonyl chloride (0.041 mL, 0.527 mmol) dissolved in 0.6 mL of DCM was added. The mixture was kept at -78˚C for 2 h, and then warmed to rt and diluted with water. The mixture was extracted using DCM (3 x 5 mL) and the combined organic layers were washed with sat. aq. NaCl solution. The organic layer was then dried over anhydrous Na$_2$SO$_4$, filtered and concentrated. The residue was purified via silica gel chromatography (30% EA: 70% hexanes) yielding sulfonamide **15** a white powder (0.091 g, 46%). TLC R$_f$ = 0.22 (30% EA: 70% hexanes); IR (ATR) 3659, 3287, 2980, 2919, 1463, 1440, 1313, 1145, cm^{-1}; ^{1}H NMR (400 MHz, CDCl$_3$) δ 7.59 (s, 1H), 7.43 (d, *J* = 7.3 Hz, 1H), 7.16-7.20 (m, 2H), 7.06-7.11 (m, 2H), 6.24 (d, *J* = 7.3 Hz, 1H), 5.36 (s, 2H), 4.42 (bs, 1H), 3.43 (m, 2H), 3.07 (m, 2H), 2.89 (s, 3H), 2.55 (s, 3H), 2.33 (s, 3H); ^{13}C{^{1}H} NMR (100 MHz, CD$_3$OD) δ 135.3, 135.0, 134.9, 131.9, 129.5, 128.7, 128.4, 128.0, 127.4, 126.7, 123.3, 118.6, 109.8, 107.3, 44.5, 43.6, 40.4, 25.7, 18.7, 10.2

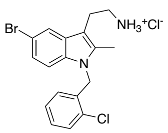

2-(2-{5-Bromo-1-[(2-chlorobenzyl)-2-methyl-1H-indol-3-yl)ethanaminium chloride (**2.39**)

Indole **2.27** (0.50g, 1.30 mmol) was dissolved in acetonitrile (22 mL, 0.06 M). Cs_2CO_3 (2.55 g, 7.83 mmol)) and 2-chlorobenzyl chloride (0.50 mL, 3.91 mmol) were added and the mixture was heated to 80˚C for 18 h. The mixture was cooled to rt, and then filtered to remove the remaining Cs_2CO_3 and other salts. The filtrate was poured into brine and extracted with DCM. The combined organic extracts were dried over anhydrous Na_2SO_4, filtered, and concentrated. The crude mixture (0.290g, 0.571 mmol) was dissolved in methanol (7 mL, 0.1 M) and hydrazine hydrate (0.139 mL, 2.86 mmol) was added. The reaction mixture was brought to reflux at 75˚C for 30 min. The mixture was then allowed to cool, filtered, and concentrated under vacuum. The residue was purified via silica gel column chromatography using an 95% DCM: 5% methanol: 1% conc. aq. NH_4OH. The resulting tryptamine **2.35** (0.072 g, 0.19 mmol) was then dissolved in ethyl ether (0.8 mL, 0.2M) and added to a solution of 2M ethyl ether-hydrochloric acid (0.02 mL) and allowed to stir for 30 min. The mixture was concentrated under vacuum and purified via recrystallization from ether/methanol resulting in a brown powder (0.074 g, 14%)%). IR (ATR) 3628, 3406, 2922, 1611, 1573, 1464, 1046, 747 cm^{-1}; ^1H NMR (400 MHz, CD_3OD) δ 7.77 (s, 1H), 7.48 (d, *J* = 7.8 Hz, 1H), 7.20-7.28 (m, 2H), 7.09-7.17 (m, 2H), 6.24 (d, *J* = 7.8 Hz, 1H), 5.48 (s, 2H), 3.09-3.18 (m, 4H), 2.34 (s, 3H); $^{13}C\{^1H\}$ NMR (100 MHz, CD_3OD) δ 135.9, 135.4, 134.9, 131.7, 129.2, 129.2, 128.6, 127.1, 126.5, 123.8, 119.8, 112.6, 110.7, 105.8, 43.9, 39.7, 22.1, 8.6.

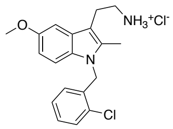

2-(2-{5-Methoxy-1-[(2-chlorobenzyl)-2-methyl-1H-indol-3-yl)ethanaminium chloride (**2.41**)

Indole **2.29** (0.34 g, 1.02 mmol) was dissolved in acetonitrile (18 mL, 0.06 M). Cs_2CO_3 (1.99 g, 6.10 mmol)) and 2-chlorobenzyl chloride (0.39 mL, 3.05 mmol) were added and the mixture was heated to 80˚C for 18 h. The mixture was cooled to rt, and then filtered to remove the remaining Cs_2CO_3 and other salts. The filtrate was poured into brine and extracted with DCM. The combined organic extracts were dried over anhydrous Na_2SO_4, filtered, and concentrated. The crude mixture (0.30g, 0.65 mmol) was dissolved in methanol (8 mL, 0.1 M) and hydrazine hydrate (0.160 mL, 3.27 mmol) was added. The reaction mixture was brought to reflux at 75˚C for 30 min. The mixture was then allowed to cool, filtered, and concentrated under vacuum. The residue was purified via silica gel column chromatography using an 95% DCM: 5% methanol: 1% conc. aq. NH_4OH. The resulting tryptamine **2.37** (0.070 g, 0.21 mmol) was then dissolved in ethyl ether (1.0 mL, 0.2M) and added to a solution of 2M ethyl ether-hydrochloric acid (0.02 mL) and allowed to stir for 30 min. The mixture was concentrated under vacuum and purified via recrystallization from ether/methanol resulting in a brown powder (0.050 g, 13%)%). IR (ATR) 2953, 2908, 2829, 1619, 1588, 1484, 1234, 1038, 750 cm^{-1}; ^{1}H NMR (400 MHz, CD_3OD) δ 7.45 (d, *J* = 7.2 Hz, 1H), 7.23 (t, *J* = 7.2 Hz, 1H), 7.12 (d, *J* = 2.3 Hz, 1H), 7.05-7.09 (m, 2H), 6.75 (dd, *J* = 2.3, 8.8 Hz, 1H), 6.23 (d, *J* = 7.7, 1H), 5.40 (s, 2H), 3.86 (s, 3H), 3.13-3.20 (m, 4H), 2.31 (s, 3H); $^{13}C\{^1H\}$ NMR (100 MHz, CD_3OD) δ 154.5, 135.4, 134.6, 131.9, 131.6, 129.1, 128.4, 127.9, 127.0, 126.6, 110.6, 109.6, 105.7, 99.9, 55.0, 43.9, 39.8, 22.3, 8.7.

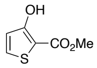

Methyl 3-hydroxy-2-thiophenecarboxylate (**2.55**)

To a solution of $NaHCO_3$ (7.120 g, 84.78 mmol) suspended in 20mL methanol, was added methyl thioglycolate (2.00 g, 18.84 mmol) and methyl-2,3-dichloropropionate (2.960 g, 18.84 mmol). The mixture was brought to reflux at 73˚C and was stirred overnight. The reaction mixture was then cooled to r.t. and brought to a pH of 1 using 1M hydrochloric acid. The aqueous phase was washed with dichloromethane (4x), and the organic fractions were dried over Na_2SO_4 and concentrated down under vacuum. The crude brown oil was purified via silica gel column chromatography using a gradient of 90% hexanes:10% ethyl acetate to 80% hexanes:20% ethyl acetate yielding an off-white crystal (0.7344 g, 24.6%). MP = 42-45˚C TLC $R_f = 0.66$ (hexane: ethyl acetate, 80%:20%); ^1H NMR (400 MHz, $CDCl_3$) δ 3.88 (s, 3H), 6.71-6.74 (m, 1H), 7.34-7.37 (m, 1H), 9.56 (s, 1H); ^{13}C NMR (400 MHz, $CDCl_3$) δ 166.7, 164.6, 131.5, 119.2, 103.7, 77.4, 77.1, 76.8, 51.9, 29.7

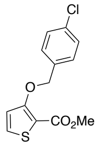

Methyl-3-[(4-chlorophenyl)]thiophene-2-carboxylate (**2.56**)

To a solution of 4-chlorobenzyl chloride (0.897 g, 5.57 mmol) suspended in 12mL of 2-butanone, was added methyl-3-hydroxy-2-thiophenecarboxylate (0.734 g, 4.65 mmol) and potassium carbonate (0.925 g, 7.00 mmol). The mixture was brought to reflux at 88˚C and was stirred overnight. The reaction mixture was diluted in 50 mL of ethyl acetate and 50 mL of deionized water. The organic layer was recovered and washed with 15 mL of hydrochloric acid and 15 mL of brine solution. The organic layer was recovered, dried over Na_2SO_4, and concentrated down under vacuum. The crude product was purified via silica gel column chromatography using a gradient of 95% hexanes:5% ethyl acetate to 80% hexanes:20% ethyl acetate yielding the desired product (0.6771 g, 51.5%). m.p. = 106-108˚C, TLC R_f = 0.55 (hexane: ethyl acetate, 80%:20%); ^{1}H NMR (400 MHz, $CDCl_3$) δ 7.32-7.41 (m, 5H), 6.80 (d, *J* = 5.2 Hz, 1H), 5.21 (s, 2H), 3.86 (s, 3H); ^{13}C NMR (400 MHz, $CDCl_3$) δ 162.0, 160.5, 135.0, 133.9, 130.6, 128.8, 128.3, 117.5, 110.9, 72.6, 51.7

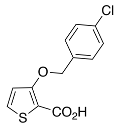

3-((4-Chlorobenzyl)oxy)thiophene-2-carboxylic acid (**2.57**)

To a solution of methyl-3-[(4-chlorophenyl)]thiophene-2-carboxylate (0.500 g, 1.77 mmol) suspended in 4 mL of tetrahydrofuran and 5 mL of methanol was added sodium hydroxide (2M, 2.64 mL). The reaction mixture was brought to 50˚C and was stirred overnight under argon. The mixture was then diluted in 6 mL of ethyl acetate and 10 mL of 1M hydrochloric acid. The organic layer was collected, washed with brine, and dried over Na_2SO_4. The dried organic layer was concentrated down under vacuum yielding the pure desired product (0.400 g, 84.0%). TLC R_f = 0.64 (hexane: ethyl acetate, 90%:10%); ^{1}H NMR (400 MHz, $CDCl_3$) δ 7.53 (dd, *J* = 1.2, 5.6 Hz, 1H), 7.35-7.41 (m, 4H), 6.87 (dd, *J* = 1.2, 5.2 Hz, 1H), 5.26 (s, 2H); ^{13}CNMR (400 MHz, CDCl3) δ 162.0, 159.0, 134.9, 133.4, 132.6, 129.3, 128.9, 116.3, 109.7, 73.6

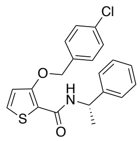

AS1949490 (**2.3**)

To 12 mL dichloromethane was added 3-((4-chlorobenzyl)oxy)thiophene-2-carboxylic acid (0.400 g, 1.49 mmol), EDCI (0.573 g, 2.98 mmol) and (S)-1-Ephenylethylamine (0.234 mL, 1.49 mmol) and a catalytic amount of DMAP. The mixture was stirred overnight at r.t. After approximately 18 h, hydrochloric acid (1M, 50 mL) was added and the aqueous layer was washed with dichloromethane (3x). The organic layer was dried over Na_2SO_4 and concentrated down under vacuum. The crude product was purified via silica gel column chromatography using 60% hexanes:40% ethyl acetate yielding a yellow powder (0.4628 g, 77.0%). m.p. = 91-94˚C, TLC R_f = 0.46 (hexane: ethyl acetate, 80%:20%); ^{1}H NMR (400 MHz, $CDCl_3$) δ 7.44 (d, *J* = 6.8 Hz, 1H), 7.38 (d, *J* = 5.6 Hz, 1H), 7.27-7.34 (m, 3H), 7.18-7.25 (m, 5H), 6.88 (d, *J* = 5.2 Hz, 1H), 5.22 (dq, *J* = 6.8, 6.8 Hz, 1H), 5.11 (dd, *J* = 11.2, 14.0 Hz, 2H), 1.46 (d, *J* = 6.8 Hz, 3H); ^{13}C NMR (400 MHz, $CDCl_3$) δ 160.8, 154.9, 143.3, 134.8, 133.9, 129.3, 129.1, 129.0, 128.7, 127.3, 126.1, 118.2, 116.1, 73.2, 48.9, 22.4

2.6 References

(1) Hoekstra, E.; Das, A. M.; Willemsen, M.; Swets, M.; Kuppen, P. J. K.; van der Woude, C. J.; Bruno, M. J.; Shah, J. P.; Ten Hagen, T. L. M.; Chisholm, J. D.; et al. Lipid Phosphatase SHIP2 Functions as Oncogene in Colorectal Cancer by Regulating PKB Activation. *Oncotarget* **2016**, *7* (45), 1–16.

(2) Majerus, P. W.; Kisseleva, M. V.; Anderson Norris, F. The Role of Phosphatases in Inositol Signaling Reactions. *J. Biol. Chem.* **1999**, *274* (16), 10669–10672.

(3) Fuhler, G.; Brooks, R. Therapeutic Potential of SH2 Domain-Containing Inositol-5′-Phosphatase 1 (SHIP1) and SHIP2 Inhibition in Cancer. *Mol. Med.* **2012**, *18* (1), 1.

(4) Viernes, D. R.; Choi, L. B.; Kerr, W. G.; Chisholm, J. D. Discovery and Development of Small Molecule SHIP Phosphatase Modulators. *Med. Res. Rev.* **2014**, *34* (4), 795–824.

(5) Gericke, A.; Leslie, N. R.; Lösche, M.; Ross, A. H. PtdIns(4,5)P2-Mediated Cell Signaling: Emerging Principles and PTEN as a Paradigm for Regulatory Mechanism. In *Lipid-mediated Protein Signaling*; Capelluto, D. G. S., Ed.; Springer Netherlands: Dordrecht, 2013; pp 85–104.

(6) Brooks, R.; Fuhler, G. M.; Iyer, S.; Smith, M. J.; Park, M.-Y.; Paraiso, K. H. T.; Engelman, R. W.; Kerr, W. G. SHIP1 Inhibition Increases Immunoregulatory Capacity and Triggers Apoptosis of Hematopoietic Cancer Cells. *J. Immunol.* **2010**, *184* (7), 3582–3589.

(7) Liu, P.; Cheng, H.; Roberts, T. M.; Zhao, J. J. Targeting the Phosphoinositide 3-Kinase Pathway in Cancer. *Nat. Rev. Drug Discov.* **2009**, *8* (8), 627–644.

(8) Wu, P.; Hu, Y. Small Molecules Targeting Phosphoinositide 3-Kinases. *Medchemcomm* **2012**, *3* (11), 1337.

(9) Marone, R.; Cmiljanovic, V.; Giese, B.; Wymann, M. P. Targeting Phosphoinositide 3-Kinase—Moving towards Therapy. *Biochim. Biophys. Acta - Proteins Proteomics* **2008**, *1784* (1), 159–185.

(10) Elkabets, M.; Vora, S.; Juric, D.; Morse, N.; Mino-Kenudson, M.; Muranen, T.; Tao, J.; Campos, A. B.; Rodon, J.; Ibrahim, Y. H.; et al. MTORC1 Inhibition Is Required for Sensitivity to PI3K P110α Inhibitors in PIK3CA -Mutant Breast Cancer. *Sci. Transl. Med.* **2013**, *5* (196).

(11) Brown, K. K.; Toker, A. The Phosphoinositide 3-Kinase Pathway and Therapy Resistance in Cancer. *F1000Prime Rep.* **2015**, *7.*

(12) Park, S.; Kim, Y. S.; Kim, D. Y.; So, I.; Jeon, J.-H. PI3K Pathway in Prostate Cancer: All Resistant Roads Lead to PI3K. *Biochim. Biophys. Acta - Rev. Cancer* **2018**, *1870* (2), 198–206.

(13) Brooks, R.; Fuhler, G. M.; Iyer, S.; Smith, M. J.; Park, M.-Y.; Paraiso, K. H. T.; Engelman, R. W.; Kerr, W. G. SHIP1 Inhibition Increases Immunoregulatory Capacity and Triggers Apoptosis of Hematopoietic Cancer Cells. *J. Immunol.* **2010**, *184* (7), 3582–3589.

(14) Prasad, N. K.; Decker, S. J. SH2-Containing 5′-Inositol Phosphatase, SHIP2, Regulates Cytoskeleton Organization and Ligand-Dependent Down-Regulation of the Epidermal Growth Factor Receptor. *J. Biol. Chem.* **2005**, *280* (13), 13129–13136.

(15) Prasad, N. K.; Tandon, M.; Handa, A.; Moore, G. E.; Babbs, C. F.; Snyder, P. W.; Bose, S. High Expression of Obesity-Linked Phosphatase SHIP2 in Invasive Breast Cancer Correlates with Reduced Disease-Free Survival. *Tumor Biol.* **2008**, *29* (5), 330–341.

(16) Helgason, C. D.; Damen, J. E.; Rosten, P.; Grewal, R.; Sorensen, P.; Chappel, S. M.;

Borowski, A.; Jirik, F.; Krystal, G.; Humphries, R. K. Targeted Disruption of SHIP Leads to Hemopoietic Perturbations, Lung Pathology, and a Shortened Life Span. *Genes Dev.* **1998**, *12* (11), 1610–1620.

(17) Song, M. S.; Salmena, L.; Pandolfi, P. P. The Functions and Regulation of the PTEN Tumour Suppressor. *Nat. Rev. Mol. Cell Biol.* **2012**, *13* (5), 283–296.

(18) Blunt, M. D.; Ward, S. G. Targeting PI3K Isoforms and SHIP in the Immune System: New Therapeutics for Inflammation and Leukemia. *Curr. Opin. Pharmacol.* **2012**, *12* (4), 444–451.

(19) Franke, T. F.; Kaplan, D. R.; Cantley, L. C.; Toker, A. Direct Regulation of the Akt Proto-Oncogene Product by Phosphatidylinositol-3,4-Bisphosphate. *Science (80-.).* **1997**, *275* (5300), 665–668.

(20) Jain, S.; Susa, M.; Keeler, M.; Carlesso, N.; Druker, B.; Varticovski, L. PI 3-Kinase Activation in BCR/Abl-Transformed Hematopoietic Cells Does Not Require Interaction of P85 SH2 Domains with P210 BCR/Abl. *Blood* **1996**, *88* (5), 1542–1550.

(21) Gewinner, C.; Wang, Z. C.; Richardson, A.; Teruya-Feldstein, J.; Etemadmoghadam, D.; Bowtell, D.; Barretina, J.; Lin, W. M.; Rameh, L.; Salmena, L.; et al. Evidence That Inositol Polyphosphate 4-Phosphatase Type II Is a Tumor Suppressor That Inhibits PI3K Signaling. *Cancer Cell* **2009**, *16* (2), 115–125.

(22) Ivetac, I.; Gurung, R.; Hakim, S.; Horan, K. A.; Sheffield, D. A.; Binge, L. C.; Majerus, P. W.; Tiganis, T.; Mitchell, C. A. Regulation of PI(3)K/Akt Signalling and Cellular Transformation by Inositol Polyphosphate 4-phosphatase-1. *EMBO Rep.* **2009**, *10* (5), 487–493.

(23) Kennah, M.; Yau, T. Y.; Nodwell, M.; Krystal, G.; Andersen, R. J.; Ong, C. J.; Mui, A.

L.-F. Activation of SHIP via a Small Molecule Agonist Kills Multiple Myeloma Cells. *Exp. Hematol.* **2009**, *37* (11), 1274–1283.

(24) Perez, L. E.; Desponts, C.; Parquet, N.; Kerr, W. G. SH2-Inositol Phosphatase 1 Negatively Influences Early Megakaryocyte Progenitors. *PLoS One* **2008**, *3* (10), e3565.

(25) Prasad, N. K. SHIP2 Phosphoinositol Phosphatase Positively Regulates EGFR-Akt Pathway, CXCR4 Expression, and Cell Migration in MDA-MB-231 Breast Cancer Cells. *Int. J. Oncol.* **2009**, *34* (1), 97–105.

(26) Hillmann, P.; Fabbro, D. PI3K/MTOR Pathway Inhibition: Opportunities in Oncology and Rare Genetic Diseases. *Int. J. Mol. Sci.* **2019**, *20* (22), 5792.

(27) Obst, J.; Bradshaw, W.; Roberts, H. H.; Priestley, R.; Jimenez-Antunez, C.; Cowley, S. A.; Gileadi, O.; Mead, E.; Daniel, E. Di; Davis, J. B. Targeting SHIP1 for Therapeutic Intervention in Alzheimer's Disease. *Alzheimer's Dement.* **2020**, *16* (S9).

(28) Fernandes, S.; Brooks, R.; Gumbleton, M.; Park, M.-Y.; Russo, C. M.; Howard, K. T.; Chisholm, J. D.; Kerr, W. G. SHIPi Enhances Autologous and Allogeneic Hematopoietic Stem Cell Transplantation. *EBioMedicine* **2015**, *2* (3), 205–213.

(29) Brooks, R.; Iyer, S.; Akada, H.; Neelam, S.; Russo, C. M.; Chisholm, J. D.; Kerr, W. G. Coordinate Expansion of Murine Hematopoietic and Mesenchymal Stem Cell Compartments by SHIPi. *Stem Cells* **2015**, *33* (3), 848–858.

(30) Sosič, I.; Anderluh, M.; Sova, M.; Gobec, M.; Mlinarič Raščan, I.; Derouaux, A.; Amoroso, A.; Terrak, M.; Breukink, E.; Gobec, S. Structure-Activity Relationships of Novel Tryptamine-Based Inhibitors of Bacterial Transglycosylase. *J. Med. Chem.* **2015**, *58* (24), 9712–9721.

(31) Kerr, W. G.; Pedicone, C.; Dormann, S.; Pacherille, A.; Chisholm, J. D. Small Molecule

Targeting of SHIP1 and SHIP2. *Biochem. Soc. Trans.* **2020**, *48* (1), 291–300.

(32) Suwa, a; Yamamoto, T.; Sawada, a; Minoura, K.; Hosogai, N.; Tahara, a; Kurama, T.; Shimokawa, T.; Aramori, I. Discovery and Functional Characterization of a Novel Small Molecule Inhibitor of the Intracellular Phosphatase, SHIP2. *Br. J. Pharmacol.* **2009**, *158* (3), 879–887.

(33) Wada, T.; Tsuneki, H.; Hosoh, S.; Toyooka, N.; Kagawa, S.; Takamura, Y.; Muranaka, H.; Wang, X.; Sasaoka, T.; Ichihara, Y.; et al. The Inositol Phosphatase SHIP2 Negatively Regulates Insulin/IGF-I Actions Implicated in Neuroprotection and Memory Function in Mouse Brain. *Mol. Endocrinol.* **2010**, *24* (10), 1965–1977.

(34) Tsuneki, H.; Yoshida, H.; Okamoto, K.; Yamaguchi, M.; Endo, K.; Nakano, A.; Tsuda, M.; Toyooka, N.; Wada, T.; Sasaoka, T. AS1949490, an Inhibitor of 5'-Lipid Phosphatase SHIP2, Promotes Protein Kinase C-Dependent Stabilization of Brain-Derived Neurotrophic Factor MRNA in Cultured Cortical Neurons. *Eur. J. Pharmacol.* **2019**, *157*, 405–422.

(35) Lim, J. W.; Kim, S. K.; Choi, S. Y.; Kim, D. H.; Gadhe, C. G.; Lee, H. N.; Kim, H.-J.; Kim, J.; Cho, S. J.; Hwang, H.; et al. Identification of Crizotinib Derivatives as Potent SHIP2 Inhibitors for the Treatment of Alzheimer's Disease. *Eur. J. Med. Chem.* **2018**, *157*, 405–422.

(36) Maehama, T.; Taylor, G. S.; Slama, J. T.; Dixon, J. E. A Sensitive Assay for Phosphoinositide Phosphatases. *Anal. Biochem.* **2000**, *279* (2), 248–250.

(37) Feng, J.; Chen, Y.; Pu, J.; Yang, X.; Zhang, C.; Zhu, S.; Zhao, Y.; Yuan, Y.; Yuan, H.; Liao, F. An Improved Malachite Green Assay of Phosphate: Mechanism and Application. *Anal. Biochem.* **2011**, *409* (1), 144–149.

(38) Mosmann, T. Rapid Colorimetric Assay for Cellular Growth and Survival: Application to Proliferation and Cytotoxicity Assays. *J. Immunol. Methods* **1983**, *65* (1–2), 55–63.

(39) Prasad, N. K.; Tandon, M.; Badve, S.; Snyder, P. W.; Nakshatri, H. Phosphoinositol Phosphatase SHIP2 Promotes Cancer Development and Metastasis Coupled with Alterations in EGF Receptor Turnover. *Carcinogenesis* **2008**, *29* (1), 25–34.

(40) Daina, A.; Michielin, O.; Zoete, V. SwissADME: A Free Web Tool to Evaluate Pharmacokinetics, Drug-Likeness and Medicinal Chemistry Friendliness of Small Molecules. *Sci. Rep.* **2017**, *7* (1), 42717.

(41) MORIGUCHI, I.; HIRONO, S.; NAKAGOME, I.; HIRANO, H. Comparison of Reliability of Log P Values for Drugs Calculated by Several Methods. *Chem. Pharm. Bull.* **1994**, *42* (4), 976–978.

(42) Lipinski, C. A.; Lombardo, F.; Dominy, B. W.; Feeney, P. J. Experimental and Computational Approaches to Estimate Solubility and Permeability in Drug Discovery and Development Settings 1PII of Original Article: S0169-409X(96)00423-1. The Article Was Originally Published in Advanced Drug Delivery Reviews 23 (1997). *Adv. Drug Deliv. Rev.* **2001**, *46* (1–3), 3–26.

(43) Eriks, J. C.; Van der Goot, H.; Sterk, G. J.; Timmerman, H. Histamine H2-Receptor Agonists. Synthesis, in Vitro Pharmacology, and Qualitative Structure-Activity Relationships of Substituted 4- and 5-(2-Aminoethyl)Thiazoles. *J. Med. Chem.* **1992**, *35* (17), 3239–3246.

(44) Ahlström, M. M.; Ridderström, M.; Zamora, I.; Luthman, K. CYP2C9 Structure−Metabolism Relationships: Optimizing the Metabolic Stability of COX-2 Inhibitors. *J. Med. Chem.* **2007**, *50* (18), 4444–4452.

(45) Fink, D. M. Cesium Carbonate Promoted N-Alkylation of Indoles. *Synlett* **2004**, No. 13, 2394–2396.

(46) Righi, M.; Topi, F.; Bartolucci, S.; Bedini, A.; Piersanti, G.; Spadoni, G. Synthesis of Tryptamine Derivatives via a Direct, One-Pot Reductive Alkylation of Indoles. *J. Org. Chem.* **2012**, *77* (14), 6351–6357.

Chapter 3: The Design, Synthesis and SAR of Bis-Sulfonamide SHIP1 Agonists

Abstract

The SHIP enzyme is known to resist the activity of PI3K, and subsequently is of interest in the treatment of inflammatory disorders like Crohn's disease, IBD and Alzheimer's disease. SHIP1 is allosterically stimulated by its own product PI(3,4)P_2, which binds to the enzyme resulting in an increase in the enzymatic activity. This increased activity of SHIP1 promotes an increased rate of hydrolysis of PI(3,4,5)P_3, leading to a reduction in the activation of AKT from PI(3,4,5)P_3 but an increase in the signaling interactions of PI(3,4)P_2 and AKT. Small molecules that increase SHIP1 activity may have benefits in these areas. We recently uncovered a bis-sulfonamide found to increase the activity of SHIP1. Additionally, studies were pursued leading to the design and synthesis of new sulfonamide-based SHIP1 agonists. These newly developed agonists were then evaluated for their potential to increase SHIP1 activity. Structure-activity relationships were also explored with the goal of developing more potent agonists that are less prone to biodegradation by CYP enzymes.

3.1 Introduction & Background

SHIP1 has surfaced as a promising therapeutic target due to its vital role in immune cells, but also for its involvement in the survival of certain cancers.[1] SHIP inhibitors, specifically SHIP1 selective inhibitors, have been shown to induce apoptosis in multiple myeloma cell lines.[2] In addition, pulsatile dosing of the SHIP1 inhibitors promotes immune responses against tumor cells, allowing them to serve as potential chemotherapeutic adjuvants against B lymphoid cancers.[3] Small molecule SHIP1 inhibitors also stimulate engraftment of autologous and allogeneic hematopoietic stem cells in murine models of bone marrow transplantation, and therefore could potentially be used to improve the outcome of these treatments. Additionally, some pan-SHIP1/2 inhibitors have also been found to exhibit cytotoxic properties against breast cancer and prostate cancer cell lines.[4,5] These pan-inhibitors have also shown the potential to upregulate the phagocytic function of microglia in the central nervous system, providing a potential therapeutic target for neurogenic disorders.[6]

Furthermore, the discovery that PI(3,4)P_2 binds to the SHIP1 C2 domain resulting in an increase in the catalytic activity by means of a feed-forward process led to the development and identification of SHIP1 agonists. These initial SHIP1 agonists were based on the natural product pelorol, and were found to be effective at reducing proinflammatory functions of macrophages, both in vitro and in vivo.[7–10] This work resulted in the synthesis of two potent SHIP1 agonists, AQX-MN100 (**3.1**) and AQX-16A (**3.2, Figure 3.1.1**), however these molecules suffered from poor water solubility and low bioavailability. This led to the advancement of AQX-1125 (**3.3**), an indane derivative found to selectively agonize SHIP1 while also possessing anti-inflammatory properties. AQX-1125 (**3.3**) was evaluated in the clinic, proceeding to phase III trials for the treatment of inflammatory bladder disease before ultimately being discontinued.[11] Recently, the ability of AQX-1125 (**3.3**) to increase SHIP1 activity was reevaluated, with the major findings showing the failed trial was likely correlated to the poor potency of the molecule.[7]

Figure 3.1.1: Aquinox Pharmaceutical SHIP1 Agonists

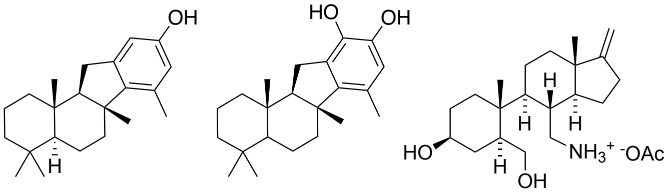

3.1 **3.2** **3.3**

Recent results showing a correlation between single nucleotide polymorphisms in the SHIP1 gene INPP5D and Alzheimer's Disease has led to an increased interest in the modulation of SHIP1 activity. SHIP1 inhibition is being investigated for its potential to increase microglial functions stimulated by the SHIP1-regulated TREM2 receptor, most notable to decrease amyloid burden in the central nervous system.[12] Further analysis confirmed pan-SHIP1/2 inhibitors were capable of promoting phagocytosis in microglia both in in vitro and in vivo testing, including phagocytosis of pathogenic Ab42.[6] Other studies have shown decreased SHIP1 expression to be part of a seven gene Alzheimer's Disease risk cassette in a murine model suggesting that SHIP1 agonism could also prove to be a viable therapeutic strategy in some settings.[13] This brings about an interesting paradox in that SHIP1 may need to be both inhibited or upregulated depending upon the stage of disease. SHIP1 antagonism in early-stage disease may allow for enhanced microglial homeostatic function, while agonism could prove beneficial in late-stages of the disease to reduce the inflammation caused by dysfunctional microglia.

SHIP1 agonists may also be effective in the treatment of inflammatory diseases, such as IBD and Crohn disease, as SHIP1 knock-out mice develop ileitis that closely resembles human Crohn's disease.[14] Further supporting these studies, it was found 15% of patients with IBD are SHIP1-deficient at the protein level.[15,16] This same subset of IBD patients was found to suffer from a more severe case of the disease, typically requiring surgical resections or biological treatment when compared to SHIP1-sufficient IBD patients.[15] SHIP1 agonism may be a viable treatment for those who express low levels of SHIP1when compared against healthy individuals.[7]

While several SHIP1 agonists are known, most suffer from poor bioavailability and/or low efficacy. New agonist leads were discovered using a high-throughput virtual screening approach performed on the SHIP1 active site, aided by the use of an AI based algorithm to improve scoring.

Due to a lack of SHIP1 crystal structures at the time of screening, this screening was performed by threading the SHIP1 amino resides into the SHIP2 active site crystal structure providing an estimated model of the SHIP1 phosphatase domain. The screening of this active site model turned up 76 potentially active structures. Purchasing these molecules and evaluating their effects on SHIP1 was then undertaken employing the malachite green assay for phosphatase activity. This testing yielded four compounds showing potent SHIP1 agonism identified as **3.4**, **3.5**, **3.6**, and **3.7** (**Figure 3.1.2**).[17,18] While this screening was performed on the SHIP active site in the hopes of uncovering potential SHIP inhibitors, it was not unexpected to find SHIP agonists due to the similarity of the SHIP active site and the allosteric site, as the active site binds PI(3,4,5)P_2 while the allosteric site binds PI(3,4)P_2, and these inositols have extremely similar structures.

Figure 3.1.2: SHIP1 Agonists Identified Via Virtual Screening

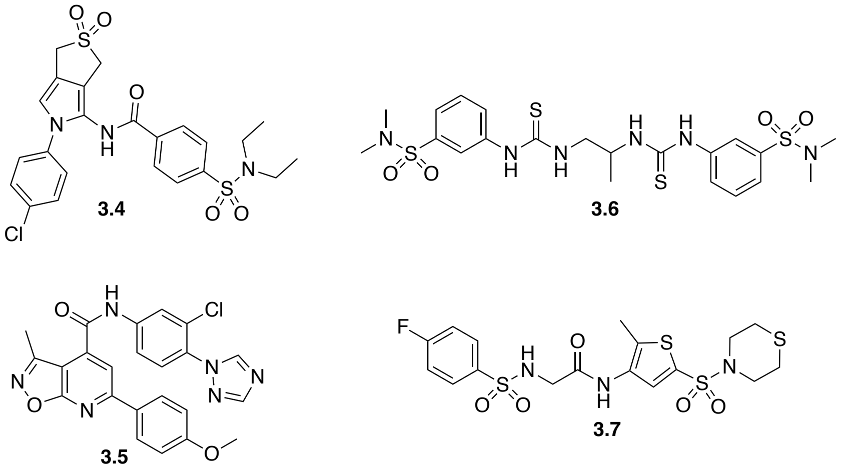

All four compounds induced significant increases in SHIP1 activity in the malachite green assay, however; **3.7** and **3.5** also showed strong agonism of SHIP2 but only at 0.5 mM and 0.0625 mM concentrations, respectively.[18] These compounds were next evaluated for potential biological activity in cells, examining their capacity to suppress LPS-induced production of TNF-α as well as IL-6 in microglial cells. SHIP1 is known to restrict production of both TNF-α and IL-6 in LPS-stimulated macrophages, which was further supported by increased suppression of these inflammatory cytokines when subjected to the SHIP1 agonist AQX-MN100 (**3.1**). This test would also provide some information about the ability of these molecules to cross a cell membrane. Testing of the four potential agonists versus LPS-stimulated BV2 cells showed only reductions in both TNF-α and IL-6 production by the **3.7** molecule (**Figure 3.1.3**).[8,18] This may be due to the other molecules being unable to cross the cell membrane.

Figure 3.1.3: SHIP1 Agonists vs. LPS-stimulated BV2 cell TNF-α and IL-6 Production

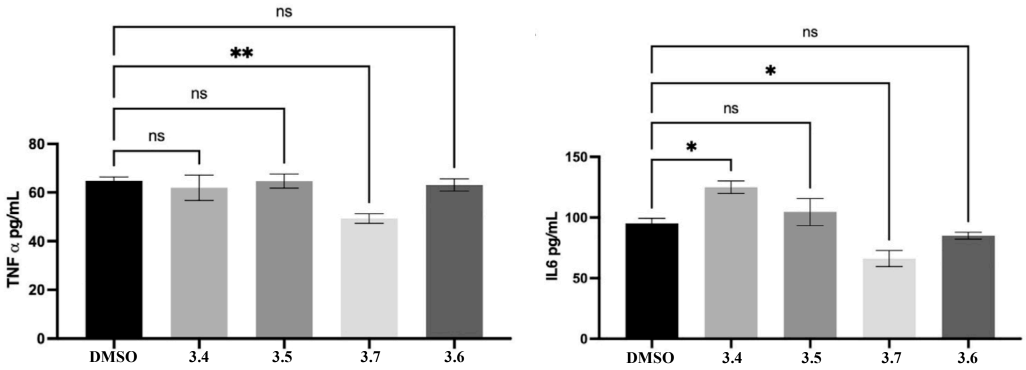

Figure 3.1.3: (A) IL-6 and (B)TNF-a production by BV2 microglia cells stimulated with LPS for 6 h or 2 h, respectively, as measured from supernatants by ELISA. (Representative results of two independent comparisons of all potential agonists at 5mM). All cells were treated with agonists or vehicle control 1 h before LPS challenge. Bars indicate mean GSEM. Statistical analysis was performed with one-way ANOVA with Dunnett correction for multiple comparisons versus control (DMSO), **$p < 0.01$, *$p < 0.05$).

Bis-sulfonamide **3.7** was found to increase SHIP1 activity 30% when tested at 500 µM concentrations and 6% when tested at 250 µM concentrations. It was also found to possess an EC$_{50}$ of 0.2051 µM, while the previously know SHIP1 selective agonist, AQX-MN100 (**3.1**), only agonizes SHIP1 at an EC$_{50}$ of 0.5896 µM. Analog **3.7** was also found to possess an EC$_{50}$ of 0.1192 µM against SHIP1 compared to an EC$_{50}$ of 1.169 µM against SHIP2 when tested on recombinant SHIP1 and SHIP2, marking a 10-fold preference for SHIP1 agonism over SHIP2.[18] These results would indicate **3.7** is both a more selective and potent SHIP1 agonist than **3.1**. In addition to being a more potent and selective agonist, **3.7** is also believed to operate by a different mechanism of action than the pelorol-based SHIP agonists. The pelorol-based agonists, like AQX-MN100 (**3.1**), have been shown to require the C2 domain of SHIP1 be present in order to increase SHIP1 activity.[8] However, examination of **3.7**'s agonism showed little dependency on the presence of this domain. When **3.1** and **3.7** were tested against a SHIP1 protein mutant lacking the C2 domain, **3.1** no longer gave any increase in SHIP1 activity, while **3.7** remained able to increase SHIP1 activity. These results show that the **3.7** agonism of SHIP1 is not dependent on the C2 domain, supporting the claim that the agonism of SHIP1 by **3.7** occurs by a different mechanism of action and depend on a different allosteric binding site.[18]

One potential issue with the **3.7** structure is the presence of oxidizable sulfide groups, which may be targeted by cytochrome P450 oxidases present in cells, including microglia. This oxidation, may lead to premature degradation of the molecule in cells, reducing the half-life of the effects. Therefore, the synthesis of **3.7** analogs has been undertaken in order to replace these potentially oxidizable groups with more stable isosteres, while also focusing on maintaining or increasing the agonistic potential of the newly formed analogs. The synthesis of **3.7** analogs, and the subsequent testing, also allows for further probing of the structure-activity relationships of **3.7** and the newly discovered allosteric site, with the goal to increase the potency, bioavailability, and stability of the SHIP1 agonists.

3.2 Objectives

The primary objective of this project was to synthesize the selective SHIP1 agonist **3.7** for initial testing on BV2 microglial cells as well as to modify the **3.7** structure to find an analog with increased potency, bioavailability, and stability. This goal was achieved by performing structure activity relationship testing on analogs where the four distinct **3.7** quadrants were changed sequentially; the aryl sulfonyl quadrant (quadrant A), the amino acid quadrant (quadrant B), the aromatic core quadrant (quadrant C), and the sulfonamide quadrant (quadrant D).

Figure 3.2.1: Sections of Bis-sulfonamide 3.7 to be Modified in SAR studies

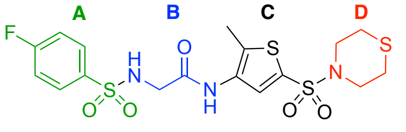

3.7

Once the most active component at each quadrant was determined through the use of the malachite green assay, hybrid molecules may be designed that could have even greater potency.

3.3 Results & Discussion

Initially the synthesis of the bis-sulfonamide **3.7** structure was undertaken. This synthesis begins with the sulfonation of 2-methylthiophene (**3.8**) using sulfuryl chloride and DMF yielding sulfonyl chloride **3.9** in 63% yield. DMF plays a vital role in this reaction serving as both the solvent and a reagent, forming a white crystalline DMF-SO_2Cl_2 complex that acts as the chlorosulfonating agent in this reaction.[19] Sulfonyl chloride **3.9** then underwent nitration in the presence of fuming nitric acid and acetic anhydride yielding nitrothiophene **3.10**.[20] Nitrothiophene **3.10** is then used to form a sulfonamide with thiomorpholine producing the desired intermediate **3.11** in near quantitative yields. Reduction of the nitro group by iron powder and acetic acid then leads to amine **3.12** in an 89% yield. The amine **3.12** then undergoes an amide coupling with Boc-glycine mediated by HATU and diisopropylamine forming amide **3.13**. The Boc-protecting group was removed by stirring amide **3.13** in TFA yielding the TFA salt **3.14**. Amine salt **3.14** then underwent an N-sulfonylation with 4-fluorobenzenesulfonyl chloride providing the desired bis-sulfonamide **3.7** in a 65% yield with an overall yield of 28% across the 7-step synthesis sequence.

Scheme 3.3.1: Synthetic Route for the SHIP1 Agonist **3.7**

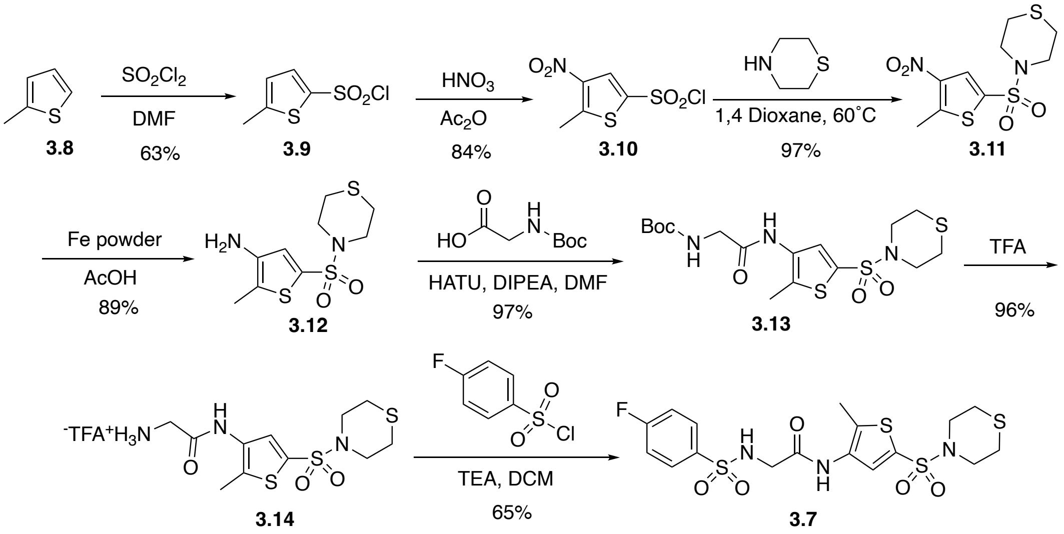
SO2Cl2
DMF
63%
3.8
SO2Cl
3.9
HNO3
Ac2O
84%
O2N
3.10
HN S
1,4 Dioxane, 60˚C
97%
3.11
Fe powder
AcOH
89%
H2N
3.12
HO N Boc
HATU, DIPEA, DMF
97%
Boc
3.13
TFA
96%
-TFA+H3N
3.14
F
Cl
TEA, DCM
65%
3.7

Initial testing of the synthesized agonist **3.7** confirmed the strong agonistic properties, with increases in enzymatic activity of 33% and 6% when tested at 500 μM and 250 μM concentrations, respectively. However, it also showed **3.7** suffered a short-half life in mice, requiring a multiple dosing regimen in order to achieve the agonistic and anti-inflammatory responses reported earlier.[18] This is believed to be due to rapid oxidation of the sulfur in the thiomorpholine ring by cytochrome P450 enzymes.[21] In order to test this hypothesis two analogs, sulfoxide **3.15** and sulfone **3.16**, were synthesized as described below to confirm the lack of activity. As expected **3.15** showed no agonistic activity in malachite green testing, while **3.16** suffered from poor water solubility and was therefore impossible to test. This is consistent with oxidation of the sulfur being a problem that needs to be addressed in this class of SHIP1 agonists.

Figure 3.3.1: Sulfoxide and Sulfone Analogs

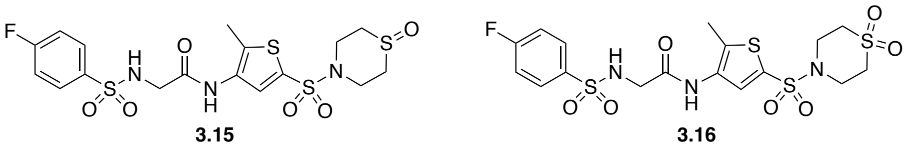
3.15 **3.16**

In order to gain further data on the structure-activity relationships of agonist **3.7** and its new allosteric site, additional analogs were synthesized. Bis-sulfonamide **3.7** can essentially be broken down into four main quadrants, the aryl sulfonyl quadrant, in green, the amino acid quadrant, in blue, the aromatic core quadrant, in black, and lastly the sulfonamide quadrant, in red (**Figure 3.3.2**).

Figure 3.3.2: Design and Development of Bis-sulfonamide **3.7** Analogs

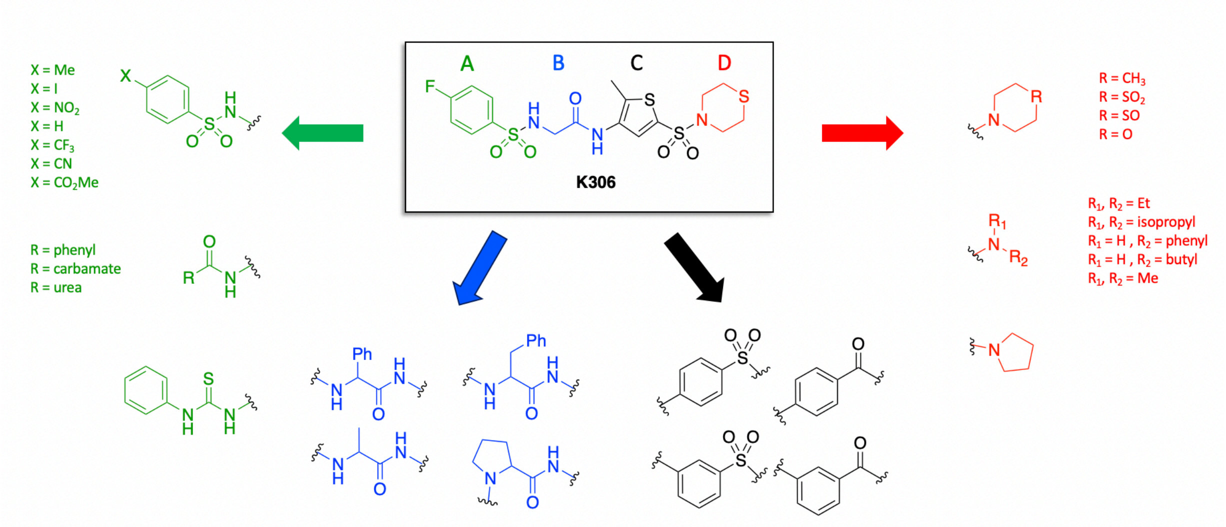
X = Me
X = I
X = NO_2
X = H
X = CF_3
X = CN
X = CO_2Me
R = phenyl
R = carbamate
R = urea
A
B
C
D
K306
R = CH_3
R = SO_2
R = SO
R = O
R_1, R_2 = Et
R_1, R_2 = isopropyl
R_1 = H , R_2 = phenyl
R_1 = H , R_2 = butyl
R_1, R_2 = Me

Swapping out individual quadrants, while keeping the remaining three constant, will allow for the essential functionality required for activity to be determined. With the basis of **3.15** and **3.16** as a backdrop, modification of the sulfonamide quadrant D was undertaken. Using previously synthesized nitrothiophene **3.10** and the desired amine, *N*-sulfonylation was achieved yielding intermediates **3.17-3.26** in moderate to high yields.

Table 3.3.1: Quadrant D Sulfonamide formation via *N*-sulfonylation of **3.10**

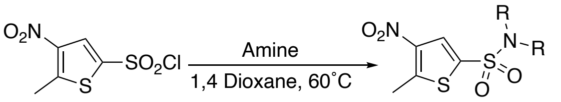
O2N
SO2Cl
Amine
1,4 Dioxane, 60˚C
O2N
R
N
R
S
O
O

3.10 **3.17-3.26**

Entry	Amine	Product	% Yield
1	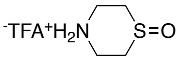	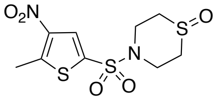 **3.17**	59%
2	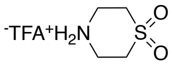	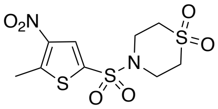 **3.18**	71%
3	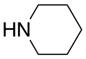	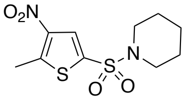 **3.19**	73%
4	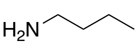	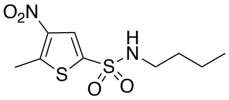 **3.20**	62%
5	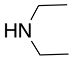	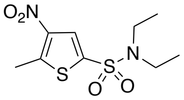 **3.21**	41%
6	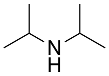	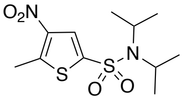 **3.22**	45%
7	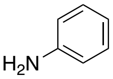	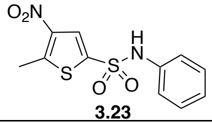 **3.23**	42%
8	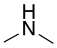	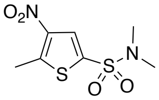 **3.24**	57%
9	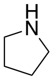	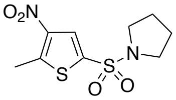 **3.25**	59%
10	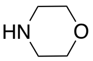	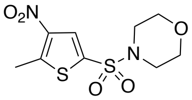 **3.26**	73%

Reduction of the nitro group in each of these sulfonamides was accomplished by iron powder and acetic acid providing the desired amines **3.27-3.36**. The yields for these reactions are summarized in **Table 3.3.2**. The lower yielding amines resulted from a slurry like formation during the reaction period, making the work up and product recovery difficult due to solubility issues.

Table 3.3.2: Nitro Reduction of Quadrant D Analogs

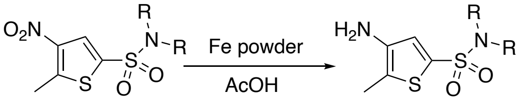

3.17-3.26 **3.27-3.36**

Entry	Amine	Product	% Yield
1	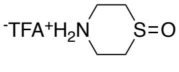	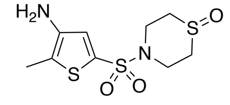 **3.27**	99%
2	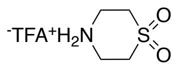	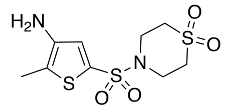 **3.28**	20%
3	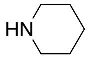	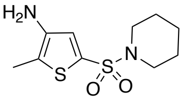 **3.29**	70%
4	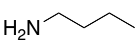	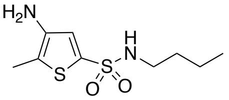 **3.30**	51%
5	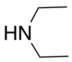	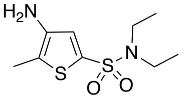 **3.31**	29%
6	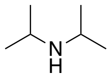	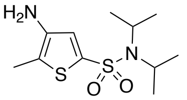 **3.32**	47%
7	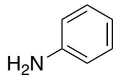	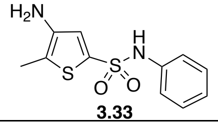 **3.33**	42%
8	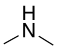	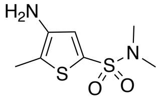 **3.34**	39%
9	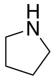	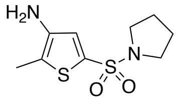 **3.35**	58%
10	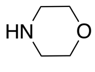	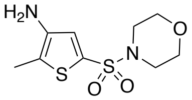 **3.36**	89%

Amines **3.27-3.36** were then subjected to amide coupling conditions using Boc-glycine, HATU, and DIPEA providing amides **3.37-3.46**. These amides were then stirred in trifluoroacetic acid, removing the Boc protecting group, yielding the TFA amine salts **3.47-3.56** in high yields.

Table 3.3.3: Coupling and Deprotection of Quadrant D Analogs

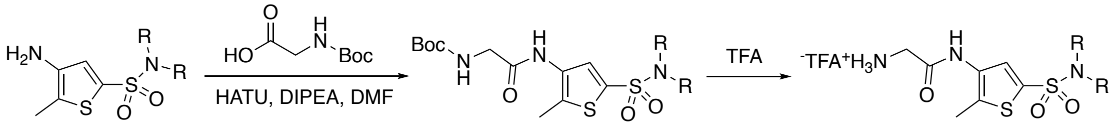

3.27-3.36 **3.37-3.46** **3.47-3.56**

Entry	Amine	Product	% Yield^a
1	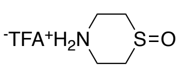	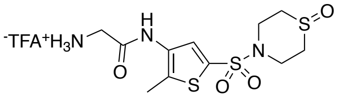 **3.47**	64%
2	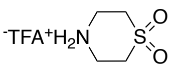	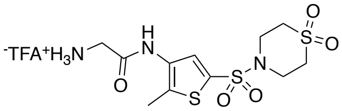 **3.48**	40%
3	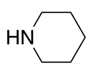	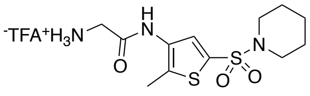 **3.49**	58%
4	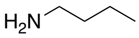	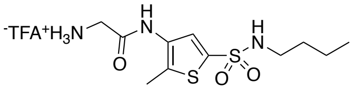 **3.50**	64%
5	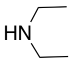	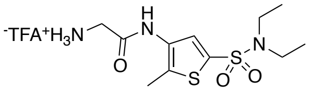 **3.51**	49%
6	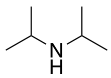	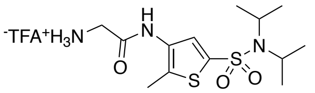 **3.52**	70%
7	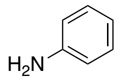	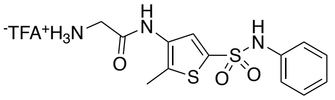 **3.53**	70%
8	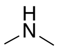	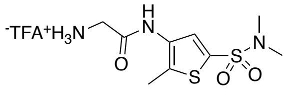 **3.54**	59%
9	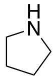	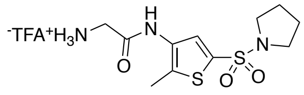 **3.55**	52%
10	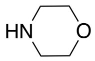	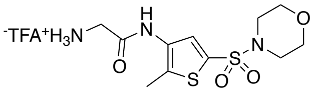 **3.56**	71%

Note: ^{a}Yield is over two steps

The desired analogs **3.57-3.66** were then obtained following the *N*-sulfonylation of the TFA amine salts **3.47-3.56** with 4-fluorobenzenesulfonyl chloride and triethylamine. The yields varied greatly in response to the solubility of the amine after free basing. Notable **3.57**, **3.58**, **3.63** and **3.65** required initial heating to dissolve the free based amine, the solubility issues are believed to be directly correlated to the lower yields obtained.

Table 3.3.4: *N*-Sulfonylation Reactions of Quadrant D Analogs

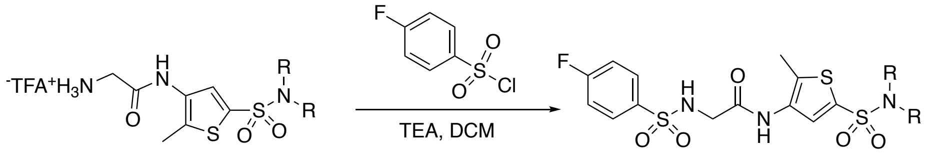

3.47-3.56 **3.57-3.66**

Number	Amine	Product	% Yield
1	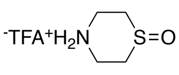	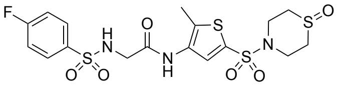 **3.57**	13%
2	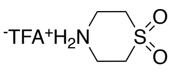	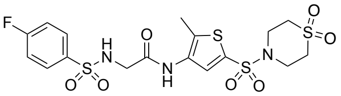 **3.58**	12%
3	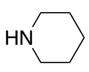	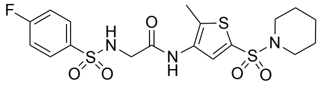 **3.59**	37%
4	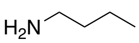	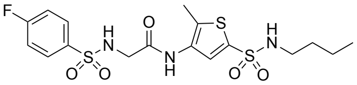 **3.60**	42%
5	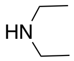	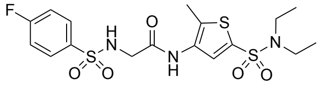 **3.61**	80%
6	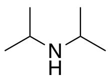	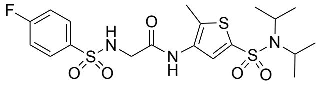 **3.62**	31%
7	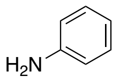	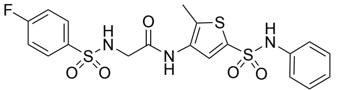 **3.63**	12%
8	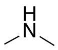	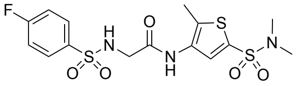 **3.64**	51%
9	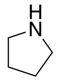	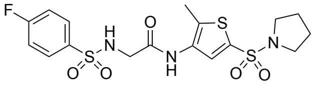 **3.65**	10%
10	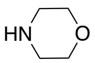	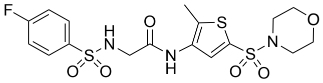 **3.66**	30%

The above quadrant D sulfonamide derivatives have undergone evaluation in the malachite green phosphatase assay. This initial testing provided us with a rough blueprint of the most active functionality for future hybrid derivatives. Given the results of analog **3.66**, the morpholine derivative, it was determined non-polar groups were preferred for the amine fragment, in contrast to the oxygen containing morpholine. Various "greasy" hydrocarbon amines that were used to replace morpholine provided a marked improvement in the agonistic activity. **3.59** and **3.63** both showed strong increases in activity at 500 μM, and maintained this increase when decreased to a 250 μM. Interestingly, **3.60** showed an approximate 25% increase in activity maintained across 500 μM, 250 μM, and 125 μM concentrations, showing high increases at lower concentrations. **3.61** and **3.64** showed little activity. Based off these results it was concluded nonpolar sulfonamide derivatives that were not too large similar to **3.59**, **3.60** and **3.63** were preferred.

Table 3.3.5: Malachite Green Assay Results for Sulfonamide Quadrant D

Entry	**Compound**	**% Activity**		
		SHIP1 500 µM	SHIP1 250 µM	SHIP1 125 µM
1	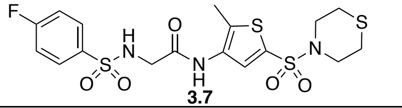 **3.7**	30%	6%	-5%
2	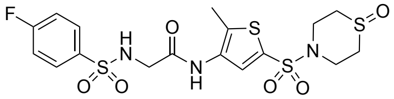 **3.57**	-20%	-11%	-2%
3	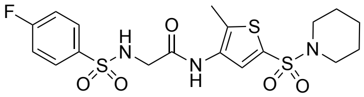 **3.59**	41%	40%	32%
4	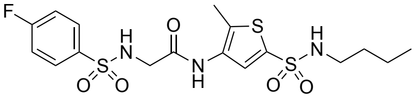 **3.60**	22%	24%	24%
5	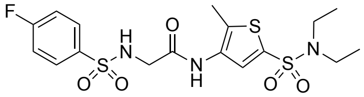 **3.61**	9%	-7%	1%
6	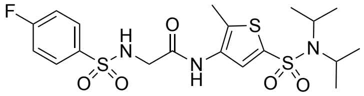 **3.62**	40%	2%	6%
7	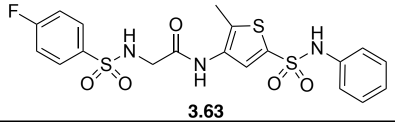 **3.63**	51%	23%	0%
8	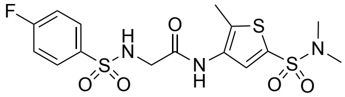 **3.64**	-6%	3%	0%
9	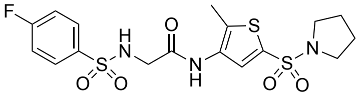 **3.65**	-10%	-3%	0%
10	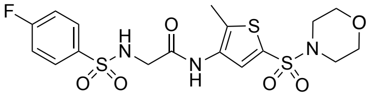 **3.66**	-6%	-7%	n/d

Analogs were also synthesized by varying the aryl sulfonyl quadrant A. Again, keeping the other three quadrants constant in order to isolate the quadrant of interest to determine the importance in binding activity, so the thiomorpholine sulfonamide **3.14** was used as the coupling partner in these reactions. Along with some sulfonyl chlorides , an isocyanate, isothiocyanate, and acid chlorides were employed in the presence of TEA. This allowed for the formation of a number of functional groups other than sulfonamides, like a urea, thiourea, amide and carbamate analog to be formed for evaluation (**Table 3.3.6**).

Table 3.3.6: Aryl Sulfonyl Quadrant A Derivatives

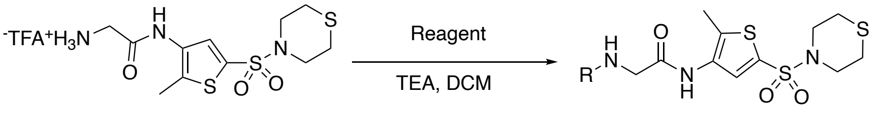

3.14 **3.67-3.78**

Number	Reagent	Product	% Yield
1	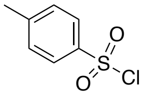	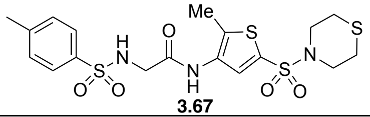 **3.67**	12%
2	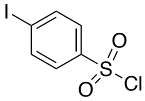	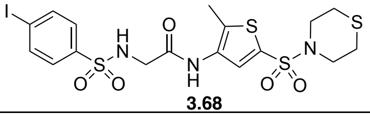 **3.68**	27%
3	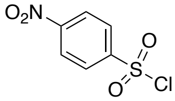	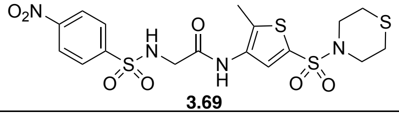 **3.69**	20%
4	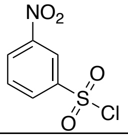	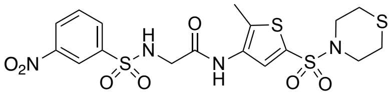 **3.70**	53%
5	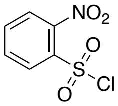	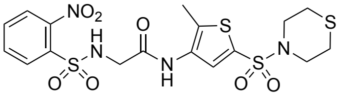 **3.71**	47%
6	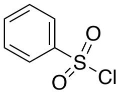	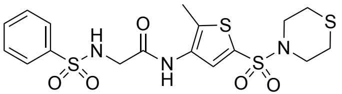 **3.72**	27%
7	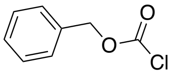	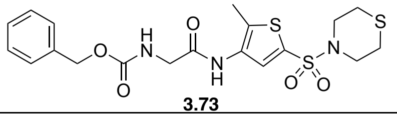 **3.73**	54%
8	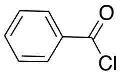	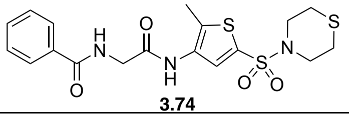 **3.74**	31%
9	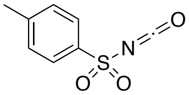	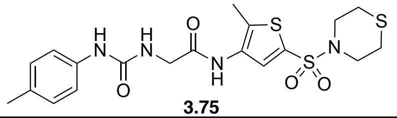 **3.75**	12%
10	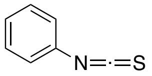	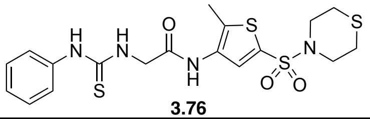 **3.76**	14%

11	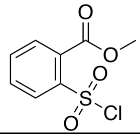	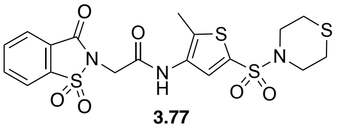 **3.77**	36%
12	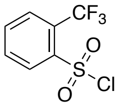	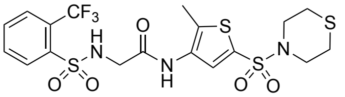 **3.78**	24%

Evaluation of the malachite green assay results for the aryl sulfonyl quadrant provided some clear characteristics of the preferred aromatic functionality. **3.69** and **3.71** showed strong increases in enzyme activity, with a corresponding dose-response to the decreasing concentrations. Both of these analogs contain polar nitro groups, with **3.69** possessing a para substituted nitro group and **3.71** possessing an ortho substituted nitro. While these nitro groups do show strong enzymatic increases, they also raise the possibility of in vivo mutagenesis. Nitro groups have the potential to be reduced to nitroso groups in vivo which are known DNA-alkylators, however; the steric hindrance of the ortho-nitro in **3.71** may help to prevent possible nitro reductions.[22,23] Additionally, analogs **3.76**, **3.75** and **3.77** all showed strong increases in enzymatic activity, with all three also showing good dose-responses. **3.76** and **3.75** are of interest as the sulfonyl group itself was replaced ,with a thiourea linker in **3.76** and a urea linker in **3.75**, while **3.77** contains the sulfonyl linker within a carbonyl sulfonimide ring structure. All three of these analogs provide evidence the sulfonyl linker may not be vital for activity and could possibly be removed in favor of other functionality. These results as a whole show the aryl sulfonyl quadrant should possess smaller, polar, electronegative substituents to maximize activity. They also give reason to believe the sulfonyl linker can be omitted without seeing major decreases in the agonistic effect.

Table 3.3.7: Malachite Green Assay Results for Aryl Sulfonyl Quadrant A

Entry	**Compound**	**% Activity**		
		SHIP1 500 µM	SHIP1 250 µM	SHIP1 125 µM
1	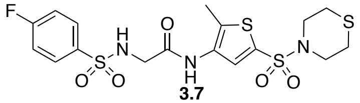 **3.7**	30%	6%	-5%
2	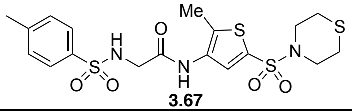 **3.67**	5%	3%	5%
3	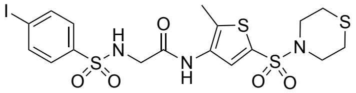 **3.68**	19%	-17%	-1%
4	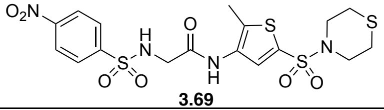 **3.69**	50%	15%	8%
5	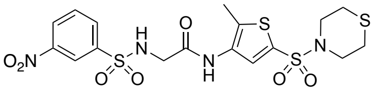 **3.70**	6%	2%	n/d
6	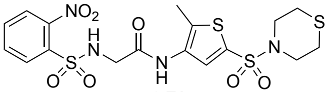 **3.71**	63%	33%	17%
7	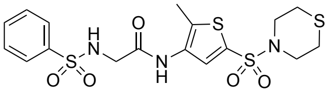 **3.72**	7%	6%	4%
8	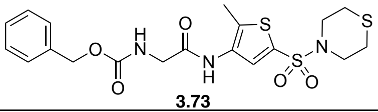 **3.73**	5%	2%	-7%
9	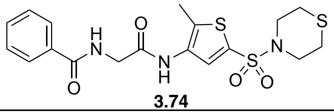 **3.74**	-17%	-6%	-3%
10	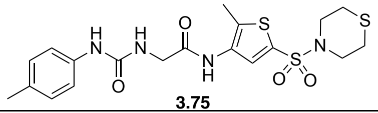 **3.75**	50%	12%	4%
11	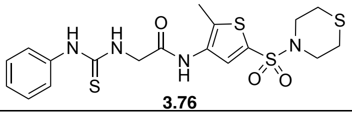 **3.76**	54%	20%	11%
12	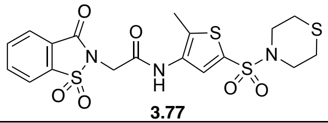 **3.77**	61%	31%	9%
13	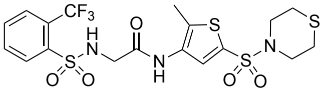 **3.78**	39%	8%	6%
14	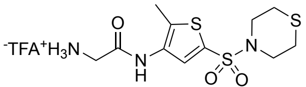 **3.14**	7%	4%	3%

Fellow lab members, Rob Anderson and Angela Pacherille, assisted in the synthesis of the amino acid quadrant analogs. They successfully synthesized the analogs by replacing the glycine linker in favor of both the L and D stereoisomers of alanine (L-**3.79**, D-**3.80**) phenylalanine (L-**3.83**, D-**3.84**), phenyl glycine (L-**3.81**, D-**3.82**), and proline (L-**3.85**, D-**3.86**; **Figure 3.3.3**).

Figure 3.3.3: Bis-Sulfonamide **3.7** Amino Acid Analogs

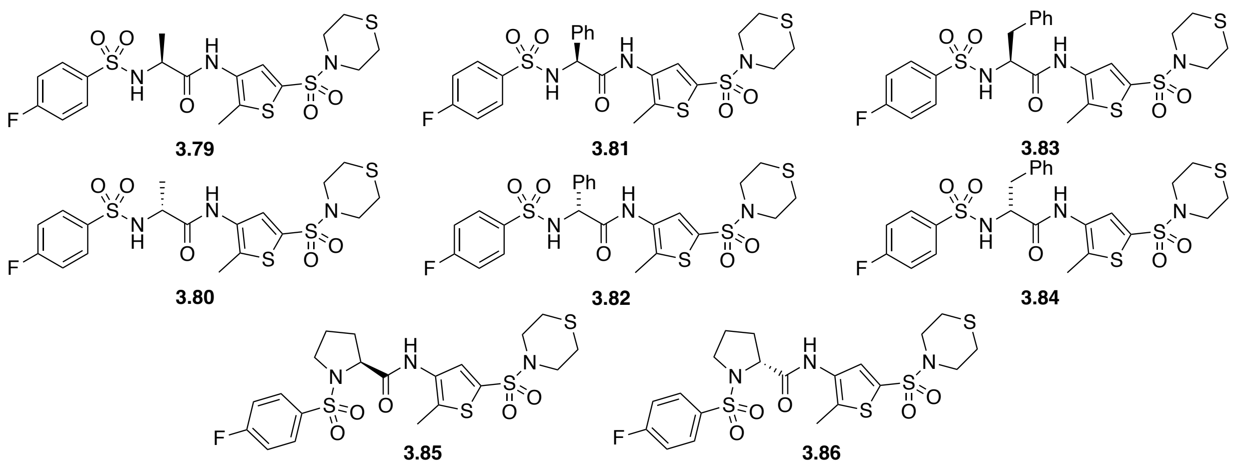

These analogs also underwent evaluation in the malachite green assay providing initial results on the activity of the various amino acid analogs. This provided some noteworthy results, giving further information into how these analogs may possibly be interacting with the allosteric site. **3.79**, **3.80**, **3.81**, **3.82**, **3.83**, **3.84**, and **3.86** showed small to no increases in the enzymatic activity. None of these analogs provided a benefit over using the glycine already present in **3.7**. While **3.81** does appear to show a strong increase in activity at 500 μM, precipitation was observed leading to higher and unreliable readings. At lower concentrations the compound remained in solution and the activity was significantly lower. **3.85**, the L-proline analog, showed a major improvement in the enzymatic activity when compared to the glycine of **3.7**. Additionally, there was a dose response observed over the decreasing concentration. The positive results of the proline analog provided some valuable details regarding the structure-activity relationship between these small molecules and the allosteric site. Proline forces the structure to have a "kink" or bend, keeping the molecule more rigid while also locking it in that bent conformation. This conformation is tolerated in the agonist, and therefore it may be worth pursuing other amino acids or structures that induce a similar conformational change. The other amino acids tested: glycine, phenyl glycine, alanine, and phenylalanine; all are generally linear and allow for a wide range of flexibility. Therefore, the rigidity of the proline, and the locked conformation, keeps the active portions of the molecule in a more accessible position, allowing for easier and stronger binding to occur.

Table 3.3.8: Malachite Green Assay Results for Amino Acid Quadrant B

Entry	**Compound**	**% Activity**		
		SHIP1 500 µM	SHIP1 250 µM	SHIP1 125 µM
1	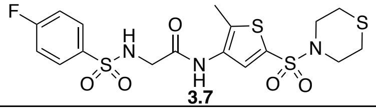 **3.7**	30%	6%	-5%
2	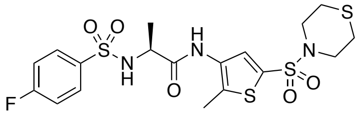 **3.79**	16%	8%	n/d
3	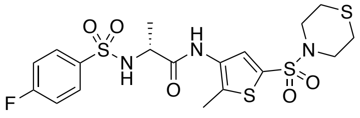 **3.80**	32%	18%	-11%
4	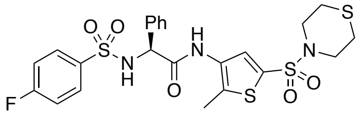 **3.81**	93%[a]	26%	8%
5	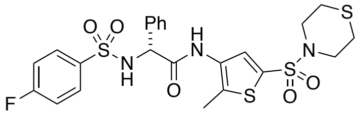 **3.82**	34%[a]	7%	-6%
6	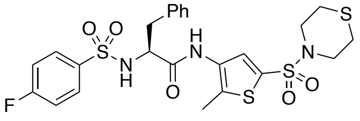 **3.83**	6%	6%	12%
7	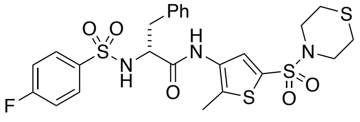 **3.84**	30%	-26%	-29%

8	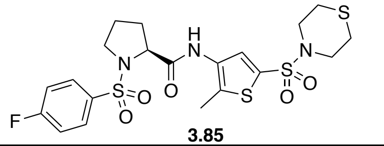 **3.85**	59%	17%	6%
9	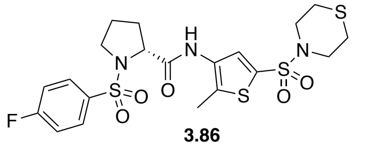 **3.86**	30%	27%	7%

Note *a*: precipitation was observed

The fourth quadrant was the aromatic core, originally a thiophene in the parent **3.7** structure. The goal with these modifications was again to optimize for agonist activity but also to replace the sulfur containing thiophene. As was previously stated sulfur containing compounds present the potential for oxidation when in vivo, however; thiophene is aromatic with the sulfur's lone pairs being delocalized among the aromatic pi system. While this aromaticity should make the thiophene more stable, and therefore less likely to oxidize, removal of this group would remove any question of oxidative degradation. To achieve this, various aromatic core analogs were synthesized replacing the thiophene group with other aromatic rings, as well as an additional thiophene derivative to flesh out structure-activity information (**Table 3.3.9**). The synthesis of these analogs began with the desired aromatic sulfonyl chlorides: 5-chloro-4-nitrothiophene-2-sulfonyl chloride (**3.87**), 3-nitrobenzenesulfonyl chloride (**3.88**) and 4-nitrobenzenesulfonyl chloride (**3.89**) and followed closely the synthesis of the original **3.7** agonist. The thiomorpholine was incorporated via an *N*-sulfonylation yielding sulfonamide intermediates **3.90-3.91**. The nitro group was then reduced utilizing iron powder and acetic acid returning the aromatic amines of **3.93-3.95**. These amines then underwent an HATU coupling with Boc-glycine followed by removal of the Boc group using TFA leading to amine salts **3.99-3.101**. *N*-sulfonylation of these TFA amine salts with 4-flurobenzensulfonyl chloride yielded the desired analogs **3.102-3.104**

Table 3.3.9: Quadrant C Aromatic Core Analogs

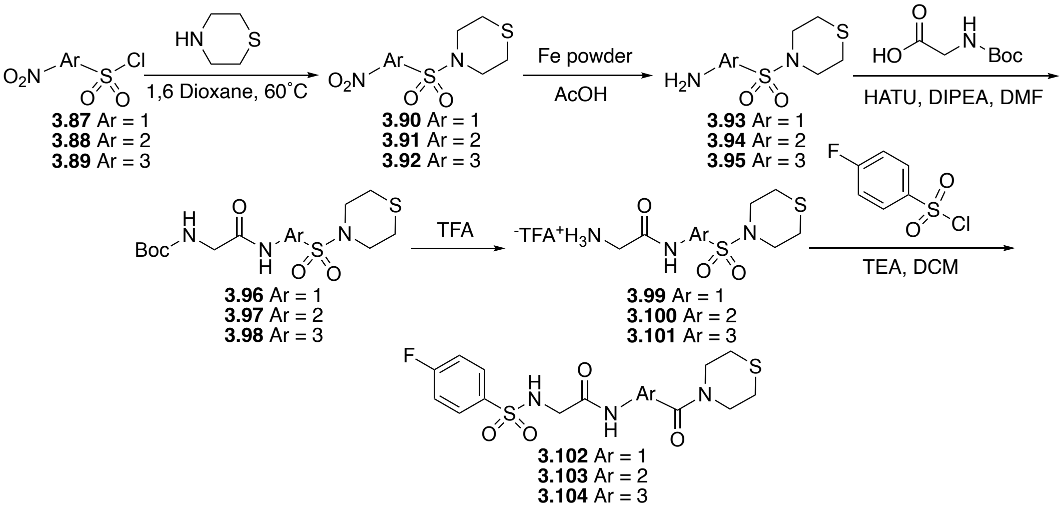
1,6 Dioxane, 60˚C
Fe powder
AcOH
HATU, DIPEA, DMF
TFA
TEA, DCM
3.87 Ar = 1
3.88 Ar = 2
3.89 Ar = 3
3.90 Ar = 1
3.91 Ar = 2
3.92 Ar = 3
3.93 Ar = 1
3.94 Ar = 2
3.95 Ar = 3
3.96 Ar = 1
3.97 Ar = 2
3.98 Ar = 3
3.99 Ar = 1
3.100 Ar = 2
3.101 Ar = 3
3.102 Ar = 1
3.103 Ar = 2
3.104 Ar = 3

Entry	Aryl Group	Sulfonylation % Yield	Reduction % Yield	Coupling % Yield	Deprotection % Yield	Sulfonylation % Yield
1	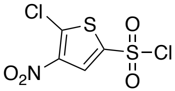 **3.87**	50%	69%	82%	97%	12%
2	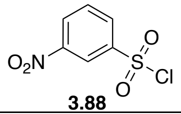 **3.88**	47%	69%	48%	88%	72%
3	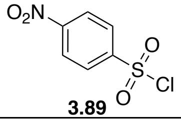 **3.89**	66%	77%	21%	99%	36%

Additionally, an analog with a modified aromatic ring was made where the sulfonamide was replaced in favor of an amide group allowing for SAR studies to be performed on the importance of the sulfonamide, both for activity and binding potential (**Scheme 3.3.2**). Starting with 3-nitrobenzoic acid (**3.105**) and thiomorpholine, an amide coupling was performed using HATU and DIPEA yielding amide **3.106** in high yields. Reduction of the nitro group by means of iron power and acetic acid yielded aniline **3.107** at a 53% yield, followed by a second amide coupling using Boc-protected glycine yielding in intermediate **3.108**. Removal of the Boc protecting group using TFA returned amine salt **3.109** in quantitative yields. Amine **3.109** then underwent *N*-sulfonylation with 4-fluorobenzenesulfonyl chloride producing the desired analog **3.110**.

Scheme 3.3.2: Aromatic Core Amide Linker Derivative

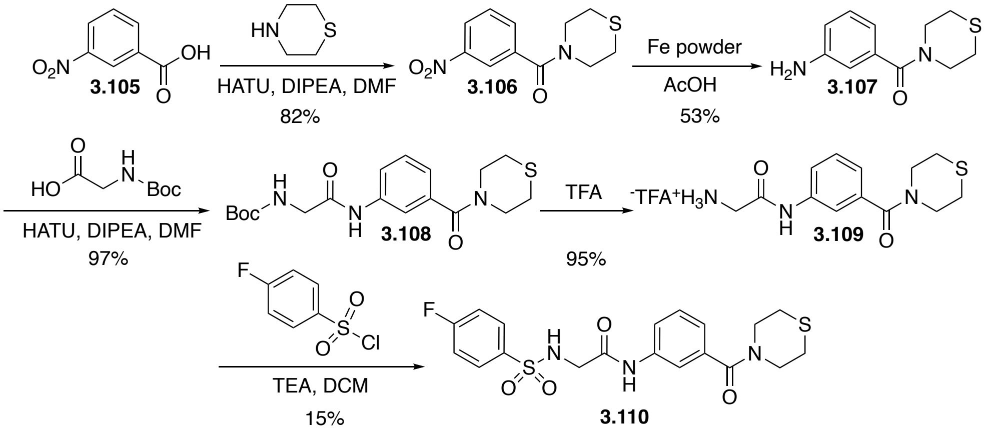

Two additional amide replacements were synthesized by Chisholm lab member Rob Anderson, each with various aryl functionality, as well as a shift to a para substituted amide rather than the initial meta substitution. The first analog, **3.111**, incorporates a chlorine ortho to the amide, while the second analog, **3.112**, features a methyl group at the position meta to the amide (**Figure 3.3.4**). These groups will help to mimic the methyl present on the original **3.7** thiophene core. These two, along with **3.110**, will allow for SAR studies to be performed on both the importance of the sulfonamide incorporation, as well as the importance of the thiophene sulfur.

Figure 3.3.4: Functionalized Aromatic Core Analogs

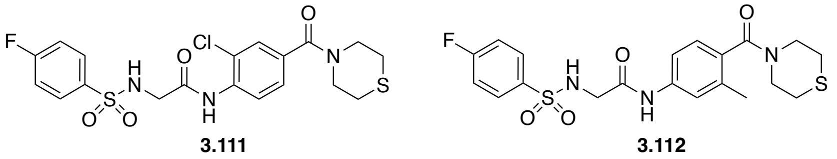

With these six analogs successfully synthesized, malachite green testing was again performed in order to assess the relative activity of the new cyclic cores. The results of the malachite testing failed to provide any plausible substitutions for the thiophene core. All six analogs tested displayed decreases or little change in activity across all concentrations when compared to the **3.7** parent. Four of the analogs: **3.103**, **3.110**, **3.111**, and **3.112** showed no agonist activity, with all of them actually inhibiting the enzyme at various concentrations. **3.102** did show a slight increase in agonist activity with a 25%, 9%, 2% response curve, however, these numbers closely match that of **3.7** and provide little or no potential benefit over the thiophene present. The last analog, **3.104** also showed activity that modeled that of **3.7**, however displaying no improved activity compared to **3.7**. However, in the event the sulfur containing thiophene had to be removed due to possible oxidation issue, the analog **3.104** could provide a solution without any loss in the agonist activity. Work continues on developing additional analogs to replace the thiophene core to optimize the activity provided from this quadrant.

Table 3.3.10: Malachite Green Assay Results for Aromatic Core Quadrant C

Entry	**Compound**	**% Activity**		
		SHIP1 500 µM	SHIP1 250 µM	SHIP1 125 µM
1	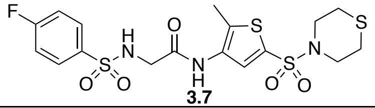 **3.7**	30%	6%	-5%
2	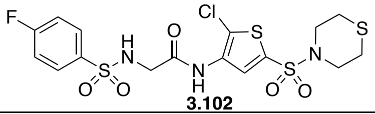 **3.102**	25%	9%	2%
3	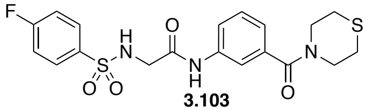 **3.103**	7%	2%	-1%
4	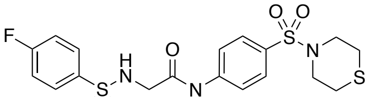 **3.104**	30%	5%	12%
5	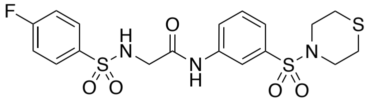 **3.110**	7%	-3%	-6%
6	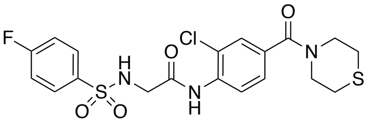 **3.111**	-5%	-3%	0%
7	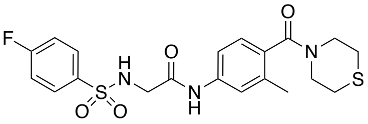 **3.112**	-15%	-3%	0%

With analogs successfully synthesized for all four unique quadrants, and with suitable alternatives for three of the four quadrants, testing in cells was performed utilizing the top hits for each quadrant. Previously **3.7** had been shown to reduce inflammatory gene expression in a study performed on inducible nitrite synthase (iNOS) expression. It was found **3.7** was able to reduce lipopolysaccharide (LPS) mediated induction of iNOS in LPS stimulated BV2 cells when treated both before and after LPS stimulation occurred (**Figure 3.3.5**).[18] These findings were some of the first to prove SHIP1 agonism has the potential to reduce inflammatory cytokines, as well as reduce the enzyme responsible for nitrite production in microglial. This proved significant as nitrate production generated from iNOS has been shown to promote glioblastoma proliferation and invasion, as well as aid in the resistance of glioblastoma to both radio and chemotherapy.[24,25]

Figure 3.3.5: Bis-sulfonamide **3.7** iNOS Expression Study

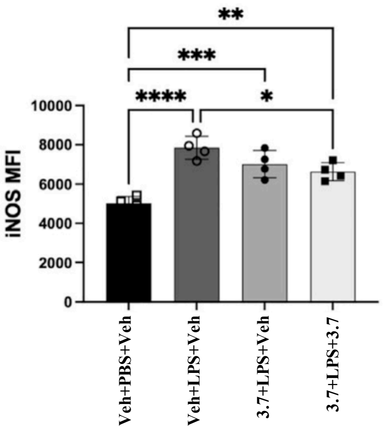

*Figure 3.3.5: **3.7** reduces induction of iNOS in microglia. Mean fluorescence intensity (MFI) for iNOS staining of vehicle or **3.7** LPS-stimulated BV2 cells. BV2 cells were plated and treated for 1 h with Veh (0.25%DMSO) or **3.7** (10mM in Veh) prior to addition of LPS (100 ng/mL). Unstimulated BV2 cells treated with Veh are shown as an additional control to assess LPS induction of iNOS (lane 1). After a 1 h incubation with LPS, Veh (0.25% DMSO) or **3.7** (10mM in Veh) was again added to the indicated samples and incubation was continued for 16 h (Final DMSO concentration in each well was 0.5% DMSO and 0mM (lane 1 and 2), 10mM (lane 3), or 20mM **3.7** (lane 4). Cells were harvested and expression of iNOS was analyzed by intracellular spectral flow cytometry. A one-way ANOVA with Tukey's multiple comparison test was used to compare all-pairs of columns. Shown is one representative experiment of 4 independent experiments with 4 replicate wells/condition.*

Based off this study, analogs were selected from each quadrant, with the exception of the aromatic core where a more active alternative has not yet been found. These analogs underwent the same iNOS detection studies where nitrite production in LPS stimulated BV2 cells were measured that the initial **3.7** agonist parent underwent. For the sulfonamide quadrant the initial analogs selected were **3.59**, **3.60** and **3.63**. The amino acid quadrant had three analogs submitted, both proline derivates **3.85** and **3.86**, as well as D-alanine analog **3.80**. The final analogs selected from the aryl sulfonyl quadrant were the two nitro containing analogs **3.69** and **3.71**, as well as the thiourea containing **3.75**. The results of the in vivo study showed that while all nine analogs did possess the ability to inhibit nitrite production, few were able to do it as well or even better than the original agonist **3.7** (**Figure 3.3.6**). However, there were some significant results from each of the three quadrants tested.

Figure 3.3.6: Evaluation of Bis-Sulfonamides in the iNOS Expression Assay

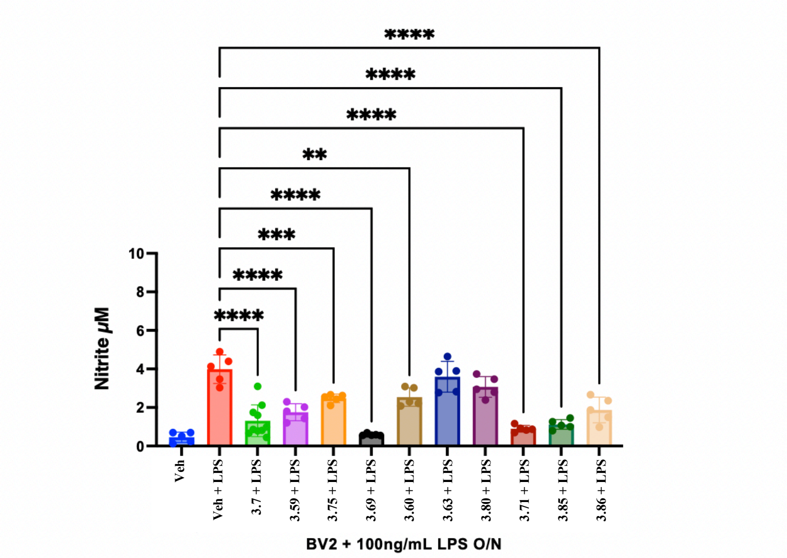

Figure 3.3.6: SHIP1 Agonists reduce induction of iNOS in microglia. Mean fluorescence intensity (MFI) for iNOS staining of vehicle or compound LPS-stimulated BV2 cells. BV2 cells were plated and treated for 1 h with Veh (0.25%DMSO) or compound (10mM in Veh) prior to addition of LPS (100 ng/mL). Unstimulated BV2 cells treated with Veh are shown as an additional control to assess LPS induction of iNOS (lane 1). After a 1 h incubation with LPS, Veh (0.25% DMSO) or ***3.7*** *(10mM in Veh) was again added to the indicated samples and incubation was continued for 16 h (Final DMSO concentration in each well was 0.5% DMSO and 0mM (lane 1 and 2), 10mM (lane 3), or 20mM compound (lane 4). Cells were harvested and expression of iNOS was analyzed by intracellular spectral flow cytometry. A one-way ANOVA with Tukey's multiple comparison test was used to compare all-pairs of columns. Shown is one representative experiment of 4 independent experiments with 4 replicate wells/condition.*

Analog **3.69**, containing a 4-nitrophenylsulfonamide, showed promising results for the aryl sulfonyl quadrant A, displaying a significant improvement in nitrite suppression when compared to **3.7**. **3.71**, the ortho nitro analog also displayed an increased nitrite suppression when compared to **3.7**. These results further supported those obtained from the malachite green testing, which also identified the nitrophenylsulfonamide containing compounds as the most potent agonists. When evaluating the analogs of the sulfonamide quadrant, **3.63** showed almost no nitrite reduction when compared to the vehicle, while **3.60** did have significant reduction compared to the vehicle but failed to approach the levels of nitrite reduction seen by **3.7**. Analog **3.59**, however; was able to reduce nitrite production on a level that closely matched that of **3.7**, further supporting the notion that a piperidine could be a suitable replacement for the oxidizable thiomorpholine. The amino acid quadrant also produced some noteworthy results, with none of the three analogs tested showing any significant advantage over the glycine of **3.7**. Analog **3.80** showed a very minor reduction in nitrite production when compared to the vehicle. The proline derivatives, **3.85** and **3.86**, both showed significant reduction when compared to the vehicle but failed to surpass that seen by **3.7**. These results overall further supported the initial beliefs formed after the malachite assay testing. The nitro containing compounds continued to perform well, as well as the piperidine in replacing of the thiomorpholine. While the proline analogs tested better than **3.7** in the malachite, they failed to display similar results when tested in-vivo.

Based off this body of work, and the data obtained from both the in vivo and in vitro testing and initial hybrid molecule was synthesized utilizing the most active component from each quadrant. Piperidine was chosen for the sulfonamide quadrant, after testing strongly in both the malachite and BV2 cell studies. This would also remove the oxidizable sulfur present in the thiomorpholine of **3.7**, which was responsible for the limited potency. The thiophene core and glycine amino acid linker were left as is, as no beneficial replacements were discovered. The para-nitro group was chosen for the aryl sulfonyl quadrant, again after strong testing in both the malachite and the BV2 cell studies. The synthesis of the hybrid analog began with sulfonyl chloride

3.10. The piperidine was installed by means of *N*-sulfonylation retuning sulfonamide **3.19**. After exposure to iron powder and acetic acid the nitro group was converted amine **3.29**, which then underwent a peptide coupling with Boc-glycine producing intermediate **3.39**. Removal of the Boc protecting group using TFA allowed for *N*-sulfonylation of the amine salt to be employed with 4-nitrobenzenesulfonyl chloride yielding the desired hybrid analog **3.113** (**Scheme 3.3.3**).

Scheme 3.3.3: Hybrid Analog Synthesis

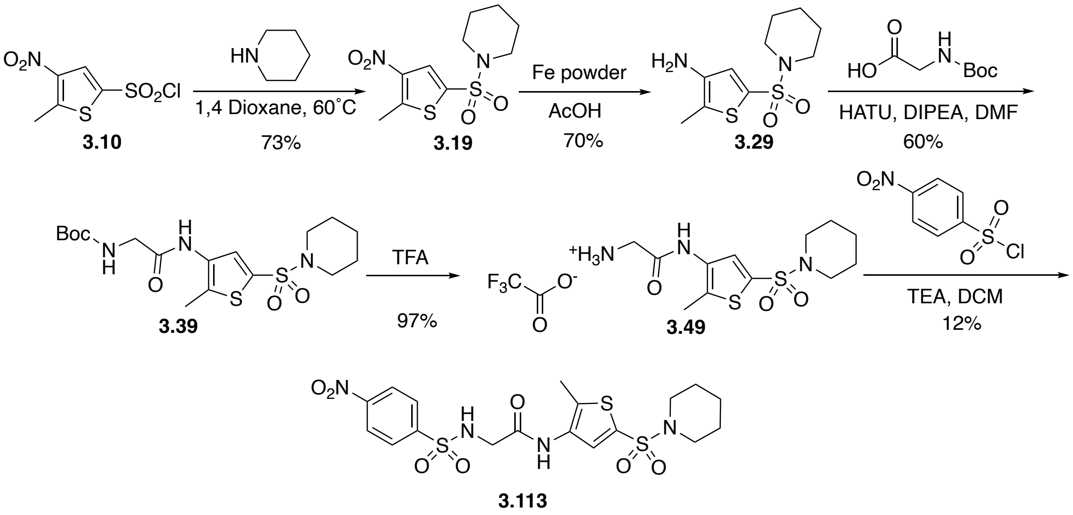

With the first analog successfully synthesized malachite green assay testing was performed to assess how well the hybrid was able to agonize SHIP1. With the idea it was designed to have the most active analog at each quadrant, it was expected to significantly agonize SHIP1 better than the **3.7** agonist parent.

Table 3.3.11: Malachite Green Assay Results for Hybrid Analog

Entry	**Compound**	**% Activity**		
		SHIP1 500 µM	SHIP1 250 µM	SHIP1 125 µM
1	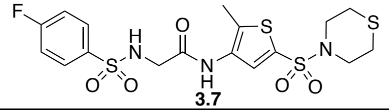 **3.7**	30%	6%	-5%
2	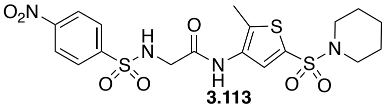 **3.113**	64%	30%	10%

The hybrid analog, **3.113**, was found to possess a 64% activity at 500 µM, a 2-fold increase when compared to **3.7** at the same concentration. Upon dilution to 250 µM, **3.113** still possessed a 30% activity, a 5-fold increase over **3.7**. When diluted to 125 µM, **3.113** was still shown to possess a 10% activity, whereas **3.7** no longer exhibited any agonistic activity. These results confirm the newly synthesized hybrid is a more potent and active SHIP1 agonist, and that removal of the oxidizable thiomorpholine sulfur and altering of the aryl sulfonyl substituents can lead to increasingly active agonists.

3.4 Conclusion &Future Work

The synthesis of SHIP1 selective agonist **3.7** and numerous agonist analogs has successfully been completed, along with initial rounds of in vivo and in vitro testing. Using the SAR and agonistic data obtained from these studies, an initial hybrid analog was synthesized, which showed superior activity and dose-response when compared to **3.7**. Building off these initial results, future work will be focused on finding a suitable replacement for the thiophene core. Work is underway to find a replacement that could eliminate the sulfur, along with any potential oxidization issues. Furthermore, a suitable substitute would display an increased percent activity while also showing an observable dose-response. The final, and arguably most important, criteria still in search of a suitable replacement would be the continued ability to pass through cellular membranes. Work is also underway to synthesize additional hybrid analogs, incorporating additional hits from each quadrant. Currently a hybrid is being developed incorporating proline as the amino acid linker. The final area of exploration currently being pursued is the development of a binding assay utilizing bis-sulfonamide analogs. Work is underway to develop specialized analogs that would allow for a binding assay to be produced allowing for EC_{50}s to easily be obtained for future SHIP based therapeutics.

3.5 Experimental

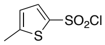

5-methylthiophene-2-sulfonyl chloride (**3.9**)

Lit Ref: Sone, T.; Abe, Y.; Sato, N.; Ebina, M. The Use of N , N -Dimethylformamide–Sulfonyl Chloride Complex for the Preparation of Thiophenesulfonyl Chlorides. *Bull. Chem. Soc. Jpn.* **1985**, *58* (3), 1063–1064.

Dry DMF (1.02 mL, 13.23 mmol) was added to a flame-dried round bottom flask under argon and cooled to 0˚C. Sulfuryl Chloride (1.07 mL, 13.23 mmol) was added dropwise to the solution and stirred for 40 min at 0˚C forming a white crystal complex. 2-methylthiophene (**1**) (1.00 mL, 10.19 mmol) was then added dropwise to the complex and heated to 100˚C and stirred for 1 h. The mixture was poured into ice-water and extracted with $CHCl_3$ (3x25 mL). The organics were washed with a 5% $NaHCO_3$ solution followed by water, dried over Na_2SO_4, and concentrated yielding the pure black oil (1.24g, 63%). TLC R_f = 0.655 (hexane: ethyl acetate, 80%:20%); ^{1}H NMR (400 MHz, $CDCl_3$) δ 7.70 (d, *J* = 4.0 Hz, 1H), 6.85 (d, *J* = 3.9 Hz, 1H), 2.61 (s, 3H); $^{13}C\{^1H\}$ NMR (100 MHz, $CDCl_3$) δ 152.6, 140.7, 135.5, 126.3, 12.9

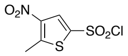

5-methyl-4-nitrothiophene-2-sulfonyl chloride (**3.10**)

Lit Ref: Gronowitz, S.; Ander, I.; Lund, H.; Nimmich, W.; Servin, R.; Sternerup, H. On the Base-Catalyzed Reaction of Some Methyl Nitrothiophenes with Aldehydes. An Unexpected Cyclobutane Formation. *Acta Chem. Scand.* **1975**, *29b*, 513–523.

Cooled fuming nitric acid (1.53 mL, 42.58) was added dropwise to a round bottom flask of acetic anhydride (1.66 mL, 17.57 mmol) and stirred at 0˚C. A solution of sulfonyl Chloride **76** (0.58 g, 2.95 mmol) in acetic anhydride (1.66 mL, 17.57 mmol) was added dropwise over a 30 min period. The temperature of the mixture was raised to 15˚C and stirred for 3 hr. After stirring, the mixture was poured over crushed-ice, extracted with diethyl ether (3x15 mL), and washed with saturated $NaHCO_3$ until a neutral pH was achieved. The organics were collected and dried over Na_2SO_4, filtered and concentrated yielding a pure orange powder (0.50 g, 70.4%). mp = 77.8-83.1˚C; TLC $R_f = 0.491$ (30% EA/70% hexanes); IR (ATR) 3657, 3103, 2980, 1543, 1369, 1316, 1160, 1008, 541 cm^{-1}; 1H NMR ($CDCl_3$, 400 MHz) δ 8.19 (s, 1H), 2.86 (s, 3H); $^{13}C\{^1H\}$ NMR ($CDCl_3$, 100 MHz) δ 152.3, 143.2, 138.8, 130.8, 16.2. Anal. Calcd for $C_5H_4ClNO_4S_2$: C, 55.49; H, 6.81; N, 4.98. Found: C, 55.11; H, 6.44; N, 4.90.

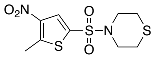

4-[(5-methyl-4-nitrothiophene-2-yl)sulfonyl]thiomorpholine (**3.11**)

Thiomorpholine (0.46 mL, 4.55 mmol) and nitrothiophene **77** (0.50 g, 2.07 mmol) was dissolved in 2 mL of dry 1,4-dioxane and heated to 60˚C. The mixture was stirred for 1 h at 60˚C, after which the reaction was cooled to rt and 20 mL of water was added. The mixture was extracted with DCM (3x20 mL), and the organics were dried over $MgSO_4$, filtered and concentrated. The crude mixture was purified via silica gel chromatography in 70% hexanes:30% ethyl acetate yielding a maroon solid (0.490g, 78%). mp = 142.7-147.0˚C; TLC $R_f = 0.531$ (30% EA/70% hexanes); IR (ATR) 3655, 3117, 2980, 2913, 1545, 1507, 1368, 1163, 1153, 569 cm^{-1}; 1H NMR ($CDCl_3$, 400 MHz) δ 7.94 (s, 1H), 3.43 (t, *J* = 4.8 Hz, 4H), 2.86 (s, 3H), 2.76 (t, *J* = 4.8, 4H); $^{13}C\{^1H\}$ NMR ($CDCl_3$, 100 MHz) δ 149.3, 143.7, 133.1, 127.9, 48.0, 27.3, 16.0. Anal. Calcd for $C_9H_{12}N_2O_4S_3$: C, 35.05; H, 3.92; N, 9.08. Found: C, 35.13; H, 4.06; N, 8.91.

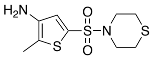

2-methyl-5-thiomorpholine-4-sulfonyl)thiophen-3-amine (**3.12**)

Nitrothiophene **78** (0.49 g, 1.59 mmol) was dissolved in acetic acid (5.3 mL, 92.67 mmol) and iron powder (0.44 g, 7.95 mmol) was added. The mixture was heated to 60˚C and stirred for 1 h, after which the acetic acid was removed via vacuo. The residue was dissolved in ethyl acetate and washed with saturated $NaHCO_3$ until a pH of 8 was reached. The organics were washed with brine, dried over $MgSO_4$, filtered and concentrated. The crude mixture was purified via silica gel chromatography in a gradient of 70% hexanes:30% ethyl acetate to 50% hexanes:50% ethyl acetate yielding a dark solid (0.230g, 52%). mp = 139.7-146.7˚C; TLC R_f = 0.121 (30% EA/70% hexanes); IR (ATR) 3361, 2913, 2852, 1565, 1348, 1327, 1144, 898, 699 cm^{-1}; 1H NMR ($CDCl_3$, 400 MHz) δ 7.54 (s, 1H), 3.72 (br s, 2H), 3.64 (t, *J* = 4.6 Hz, 4H), 3.01 (t, *J* = 4.8, 4H), 2.54 (s, 3H); $^{13}C\{^1H\}$ NMR ($CDCl_3$, 100 MHz) δ 140.0, 130.5, 125.6, 122.0, 48.0, 27.3, 11.8. Anal. Calcd for $C_9H_{14}N_2O_2S_3$: C, 38.83; H, 5.09; N, 10.06. Found: C, 39.17; H, 4.73; N, 9.84.

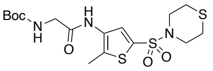

tert-butyl N-({[2-methyl-5-(thiomorpholine-4-sulfonyl)thiophen-3-yl]carbamoyl}methyl)carbamate (**3.13**)

Boc-glycine (0.159g , 0.905 mmol), amine **79** (0.210 g, 0.754 mmol), HATU (0.574 g, 1.509 mmol) and DIPEA (0.262 mL, 1.509) were dissolved in 10.5 mL of dry DMF under argon. The mixture was stirred for 24 h at rt. The reaction was diluted with ethyl acetate, washed with NH_4Cl (3x15 mL) and brine. The organics were dried over $MgSO_4$, filtered and concentrated. The crude mixture was purified via silica gel chromatography using 50% hexanes:50% ethyl acetate yielding a yellow oil (0.250g, 76%). TLC R_f = 0.308 (50% EA/50% hexanes); IR (ATR)

3656, 3254, 2980, 2971, 1665, 1350, 1154, 1141 cm^{-1}; 1H NMR ($CDCl_3$, 400 MHz) δ 8.55 (br s, 1H), 7.78 (s, 1H), 5.60 (t, *J* = 5.7 Hz, 1H), 3.89 (d, *J* = 5.6 Hz, 2H), 3.32 (t, *J* = 4.0 Hz, 4H), 2.68 (t, *J* = 5.2, 4H), 2.32 (s, 3H), 1.43 (s, 9H); $^{13}C\{^1H\}$ NMR ($CDCl_3$, 100 MHz) δ 168.0, 156.9, 132.8, 132.2, 130.9, 128.6, 80.9, 47.9, 45.1, 28.3, 27.2, 12.4.

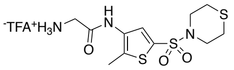

2-aminotrifluoroacetate-N-[2-methyl-5-(thiomorpholine-4-sulfonyl)thiophene-3-yl]acetamide (**3.14**)

Boc protected amine **80** was dissolved in TFA and stirred at rt for 0.5 h. The solvent was removed under vacuo and a pure off-white solid was recovered (1.57g, 96.3%). mp = 190˚C dc; IR (ATR) 3255, 2980, 2915, 1665, 1350, 1329, 1153 cm^{-1}; 1H NMR (CD_3OD, 400 MHz) δ 7.79 (s, 1H), 3.93 (s, 2H), 3.37 (t, *J* = 5.0 Hz, 4H), 2.74 (t, *J* = 5.2, 4H), 2.45 (s, 3H); $^{13}C\{^1H\}$ NMR (CD_3OD, 100 MHz) δ 164.5, 138.9, 134.7, 131.7, 131.4, 128.9, 40.4, 26.7, 11.1. Anal. Calcd for $C_{13}H_{18}F_3N_3O_5S_3$: C, 34.74; H, 4.04; N, 9.35. Found: C, 34.97; H, 4.16; N, 8.96.

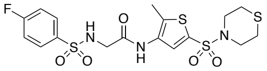

2-(4-fluorobenzenesulfonamido)-N-[2-methyl-5-(thiomorpholine-4-sulfonyl)thiophen-3-yl]acetamide (**3.7**)

Amine salt **81** (0.600g, 1.384 mmol) was dissolved in dry dichloromethane (2.15 mL) and dry TEA (0.425 mL, 3.045 mmol) and stirred at rt. 4-fluorobenzenesulfonyl chloride (0.296g, 1.523 mmol) was added and the mixture was stirred at rt for 24 h. The mixture was washed with water (3x 5 mL) followed by a 5% HCl solution. The organics were collected, dried over $MgSO_4$, filtered and concentrated. The crude mixture was purified by precipitation from dichloromethane

yielding a white powder (0.213g, 31.2%). mp = 177.2-180.3˚C; TLC R_f = 0.371 (1% MeOH/99% DCM); IR (ATR) 3301, 3259, 2959, 2915, 1665, 1352, 1324, 1166, 1141 cm^{-1}; 1H NMR (DMSO-d_6, 400 MHz) δ 7.82 (dd, *J* = 5.0, 8.5 Hz, 2H), 7.60 (s, 1H), 7.36 (t, *J* = 8.7 Hz, 2H), 3.63 (s, 2H), 3.19 (t, *J* = 4.4, 4H), 2.68 (t, *J* = 4.4 Hz, 4H), 2.31 (s, 3H); $^{13}C\{^1H\}$ NMR (DMSO-d_6, 100 MHz) δ.167.7, 138.5, 133.4, 133.2, 130.1, 130.0, 129.9, 129.3, 116.5, 116.3, 48.3, 26.8, 12.8; Anal. Calcd for $C_{17}H_{20}FN_3O_5S_4$: C, 41.37; H, 4.08; N, 8.51. Found: C, 41.66; H, 3.80; N, 8.87.

General Procedure for Sulfonamide Formation

The desired amine (2 eq) and 5-methyl-4-nitrothiophene-2-sulfonyl chloride (**3**) (1eq) was dissolved in 1,4-dioxane (1.0M) and heated to 60˚C. The mixture was stirred for 1 h at 60˚C, after which the reaction was cooled to rt and 20 mL of water was added. The mixture was extracted with DCM (3x20 mL), and the organics were dried over $MgSO_4$, filtered and concentrated. The crude mixture was purified via silica gel chromatography yielding the desired product.

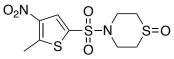

4-[(5-methyl-4-nitrothiophen-2-yl)sulfonyl]-1-thiomorpholin-1-one (**3.17**)

The crude mixture was purified via trituration from DCM yielding a white solid (0.93g, 59%). mp = 212.8-216.5˚C; TLC R_f = 0.40 (50% EA/50% hexanes); IR (ATR) 3114, 3000, 2942, 2862, 1546, 1505,1374, 1365, 1037 cm^{-1}; 1H NMR (MeOD, 400 MHz) δ 8.12 (s, 1H), 3.85 (d, *J* = 13.4 Hz, 2H), 3.42 (dt, *J* = 7.2, 13.7 Hz, 2H), 3.02-3.07 (m, 4H), 2.88 (s, 3H); $^{13}C\{^1H\}$ NMR

(MeOD, 100 MHz) δ 151.1, 144.3, 131.5, 128.9, 43.9, 37.9, 16.0.; Anal. Calcd for $C_9H_{12}N_2O_5S_3$: C, 33.32; H, 3.73; N, 8.64. Found: C, 33.30; H, 3.87; N, 8.55.

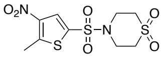

4-[(5-methyl-4-nitrothiophen-2-yl)sulfonyl]-1-thiomorpholin-1,1-dione (**3.18**)

The crude oil was purified via silica gel column chromatography using a 50% hexanes:50% ethyl acetate eluent yielding an off-white solid (1.34g, 71%). mp = 247.9-248.8˚C; TLC R_f = 0.46 (50% EA/50% hexanes); IR (ATR) 3111, 2988, 2933, 1540, 1504, 1365, 1337, 1300, 1124 cm^{-1}; 1H NMR (DMSO, 400 MHz) δ 8.18 (s, 1H), 3.57-3.62 (m, 4H), 3.33-3.67 (m, 4H), 2.83 (s, 3H); $^{13}C\{^1H\}$ NMR (DMSO, 100 MHz) δ 151.2, 144.3, 131.9, 129.1, 50.5, 45.6, 16.0; Anal. Calcd for $C_9H_{12}N_2O_6S_3$: C, 31.76; H, 3.55; N, 8.23. Found: C, 31.65; H, 3.71; N, 7.87.

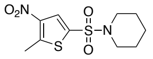

1-[(5-methyl-4-nitrothiophen-2-yl)sulfonyl]piperidine (**3.19**)

The crude oil was purified via silica gel column chromatography using a 70% hexanes:30% ethyl acetate eluent yielding a tan solid (0.88g, 73%). mp = 131.2-134.7˚C; TLC R_f = 0.56 (30% EA/70% hexanes); IR (ATR) 3107, 2952, 2919, 2860, 1540, 1499, 1313, 1144, 929, 568 cm^{-1}; 1H NMR ($CDCl_3$, 400 MHz) δ 7.93 (s, 1H), 3.10 (t, *J* = 5.6 Hz, 4H), 2.85 (s, 3H), 1.70 (quin, *J* = 5.8 Hz, 4H), 1.50 (quin, *J* = 5.8 Hz, 2H); $^{13}C\{^1H\}$ NMR ($CDCl_3$, 100 MHz) δ 148.9, 143.7, 132.8, 127.7, 47.02, 25.03, 23.3, 15.9.; Anal. Calcd for $C_{10}H_{14}N_2O_4S_2$: C, 41.37; H, 4.86; N, 9.65. Found: C, 41.18; H, 4.54; N, 9.80.

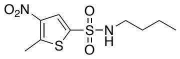

N-butyl-5-methyl-4-nitrothiophenene-2-sulfonamide (**3.20**)

The crude oil was purified via silica gel column chromatography using a 70% hexanes:30% ethyl acetate eluent yielding a tan solid (0.85g, 72%). mp = 69.4-71.7˚C; TLC $R_f = 0.56$ (30% EA/70% hexanes); IR (ATR) 3278, 2958, 2930, 2871, 1547, 1505, 1315, 1145 cm^{-1}; 1H NMR ($CDCl_3$, 400 MHz) δ 8.02 (s, 1H), 4.56 (bs, 1H), 3.09 (q, *J* = 6.5 Hz, 2H), 2.85 (s, 3H), 1.53 (quin, *J* = 7.0 Hz, 2H), 1.35 (sex, *J* = 7.0 Hz, 2H), 0.91 (t, *J* = 7.4 Hz, 3H); $^{13}C\{^1H\}$ NMR ($CDCl_3$, 100 MHz) δ 149.0, 143.3, 136.8, 127.8, 43.3, 31.6, 19.7, 15.9, 13.5; Anal. Calcd for $C_9H_{14}N_2O_4S_2$: C, 38.84; H, 5.07; N, 10.06. Found: C, 39.15; H, 4.73; N, 9.89.

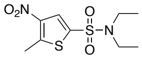

N,N-diethyl-5-methyl-4-nitrothiophenene-2-sulfonamide (**3.21**)

The crude oil was purified via silica gel column chromatography using a 70% hexanes:30% ethyl acetate eluent yielding a yellow solid (0.57g, 41%). mp = 70.3-72.1˚C; TLC $R_f = 0.50$ (30% EA/70% hexanes); IR (ATR) 3277, 2958, 2929, 2870, 2360, 2342, 1546, 1506, 1315, 1145 cm^{-1}; 1H NMR ($CDCl_3$, 400 MHz) δ 7.95 (s, 1H), 3.28 (q, *J* = 7.3, 4H), 2.84 (s, 3H), 1.22 (t, *J* = 6.9 Hz, 6H); $^{13}C\{^1H\}$ NMR ($CDCl_3$, 100 MHz) δ 148.4, 143.4, 136.8, 127.0, 42.8, 15.9, 14.3; Anal. Calcd for $C_7H_{14}N_2O_4S_2$: C, 38.84; H, 5.07; N, 10.06. Found: C, 38.74; H, 5.04; N, 9.81.

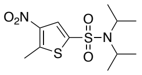

5-methyl-4-nitro-N,N-bis(propan-2-yl)thiophenene-2-sulfonamide (**3.22**)

The crude oil was purified via silica gel column chromatography using a 70% hexanes:30% ethyl acetate eluent yielding an orange solid (0.68g, 45%). mp = 109.3.3-109.9˚C; TLC $R_f = 0.69$ (30% EA/70% hexanes); IR (ATR) 3118, 2983, 2935, 2876 1544, 1502, 1335, 1131 cm^{-1}; 1H NMR ($CDCl_3$, 400 MHz) δ 7.97 (s, 1H), 3.79 (sep, *J* = 6.9, 2H), 2.83 (s, 3H), 1.32 (d, *J* = 7.0, 12H); $^{13}C\{^1H\}$ NMR ($CDCl_3$, 100 MHz) δ 148.1, 143.0, 139.9, 127.1, 49.5, 21.9, 15.9; Anal. Calcd for $C_{11}H_{18}N_2O_4S_2$: C, 43.12; H, 5.92; N, 9.14. Found: C, 43.12; H, 5.83; N, 9.30.

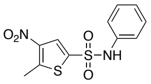

5-methyl-4-nitro-N-phenylthiophenene-2-sulfonamide (**3.23**)

The crude oil was purified via silica gel column chromatography using a 70% hexanes:30% ethyl acetate eluent yielding an orange solid (0.99g, 67%). mp = 141.3-143.9°C; TLC R_f = 0.42 (30% EA/70% hexanes); IR (ATR) 3243, 3107, 2968, 2939, 2874, 1540, 1501, 1366, 1314, 1143 cm^{-1}; 1H NMR ($CDCl_3$, 400 MHz) δ 7.94 (s. 1H), 7.34 (t, *J* = 7.5 Hz, 2H), 7.23 (t, *J* = 7.4 Hz, 1H), 7.16 (d, *J* = 7.5 Hz, 2H), 2.78 (s, 3H); $^{13}C\{^1H\}$ NMR ($CDCl_3$, 100 MHz) 149.7, 143.3, 135.2, 134.9, 129.8, 128.7, 126.6, 122.1, 16.0; Anal. Calcd for $C_{11}H_{10}N_2O_4S_2$: C, 44.29; H, 3.38; N, 9.39. Found: C, 43.93; H, 3.01; N, 9.04.

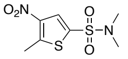

N,N,5-trimethyl-4-nitrothiophenene-2-sulfonamide (**3.24**)

The crude oil was purified via silica gel column chromatography using a 70% hexanes:30% ethyl acetate eluent yielding a light-brown solid (0.71g, 57%). mp = 133.2-135.4°C; TLC R_f = 0.37 (30% EA/70% hexanes); IR (ATR) 3100, 2980, 2884, 1548, 1506, 1340, 1319, 1152, 1139 cm^{-1}; 1H NMR ($CDCl_3$, 400 MHz) δ 7.96 (s, 1H), 2.86 (s, 3H), 2.82 (s, 6H); $^{13}C\{^1H\}$ NMR ($CDCl_3$, 100 MHz) 149.0, 143.8, 131.9, 127.9, 37.9, 15.9; Anal. Calcd for $C_7H_{10}N_2O_4S_2$: C, 33.59; H, 4.03; N, 11.19. Found: C, 33.50; H, 3.78; N, 10.82.

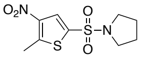

1-[(5-methyl-4-nitrothiophen-2-yl)sulfonyl]pyrrolidine (**3.25**)

The crude oil was purified via silica gel column chromatography using a 70% hexanes:30% ethyl acetate eluent yielding a light-orange solid (0.70g, 51%). mp = 131.6-133.7˚C; TLC R_f = 0.42 (30% EA/70% hexanes); IR (ATR) 3110, 2959, 2886, 1543, 1499, 1341, 1315, 1147cm^{-1}; 1H NMR ($CDCl_3$, 400 MHz) δ 8.02 (s, 1H), 3.35 (m, 4H), 2.88 (s, 3H), 1.89 (m, 4H); $^{13}C\{^1H\}$ NMR ($CDCl_3$, 100 MHz) 148.7, 143.6, 133.2, 127.7, 48.3, 25.4, 15.9; Anal. Calcd for $C_9H_{12}N_2O_4S_2$: C, 39.12; H, 4.38; N, 10.14. Found: C, 39.37; H, 4.71; N, 10.43.

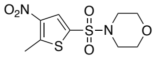

4-[(5-methyl-4-nitrothiophen-2-yl)sulfonyl]morpholine (**3.26**)

The crude mixture was purified via silica gel chromatography in 70% hexanes:30% ethyl acetate yielding an off-white solid (0.220g, 73%). mp = 149.1-152.6˚C; TLC R_f = 0.28 (30% EA/70% hexanes); IR (ATR) 3104, 2981, 2912, 2860, 1540, 1499, 1348, 1219, 1164, 1110, 568 cm^{-1}; 1H NMR ($CDCl_3$, 400 MHz) δ 7.97 (s, 1H), 3.80 (t, J = 4.5 Hz, 4H), 3.12 (t, J = 4.5, 4H), 2.87 (s, 3H); $^{13}C\{^1H\}$ NMR ($CDCl_3$, 100 MHz) δ 149.7, 143.8, 131.3, 128.5, 65.9, 45.9, 16.0.; Anal. Calcd for $C_9H_{12}N_2O_5S_2$: C, 36.98; H, 4.14; N, 9.58. Found: C, 36.72; H, 4.22; N, 9.23.

General Procedure for Amine Formation

The desired nitrothiophene (1 eq) was dissolved in acetic acid (0.3M) and iron power (5 eq) was added. The mixture was heated to 60˚C and stirred for 1.5 hr followed by removal of acetic acid via rotary evaporation. The residue was dissolved in ethyl acetate and the iron powder was filtered away. The solution was washed with saturated $NaHCO_3$ until a pH of 8 was reached. The organics were dried over Na_2SO_4, filtered, and concentrated. The crude product was purified via silica gel chromatography yielding the desired amine.

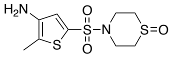

4-[(4-amino-5-methylthiophen-2-yl)sulfonyl]-1-thiomorpholin-1-one (**3.27**)

The crude oil was purified via silica gel column chromatography using a 50% dichloromethane: 50% methanol eluent yielding a yellow solid (0.161g, 99%). mp = 151.1-154.7˚C; TLC R_f = 0.54 (50% DCM/50% MeOH); IR (ATR) 3386, 3322, 3220, 2917, 2858, 1334, 1153, 1017 cm^{-1}; 1H NMR (CD_3OD, 400 MHz) δ 7.11 (s, 1H), 3.69-3.73 (m, 2H), 3.28-3.34 (m, 2H), 2.97-3.00 (m, 4H), 2.27 (s, 3H); $^{13}C\{^1H\}$ NMR (CD_3OD, 100 MHz) 142.8, 128.7, 126.3, 120.7, 44.0,36.7, 10.16; Anal. Calcd for $C_9H_{14}N_2O_3S_3$: C, 36.72; H, 4.79; N, 9.52. Found: C, 36.43; H, 4.73; N, 9.32.

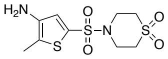

4-[(4-amino-5-methylthiophen-2-yl)sulfonyl]-1-thiomorpholine-1,1-dione (**3.28**)

The crude oil was purified via silica gel column chromatography using a 50% hexanes:50% ethyl acetate eluent yielding a yellow solid (0.237, 19%). mp = 194.3-199.4˚C; TLC R_f = 0.11 (50% EA/50% hexanes); IR (ATR) 3448, 3371, 3071, 3003, 2930, 2852, 1627, 1561, 1351, 1296, 1124, 1115 cm^{-1}; 1H NMR (CD_3OD, 400 MHz) δ 7.13 (s, 1H), 3.59-3.61 (m, 4H), 3.22 (t, *J* = 5.4 Hz, 4H), 2.29 (s, 3H); $^{13}C\{^1H\}$NMR (CD_3OD, 100 MHz) 142.8, 129.3, 126.4, 121.0, 50.4, 45.1, 10.2; Anal. Calcd for $C_9H_{14}N_2O_4S_3$: C, 34.83; H, 4.55; N, 9.03. Found: C, 34.99; H, 4.19; N, 8.86

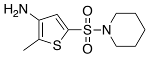

2-methyl-5-(piperidine-1-sulfonyl)thiophen-3-amine (**3.29**)

The crude oil was purified via silica gel column chromatography using a 50% hexanes:50% ethyl acetate eluent yielding a tan solid (0.63g, 70%). mp = 96.1-101.2°C; TLC R_f = 0.30 (50% EA/50% hexanes); IR (ATR) 3426, 3349, 2979, 2949, 2851, 1618, 1566, 1543, 1334, 1322, 572 cm^{-1}; 1H NMR (CDCl$_3$, 400 MHz) δ 7.02 (s, 1H), 3.75 (bs, 2H), 3.01 (t, *J* = 5.5 Hz, 4H), 2.29 (s, 3H), 1.67 (quin, *J* = 5.8 Hz, 4H), 1.45 (quin, *J* = 6.0 Hz, 2H); ^{13}C{^{1}H} NMR (CDCl$_3$, 100 MHz) 139.5, 130.3, 125.6, 121.9, 47.0, 25.1, 23.5, 11.8; Anal. Calcd for $C_{10}H_{16}N_2O_2S_2$: C, 46.13; H, 6.19; N, 10.76. Found: C, 46.00; H, 6.45; N, 10.66.

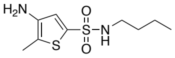

4-amino-N-butyl-5-methylthiophene-2-sulfonamide (**3.30**)

The crude oil was purified via silica gel column chromatography using a 50% hexanes:50% ethyl acetate eluent yielding an off-white solid (0.384g, 50.6%). mp = 65.3-66.9°C; TLC R_f = 0.325 (50% EA/50% hexanes); IR (ATR) 3371, 3313, 3094, 2967, 2869, 1449, 1316,1148, 1135 cm^{-1}; 1H NMR (CDCl$_3$, 400 MHz) δ 7.06 (s, 1H), 4.86 (t, *J* =5.9 Hz, 1H), 3.65 (bs, 2H), 2.96 (q, *J* = 6.8Hz, 2H), 2.23 (s, 3H), 1.45 (p, *J* = 7.1 Hz, 2H), 1.29 (sext, *J* = 7.2 Hz, 2H), 0.86 (t, *J* = 7.4 Hz, 3H); ^{13}C{^{1}H} NMR (CDCl$_3$, 100 MHz) 140.8, 133.9, 125.6, 120.3, 43.2, 31.4, 19.8, 13.6, 11.7; Anal. Calcd for $C_9H_{16}N_2O_2S_2$: C, 43.53; H, 6.49; N, 11.28. Found: C, 43.63; H, 6.79; N, 11.04.

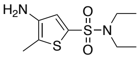

4-amino-N,N-diethyl-5-methylthiophene-2-sulfonamide (**3.31**)

The crude oil was purified via silica gel column chromatography using a 50% hexanes:50% ethyl acetate eluent yielding an orange solid (0.150g, 30%). mp = 71.9-74.3˚C; TLC R_f = 0.26 (50% EA/50% hexanes); IR (ATR) 3434, 3356, 2982, 2937, 1320, 1133 cm^{-1}; 1H NMR ($CDCl_3$, 400 MHz) δ 6.98 (s, 1H), 3.52 (bs, 2H), 3.16 (q, *J* = 7.2 Hz, 4H), 2.20 (s, 3H), 1.13 (t, *J* = 7.2 Hz, 6H); $^{13}C\{^1H\}$NMR ($CDCl_3$, 100 MHz) 140.8,133.7, 125.1, 119.5, 42.7, 14.3, 11.6; Anal. Calcd for $C_9H_{16}N_2O_2S_2$: C, 43.53; H, 6.49; N, 11.28. Found: C, 43.18; H, 6.19; N, 11.48.

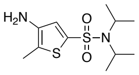

4-amino-5-methyl-N,N-bis(propan-2-yl)thiophene-2-sulfonamide (**3.32**)

The crude oil was purified via silica gel column chromatography using a 50% hexanes:50% ethyl acetate eluent yielding an brown solid (0.290g, 47%). mp = 161.3-163.6˚C; TLC R_f = 0.30 (50% EA/50% hexanes); IR (ATR) 3438, 3364, 2973, 2933, 1311, 1131, 1118 cm^{-1}; 1H NMR ($CDCl_3$, 400 MHz) δ 7.16 (s, 1H), 3.76 (hept, *J* = 6.8 Hz, 2H), 2.33 (s, 3H), 1.31 (d, *J* = 6.9 Hz, 12H); $^{13}C\{^1H\}$NMR ($CDCl_3$, 100 MHz) 138.5, 136.9, 125.5, 122.8, 49.0, 21.9, 11.9; Anal. Calcd for $C_{11}H_{20}N_2O_2S_2$: C, 47.80; H, 7.29; N, 10.13. Found: C, 48.04; H, 7.37; N, 10.03.

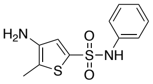

4-amino-5-methyl-N-phenylthiophene-2-sulfonamide (**3.33**)

The crude oil was purified via silica gel column chromatography using a 50% hexanes:50% ethyl acetate eluent yielding a light-orange solid (0.370g, 42%). mp = 141.3-143.6˚C; TLC R_f = 0.46 (50% EA/50% hexanes); IR (ATR) 3386, 3321, 3113, 3069, 2970, 2882, 2846, 2774, 1598, 1495, 1340, 1143 cm^{-1}; 1H NMR (CD_3OD, 400 MHz) δ 7.24 (t, *J* =7.3 Hz, 2H), 7.13 (d, *J* = 7.6 Hz, 2H), 7.08 (t, *J* = 7.1 Hz, 1H), 6.97 (s, 1H), 2.18 (s, 3H); $^{13}C\{^1H\}$NMR (CD_3OD, 100 MHz) 141.5, 137.6, 133.1, 128.7, 126.0, 124.4, 120.9, 120.3, 10.1; Anal. Calcd for $C_{11}H_{12}N_2O_2S_2$: C, 49.23; H, 4.51; N, 10.44. Found: C, 49.05; H, 4.27; N, 10.06

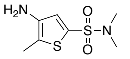

4-amino-N,N,5-trimethylthiophene-2-sulfonamide (**3.34**)

The crude oil was purified via silica gel column chromatography using a 50% hexanes:50% ethyl acetate eluent yielding a light-yellow solid (0.240g, 39%). mp = 143.9-146.2˚C; TLC R_f = 0.46 (50% EA/50% hexanes); IR (ATR) 3454, 3372, 3236, 3063, 2975, 2908, 1630, 1563, 1324, 1138 cm^{-1}; 1H NMR (CD_3OD, 400 MHz) δ 7.06 (s, 1H), 2.69 (s, 6H), 2.27 (s, 3H); $^{13}C\{^1H\}$NMR (CD_3OD, 100 MHz) 142.3, 127.8, 126.2, 120.1, 37.0, 10.1; Anal. Calcd for $C_7H_{12}N_2O_2S_2$: C, 38.16; H, 5.49; N, 12.72. Found: C, 38.09; H, 5.76; N, 12.85

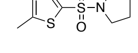

2-methyl-5-(pyrrolidine-1-sulfonyl)thiophen-3-amine (**3.35**)

The crude oil was purified via silica gel column chromatography using a 50% hexanes:50% ethyl acetate eluent yielding an tan solid (0.410g, 58%). mp = 151.8-154.7˚C; TLC R_f = 0.22 (50% EA/50% hexanes); IR (ATR) 3452, 3367, 2980, 2863, 1627, 1569, 1326, 1144 cm^{-1}; 1H NMR (CD_3OD, 400 MHz) δ 7.09 (s, 3H), 3.24 (t, *J* = 6.6 Hz 4H), 2.27 (s, 3H), 1.77 (pent, *J* = 6.8 Hz, 4H); $^{13}C\{^1H\}$NMR ($CDCl_3$, 100 MHz) 136.2, 131.4, 129.2, 126.0, 48.2, 25.4, 12.1; Anal. Calcd for $C_9H_{14}N_2O_2S_2$: C, 43.88; H, 5.73; N, 11.34. Found: C, 43.60; H, 5.36; N, 11.20.

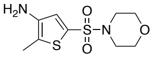

2-methyl-5-(morpholine-4-sulfonyl)thiophen-3-amine (**3.36**)

The crude oil was purified via silica gel column chromatography using a 3% MeOH:97% $CHCl_3$ eluent yielding an orange solid (0.800g, 89%).TLC $R_f = 0.22$ (3% MeOH/97% $CHCl_3$); 1H NMR ($CDCl_3$, 400 MHz) δ 7.00 (s, 1H), 3.76 (t, *J* = 4.7 Hz 4H), 3.45 (bs, 2H), 3.04 (t, *J* = 4.8 Hz, 4H), 2.27 (s, 3H); $^{13}C\{^1H\}$NMR ($CDCl_3$, 100 MHz) 141.2, 128.5, 126.0, 121.1, 66.1, 46.0, 11.7.

General Procedure for Amide Formation

The desired boc-protected amino acid (1.2 eq), thioamine (1 eq), HATU (2eq) and DIPEA (2 eq) were dissolved in dry DMF (0.08M) under argon. The mixture was stirred for 24 h at rt. The reaction was diluted with ethyl acetate, washed with NH_4Cl (3x15 mL) and brine. The organics were dried over $MgSO_4$, filtered and concentrated. The crude mixture was purified via silica gel chromatography yielding the desired amide product.

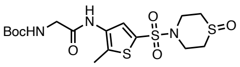

tert-butyl-N-[({2-methyl-5-[(1-oxo-1-thiomorpholin-4-yl)sulfonyl]thiophen-3-yl}carbamoyl) methyl]carbamate (**3.37**)

The crude mixture was purified via silica gel column chromatography using an 100% EA eluent yielding a clear oil (0.200g, 73%). TLC $R_f = 0.17$ (100% EA); IR (ATR) 3283, 2979, 2929, 2861, 1683, 1150, 1021 cm^{-1}; 1H NMR ($CDCl_3$, 400 MHz) δ 8.55 (bs, 1H), 8.04 (s, 1H), 5.25

(bs, 1H), 3.89 (d, *J* = 4.5 Hz, 2H), 3.80 (d, *J* = 13.3 Hz, 2H), 3.45 (t, *J* = 11.5 Hz, 2H), 2.94 (d, *J* = 13.9 Hz, 2H), 2.79-2.86 (m, 2H), 2.38 (s, 3H), 1.49 (s, 9H); $^{13}C\{^1H\}$ NMR (CD_3OD, 100 MHz) 171.2, 169.6, 136.0, 132.5, 130.3, 130.1, 79.4, 44.0, 43.3, 36.7, 27.3, 11.2.; Anal. Calcd for $C_{16}H_{25}N_3O_6S_3$: C, 42.56; H, 5.58; N, 9.34. Found: C, 42.28; H, 5.63 N, 9.70.

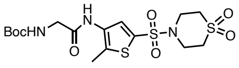

tert-butyl-N-[({5-[(1,1-dioxo-1-thiomorpholine-4-yl)sulfonyl]-2-methylthiophen-3-yl} carbamoyl)methyl]carbamate (**3.38**)

The crude oil was purified via silica gel column chromatography using a 70% hexanes:30% ethyl acetate eluent yielding a light-yellow powder (0.140, 39%). mp = 187.1-190.3°C; TLC R_f = 0.51 (30% EA/70% hexanes); IR (ATR) 3273, 2987, 2928, 2395, 1689, 1670, 1308, 1150, 1125 cm^{-1}; 1H NMR (CD_3OD, 400 MHz) δ 7.74 (s, 1H), 3.88 (s, 2H), 3.65 (bs, 4H), 3.23 (t, *J* = 5.4 Hz, 4H), 2.42 (s, 3H), 1.47 (s, 9H); $^{13}C\{^1H\}$NMR (CD_3OD, 100 MHz) 169.8, 157.2, 136.5, 132.5, 130.8, 130.4, 79.4, 50.5, 45.1, 43.3, 27.3, 11.2.; Anal. Calcd for $C_{16}H_{25}N_3O_7S_3$: C, 41.10; H, 5.39; N, 8.99. Found: C, 39.89; H, 5.30; N, 9.34

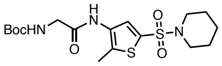

tert-butyl-N-[({2-methyl-5-(piperidine-1-sulfonyl)thiophen-3-yl}carbamoyl) methyl]carbamate (**3.39**)

The crude oil was purified via silica gel column chromatography using a 50% hexanes:50% ethyl acetate eluent yielding a yellow solid (0.220g, 47%). mp = 156.1-160.3°C; TLC R_f = 0.30 (50% EA/50% hexanes); IR (ATR) 3321, 2935, 2856, 1685, 1676, 1159, 1142 cm^{-1}; 1H NMR (Acetone-*d$_6$*, 400 MHz) δ 9.01 (s, 1H), 7.82 (s, 1H), 6.37 (s, 1H), 3.90 (d, *J* = 5.8 Hz 2H), 3.00

(t, *J* = 5.4 Hz, 4H), 2.40 (s, 3H), 1.65 (p, *J* = 5.8 Hz, 4H), 1.44-1.49 (m, 11H); $^{13}C\{^{1}H\}$NMR (Acetone-d_6, 100 MHz) 167.8, 156.3, 133.1, 132.0, 130.5, 128.8, 78.7, 46.9, 44.1, 27.7, 25.0, 23.1, 11.6; Anal. Calcd for $C_{17}H_{27}N_3O_5S_2$: C, 48.90; H, 6.52; N, 10.06. Found: C, 48.63; H, 6.29; N, 10.03.

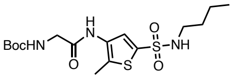

tert-butyl-N-[({5-(butylsulfamoyl)-2-methylthiophen-3-yl}carbamoyl)methyl]carbamate (**3.40**)

The crude oil was purified via silica gel column chromatography using a 50% hexanes:50% ethyl acetate eluent yielding an off-white solid (0.320g, 70%). mp = 64.6-66.7˚C; TLC R_f = 0.33 (50% EA/50% hexanes); IR (ATR) 3657, 3217, 2980, 1676, 1505, 1146 cm^{-1}; 1H NMR ($CDCl_3$, 400 MHz) δ 8.44 (bs, 1H), 7.83 (bs, 1H), 7.25 (s, 1H), 5.44 (bs, 1H), 3.91 (s, 2H), 3.01 (t, *J* =6.6 Hz, 2H), 2.33 (s, 3H), 1.43-1.53 (m, 11H), 1.32 (sext, *J* = 7.0 Hz, 2H), 0.88 (t, *J* = 7.3 Hz, 3H); $^{13}C\{^{1}H\}$ NMR ($CDCl_3$, 100 MHz) 167.9, 156.9, 135.2, 131.7, 128.0, 128.0, 81.0, 45.3, 43.3, 31.5, 28.3, 19.7, 13.6, 12.4; Anal. Calcd for $C_9H_{27}N_3O_5S_2$: C, 47.39; H, 6.71; N, 10.36. Found: C, 47.43; H, 6.40; N, 10.49.

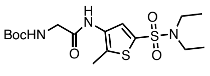

tert-butyl-N-[({5-(diethylsulfamoyl)-2-methylthiophen-3-yl}carbamoyl)methyl]carbamate (**3.41**)

The crude oil was purified via silica gel column chromatography using a 50% hexanes:50% ethyl acetate eluent yielding an orange solid (0.120g, 49%). mp = 46.7-49.1˚C; TLC R_f = 0.31 (50% EA/50% hexanes); IR (ATR) 3309, 2978, 2935, 1679, 1501, 1140, 1015 cm^{-1}; 1H NMR (CD_3OD, 400 MHz) δ 7.64 (s, 1H), 3.86 (bs, 2H), 3.22 (q, *J* = 7.4 Hz, 4H), 2.38 (s, 3H), 1.47 (s, 9H), 1.17 (t, *J* = 7.2 Hz, 6H); $^{13}C\{^{1}H\}$NMR (CD_3OD, 100 MHz) 169.7, 157.2, 134.6, 134.4, 131.8, 128.9, 79.4, 43.3, 42.6, 27.3, 13.4, 11.1; Anal. Calcd for $C_{16}H_{27}N_3O_5S_2$: C, 47.39; H, 6.71; N, 10.36. Found: C, 47.58; H, 6.42; N, 10.34.

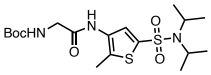

tert-butyl-N-[({5-[bis(propan-2-yl)sulfamoyl]-2-methylthiophen-3-yl}carbamoyl)methyl] carbamate (**3.42**)

The crude oil was purified via silica gel column chromatography using a 50% hexanes:50% ethyl acetate eluent yielding an brownish solid (0.220g, 74%). mp = 66.3-69.1˚C; TLC $R_f = 0.26$ (50% EA/50% hexanes); IR (ATR) 3305, 2975, 2935, 1680, 1505, 1166, 1133 cm^{-1}; 1H NMR (CD_3OD, 400 MHz) δ 7.65 (s, 1H), 3.86 (s, 2H), 3.78 (hept, *J* = 6.7 Hz, 2H), 2.37 (s, 3H), 1.47 (s, 9H), 1.28 (d, *J* = 6.7 Hz, 12H); $^{13}C\{^1H\}$NMR (CD_3OD, 100 MHz) 171.0, 158.6, 139.2, 125.6, 132.8, 130.5, 80.8, 50.3, 44.7, 28.7, 22.1, 12.5.; Anal. Calcd for $C_{18}H_{31}N_3O_5S_2$: C, 49.86; H, 7.21; N, 9.69. Found: C, 49.91; H, 7.15; N, 9.96.

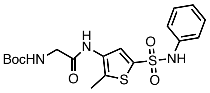

tert-butyl-N-[({2-methyl-5-(phenylsulfamoyl)thiophen-3-yl}carbamoyl)methyl] carbamate (**3.43**)

The crude oil was purified via silica gel column chromatography using a 50% hexanes:50% ethyl acetate eluent yielding a off-white solid (0.173g, 30%). mp = 83.7-87.6˚C; TLC $R_f = 0.30$ (50% EA/50% hexanes); IR (ATR) 3270, 2978, 2933, 1676, 1496, 1146 cm^{-1}; 1H NMR (CD_3OD, 400 MHz) δ 7.59 (s, 1H), 7.24 (t, *J* =8.4 Hz, 2H), 7.14 (d, *J* = 7.4 Hz, 2H), 7.08 (t, *J* = 7.4 Hz, 1H), 3.82 (s, 2H), 2.30 (s, 3H), 1.46 (s, 9H); $^{13}C\{^1H\}$NMR (CD_3OD, 100 MHz) 169.5, 157.2, 137.4, 135.2, 134.5, 131.5, 129.4, 128.7, 124.6, 121.0, 79.4, 43.2, 27.3, 11.2.; Anal. Calcd for $C_{18}H_{23}N_3O_5S_2$: C, 50.81; H, 5.45; N, 9.88. Found: C, 50.85; H, 5.78; N, 9.51

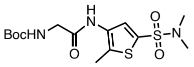

tert-butyl-N-[({5-(dimethylsulfamoyl)-2-methylthiophen-3-yl}carbamoyl)methyl] carbamate **(3.44)**

The crude oil was purified via silica gel column chromatography using a 50% hexanes:50% ethyl acetate eluent yielding an orange solid (0.230g, 67%). mp = 87.7-92.9°C; TLC R_f = 0.20 (50% EA/50% hexanes); IR (ATR) 3314, 2974, 2928, 1677, 1502, 1341, 1142 cm^{-1}; 1H NMR (CD_3OD, 400 MHz) δ 7.64 (s, 1H), 3.87 (bs, 2H), 2.72 (s, 6H), 2.40 (s, 3H), 1.47 (s, 9H); $^{13}C\{^1H\}$NMR (CD_3OD, 100 MHz) 169.7, 165.3, 135.6, 132.2, 129.8, 129.3, 78.1, 43.3, 36.9, 27.3, 11.2.; Anal. Calcd for $C_{14}H_{23}N_3O_5S_2$: C, 44.55; H, 6.14; N, 11.13. Found: C, 44.67; H, 6.31; N, 10.88

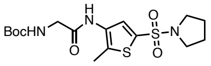

tert-butyl-N-[({2-methyl-5-(pyrrolidine-1-sulfonyl)thiophen-3-yl}carbamoyl)methyl] carbamate **(3.45)**

The crude oil was purified via silica gel column chromatography using a 50% hexanes:50% ethyl acetate eluent yielding an tan solid (0.280g, 64%). mp = 62.5-66.8°C; TLC R_f = 0.24 (50% EA/50% hexanes); IR (ATR) 3317, 2975, 2930, 2873, 1679, 1503, 1344, 1147 cm^{-1}; 1H NMR (CD_3OD, 400 MHz) δ 7.67 (s, 1H), 3.87 (s, 2H), 3.24-3.28 (m, 4H), 2.39 (s, 3H), 1.77-1.80 (m, 4H), 1.47 (s, 9H); $^{13}C\{^1H\}$NMR ($CDCl_3$, 100 MHz) 171.1, 158.6, 136.0, 135.8, 133.2, 130.3, 80.8, 44.7, 44.0, 28.7, 14.8, 12.5; Anal. Calcd for $C_{16}H_{25}N_3O_5S_2$: C, 47.63; H, 6.25; N, 10.41. Found: C, 47.30; H, 5.93; N, 10.14.

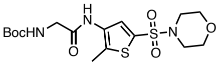

tert-butyl-N-[({2-methyl-5-(morpholine-4-sulfonyl)thiophen-3-yl}carbamoyl)methyl] carbamate (**3.46**)

The crude oil was purified via silica gel column chromatography using a 50% EA/ 50% hexanes eluent yielding an off-white solid (0.370g, 86%). mp = 124.4-128.3˚C; TLC R_f = 0.21 (50% EA/ 50% hexanes); IR (ATR) 3623, 3313, 2976, 2924, 2859, 1681, 1504, 1348, 1152, 941 cm^{-1}; 1H NMR ($CDCl_3$, 400 MHz) δ 8.48 (bs, 1H), 7.92 (s, 1H), 5.27 (bs, 1H), 3.91 (d, *J* = 4.2 Hz, 2H), 3.77 (t, *J* = 4.2 Hz 4H), 3.06 (t, *J* = 4.2 Hz, 4H), 2.38 (s, 3H), 1.49 (s, 9H); $^{13}C\{^1H\}$NMR ($CDCl_3$, 100 MHz) 167.9, 156.8, 132.7, 132.1, 130.8, 128.5, 80.8, 47.8, 45.0, 28.2, 27.1, 12.3.; Anal. Calcd for $C_{16}H_{25}N_3O_6S_2$: C, 45.81; H, 6.01; N, 10.02. Found: C, 45.61; H, 6.04; N, 9.73.

General Procedure for Amine Salt Formation

To a solution of Boc-protected amide (1 equiv) dissolved in methanol (0.3 M) was added TFA. The reaction mixture was stirred at rt for 30 min and the mixture was concentrated under vacuum. The recovered solid was used without further purification.

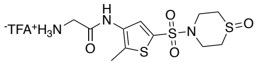

2-aminotrifluoroacetate-N-[2-methyl-5-[(1-oxo-1-thiomorpholin-4-yl)sulfonyl]thiophen-3-yl]acetamide (**3.47**)

Boc protected amine **3.37** (0.200 g, 0.443 mmol) was dissolved in TFA and stirred at rt for 0.5 h. The solvent was removed under vacuo and a pure white solid was recovered (0.180 g, 87%). mp = 188.4-192.5°C; IR (ATR) 3218, 2980, 2651, 1702, 1673, 1591, 1407, 1204, 1154, 1134, 1018 cm^{-1}; 1H NMR (CD_3OD, 400 MHz) δ 7.87 (s, 1H), 3.91 (s, 2H), 3.77 (d, *J* = 13.1 Hz, 2H), 3.31-3.36 (m, 2H), 3.00 (bs, 4H), 2.44 (s, 3H); $^{13}C\{^{1}H\}$ NMR (CD_3OD, 100 MHz) 164.4, 135.1, 132.0, 130.6, 129.3, 43.9, 40.4, 36.5, 11.2.; Anal. Calcd for $C_{13}H_{18}F_3N_3O_6S_3$: C, 33.54; H, 3.90; N, 9.03. Found: C, 33.85; H, 4.22 N, 8.98.

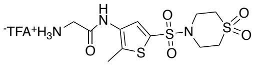

2-aminotrifluoroacetate-N-[1,1-dioxo-1-thiomorpholine-4-yl)sulfonyl)sulfonyl]thiophen-3-yl]acetamide (**3.48**)

Boc protected amine **3.38** (0.140 g, 0.299 mmol) was dissolved in TFA and stirred at rt for 0.5 h. The solvent was removed under vacuo and a pure off-white solid was recovered (0.143 g, 99%). mp = 214.7-218.4°C; IR (ATR) 3313, 3182, 3004, 1783, 1679, 1188, 1143, 1115, 700 cm^{-1}; 1H NMR (CD_3OD, 400 MHz) δ 7.87 (s, 1H), 3.91 (s, 2H), 3.65 (bs, 4H), 3.24 (t, *J* = 5.6 Hz, 4H), 2.45 (s, 3H); $^{13}C\{^{1}H\}$ NMR (CD_3OD, 100 MHz) 164.5, 135.4, 132.0, 131.3, 129.4, 50.4, 45.1, 40.4, 11.2.; Anal. Calcd for $C_{13}H_{18}F_3N_3O_7S_3$: C, 32.43; H, 3.77; N, 8.73. Found: C, 32.61; H, 4.08 N, 8.42.

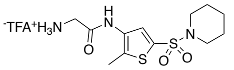

2-aminotrifluoroacetate-N-[2-methyl-5-(piperidine-1-sulfonyl)thiophen-3-yl]acetamide (**3.49**)

Boc protected amine **3.39** was dissolved in TFA and stirred at rt for 0.5 h. The solvent was removed under vacuo and a pure beige solid was recovered (0.220g, 94%). mp = 155.4-157.0°C;

IR (ATR) 3264, 3152, 2935, 2855, 2605, 1666, 1143, 1119 cm^{-1}; 1H NMR (CD$_3$OD, 400 MHz) δ 7.73 (s, 1H), 3.91 (s, 2H), 3.01 (t, *J* = 5.1 Hz, 4H), 2.42 (s, 3H), 1.66 (p, *J* = 5.3 Hz, 4H), 1.44-1.40 (m, 2H); ^{13}C{^{1}H}NMR (CD$_3$OD, 100 MHz) 164.5, 134.4, 131.6, 130.9, 128.9, 46.8, 40.4, 24.9, 23.1, 11.1.; Anal. Calcd for $C_{14}H_{20}F_3N_3O_5S_2$: C, 38.97; H, 4.67; N, 9.74. Found: C, 39.28; H, 4.69; N, 10.05.

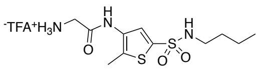

2-aminotrifluoroacetate-N-[5-(butylsulfamoyl)-2-methylthiophen-3-yl]acetamide (**3.50**)

Boc protected amine **3.40** (0.420 g, 1.036 mmol) was dissolved in TFA and stirred at rt for 0.5 h. The solvent was removed under vacuo and a pure off-white solid was recovered (0.400g, 92%). mp = 166.0-169.7˚C; IR (ATR) 3208, 2970, 2641, 1662, 1577, 1430, 1143 cm^{-1}; 1H NMR (CD$_3$OD, 400 MHz) δ 7.77 (s, 1H), 3.90 (s, 2H), 2.92 (t, *J* =7.0 Hz, 2H), 2.41 (s, 3H), 1.46 (p, *J* = 6.4 Hz, 2H), 1.33 (sext, *J* = 7.4 Hz, 2H), 0.89 (t, *J* = 7.4 Hz, 3H); ^{13}C{^{1}H} NMR (CD$_3$OD, 100 MHz) 164.4, 136.2, 133.5, 131.0, 128.2, 42.6, 40.3, 31.2, 19.4, 12.5, 11.1; Anal. Calcd for $C_{13}H_{20}F_3N_3O_5S_2$: C, 37.23; H, 4.81; N, 10.02. Found: C, 37.21; H, 4.89; N, 9.64.

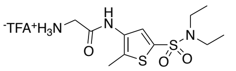

2-aminotrifluoroacetate-N-[5-(diethylsulfamoyl)-2-methylthiophen-3-yl]acetamide (**3.51**)

Boc protected amine **3.41** (0.120 g, 0.296 mmol) was dissolved in TFA and stirred at rt for 0.5 h. The solvent was removed under vacuo and a pure off-white solid was recovered (0.122g, 99%). mp = 43.9-47.4˚C; IR (ATR) 2980, 2938, 2641, 1669, 1590, 1198, 1133, 1014 cm^{-1}; 1H NMR (CD$_3$OD, 400 MHz) δ 7.77 (s, 1H), 3.90 (s, 2H), 3.22 (q, *J* =7.2 Hz, 4H), 2.41 (s, 3H), 1.17 (t, *J* = 7.1 Hz, 6H); ^{13}C{^{1}H} NMR (CDCl$_3$, 100 MHz) 164.4, 134.9, 133.6, 131.3, 128.2, 42.6, 40.3, 13.3, 11.0; Anal. Calcd for $C_{13}H_{20}F_3N_3O_5S_2$: C, 37.23; H, 4.81; N, 10.02. Found: C, 37.03; H, 4.99; N, 9.81.

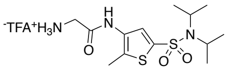

2-aminotrifluoroacetate-N-[5-{bis(propan-2-yl)sulfamoyl}-2-methylthiophen-3-yl]acetamide (**3.52**)

Boc protected amine **3.42** (0.120 g, 0.296 mmol) was dissolved in TFA and stirred at rt for 0.5 h. The solvent was removed under vacuo and a pure orange solid was recovered (0.214g, 92%). mp = 52.6-54.9°C; IR (ATR) 3083, 2976, 2936, 2648, 1670, 1169, 1125, 1012 cm^{-1}; 1H NMR (CD_3OD, 400 MHz) δ 7.77 (s, 1H), 3.89 (s, 2H), 3.79 (hept, *J* = 6.6, 2H), 2.41 (s, 3H), 1.28 (d, *J* = 6.6 Hz, 12 H); $^{13}C\{^1H\}$NMR (CD_3OD, 100 MHz) 164.3, 138.3, 133.2, 130.9, 128.4, 48.9, 40.3, 20.7, 11.0.; Anal. Calcd for $C_{15}H_{26}F_3N_3O_5S_2$: C, 41.64; H, 5.68; N, 9.11. Found: C, 41.49; H, 5.30; N, 9.38

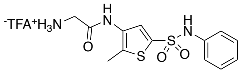

2-aminotrifluoroacetate-N-[2-methyl-5-(phenylsulfamoyl)thiophen-3-yl]acetamide (**3.53**)

Boc protected amine **3.43** (0.173 g, 0.407 mmol) was dissolved in TFA and stirred at rt for 0.5 h. The solvent was removed under vacuo and a pure tan powder was recovered (0.169g, 94%). mp = 68.1-71.7°C; IR (ATR) 3152, 3080, 2964, 1667, 1594, 1495, 1187, 1139 cm^{-1}; 1H NMR (CD_3OD, 400 MHz) δ 7.70 (s, 1H), 7.24 (t, *J* =7.8 Hz, 2H), 7.14 (d, *J* = 7.8 Hz, 2H), 7.08 (t, *J* = 7.5 Hz, 1H), 3.85 (s, 2H), 2.34 (s, 3H); $^{13}C\{^1H\}$NMR (CD_3OD, 100 MHz) 164.2, 137.2, 134.8, 134.2, 131.0, 128.8, 128.7, 124.6, 120.9, 40.3, 11.1.; Anal. Calcd for $C_{15}H_{16}F_3N_3O_5S_2$: C, 41.00; H, 3.67; N, 9.56. Found: C, 39.88; H, 3.89; N, 9.85.

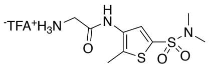

2-aminotrifluoroacetate-N-[5-(dimethylsulfamoyl)-2-methylthiophen-3-yl]acetamide (**3.54**)

Boc protected amine **3.44** (0.173 g, 0.407 mmol) was dissolved in TFA and stirred at rt for 0.5 h. The solvent was removed under vacuo and a pure off-white solid was recovered (0.169g, 94%). mp = 181.3-185.9˚C; IR (ATR) 3259, 3159, 3044, 2921, 2609, 1666, 1339, 1144, 1120 cm^{-1}; 1H NMR (CD_3OD, 400 MHz) δ 7.78 (s, 1H), 3.91 (s, 2H), 2.72 (s, 6H), 2.43 (s, 3H); $^{13}C\{^1H\}$NMR (CD_3OD, 100 MHz) 164.5, 134.5, 131.7, 129.7, 129.1, 40.4, 36.9, 11.1.; Anal. Calcd for $C_{11}H_{16}F_3N_3O_5S_2$: C, 33.76; H, 4.12; N, 10.74. Found: C, 33.69; H, 3.83; N, 10.47

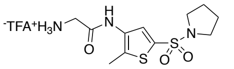

2-aminotrifluoroacetate-N-[2-methyl-5-(pyrrolidine-1-sulfonyl)thiophen-3-yl]acetamide (**3.55**)

Boc protected amine **3.45** (0.200 g, 0.496 mmol) was dissolved in TFA and stirred at rt for 0.5 h. The solvent was removed under vacuo and a pure light orange solid was recovered (0.170g, 82%). mp = 174.3-179.0˚C; IR (ATR) 3260, 3161, 2985, 2705, 2603, 1666, 1432, 1343, 1203, 1146, 1119 cm^{-1}; 1H NMR (CD_3OD, 400 MHz) δ 7.80 (s, 1H), 3.91 (s, 2H), 3.25-3.28 (m, 4H), 2.43 (s, 3H), 1.77-1.81 (m, 4H); $^{13}C\{^1H\}$NMR (CD_3OD, 100 MHz) 164.5, 134.1, 131.5, 131.1, 128.8, 47.8 (obscured by solvent peak), 40.4, 24.4, 11.1; Anal. Calcd for $C_{13}H_{18}F_3N_3O_5S_2$: C, 37.41; H, 4.35; N, 10.07. Found: C, 37.43; H, 4.09; 9.74.

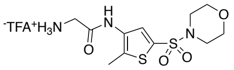

2-aminotrifluoroacetate-N-[2-methyl-5-(morpholine-4-sulfonyl)thiophen-3-yl]acetamide (**3.56**)

Boc protected amine **3.46** (0.370 g, 0.882 mmol) was dissolved in TFA and stirred at rt for 0.5 h. The solvent was removed under vacuo and a pure white solid was recovered (0.300 g, 84%). mp = 241.3-245.7°C; IR (ATR) 3255, 2890, 2856, 2638, 1670, 1588, 1522, 1159, 1110 cm^{-1}; 1H NMR (CD_3OD, 400 MHz) δ 7.79 (s, 1H), 3.91 (s, 2H), 3.74 (t, *J* = 4.6 Hz 4H), 3.01 (t, *J* = 4.6 Hz, 4H), 2.44 (s, 3H); $^{13}C\{^1H\}$NMR (CD_3OD, 100 MHz) 164.5, 135.1, 131.8, 129.6, 129.5, 65.7, 46.0, 40.4, 11.1.; Anal. Calcd for $C_{13}H_{18}F_3N_3O_6S_2$: C, 36.03; H, 4.19; N, 9.70. Found: C, 35.69; H, 4.31; N, 9.58.

General Procedure for N-sulfonylation

The desired amine (1 eq) was dissolved in dry DCM (0.7M) and dry TEA was added (2.2 eq). The desired sulfonyl chloride or benzyl chloride (1.1 eq) was added and the mixture was stirred at rt for 24 h under argon. The reaction was washed with H_2O, followed by a 5% HCl solution. The organics were collected and dried over Na_2SO_4, filtered, and concentrated. The crude mixture was then purified by trituration from DCM or by silica gel chromatography yielding the pure product.

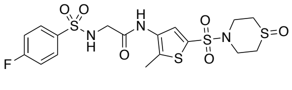

2-(4-fluorobenzenesulfonamido)-N-{2-methyl-5-[1-oxo-1-thiomorpholin-4-yl)sulfonyl]thiophen-3-yl}acetamide (**3.57**)

The crude oil was purified via trituration from DCM yielding a white solid (0.021g, 13%). mp = 209.5-211.8˚C; TLC R_f = 0.49 (95% DCM/5% MeOH); IR (ATR) 3360, 3267, 3106, 2927, 2858, 1685, 1670,1352, 1328, 1154 cm^{-1}; 1H NMR (DMSO-d_6, 400 MHz) δ 9.77 (s, 1H), 8.17 (bs, 1H), 7.89 (m, 2H), 7.65 (s, 1H), 7.44 (t, *J* = 8.4Hz, 2H), 3.73 (d, *J* = 4.8 Hz, 2H), 3.60 (d, *J* = 12.4 Hz, 2H), 3.05-3.10 (m, 2H), 2.90-2.99 (m, 4H), 2.35 (s, 3H); $^{13}C\{^1H\}$NMR (DMSO-d_6, 100 MHz) 166.8, 163.4, 137.2 (d, *J* = 3Hz), 134.5, 133.3, 130.1 (d, *J* = 9.7 Hz), 129.9, 129.2, 116.7 (d, *J* =23.2 Hz), 45.6, 43.9, 36.9, 12.9; Anal. Calcd for $C_{17}H_{20}FN_3O_6S_4$: C, 40.07; H, 3.96; N, 8.25. Found: C, 39.93; H, 4.24; N, 8.08.

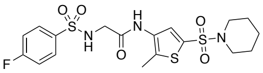

2-(4-fluorobenzenesulfonamido)-N-[2-methyl-5-(piperidine-1-sulfonyl)thiophen-3-yl]acetamide (**3.59**)

The crude oil was purified via silica gel column chromatography using a 50% hexanes:50% ethyl acetate eluent yielding a white solid (0.092g, 37%). mp = 79.8-84.2˚C; TLC R_f = 0.21 (50% EA/50% hexanes); IR (ATR) 3300, 2939, 2853, 1686, 1589, 1335, 1154, 1143 cm^{-1}; 1H NMR (CD_3OD, 400 MHz) δ 7.95 (m, 2H), 7.48 (s, 1H), 7.31 (t, *J* = 8.7 Hz, 2H), 3.77 (s, 2H), 3.00 (t, *J* = 5.2 Hz, 4H), 2.35 (s, 3H), 1.62-1.69 (m, 4H), 1.47-1.50 (m, 2H); $^{13}C\{^1H\}$NMR (CD_3OD, 100 MHz) 166.7, 164.6 (d, *J* = 250.4 Hz), 137.3 (d, *J* = 2.9 Hz), 133.5, 133.1, 130.1 (d, *J* = 9.4Hz), 129.7, 129.4, 116.6 (d, *J* = 23.1 Hz), 47.1, 45.6, 25.0, 23.2, 12.9; Anal. Calcd for $C_{18}H_{22}FN_3O_5S_3$: C, 45.46; H, 4.66; N, 8.84. Found: C, 45.47; H, 4.92; N, 8.99.

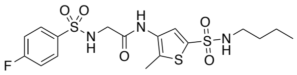

N-[5-(butylsulfamoyl)-2-methylthiophen-3-yl]-2-(4-fluorobenzenesulfonamido)acetamide (**3.60**)

The crude oil was purified via trituration from DCM yielding a white solid (0.185g, 13%). mp = 161.2-164.4˚C; TLC R_f = 0.19 (50% EA/50% Hexane); IR (ATR) 3247, 2964, 2934, 2876, 1652, 1325, 1151 cm^{-1}; 1H NMR (CD_3OD, 400 MHz) δ 7.94-8.00 (m, 2H), 7.56 (s, 1H), 7.30-7.35 (m, 2H), 3.78 (s, 2H), 2.93 (t, *J* = 7.0 Hz, 2H), 2.36 (s 3H), 1.48 (pent, *J* = 6.9Hz, 2H), 1.35 (sext, *J* = 7.0 Hz, 2H), 0.91 (t, *J* = 7.2, 3H); $^{13}C\{^1H\}$NMR (CD_3OD, 100 MHz) 167.8, 163.9, 136.2 (d, *J* = 3.4 Hz), 135.8, 134.6, 131.2, 129.8 (d, *J* = 9.3Hz), 128.6, 115.8 (d, *J* = 23.1 Hz), 45.1, 42.6, 31.2, 19.4, 12.5, 11.1; Anal. Calcd for $C_{17}H_{22}FN_3O_5S_3$: C, 44.05; H, 4.78; N, 9.06. Found: C, 44.10; H, 4.70; N, 9.05.

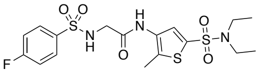

N-[5-(diethylsulfamoyl)-2-methylthiophen-3-yl]-2-(4-fluorobenzenesulfonamido)acetamide **(3.61)**

The crude oil was purified via silica gel column chromatography using a 50% hexanes:50% ethyl acetate eluent yielding an orange solid (0.108g, 80%). mp = 44.3-48.1˚C; TLC R_f = 0.18 (50% EA/50% Hexane); IR (ATR) 3309, 2977, 2934, 2360, 2343, 1685, 1590, 1494, 1327, 1141 cm^{-1}; 1H NMR (CD_3OD, 400 MHz) δ 7.95 (m, 2H), 7.52 (s, 1H), 7.30 (t, *J* = 8.6 Hz, 2H), 3.76 (s, 2H), 3.20 (q, *J* = 7.2 Hz, 4H), 2.33 (s, 3H), 1.16 (t, *J* = 7.2 Hz, 6H); $^{13}C\{^1H\}$NMR (CD_3OD, 100 MHz) 167.7, 165.0 (d, *J* = 250 Hz), 136.2 (d, *J* = 2.5 Hz), 134.6, 134.5, 131.5, 129.9 (d, *J* = 9.4Hz), 128.6, 115.8 (d, *J* = 23.8 Hz), 45.1, 42.6, 13.4, 11.1; Anal. Calcd for $C_{17}H_{22}FN_3O_5S_3$: C, 44.05; H, 4.78; N, 9.06. Found: C, 44.12; H, 4.99; N, 8.79.

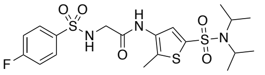

N-{5-[bis(propan-2-yl)sulfamoyl]-2-methylthiophen-3-yl}-2-(4-fluorobenzenesulfonamido) acetamide (**3.62**)

The crude oil was purified via silica gel column chromatography using a 50% hexanes:50% ethyl acetate eluent yielding a pink solid (0.073g, 31%). mp = 61.1-63.5˚C; TLC R_f = 0.32 (50% EA/50% Hexane); IR (ATR) 3304, 2974, 2930, 2466, 1685, 1591, 1403, 1325, 1154, 1132cm^{-1}; 1H NMR (CD_3OD, 400 MHz) δ 7.93-8.00 (m, 2H), 7.54 (s, 1H), 7.28-7.32 (m, 2H), 3.74-3.81 (m, 4H), 2.33 (s, 3H), 1.27 (d, *J* = 6.9 Hz, 12H); $^{13}C\{^1H\}$NMR (CD_3OD, 100 MHz) 167.7, 165.0 (d, *J* = 251.0 Hz), 137.9, 136.2 (d, *J* = 2.9 Hz), 134.1, 131.0, 129.9 (d, *J* = 9.7Hz), 128.8, 115.8 (d, *J* = 23.0 Hz), 48.9, 45.1, 20.7, 11.1; Anal. Calcd for $C_{19}H_{26}FN_3O_5S_3$: C, 46.42; H, 5.33; N, 8.55. Found: C, 46.05; H, 5.09; N, 8.23.

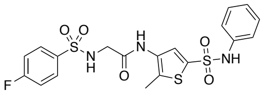

2-(4-fluorobenzenesulfonamido)-N-[2-methyl-5-(phenylsulfamoyl)thiophen-3-yl]acetamide (**3.63**)

The crude oil was purified via silica gel column chromatography using a 5% methanol:95% chloroform eluent yielding a white solid (0.022g, 12%). mp = 143.7-146.4˚C; TLC R_f = 0.37 (5% MeOH/95% $CHCl_3$); IR (ATR) 3366, 3321, 3139, 2966, 2900, 2851, 2360, 2342, 1637, 1582, 1491, 1339, 1146 cm^{-1}; 1H NMR (CD_3OD, 400 MHz) δ 7.90-7.95 (m, 2H), 7.49 (s, 1H), 7.23-7.31 (m, 4H), 7.07-7.15 (m, 3H), 3.72 (s, 2H), 2.26 (s, 3H); $^{13}C\{^1H\}$NMR (CD_3OD, 100

MHz) 167.7, 166.4, 136.2 (d, *J* = 3.5 Hz), 135.3, 134.6, 131.2, 129.8 (d, *J* = 9.3 Hz), 129.2, 128.8, 124.6, 121.0, 115.8 (d, *J* = 23.0 Hz), 78.1, 45.0, 11.1; Anal. Calcd for $C_{19}H_{18}FN_3O_5S_3$: C, 47.19; H, 3.75; N, 8.69. Found: C, 47.48; H, 4.06; N, 8.78.

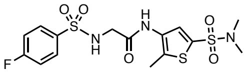

N-[5-(dimethylsulfamoyl)-2-methylthiophen-3-yl]-2-(4-fluorobenzenesulfonamido)acetamide **(3.64)**

The crude oil was purified via silica gel column chromatography using a 50% hexanes:50% EA eluent yielding a white solid (0.120g, 51%). mp = 123.0-127.8˚C; TLC R_f = 0.21 (50% EA/50% Hexanes); IR (ATR) 3321, 3278, 3107, 2928, 1658, 1590, 1342, 1155, 1137 cm^{-1}; 1H NMR (CD_3OD, 400 MHz) δ 7.93-7.97 (m, 2H), 7.52 (s, 1H), 7.31 (t, *J* = 8.1 Hz, 2H), 3.77 (s, 2H), 2.71 (s, 6H), 2.36 (s, 3H); $^{13}C\{^1H\}$NMR (CD_3OD, 100 MHz) 167.8, 165.2 (d, *J* = 251.5), 136.2 (d, *J* = 3.1 Hz), 135.6, 131.8, 129.9 (d, *J* = 9.4 Hz), 129.6, 129.4, 115.8 (d, *J* = 24.3 Hz), 45.1, 36.9, 11.1.; Anal. Calcd for $C_{15}H_{18}FN_3O_5S_3$: C, 41.37; H, 4.17; N, 9.65. Found: C, 41.24; H, 4.28; N, 9.36.

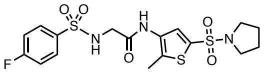

2-(4-fluorobenzenesulfonamido)-N-[2-methyl-5-(pyrrolidine-1-sulfonyl)thiophen-3-yl]acetamide **(3.65)**

The crude oil was purified via silica gel column chromatography using a 50% hexanes:50% EA eluent yielding a white solid (0.020g, 10%). mp = 158.9-163.5˚C; TLC R_f = 0.18 (50% EA/50% Hexanes); IR (ATR) 3360, 3239, 3099, 2885, 1676, 1508, 1328, 1151 cm^{-1}; 1H NMR (CD_3OD, 400 MHz) δ 7.94-7.97 (m, 2H), 7.55 (s, 1H), 7.31 (t, *J* = 8.5 Hz, 2H), 3.77 (s, 2H), 3.25 (bs, 3H), 2.35 (s, 3H), 1.79 (bs, 4H); $^{13}C\{^1H\}$NMR (CD_3OD, 100 MHz) 167.8, 165.2 (d, *J* = 251.6), 136.2 (d, *J* = 2.7 Hz), 135.2, 131.7, 130.7, 129.9 (d, *J* = 9.5 Hz), 129.3, 115.8 (d, *J* = 23.4 Hz), 47.8, 45.1, 24.9, 11.1.; Anal. Calcd for $C_{17}H_{20}FN_3O_5S_3$: C, 44.24; H, 4.37; N, 9.10. Found: C, 44.21; H, 4.44; N, 8.97.

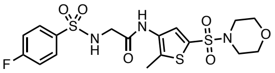

2-(4-fluorobenzenesulfonamido)-N-[2-methyl-5-(morpholine-4-sulfonyl)thiophen-3-yl]acetamide (**3.66**)

The crude oil was purified via silica gel column chromatography using a 50% hexanes:50% EA eluent yielding a white solid (0.104g, 30%). mp = 173.4-177.3˚C; TLC R_f = 0.28 (50% EA/50% Hexanes); IR (ATR) 3650, 3395, 3233, 2980, 2890, 2856, 1673, 1345, 1153 cm^{-1}; 1H NMR (CD_3OD, 400 MHz) δ 8.19 (s, 1H), 7.91-7.94 (m, 2H), 7.77 (s, 1H), 7.23-7.28 (m, 2H), 5.45 (t, *J* = 5.9 Hz, 1H), 3.72-3.78 (m, 6H), 3.02-3.06 (m, 4H), 2.40 (s, 3H); $^{13}C\{^1H\}$NMR (CD_3OD, 100 MHz) 166.9, 165.6, 134.2, 133.9, 131.5, 130.1 (d, *J* = 9.9 Hz), 129.8, 128.8, 116.8 (d, *J* = 23.1 Hz), 66.0, 46.3, 46.0, 12.5.; Anal. Calcd for $C_{17}H_{20}FN_3O_6S_3$: C, 42.76; H, 4.22; N, 8.80. Found: C, 42.82; H, 4.24; N, 8.52.

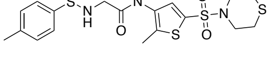

N-[2-methyl-5-(thiomorpholine-4-sulfonyl)thiophen-3-yl]-2-(4-methylbenzenesulfonamido) acetamide (**3.67**)

The crude mixture was purified by precipitation from dichloromethane yielding a white powder (0.053g, 20.9%). mp = 205.8-209.3˚C; TLC R_f = 0.244 (50% EA/50% hexane); IR (ATR) 3290, 2913, 1685, 1578, 1332, 1152 cm^{-1}; 1H NMR (Acetone-d_6, 400 MHz) δ 9.03 (s, 1H), 7.79 (d, *J* =

7.9 Hz, 2H), 7.70 (s, 1H), 7.41 (d, *J* = 7.5 Hz, 2H), 6.87 (t, *J* = 5.6 Hz, 1H), 3.79 (d, *J* = 5.8 Hz, 2H), 3.32 (t, *J* = 4.8 Hz, 4H), 2.75 (t, *J* = 5.0 Hz, 4H), 2.42 (s, 3H), 2.39 (s, 3H); ^{13}C{^{1}H} NMR (Acetone-*d*$_6$, 100 MHz) 166.2, 143.5, 137.2, 133.3, 132.7, 130.9, 129.6, 129.0, 127.2, 48.1, 45.8, 26.8, 20.5, 11.6. Anal. Calcd for $C_{18}H_{23}N_3O_5S_4$: C, 44.15; H, 4.73; N, 8.58. Found: C, 44.08; H, 4.72; N, 8.30.

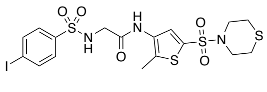

2-(4-iodobenzenesulfonamido)-N-[2-methyl-5-(thiomorpholine-4-sulfonyl)thiophen-3-yl] acetamide (**3.68**)

The crude mixture was purified by precipitation from dichloromethane yielding a white powder (0.094g, 26.9%). mp = 197.6-201.9°C; TLC R_f = 0.513 (50% EA/50% hexane); IR (ATR) 3381, 3156, 2979, 2907, 2865, 1655, 1335, 1327, 1164, 1148 cm^{-1}; 1H NMR (DMSO-*d*$_6$, 400 MHz) δ 9.73 (s, 1H), 8.20 (t, *J* = 5.9 Hz, 1H), 7.97 (d, *J* = 8.1 Hz, 2H), 7.59 (d, *J* = 5.0 Hz, 2H), 7.57 (s, 1H), 3.71 (d, *J* = 6.2 Hz, 2H), 3.22 (t, *J* = 4.6 Hz, 4H), 2.71 (t, *J* = 4.6 Hz, 4H), 2.32 (s, 3H); ^{13}C{^{1}H} NMR (DMSO-*d*$_6$, 100 MHz) 166.8, 140.5, 138.5, 134.1, 133.2, 130.1, 129.6, 128.8, 101.0, 48.3, 45.6, 26.8, 12.9.; Anal. Calcd for $C_{17}H_{20}IN_3O_5S_4$: C, 33.95; H, 3.35; N, 6.99. Found: C, 33.93; H, 3.42; N, 6.65.

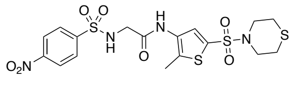

N-[2-methyl-5-(thiomorpholine-4-sulfonyl)thiophen-3-yl]-2-(4-nitrobenzenesulfonamido) acetamide (**3.69**)

The crude mixture was purified by precipitation from dichloromethane yielding a white powder (0.059g, 19.6%). mp = 209.3-212.4˚C; TLC R_f = 0.189 (50% EA/50% hexane); IR (ATR) 3380, 3247, 3105, 3063, 2980, 2914, 2853, 1668, 1531, 1349, 1332, 1150 cm^{-1}; 1H NMR (Acetone-*d*$_6$, 400 MHz) δ 9.73 (s, 1H), 8.21 (t, *J* = 5.6 Hz, 1H), 7.98 (d, *J* = 7.5 Hz, 2H), 7.60 (d, *J* = 5.7 Hz, 2H), 7.57 (s, 1H), 3.72 (d, *J* = 5.3 Hz, 2H), 3.22 (t, *J* = 4.1 Hz, 4H), 2.71 (t, *J* = 4.7 Hz, 4H), 2.32 (s, 3H); ^{13}C{^{1}H} NMR (Acetone-*d*$_6$, 100 MHz) 166.8, 140.5, 138.5, 134.1, 133.2, 130.1, 129.5, 128.8, 101.0, 48.3, 45.6, 26.8, 12.9.; Anal. Calcd for $C_{17}H_{20}N_4O_7S_4$: C, 39.22; H, 3.87; N, 10.76. Found: C, 39.14; H, 3.84; N, 11.14.

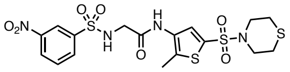

N-[2-methyl-5-(thiomorpholine-4-sulfonyl)thiophen-3-yl]-2-(3-nitrobenzenesulfonamido) acetamide (**3.70**)

The crude mixture was purified via silica gel chromatography using 50% EA/50% hexanes yielding a white powder (0.16g, 53%). mp = 141.0-144.2˚C; TLC R_f = 0.19 (50% EA/50% hexanes); IR (ATR) 3365, 3217, 3104, 2927, 2851, 1677, 1528, 1426, 1349, 1337, 1161 cm^{-1}; 1H NMR (Acetone-*d*$_6$, 400 MHz) δ 9.13 (s, 1H), 8.68 (t, *J* = 1.8 Hz, 1H), 8.50 (dd, *J* = 1.3, 8.3 Hz, 1H), 8.32 (d, *J* = 7.8 Hz, 1H), 7.93 (t, *J* = 7.9 Hz, 1H), 7.63 (s, 1H), 7.37 (bs, 1H), 4.00 (d, *J* = 5.5 Hz, 2H), 3.29 (t, *J* = 4.9 Hz, 4H), 2.75 (t, *J* = 4.9 Hz, 4H), 2.37 (s, 3H); ^{13}C{^{1}H} NMR (Acetone-*d*$_6$, 100 MHz) 165.8, 148.3, 142.4, 133.1, 133.0, 132.6, 131.0, 130.9, 128.8, 127.1, 122.1, 48.1, 45.6, 26.8, 11.6.; Anal. Calcd for $C_{17}H_{20}N_4O_7S_4$: C, 39.22; H, 3.87; N, 10.76. Found: C, 39.23; H, 3.91; N, 10.94.

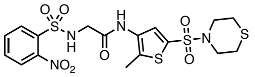

N-[2-methyl-5-(thiomorpholine-4-sulfonyl)thiophen-3-yl]-2-(2-nitrobenzenesulfonamido) acetamide (**3.71**)

The crude mixture was purified via silica gel chromatography using 50% EA/50% hexanes yielding an orange powder (0.140g, 47%). mp = 101.1-104.4°C; TLC $R_f = 0.19$ (50% EA/50% hexanes); IR (ATR) 3325, 3097, 2917, 2490, 1686, 1537, 1336, 1149 cm^{-1}; 1H NMR (CD_3OD, 400 MHz) δ 8.11-8.15 (m, 1H), 7.90-7.93 (m, 1H), 7.79 (s, 1H), 4.03 (s, 2H), 3.31-3.33 (m, 4H), 2.72 (t, *J* = 5.2 Hz, 4H), 2.36 (s, 3H); $^{13}C\{^1H\}$ NMR (CD_3OD, 100 MHz) 167.8, 148.0, 135.4, 133.8, 133.4, 132.4, 131.9, 131.0, 130.3, 129.3, 124.8, 48.0, 45.4, 26.7, 11.2.; Anal. Calcd for $C_{17}H_{20}N_4O_7S_4$: C, 39.22; H, 3.87; N, 10.76. Found: C, 39.60; H, 4.11; N, 10.48.

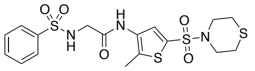

2-benzenesulfonamido-N-[2-methyl-5-(thiomorpholine-4-sulfonyl)thiophen-3-yl]acetamide (**3.72**)

The crude mixture was purified by precipitation from dichloromethane yielding a white powder (0.074g, 26.8%). mp = 172.3-175.9°C; TLC $R_f = 0.263$ (50% EA/50% hexane); IR (ATR) 3352, 3160, 2980, 2889, 1682, 1587, 1329, 1156 cm^{-1}; 1H NMR (DMSO-d_6, 400 MHz) δ 9.72 (s, 1H), 8.12 (t, *J* = 6.4 Hz, 1H), 7.82 (d, *J* = 7.5 Hz, 2H), 7.55-7.65 (m, 4H), 3.70 (d, *J* = 6.2 Hz,, 2H), 3.20 (t, *J* = 4.8 Hz, 4H), 2.71 (t, *J* = 4.5 Hz, 4H), 2.32 (s, 3H); $^{13}C\{^1H\}$ NMR (DMSO-d_6, 100 MHz) 166.9, 140.8, 134.0, 133.2, 133.0, 130.0, 129.6, 129.6, 127.1, 48.3, 45.7, 26.8, 12.9.;Anal. Calcd for $C_{17}H_{21}N_3O_5S_4$: C, 42.93; H, 4.45; N, 8.84. Found: C, 42.65; H, 4.06; N, 8.50.

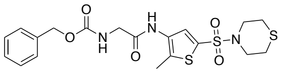

benzyl N-({[2-methyl-5-(thiomorpholine-4-sulfonyl)thiophen-3-yl]carbamoyl}methyl)carbamate (**3.73**)

The crude mixture was purified by precipitation from dichloromethane yielding a white powder (0.079g, 31.3%). mp = 69.3-73.7˚C; TLC R_f = 0.21% (50% ethyl acetate/ 50% hexanes); IR (ATR) 3309, 3098, 3066, 2962, 2907, 2860, 2466, 1676, 1636, 1556, 1350, 1333, 1137cm^{-1}; 1H NMR (DMSO-*d*$_6$, 400 MHz) δ 9.78 (s, 1H), 7.74 (s, 1H), 7.58 (t, *J* = 5.9 Hz, 1H), 7.31-7.38 (m, 5H), 5.06 (s, 2H), 3.85 (d, *J* = 5.8 Hz, 2H), 3.23 (t, *J* = 4.6 Hz, 4H), 2.71 (t, *J* = 4.6 Hz, 4H), 2.39 (s, 3H); $^{13}C\{^1H\}$ NMR (DMSO-*d*$_6$, 100 MHz) 168.5, 157.1, 137.5, 133.7, 133.5, 129.9, 129.7, 128.8, 128.3, 128.2, 66.0, 48.3, 44.0, 26.8, 13.0.; Anal. Calcd for $C_{18}H_{21}N_3O_4S_3$: C, 49.18; H, 4.82; N, 9.56. Found: C, 49.00; H, 5.02; N, 9.22.

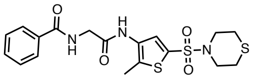

N-[2-methyl-5-(thiomorpholine-4-sulfonyl)thiophen-3-yl]-2-(phenylformamido)acetamide (**3.74**)

The crude mixture was purified by precipitation from dichloromethane yielding a white powder (0.079g, 31%). mp = 189.3-193.1˚C; TLC R_f = 0.53 (95% DCM/5% MeOH); IR (ATR) 3309, 3098, 3066, 2907, 2860, 2467, 1675, 1636, 1556, 1137, 1072, 909 cm^{-1}; 1H NMR (Acetone-*d*$_6$, 400 MHz) δ 9.70 (s, 1H), 8.65 (s, 1H), 8.41 (d, *J* = 7.5 Hz, 2H), 8.30 (s, 1H), 8.01 (t, *J* = 7.5 Hz, 1H), 7.94 (t, *J* = 7.1 Hz, 2H), 4.68 (d, *J* = 5.2 Hz, 2H), 3.77 (t, *J* = 4.9 Hz, 4H), 3.19 (t, *J* = 4.9 Hz, 4H), 2.87 (s, 3H); $^{13}C\{^1H\}$ NMR (Acetone-*d*$_6$, 100 MHz) 167.5, 167.3, 134.2, 133.2, 132.7, 131.5, 130.9, 129.0, 128.4, 127.3, 48.2, 43.6, 26.8, 11.7.; Anal. Calcd for $C_{18}H_{21}N_3O_4S_3$: C, 49.18; H, 4.82; N, 9.56. Found: C, 49.00; H, 5.02; N, 9.22.

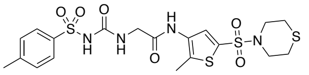

N-[2-methyl-5-(thiomorpholine-4-sulfonyl)thiophen-3-yl]-2-{[(4-methylbenzenesulfonyl) carbamoyl]amino}acetamide (**3.75**)

The crude mixture was purified by precipitation from DCM yielding a white powder (0.037g, 12%). mp = 192.2-195.7˚C; TLC R_f = 0.39 (90% DCM/10% MeOH); IR (ATR) 3657, 3329, 3107, 2980, 2889, 2473, 1708, 1655, 1333, 1148 cm^{-1}; 1H NMR (Acetone-*d₆*, 400 MHz) δ 9.08 (s, 1H), 7.92 (d, *J* = 8.3 Hz, 2H), 7.83 (s, 1H), 7.41 (d, *J* = 8.4 Hz, 2H), 6.97 (bs, 1H), 4.04 (d, *J* = 5.0 Hz, 4H), 3.33 (t, *J* = 5.0 Hz, 4H), 2.75 (t, *J* = 5.0 Hz, 4H), 2.43 (s, 3H), 2.37 (s, 3H); $^{13}C\{^1H\}$ NMR (Acetone-*d₆*, 100 MHz) 167.1, 151.4, 144.3, 137.7, 132.9, 132.8, 130.9, 129.5, 129.0, 127.5, 48.2, 43.2, 26.8, 20.6, 11.6.; Anal. Calcd for $C_{19}H_{24}N_4O_6S_4$: C, 48.60; H, 4.94; N, 8.95. Found: C, 48.85; H, 4.64; N, 9.07.

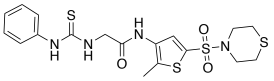

N-[2-methyl-5-(thiomorpholine-4-sulfonyl)thiophen-3-yl]-2-[(phenylcarbamothioyl)amino] acetamide (**3.76**)

The crude mixture was purified by silica gel chromatography yielding a white powder (0.035g, 13.7%). mp = 179.8-183.0˚C; TLC R_f = 0.275 (50% EA/50% hexane); IR (ATR) 3596, 3439, 3217, 3058, 2909, 1660, 1590, 1521, 1493, 1336, 1148 cm^{-1}; 1H NMR (Acetone-*d₆*, 400 MHz) δ 9.22-9.25 (m, 1H), 7.87 (s, 1H), 7.51 (d, *J* = 7.9 Hz, 2H), 7.40 (t, *J* = 8.2 Hz, 2H), 7.21 (t, *J* = 7.4 Hz, 1H), 4.49 (s, 2H), 3.32 (t, *J* = 5.0 Hz, 4H), 2.74 (t, *J* = 5.0 Hz, 4H), 2.45 (s, 3H); $^{13}C\{^1H\}$ NMR (CD_3OD, 100 MHz) 181.8, 169.0, 138.0, 135.7, 132.3, 130.9, 129.7, 129.0, 125.6, 124.2, 48.3, 47.3, 26.7, 11.4.; Anal. Calcd for $C_{18}H_{22}N_4O_3S_4$: C, 45.94; H, 4.71; N, 11.90. Found: C, 46.06; H, 4.55; N, 12.26.

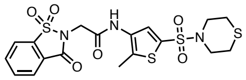

N-[2-methyl-5-(thiomorpholine-4-sulfonyl)thiophen-3-yl]-2-(1,1,3-trioxo-2,3-dihydro-1-benzothiazol-2-yl)acetamide (**3.77**)

The crude mixture was purified via silica gel chromatography using 50% EA/50% hexanes yielding an white powder (0.041g, 36%). mp = 233.7-237.4˚C; TLC R_f = 0.28 (50% EA/50% hexanes); IR (ATR) 3264, 2980, 2918, 1743, 1671, 1335, 1150, 585 cm^{-1}; 1H NMR (Acetone-*d$_6$*, 400 MHz) δ 9.32 (s, 1H), 8.22 (d, *J* = 7.7 Hz, 1H), 8.05-8.17 (m, 3H), 7.80 (s, 1H), 4.64 (s, 2H), 3.31 (bs, 4H), 2.74 (t, *J* = 5.0 Hz, 4H), 2.44 (s, 3H); $^{13}C\{^1H\}$ NMR (Acetone-*d$_6$*, 100 MHz) 163.4, 158.9, 137.9, 135.7, 135.0, 133.8, 132.6, 131.1, 129.0, 127.2, 125.1, 121.3, 48.2, 40.4, 26.8, 11.7.; Anal. Calcd for $C_{18}H_{19}N_3O_6S_4$: C, 43.10; H, 3.82; N, 8.38. Found: C, 43.35; H, 3.98; N, 8.17.

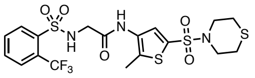

N-[2-methyl-5-(thiomorpholine-4-sulfonyl)thiophen-3-yl]-2-(2-trifluoromethylbenzene sulfonamido)acetamide (**3.78**)

The crude mixture was purified via silica gel chromatography using 50% EA/50% hexanes yielding an off-white solid (0.030g, 24%). mp = 88.7-92.9˚C; TLC R_f = 0.32 (50% EA/50% hexanes); IR (ATR) 3329, 2980, 1685, 1581, 1307, 1143, 1116, 587 cm^{-1}; 1H NMR (Acetone-*d$_6$*, 400 MHz) δ 9.07 (s, 1H), 8.27 (dd, *J* = 3.7, 5.0 Hz, 1H), 8.00 (dd, *J* = 3.7, 5.5 Hz, 1H), 7.86 (dd, *J* = 3.7, 6.0, 1H), 7.65 (bs, 1H), 3.99 (d, *J*= 6.0 Hz, 2H), 3.30 (t, *J* = 4.6 Hz, 4H), 2.74 (t, *J* = 5.0

Hz, 4H), 2.37 (s, 3H); $^{13}C\{^1H\}$ NMR (Acetone-d_6, 100 MHz) 166.0, 138.9, 133.1, 132.9 (d, *J* = 59.4 Hz), 132.8, 131.0, 130.1 (d, *J* = 234.4 Hz), 128.5 (q, *J* = 6.3 Hz), 127.5 (d, *J* = 42.6 Hz), 127.2 (d, *J* = 33.1 Hz), 126.6, 123.3 (d, *J* = 273.1 Hz), 48.1, 45.7, 26.8, 11.7.; Anal. Calcd for $C_{18}H_{20}F_3N_3O_5S_4$: C, 39.77; H, 3.71; N, 7.73. Found: C, 39.74; H, 3.95; N, 7.42.

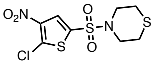

4-[(5-chloro-4-nitrothiophen-2-yl)sulfonyl]thiomorpholine (**3.90**)

Thiomorpholine (0.086 mL, 0.859 mmol), and DIPEA (0.149 mL, 0.859 mmol) was dissolved in dry DCM (11.8 mL,0.08M) and cooled to 0˚C. 2-chloro-3-nitrothiophene-5-sulfonyl chloride (0.250 g, 0.954 mmol) was added dropwise to and the mixture was heated to r.t. and stirred for 1hr until TLC indicated reaction was completed. The mixture was diluted in DCM, washed with sat. $NaHCO_3$, followed by brine and the organics were dried over Na_2SO_4, filtered and concentrated. The crude mixture was purified via silica gel chromatography using a 20% EA/ 80% hexanes eluent yielding the desired product (0.157g, 50%). mp = 139.1-143.1˚C; TLC R_f = 0.50 (20% EA/80% hexanes); IR (ATR) 3106, 2972, 2906, 1531, 1358, 1152, 566, 552 cm^{-1}; 1H NMR (Acetone-d_6, 400 MHz) δ 8.06 (s, 1H), 3.50 (t, *J* = 4.0 Hz, 4H), 2.79 (t, *J* = 5.1 Hz, 4H); $^{13}C\{^1H\}$ NMR (DMSO-d_6, 100 MHz) 143.9, 137.4, 133.2, 128.2, 48.2, 26.8.; Anal. Calcd for $C_8H_9ClN_2O_4S_3$: C, 29.22; H, 2.76; N, 8.52. Found: C, 29.42; H, 2.40; N, 8.35.

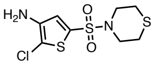

2-chloro-5-(thiomorpholine-4-sulfonyl)thiophene-3-amine (**3.93**)

4-[(5-chloro-4-nitrothiophen-2-yl)sulfonyl]thiomorpholine (0.67 g, 2.04 mmol) was dissolved in acetic acid (6.8 mL, 0.3M) and iron powder (0.57 g, 10.19 mmol) was added. The mixture was heated to 60˚C and stirred for 1 h, after which the acetic acid was removed via vacuo. The residue was dissolved in ethyl acetate and washed with saturated $NaHCO_3$ until a pH of 8 was reached. The organics were washed with brine, dried over $MgSO_4$, filtered and concentrated. The crude mixture was purified via silica gel chromatography using a 50% EA/ 50% hexanes eluent yielding the desired product (0.420g, 69%). mp = 137.9-140.3˚C; TLC R_f = 0.58 (50% EA/50% hexanes); IR (ATR) 3448, 3360, 2903, 2852, 1611, 1569, 1405, 1334, 1149, 897, 578 cm^{-1}; 1H NMR (Acetone-*d₆*, 400 MHz) δ 7.16 (s, 1H), 5.00 (bs, 2H), 3.36 (t, *J* = 4.9 Hz, 4H), 2.77 (t, *J* = 5.3 Hz, 4H); $^{13}C\{^1H\}$ NMR (DMSO-*d₆*, 100 MHz) 143.9, 131.6, 124.5, 106.7, 48.1, 26.8.; Anal. Calcd for $C_8H_{11}ClN_2O_2S_3$: C, 32.16; H, 3.71; N, 9.37. Found: C, 32.31; H, 3.40; N, 9.11.

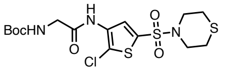

tert-butyl-N-({[2-chloro-5-(thiomorpholine-4-sulfonyl)thiophen-3-yl]carbamoyl}methyl) carbamate (**3.96**)

Boc-glycine (0.300g , 1.69 mmol), 2-chloro-5-(thiomorpholine-4-sulfonyl)thiophene-3-amine (0.420 g, 1.41 mmol), HATU (1.069 g, 2.81 mmol) and DIPEA (0.49 mL, 2.81) were dissolved in 7 mL of dry DMAc under argon. The mixture was stirred for 24 h at rt. The reaction was diluted with ethyl acetate, washed with NH_4Cl (3x15 mL) and brine. The organics were dried over $MgSO_4$, filtered and concentrated. The crude mixture was purified via silica gel chromatography using 50% hexanes:50% ethyl acetate yielding a yellow solid (0.400g, 63%). mp = 143.4-147.7˚C; TLC R_f = 0.36 (50% EA/50% hexanes); IR (ATR) 3297, 2982, 2915, 1693, 1147, 600, 583 cm^{-1}; 1H NMR (DMSO-*d₆*, 400 MHz) δ 10.01 (s, 1H), 7.93 (s, 1H), 7.12 (t, *J* = 6.1 Hz, 1H), 3.80 (d, *J* = 5.7 Hz, 2H), 3.29 (t, *J* = 4.4 Hz, 4H), 2.72 (t, *J* = 5.0, 4H), 1.40 (s, 9H); $^{13}C\{^1H\}$ NMR (DMSO-*d₆*, 100 MHz) δ 169.2, 156.4, 134.8, 131.9, 128.4, 120.8, 78.7, 48.3, 43.7, 28.7, 26.8. Anal. Calcd for $C_{15}H_{22}ClN_3O_5S_3$: C, 39.51; H, 4.86; N, 9.22. Found: C, 39.73; H, 4.62; N, 9.07.

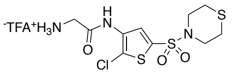

2-aminotrifluoroacetate-N-[2-chloro-5-(thiomorpholine-4-sulfonyl)thiophen-3-yl]acetamide (**3.99**)

Boc protected amine **3.96** (0.250 g, 0.532 mmol) was dissolved in TFA and stirred at rt for 0.5 h. The solvent was removed under vacuo and an off-white solid was recovered (0.250 g, 61%). mp = 177.1-181.4°C; IR (ATR) 3354, 2916, 1671, 1584, 1372, 1146, 1121, 584 cm^{-1}; 1H NMR (DMSO-*d*$_6$, 400 MHz) δ 10.65 (bs, 1H), 8.15 (bs, 3H), 7.93 (s, 1H), 3.88 (s, 2H), 3.30 (t, *J* = 3.9 Hz, 4H), 2.72 (t, *J* = 4.2, 4H); $^{13}C\{^1H\}$ NMR (DMSO-*d*$_6$, 100 MHz) δ 166.0, 134.0, 132.4, 127.9, 121.6, 48.3, 41.2, 26.8. Anal. Calcd for $C_{12}H_{15}ClN_3F_3O_5S_3$: C, 30.67; H, 3.22; N, 8.94. Found: C, 30.80; H, 3.41; N, 8.61.

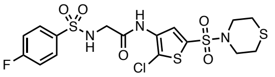

N-[2-chloro-5-(thiomorpholine-4-sulfonyl)thiophen-3-yl]-2-(4-fluorobenzenesulfonamido) acetamide (**3.102**)

tert-butyl-N-({[2-chloro-5-(thiomorpholine-4-sulfonyl)thiophen-3-yl]carbamoyl}methyl) carbamate (0.250g, 0.532 mmol) was dissolved in dry dichloromethane (0.829 mL, 0.6M) and dry TEA (0.163 mL, 1.170 mmol) and stirred at rt. 4-fluorobenzenesulfonyl chloride (0.114 g, 0.585 mmol) was added and the mixture was stirred at rt for 24 h. The mixture was washed with water (3x5 mL) followed by a 5% HCl solution. The organics were collected, dried over $MgSO_4$, filtered and concentrated. The crude mixture was purified by precipitation from dichloromethane yielding a white powder (0.032g, 12%). mp = 173.2-177.8˚C; TLC R_f = 0.24 (50% EA/50% hexanes); IR (ATR) 3274, 2917, 1664, 1576, 1392, 1332, 1141, 551 cm^{-1}; 1H NMR (CD_3OD, 400 MHz) δ 7.93-7.96 (m, 2H), 7.80 (s, 1H), 7.27-7.32 (m, 2H), 3.84 (s, 2H), 3.36 (t, *J* = 4.9, 4H), 2.73 (t, *J* = 4.9 Hz, 4H), 2.31; $^{13}C\{^1H\}$ NMR (CD_3OD, 100 MHz) δ.167.4, 165.2 (d, *J* =252.9 Hz), 136.3 (d, *J* = 3.1 Hz), 133.3, 132.7, 129.9 (d, *J* = 10.7 Hz), 127.3, 121.7, 115.8 (d, *J* = 21.4 Hz), 45.0, 29.3, 26.7; Anal. Calcd for $C_{16}H_{17}FN_3O_5S_4$: C, 37.39; H, 3.33; N, 8.18. Found: C, 37.51; H, 3.02; N, 8.12.

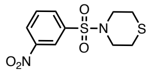

4-(3-nitrobenzenesulfonyl)thiomorpholine (**3.91**)

Thiomorpholine (2.00 mL, 19.85 mmol) and 3-nitrobenzenesulfonyl chloride (2.00 g, 9.02 mmol) was dissolved in 8.75 mL of 1,4-dioxane and heated to 60˚C. The mixture was stirred for 1 h at 60˚C, after which the reaction was cooled to rt and 20 mL of water was added. The mixture was extracted with DCM (3x20 mL), and the organics were dried over $MgSO_4$, filtered and concentrated. The crude mixture was purified via silica gel chromatography in 80% hexanes:20% ethyl acetate yielding a off-white solid (1.21g, 47%). mp = 151.3-154.7˚C; TLC R_f = 0.33 (20% EA/80% hexanes); IR (ATR) 3104, 3073, 2918, 2860, 1531, 1356, 1341, 899, 575 cm^{-1}; 1H NMR ($CDCl_3$, 400 MHz) δ 8.58 (t, *J* = 1.8 Hz, 1H), 8.47 (ddd, *J* = 0.8, 2.0, 8.3 Hz, 1H), 8.07 (dt, *J* = 0.8, 7.8 Hz, 1H), 7.78 (t, *J* = 8.1 Hz, 1H), 3.42 (t, *J* = 4.5 Hz, 4H), 2.74 (t, *J* = 4.8, 4H); $^{13}C\{^1H\}$ NMR ($CDCl_3$, 100 MHz) δ 148.5, 139.5, 132.8, 130.7, 127.4, 122.4, 47.9, 27.3. Anal. Calcd for $C_{10}H_{12}N_2O_4S_2$: C, 41.66; H, 4.20; N, 9.72. Found: C, 41.68; H, 4.46; N, 9.54.

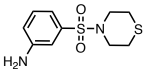

3-(thiomorpholine-4-sulfonyl)aniline (**3.94**)

4-(3-nitrobenzenesulfonyl)thiomorpholine (1.20 g, 4.16 mmol) was dissolved in acetic acid (13.9 mL, 0.3M) and iron powder (1.16 g, 20.81 mmol) was added. The mixture was heated to 60˚C and stirred for 1 h, after which the acetic acid was removed via vacuo. The residue was dissolved in ethyl acetate and washed with saturated $NaHCO_3$ until a pH of 8 was reached. The organics were washed with brine, dried over $MgSO_4$, filtered and concentrated. The recovered off-white solid was used without further purification (0.750g, 69%). mp = 149.8-152.5˚C; TLC $R_f = 0.43$ (20% EA/80% hexanes); IR (ATR) 3467, 3375, 2907, 2859, 2360, 1619, 1597, 1313, 1151, 716, 579 cm^{-1}; 1H NMR (DMSO-d_6, 400 MHz) δ 7.25 (t, *J* = 7.9 Hz, 1H), 6.91 (t, *J* = 1.9 Hz, 1H), 6.82-6.84 (m, 1H), 6.78-6.81 (m, 1H), 5.65 (bs, 2H), 3.17 (t, *J* = 4.9 Hz, 4H), 2.67 (t, *J* = 5.1, 4H); $^{13}C\{^1H\}$ NMR (DMSO-d_6, 100 MHz) δ 150.1, 136.9, 130.3, 118.4, 114.2, 111.8, 48.3, 26.9. Anal. Calcd for $C_{10}H_{14}N_2O_2S_2$: C, 46.49; H, 5.46; N, 10.84. Found: C, 46.63; H, 5.17; N, 10.96.

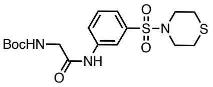

tert-butyl-N-([{3-(thiomorpholine-4-sulfonyl)phenyl]carbamoyl}methyl)carbamate (**3.97**)

Boc-glycine (0.244g , 1.39 mmol), 3-(thiomorpholine-4-sulfonyl)aniline (0.300 g, 1.16 mmol), HATU (0.883 g, 2.32 mmol) and DIPEA (0.59 mL, 2.32) were dissolved in 7 mL of dry DMAc under argon. The mixture was stirred for 24 h at rt. The reaction was diluted with ethyl acetate, washed with NH_4Cl (3x15 mL) and brine. The organics were dried over $MgSO_4$, filtered and concentrated. The crude mixture was purified via silica gel chromatography using 50% hexanes:50% ethyl acetate yielding a white solid (0.230g, 48%). mp = 169.0-172.9˚C; TLC $R_f =$ 0.44 (50% EA/50% hexanes); IR (ATR) 3657, 3436, 3267, 2980, 1702, 1673, 1499, 1163 cm^{-1};

1H NMR (CD_3OD, 400 MHz) δ 8.14 (bs, 1H), 7.77 (d, *J* = 8.0 Hz, 1H), 7.55 (t, *J* = 8.0 Hz, 1H), 7.48 (d, *J* = 7.9 Hz, 1H), 3.88 (s, 2H), 3.32-3.35 (m, 4H), 2.68 (t, *J* = 5.1, 4H), 1.47 (s, 9H); $^{13}C\{^1H\}$ NMR (CD_3OD, 100 MHz) δ 169.4, 156.4, 140.3, 137.1, 130.6, 123.7, 122.1, 117.6, 78.6, 48.3, 44.3, 28.7, 26.8. Anal. Calcd for $C_{17}H_{25}N_3O_5S_2$: C, 49.14; H, 6.06; N, 10.11. Found: C, 49.06; H, 6.35; N, 9.76.

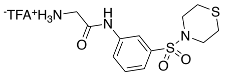

2-aminotrifluoroacetate-N-[3-(thiomorpholine-4-sulfonyl)phenyl]acetamide (**3.100**)

Boc protected amine **3.97** (0.220 g, 0.529 mmol) was dissolved in TFA and stirred at rt for 0.5 h. The solvent was removed under vacuo and a pure white solid was recovered (0.200 g, 88%). mp = 189.7-193.8°C; IR (ATR) 3189, 3081, 2980, 2854, 2639, 1670, 1322, 1201, 1139 cm^{-1}; 1H NMR (DMSO-d_6, 400 MHz) δ 10.90 (bs, 1H), 8.19 (bs, 3H), 8.13 (s, 1H), 7.80 (d, *J* = 8.3 Hz, 1H), 7.65 (t, *J* = 8.3 Hz, 1H), 7.48 (d, *J* = 7.9 Hz, 1H), 3.34 (s, 2H), 3.23 (t, *J* = 4.7 Hz, 4H), 2.68 (t, *J* = 5.0, 4H); $^{13}C\{^1H\}$ NMR (DMSO-d_6, 100 MHz) δ 166.0, 139.5, 137.4, 130.9, 123.8, 122.8, 117.7, 48.3, 41.6, 26.8. Anal. Calcd for $C_{14}H_{18}F_3N_3O_5S_3$: C, 39.16; H, 4.23; N, 9.79. Found: C, 39.55; H, 4.36; N, 9.50.

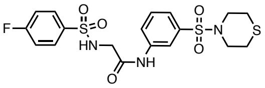

2-(4-fluorobenzenesulfonamido)-N-[3-(thiomorpholine-4-sulfonyl)phenyl]acetamide (**3.103**)

tert-butyl-N-([{3-(thiomorpholine-4-sulfonyl)phenyl]carbamoyl}methyl)carbamate (0.20g, 0.466 mmol) was dissolved in dry dichloromethane (0.700 mL, 0.6M) and dry TEA (0.143 mL, 1.025 mmol) and stirred at rt. 4-fluorobenzenesulfonyl chloride (0.100 g, 0.513 mmol) was added and the mixture was stirred at rt for 24 h. The mixture was washed with water (3x5 mL) followed by a 5% HCl solution. The organics were collected, dried over $MgSO_4$, filtered and concentrated. The crude mixture was purified by precipitation from dichloromethane yielding a white powder (0.059g, 27%). mp = 143.1-147.7˚C; TLC R_f = 0.44 (50% EA/50% hexanes); IR (ATR) 3318, 3284, 3221, 3137, 2918, 1697, 1590, 1548, 1314, 1148, 572 cm^{-1}; 1H NMR (Acetone-*d*$_6$, 400 MHz) δ 9.57 (s, 1H), 8.11 (s, 1H), 7.97-8.01 (m, 2H), 7.83 (dd, *J* = 0.9, 8.2 Hz, 1H), 7.57 (t, *J* = 7.8 Hz, 1H), 7.47 (d, *J* = 7.8 Hz, 1H), 7.33-7.37 (m, 2H), 6.99(bs, 1H), 3.86 (d, *J* = 5.9 Hz, 2H), 3.30 (t, *J* = 4.9 Hz, 4H), 2.70 (t, *J* = 4.0, 4H); $^{13}C\{^1H\}$ NMR (Acetone-*d*$_6$, 100 MHz) δ 166.7, 166.2, 139.4, 137.7, 136.6 (d, *J* = 3.1 Hz), 130.1 (d, *J* = 10.7 Hz), 129.8, 123.4, 122.4, 118.0, 116.1 (d, *J* = 23.1 Hz), 48.1, 46.3, 26.8. Anal. Calcd for $C_{18}H_{20}FN_3O_5S_3$: C, 45.65; H, 4.26; N, 8.87. Found: C, 45.43; H, 4.30; N, 8.80.

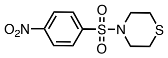

4-(4-nitrobenzenesulfonyl)thiomorpholine (**3.92**)

Thiomorpholine (2.00 mL, 19.85 mmol) and 4-nitrobenzenesulfonyl chloride (2.00 g, 9.02 mmol) was dissolved in 8.75 mL of 1,4-dioxane and heated to 60˚C. The mixture was stirred for 1 h at 60˚C, after which the reaction was cooled to rt and 20 mL of water was added. The mixture was extracted with DCM (3x20 mL), and the organics were dried over $MgSO_4$, filtered and concentrated. The crude mixture was purified via precipitation from DCM yielding a white solid (1.72g, 66%). mp = 145.6-150.3˚C; TLC R_f = 0.41 (20% EA/80% hexanes); IR (ATR) 3103, 2924, 2871, 1527, 1348, 1160, 1090, 748, 596 cm^{-1}; 1H NMR ($CDCl_3$, 400 MHz) δ 8.39 (d, *J* = 8.6 Hz, 2H), 7.93 (d, *J* =8.8 Hz, 2H), 3.31 (t, *J* = 4.6 Hz, 4H), 2.72 (t, *J* = 4.6, 4H);

$^{13}C\{^1H\}$ NMR ($CDCl_3$, 100 MHz) δ 150.2, 143.1, 128.5, 124.5, 47.9, 27.3. Anal. Calcd for $C_{10}H_{12}N_2O_4S_2$: C, 41.66; H, 4.20; N, 9.72. Found: C, 41.92; H, 4.01; N, 9.86.

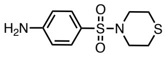

4-(thiomorpholine-4-sulfonyl)aniline (**3.95**)

4-(4-nitrobenzenesulfonyl)thiomorpholine (1.70 g, 5.90 mmol) was dissolved in acetic acid (19.7 mL, 0.3M) and iron powder (1.65 g, 29.48 mmol) was added. The mixture was heated to 60˚C and stirred for 1 h, after which the acetic acid was removed via vacuo. The residue was dissolved in ethyl acetate and washed with saturated $NaHCO_3$ until a pH of 8 was reached. The organics were washed with brine, dried over $MgSO_4$, filtered and concentrated. The recovered off-white solid was used without further purification (1.17g, 77%). mp = 176.0-179.5˚C; TLC $R_f = 0.53$ (20% EA/80% hexanes); IR (ATR) 3445, 3358, 3344, 2844, 1633, 1594, 1313, 1148, 896 cm^{-1}; 1H NMR (Acetone-d_6, 400 MHz) δ 7.74 (d, $J = 8.8$ Hz, 2H), 6.79 (d, $J = 8.8$ Hz, 2H), 5.55 (bs, 2H), 3.21 (t, $J = 5.0$ Hz, 4H), 2.68 (t, $J = 5.0$, 4H); $^{13}C\{^1H\}$ NMR (Acetone-d_6, 100 MHz) δ 152.9, 129.5, 122.8, 113.2, 48.1, 26.9. Anal. Calcd for $C_{10}H_{14}N_2O_2S_2$: C, 46.49; H, 5.46; N, 10.84. Found: C, 46.73; H, 5.64; N, 10.68.

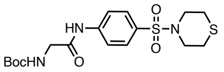

tert-butyl-N-([{4-(thiomorpholine-4-sulfonyl)phenyl]carbamoyl}methyl)carbamate (**3.98**)

Boc-glycine (0.408g , 2.32 mmol), 4-(thiomorpholine-4-sulfonyl)aniline (0.500 g, 1.94 mmol), HATU (1.472 g, 3.87 mmol) and DIPEA (0.99 mL, 3.87) were dissolved in 9.68 mL of dry DMAc under argon. The mixture was stirred for 24 h at rt. The reaction was diluted with ethyl acetate, washed with NH_4Cl (3x15 mL) and brine. The organics were dried over $MgSO_4$, filtered and concentrated. The crude mixture was purified via silica gel chromatography using 50% hexanes:50% ethyl acetate yielding a white solid (0.170g, 21%). mp = 179.5-183.8˚C; TLC R_f = 0.31 (50% EA/50% hexanes); IR (ATR) 3369, 3280, 3195, 3114, 2977, 2853, 1675, 1495, 1158 cm^{-1}; 1H NMR (CD_3OD, 400 MHz) δ 7.84 (d, *J* = 8.5 Hz, 2H), 7.73 (d, *J* = 8.5 Hz, 2H), 3.91 (s, 2H), 3.29-3.33 (m, 4H), 2.70 (t, *J* = 5.0, 4H), 1.49 (s, 9H); $^{13}C\{^1H\}$ NMR (DMSO-*d₆*, 100 MHz) δ 169.6, 156.4, 143.6, 130.1, 129.0, 119.4, 78.6, 48.2, 44.4, 28.7, 26.8. Anal. Calcd for $C_{17}H_{25}N_3O_5S_2$: C, 49.14; H, 6.06; N, 10.11. Found: C, 49.38; H, 6.32; N, 10.48.

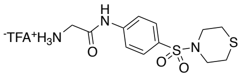

2-aminotrifluoroacetate-N-[4-(thiomorpholine-4-sulfonyl)phenyl]acetamide (**3.101**)

Boc protected amine **3.98** (0.160 g, 0.385 mmol) was dissolved in TFA and stirred at rt for 0.5 h. The solvent was removed under vacuo and a pure white solid was recovered (0.164 g, 100%). mp = 180.7-182.9˚C; IR (ATR) 3200, 3129, 2980, 2850, 1662, 1594, 1472, 1317, 1154 cm^{-1}; 1H NMR (DMSO-*d₆*, 400 MHz) δ 10.91 (s, 1H), 8.18 (bs, 3H), 7.83 (d, *J* = 8.8 Hz, 2H), 7.74 (d, *J* = 8.8 Hz, 2H), 3.84 (d, *J* = 4.0 Hz, 2H), 3.19 (bs, 4H), 2.66 (t, *J* = 4.8, 4H); $^{13}C\{^1H\}$ NMR (DMSO-*d₆*, 100 MHz) δ 166.1, 142.8, 131.0, 129.2, 119.6, 48.3, 41.6, 26.8. Anal. Calcd for $C_{14}H_{18}F_3N_3O_5S_3$: C, 39.16; H, 4.23; N, 9.79. Found: C, 39.28; H, 3.94; N, 9.43.

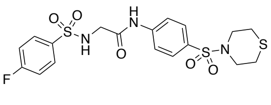

2-(4-fluorobenzenesulfonamido)-N-[4-(thiomorpholine-4-sulfonyl)phenyl]acetamide (**3.104**)

tert-butyl-N-([{4-(thiomorpholine-4-sulfonyl)phenyl]carbamoyl}methyl)carbamate (0.170g, 0.396 mmol) was dissolved in dry dichloromethane (0.595 mL, 0.6M) and dry TEA (0.121 mL, 0.871 mmol) and stirred at rt. 4-fluorobenzenesulfonyl chloride (0.085 g, 0.436 mmol) was added and the mixture was stirred at rt for 24 h. The mixture was washed with water (3x5 mL) followed by a 5% HCl solution. The organics were collected, dried over $MgSO_4$, filtered and concentrated. The crude mixture was purified by precipitation from dichloromethane yielding an off-white solid (0.068g, 36%). mp = 168.3-172.8˚C; TLC R_f = 0.39 (50% EA/50% hexanes); IR (ATR) 3650, 3326, 3288, 3209, 2980, 2888, 1700, 1589, 1540, 1147, 1090, 834, 572 cm^{-1}; 1H NMR (Acetone-*d*$_6$, 400 MHz) δ 9.61 (s, 1H), 7.97-8.00 (m, 2H), 7.83 (d, *J* = 8.6 Hz, 2H), 7.70 (d, *J* = 8.6 Hz, 2H), 7.32-7.37 (m, 2H), 6.99(bs, 1H), 3.88 (d, *J* = 5.6 Hz, 2H), 3.28 (t, *J* = 4.7 Hz, 4H), 2.69 (t, *J* = 5.0, 4H); $^{13}C\{^1H\}$ NMR (Acetone-*d*$_6$, 100 MHz) δ 166.8, 165.0 (d, *J* = 254.8 Hz), 142.6, 136.7 (d, *J* = 3.4 Hz), 131.5, 130.1 (d, *J* = 10.0 Hz), 128.6, 119.2, 116.1 (d, *J* = 23.1 Hz), 48.1, 46.3, 26.8. Anal. Calcd for $C_{18}H_{20}FN_3O_5S_3$: C, 45.65; H, 4.26; N, 8.87. Found: C, 45.34; H, 4.23; N, 8.66.

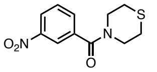

4-(3-nitrobenzoyl)thiomorpholine (**3.106**)

3-nitrobenzoic acid (3.00 g , 17.95 mmol), thiomorpholine (2.17 mL, 21.54 mmol), HATU (13.65 g, 35.90 mmol) and DIPEA (9.19 mL, 35.90) were dissolved in 90 mL of dry DMAc under argon. The mixture was stirred for 24 h at rt. The reaction was diluted with ethyl acetate, washed with NH_4Cl (3x15 mL) and brine. The organics were dried over $MgSO_4$, filtered and concentrated. The crude mixture was purified via silica gel chromatography using 50% hexanes:50% ethyl acetate yielding an off-white solid (3.70g, 82%). mp = 110.7-114.3˚C; TLC R_f = 0.38 (50% EA/50% hexanes); IR (ATR) 3093, 2919, 1632, 1526, 1438, 1351, 724 cm^{-1}; 1H NMR (CD_3OD, 400 MHz) δ 8.34 (dt, *J* = 8.2, 1.1 Hz, 1H), 8.29 (d, *J* = 1.6 Hz, 1H), 7.82 (dd, *J* =

1.1, 7.6 Hz, 1H), 7.73 (t, *J* = 7.8 Hz, 1H), 4.03 (bs, 2H), 3.67 (bs, 2H), 2.77 (bs, 2H), 2.63 (bs, 2H); $^{13}C\{^1H\}$ NMR (CD_3OD, 100 MHz) δ 168.8, 148.3, 137.2, 132.5, 129.9, 124.2, 121.6, 27.2, 26.7. Anal. Calcd for $C_{11}H_{12}N_2O_3S$: C, 52.37; H, 4.79; N, 11.10. Found: C, 52.15; H, 4.44; N, 11.14.

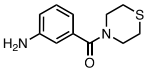

3-(thiomorpholine-4-carbonyl)aniline (**3.107**)

4-(3-nitrobenzoyl)thiomorpholine (3.00 g, 11.89 mmol) was dissolved in acetic acid (40 mL, 0.3M) and iron powder (3.33 g, 59.46 mmol) was added. The mixture was heated to 60˚C and stirred for 1 h, after which the acetic acid was removed via vacuo. The residue was dissolved in ethyl acetate and washed with saturated $NaHCO_3$ until a pH of 8 was reached. The organics were washed with brine, dried over $MgSO_4$, filtered and concentrated. The crude mixture was purified via silica gel chromatography using 100% ethyl acetate yielding a white solid (1.40g, 53%). mp = 109.3-113.1˚C; TLC R_f = 0.51 (100% EA); IR (ATR) 3430, 3340, 3228, 2965, 2911, 2859, 1598, 1578, 1432, 1224, 958, 747 cm^{-1}; 1H NMR (CD_3OD, 400 MHz) δ 7.15 (t, *J* = 7.8 Hz, 1H), 6.76 (dq, *J* = 0.9, 8.1 Hz, 1H), 6.68 (t, *J* = 1.6 Hz, 1H), 6.62 (dt, *J* = 0.9, 7.4 Hz, 1H), 3.97 (bs, 2H), 3.68 (bs, 2H), 2.71 (bs, 2H), 2.59 (bs, 2H); $^{13}C\{^1H\}$ NMR (CD_3OD, 100 MHz) δ 172.1, 148.3, 136.3, 129.1, 116.0, 114.9, 112.3, 27.4, 26.8. Anal. Calcd for $C_{11}H_{14}N_2OS$: C, 59.43; H, 6.35; N, 12.60. Found: C, 59.28; H, 6.15; N, 12.46.

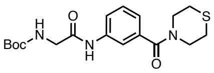

tert-butyl-N-({[3-(thiomorpholine-4-carbonyl)phenyl]carbamoyl}methyl)carbamate (**3.108**)

Boc-glycine (0.378g , 2.16 mmol), 3-(thiomorpholine-4-carbonyl)aniline (0.400 g, 1.80 mmol), HATU (1.368 g, 3.60 mmol) and DIPEA (0.63 mL, 3.60) were dissolved in 9 mL of dry DMAc under argon. The mixture was stirred for 24 h at rt. The reaction was diluted with ethyl acetate, washed with NH_4Cl (3x15 mL) and brine. The organics were dried over $MgSO_4$, filtered and concentrated. The crude mixture was purified via silica gel chromatography using 50% hexanes:50% ethyl acetate yielding an off-white solid (0.660g, 97%). mp = 58.7-62.5˚C; TLC R_f = 0.20 (50% EA/50% hexanes); IR (ATR) 3291, 3084, 2979, 2927, 1685, 1611, 1587, 1160 cm^{-1}; 1H NMR (Acetone-*d*$_6$, 400 MHz) δ 9.30 (s, 1H), 7.78 (s, 1H), 7.64 (d, *J* = 7.4 Hz, 1H), 7.37 (t, *J* = 8.1 Hz, 1H), 7.10 (d, *J* = 7.7 Hz, 1H), 6.20 (bs, 1H), 3.89 (d, *J* = 5.7 Hz, 2H), 3.80 (bs, 4H), 2.66 (bs, 4H), 1.43 (s, 9H); $^{13}C\{^1H\}$ NMR (CD_3OD, 100 MHz) δ 171.0,169.4, 169.4, 157.2, 138.7, 136.1, 129.1, 121.8, 120.9, 117.8, 79.3, 43.6, 37.5, 27.3. Anal. Calcd for $C_{18}H_{25}N_3O_4S$: C, 56.97; H, 6.64; N, 11.07. Found: C, 56.98; H, 6.73; N, 10.96.

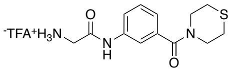

2-aminotrifluoroacetate-N-[3-(thiomorpholine-4-carbonyl)phenyl]carbamate (**3.109**)

tert-butyl-N-({[3-(thiomorpholine-4-carbonyl)phenyl]carbamoyl}methyl)carbamate (0.250 g, 0.659 mmol) was dissolved in TFA and stirred at rt for 0.5 h. The solvent was removed under vacuo and a pure off-white solid was recovered (0.247 g, 95%). mp = 155.5 – 158.3˚C; IR (ATR) 2980, 1671, 1586, 1563, 1466, 1431, 1177, 1128, 797 cm^{-1}; 1H NMR (Acetone-*d*$_6$, 400 MHz) δ 7.80 (s, 1H), 7.64 (d, *J* = 8.3 Hz, 1H), 7.40 (t, *J* = 7.7 Hz, 1H), 7.14 (d, *J* = 7.5 Hz, 1H), 4.82 (s, 2H), 3.79 (bs, 4H), 2.66 (bs, 4H); $^{13}C\{^1H\}$ NMR (CD_3CN, 100 MHz) δ 170.4, 165.1, 138.7, 137.5, 129.9, 122.9, 121.1, 118.4, 44.8, 41.8, 27.4. Anal. Calcd for $C_{15}H_{18}F_3N_3O_4S$: C, 45.80; H, 4.61; N, 10.68. Found: C, 45.99; H, 4.73; N, 10.90.

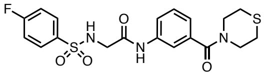

2-(4-fluorobenzenesulfonamido)-N-[3-(thiomorpholine-4-carbonyl)phenyl]acetamide (**3.110**)

2-aminotrifluoroacetate-N-[3-(thiomorpholine-4-carbonyl)phenyl]carbamate (0.200g, 0.508 mmol) was dissolved in dry dichloromethane (0.763 mL, 0.6M) and dry TEA (0.156 mL, 1.119 mmol) and stirred at rt. 4-fluorobenzenesulfonyl chloride (0.109 g, 0.559 mmol) was added and the mixture was stirred at rt for 24 h. The mixture was washed with water (3x5 mL) followed by a 5% HCl solution. The organics were collected, dried over $MgSO_4$, filtered and concentrated. The crude mixture was purified via silica gel chromatography using a solvent gradient of 50% hexanes:50% ethyl acetate to 100% ethyl acetate yielding a light orange solid (0.033g, 15%). mp = 79.1-83.3˚C; TLC $R_f = 0.53$ (100% EA); IR (ATR) 3215, 3104, 2981, 2915, 1685, 1588, 1166, 1152, 546 cm^{-1}; 1H NMR (Acetone-*d₆*, 400 MHz) δ 9.36 (s, 1H), 7.98 (q, *J* = 5.8 Hz, 2H), 7.69 (s, 1H), 7.56 (d, *J* = 8.4 Hz, 1H), 7.34 (q, *J* = 7.7 Hz, 3H), 7.11 (d, *J* = 7.3 Hz, 1H), 6.98 (bs, 1H), 3.82 (d, *J* = 5.9 Hz, 2H), 3.79 (bs, 4H), 2.65 (bs, 4H); $^{13}C\{^1H\}$ NMR (Acetone-d_6, 100 MHz) δ 169.4, 166.3, 165.0 (d, *J* = 251.8 Hz), 138.6, 137.1, 136.7 (d, *J* = 3.2 Hz), 130.1 (d, *J* = 9.9 Hz), 129.0, 122.1, 120.2, 117.8, 116.1 (d, *J* = 23.0 Hz), 46.2, 27.1. Anal. Calcd for $C_{19}H_{20}FN_3O_4S_2$: C, 52.16; H, 4.61; N, 9.60. Found: C, 52.27; H, 4.86; N, 9.45.

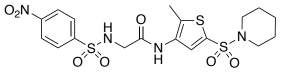

N-[2-methyl-5-(piperidine-1-sulfonyl)thiophen-3-yl]-2-(4-nitrobenzenesulfonamido)acetamide **(3.113)**

2-aminotrifluoroacetate-N-[2-methyl-5-(thiomorpholine-4-sulfonyl)thiophene-3-yl]acetamide (**3.49**) (0.200 g, 0.464 mmol) was dissolved in dry DCM (0.730 mL, 0.7M) and dry TEA (0.147 mL, 1.054 mmol) was added. 4-nitrobenzenesulfonyl chloride (0.118 g, 0.527 mmol) was added and the mixture was stirred at rt for 24 h under argon. The reaction was washed with H_2O, followed by a 5% HCl solution. The organics were collected and dried over Na_2SO_4, filtered, and concentrated. The crude mixture was purified by precipitation from dichloromethane yielding a yellow solid (0.027g, 12%). mp = 201.2-204.4˚C; TLC R_f = 0.31 (50% EA/50% hexane); IR (ATR) 3385, 3194, 3117, 2925, 2857, 1696, 1582, 1522, 1339, 1158, 1146 cm^{-1}; 1H NMR (CD_3OD, 400 MHz) δ 8.39 (d, *J* = 8.9 Hz, 2H), 8.13 (d, *J* = 8.6 Hz, 2H), 7.43 (s, 1H), 3.88 (s, 2H), 2.97 (t, *J* = 5.3 Hz, 4H), 2.34 (s, 3H), 1.65 (p, *J* = 5.4 Hz, 4H), 1.44-1.50 (m, 2H); $^{13}C\{^1H\}$ NMR (CD_3OD, 100 MHz) 167.5, 150.1, 146.1, 135.1, 131.8, 130.5, 129.2, 128.3, 123.9, 46.7, 45.0, 24.9, 23.0, 11.1.; Anal. Calcd for $C_{18}H_{22}N_4O_7S_3$: C, 43.02; H, 4.41; N, 11.15. Found: C, 43.28; H, 4.56; N, 10.93.

3.7 References

(1) Pedicone, C.; Meyer, S. T.; Chisholm, J. D.; Kerr, W. G. Targeting SHIP1 and SHIP2 in Cancer. *Cancers (Basel).* **2021**, *13* (4), 1–24.

(2) Brooks, R.; Fuhler, G. M.; Iyer, S.; Smith, M. J.; Park, M.-Y.; Paraiso, K. H. T.; Engelman, R. W.; Kerr, W. G. SHIP1 Inhibition Increases Immunoregulatory Capacity and Triggers Apoptosis of Hematopoietic Cancer Cells. *J. Immunol.* **2010**, *184* (7), 3582–3589.

(3) Saz-Leal, P.; del Fresno, C.; Brandi, P.; Martínez-Cano, S.; Dungan, O. M.; Chisholm, J. D.; Kerr, W. G.; Sancho, D. Targeting SHIP-1 in Myeloid Cells Enhances Trained Immunity and Boosts Response to Infection. *Cell Rep.* **2018**, *25* (5), 1118–1126.

(4) Fuhler, G.; Brooks, R. Therapeutic Potential of SH2 Domain-Containing Inositol-5′-Phosphatase 1 (SHIP1) and SHIP2 Inhibition in Cancer. *Mol. Med.* **2012**, *18* (1), 1.

(5) Hoekstra, E.; Das, A. M.; Willemsen, M.; Swets, M.; Kuppen, P. J. K.; van der Woude, C. J.; Bruno, M. J.; Shah, J. P.; Ten Hagen, T. L. M.; Chisholm, J. D.; et al. Lipid Phosphatase SHIP2 Functions as Oncogene in Colorectal Cancer by Regulating PKB Activation. *Oncotarget* **2016**, *7* (45), 1–16.

(6) Pedicone, C.; Fernandes, S.; Dungan, O. M.; Dormann, S. M.; Viernes, D. R.; Adhikari, A. A.; Choi, L. B.; De Jong, E. P.; Chisholm, J. D.; Kerr, W. G. Pan-SHIP1/2 Inhibitors Promote Microglia Effector Functions Essential for CNS Homeostasis. *J. Cell Sci.* **2020**, *133* (5).

(7) Chamberlain, T. C.; Cheung, S. T.; Yoon, J. S. J.; Ming-Lum, A.; Gardill, B. R.; Shakibakho, S.; Dzananovic, E.; Ban, F.; Samiea, A.; Jawanda, K.; et al. Interleukin-10 and Small Molecule SHIP1 Allosteric Regulators Trigger Anti-Inflammatory Effects

through SHIP1/STAT3 Complexes. *iScience* **2020**, *23* (8), 101433.

(8) Ong, C. J.; Ming-Lum, A.; Nodwell, M.; Ghanipour, A.; Yang, L.; Williams, D. E.; Kim, J.; Demirjian, L.; Qasimi, P.; Ruschmann, J.; et al. Small-Molecule Agonists of SHIP1 Inhibit the Phosphoinositide 3-Kinase Pathway in Hematopoietic Cells. *Blood* **2007**, *110* (6), 1942–1949.

(9) Andersen, R. J. Sponging off Nature for New Drug Leads. *Biochem. Pharmacol.* **2017**, *139*, 3–14.

(10) Yang, L.; Williams, D. E.; Mui, A.; Ong, C.; Krystal, G.; van Soest, R.; Andersen, R. J. Synthesis of Pelorol and Analogues: Activators of the Inositol 5-Phosphatase SHIP. *Org. Lett.* **2005**, *7* (6), 1073–1076.

(11) Nickel, J. C.; Moldwin, R.; Hanno, P.; Dmochowski, R.; Peters, K. M.; Payne, C.; Wein, A. Targeting the SHIP1 Pathway Fails to Show Treatment Benefit in Interstitial Cystitis/Bladder Pain Syndrome: Lessons Learned from Evaluating Potentially Effective Therapies in This Enigmatic Syndrome. *J. Urol.* **2019**, *202* (2), 301–308.

(12) Kerr, W. G.; Pedicone, C.; Dormann, S.; Pacherille, A.; Chisholm, J. D. Small Molecule Targeting of SHIP1 and SHIP2. *Biochem. Soc. Trans.* **2020**, *48* (1), 291–300.

(13) Sala Frigerio, C.; Wolfs, L.; Fattorelli, N.; Thrupp, N.; Voytyuk, I.; Schmidt, I.; Mancuso, R.; Chen, W.-T.; Woodbury, M. E.; Srivastava, G.; et al. The Major Risk Factors for Alzheimer's Disease: Age, Sex, and Genes Modulate the Microglia Response to Aβ Plaques. *Cell Rep.* **2019**, *27* (4), 1293-1306.e6.

(14) Kerr, W. G.; Park, M.-Y.; Maubert, M.; Engelman, R. W. SHIP Deficiency Causes Crohn's Disease-like Ileitis. *Gut* **2011**, *60* (2), 177–188.

(15) Fernandes, S.; Srivastava, N.; Sudan, R.; Middleton, F. A.; Shergill, A. K.; Ryan, J. C.;

Kerr, W. G. SHIP1 Deficiency in Inflammatory Bowel Disease Is Associated With Severe Crohn's Disease and Peripheral T Cell Reduction. *Front. Immunol.* **2018**, *9*.

(16) Somasundaram, R.; Fernandes, S.; Deuring, J. J.; de Haar, C.; Kuipers, E. J.; Vogelaar, L.; Middleton, F. A.; van der Woude, C. J.; Peppelenbosch, M. P.; Kerr, W. G.; et al. Analysis of SHIP1 Expression and Activity in Crohn's Disease Patients. *PLoS One* **2017**, *12* (8), e0182308.

(17) Wallach, I.; Dzamba, M.; Heifets, A. AtomNet: A Deep Convolutional Neural Network for Bioactivity Prediction in Structure-Based Drug Discovery. **2015**.

(18) Pedicone, C.; Fernandes, S.; Matera, A.; Meyer, S. T.; Loh, S.; Ha, J. H.; Bernard, D.; Chisholm, J. D.; Paolicelli, R. C.; Kerr, W. G. Discovery of a Novel SHIP1 Agonist That Promotes Degradation of Lipid-Laden Phagocytic Cargo by Microglia. *iScience* **2022**, *25* (4), 104170.

(19) Sone, T.; Abe, Y.; Sato, N.; Ebina, M. The Use of N , N -Dimethylformamide–Sulfonyl Chloride Complex for the Preparation of Thiophenesulfonyl Chlorides. *Bull. Chem. Soc. Jpn.* **1985**, *58* (3), 1063–1064.

(20) Gronowitz, S.; Ander, I.; Lund, H.; Nimmich, W.; Servin, R.; Sternerup, H. On the Base-Catalyzed Reaction of Some Methyl Nitrothiophenes with Aldehydes. An Unexpected Cyclobutane Formation. *Acta Chem. Scand.* **1975**, *29b*, 513–523.

(21) Lynch, T.; Price, A. The Effect of Cytochrome P450 Metabolism on Drug Response, Interactions, and Adverse Effects. *Am. Fam. Physician* **2007**, *76* (3), 391–396.

(22) Purohit, V.; Basu, A. K. Mutagenicity of Nitroaromatic Compounds. *Chem. Res. Toxicol.* **2000**, *13* (8), 673–692.

(23) Wang, P.; Leng, J.; Wang, Y. DNA Replication Studies of N-Nitroso Compound–Induced

O6-Alkyl-2′-Deoxyguanosine Lesions in Escherichia Coli. *J. Biol. Chem.* **2019**, *294* (11), 3899–3908.

(24) Fahey, J. M.; Stancill, J. S.; Smith, B. C.; Girotti, A. W. Nitric Oxide Antagonism to Glioblastoma Photodynamic Therapy and Mitigation Thereof by BET Bromodomain Inhibitor JQ1. *J. Biol. Chem.* **2018**, *293* (14), 5345–5359.

(25) Enoki, T.; Tominaga, T.; Takashima, F.; Ohnogi, H.; Sagawa, H.; Kato, I. Anti-Tumor-Promoting Activities of Agaro-Oligosaccharides on Two-Stage Mouse Skin Carcinogenesis. *Biol. Pharm. Bull.* **2012**, *35* (7), 1145–1149.

Appendix: Biological Testing Procedures

Malachite Green Phosphatase Release Assays

Malachite Green Phosphatase Release Assays (Echelon-Inc.) were performed with recombinant human truncated SHIP1 (tSHIP1) or tSHIP2. Briefly, serial dilutions of the compounds were dissolved in appropriate solvent (e.g. DMSO) and added to recombinant human tSHIP1 or tSHIP2 diluted in enzyme reaction buffer (50 mM Hepes pH 7.4, 150mM NaCl, 1mM $MgCl_2$, 0.25mM EDTA) in triplicate reactions in 96-well plates (22.5 µl/reaction). Reactions were incubated for 5 min at room temperature. Phosphatidylinositol 3,4,5-trisphosphate diC8 (PI(3,4,5)P3diC8) (Echelon-Inc.) was added to each reaction at a final concentration of 100 µM and the reaction were carried out for 30 min at 37℃ in a final volume of 25 µl/well. Final solvent concentration was ≤ 1%. Following incubation, 100 µL of Malachite Green Solution (Echelon-Inc.) was added to each well and plates were incubated at room temperature in the dark for 20 min. Plates were then read at 620nm.

Intracellular flow for iNOS detection

BV2 cells were plated at 5x105 cells/mL, 0.5 mL/well in 24 well plates and allowed to adhere 2-4h at 37˚C, 5% CO2. Cells were treated with **3.7** (10mM) or Vehicle (Veh: 0.25%DMSO) for 1h. LPS (100 ng/ml) or PBS were added to appropriate wells and incubation was continued for 1h. The second round of **3.7** (10mM) or Veh was added to each well such that the final concentration of DMSO was 0.5% in each well and the concentration of **3.7** was 10mM or 20mM as indicated. Cells were washed with PBS (1mL/well) and were harvested with PBS 1% EDTA. Cells were collected in FACS tubes (BD Biosciences) and washed with 2mL cold PBS and spun down 5 min at 350xg. Cell pellets were stained with Zombie Aqua (0.4mL of stock diluted 1:100 in 50mL of PBS/test) for 20min on ice, washed with 2mL cold PBS and spun down 5 min at 350xg. Pellets were re- suspended in 15mL Fc Block (TruStain FcX, Biolegend), and stained with surface antibody cocktail (CD11b-APC_Cyanine7 (Clone M1/70) and CD45-PerCP (Clone 30-F11) in 35mL FB/sample for 20min on ice. Cells were washed with 2mL cold PBS and spun down 5 min at 350xg. Cells were fixed with 200mL eBioscience IC Fixation Buffer (ThermoFisher Scientific) for 20min on ice and washed with 1XPB and spun down 5 min at 400xg. Pellets were resuspended in 25mL Fc Block in 1XPB and stained with iNOS-PE_eFlour610 (CloneCxNFT). Cells were washed twice with 2mL 1XPB and spun down 5 min at 400xg. FMO control was stained with the cocktail minus the iNOS antibody. Final pellets were resuspended in 150mL 1XPB and samples were acquired on the Cytek Aurora, after acquiring single-stained colors and unstained control cells. Samples were unmixed using SpectroFlo Version 2.2.0.2. FSC files were exported and further analyzed with FlowJo Version 10.8.1

MTT Assay Protocol for Cell Viability and Proliferation

Preincubate WEHI-164 cells at a concentration of 1 × 106 cells/ml in culture medium with 1 µg/ ml actinomycin C1 for 3 h at 37 °C and 5-6.5% CO2. Seed cells at a concentration of 5 × 104 cells/ well in 100 µl culture medium containing 1 µg/ml actinomycin C1 and various amounts of hTNF-α (final concentration e.g., 0.001–0.5 ng/ml) into microplates (tissue culture grade, 96 wells, flat bottom). Incubate cell cultures for 24 h at +37 °C and 5-6.5% CO2. After the incubation period, add 10 µl of the MTT labeling reagent (final concentration 0.5 mg/ml) to each well. Incubate the microplate for 4 h in a humidified atmosphere (e.g., +37 °C, 5-6.5% CO2). Add 100 µl of the Solubilization solution into each well. Allow the plate to stand overnight in the incubator in a humidified atmosphere (e.g., +37 °C, 5-6.5% CO2). Check for complete solubilization of the purple formazan crystals and measure the absorbance of the samples using a microplate (ELISA) reader. The wavelength to measure absorbance of the formazan product is between 550 and 600 nm according to the filters available for the ELISA reader, used. The reference wavelength should be more than 650 nm

Appendix: Spectroscopic Data

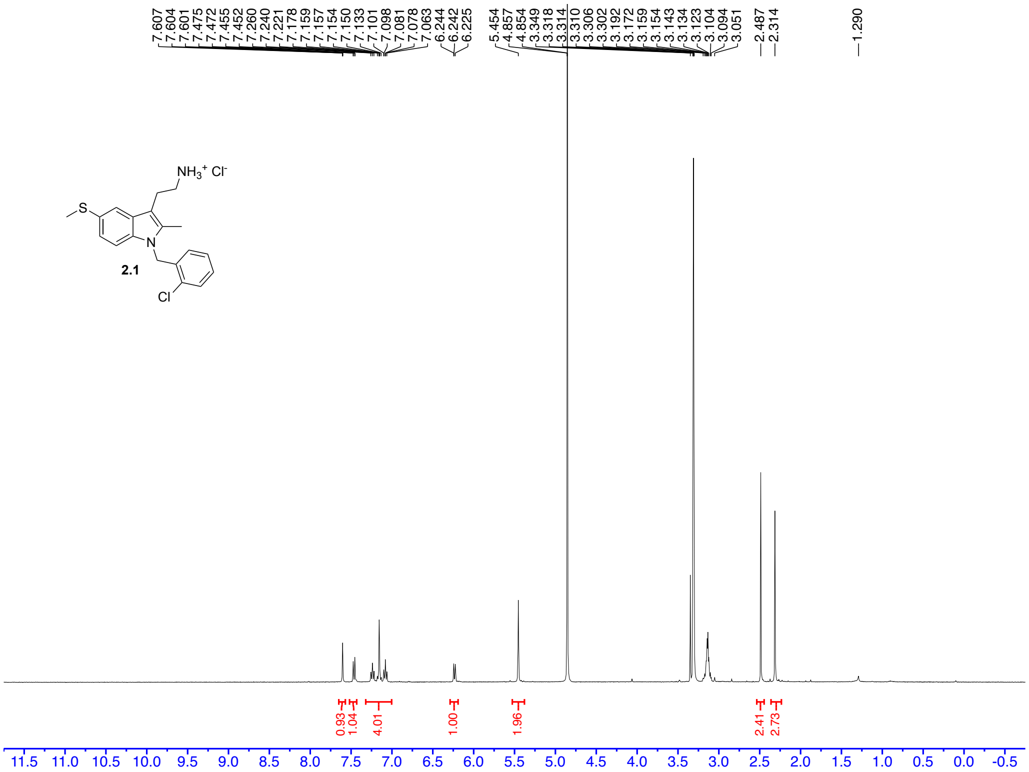

STM-2-123 - 1H NMR - 400.13 MHz - MeOD

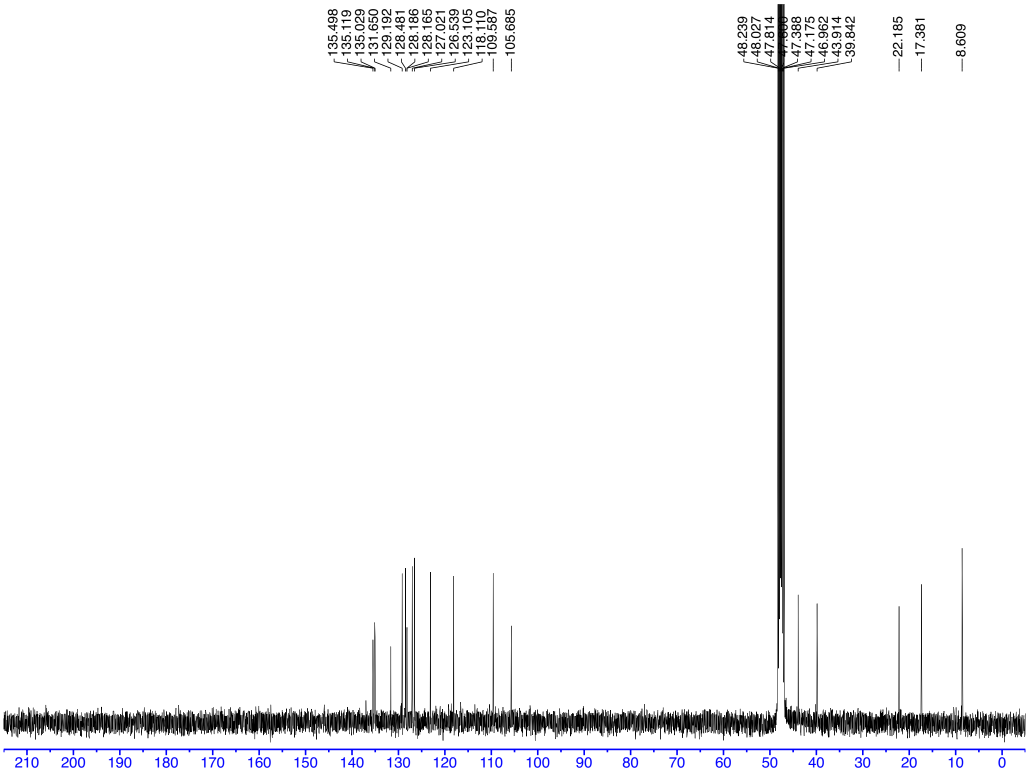

STM-2-123 CNMR (K123 Concentrated) - 13C NMR - 100.62 MHz - MeOD

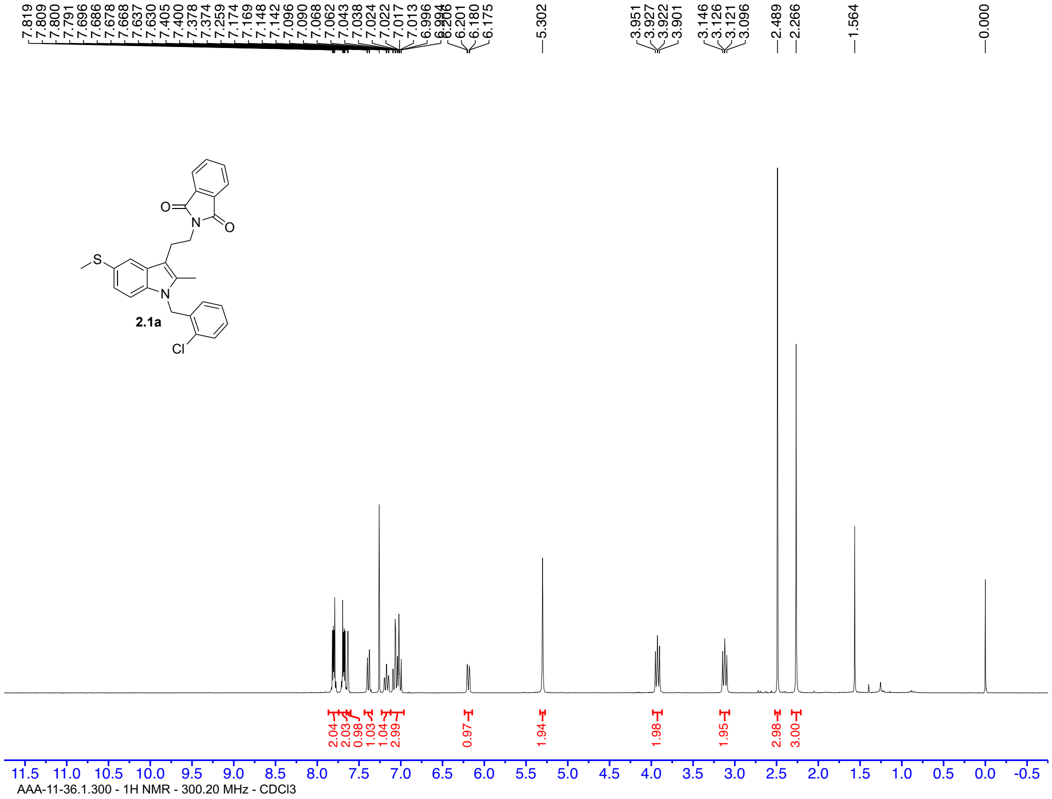
7.819
7.809
7.800
7.791
7.696
7.686
7.678
7.668
7.637
7.630
7.405
7.400
7.378
7.374
7.259
7.174
7.169
7.148
7.142
7.096
7.090
7.068
7.062
7.043
7.038
7.024
7.022
7.017
7.013
6.996
6.994
6.206
6.201
6.180
6.175
5.302
3.951
3.927
3.922
3.901
3.146
3.126
3.121
3.096
2.489
2.266
1.564
0.000
O
N
O
S
N
2.1a
Cl
2.04
2.03
0.98
1.03
1.04
2.99
0.97
1.94
1.98
1.95
2.98
3.00
11.5 11.0 10.5 10.0 9.5 9.0 8.5 8.0 7.5 7.0 6.5 6.0 5.5 5.0 4.5 4.0 3.5 3.0 2.5 2.0 1.5 1.0 0.5 0.0 -0.5
AAA-11-36.1.300 - 1H NMR - 300.20 MHz - CDCl3

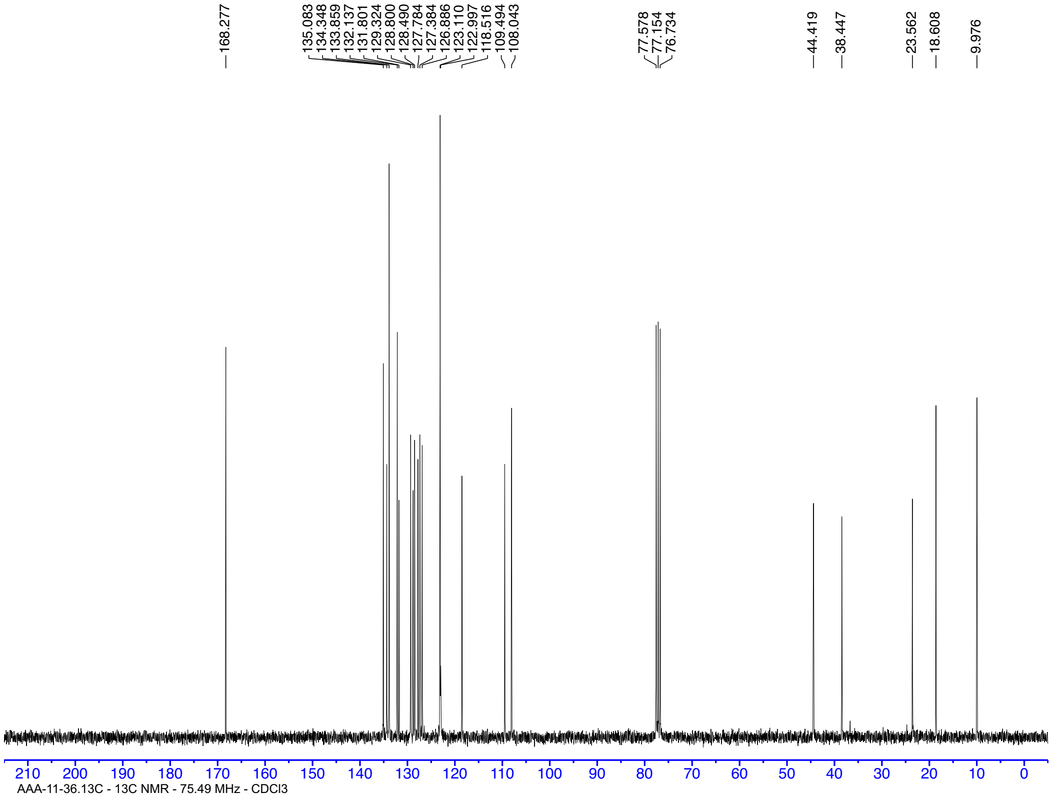
168.277
135.083
134.348
133.859
132.137
131.801
129.324
128.800
128.490
127.784
127.384
126.886
123.110
122.997
118.516
109.494
108.043
77.578
77.154
76.734
44.419
38.447
23.562
18.608
9.976
210 200 190 180 170 160 150 140 130 120 110 100 90 80 70 60 50 40 30 20 10 0
AAA-11-36.13C - 13C NMR - 75.49 MHz - CDCl3

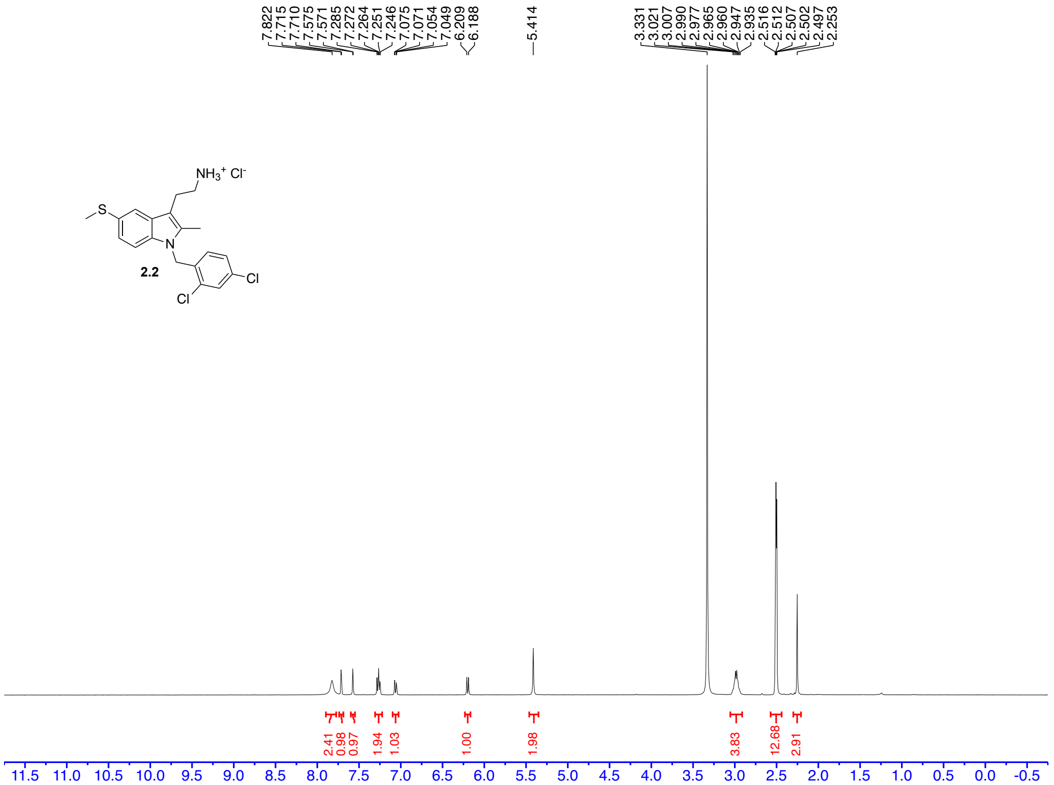

2.2

K194 Recrystalized - 1H NMR - 400.13 MHz - DMSO

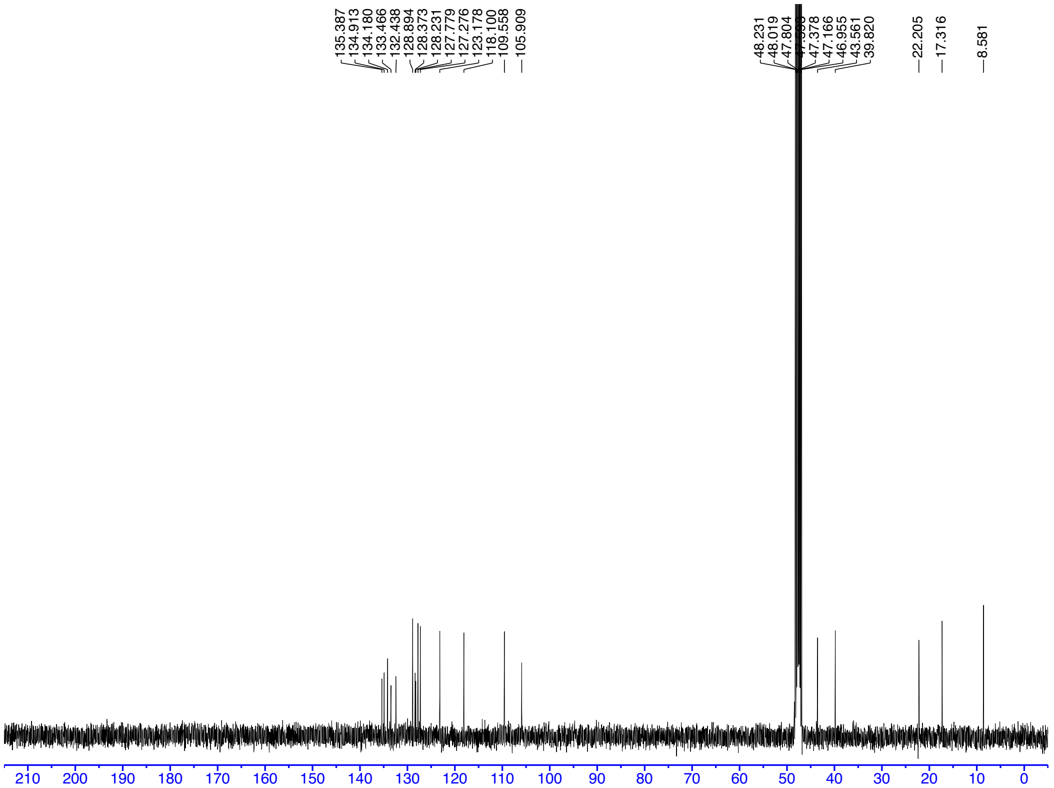

STM-2-129 CNMR - 13C NMR - 100.62 MHz - MeOD

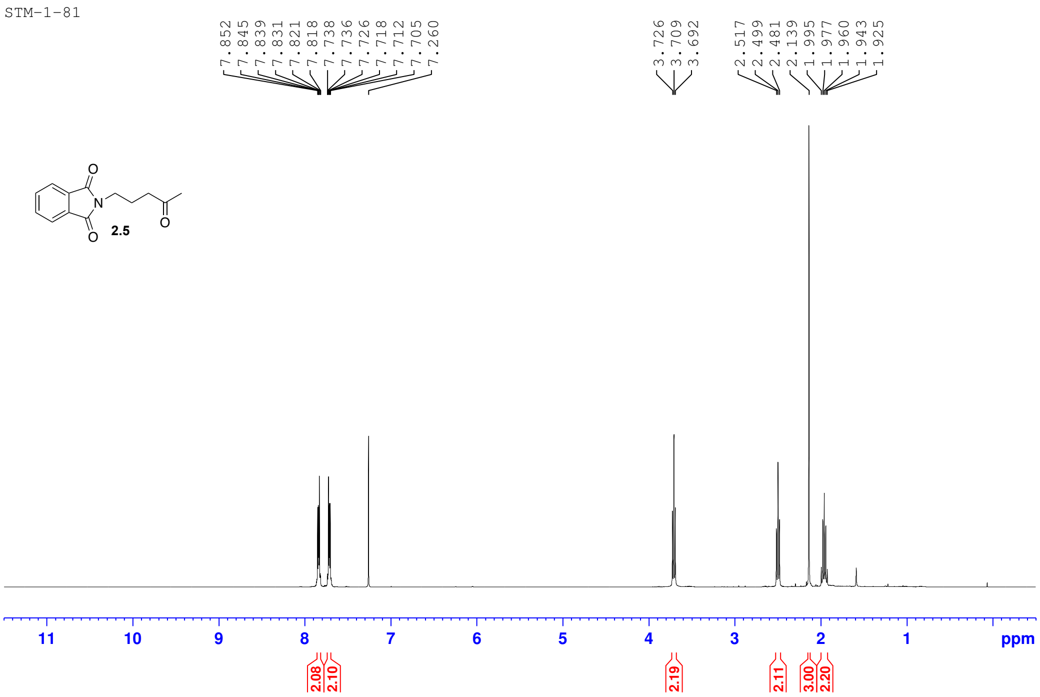
STM-1-81
7.852
7.845
7.839
7.831
7.821
7.818
7.738
7.736
7.726
7.718
7.712
7.705
7.260
3.726
3.709
3.692
2.517
2.499
2.481
2.139
1.995
1.977
1.960
1.943
1.925
O
N
O
2.5
O
11
10
9
8
7
6
5
4
3
2
1
ppm
2.08
2.10
2.19
2.11
3.00
2.20

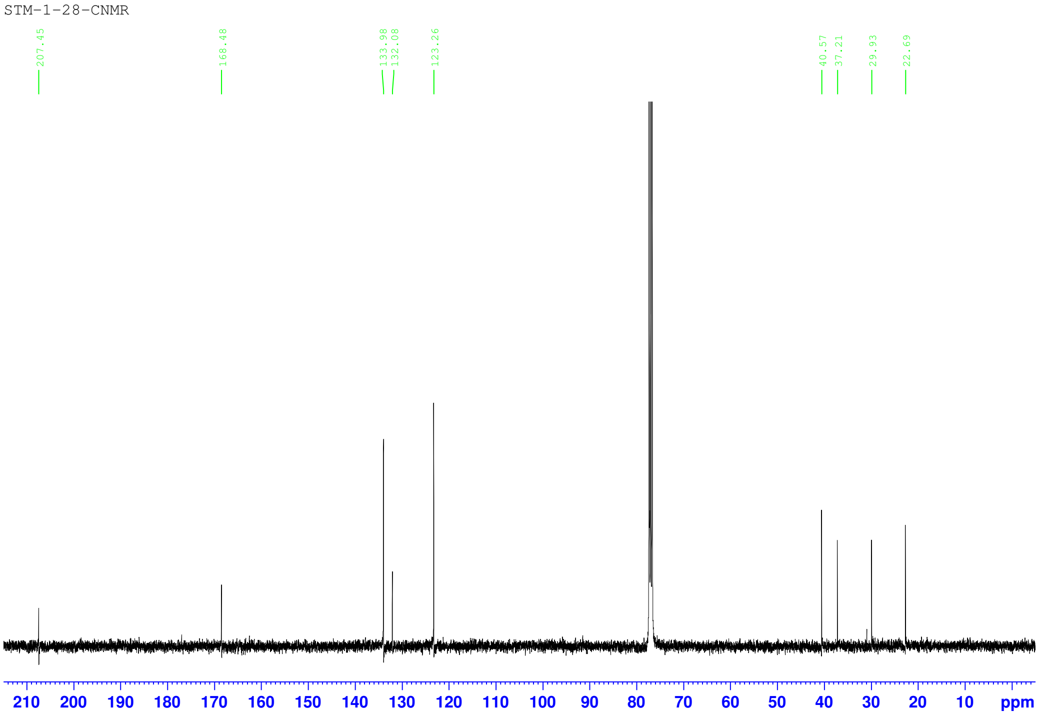
STM-1-28-CNMR
207.45
168.48
133.98
132.08
123.26
40.57
37.21
29.93
22.69
210
200
190
180
170
160
150
140
130
120
110
100
90
80
70
60
50
40
30
20
10
ppm

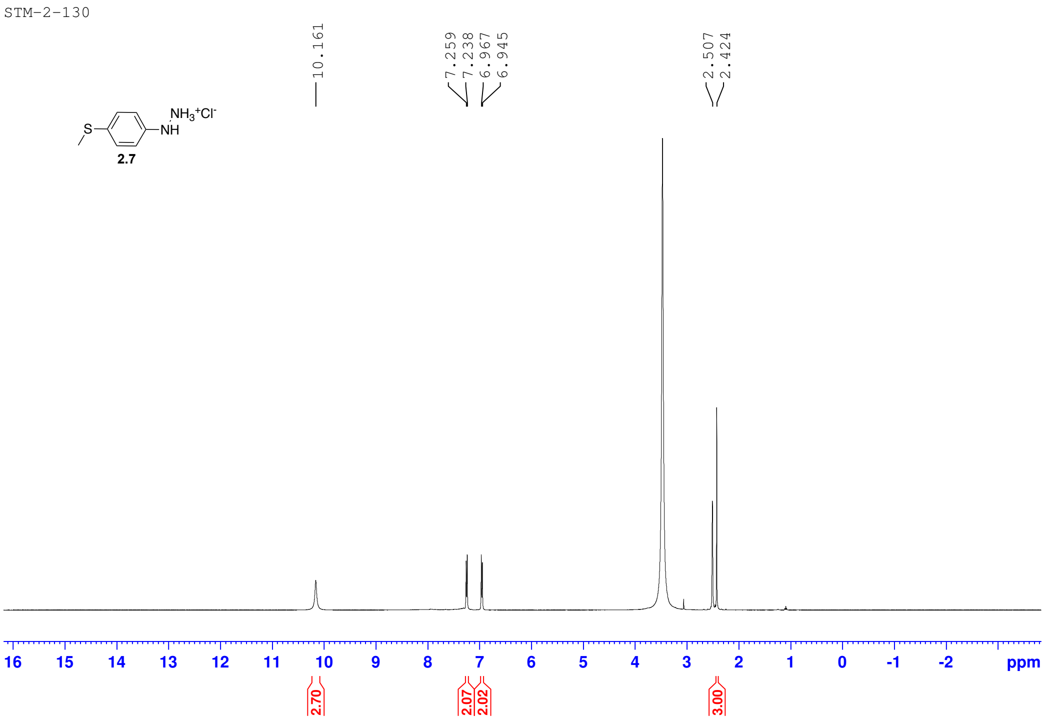
STM-2-130
10.161
7.259
7.238
6.967
6.945
2.507
2.424
S
NH
NH3+Cl-
2.7
16
15
14
13
12
11
10
9
8
7
6
5
4
3
2
1
0
-1
-2
ppm
2.70
2.07
2.02
3.00

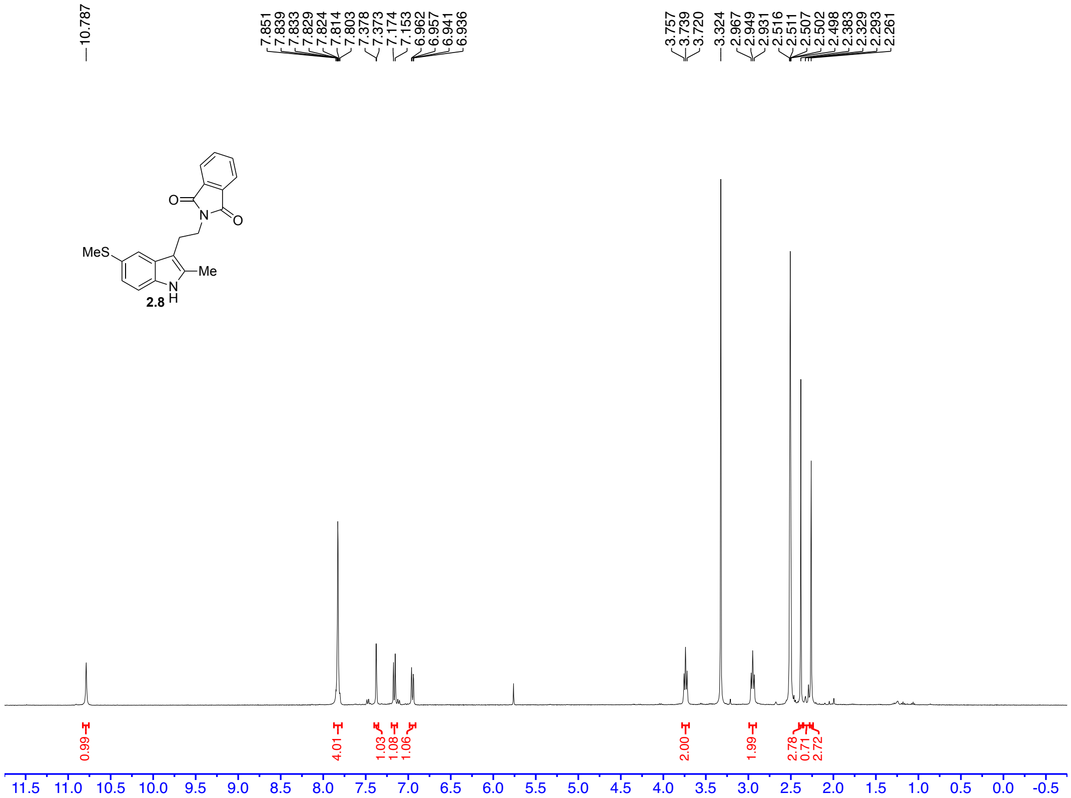

STM-2-117 - 1H NMR - 400.13 MHz - DMSO

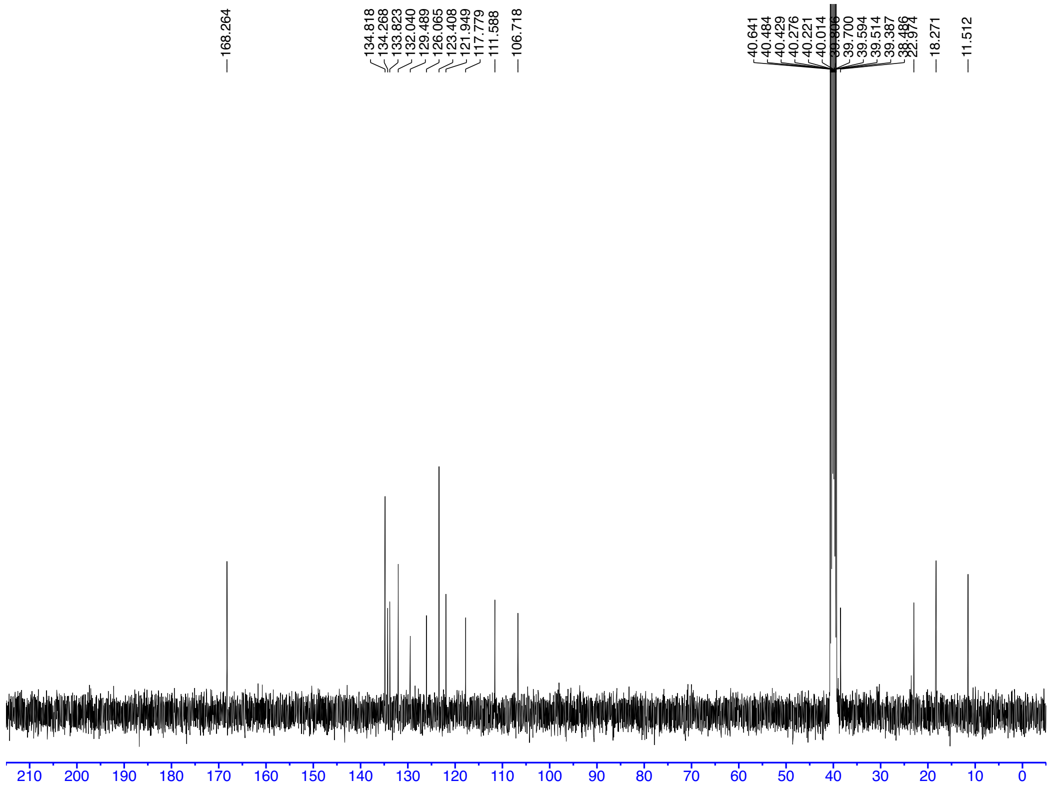

STM-2-117 CNMR - 13C NMR - 100.62 MHz - DMSO

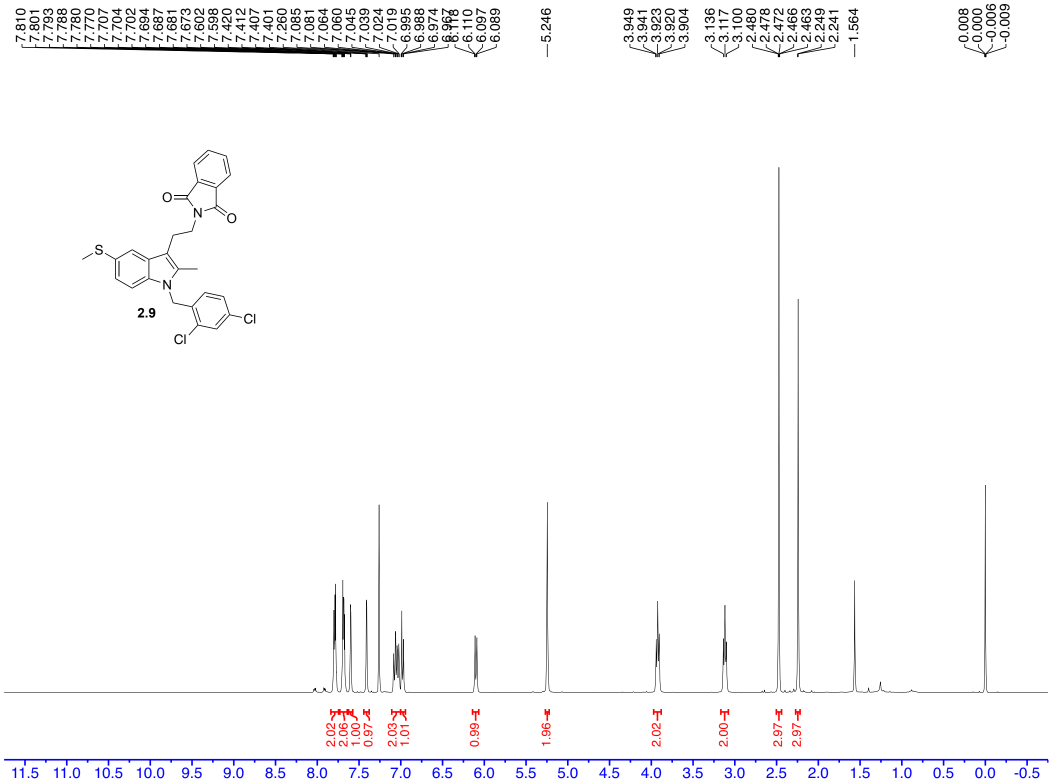

AAA-11-35.1H - 1H NMR - 400.13 MHz - CDCl3

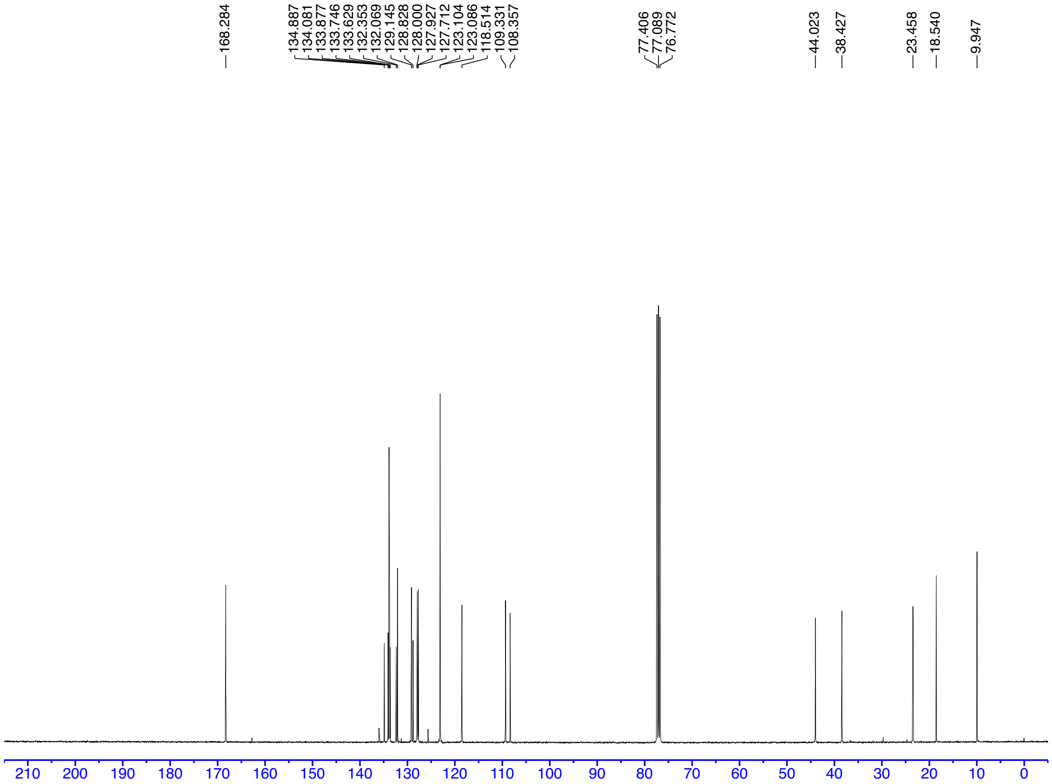

AAA-11-35.13C - 13C NMR - 100.62 MHz - CDCl3

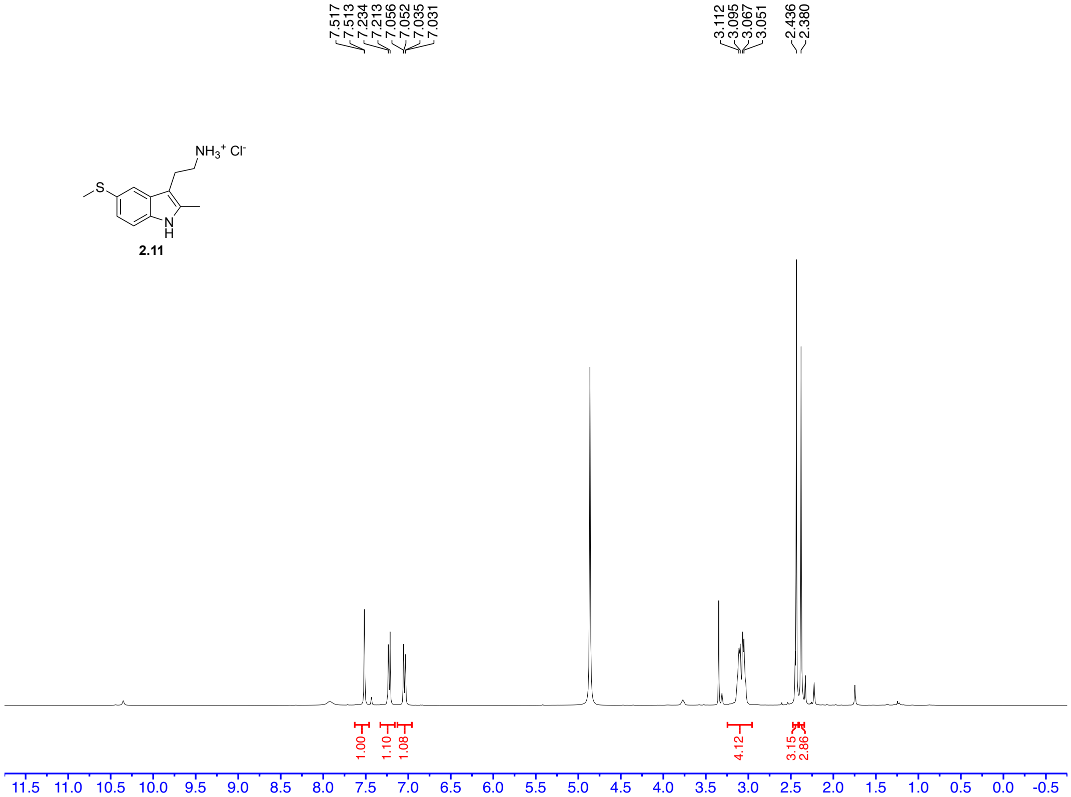

STM-3-16 Ethanol Removal - 1H NMR - 400.13 MHz - MeOD

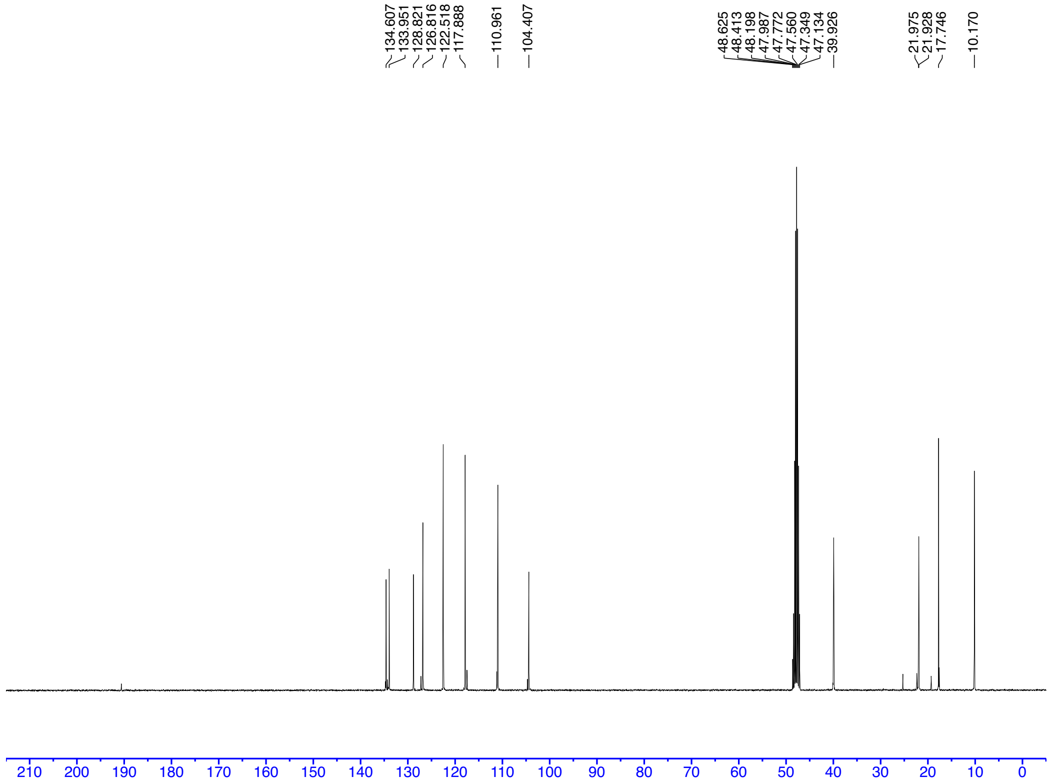

STM-3-16 CNMR Ethanol Removal - 13C NMR - 100.62 MHz - MeOD

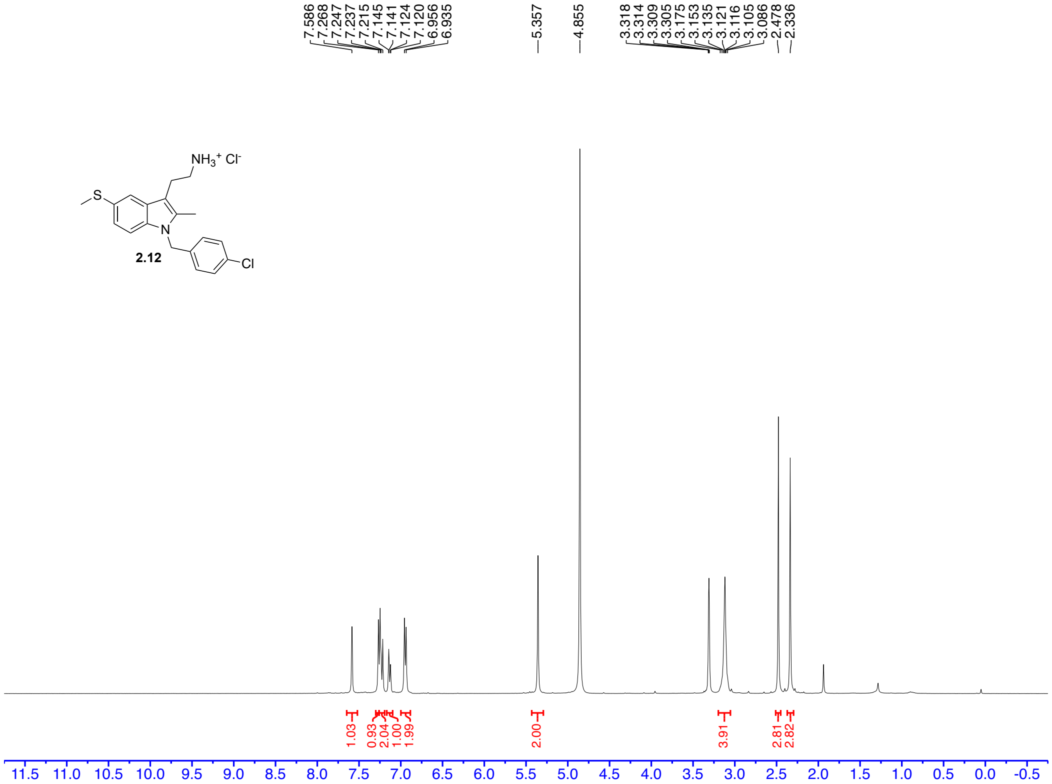

STM-2-150 diluted Second attempt - 1H NMR - 400.13 MHz - MeOD

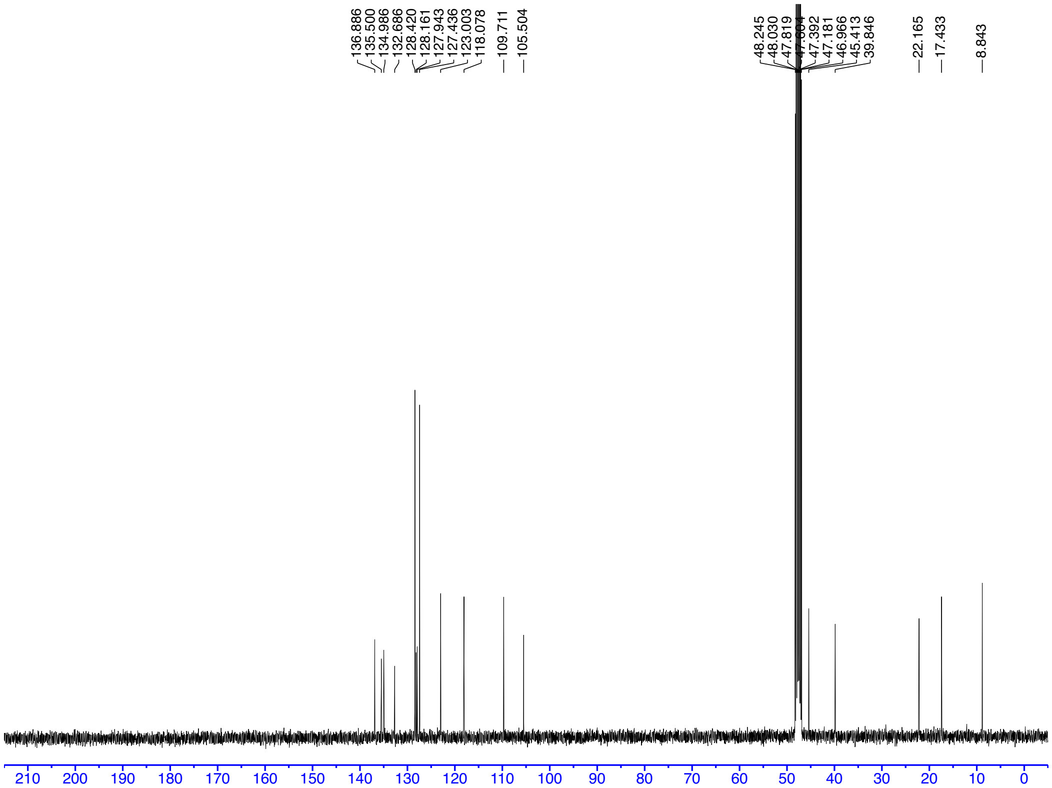

STM-2-150 CNMR - 13C NMR - 100.62 MHz - MeOD

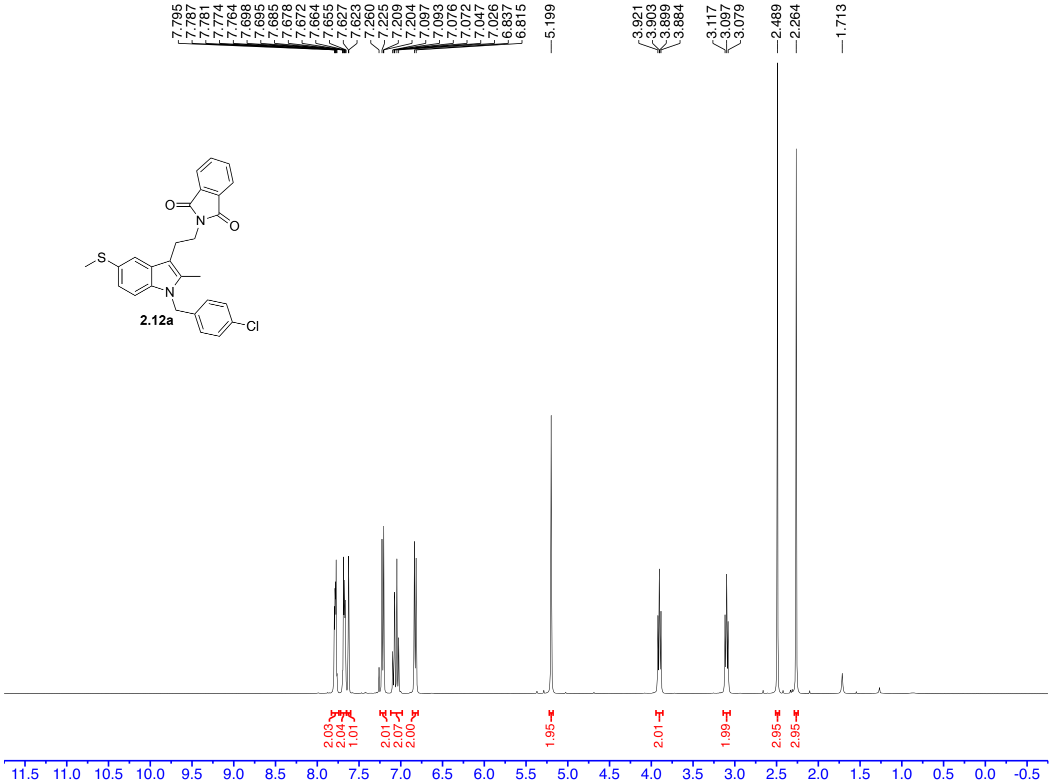

STM-2-144 Solvent pump - 1H NMR - 400.13 MHz - CDCl3

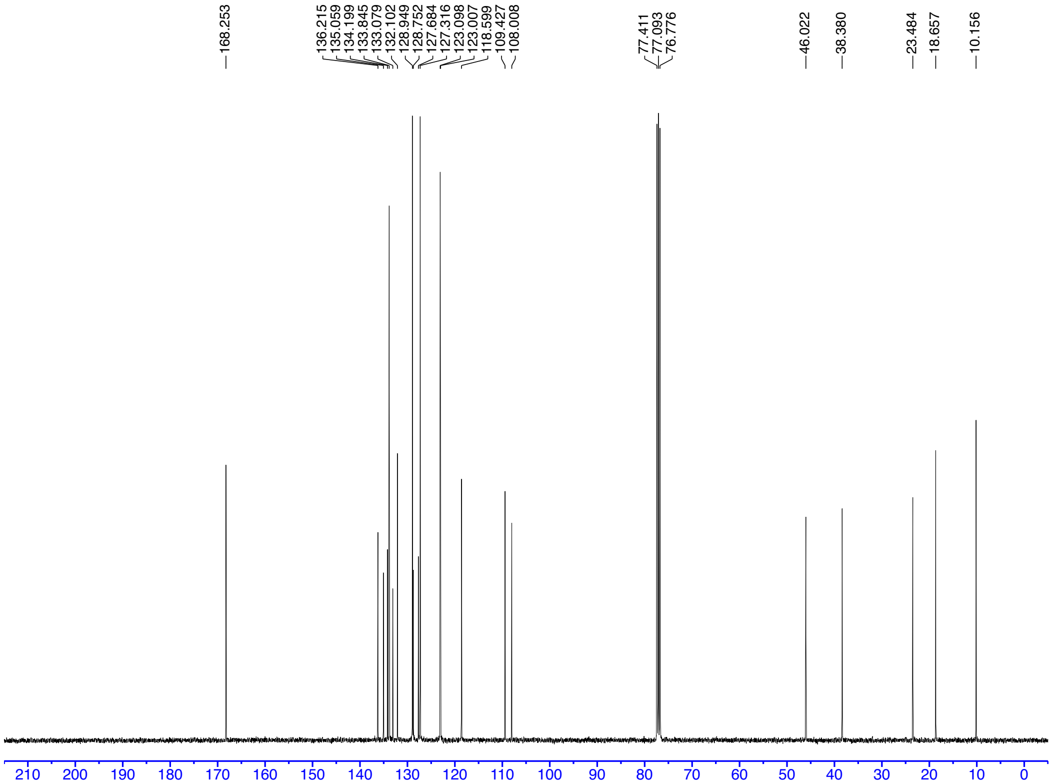

STM-2-144 Solvent pump CNMR - 13C NMR - 100.62 MHz - CDCl3

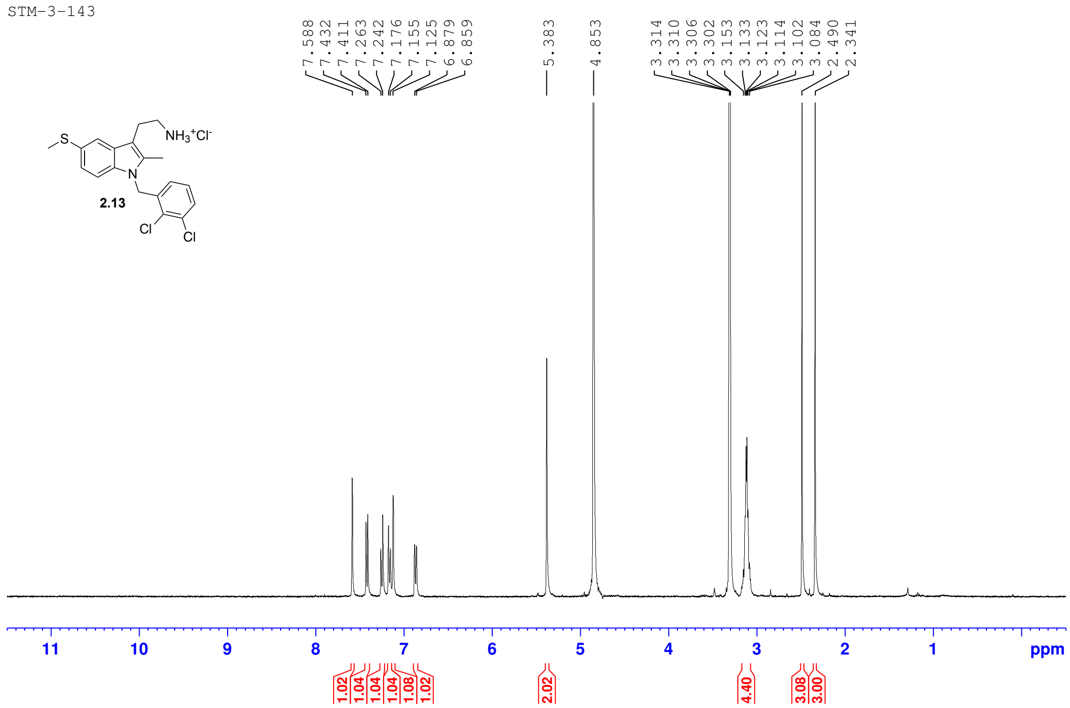
STM-3-143
7.588
7.432
7.411
7.263
7.242
7.176
7.155
7.125
6.879
6.859
5.383
4.853
3.314
3.310
3.306
3.302
3.153
3.133
3.123
3.114
3.102
3.084
2.490
2.341
S
NH3+Cl-
N
2.13
Cl
Cl
11
10
9
8
7
6
5
4
3
2
1
ppm
1.02
1.04
1.04
1.04
1.08
1.02
2.02
4.40
3.08
3.00

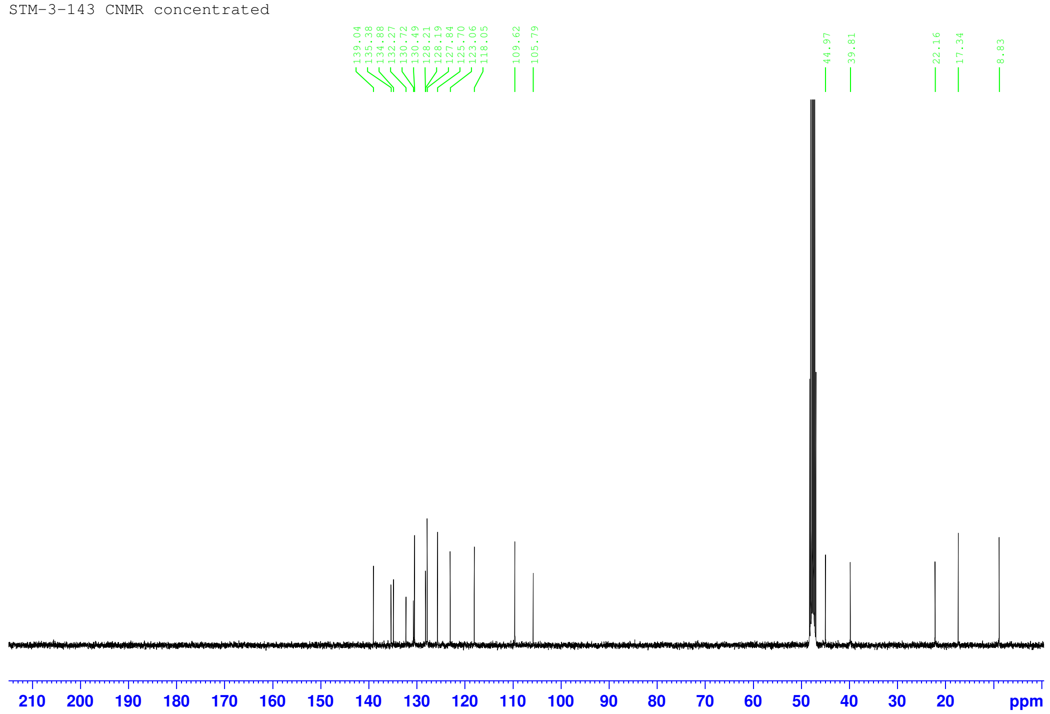
STM-3-143 CNMR concentrated
139.04
135.38
134.88
132.27
130.72
130.49
128.21
128.19
127.84
125.70
123.06
118.05
109.62
105.79
44.97
39.81
22.16
17.34
8.83
210
200
190
180
170
160
150
140
130
120
110
100
90
80
70
60
50
40
30
20
ppm

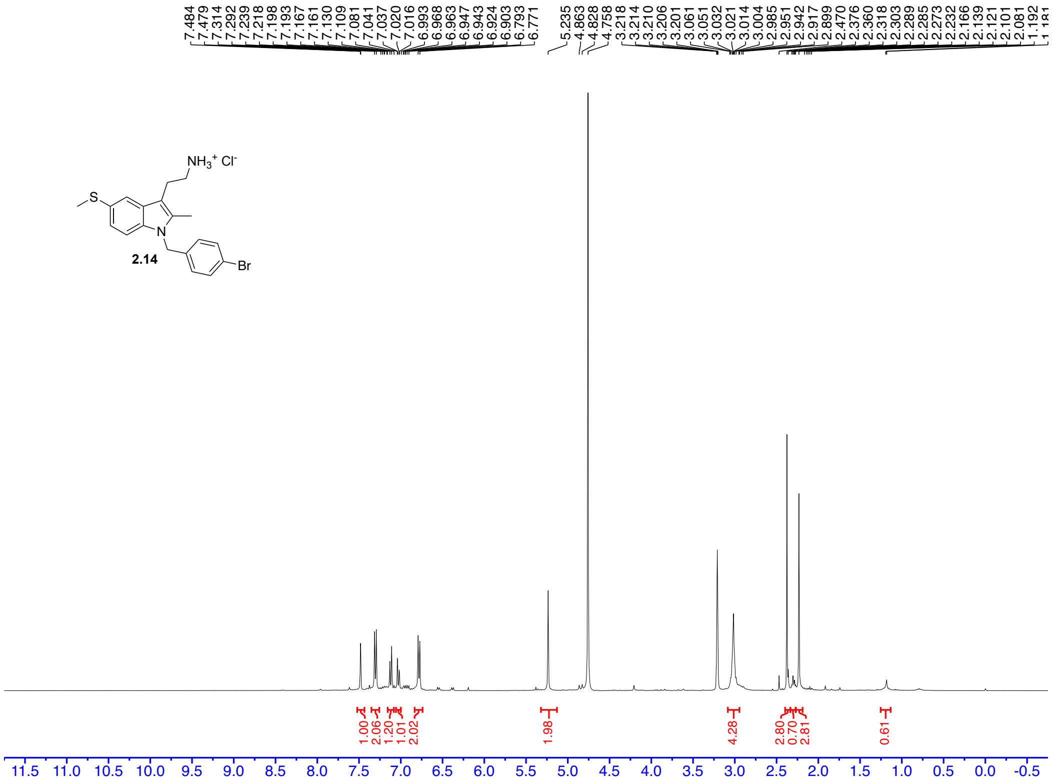

STM-3-75 CNMR - 1H NMR - 400.13 MHz - MeOD

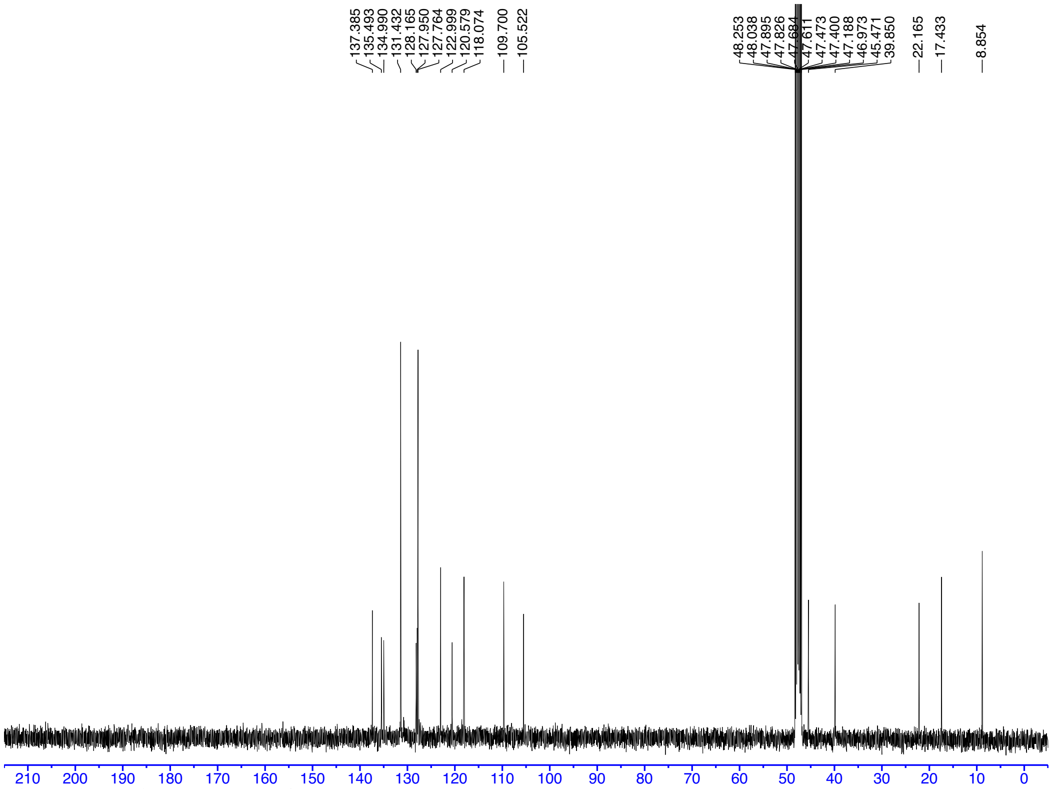

STM-3-75 CNMR - 13C NMR - 100.62 MHz - MeOD

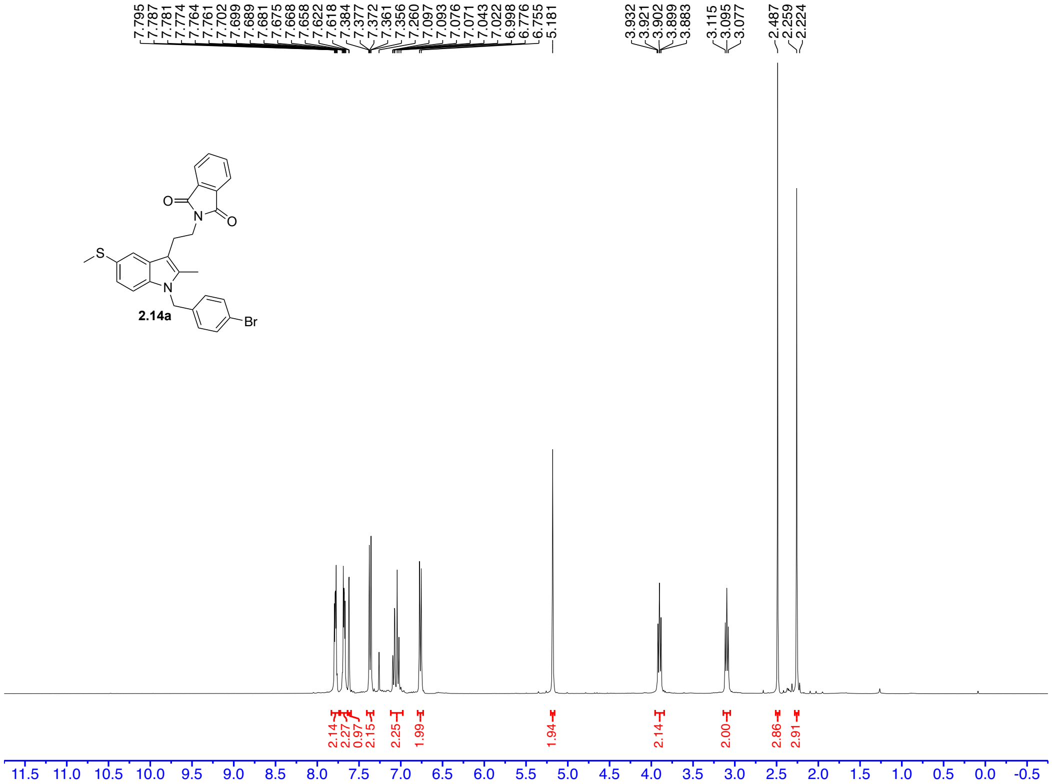

STM-3-36 Solvent Removal CNMR - 1H NMR - 400.13 MHz - CDCl3

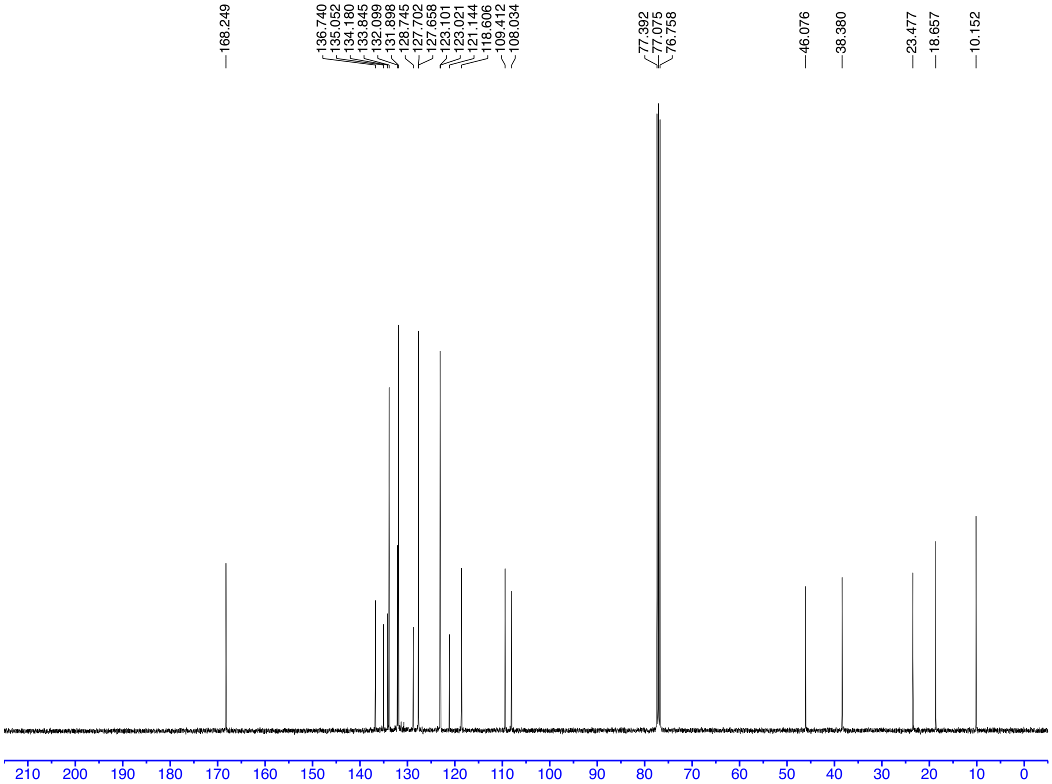

STM-3-36 Solvent Removal CNMR - 13C NMR - 100.62 MHz - CDCl3

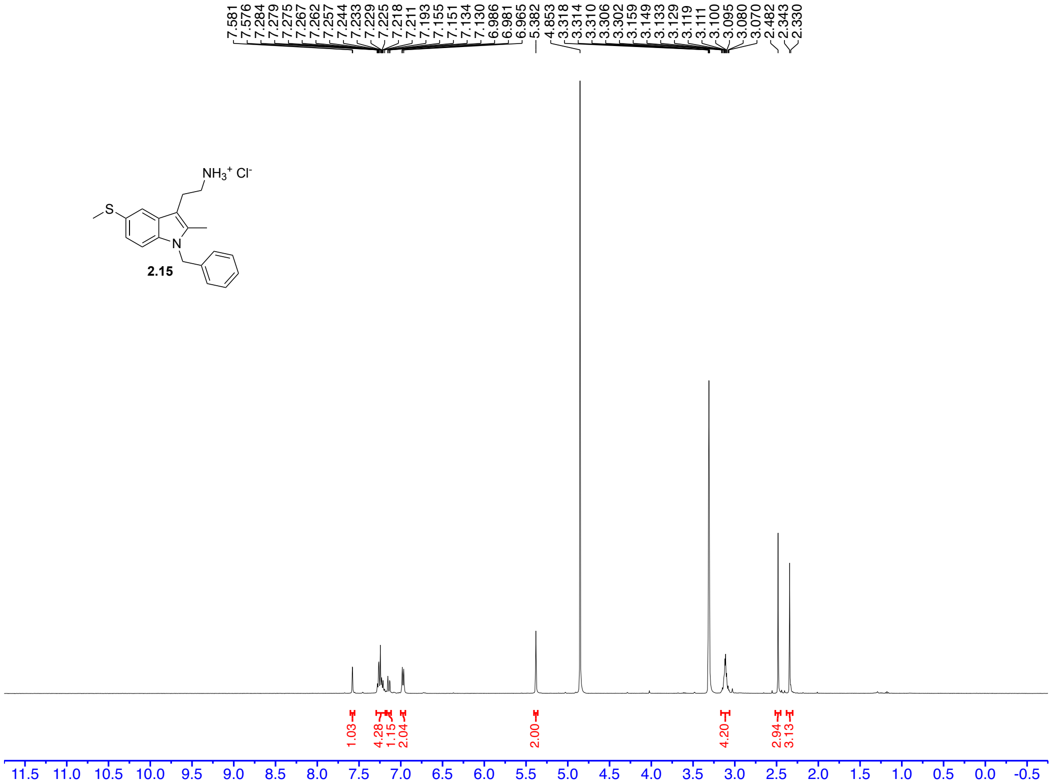

STM-3-64 - 1H NMR - 400.13 MHz - MeOD

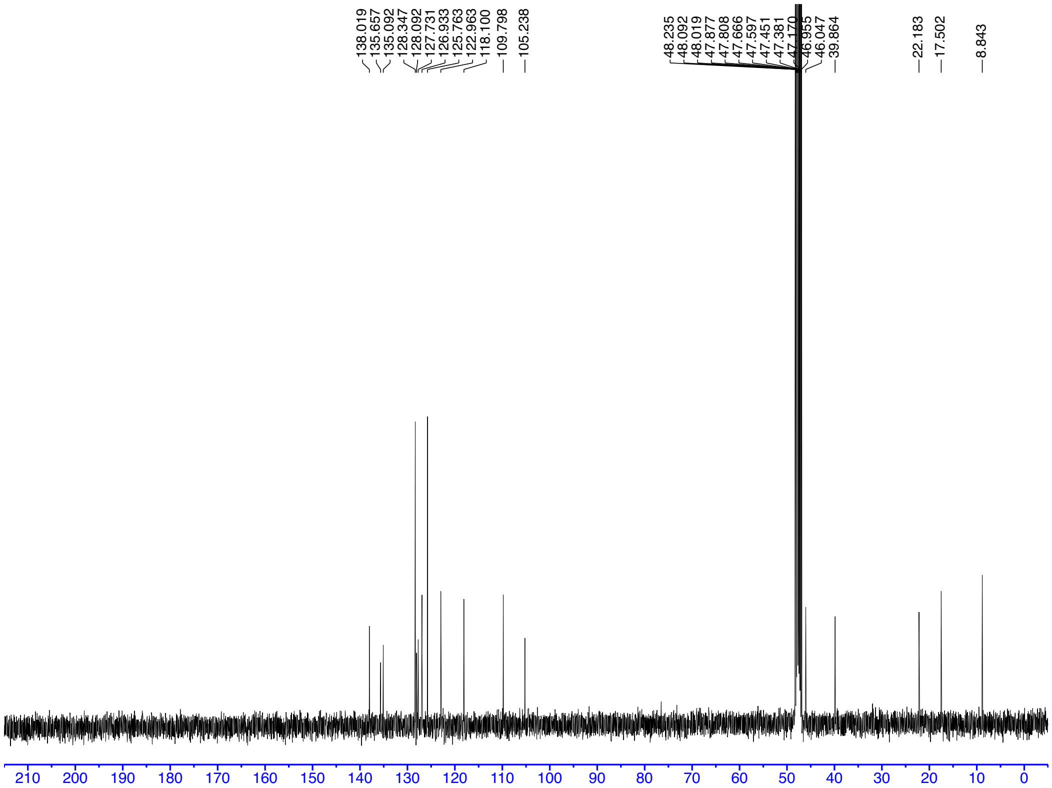

STM-3-64 Concentrated CNMR - 13C NMR - 100.62 MHz - MeOD

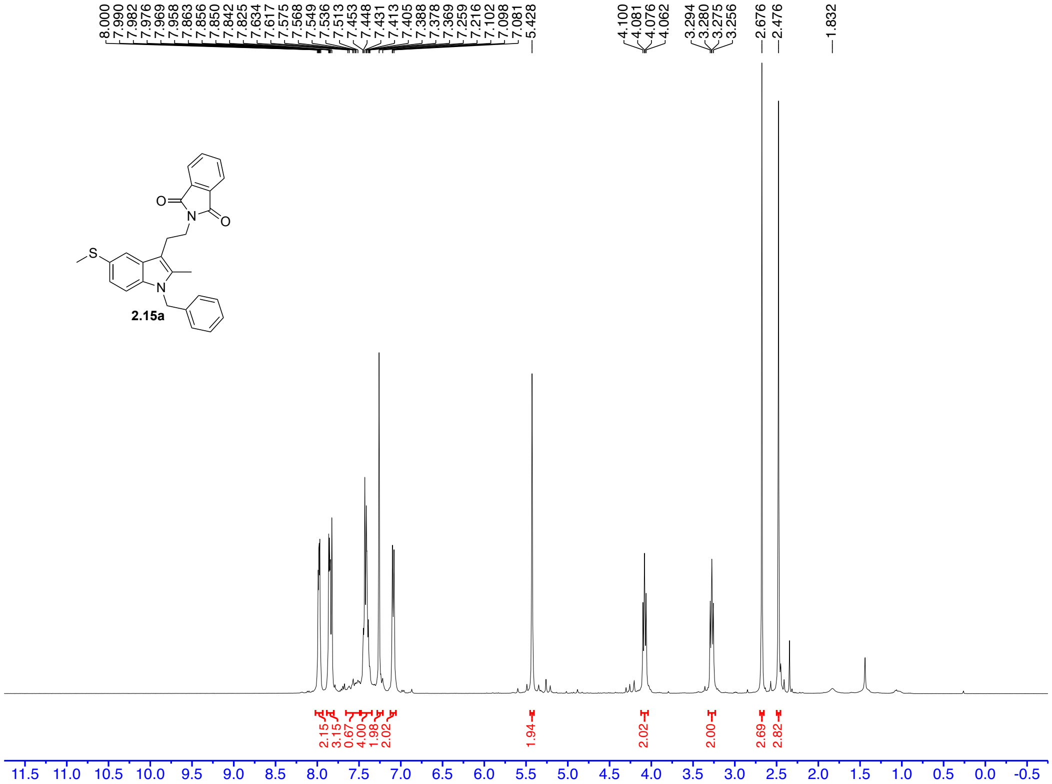

STM-3-29 2nd Column pump - 1H NMR - 400.13 MHz - CDCl3

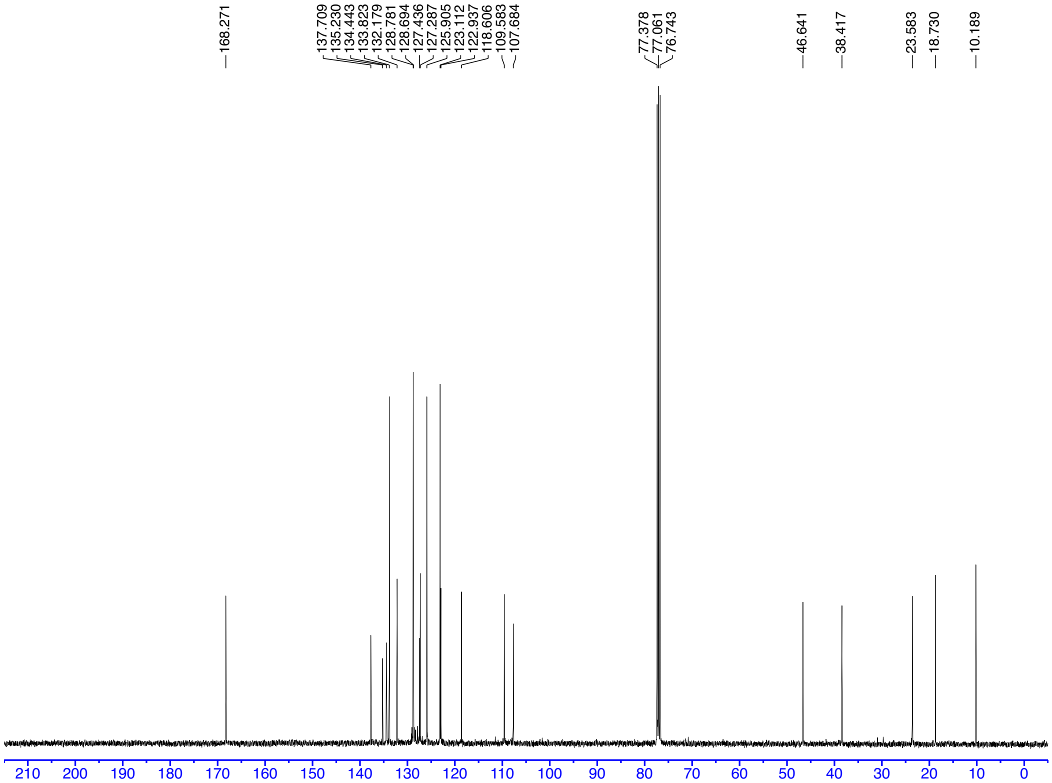

STM-3-29 2nd Column CNMR - 13C NMR - 100.62 MHz - CDCl3

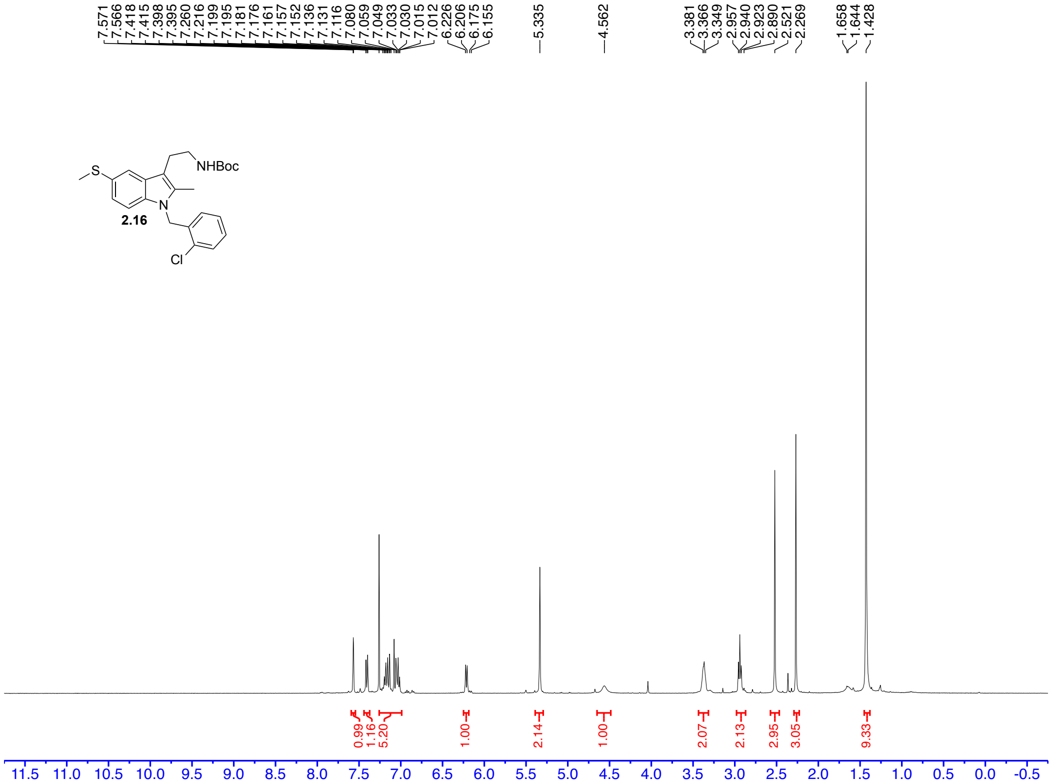

STM-3-15 - 1H NMR - 400.13 MHz - CDCl3

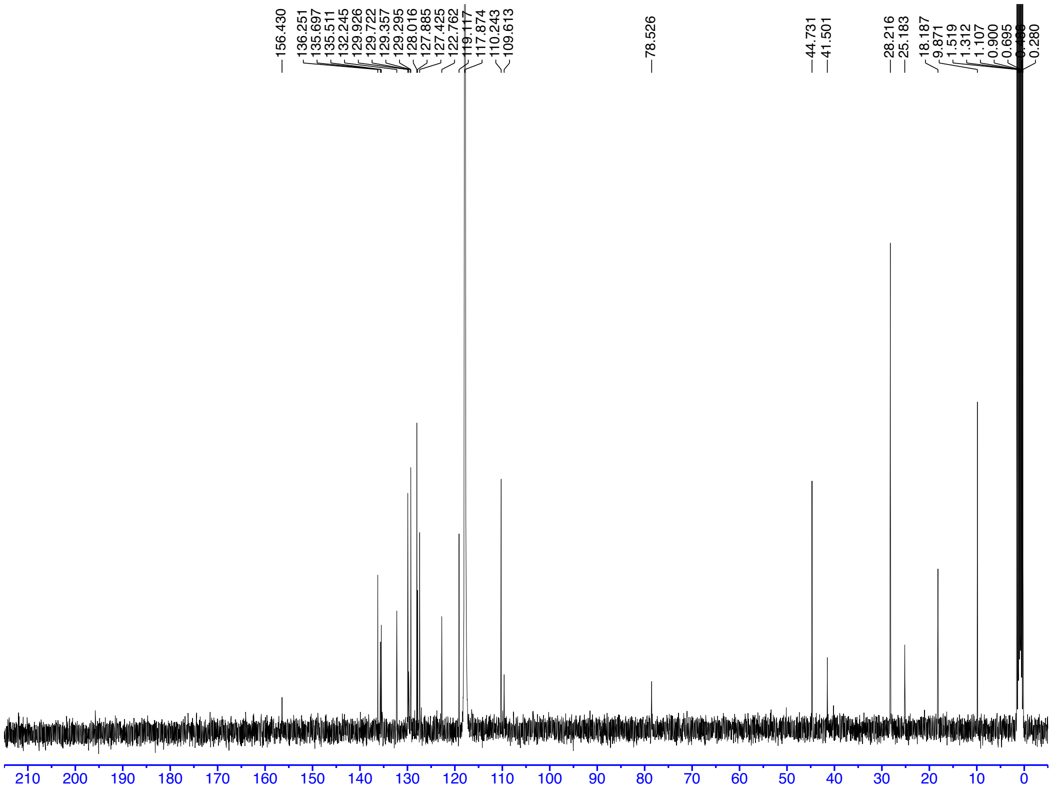

STM-3-15 CNMR MeCN - 13C NMR - 100.62 MHz - CD3CN

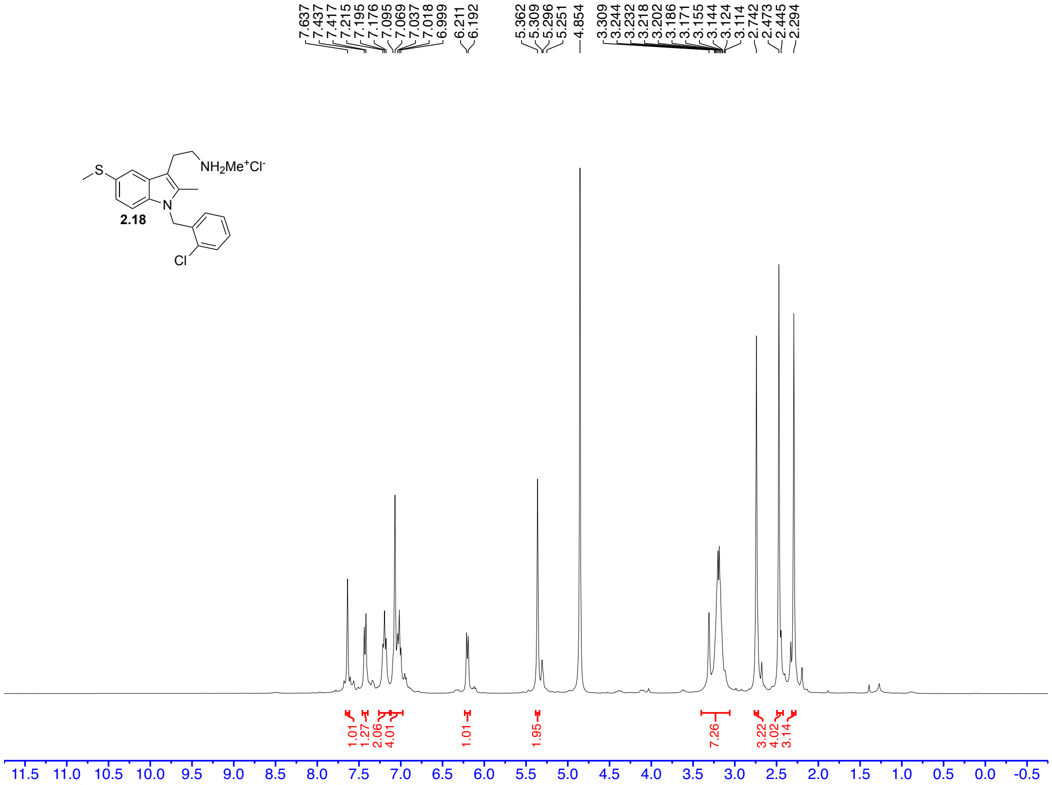

STM-3-39 Solvent Removal - 1H NMR - 400.13 MHz - MeOD

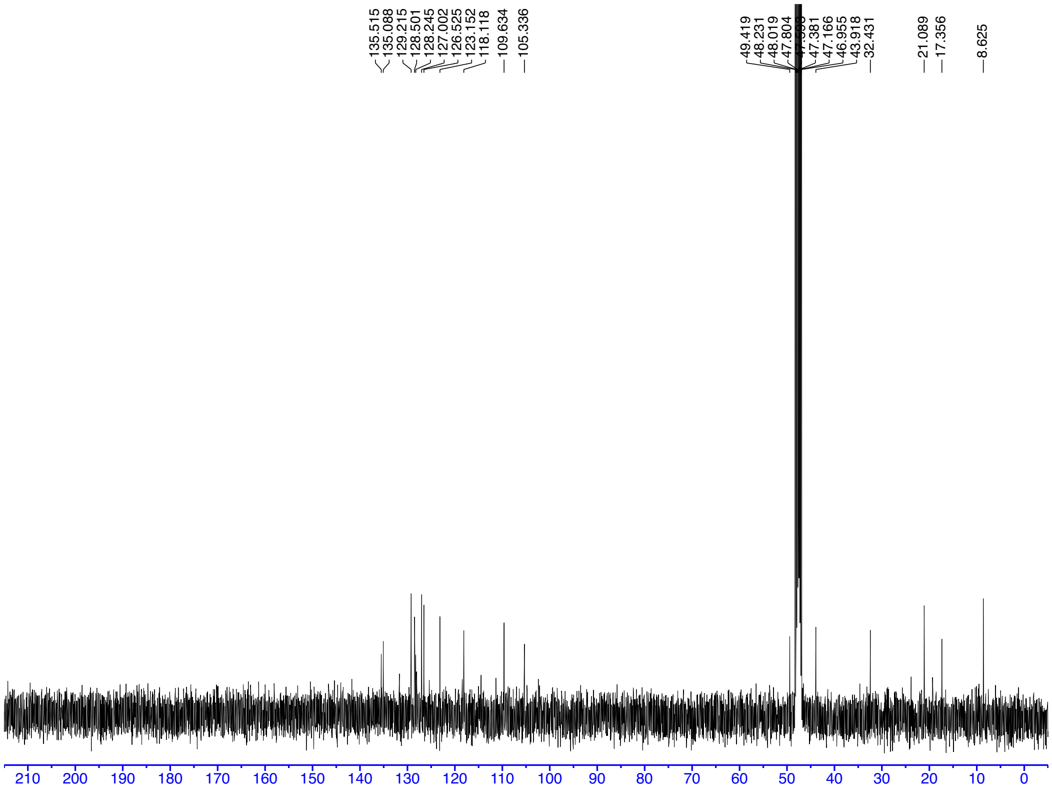

STM-3-39 Solvent Removal CNMR - 13C NMR - 100.62 MHz - MeOD

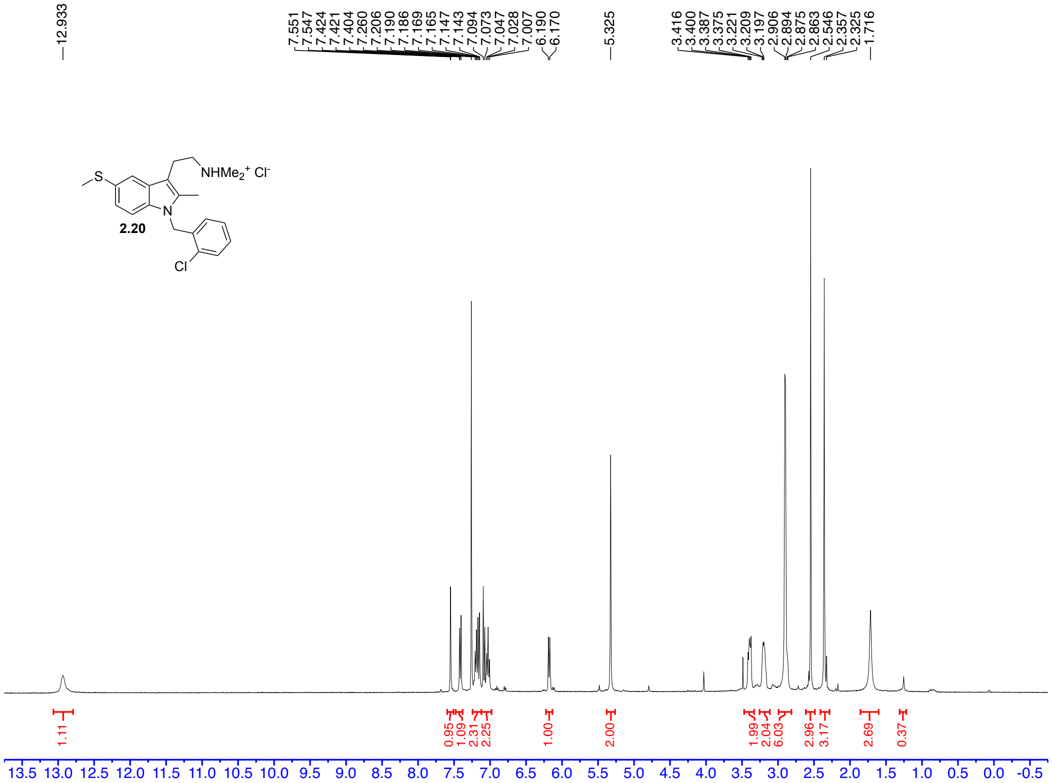

STM-3-21 CDCl3 - 1H NMR - 400.13 MHz - CDCl3

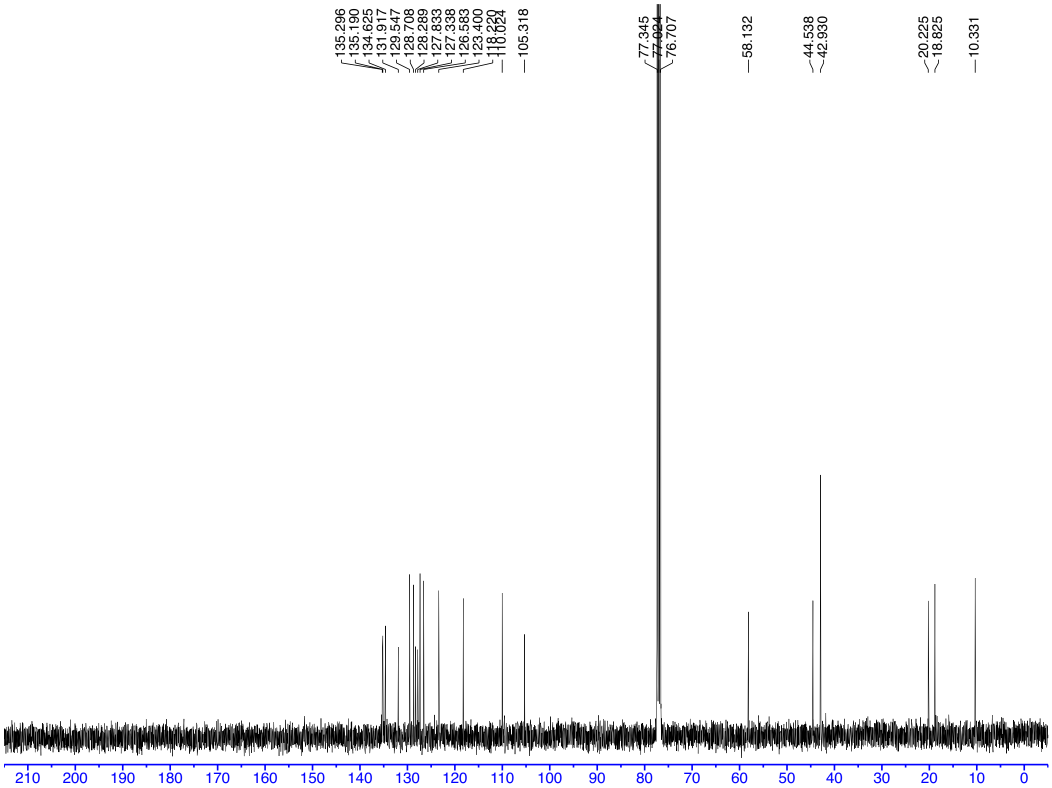

STM-3-21 CNMR concentrated - 13C NMR - 100.62 MHz - CDCl3

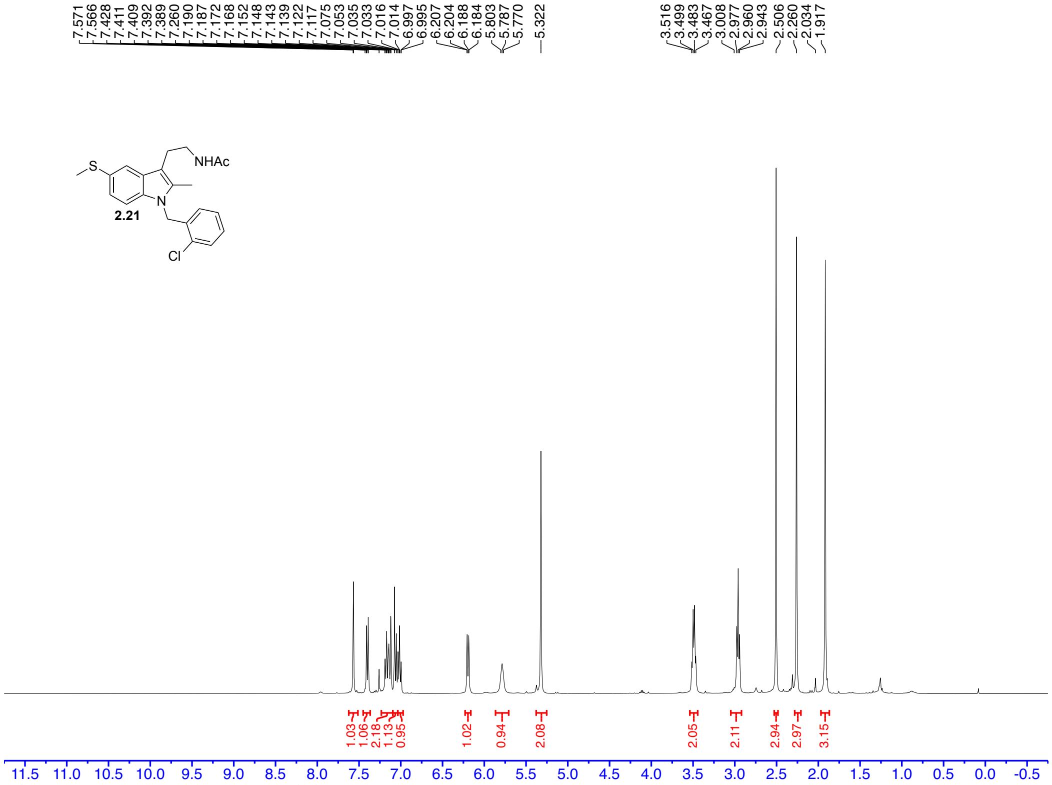

STM-2-125 Pump Pure - 1H NMR - 400.13 MHz - CDCl3

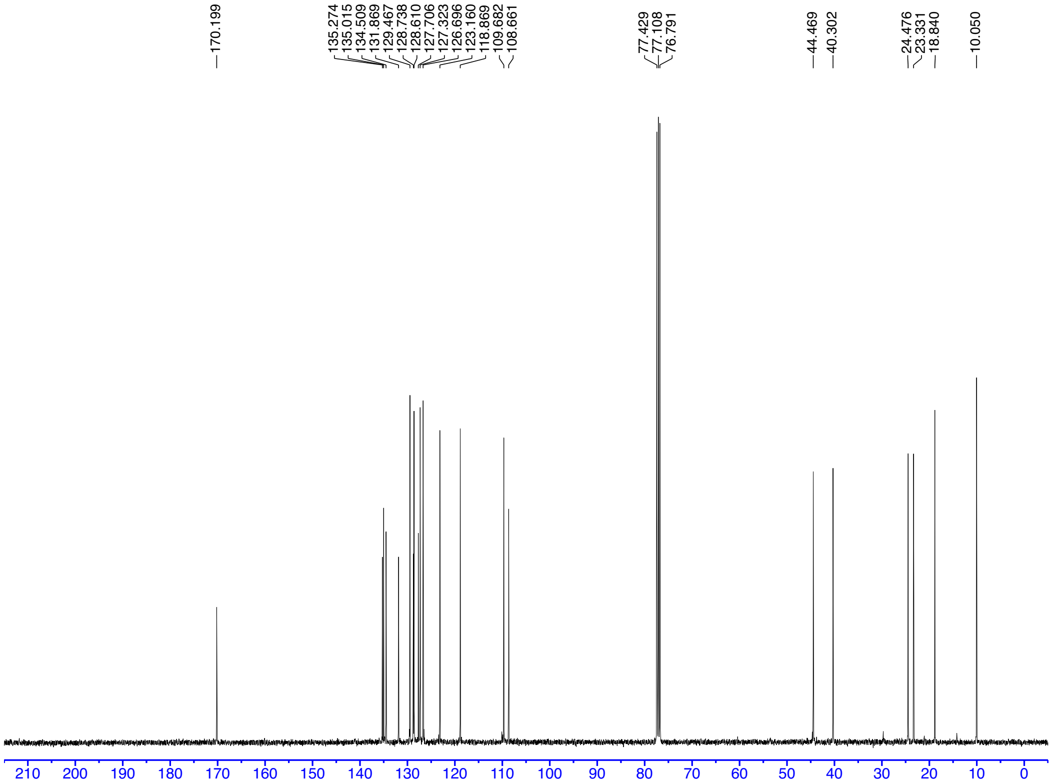

STM-2-125 Pump Pure CNMR - 13C NMR - 100.62 MHz - CDCl3

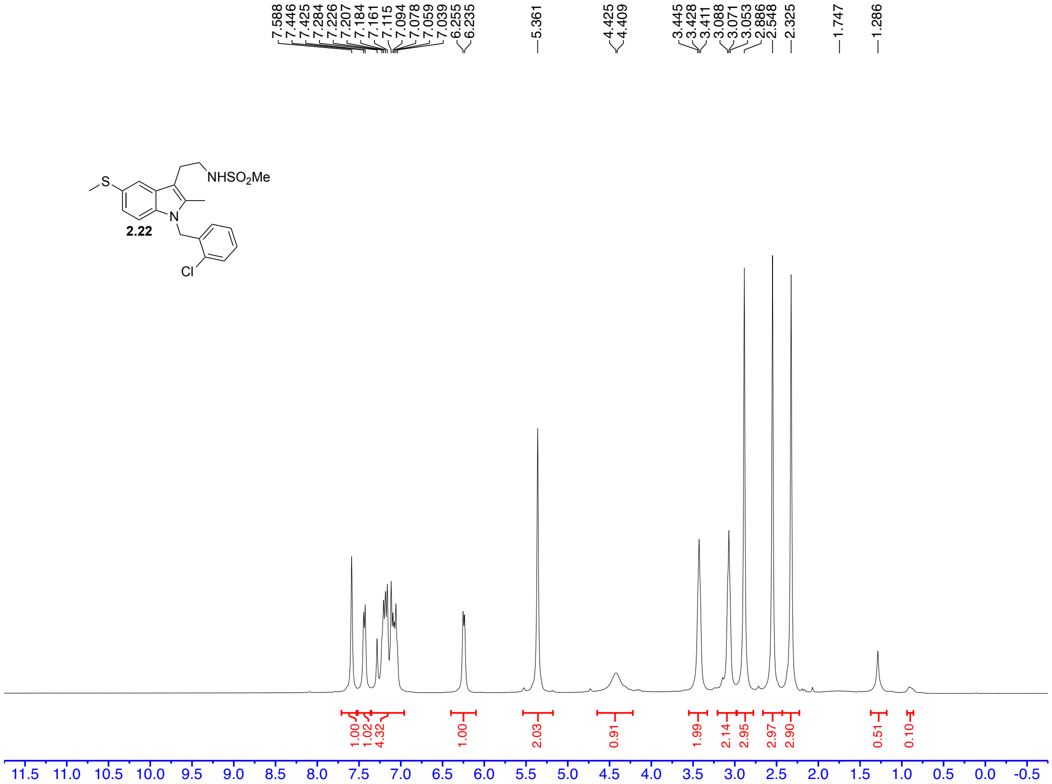

2.22

STM-3-145 - 1H NMR - 400.13 MHz - CDCl3

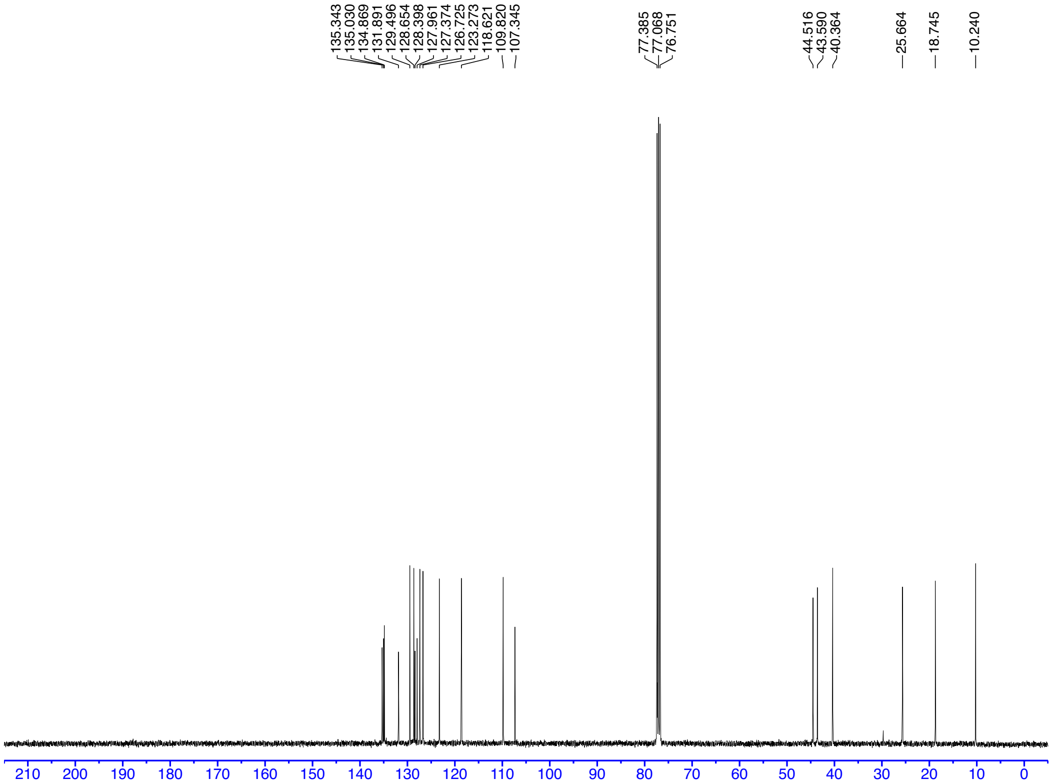

STM-3-145 CNMR - 13C NMR - 100.62 MHz - CDCl3

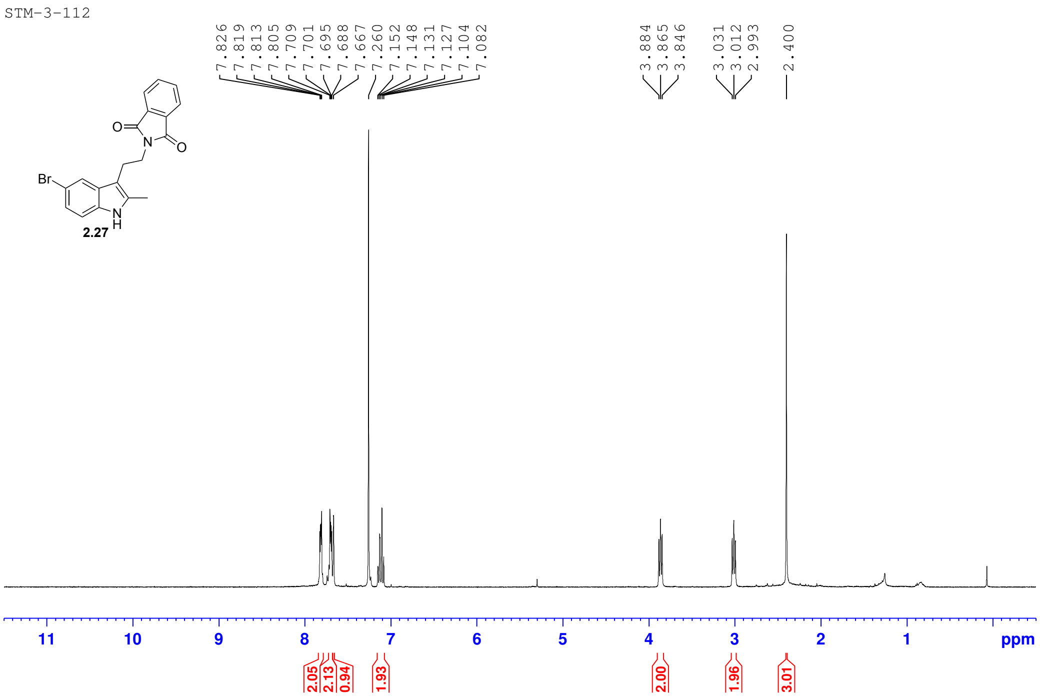
STM-3-112
7.826
7.819
7.813
7.805
7.709
7.701
7.695
7.688
7.667
7.260
7.152
7.148
7.131
7.127
7.104
7.082
3.884
3.865
3.846
3.031
3.012
2.993
2.400
Br
N
O
O
H
2.27
11
10
9
8
7
6
5
4
3
2
1
ppm
2.05
2.13
0.94
1.93
2.00
1.96
3.01

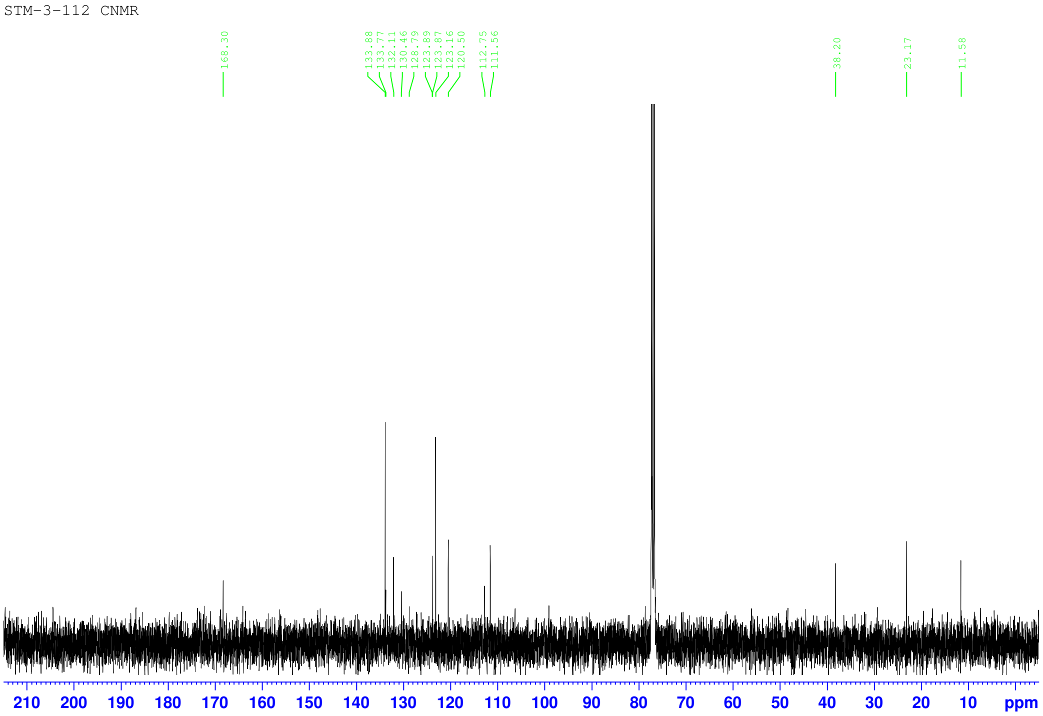
STM-3-112 CNMR
168.30
133.88
133.77
132.11
130.46
128.79
123.89
123.87
123.16
120.50
112.75
111.56
38.20
23.17
11.58
210
200
190
180
170
160
150
140
130
120
110
100
90
80
70
60
50
40
30
20
10
ppm

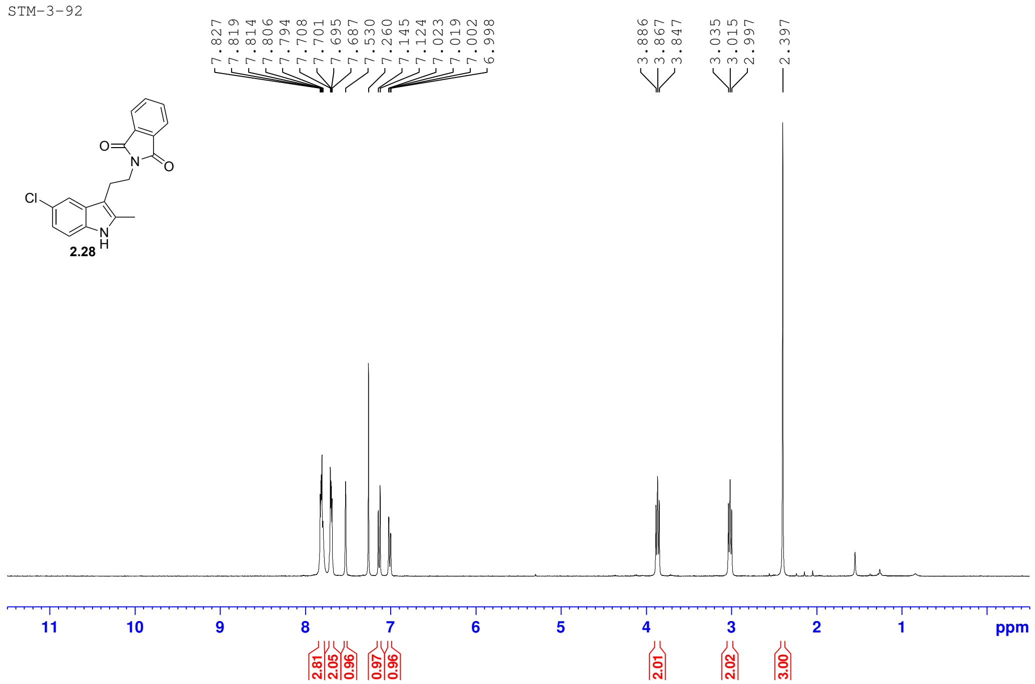
STM-3-92
7.827
7.819
7.814
7.806
7.794
7.708
7.701
7.695
7.687
7.530
7.260
7.145
7.124
7.023
7.019
7.002
6.998
3.886
3.867
3.847
3.035
3.015
2.997
2.397
O
N
O
Cl
H
N
2.28
11
10
9
8
7
6
5
4
3
2
1
ppm
2.81
2.05
0.96
0.97
0.96
2.01
2.02
3.00

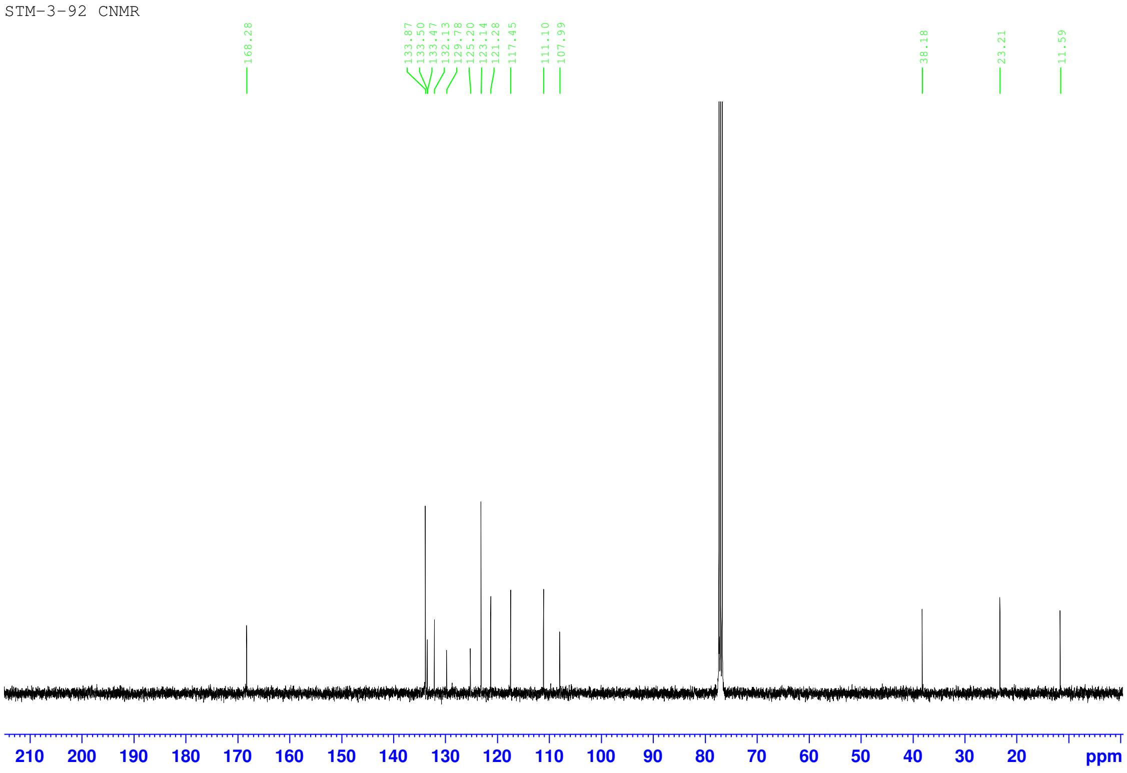
STM-3-92 CNMR
168.28
133.87
133.50
133.47
132.13
129.78
125.20
123.14
121.28
117.45
111.10
107.99
38.18
23.21
11.59
210
200
190
180
170
160
150
140
130
120
110
100
90
80
70
60
50
40
30
20
ppm

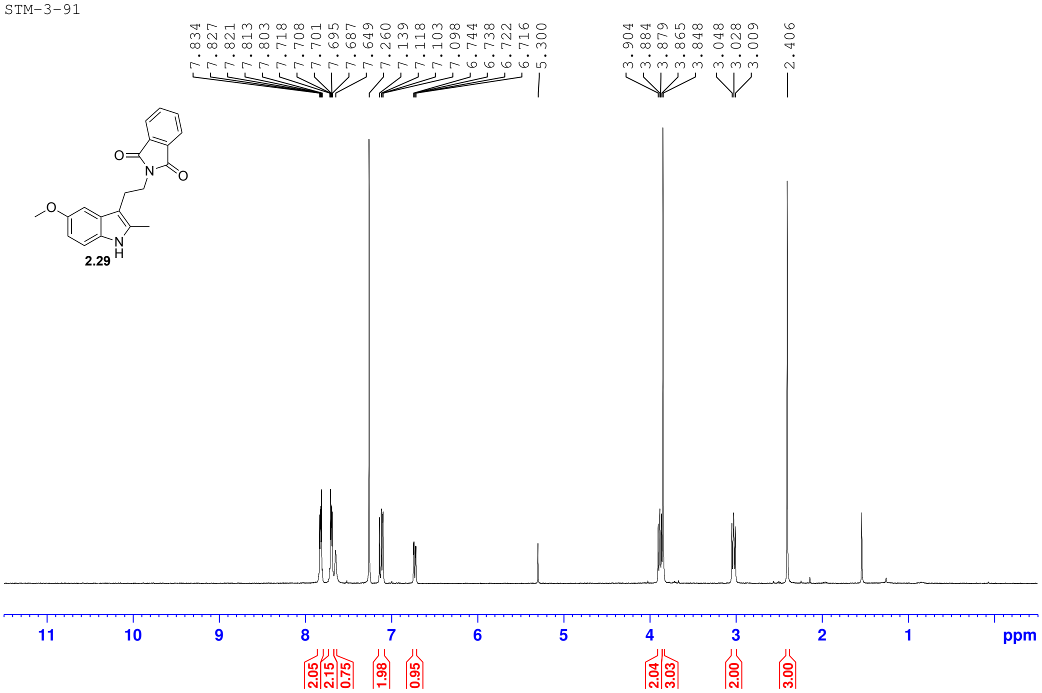
STM-3-91
7.834
7.827
7.821
7.813
7.803
7.718
7.708
7.701
7.695
7.687
7.649
7.260
7.139
7.118
7.103
7.098
6.744
6.738
6.722
6.716
5.300
3.904
3.884
3.879
3.865
3.848
3.048
3.028
3.009
2.406
O
N
O
O
N
H
2.29
11
10
9
8
7
6
5
4
3
2
1
ppm
2.05
2.15
0.75
1.98
0.95
2.04
3.03
2.00
3.00

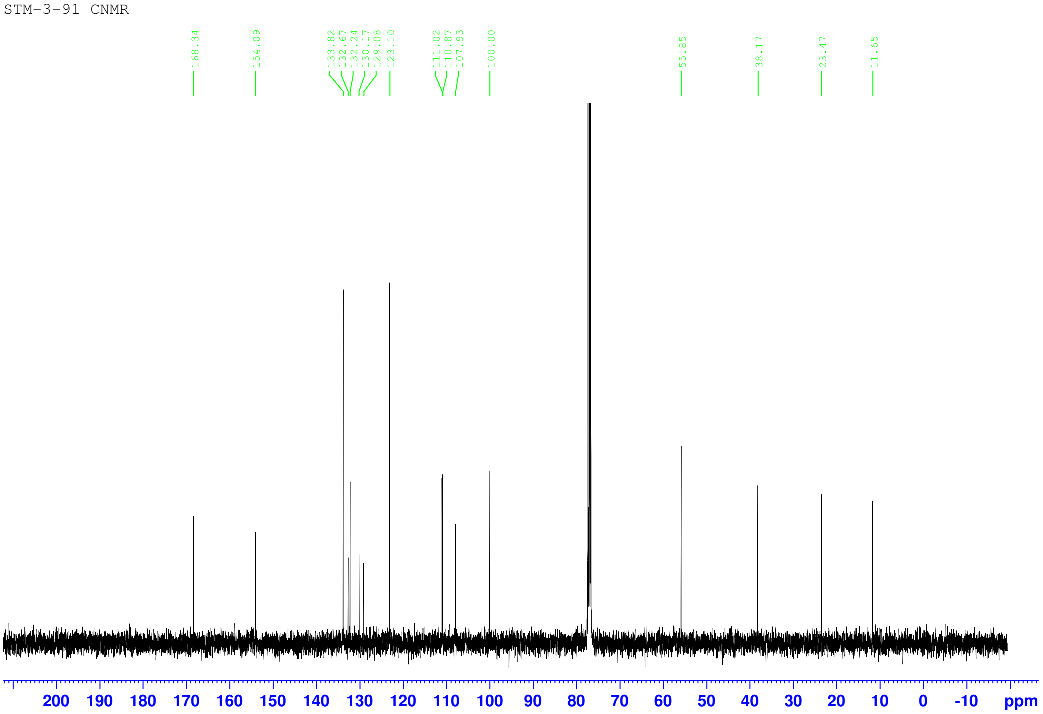
STM-3-91 CNMR
168.34
154.09
133.82
132.67
132.24
130.17
129.08
123.10
111.02
110.87
107.93
100.00
55.85
38.17
23.47
11.65
200
190
180
170
160
150
140
130
120
110
100
90
80
70
60
50
40
30
20
10
0
-10
ppm

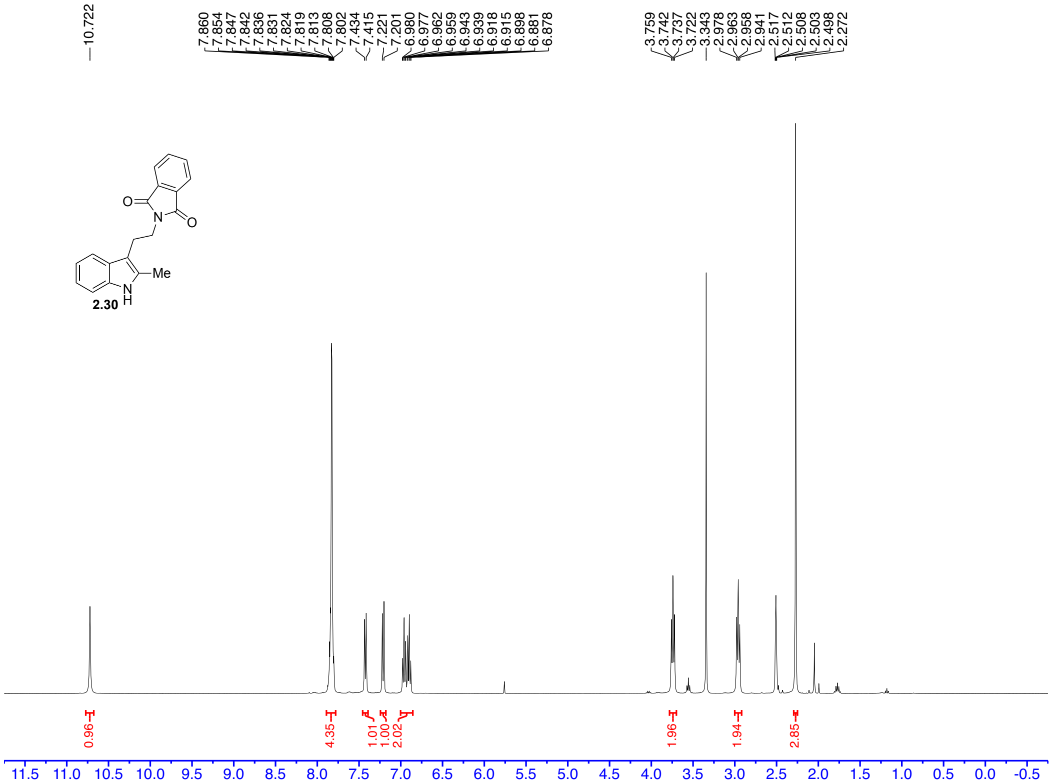

STM-3-2 (8-26-22) - 1H NMR - 400.13 MHz - DMSO

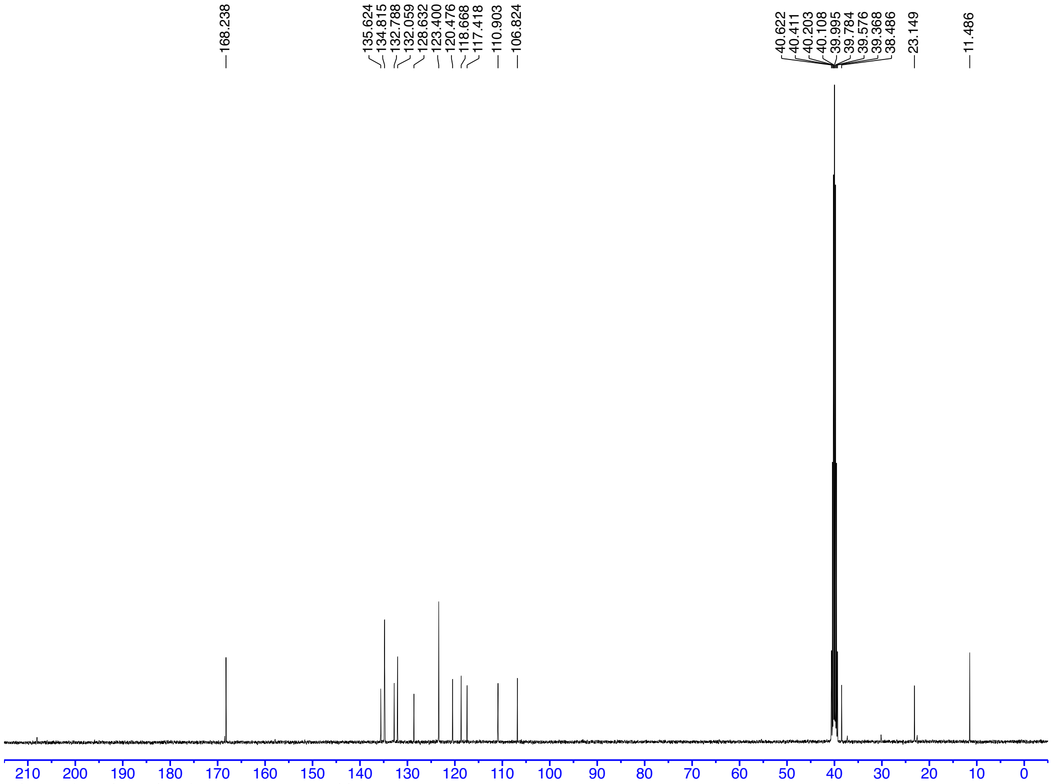

STM-3-2 CNMR (8-26-22) - 13C NMR - 100.62 MHz - DMSO

STM-3-107 2ND COLUMN PUMPED

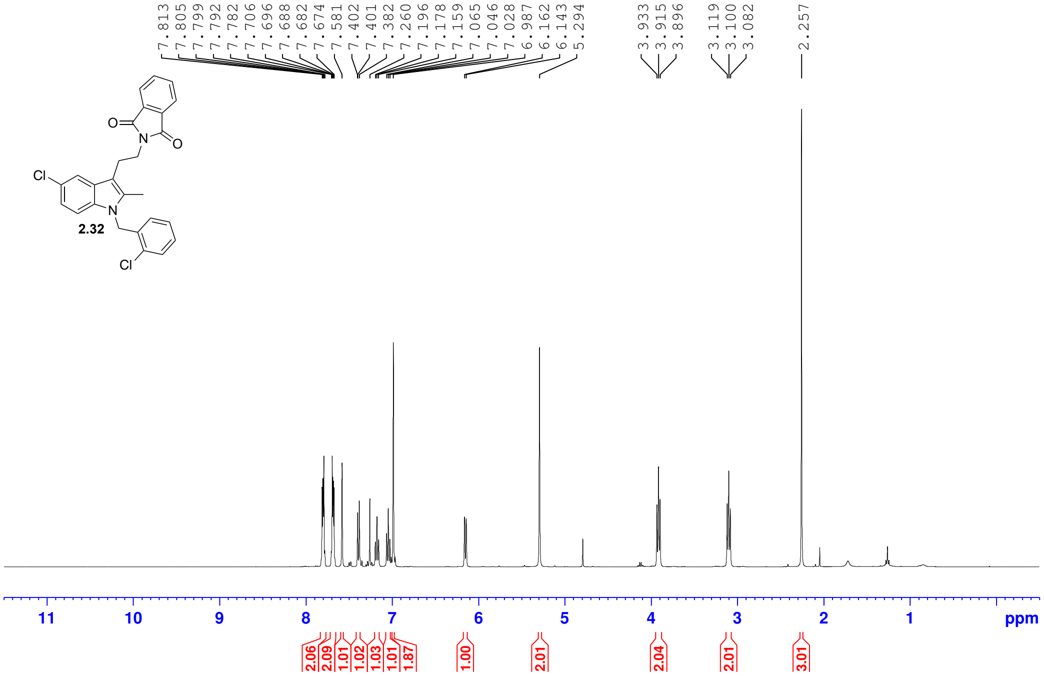

STM-3-107 2nd Column CNMR

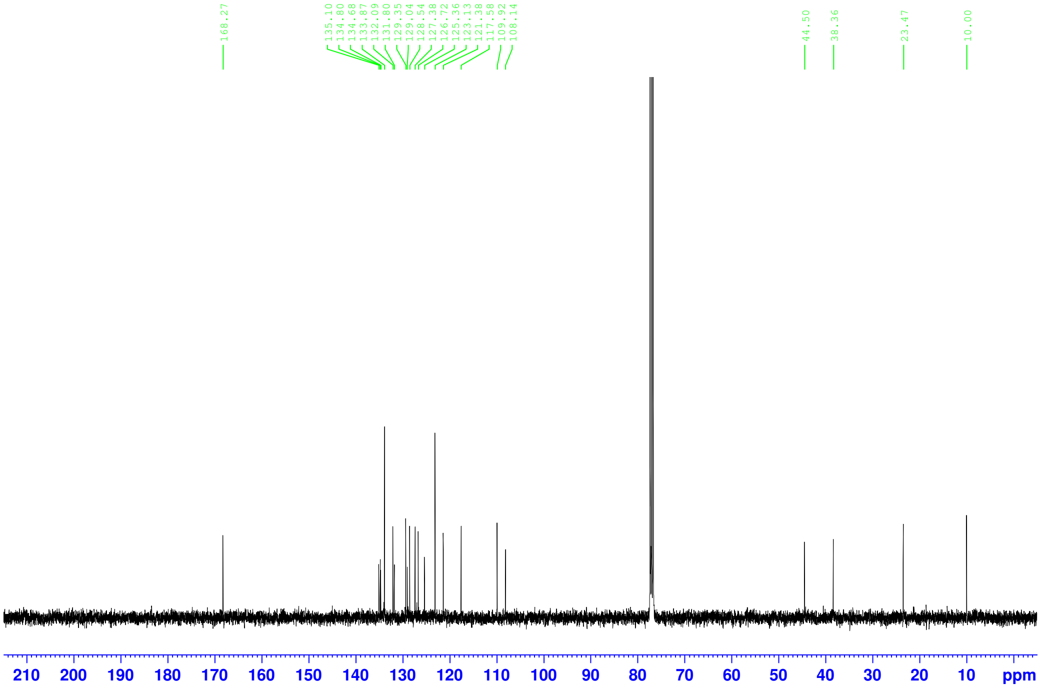

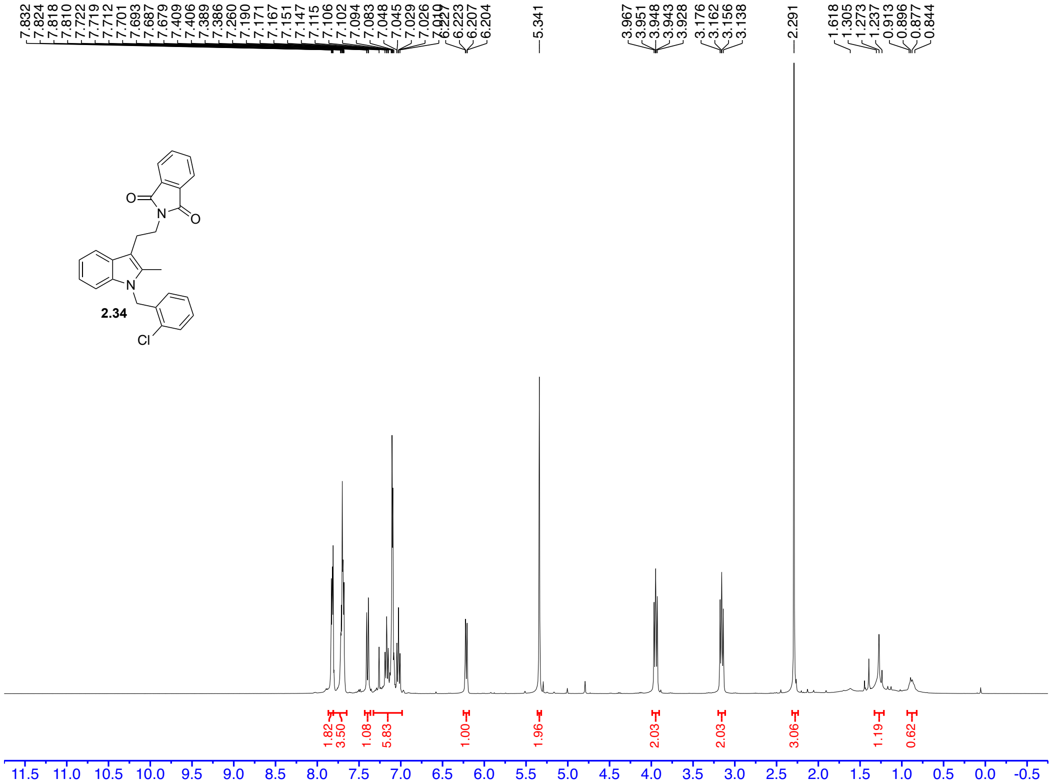

STM-3-17 - 1H NMR - 400.13 MHz - CDCl3

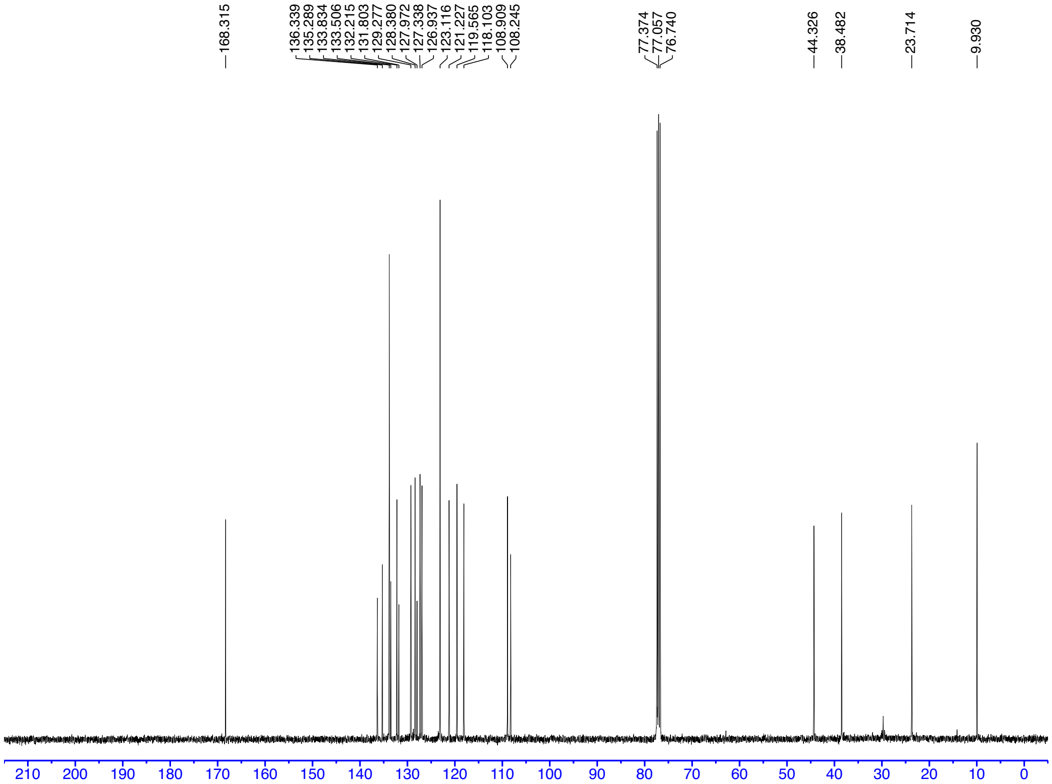

STM-3-17 CNMR - 13C NMR - 100.62 MHz - CDCl3

STM-3-124

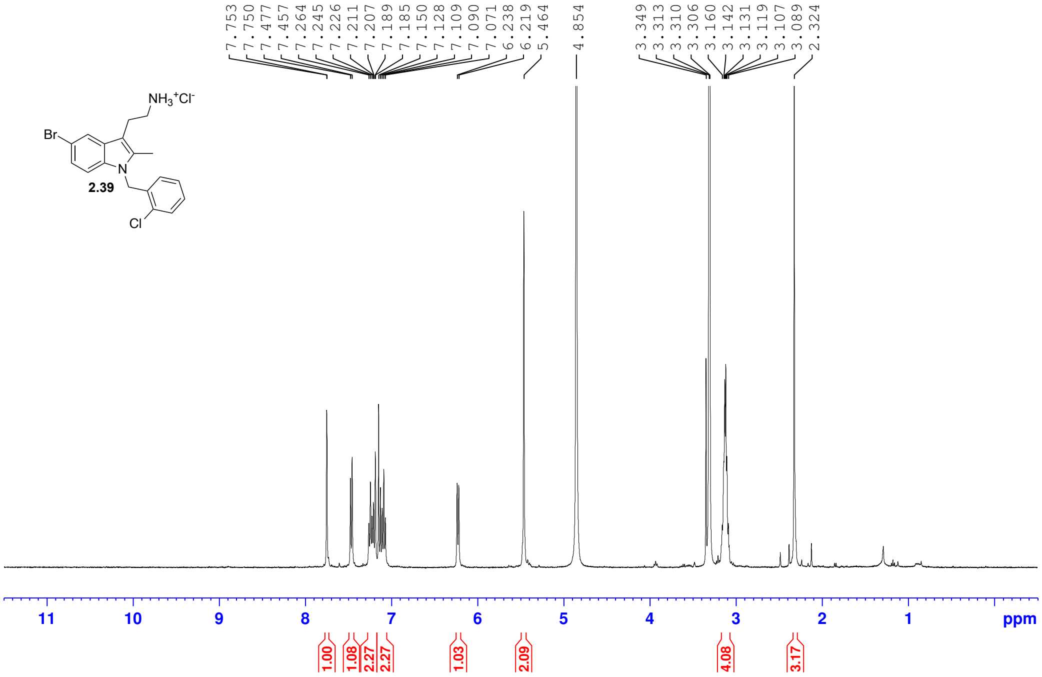

STM-3-124-CNMR

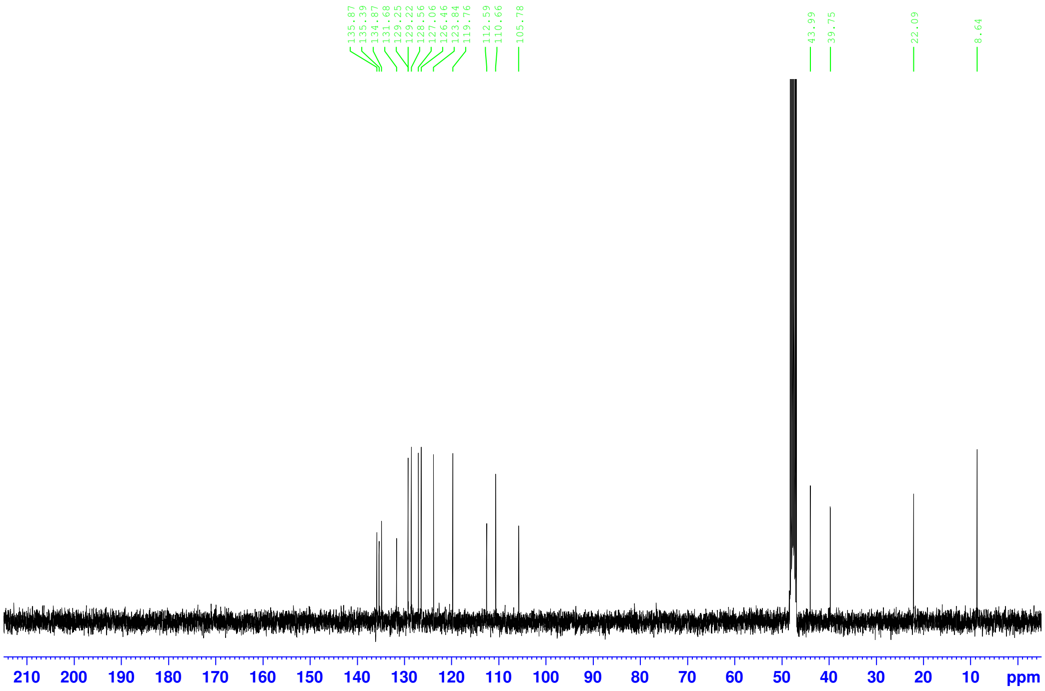

STM-3-119 Pump

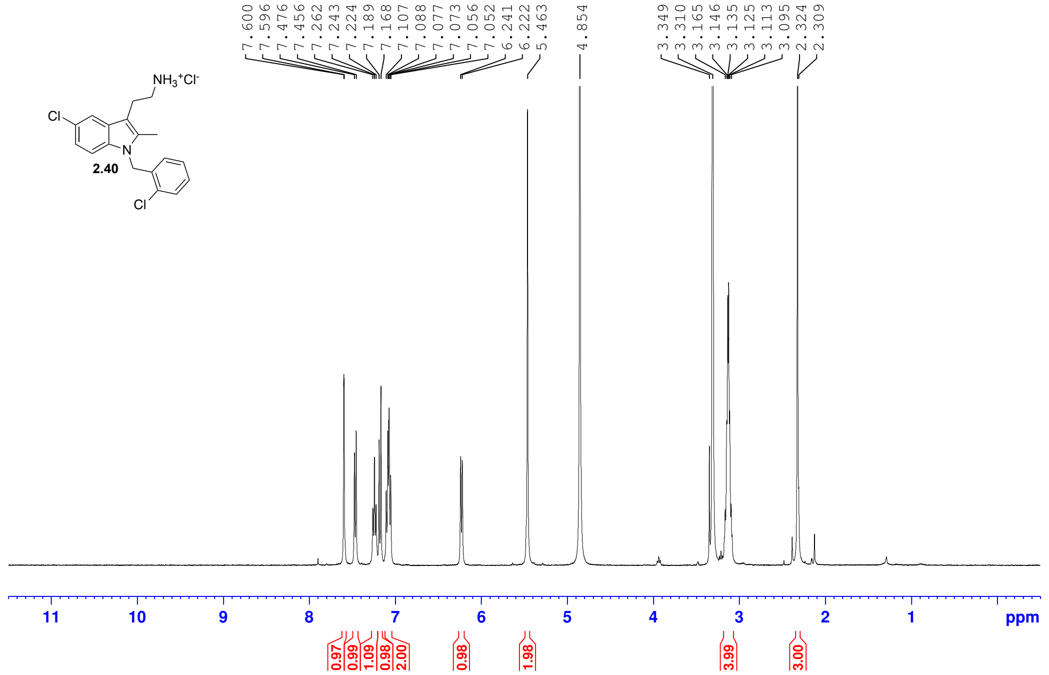

STM-3-119 Pump CNMR

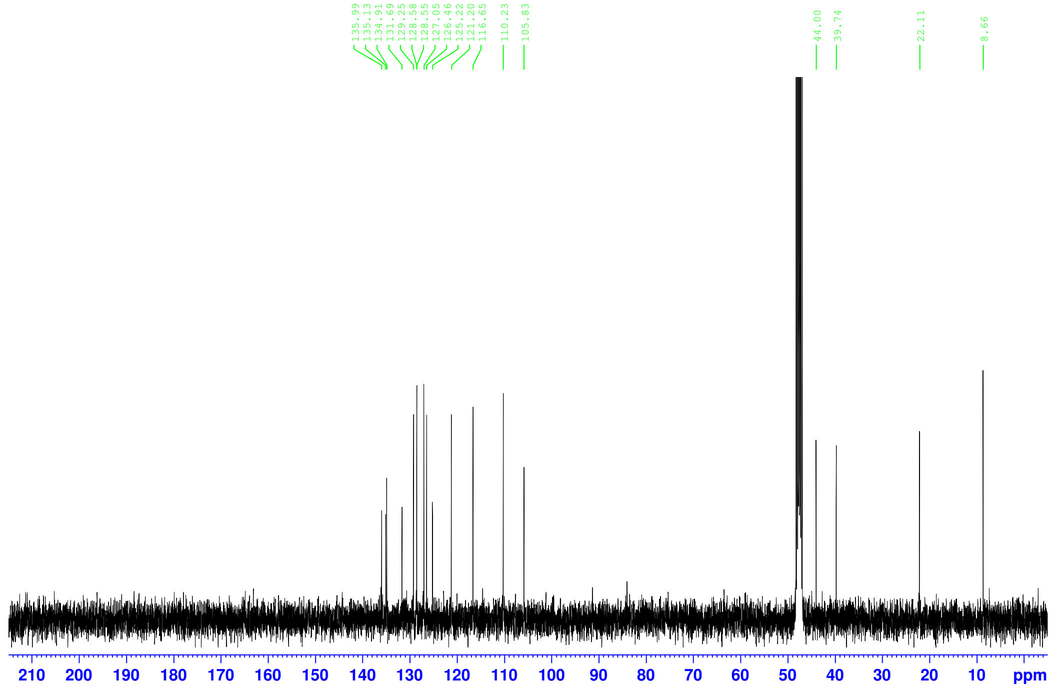

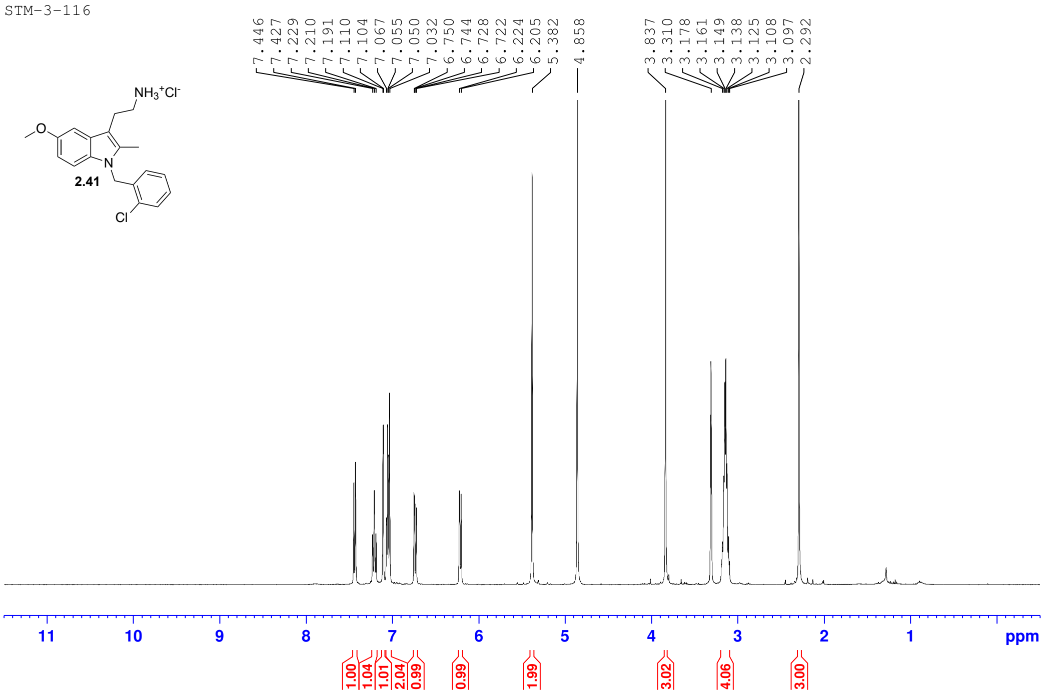
STM-3-116
NH3+Cl-
O
N
Cl
2.41
7.446
7.427
7.229
7.210
7.191
7.110
7.104
7.067
7.055
7.050
7.032
6.750
6.744
6.728
6.722
6.224
6.205
5.382
4.858
3.837
3.310
3.178
3.161
3.149
3.138
3.125
3.108
3.097
2.292
11
10
9
8
7
6
5
4
3
2
1
ppm
1.00
1.04
1.01
2.04
0.99
0.99
1.99
3.02
4.06
3.00

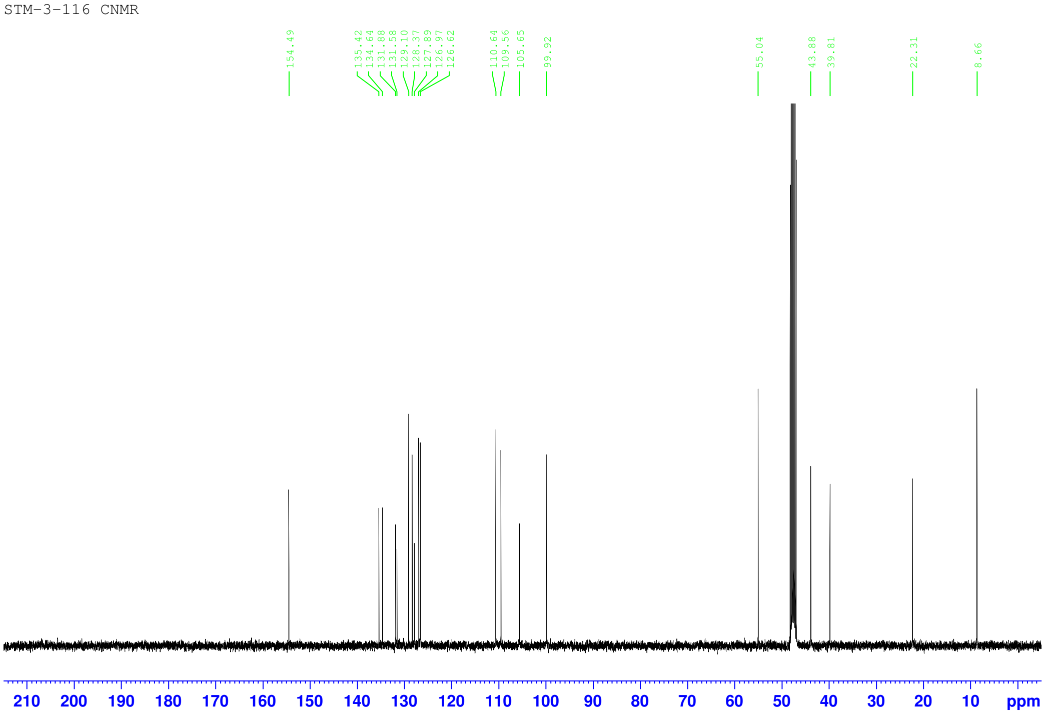
STM-3-116 CNMR
154.49
135.42
134.64
131.88
131.58
129.10
128.37
127.89
126.97
126.62
110.64
109.56
105.65
99.92
55.04
43.88
39.81
22.31
8.66
210
200
190
180
170
160
150
140
130
120
110
100
90
80
70
60
50
40
30
20
10
ppm

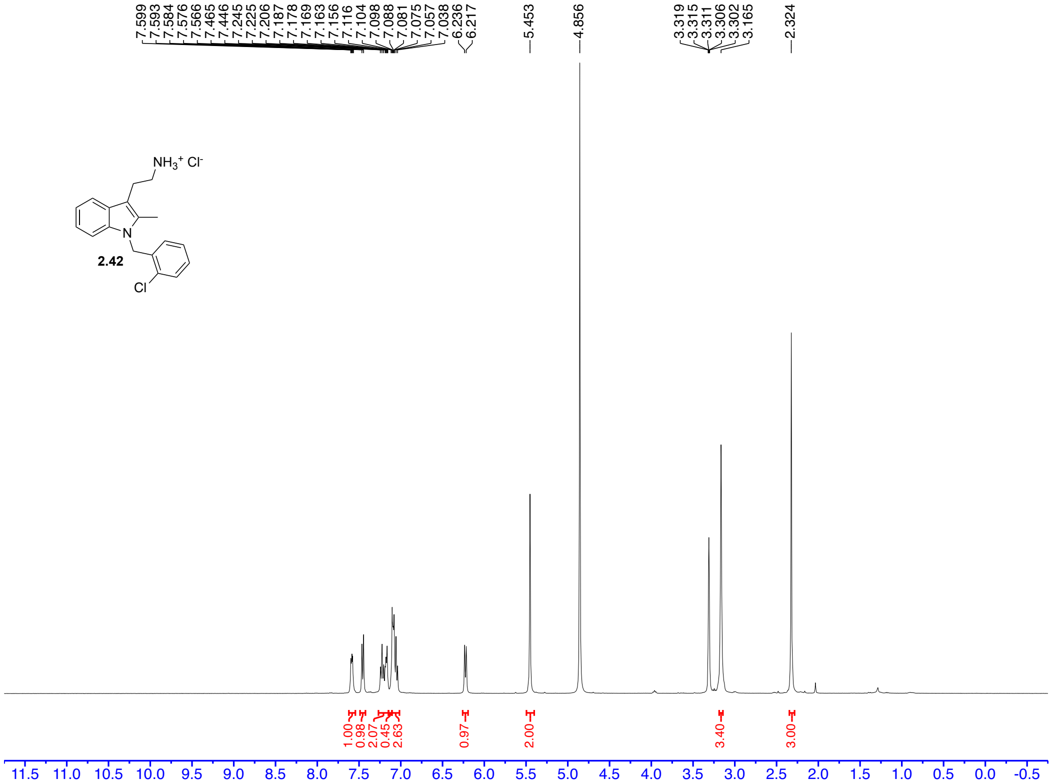

STM-3-26 - 1H NMR - 400.13 MHz - MeOD

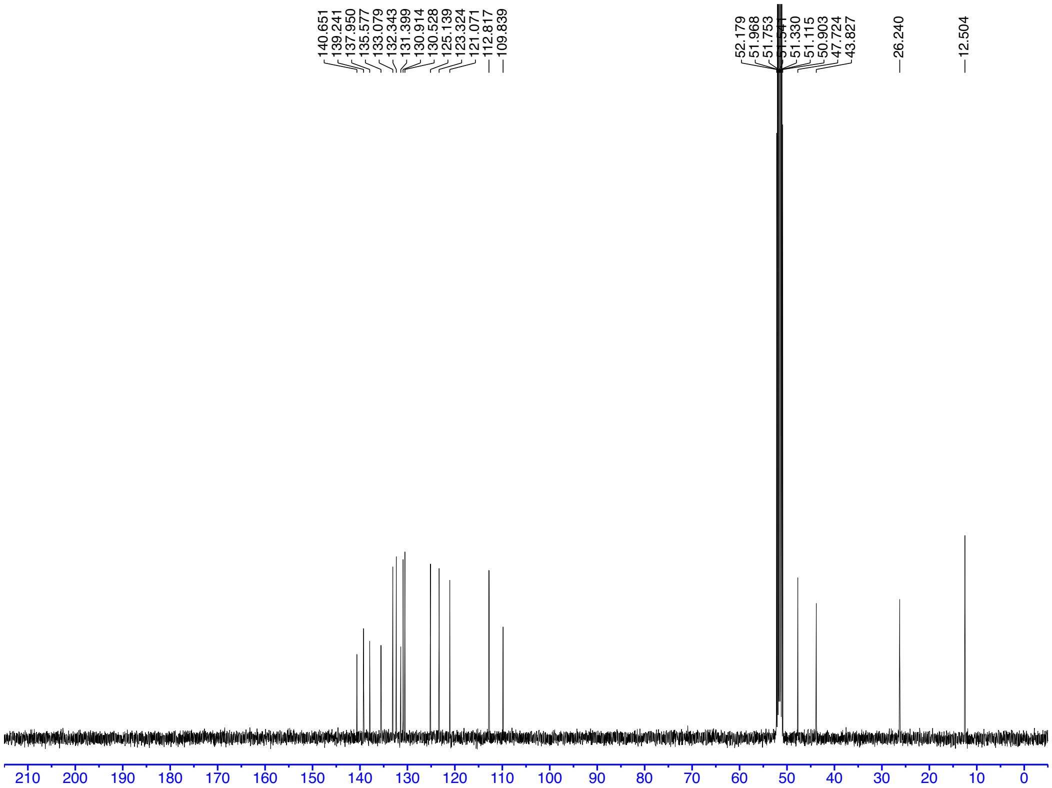

STM-3-26 CNMR - 13C NMR - 100.62 MHz - CDCl3

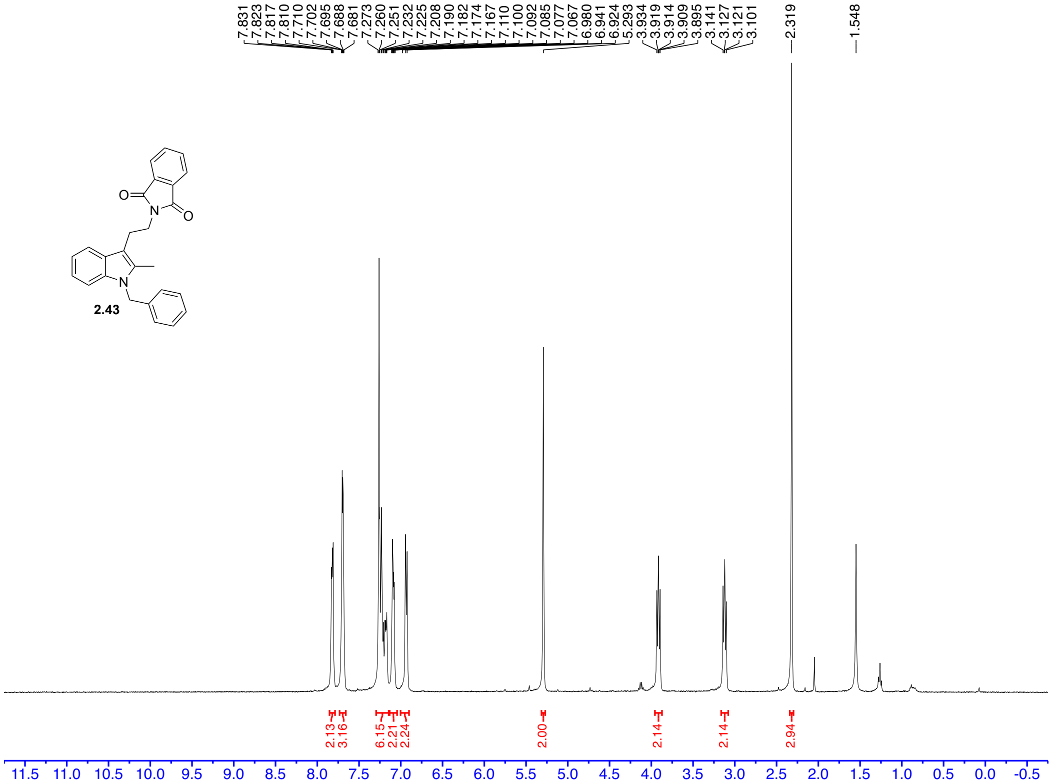

STM-3-25 - 1H NMR - 400.13 MHz - CDCl3

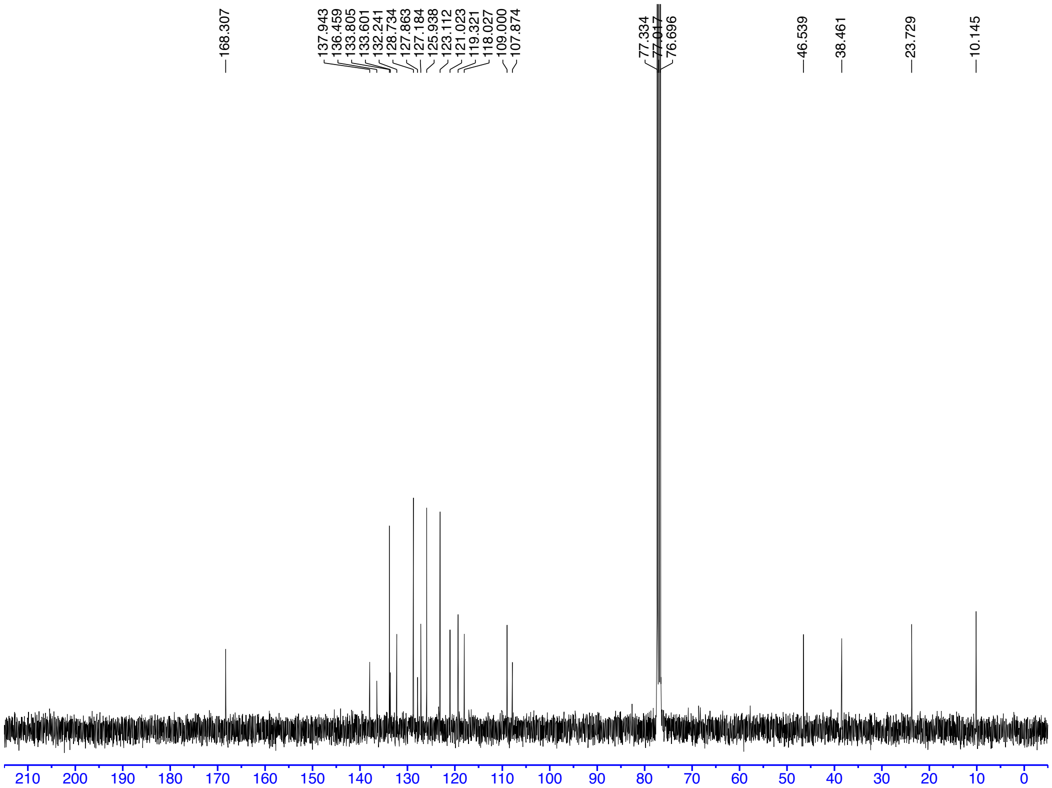

STM-3-25 CNMR - 13C NMR - 100.62 MHz - CDCl3

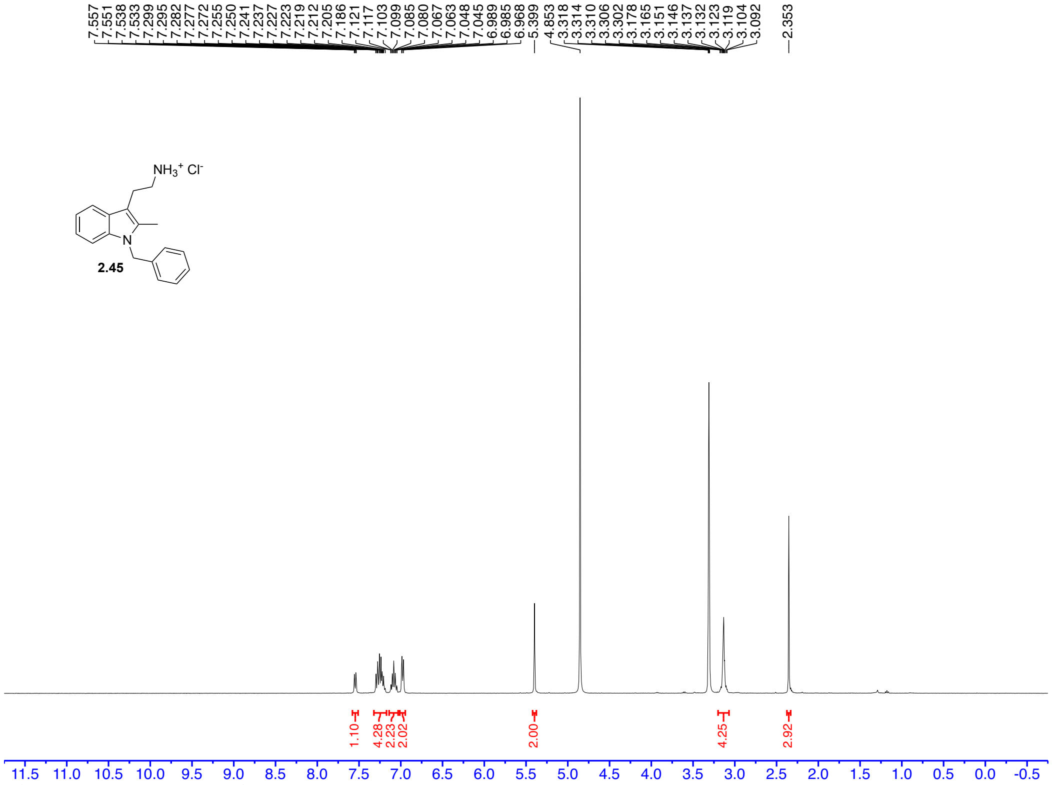

STM-3-31 - 1H NMR - 400.13 MHz - MeOD

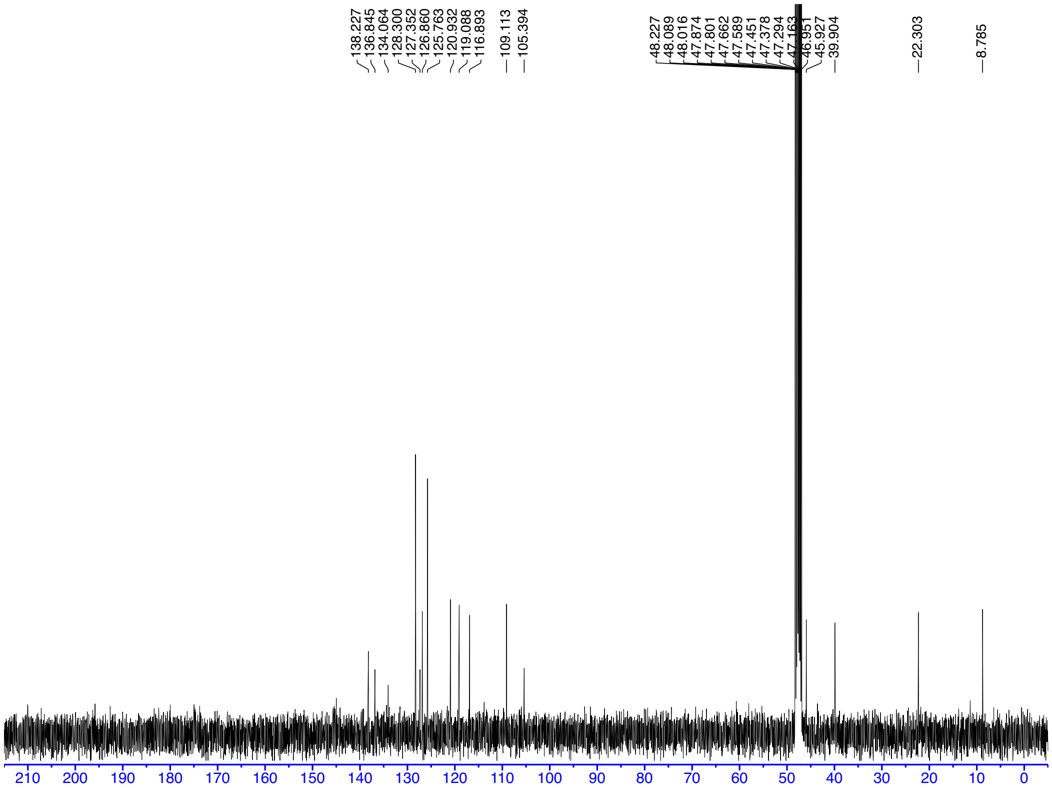

STM-3-31 CNMR - 13C NMR - 100.62 MHz - MeOD

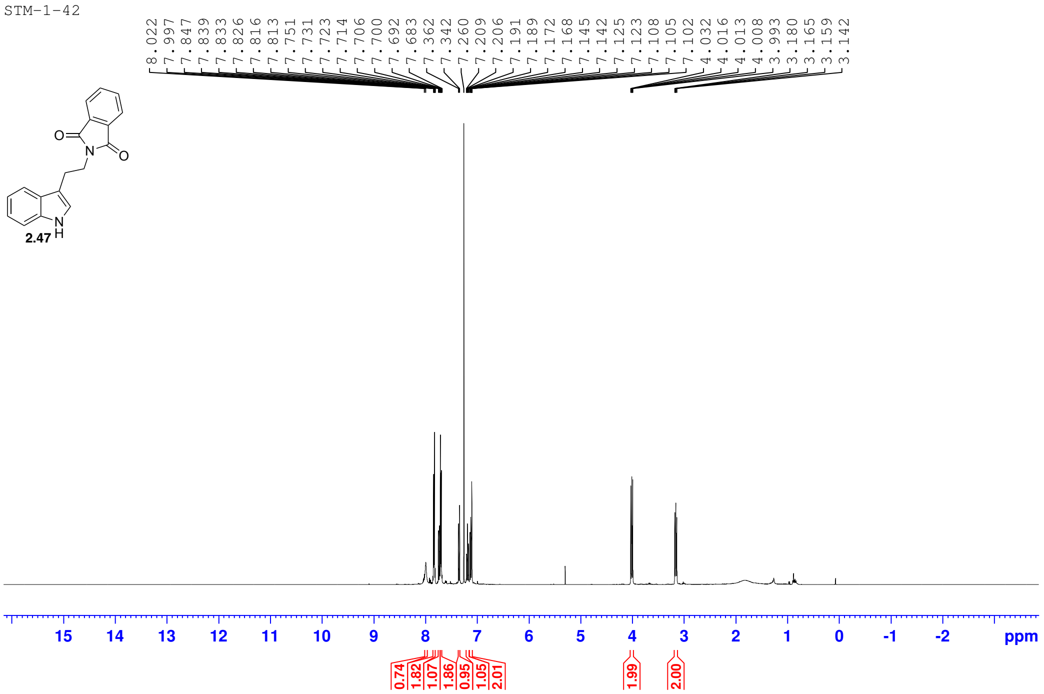
STM-1-42
2.47
8.022
7.997
7.847
7.839
7.833
7.826
7.816
7.813
7.751
7.731
7.723
7.714
7.706
7.700
7.692
7.683
7.362
7.342
7.260
7.209
7.206
7.191
7.189
7.172
7.168
7.145
7.142
7.125
7.123
7.108
7.105
7.102
4.032
4.016
4.013
4.008
3.993
3.180
3.165
3.159
3.142
15
14
13
12
11
10
9
8
7
6
5
4
3
2
1
0
-1
-2
ppm
0.74
1.82
1.07
1.86
0.95
1.05
2.01
1.99
2.00

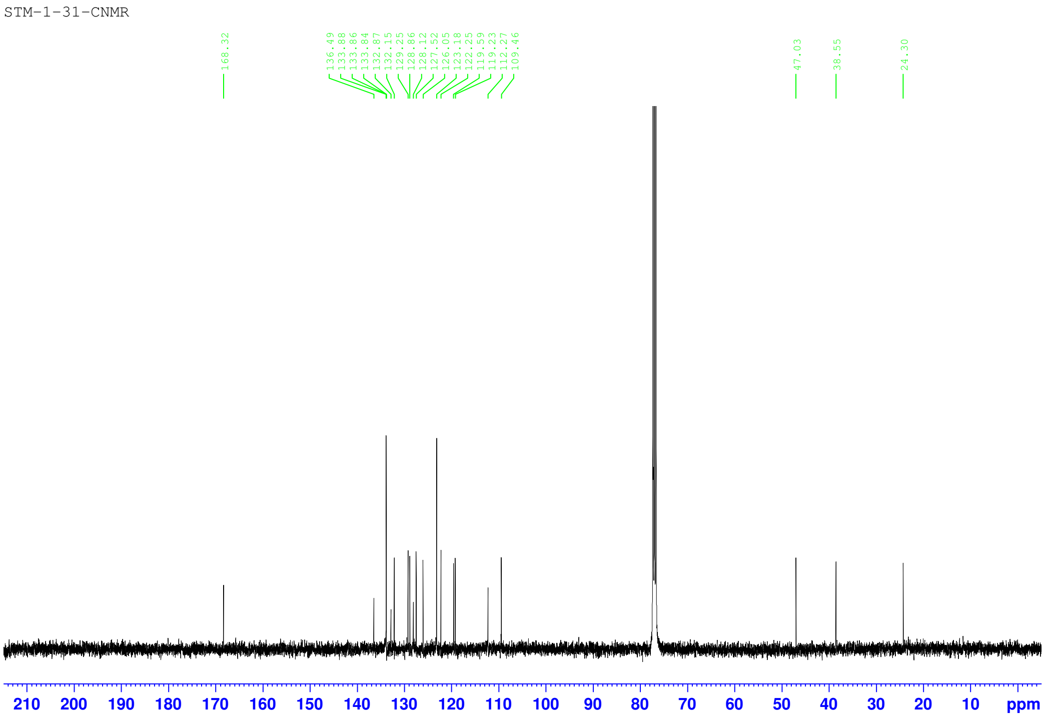
STM-1-31-CNMR
168.32
136.49
133.88
133.86
133.84
132.87
132.15
129.25
128.86
128.12
127.52
126.05
123.18
122.25
119.59
119.23
112.27
109.46
47.03
38.55
24.30
210
200
190
180
170
160
150
140
130
120
110
100
90
80
70
60
50
40
30
20
10
ppm

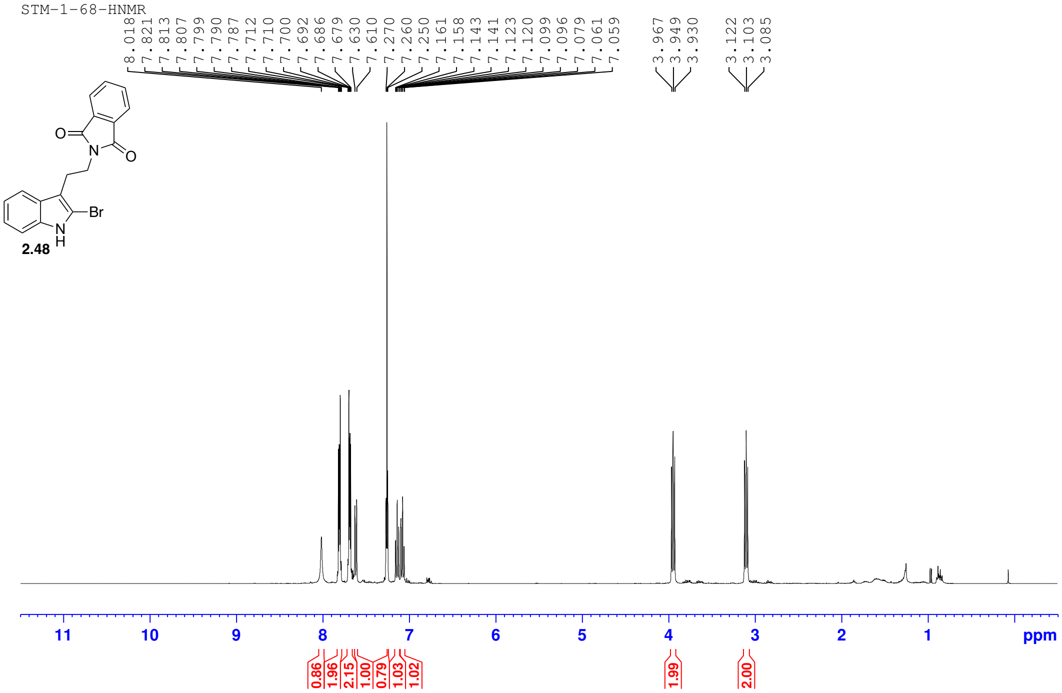
2.48
STM-1-68-HNMR
8.018
7.821
7.813
7.807
7.799
7.790
7.787
7.712
7.710
7.700
7.692
7.686
7.679
7.630
7.610
7.270
7.260
7.250
7.161
7.158
7.143
7.141
7.123
7.120
7.099
7.096
7.079
7.061
7.059
3.967
3.949
3.930
3.122
3.103
3.085
O
N
O
Br
N
H
11
10
9
8
7
6
5
4
3
2
1
ppm
0.86
1.96
2.15
1.00
0.79
1.03
1.02
1.99
2.00

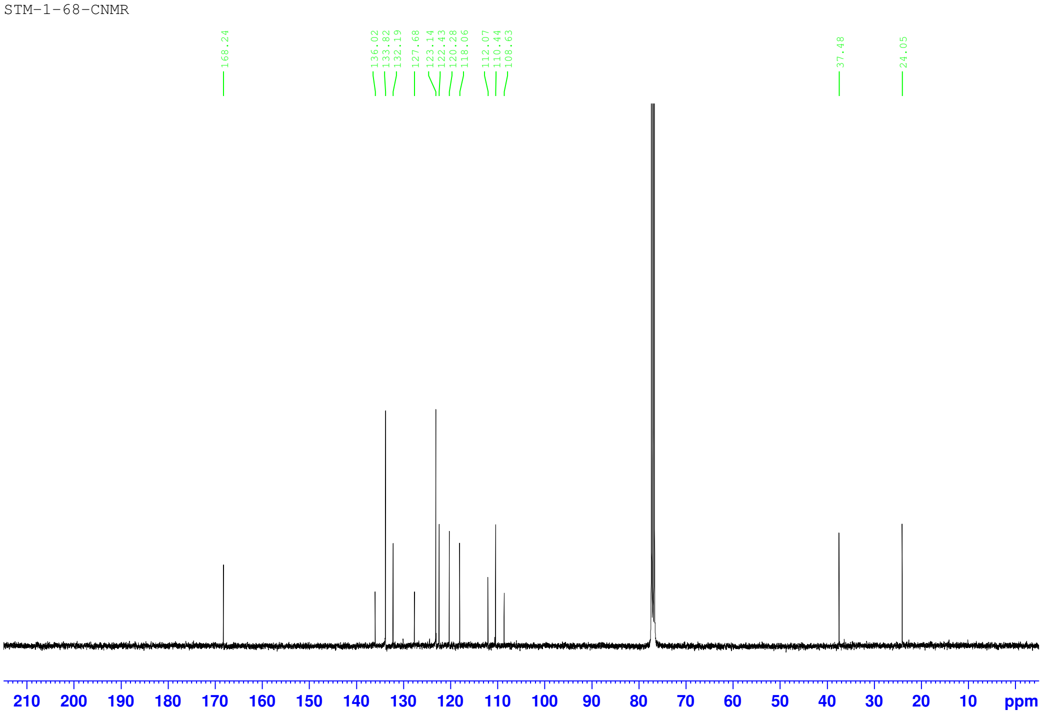
STM-1-68-CNMR
168.24
136.02
133.82
132.19
127.68
123.14
122.43
120.28
118.06
112.07
110.44
108.63
37.48
24.05
210
200
190
180
170
160
150
140
130
120
110
100
90
80
70
60
50
40
30
20
10
ppm

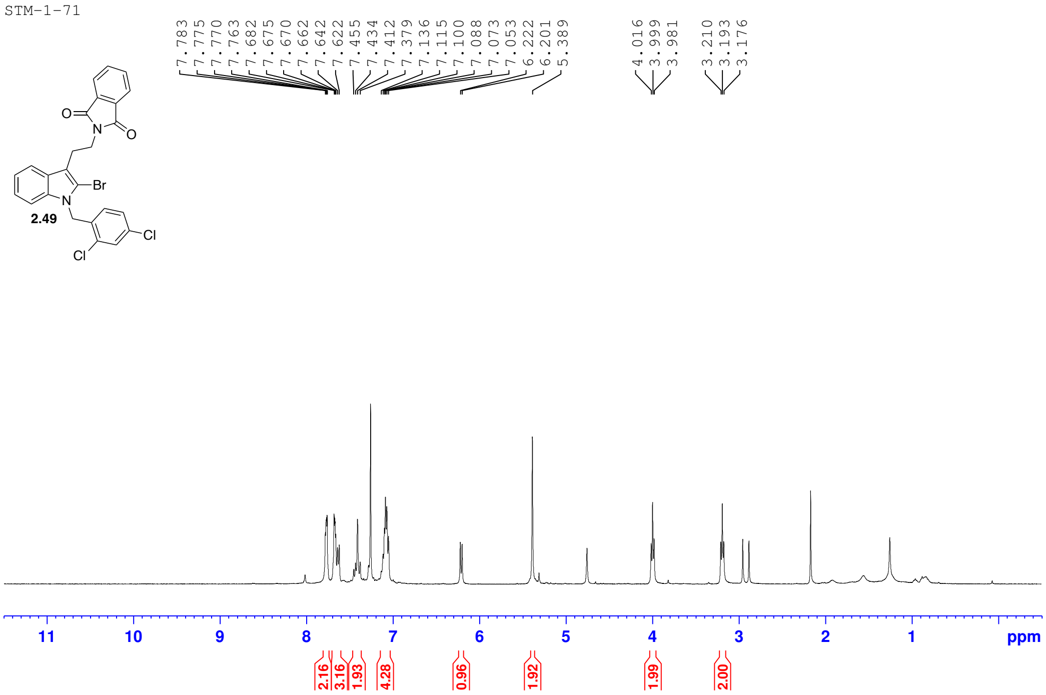
STM-1-71
O
N
O
Br
N
Cl
Cl
7.783
7.775
7.770
7.763
7.682
7.675
7.670
7.662
7.642
7.622
7.455
7.434
7.412
7.379
7.136
7.115
7.100
7.088
7.073
7.053
6.222
6.201
5.389
4.016
3.999
3.981
3.210
3.193
3.176
11
10
9
8
7
6
5
4
3
2
1
ppm
2.16
3.16
1.93
4.28
0.96
1.92
1.99
2.00

2.49

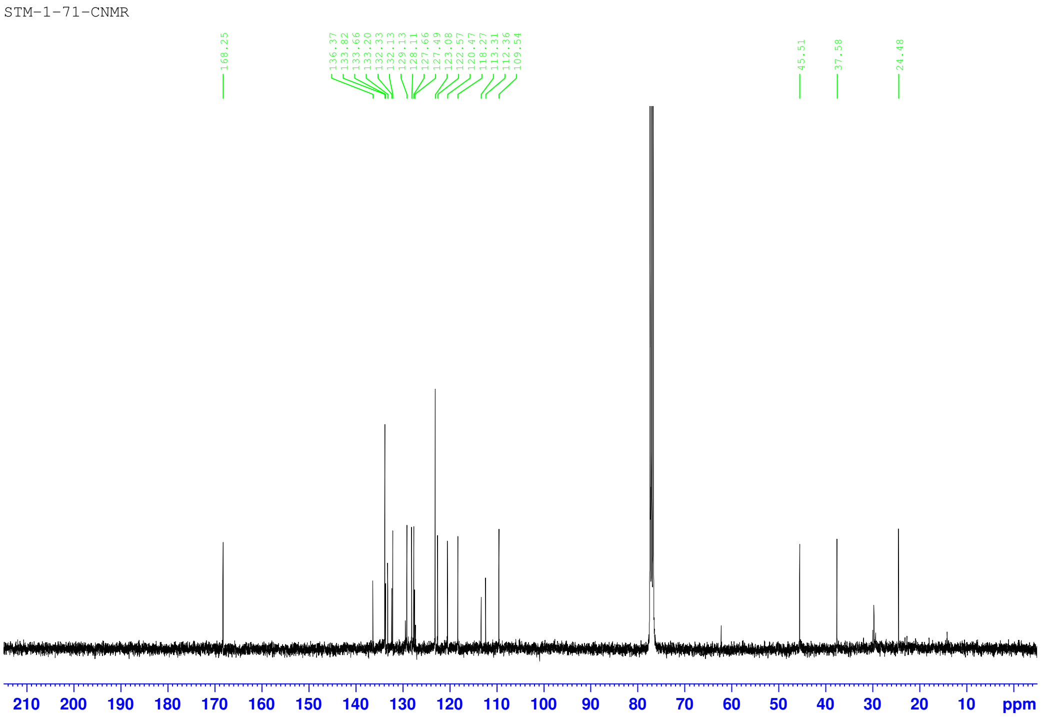
STM-1-71-CNMR
168.25
136.37
133.82
133.66
133.20
132.33
132.13
129.13
128.11
127.66
127.49
123.08
122.57
120.47
118.27
113.31
112.36
109.54
45.51
37.58
24.48
210
200
190
180
170
160
150
140
130
120
110
100
90
80
70
60
50
40
30
20
10
ppm

STM-1-53 (300MHz)

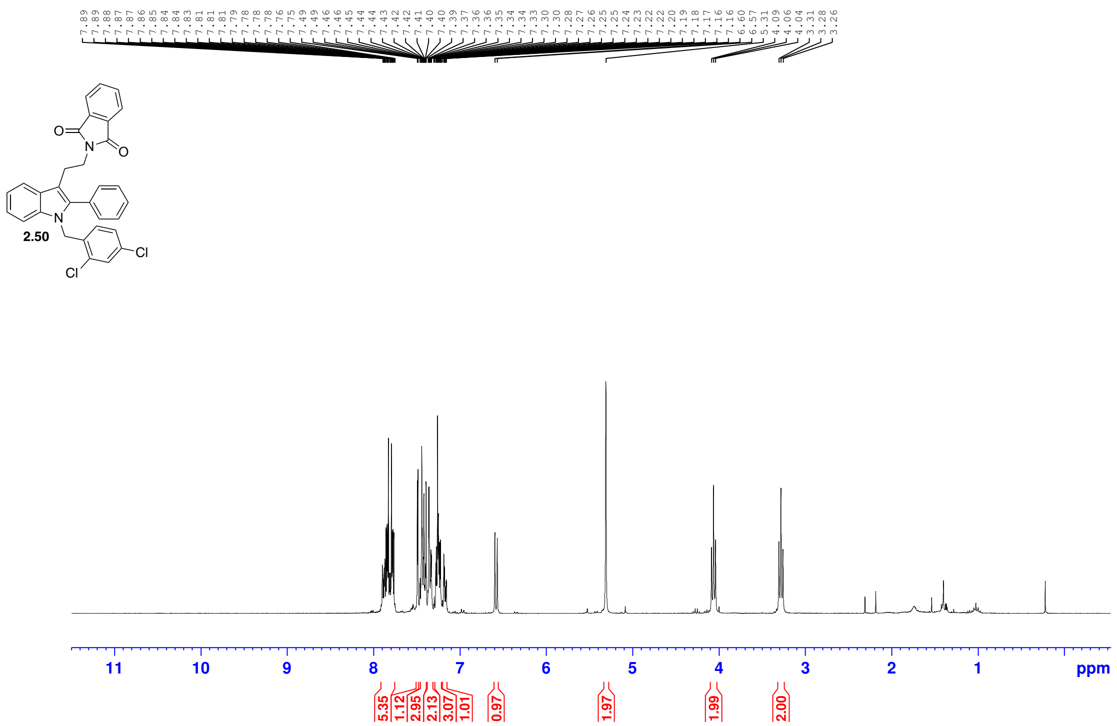

STM-1-53-CNMR (Acetone)

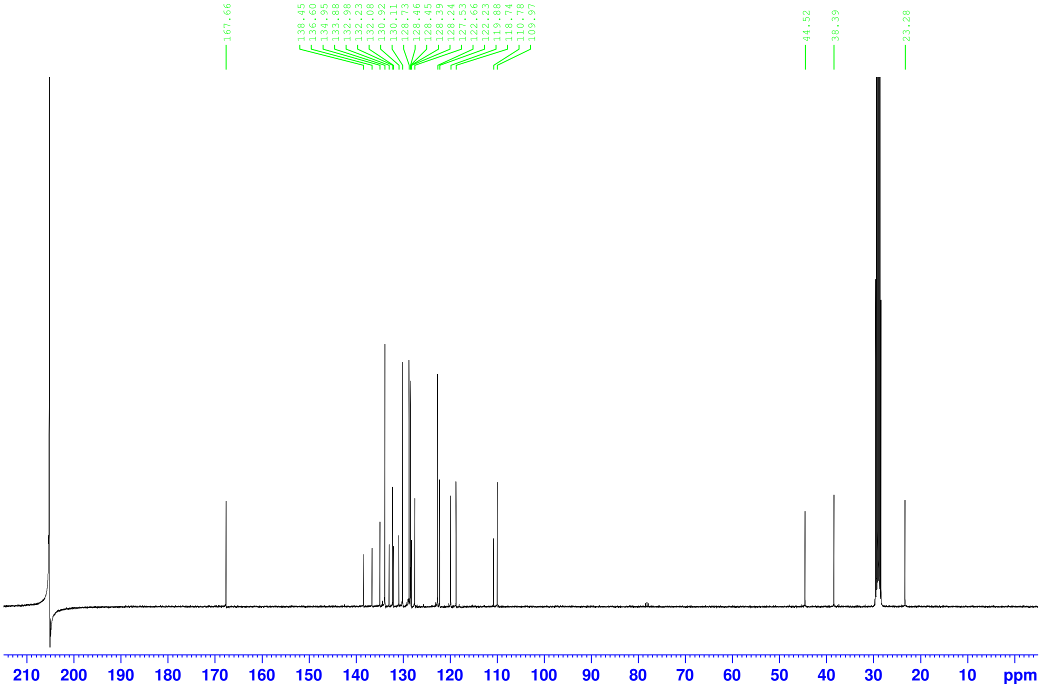

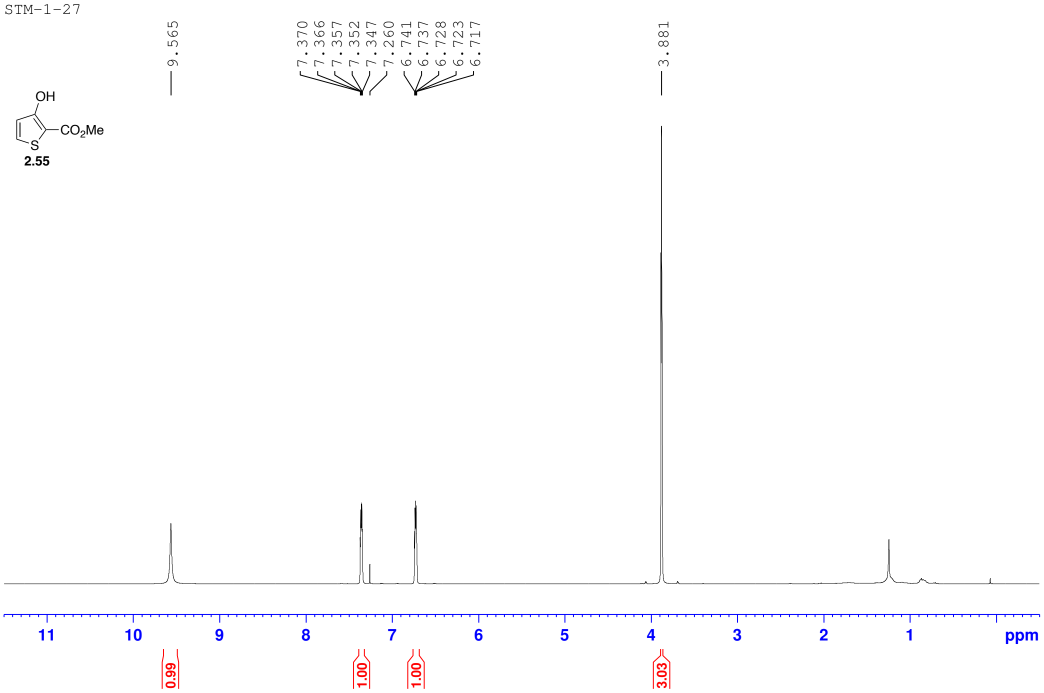
STM-1-27
OH
CO2Me
S
2.55
9.565
7.370
7.366
7.357
7.352
7.347
7.260
6.741
6.737
6.728
6.723
6.717
3.881
11
10
9
8
7
6
5
4
3
2
1
ppm
0.99
1.00
1.00
3.03

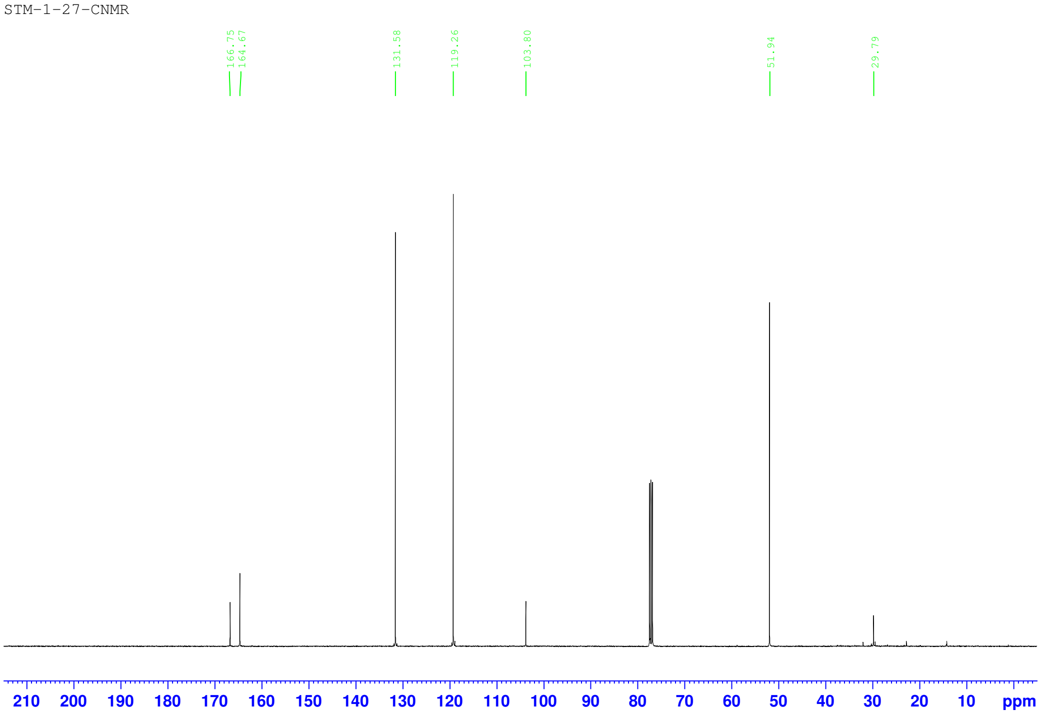
STM-1-27-CNMR
166.75
164.67
131.58
119.26
103.80
51.94
29.79
210
200
190
180
170
160
150
140
130
120
110
100
90
80
70
60
50
40
30
20
10
ppm

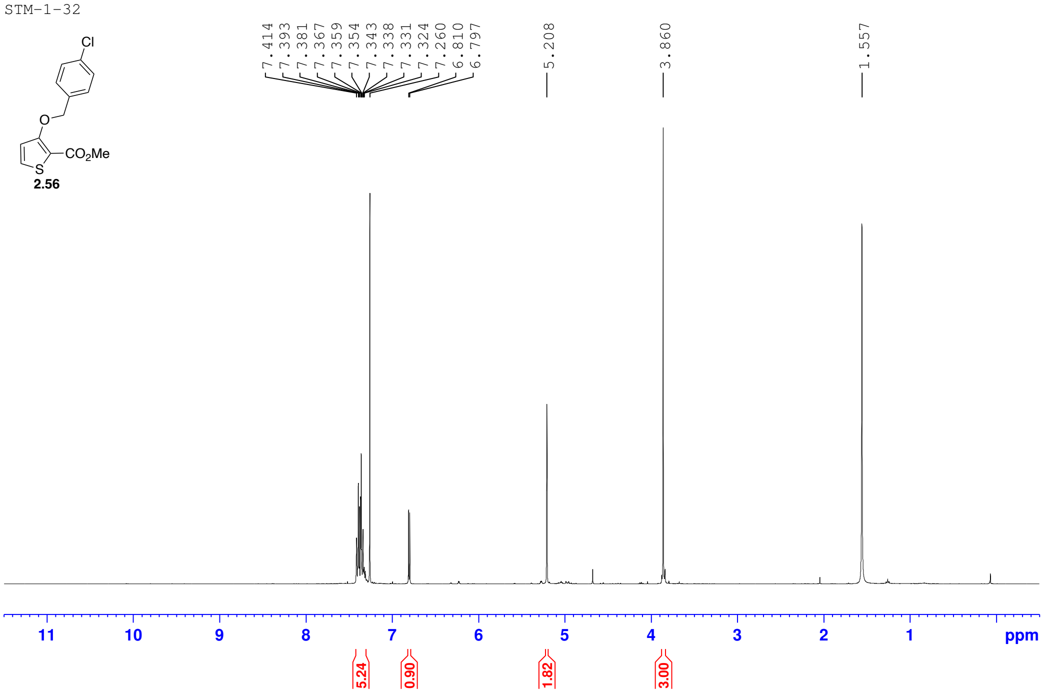
STM-1-32
Cl
O
CO$_2$Me
S
2.56
7.414
7.393
7.381
7.367
7.359
7.354
7.343
7.338
7.331
7.324
7.260
6.810
6.797
5.208
3.860
1.557
11
10
9
8
7
6
5
4
3
2
1
ppm
5.24
0.90
1.82
3.00

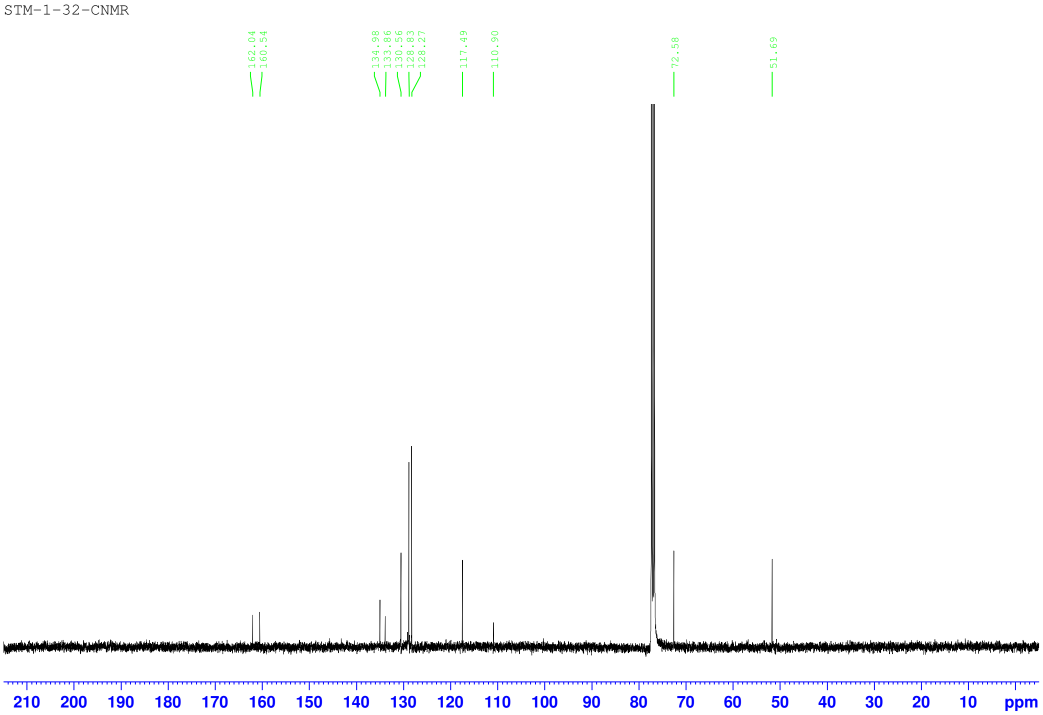
STM-1-32-CNMR
162.04
160.54
134.98
133.86
130.56
128.83
128.27
117.49
110.90
72.58
51.69
210
200
190
180
170
160
150
140
130
120
110
100
90
80
70
60
50
40
30
20
10
ppm

STM-1-36

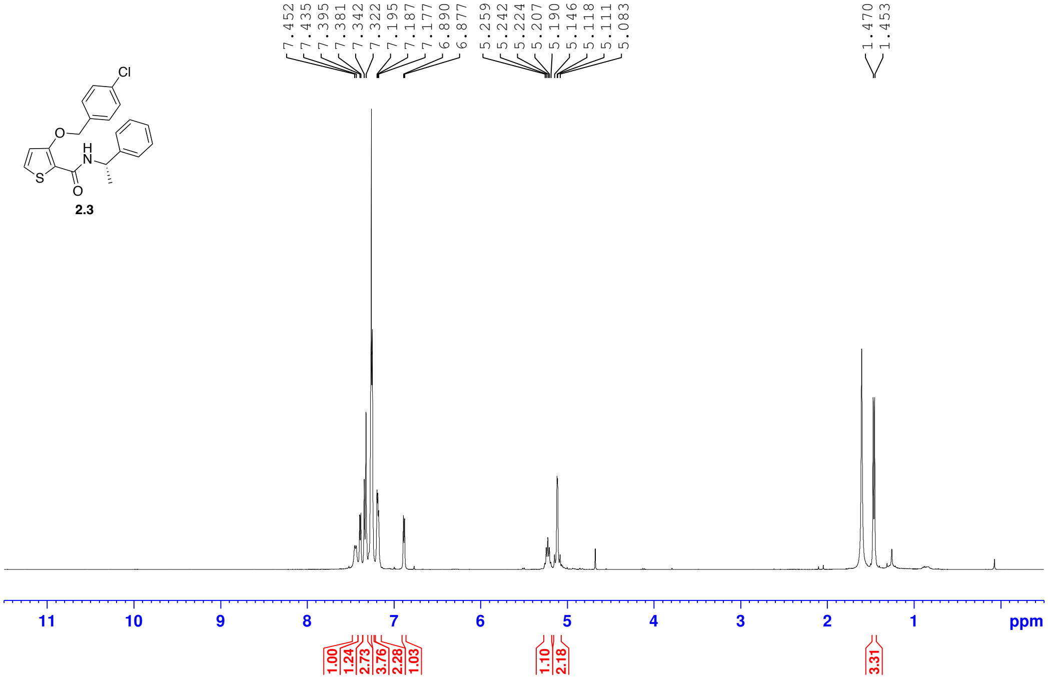

STM-1-36-CNMR

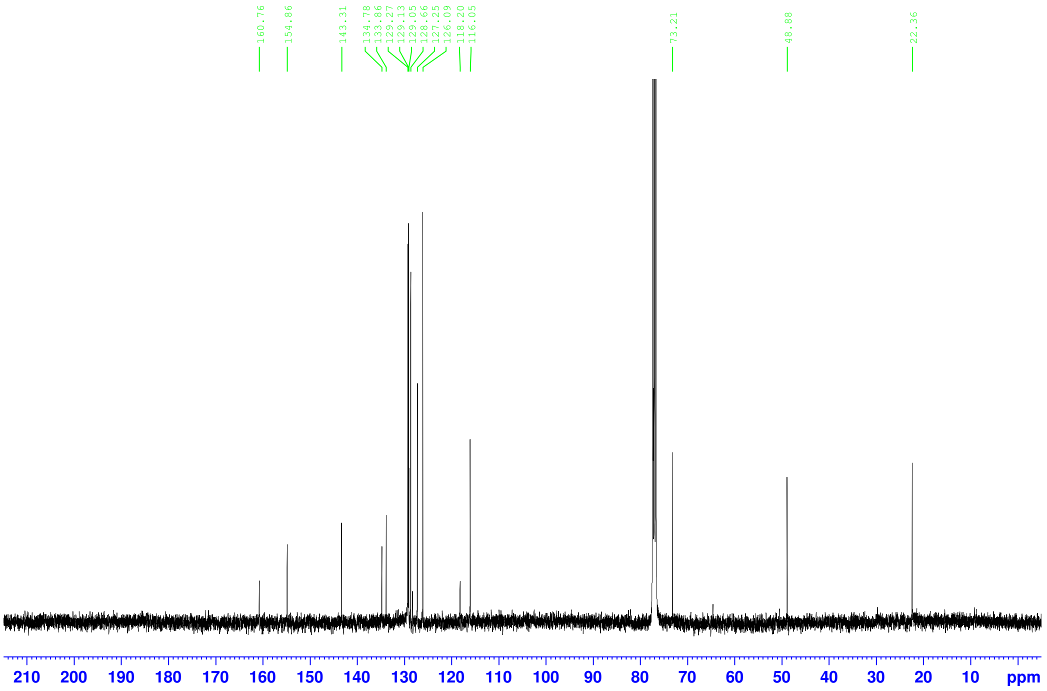

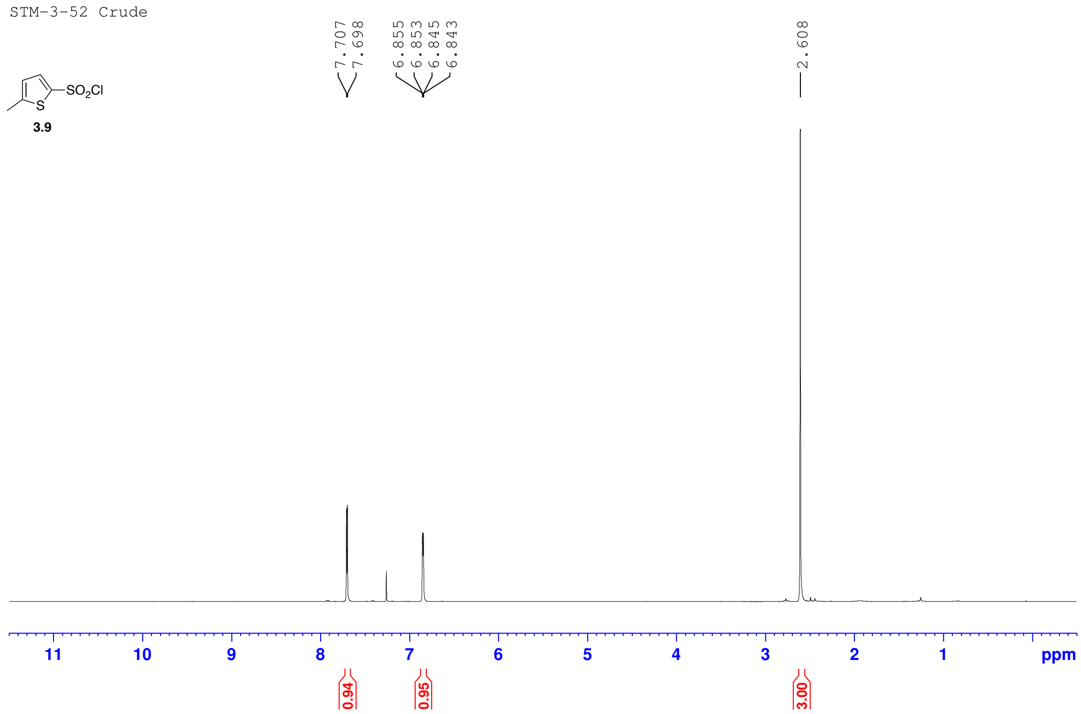
STM-3-52 Crude
SO2Cl
S
3.9
7.707
7.698
6.855
6.853
6.845
6.843
2.608
11
10
9
8
7
6
5
4
3
2
1
ppm
0.94
0.95
3.00

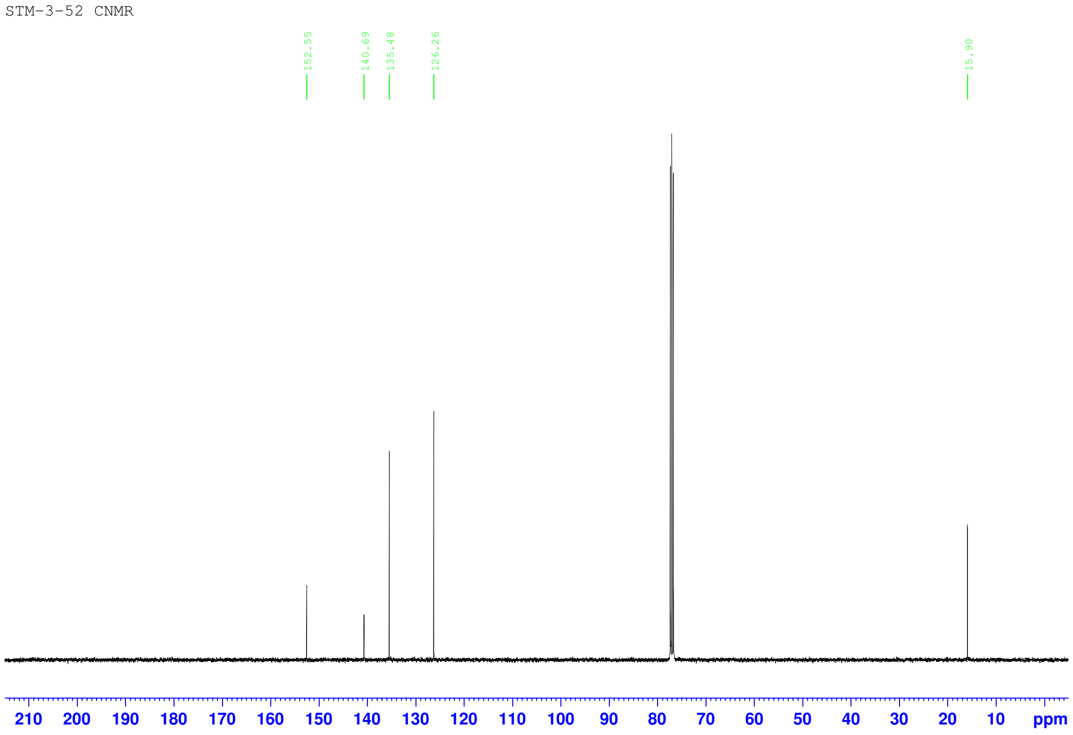
STM-3-52 CNMR
152.55
140.69
135.48
126.26
15.90
210
200
190
180
170
160
150
140
130
120
110
100
90
80
70
60
50
40
30
20
10
ppm

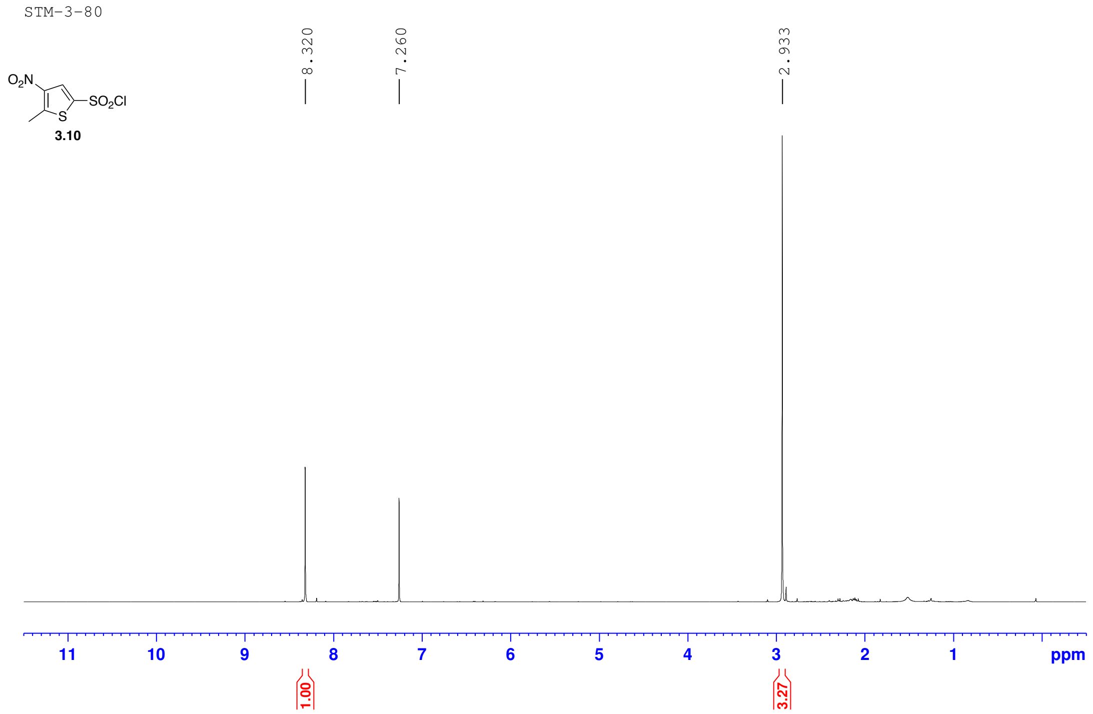
STM-3-80
O_2N
SO_2Cl
S
3.10
8.320
7.260
2.933
11
10
9
8
7
6
5
4
3
2
1
ppm
1.00
3.27

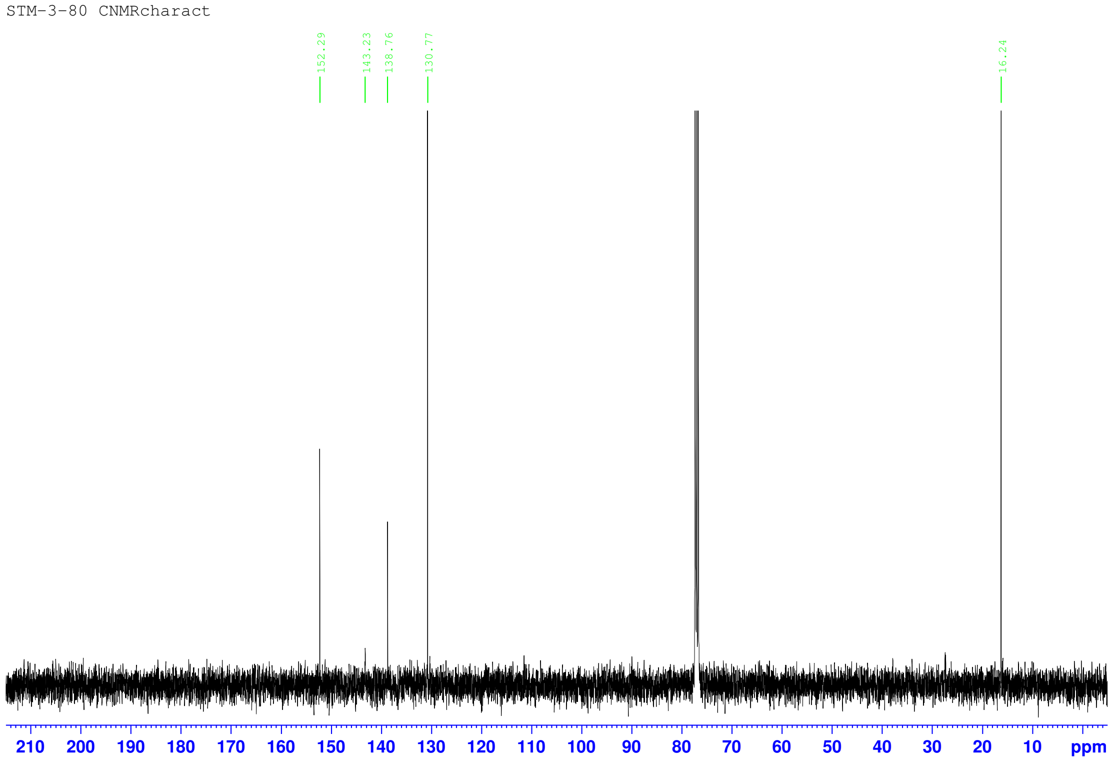
STM-3-80 CNMRcharact
152.29
143.23
138.76
130.77
16.24
210
200
190
180
170
160
150
140
130
120
110
100
90
80
70
60
50
40
30
20
10
ppm

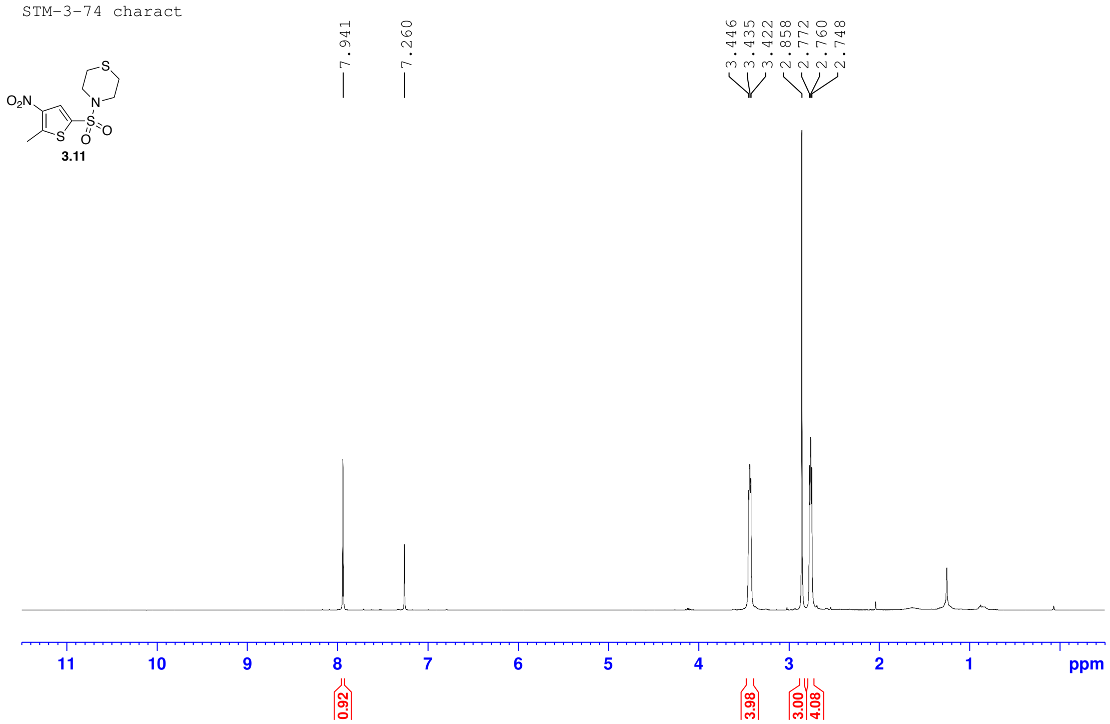
STM-3-74 charact
O_2N
S
N
S
O
O
S
3.11
7.941
7.260
3.446
3.435
3.422
2.858
2.772
2.760
2.748
11
10
9
8
7
6
5
4
3
2
1
ppm
0.92
3.98
3.00
4.08

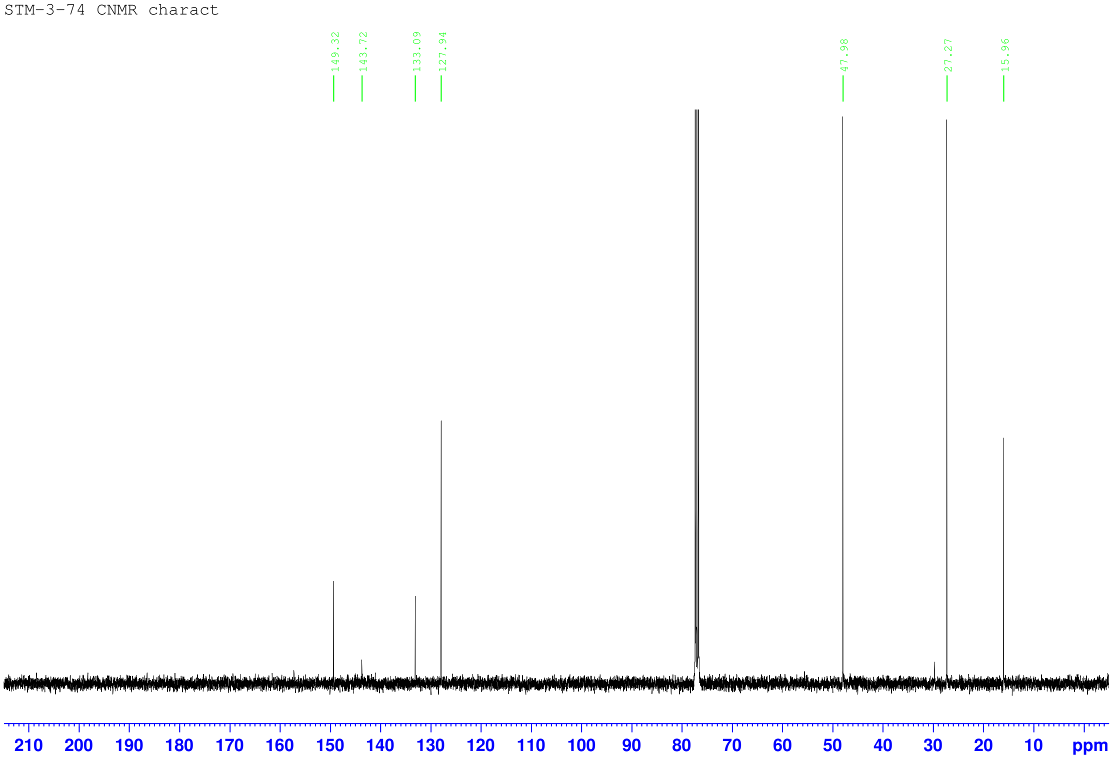
STM-3-74 CNMR charact
149.32
143.72
133.09
127.94
47.98
27.27
15.96
210
200
190
180
170
160
150
140
130
120
110
100
90
80
70
60
50
40
30
20
10
ppm

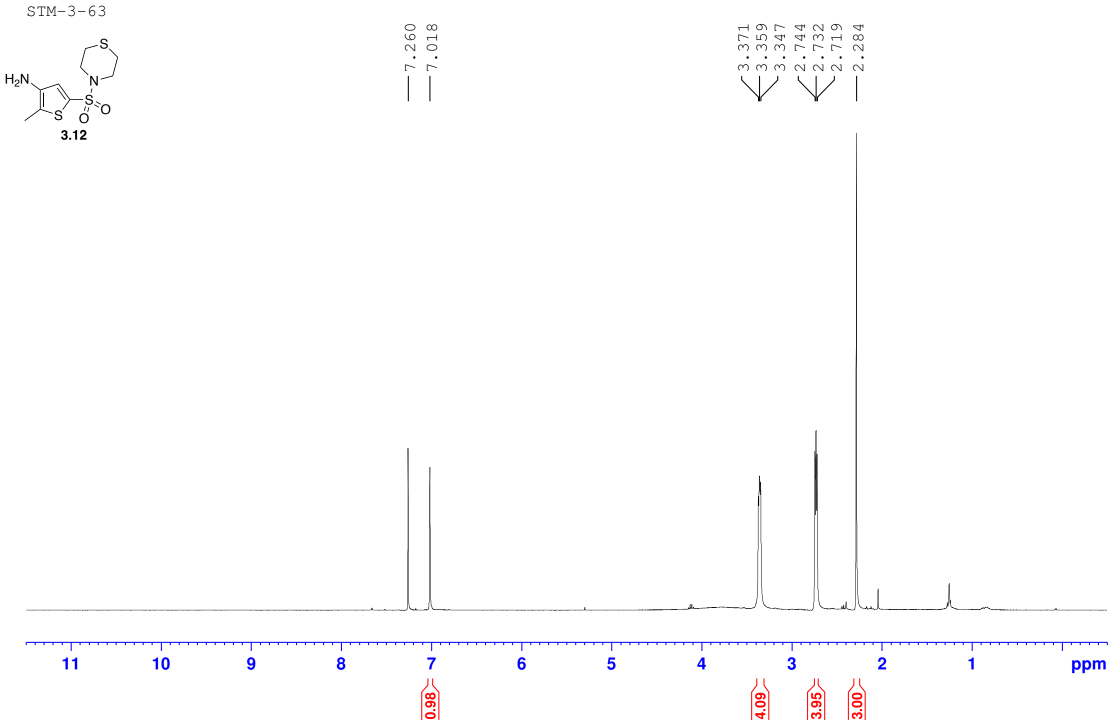
STM-3-63
H_2N
S
N
S
O
O
3.12
7.260
7.018
3.371
3.359
3.347
2.744
2.732
2.719
2.284
11
10
9
8
7
6
5
4
3
2
1
ppm
0.98
4.09
3.95
3.00

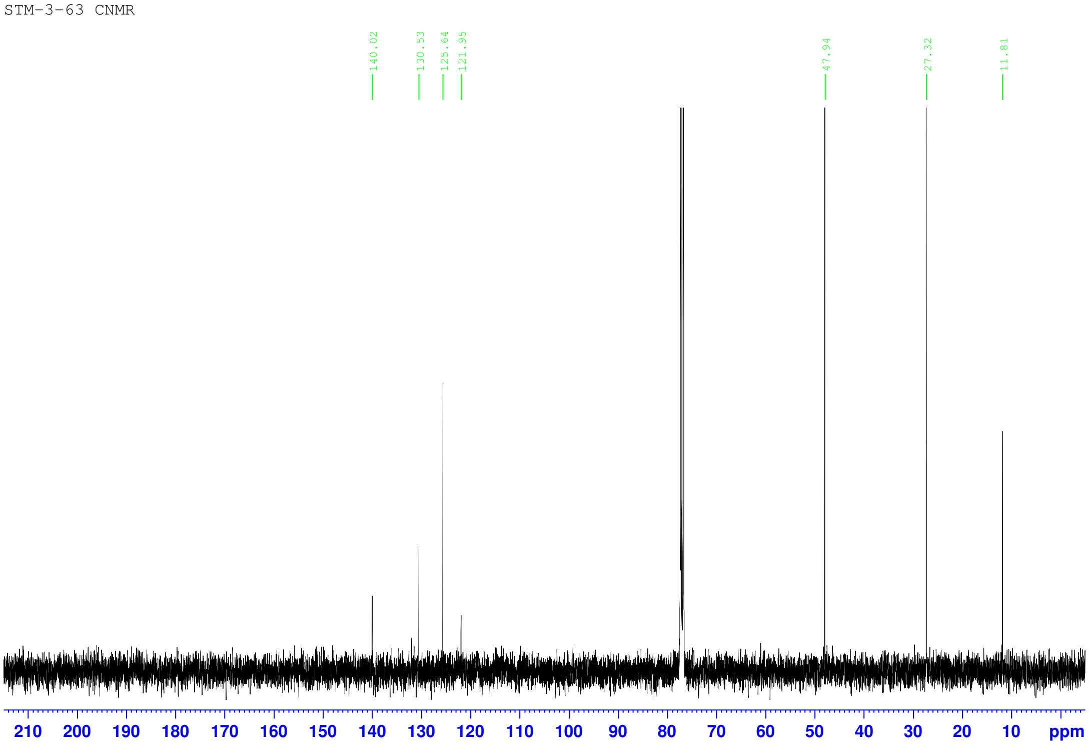
STM-3-63 CNMR
140.02
130.53
125.64
121.96
47.94
27.32
11.81
210
200
190
180
170
160
150
140
130
120
110
100
90
80
70
60
50
40
30
20
10
ppm

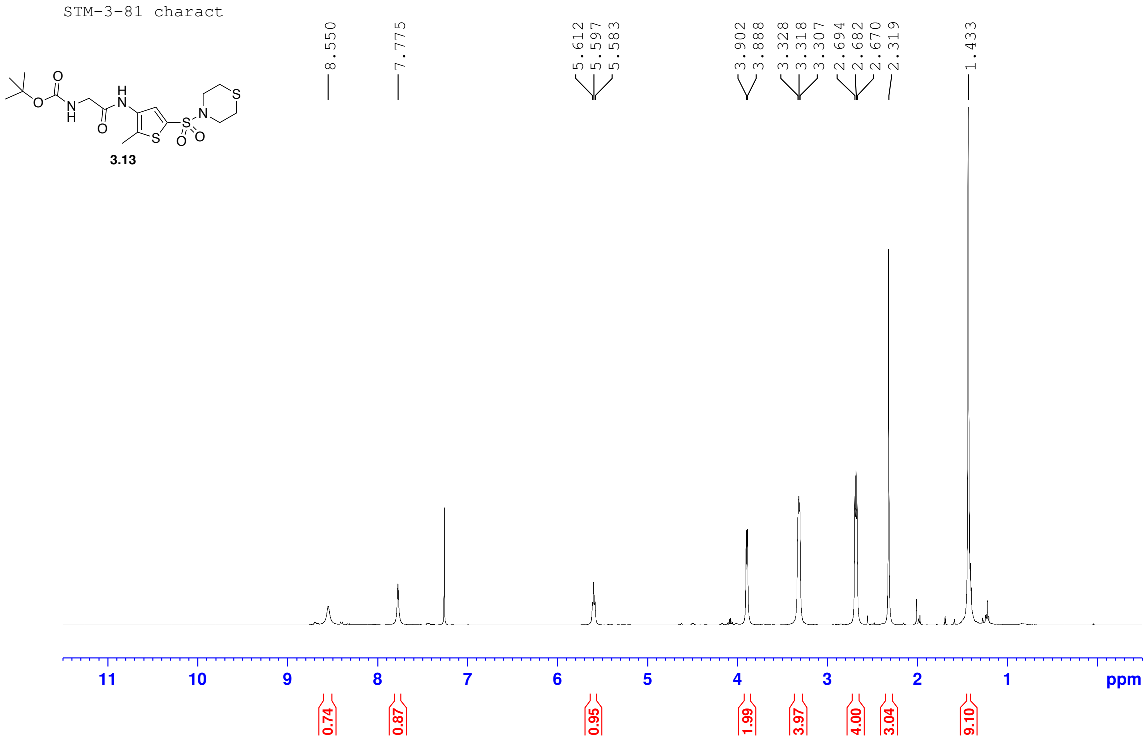
3.13
STM-3-81 charact
8.550
7.775
5.612
5.597
5.583
3.902
3.888
3.328
3.318
3.307
2.694
2.682
2.670
2.319
1.433
11
10
9
8
7
6
5
4
3
2
1
ppm
0.74
0.87
0.95
1.99
3.97
4.00
3.04
9.10
H
N
O
S

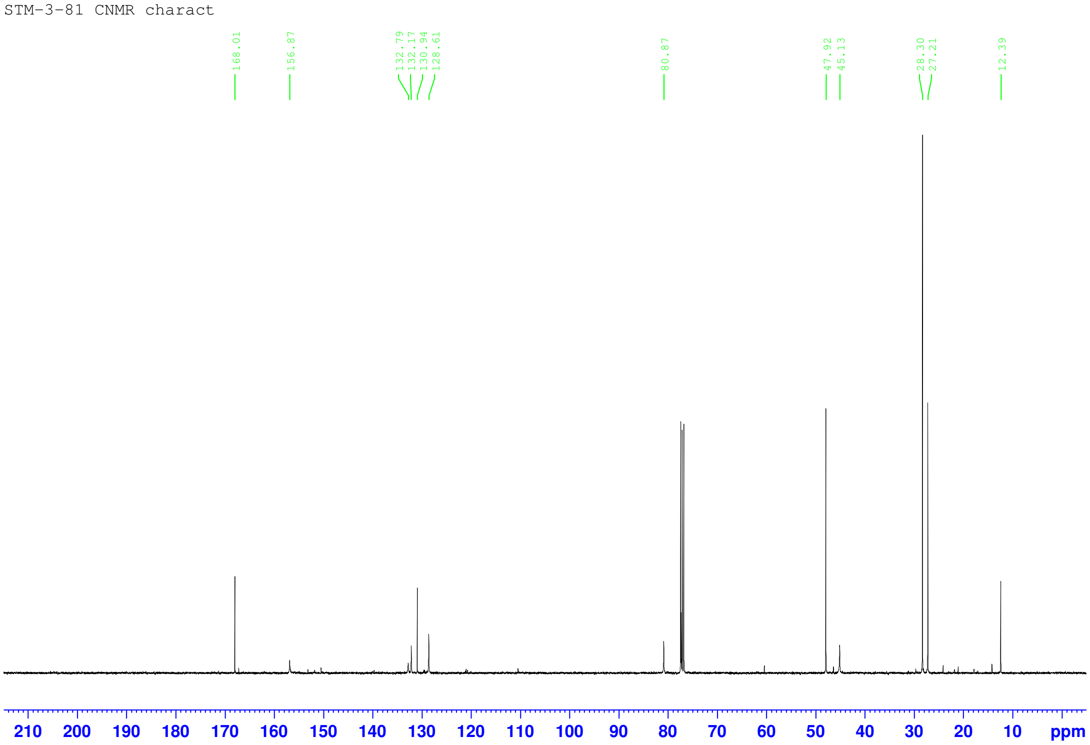
STM-3-81 CNMR charact
168.01
156.87
132.79
132.17
130.94
128.61
80.87
47.92
45.13
28.30
27.21
12.39
210
200
190
180
170
160
150
140
130
120
110
100
90
80
70
60
50
40
30
20
10
ppm

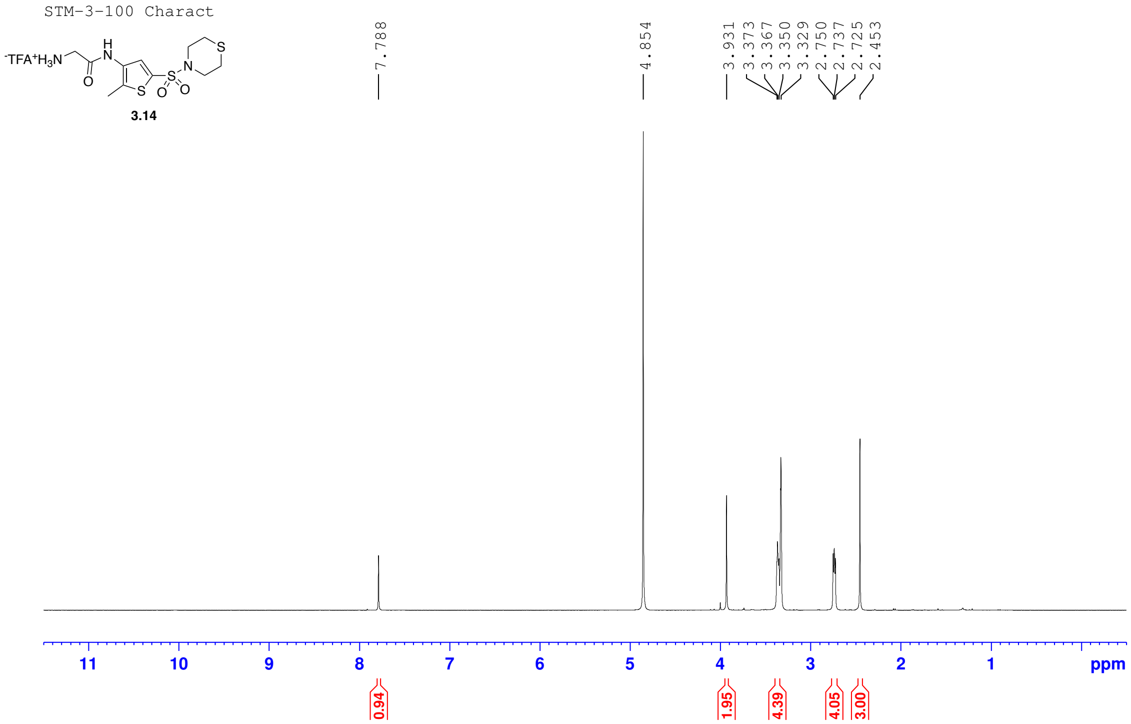
STM-3-100 Charact
-TFA+H3N
H
N
O
S
S
O
O
N
S
7.788
4.854
3.931
3.373
3.367
3.350
3.329
2.750
2.737
2.725
2.453
11
10
9
8
7
6
5
4
3
2
1
ppm
0.94
1.95
4.39
4.05
3.00

3.14

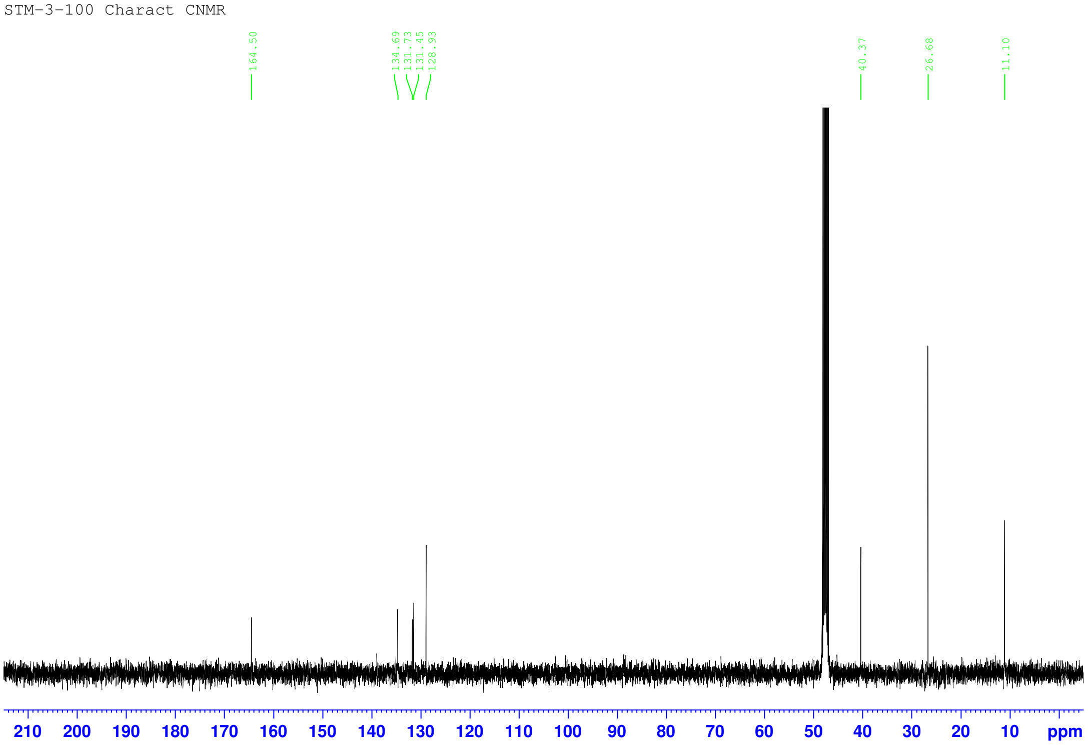
STM-3-100 Charact CNMR
164.50
134.69
131.73
131.45
128.93
40.37
26.68
11.10
210
200
190
180
170
160
150
140
130
120
110
100
90
80
70
60
50
40
30
20
10
ppm

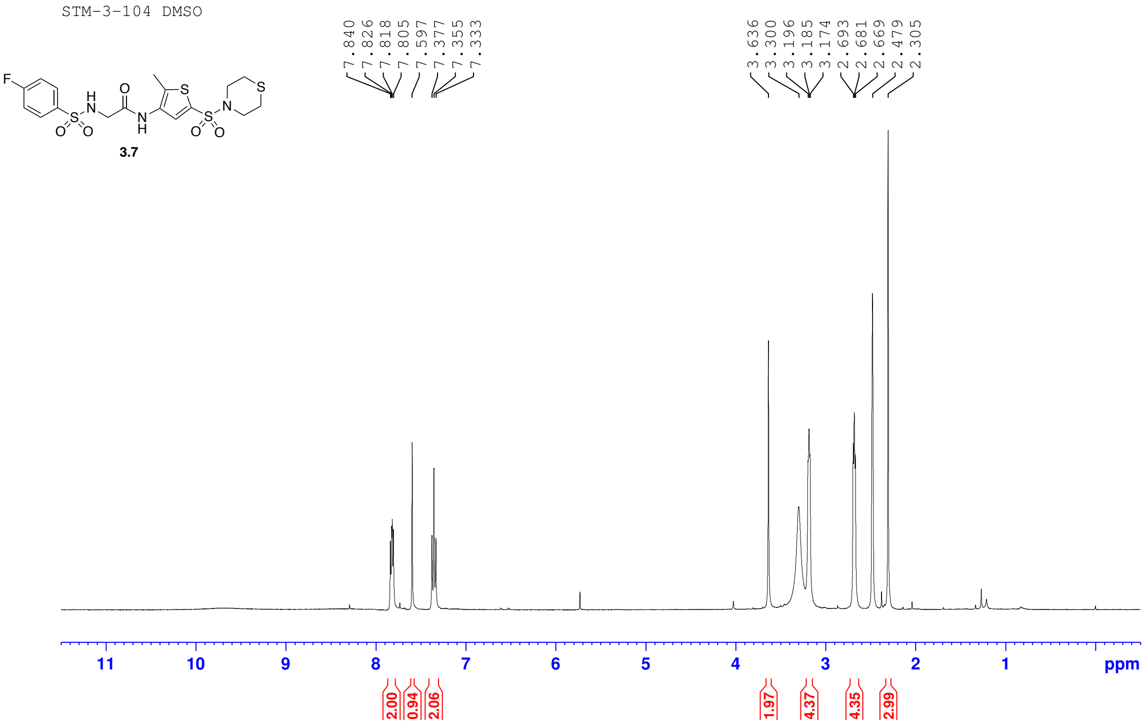
STM-3-104 DMSO
F
H
N
O
N
H
S
S
O
O
N
S
O
O
3.7
7.840
7.826
7.818
7.805
7.597
7.377
7.355
7.333
3.636
3.300
3.196
3.185
3.174
2.693
2.681
2.669
2.479
2.305
11
10
9
8
7
6
5
4
3
2
1
ppm
2.00
0.94
2.06
1.97
4.37
4.35
2.99

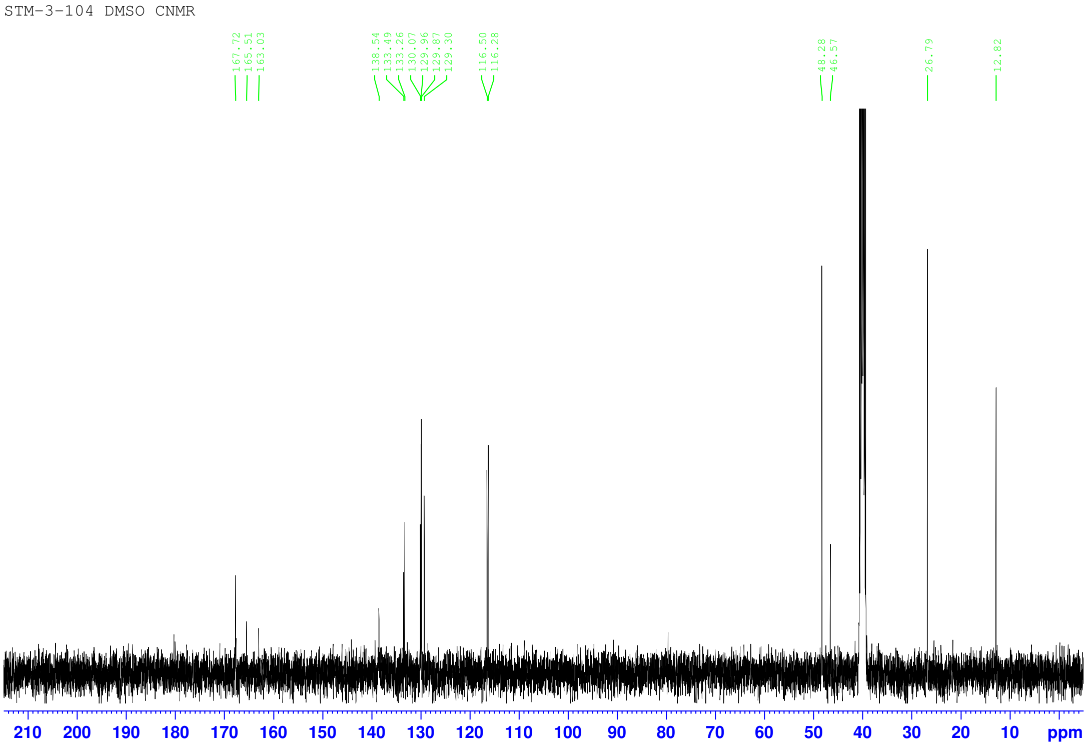
STM-3-104 DMSO CNMR
167.72
165.51
163.03
138.54
133.49
133.26
130.07
129.96
129.87
129.30
116.50
116.28
48.28
46.57
26.79
12.82
210
200
190
180
170
160
150
140
130
120
110
100
90
80
70
60
50
40
30
20
10
ppm

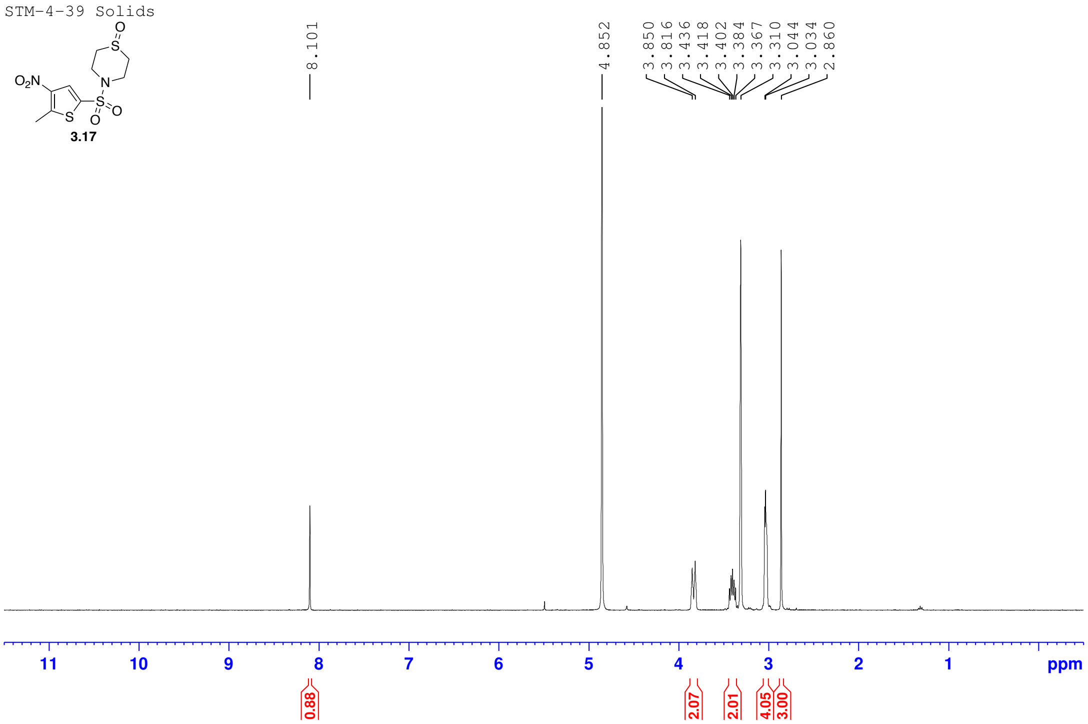
STM-4-39 Solids
O_2N
S
N
S
O
O
O
3.17
8.101
4.852
3.850
3.816
3.436
3.418
3.402
3.384
3.367
3.310
3.044
3.034
2.860
11
10
9
8
7
6
5
4
3
2
1
ppm
0.88
2.07
2.01
4.05
3.00

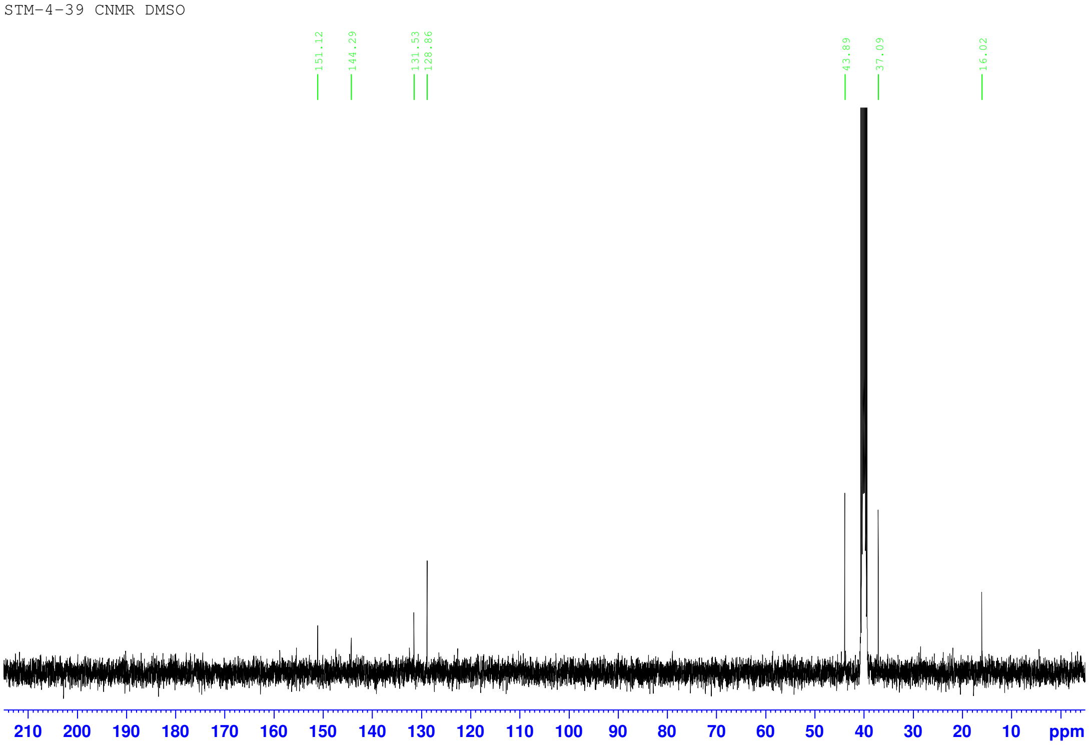
STM-4-39 CNMR DMSO
151.12
144.29
131.53
128.86
43.89
37.09
16.02
210
200
190
180
170
160
150
140
130
120
110
100
90
80
70
60
50
40
30
20
10
ppm

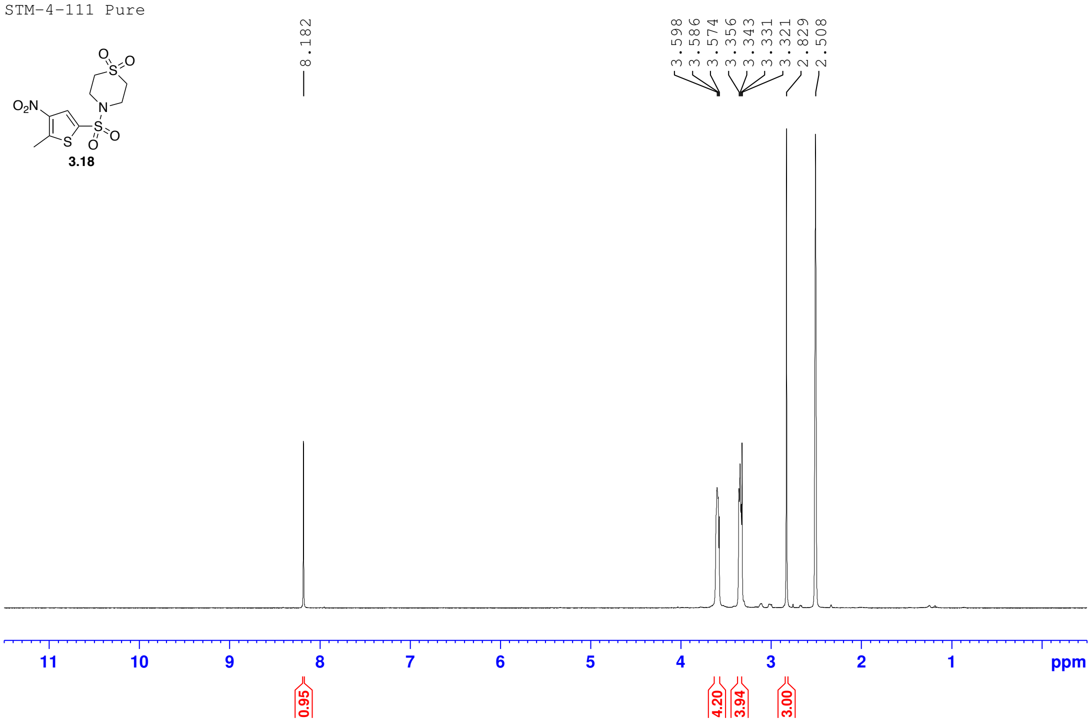
STM-4-111 Pure
O
S
O
O2N
N
S
S
O
O
3.18
8.182
3.598
3.586
3.574
3.356
3.343
3.331
3.321
2.829
2.508
11
10
9
8
7
6
5
4
3
2
1
ppm
0.95
4.20
3.94
3.00

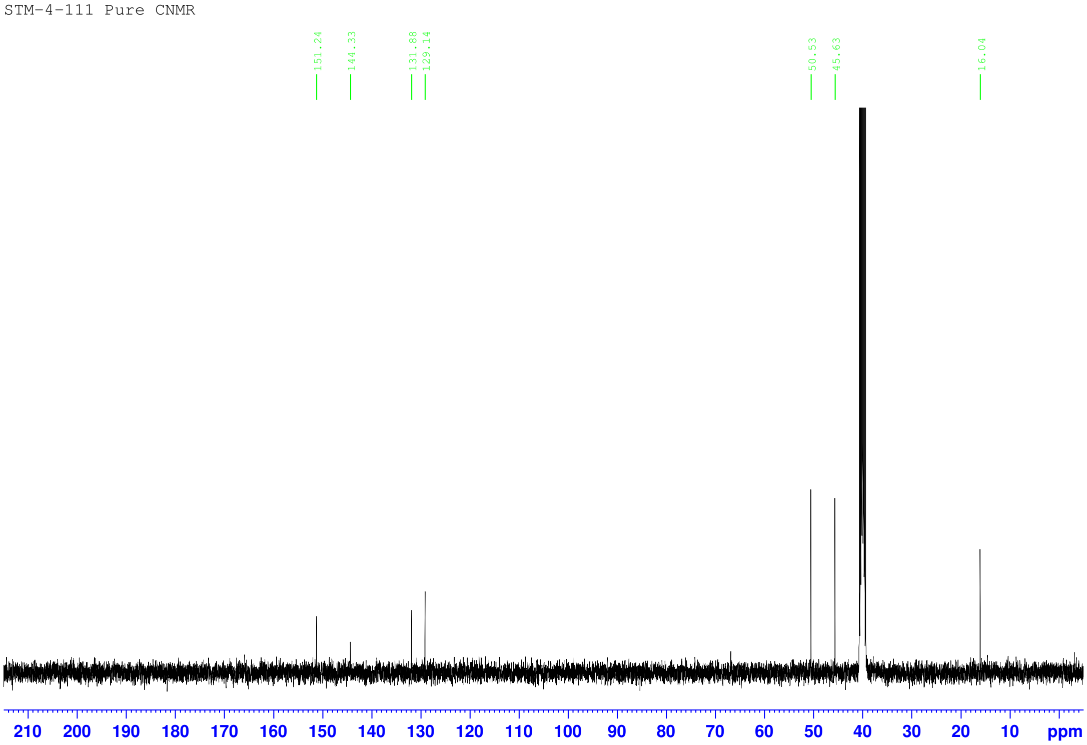
STM-4-111 Pure CNMR
151.24
144.33
131.88
129.14
50.53
45.63
16.04
210
200
190
180
170
160
150
140
130
120
110
100
90
80
70
60
50
40
30
20
10
ppm

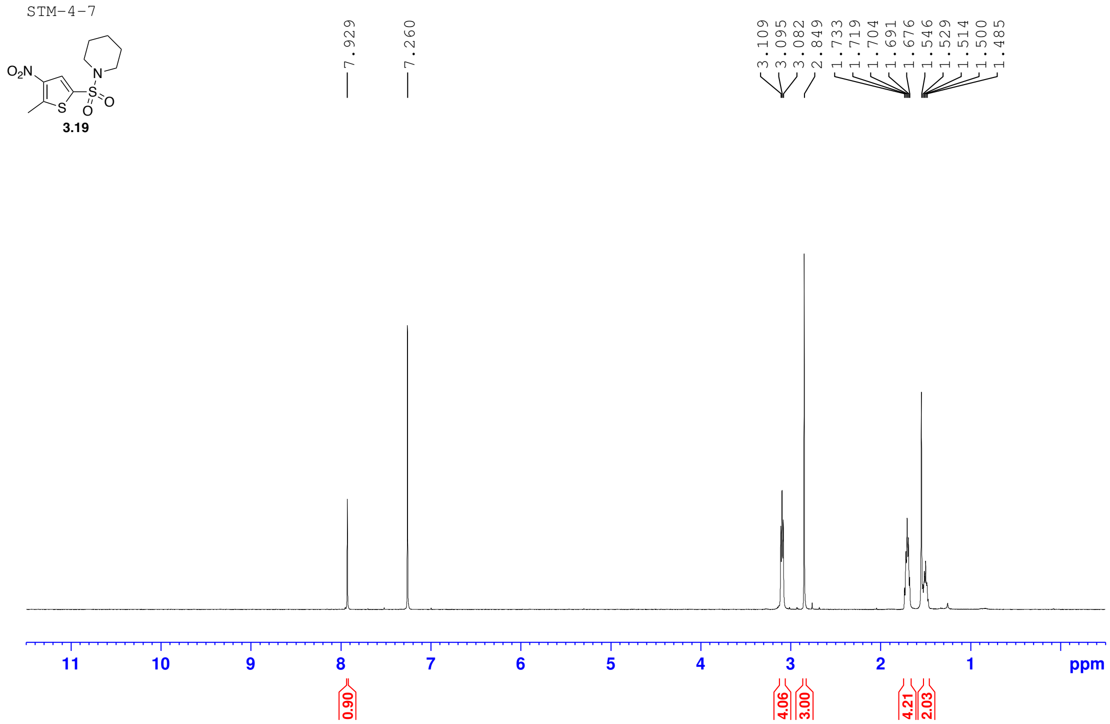
STM-4-7
O2N
N
S
O
O
S
3.19
7.929
7.260
3.109
3.095
3.082
2.849
1.733
1.719
1.704
1.691
1.676
1.546
1.529
1.514
1.500
1.485
11
10
9
8
7
6
5
4
3
2
1
ppm
0.90
4.06
3.00
4.21
2.03

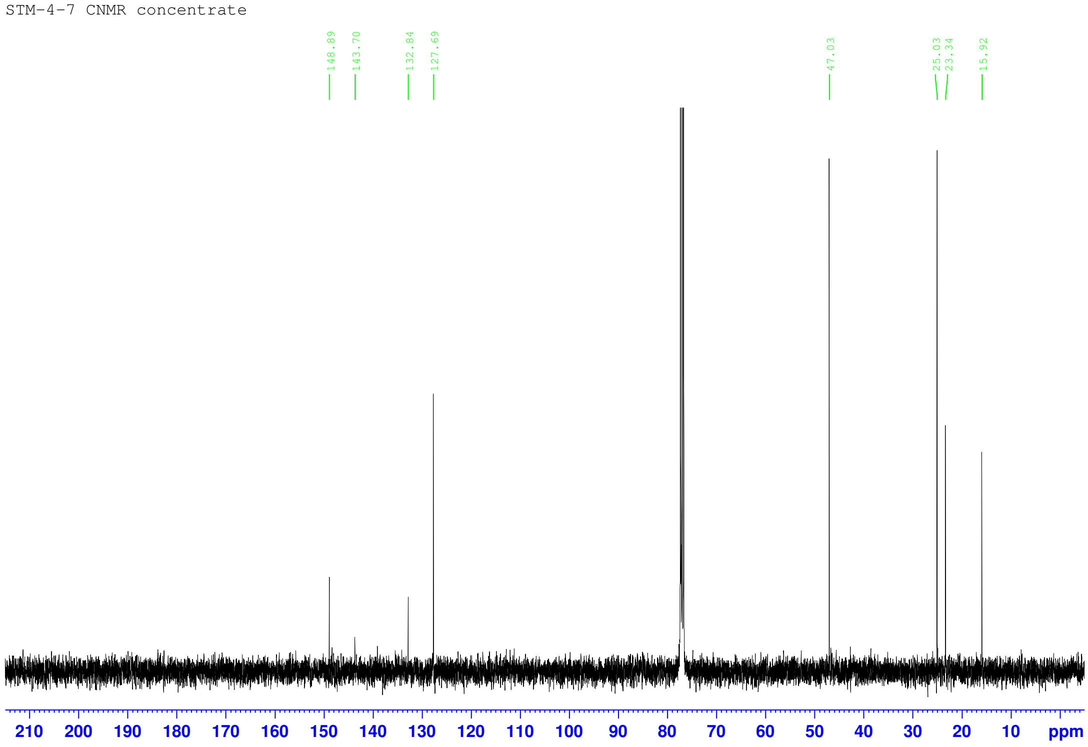
STM-4-7 CNMR concentrate
148.89
143.70
132.84
127.69
47.03
25.03
23.34
15.92
210
200
190
180
170
160
150
140
130
120
110
100
90
80
70
60
50
40
30
20
10
ppm

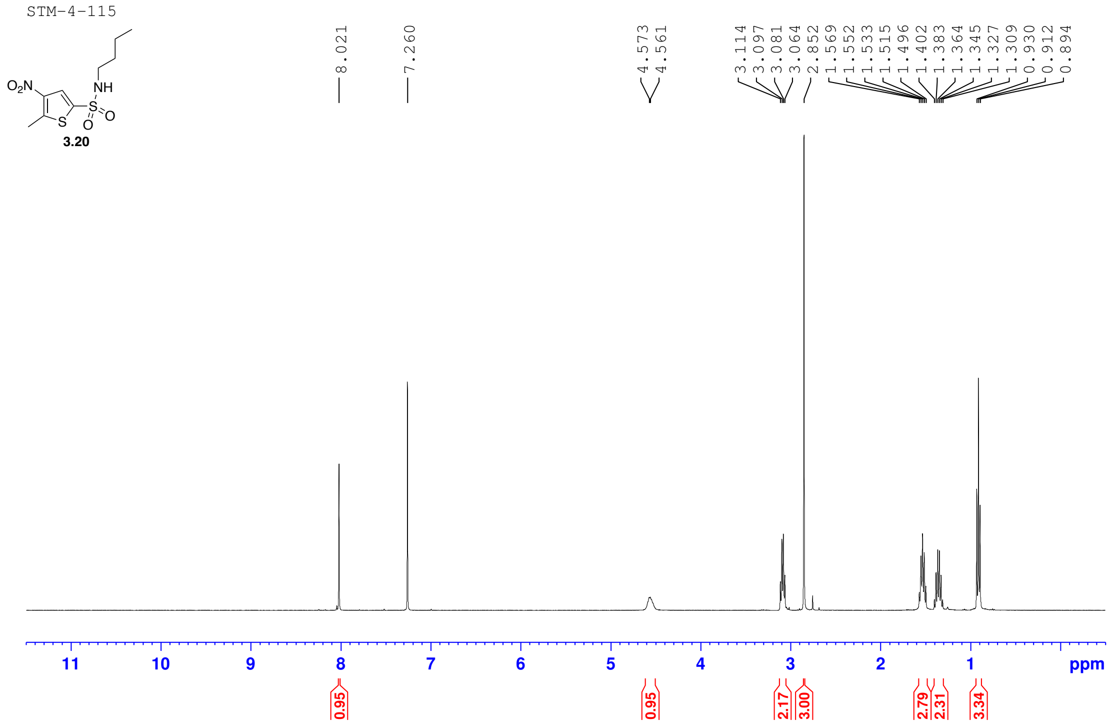
STM-4-115
O_2N
NH
S
O
O
3.20
8.021
7.260
4.573
4.561
3.114
3.097
3.081
3.064
2.852
1.569
1.552
1.533
1.515
1.496
1.402
1.383
1.364
1.345
1.327
1.309
0.930
0.912
0.894
11
10
9
8
7
6
5
4
3
2
1
ppm
0.95
0.95
2.17
3.00
2.79
2.31
3.34

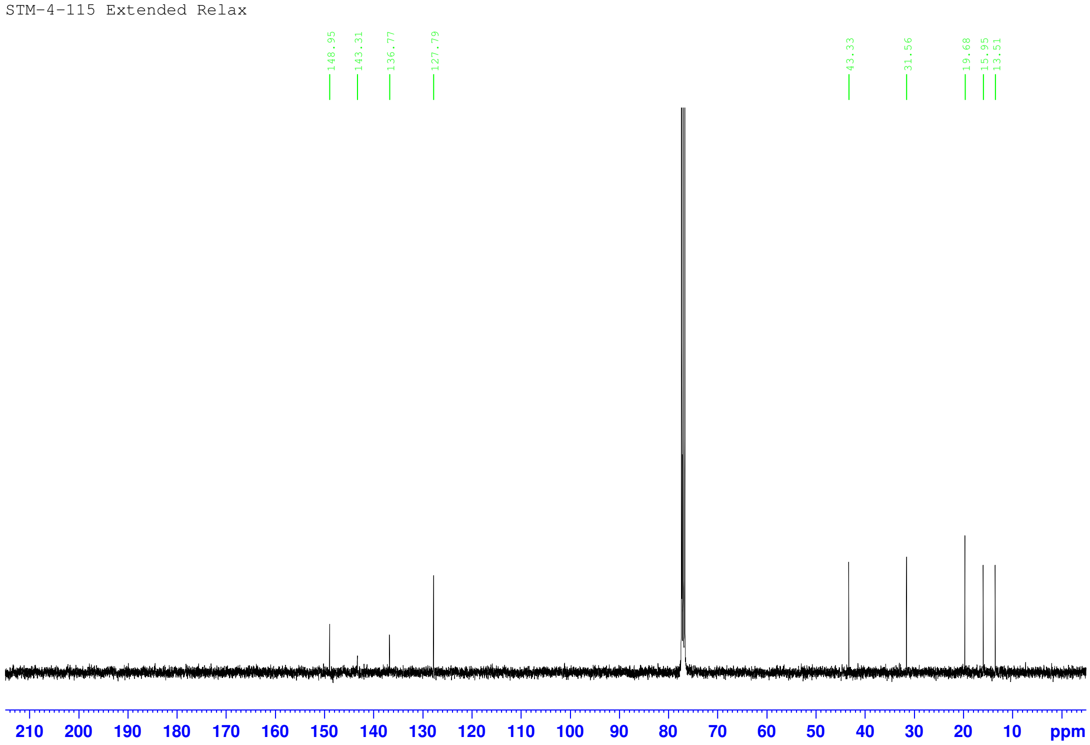
STM-4-115 Extended Relax
148.95
143.31
136.77
127.79
43.33
31.56
19.68
15.95
13.51
210
200
190
180
170
160
150
140
130
120
110
100
90
80
70
60
50
40
30
20
10
ppm

STM-4-116

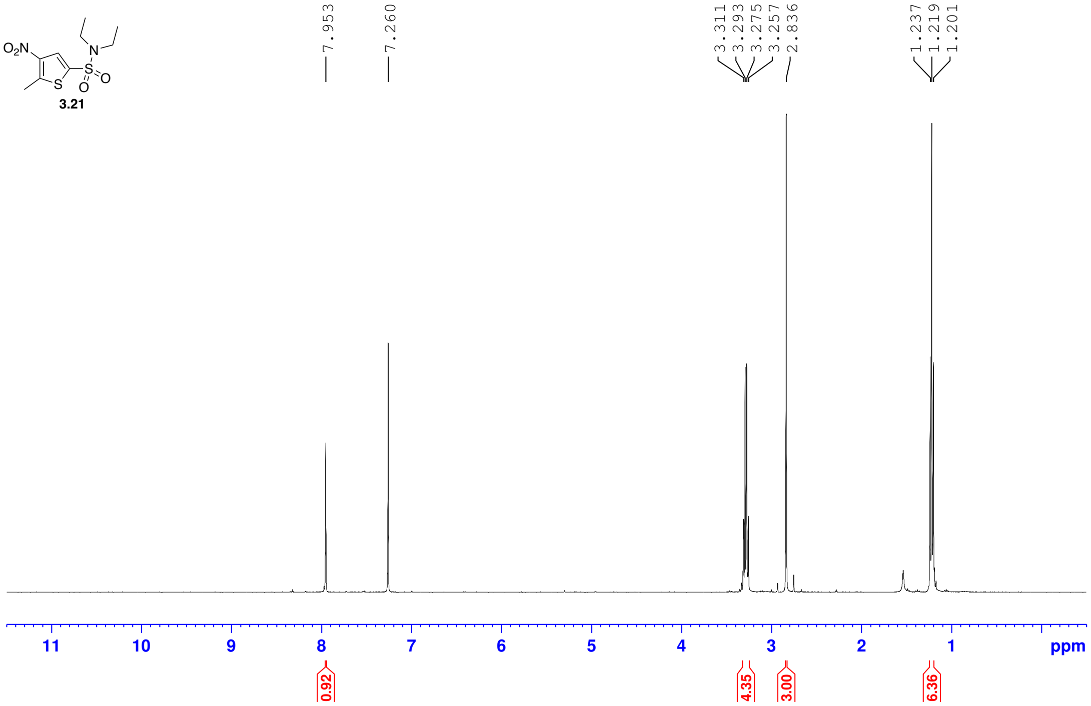

STM-4-116 CNMR Extended Relax

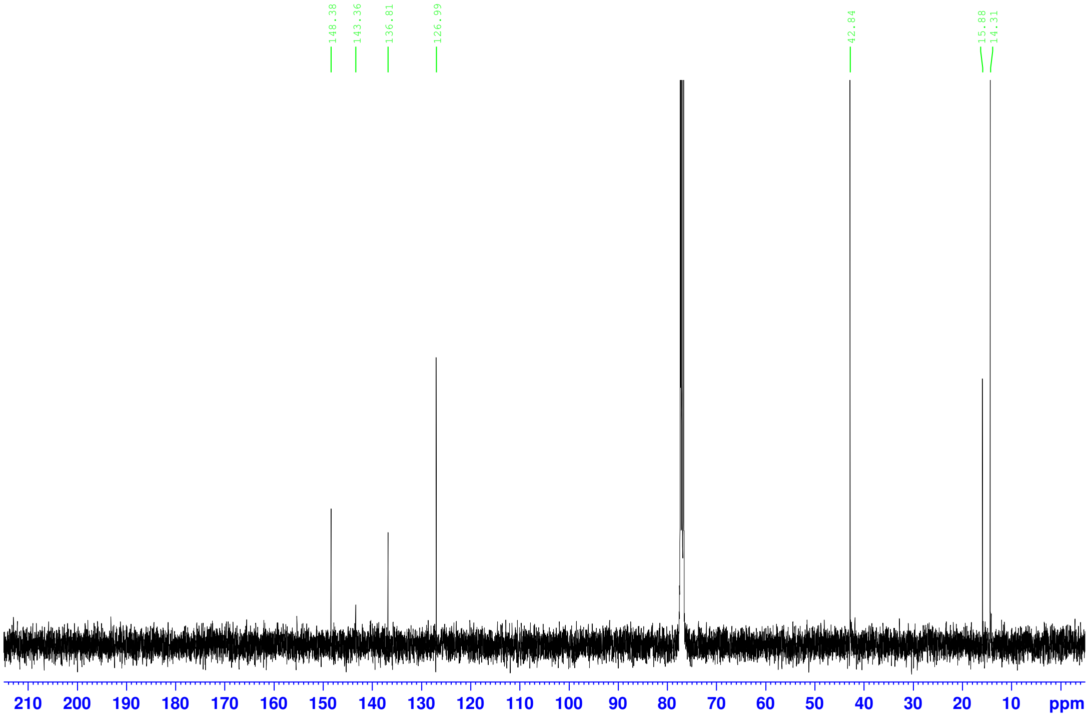

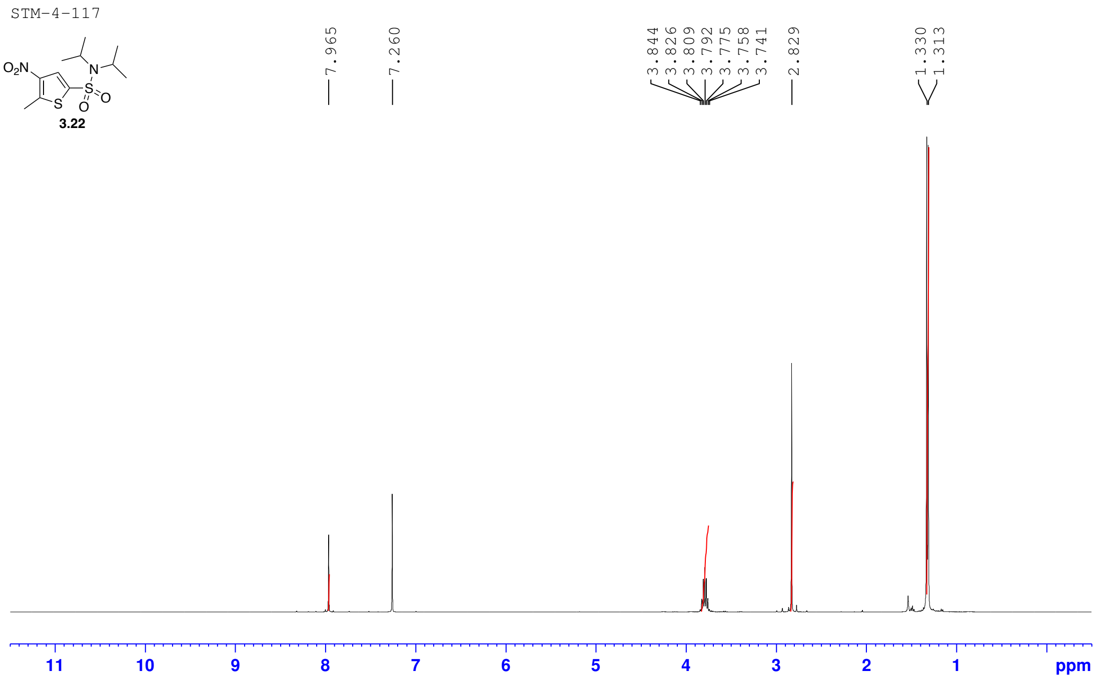
STM-4-117
O_2N
N
S
O
O
S
3.22
7.965
7.260
3.844
3.826
3.809
3.792
3.775
3.758
3.741
2.829
1.330
1.313
11
10
9
8
7
6
5
4
3
2
1
ppm

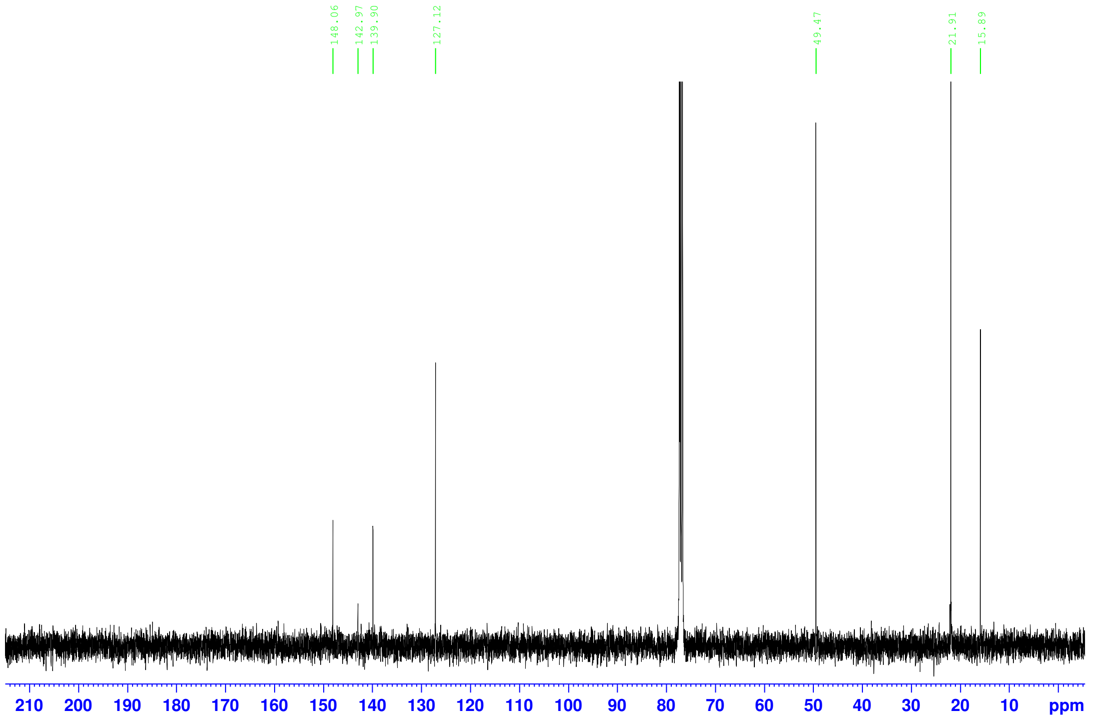
148.06
142.97
139.90
127.12
49.47
21.91
15.89
210
200
190
180
170
160
150
140
130
120
110
100
90
80
70
60
50
40
30
20
10
ppm

STM-4-118 (2-14-22)

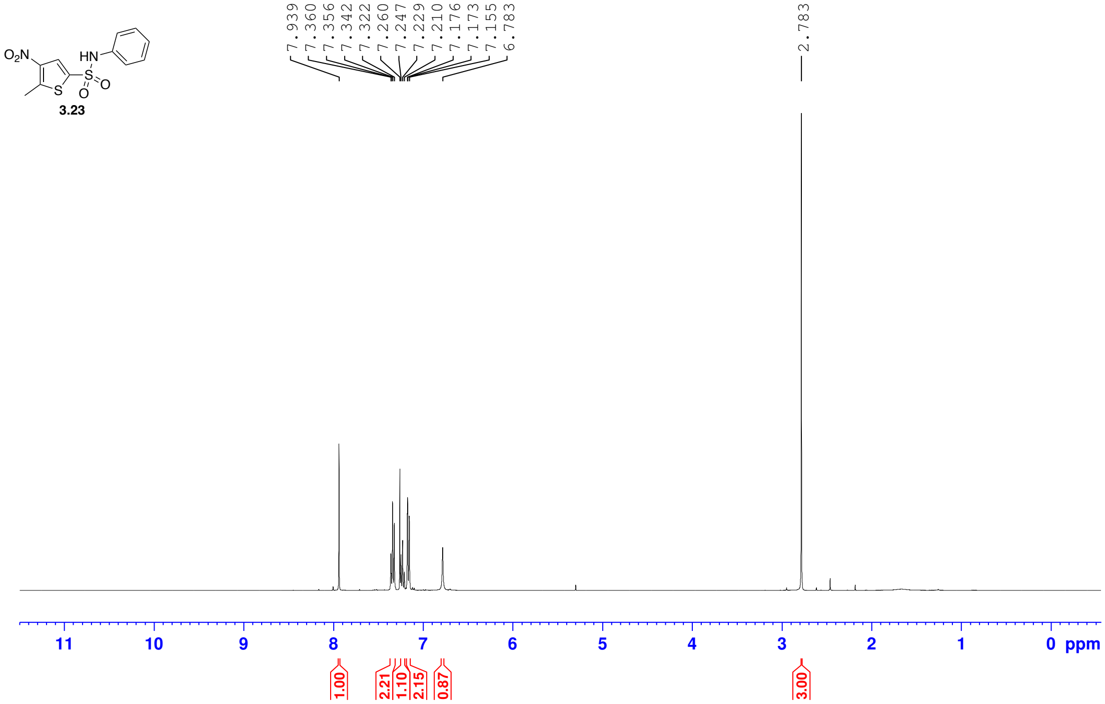

STM-4-118 CNMR (2-14-22)

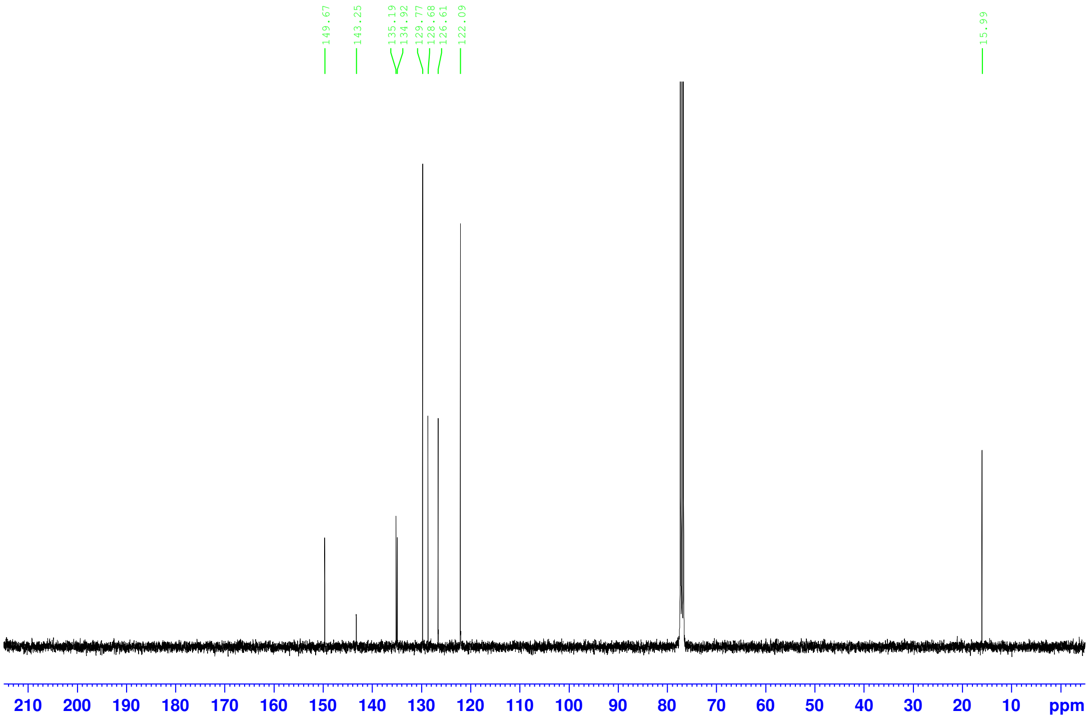

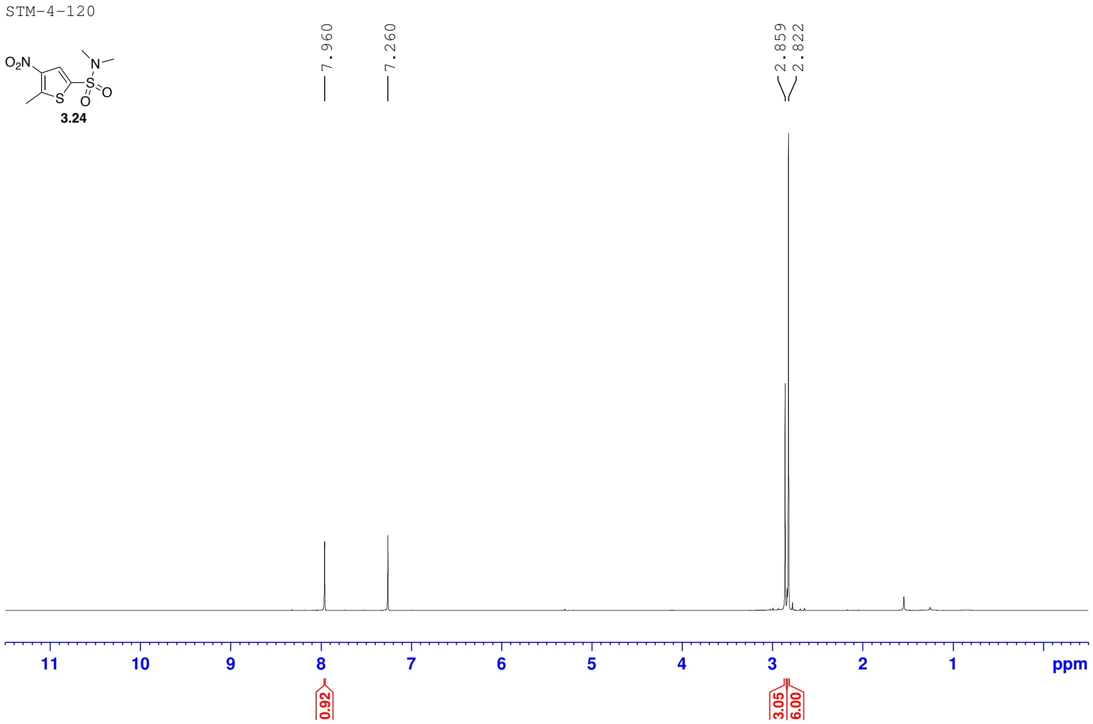
STM-4-120
O2N
N
S
O
O
3.24
7.960
7.260
2.859
2.822
11
10
9
8
7
6
5
4
3
2
1
ppm
0.92
3.05
6.00

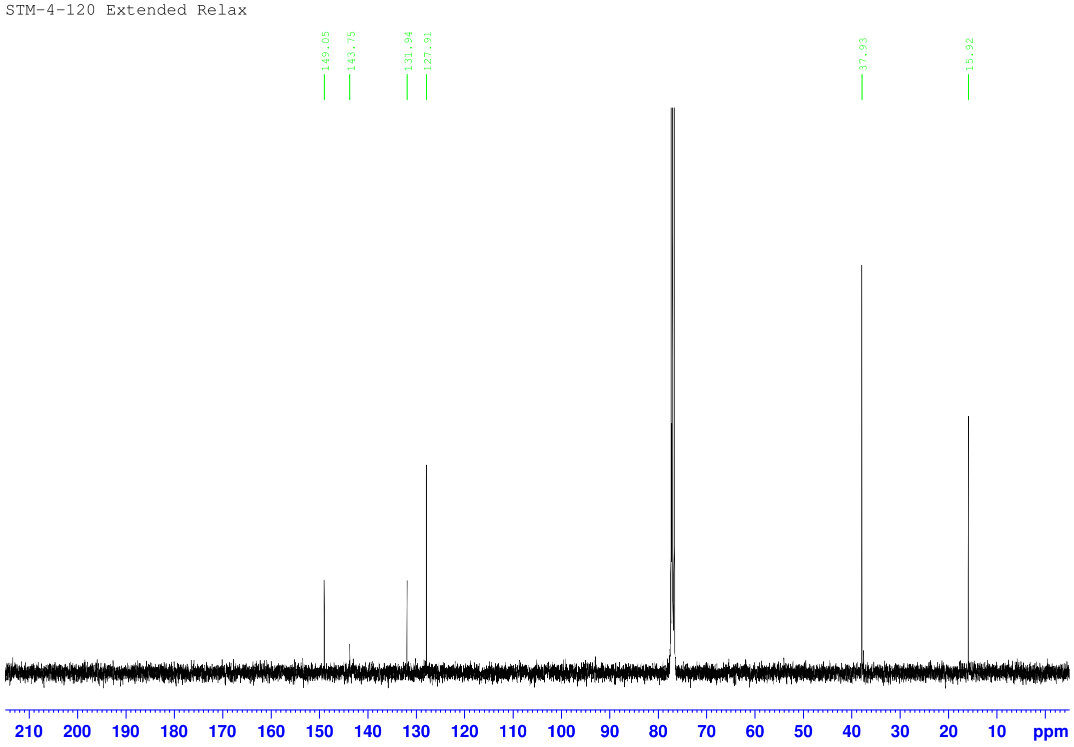
STM-4-120 Extended Relax
149.05
143.75
131.94
127.91
37.93
15.92
210
200
190
180
170
160
150
140
130
120
110
100
90
80
70
60
50
40
30
20
10
ppm

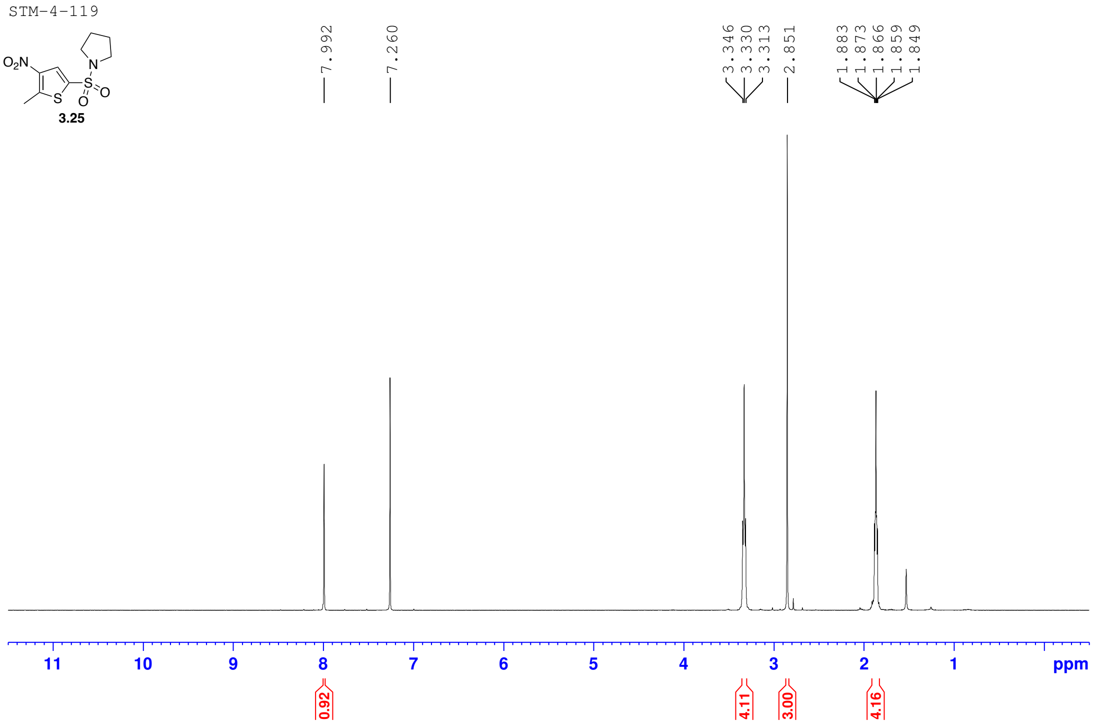
STM-4-119
O2N
N
S
O
O
3.25
7.992
7.260
3.346
3.330
3.313
2.851
1.883
1.873
1.866
1.859
1.849
11
10
9
8
7
6
5
4
3
2
1
ppm
0.92
4.11
3.00
4.16

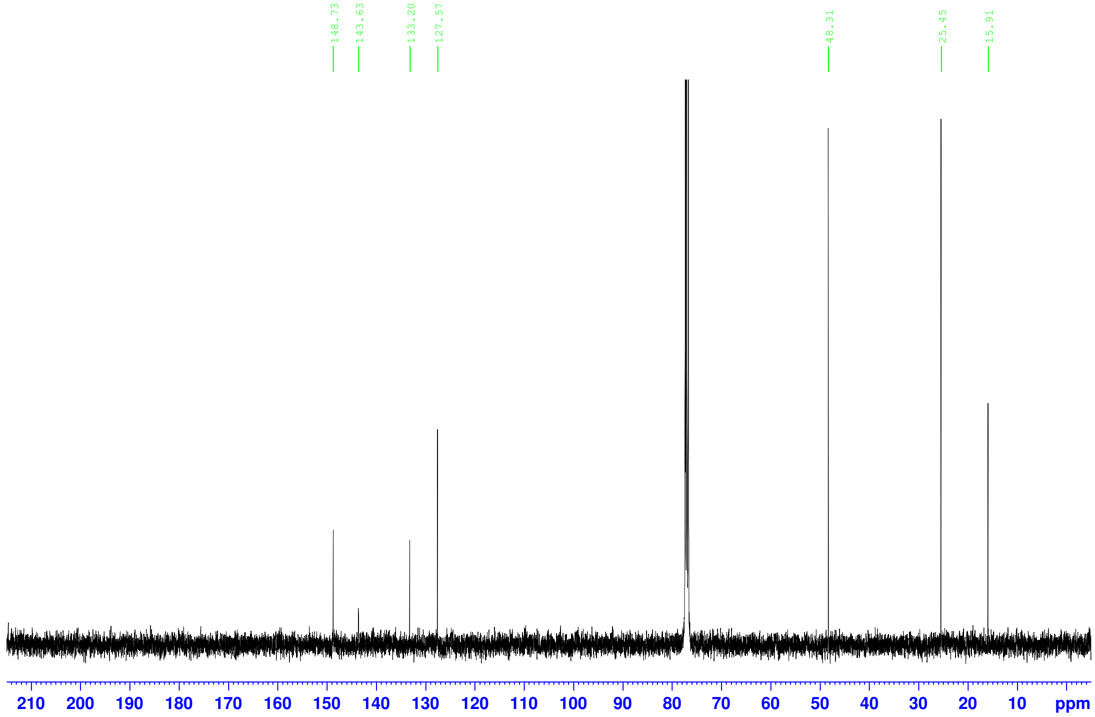
148.73
143.63
133.20
127.57
48.31
25.45
15.91
210
200
190
180
170
160
150
140
130
120
110
100
90
80
70
60
50
40
30
20
10
ppm

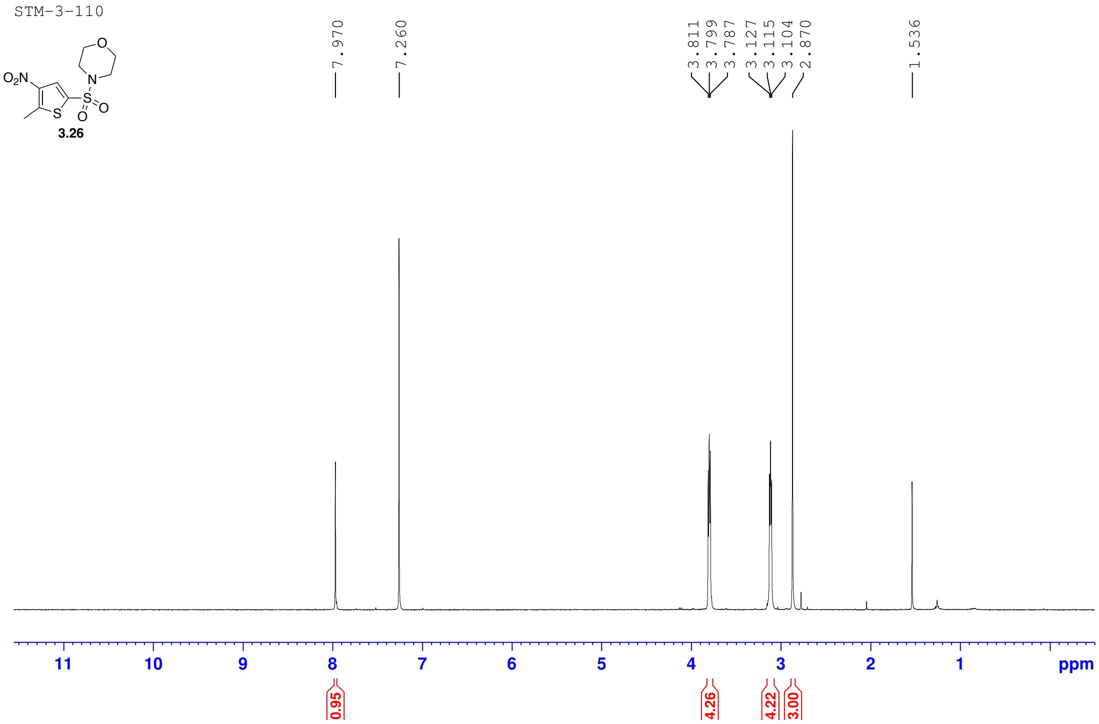
STM-3-110
O
N
O_2N
S
O
O
3.26
7.970
7.260
3.811
3.799
3.787
3.127
3.115
3.104
2.870
1.536
11
10
9
8
7
6
5
4
3
2
1
ppm
0.95
4.26
4.22
3.00

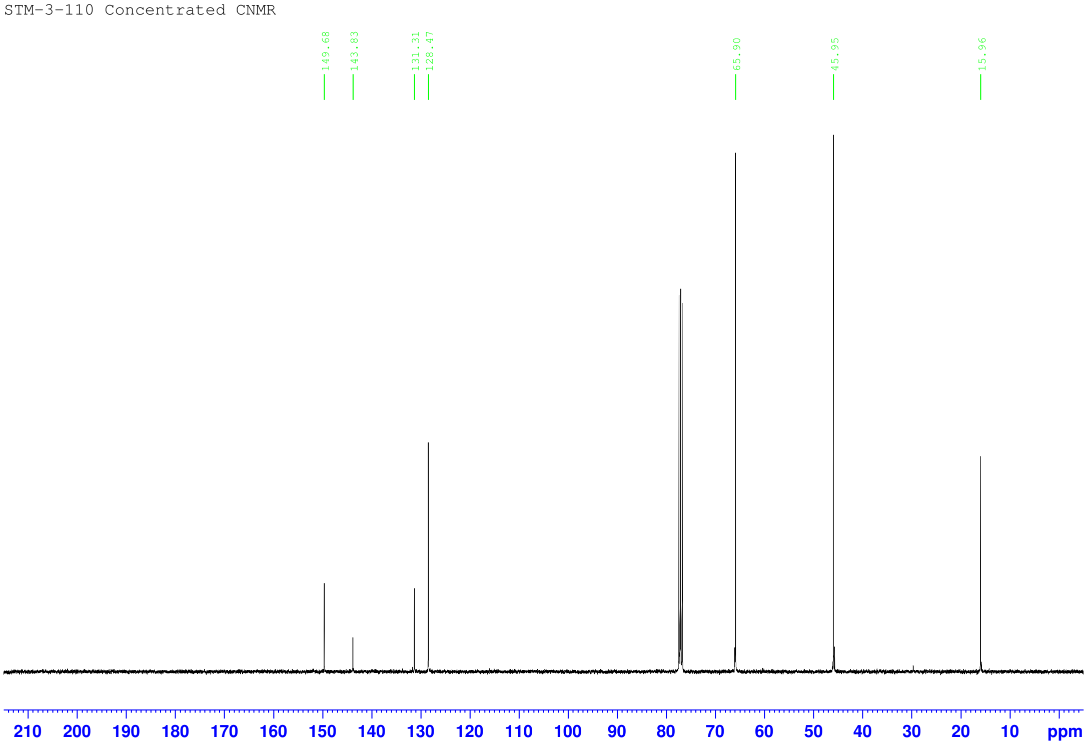
STM-3-110 Concentrated CNMR
149.68
143.83
131.31
128.47
65.90
45.95
15.96
210
200
190
180
170
160
150
140
130
120
110
100
90
80
70
60
50
40
30
20
10
ppm

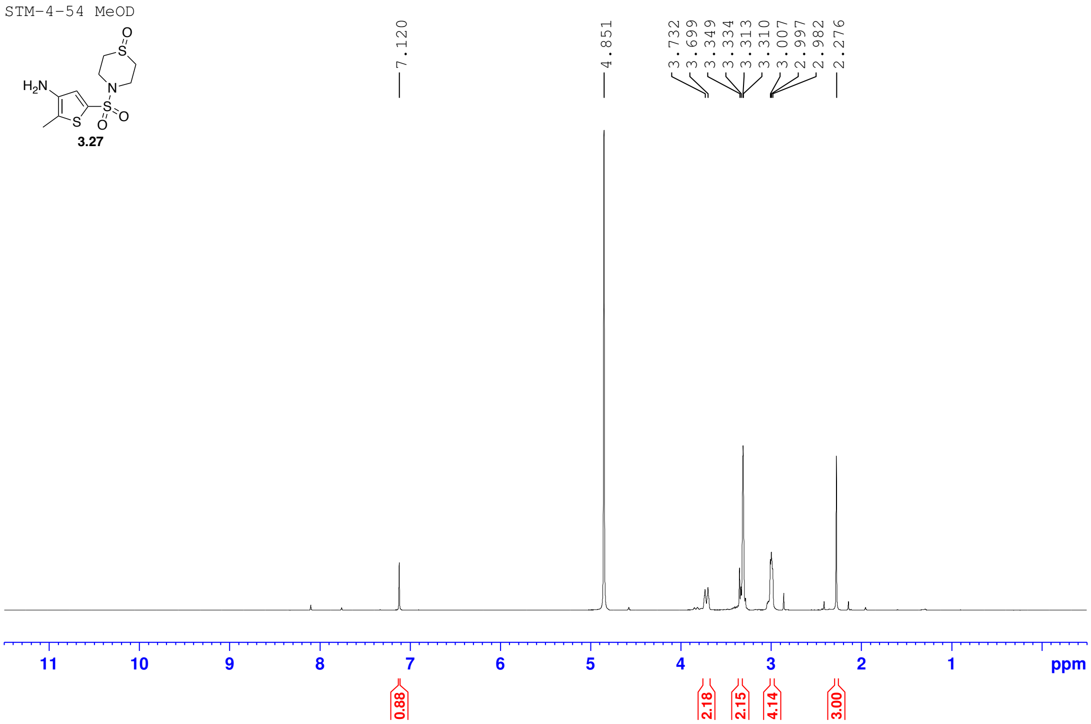
STM-4-54 MeOD
H_2N
S
N
O
3.27
7.120
4.851
3.732
3.699
3.349
3.334
3.313
3.310
3.007
2.997
2.982
2.276
11
10
9
8
7
6
5
4
3
2
1
ppm
0.88
2.18
2.15
4.14
3.00

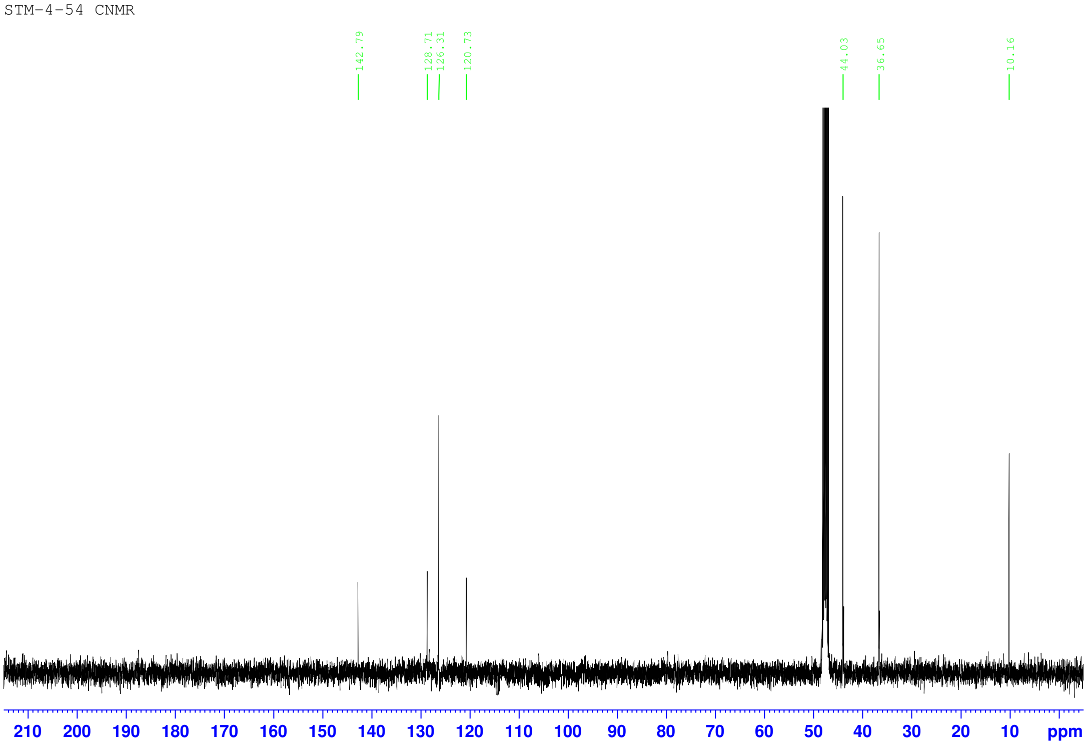
STM-4-54 CNMR
142.79
128.71
126.31
120.73
44.03
36.65
10.16
210
200
190
180
170
160
150
140
130
120
110
100
90
80
70
60
50
40
30
20
10
ppm

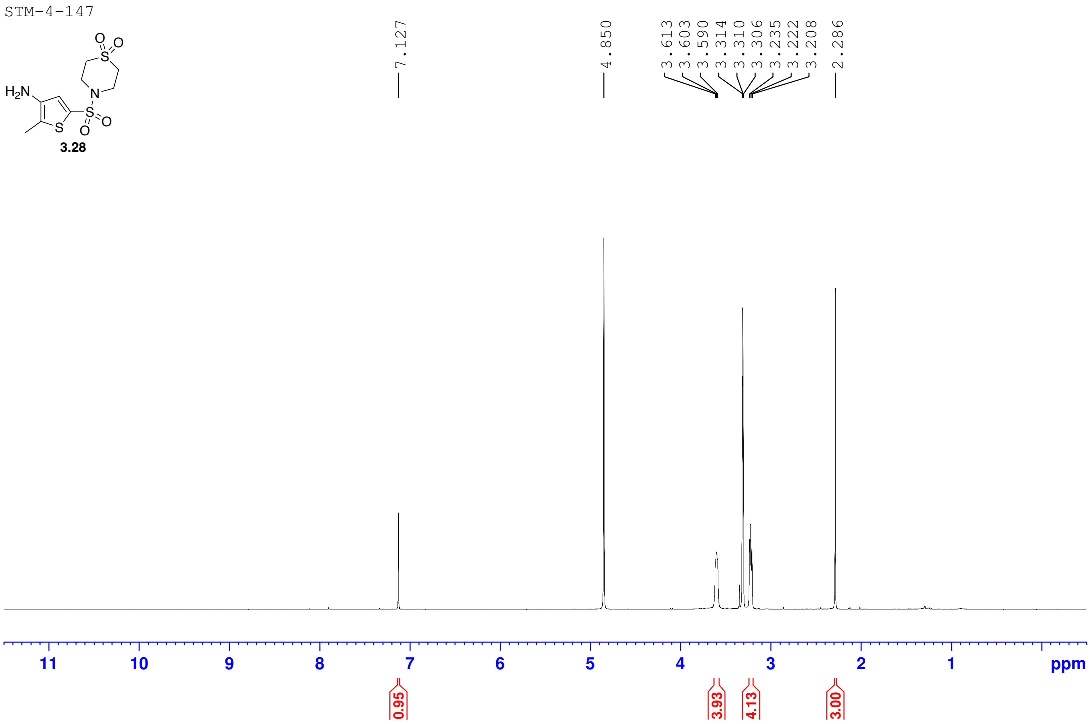
STM-4-147
H2N
S
N
O
O
S
O
O
3.28
7.127
4.850
3.613
3.603
3.590
3.314
3.310
3.306
3.235
3.222
3.208
2.286
11
10
9
8
7
6
5
4
3
2
1
ppm
0.95
3.93
4.13
3.00

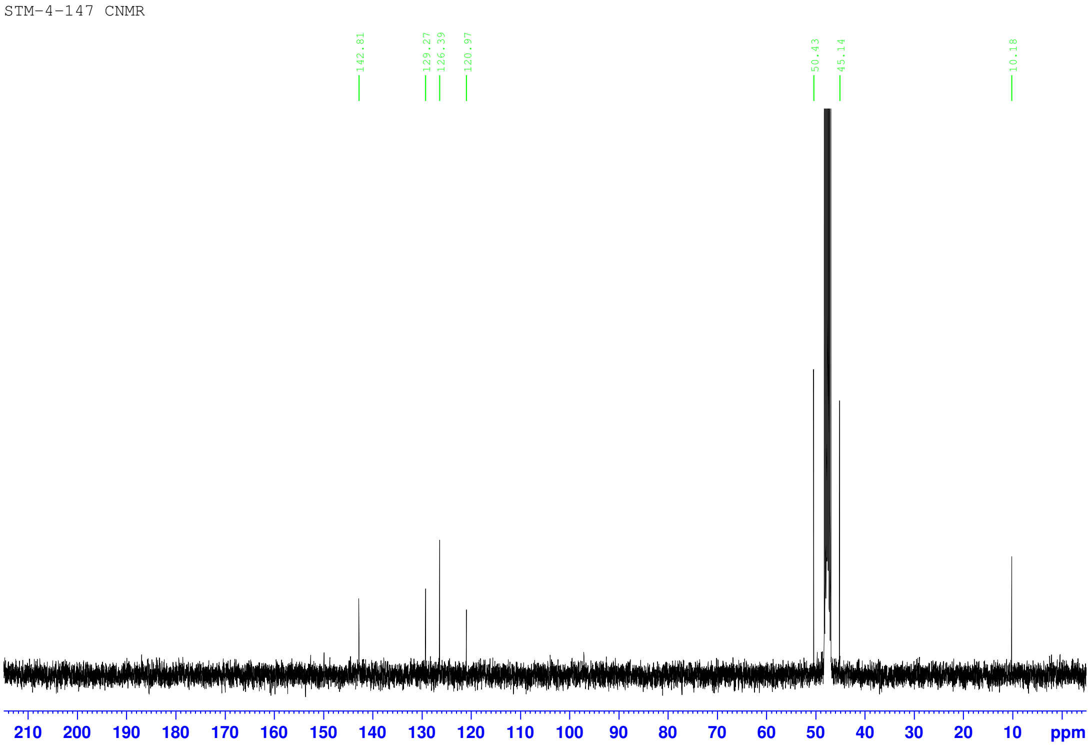
STM-4-147 CNMR
142.81
129.27
126.39
120.97
50.43
45.14
10.18
210
200
190
180
170
160
150
140
130
120
110
100
90
80
70
60
50
40
30
20
10
ppm

STM-4-9 Pure

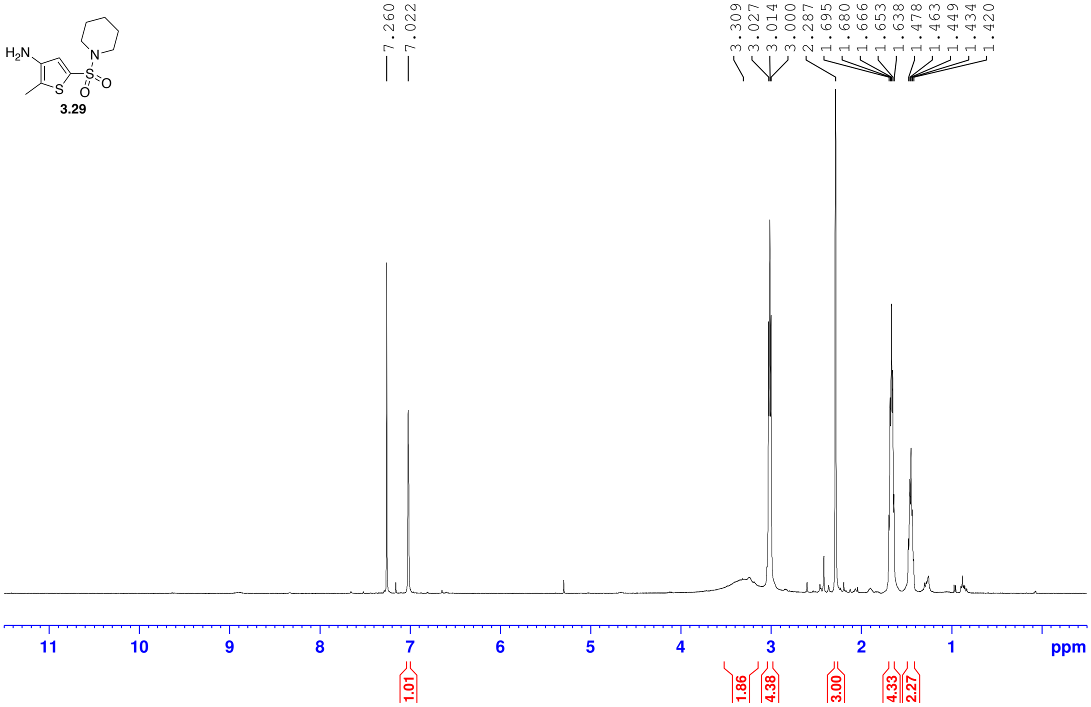

STM-4-9 CNMR

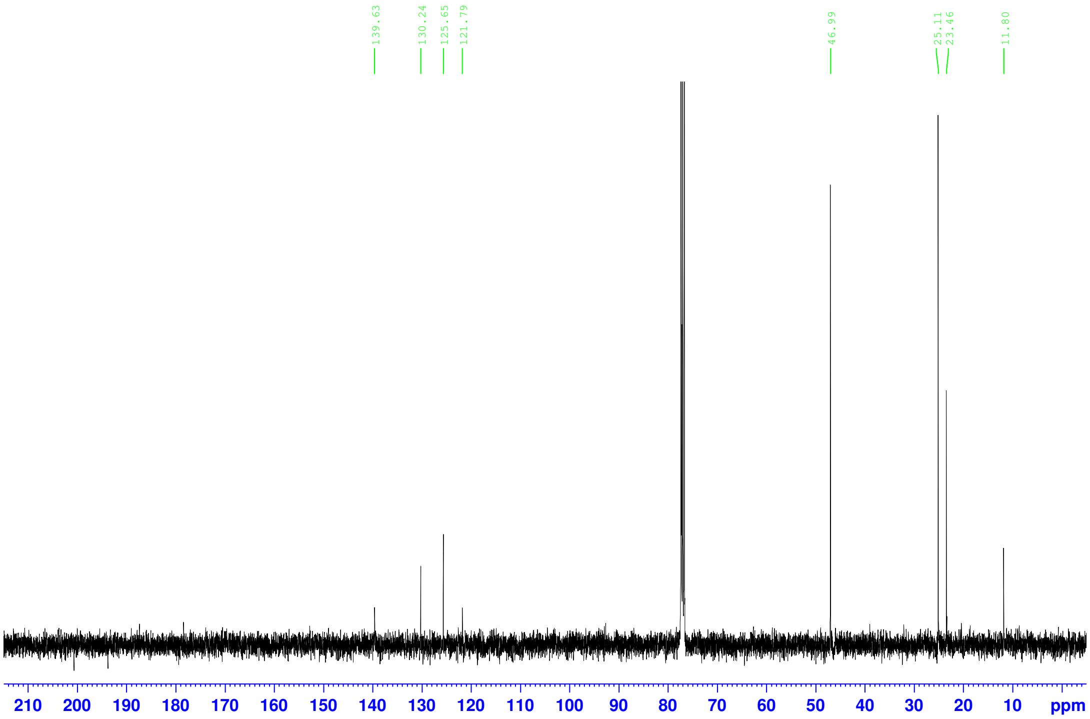

STM-4-122 Prod

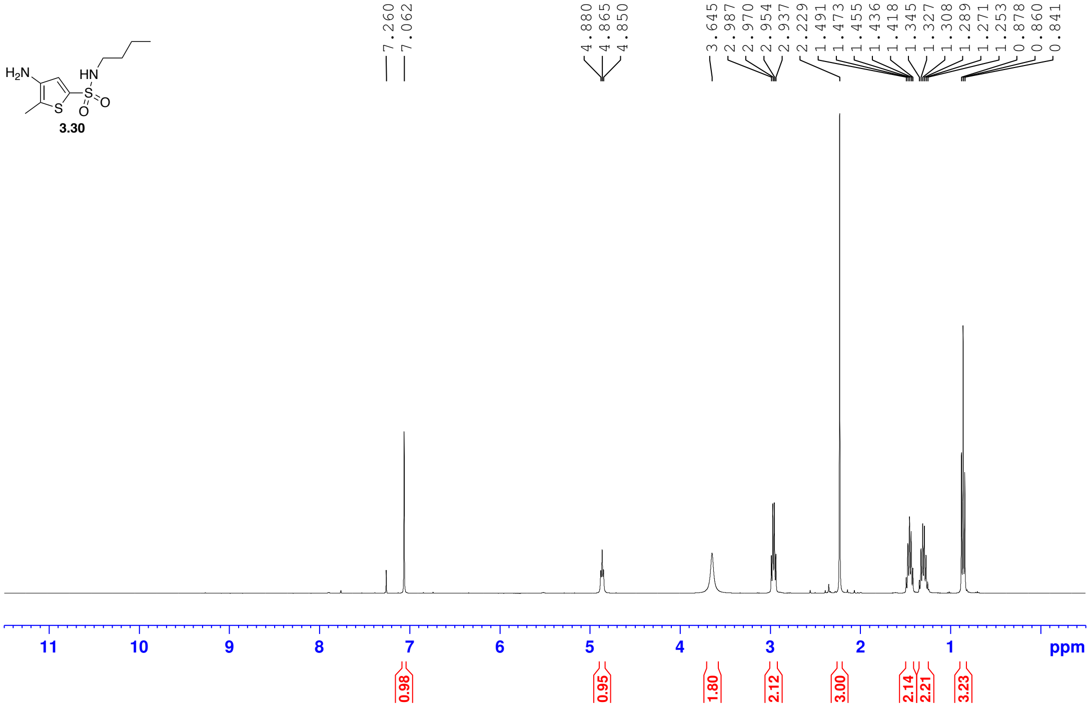

STM-4-122 CNMR Extended Relax

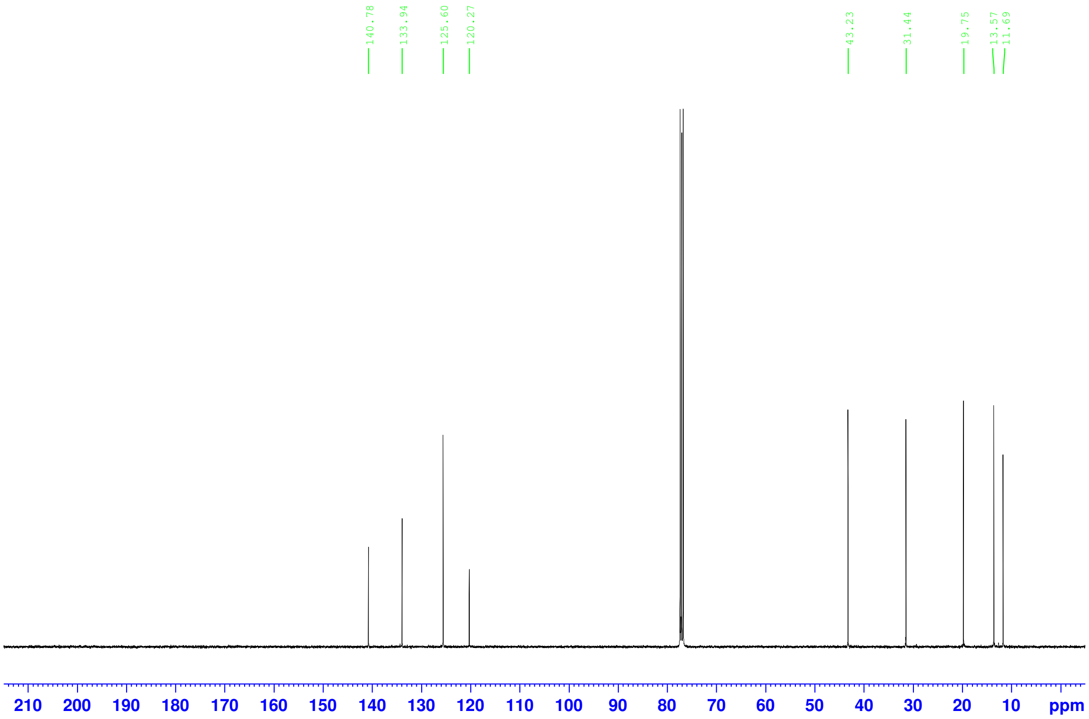

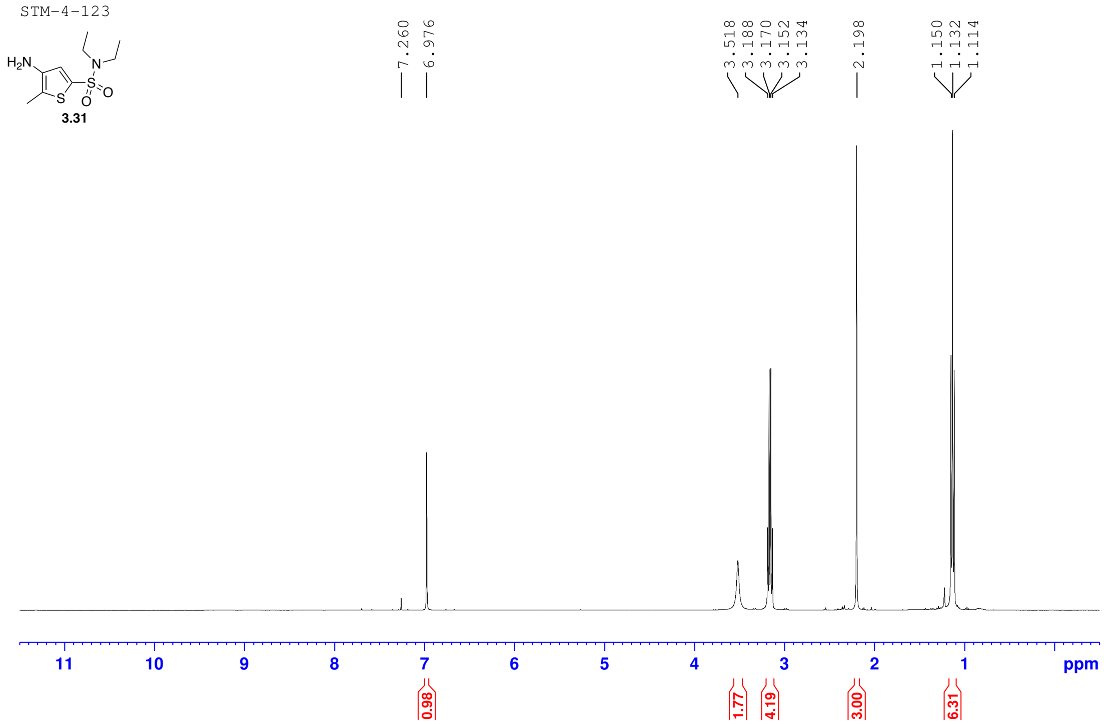
STM-4-123
H_2N
N
S
O
O
3.31
7.260
6.976
3.518
3.188
3.170
3.152
3.134
2.198
1.150
1.132
1.114
11
10
9
8
7
6
5
4
3
2
1
ppm
0.98
1.77
4.19
3.00
6.31

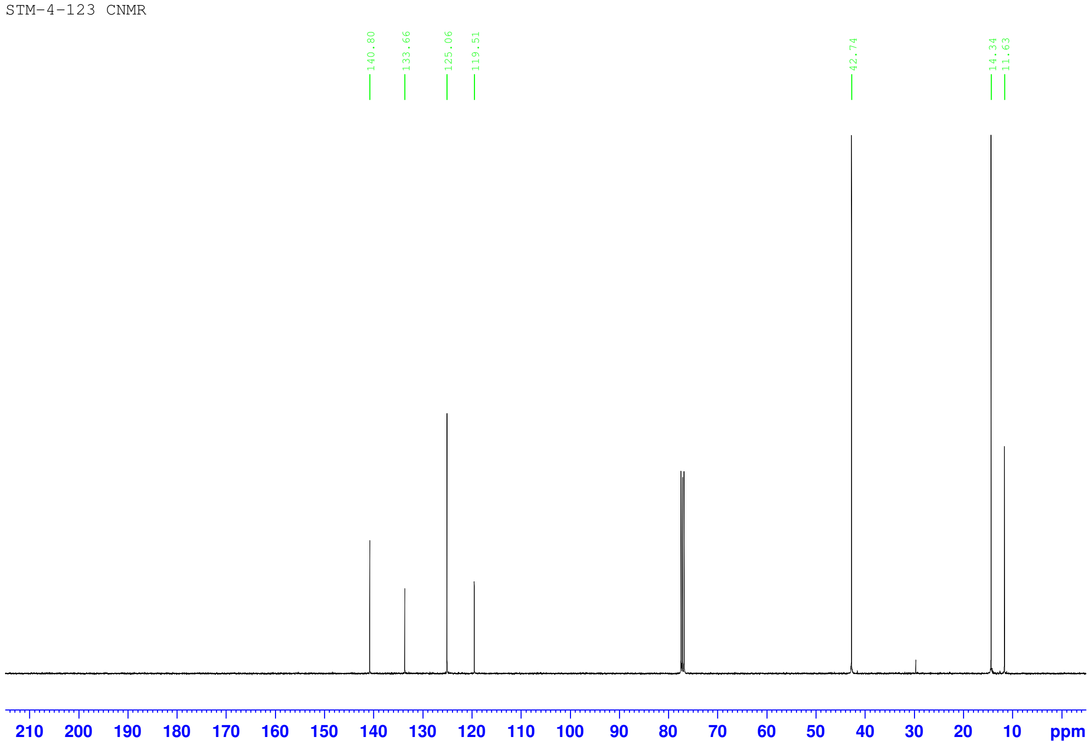
STM-4-123 CNMR
140.80
133.66
125.06
119.51
42.74
14.34
11.63
210
200
190
180
170
160
150
140
130
120
110
100
90
80
70
60
50
40
30
20
10
ppm

STM-4-128 (2-15-22)

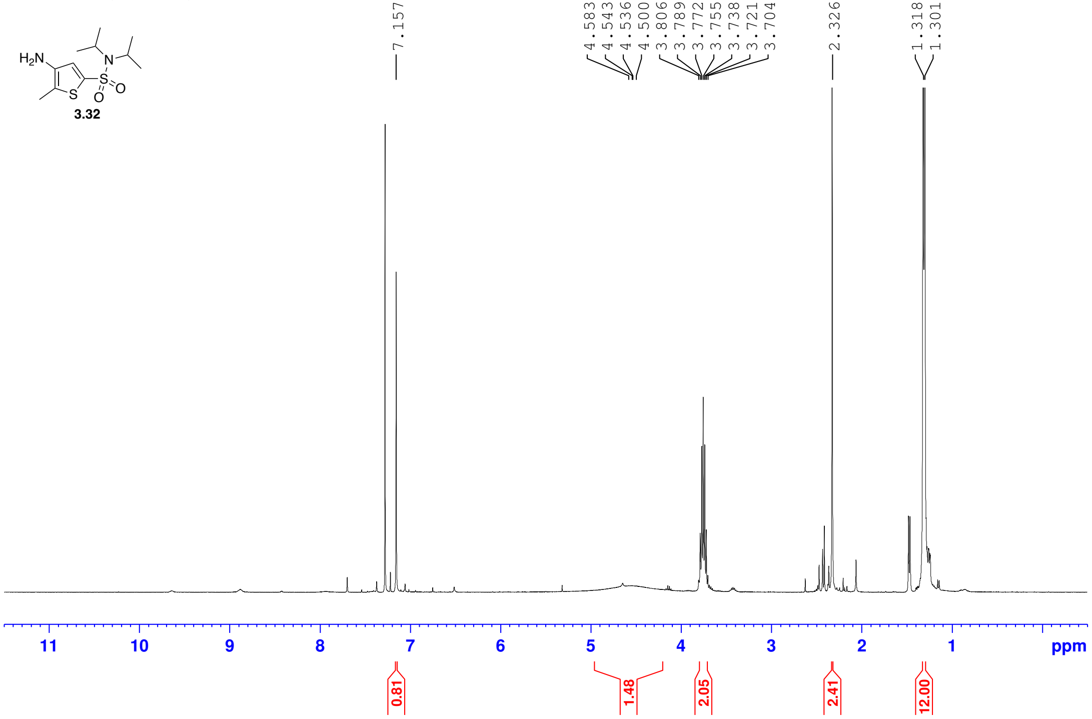

STM-4-128 CNMR (2-15-22)

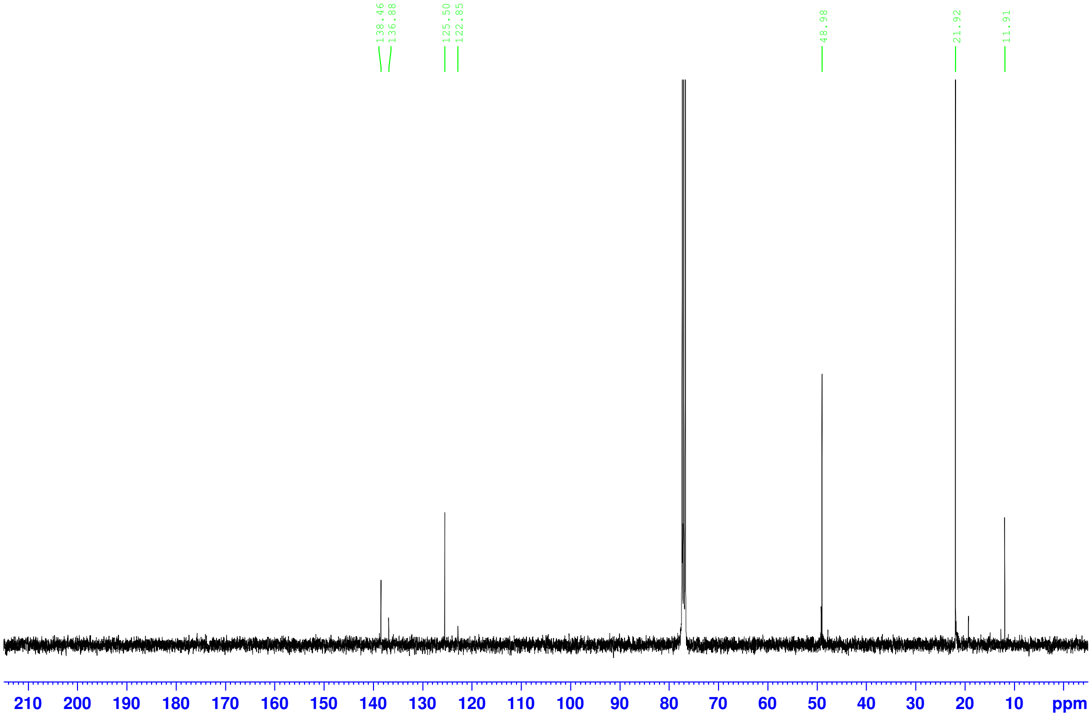

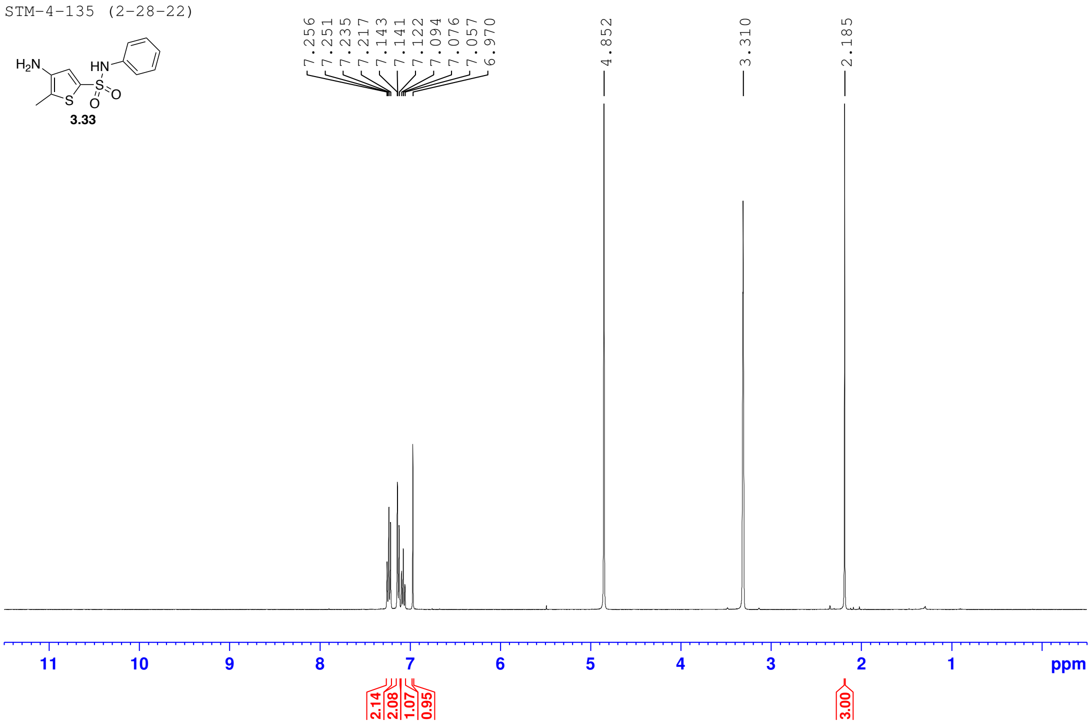
STM-4-135 (2-28-22)
H2N
HN
S
O
O
S
3.33
7.256
7.251
7.235
7.217
7.143
7.141
7.122
7.094
7.076
7.057
6.970
4.852
3.310
2.185
11
10
9
8
7
6
5
4
3
2
1
ppm
2.14
2.08
1.07
0.95
3.00

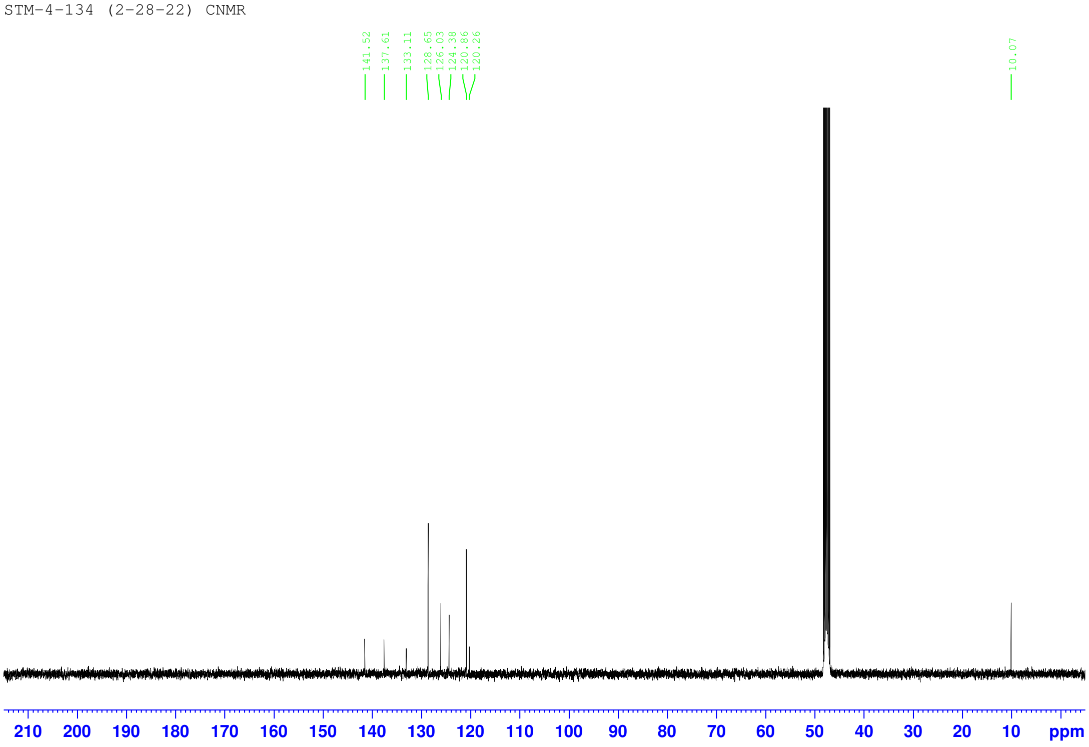
STM-4-134 (2-28-22) CNMR
141.52
137.61
133.11
128.65
126.03
124.38
120.86
120.26
10.07
210
200
190
180
170
160
150
140
130
120
110
100
90
80
70
60
50
40
30
20
10
ppm

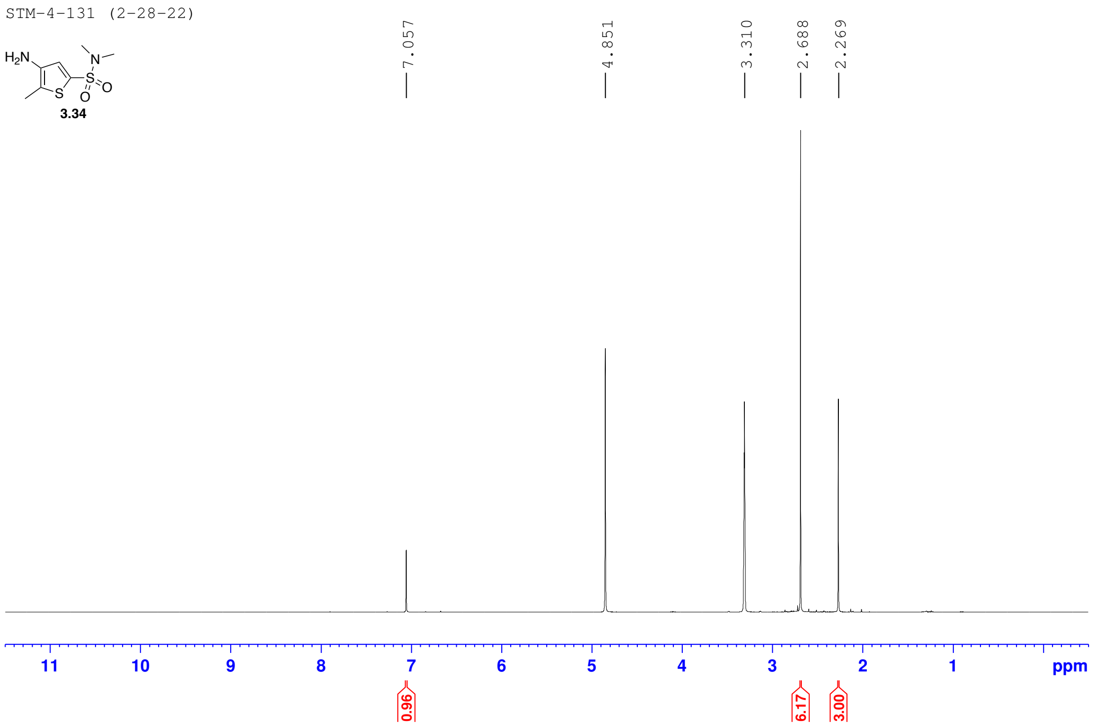
STM-4-131 (2-28-22)
H2N
N
S
O
O
S
3.34
7.057
4.851
3.310
2.688
2.269
11
10
9
8
7
6
5
4
3
2
1
ppm
0.96
6.17
3.00

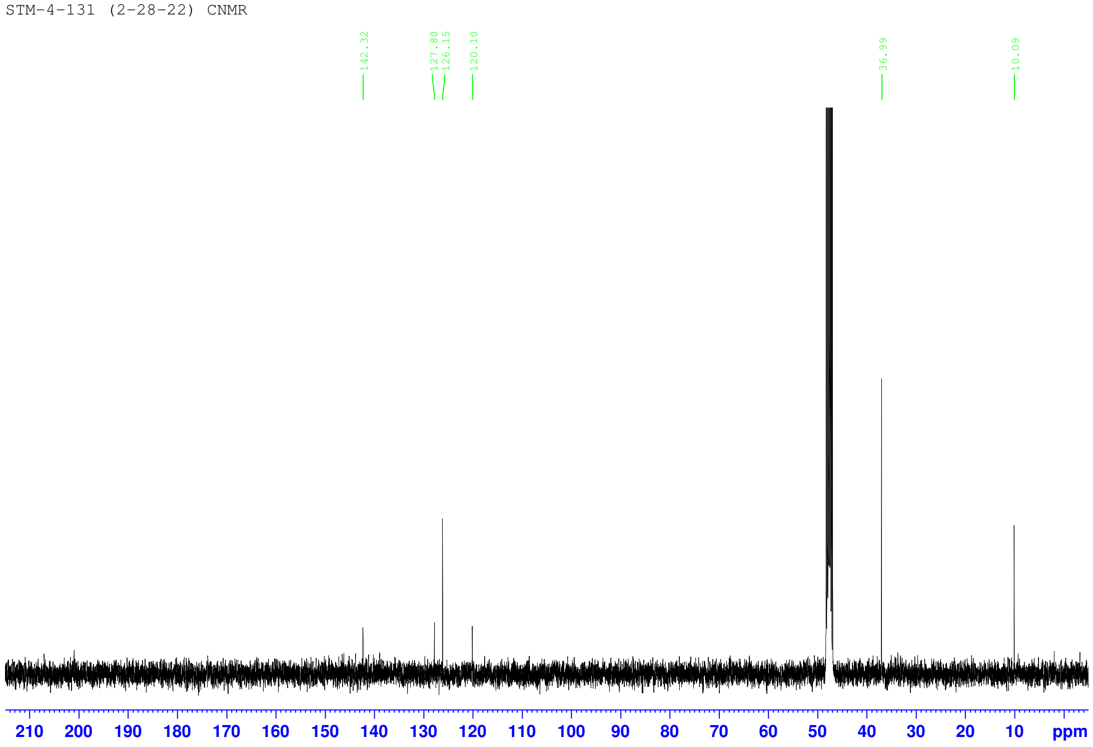
STM-4-131 (2-28-22) CNMR
142.32
127.80
126.15
120.10
36.99
10.09
210
200
190
180
170
160
150
140
130
120
110
100
90
80
70
60
50
40
30
20
10
ppm

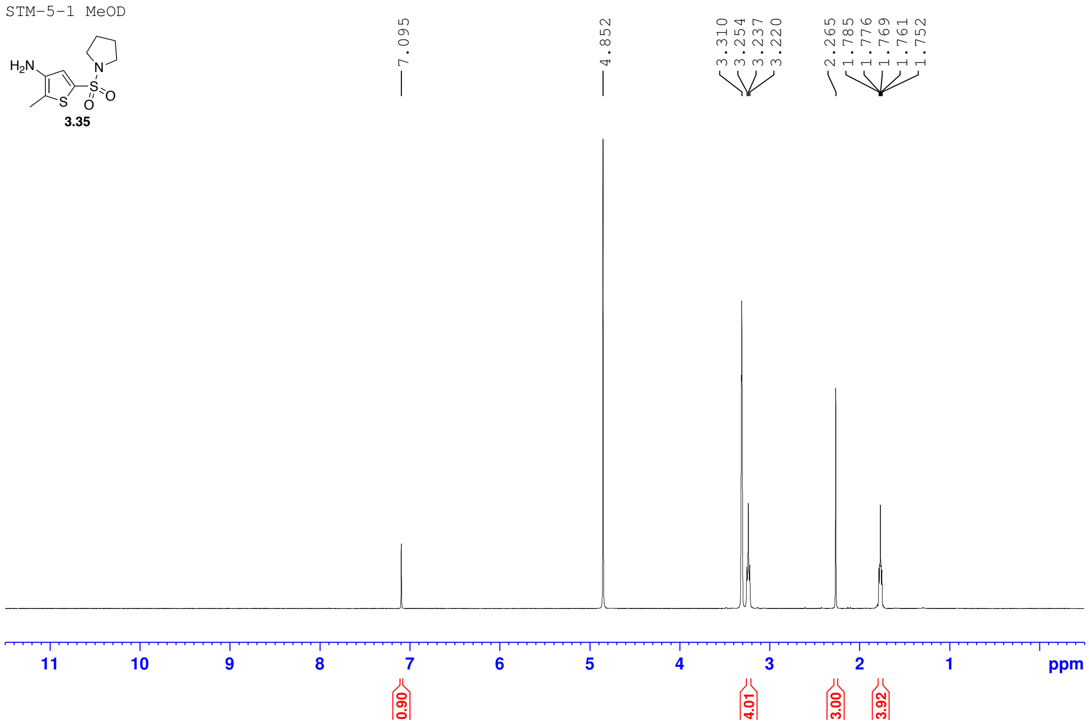
STM-5-1 MeOD
H2N
N
S
O
O
S
3.35
7.095
4.852
3.310
3.254
3.237
3.220
2.265
1.785
1.776
1.769
1.761
1.752
11
10
9
8
7
6
5
4
3
2
1
ppm
0.90
4.01
3.00
3.92

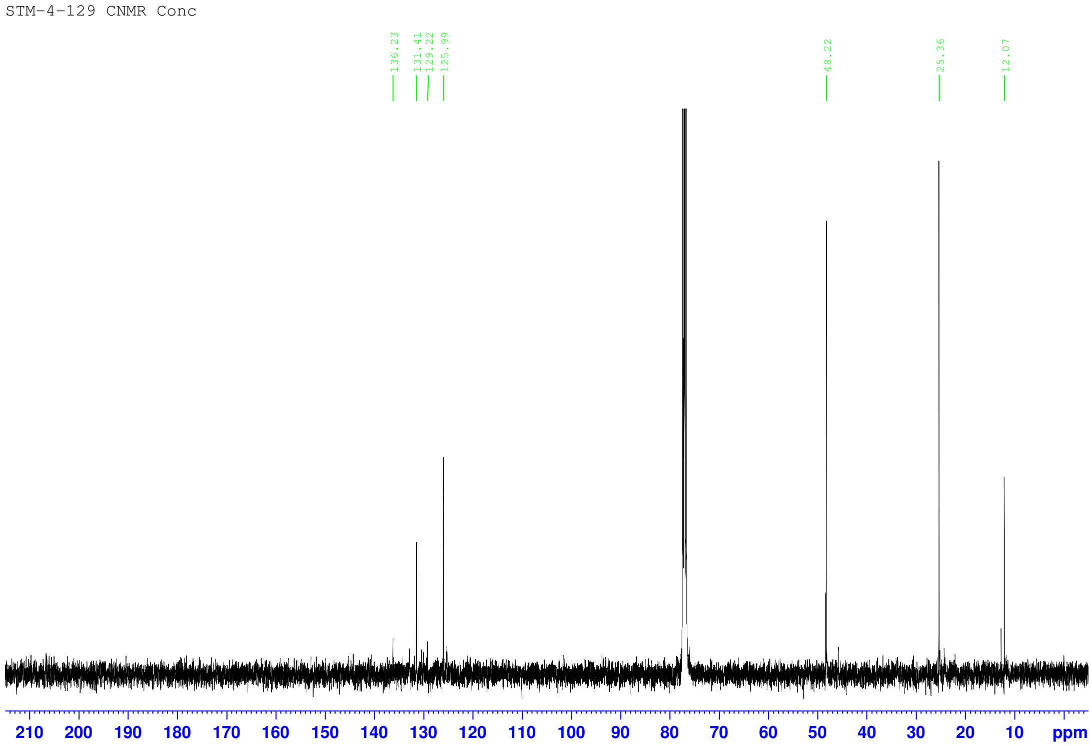
STM-4-129 CNMR Conc
136.23
131.41
129.22
125.99
48.22
25.36
12.07
210
200
190
180
170
160
150
140
130
120
110
100
90
80
70
60
50
40
30
20
10
ppm

STM-3-111

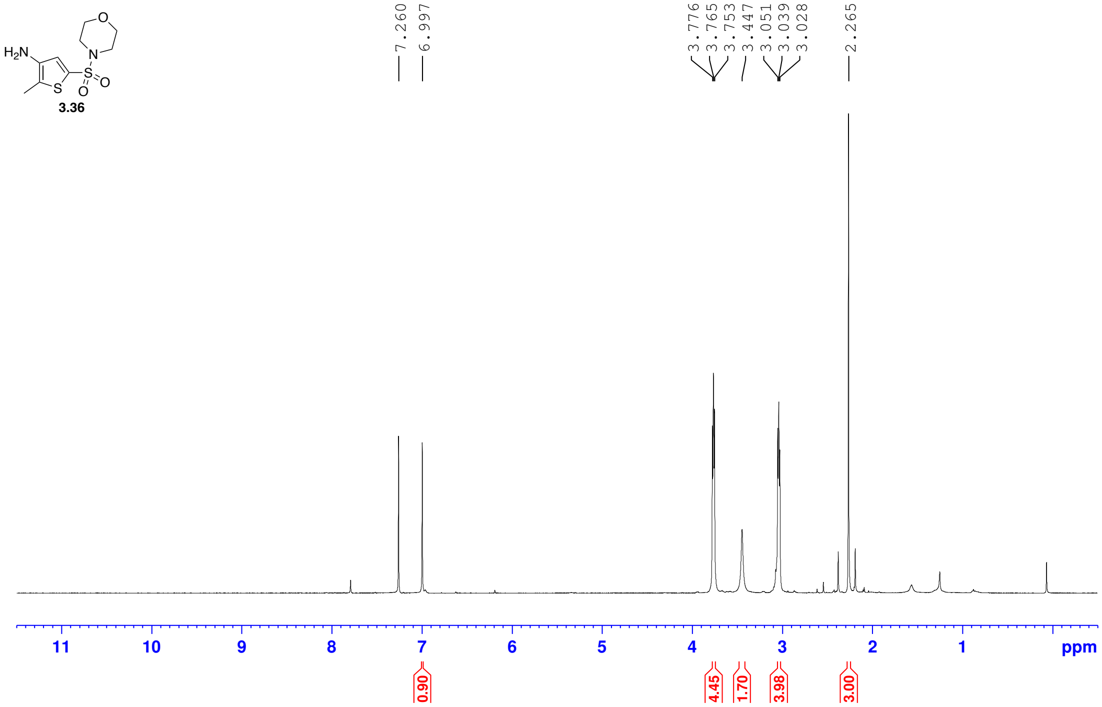

STM-3-111 CNMR

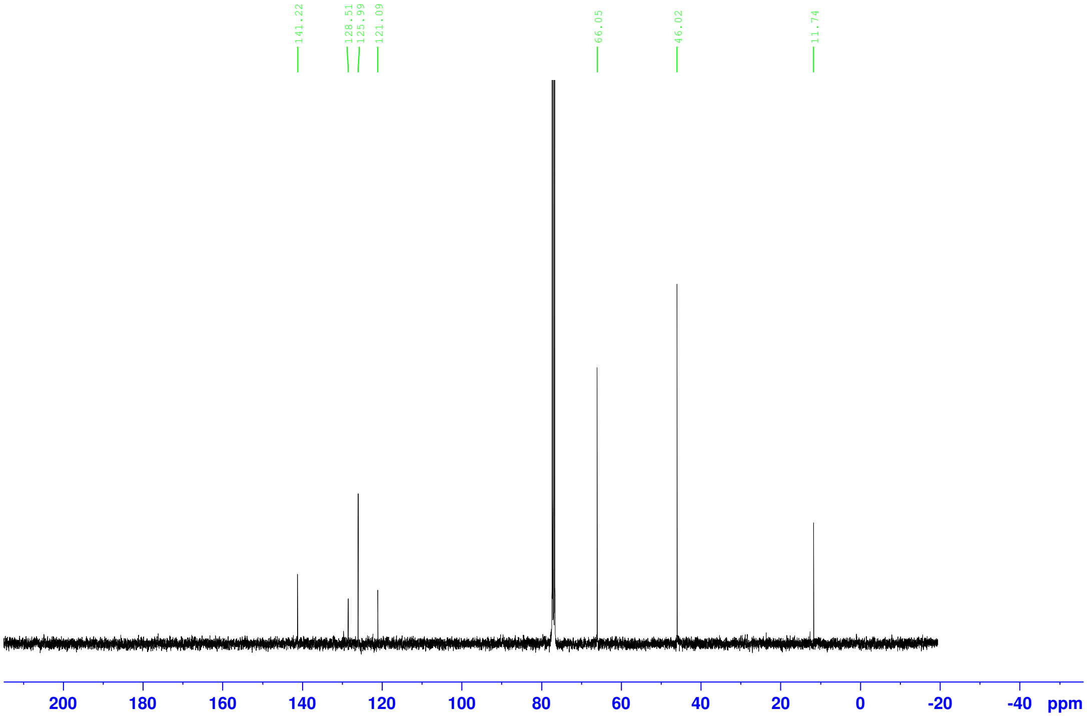

STM-4-60 Pure

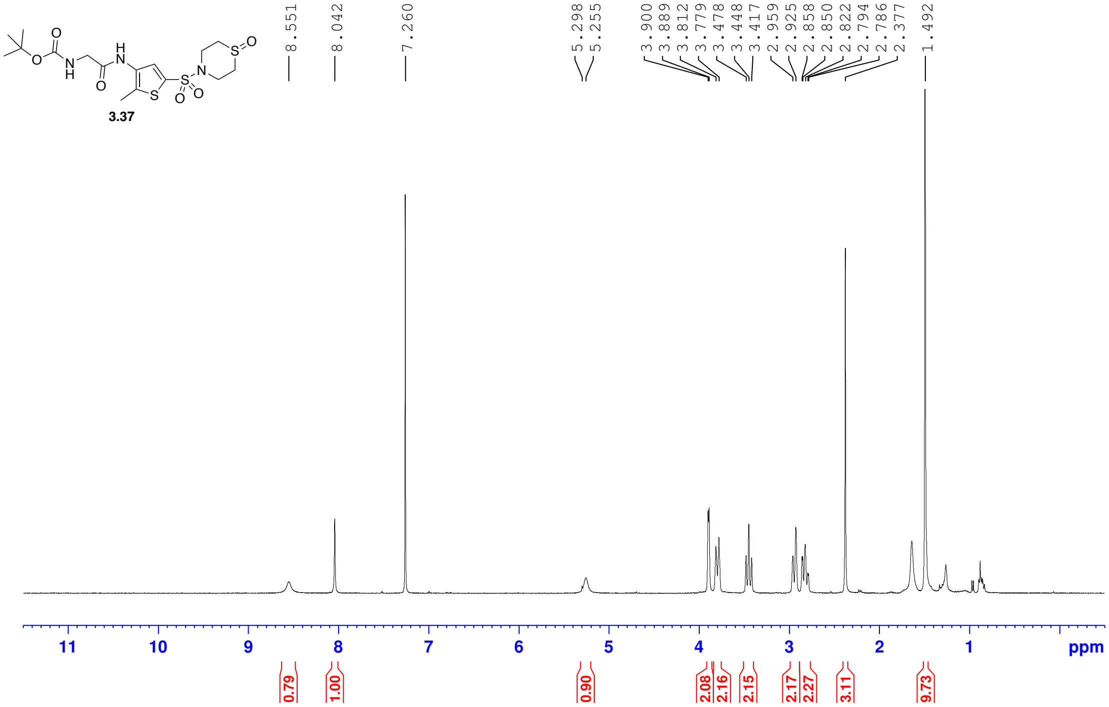

STM-4-60 MeOD CNMR

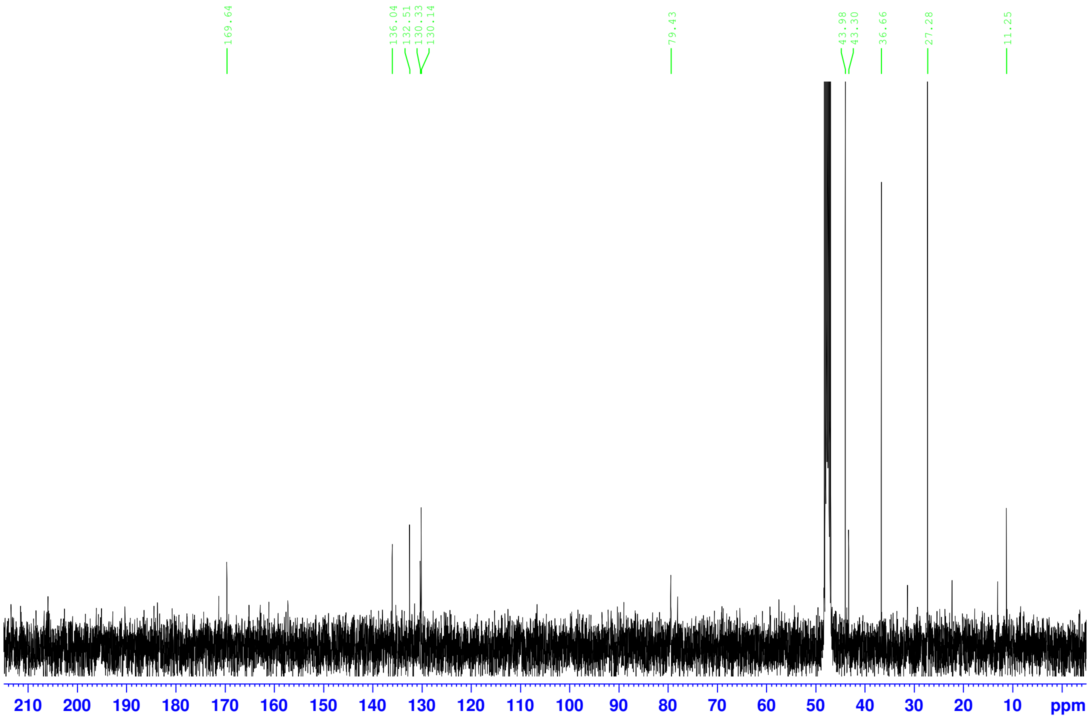

STM-5-2 (3-27-22)

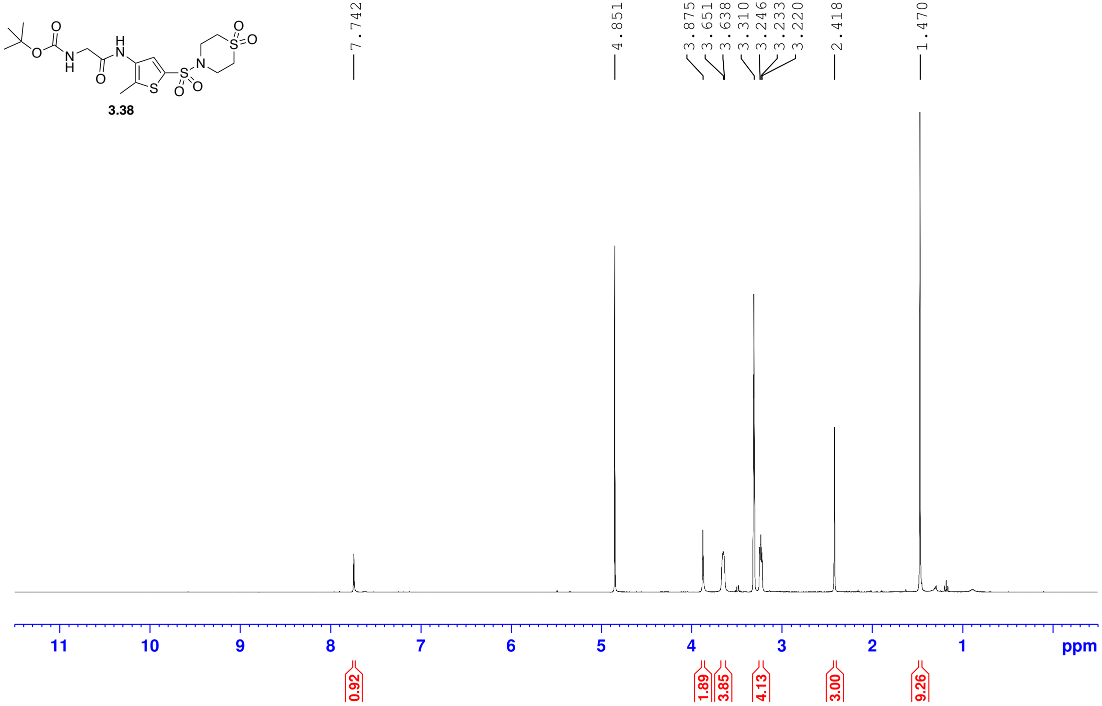

3.38

STM-5-2 (3-27-22) CNMR

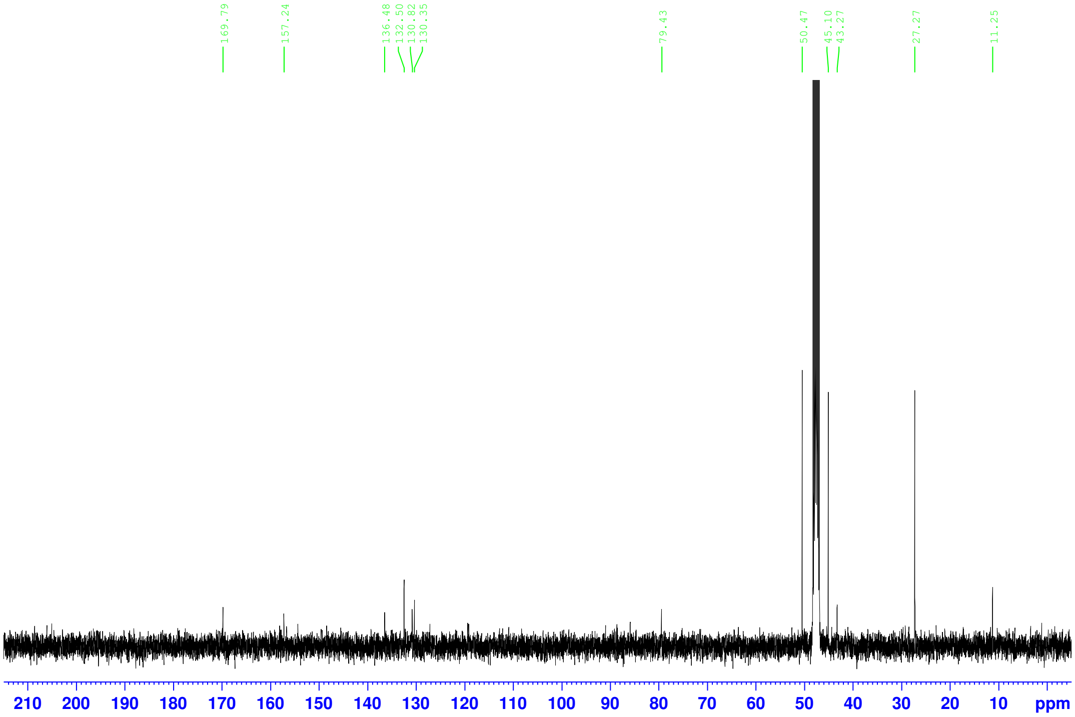

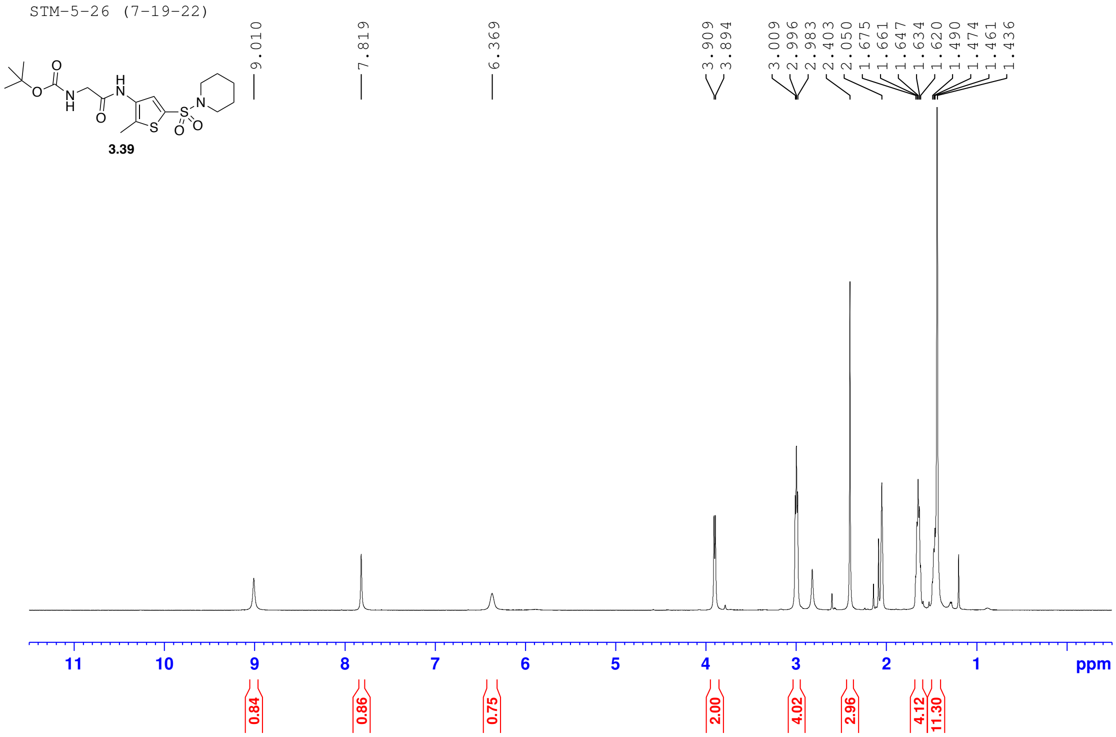
STM-5-26 (7-19-22)
3.39
9.010
7.819
6.369
3.909
3.894
3.009
2.996
2.983
2.403
2.050
1.675
1.661
1.647
1.634
1.620
1.490
1.474
1.461
1.436
11
10
9
8
7
6
5
4
3
2
1
ppm
0.84
0.86
0.75
2.00
4.02
2.96
4.12
11.30

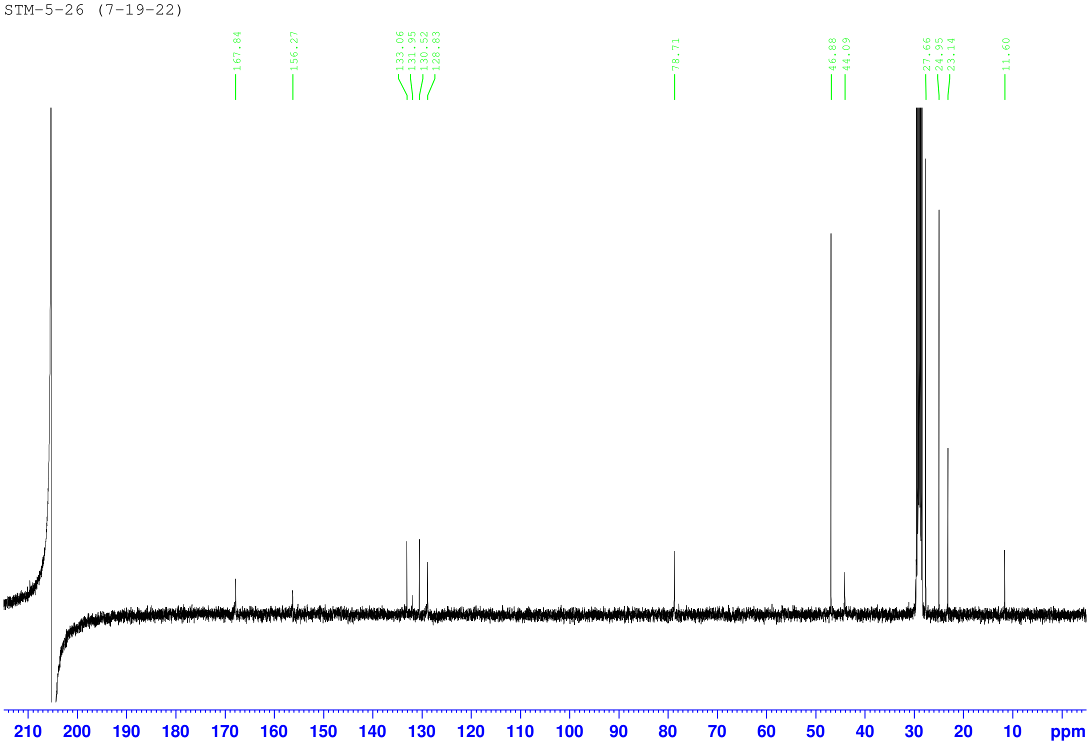
STM-5-26 (7-19-22)
167.84
156.27
133.06
131.95
130.52
128.83
78.71
46.88
44.09
27.66
24.95
23.14
11.60
210
200
190
180
170
160
150
140
130
120
110
100
90
80
70
60
50
40
30
20
10
ppm

STM-4-127 (2-14-22)

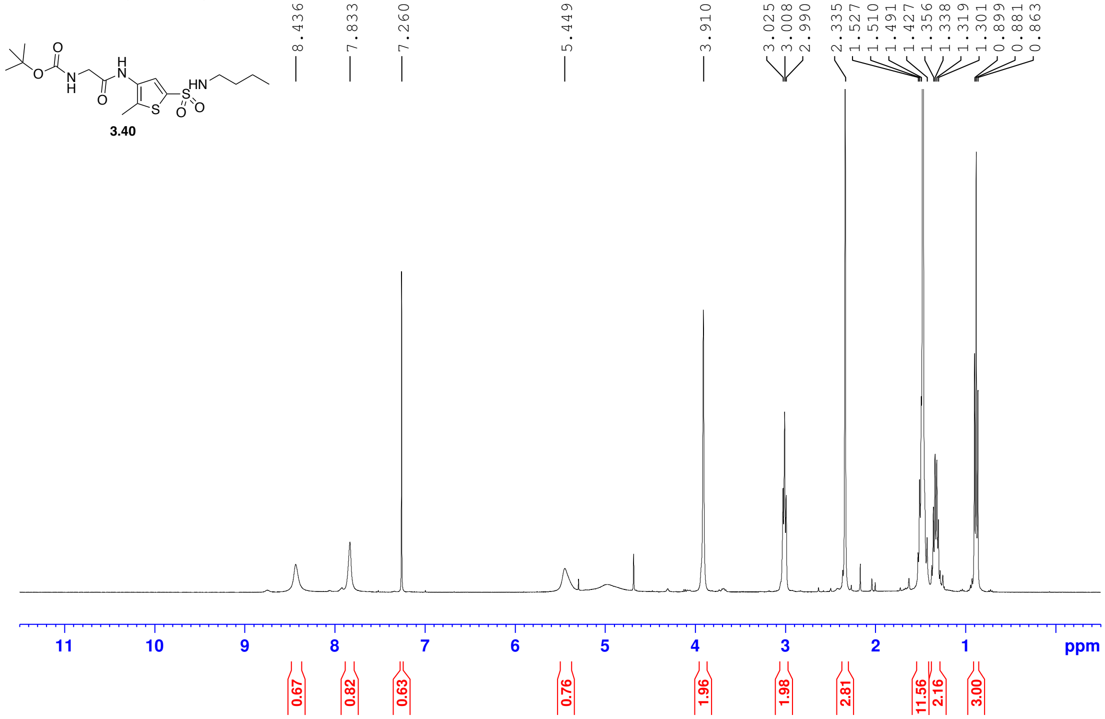

STM-4-127 CNMR (2-14-22)

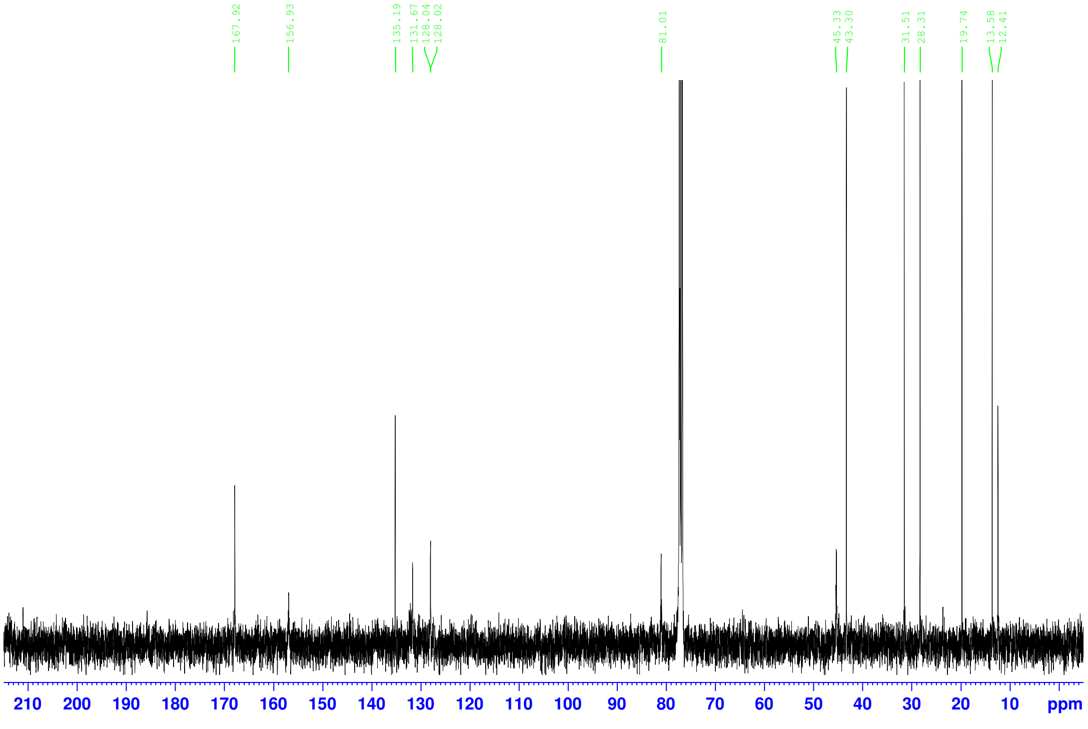

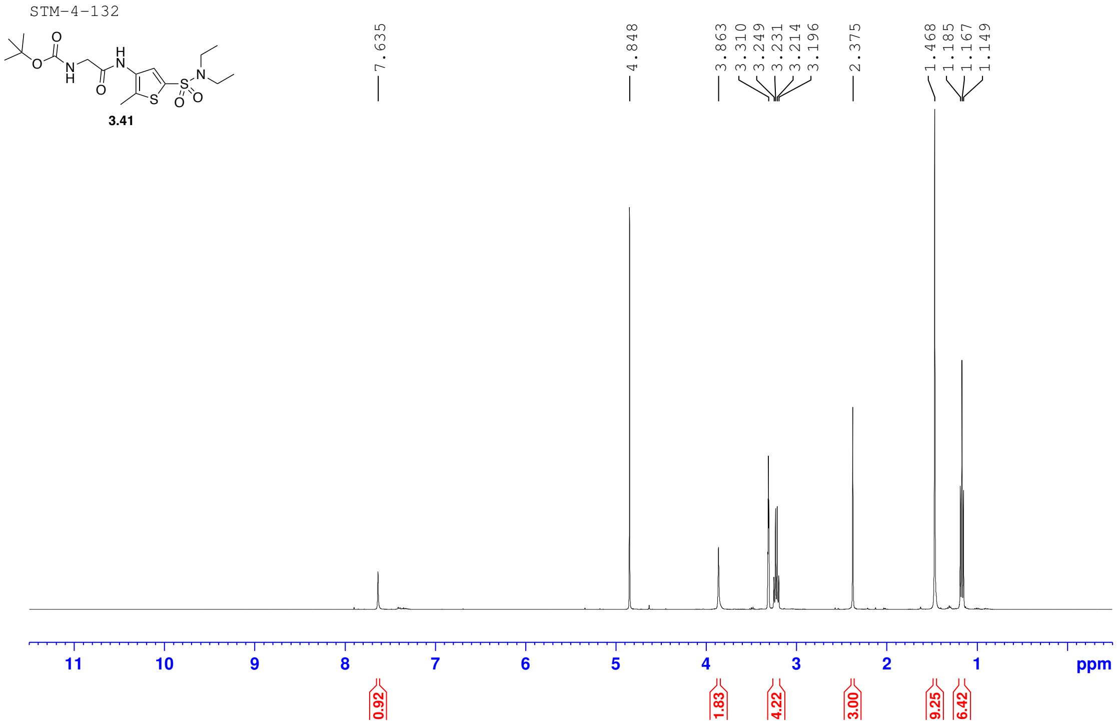
STM-4-132
3.41
7.635
4.848
3.863
3.310
3.249
3.231
3.214
3.196
2.375
1.468
1.185
1.167
1.149
11
10
9
8
7
6
5
4
3
2
1
ppm
0.92
1.83
4.22
3.00
9.25
6.42

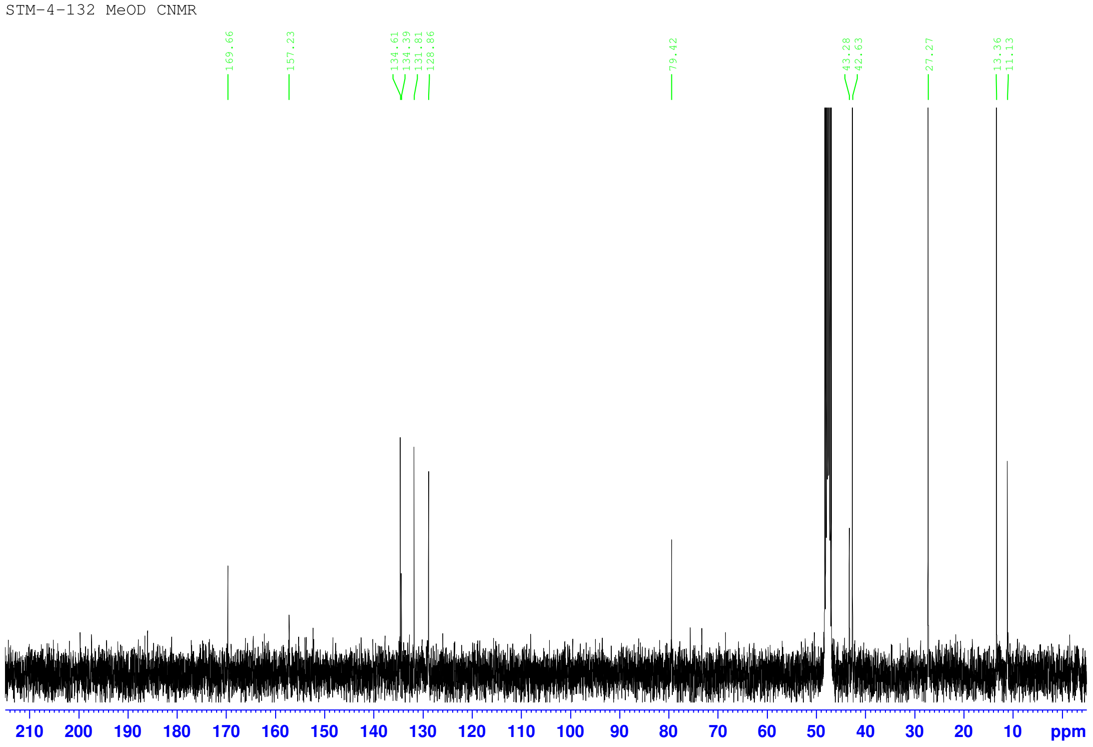
STM-4-132 MeOD CNMR
169.66
157.23
134.61
134.39
131.81
128.86
79.42
43.28
42.63
27.27
13.36
11.13
210
200
190
180
170
160
150
140
130
120
110
100
90
80
70
60
50
40
30
20
10
ppm

STM-4-133 (3-4-22)

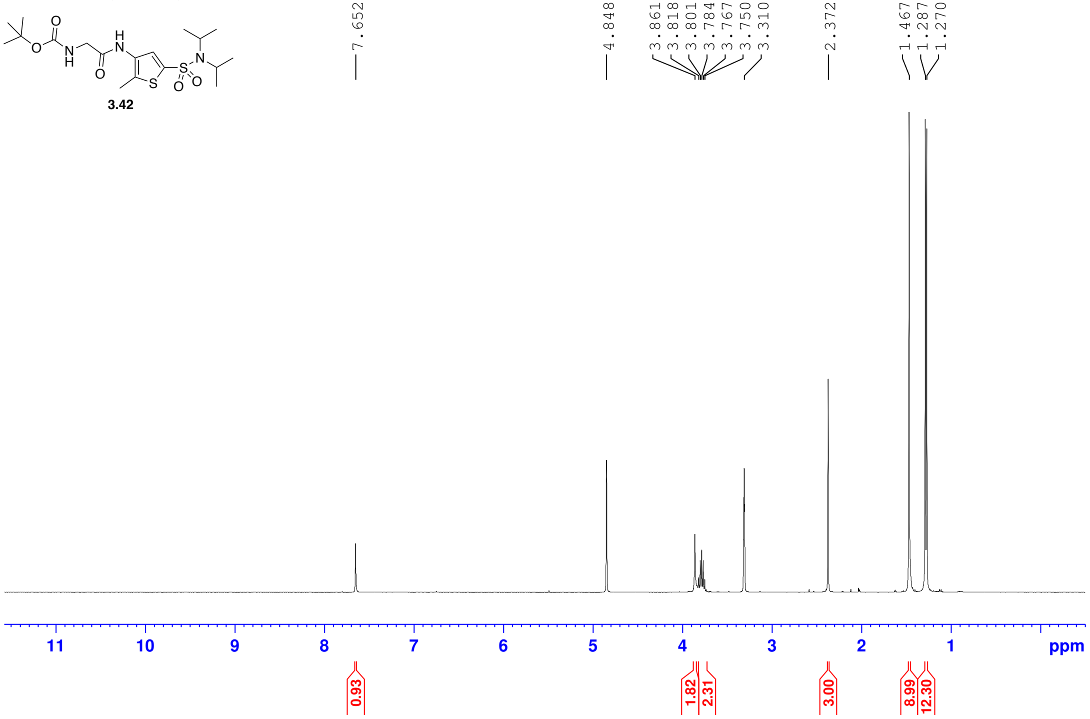

STM-4-133 (3-4-22) CNMR

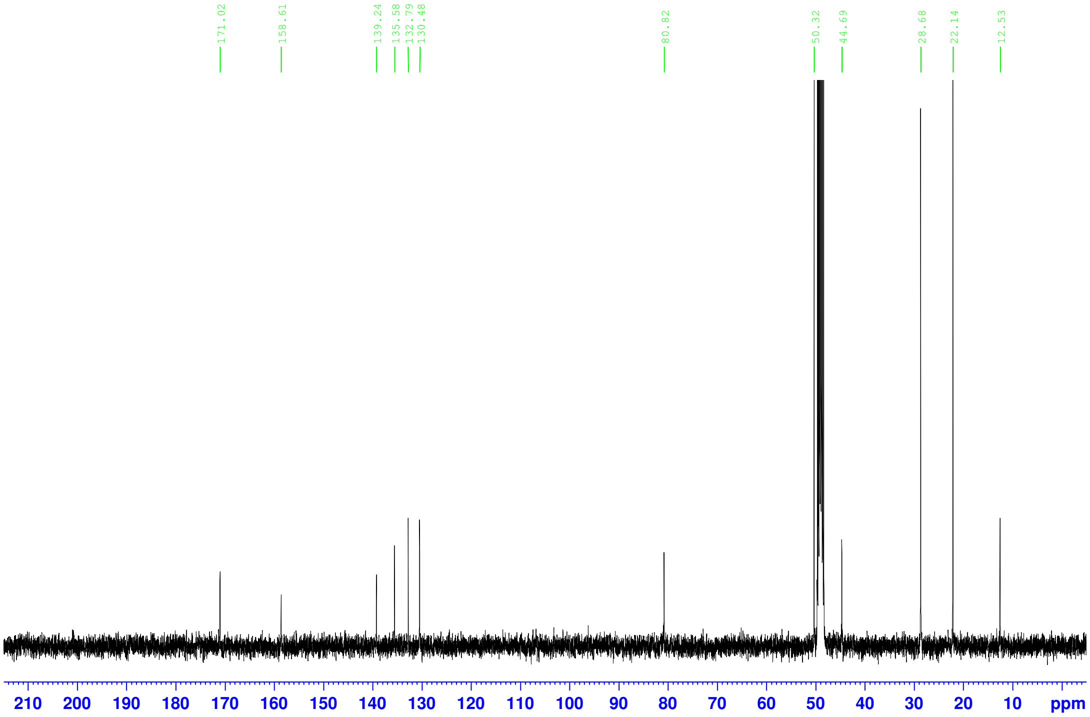

STM-4-142 (3-11-22)

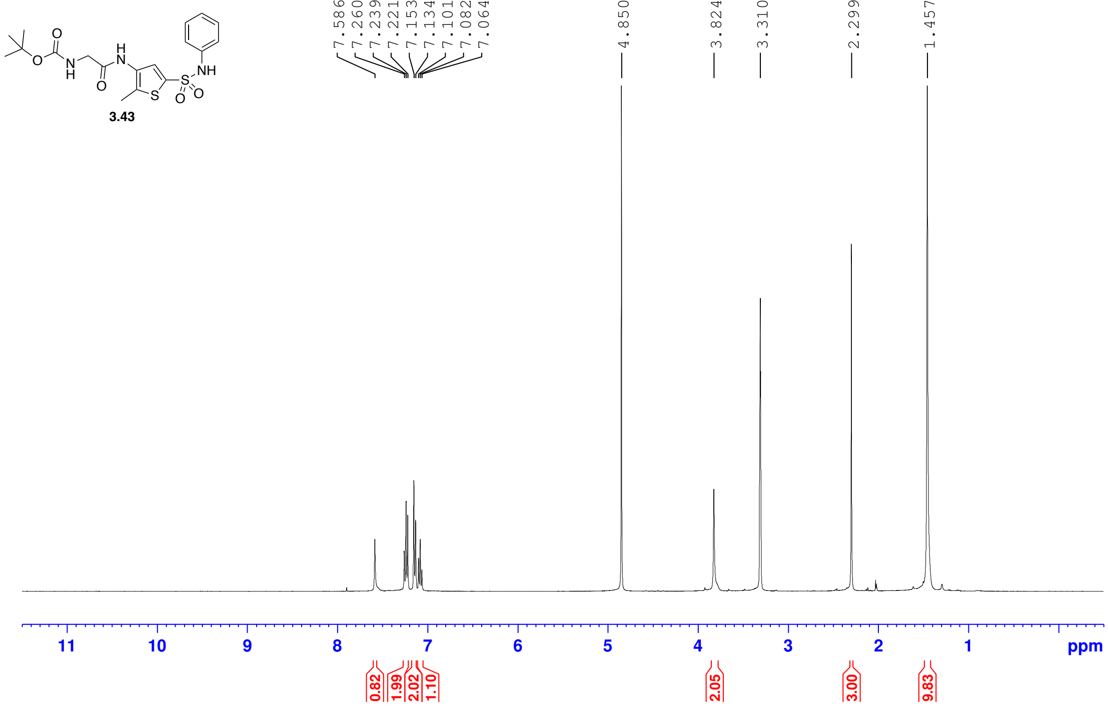

STM-4-142 (3-11-22) CNMR

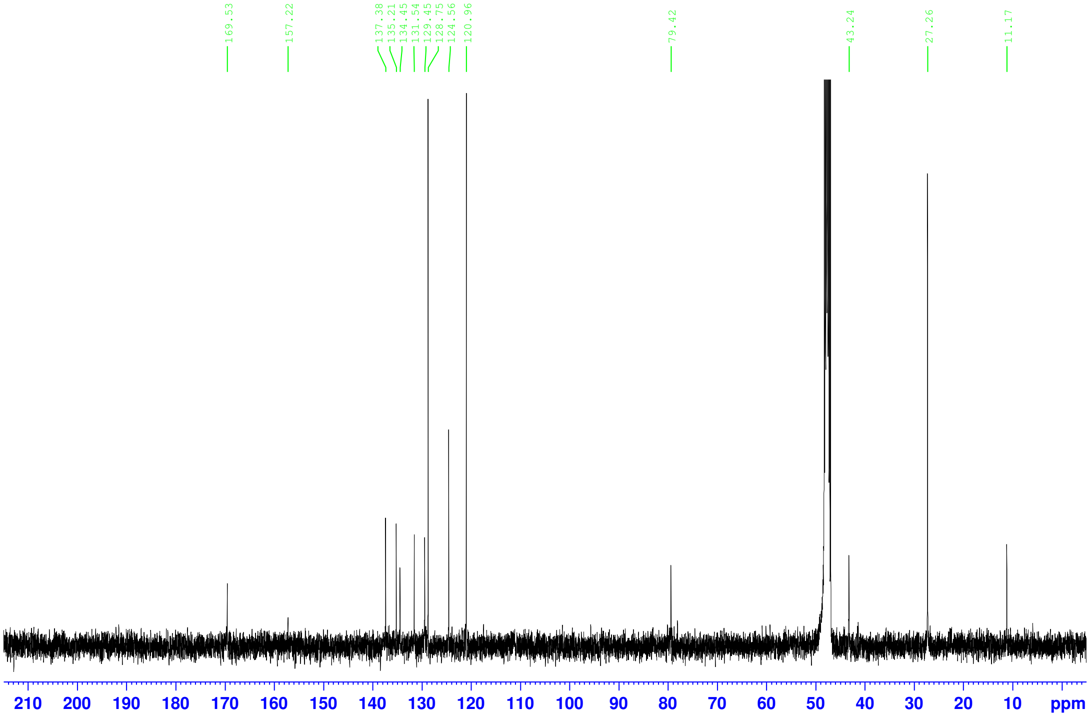

STM-5-25

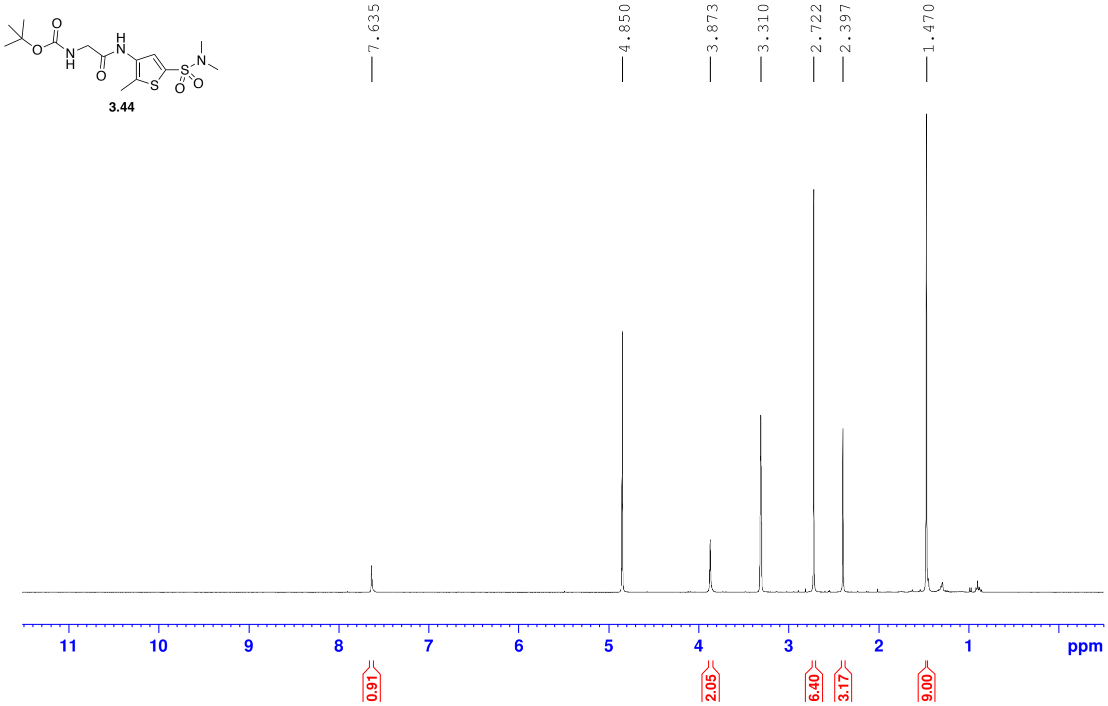

3.44

STM-5-25 CNMR

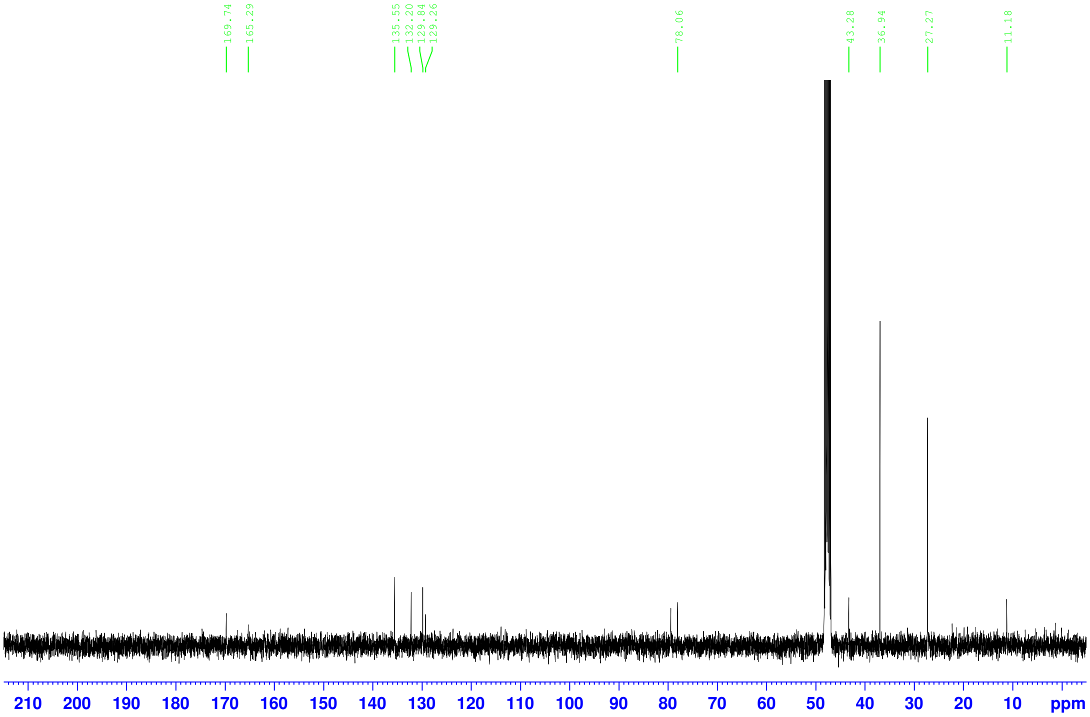

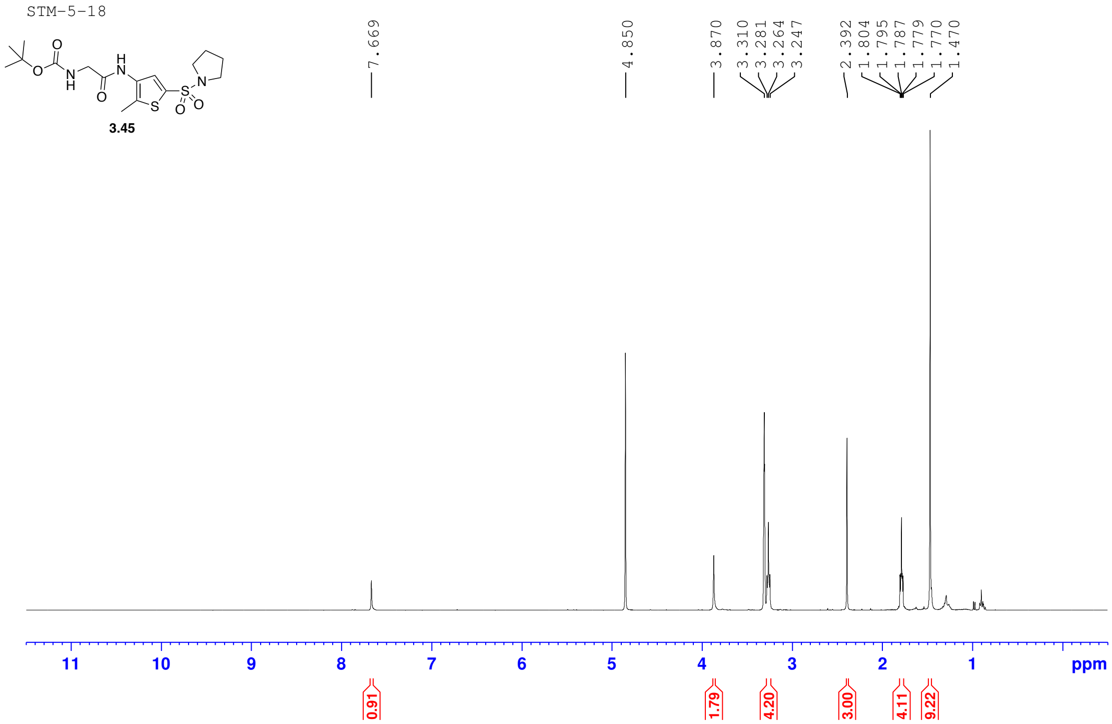
STM-5-18
3.45
7.669
4.850
3.870
3.310
3.281
3.264
3.247
2.392
1.804
1.795
1.787
1.779
1.770
1.470
11
10
9
8
7
6
5
4
3
2
1
ppm
0.91
1.79
4.20
3.00
4.11
9.22

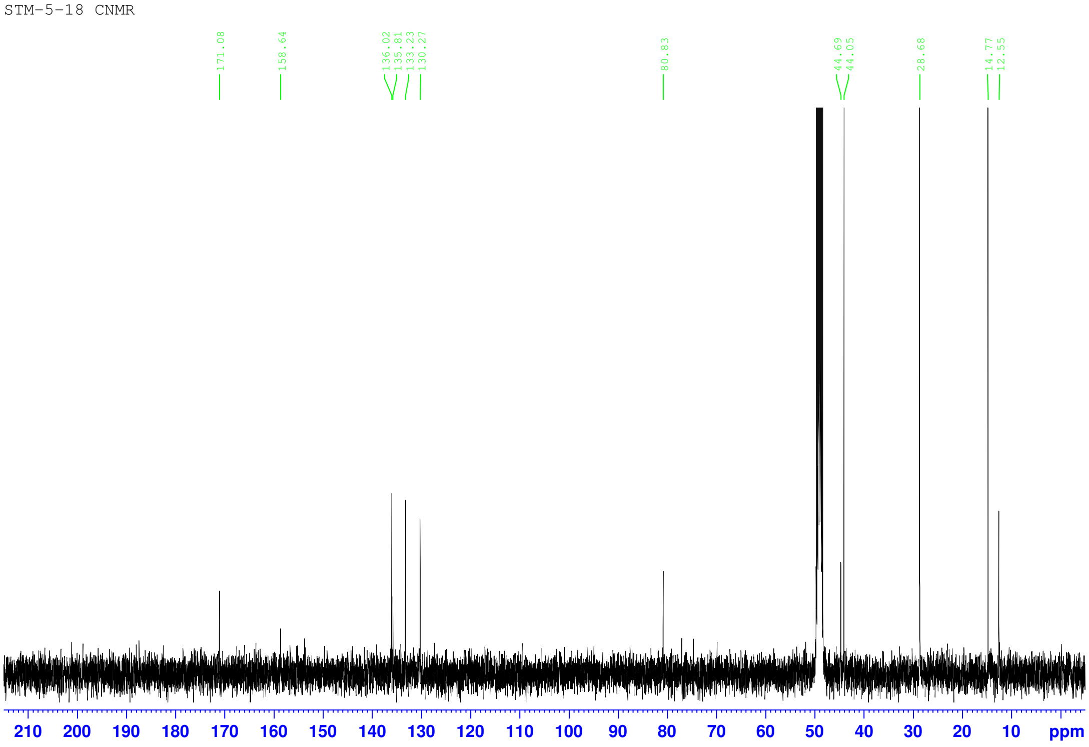
STM-5-18 CNMR
171.08
158.64
136.02
135.81
133.23
130.27
80.83
44.69
44.05
28.68
14.77
12.55
210
200
190
180
170
160
150
140
130
120
110
100
90
80
70
60
50
40
30
20
10
ppm

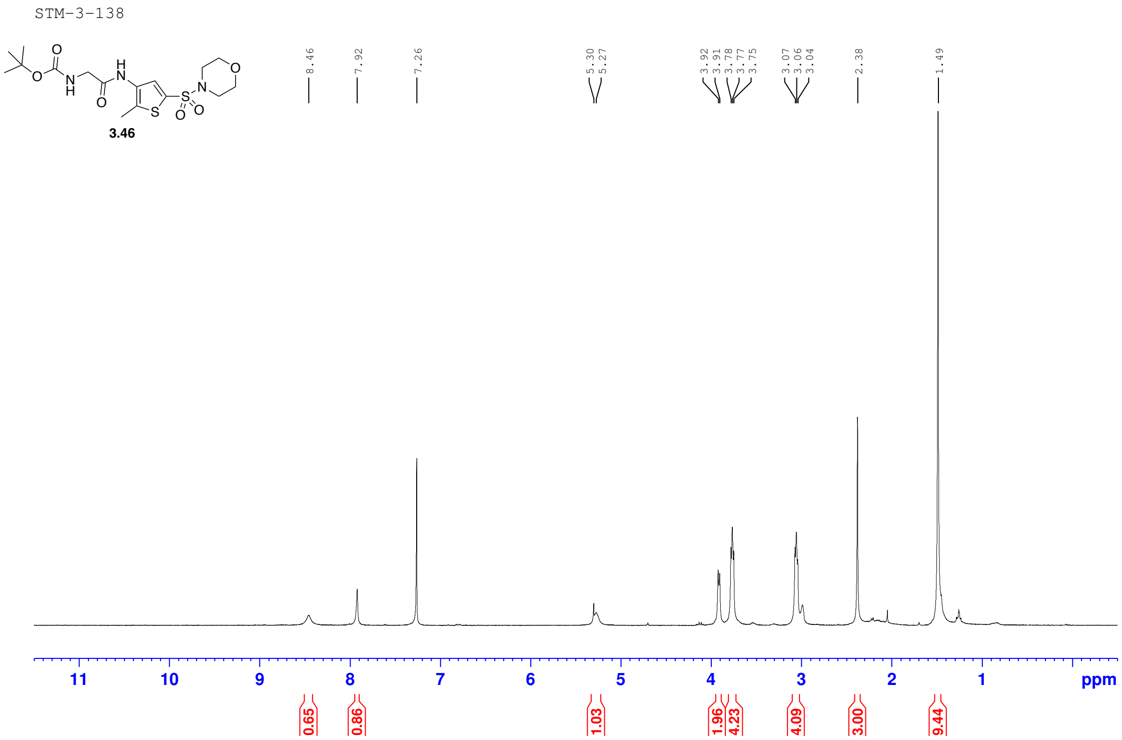
STM-3-138
3.46
8.46
7.92
7.26
5.30
5.27
3.92
3.91
3.78
3.77
3.75
3.07
3.06
3.04
2.38
1.49
0.65
0.86
1.03
1.96
4.23
4.09
3.00
9.44
11
10
9
8
7
6
5
4
3
2
1
ppm

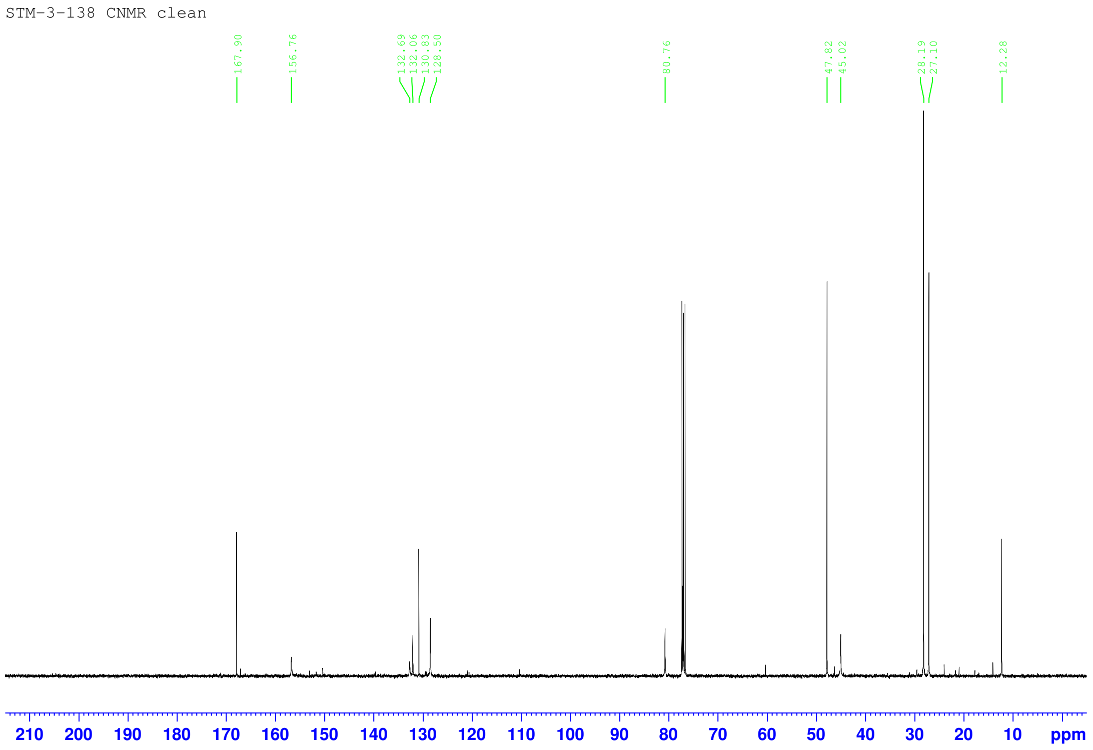
STM-3-138 CNMR clean
167.90
156.76
132.69
132.06
130.83
128.50
80.76
47.82
45.02
28.19
27.10
12.28
210
200
190
180
170
160
150
140
130
120
110
100
90
80
70
60
50
40
30
20
10
ppm

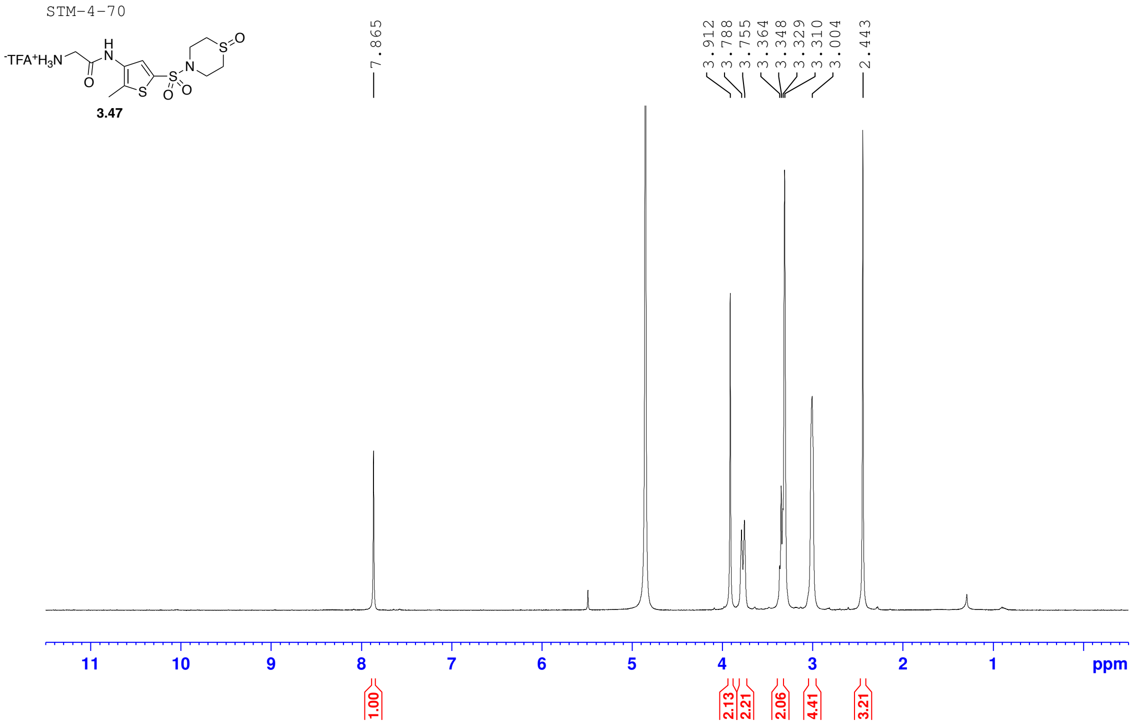
STM-4-70

3.47

STM-4-70 CNMR

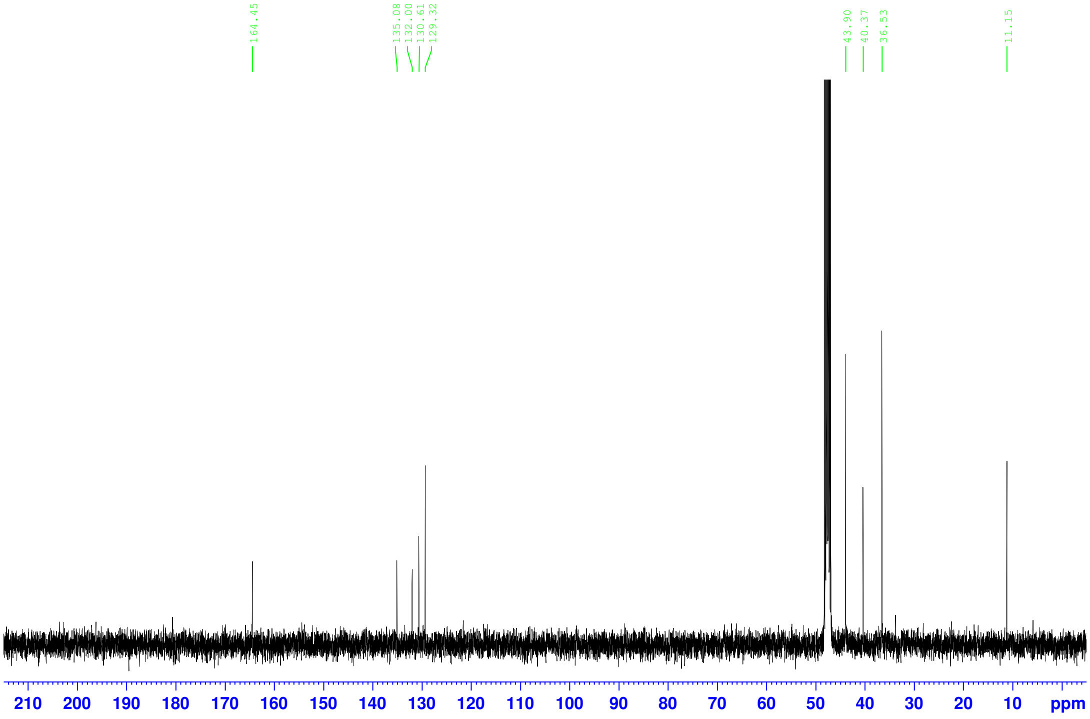

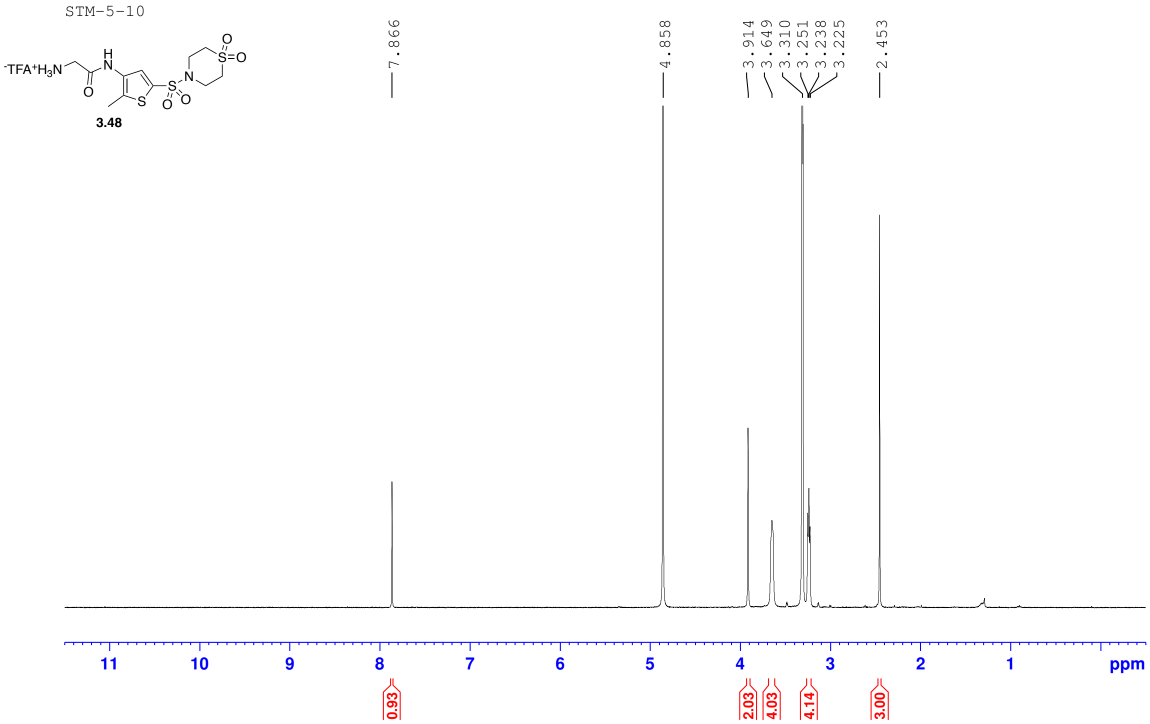
STM-5-10
-TFA+H3N
H
N
O
S
S
O
O
N
S=O
O
3.48
7.866
4.858
3.914
3.649
3.310
3.251
3.238
3.225
2.453
11
10
9
8
7
6
5
4
3
2
1
ppm
0.93
2.03
4.03
4.14
3.00

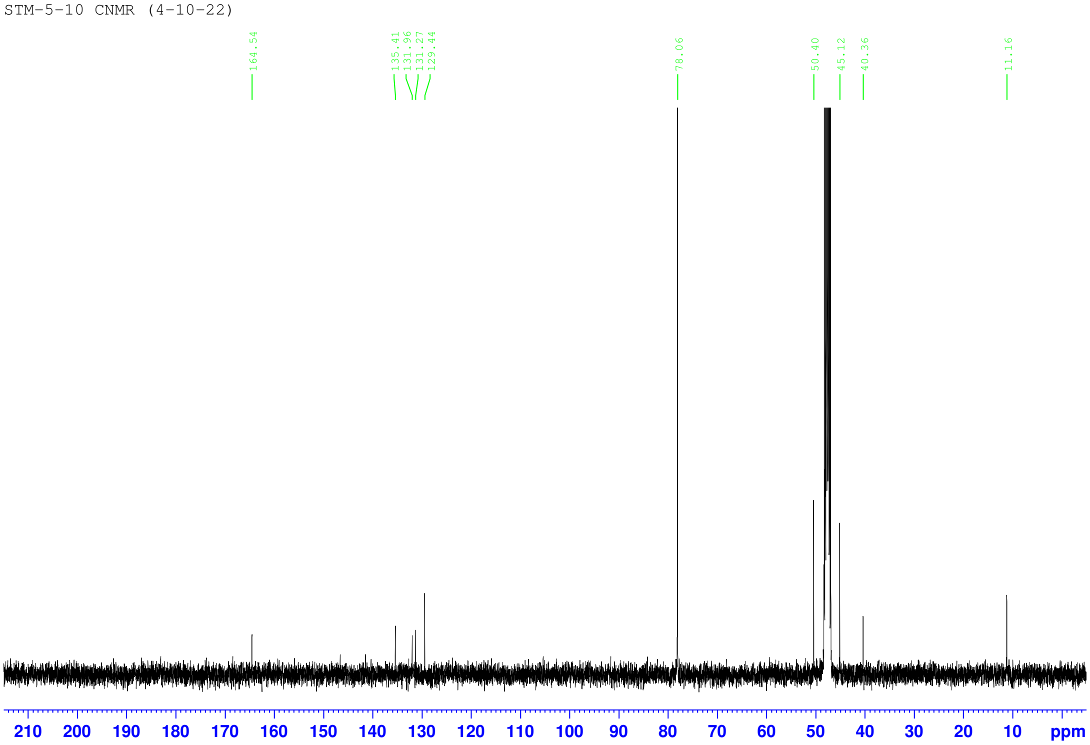
STM-5-10 CNMR (4-10-22)
164.54
135.41
131.96
131.27
129.44
78.06
50.40
45.12
40.36
11.16
210
200
190
180
170
160
150
140
130
120
110
100
90
80
70
60
50
40
30
20
10
ppm

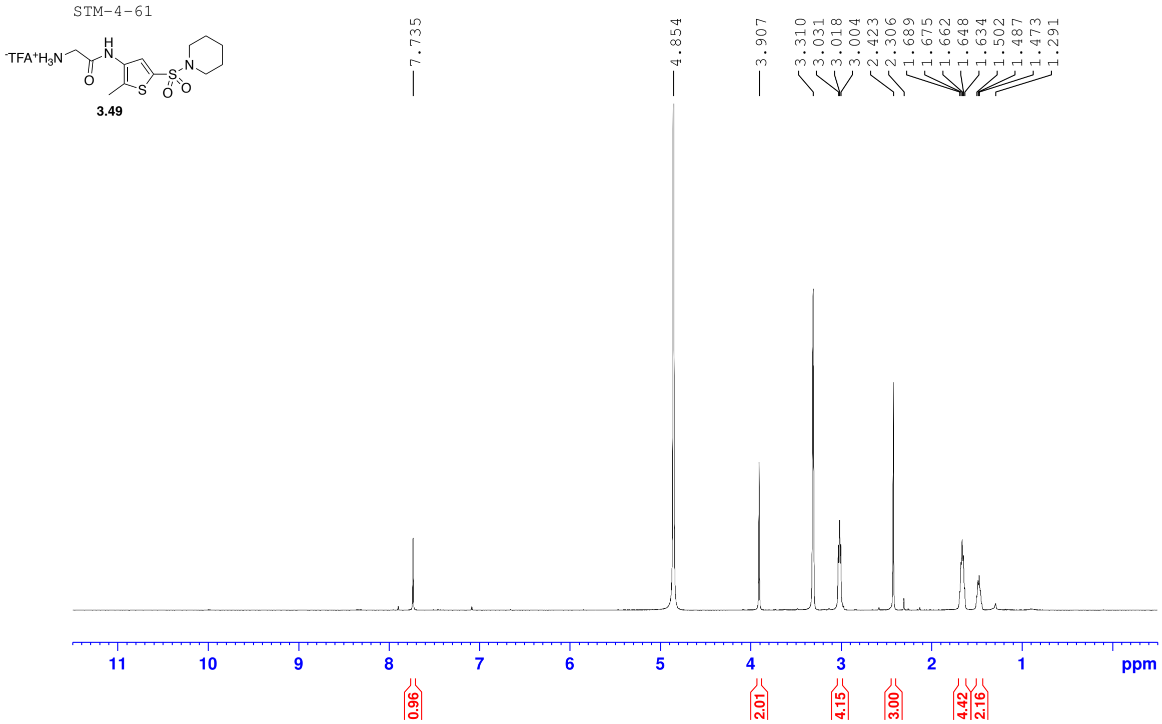
STM-4-61
-TFA+H3N
H
N
O
S
S
O
O
N
7.735
4.854
3.907
3.310
3.031
3.018
3.004
2.423
2.306
1.689
1.675
1.662
1.648
1.634
1.502
1.487
1.473
1.291
11
10
9
8
7
6
5
4
3
2
1
ppm
0.96
2.01
4.15
3.00
4.42
2.16

3.49

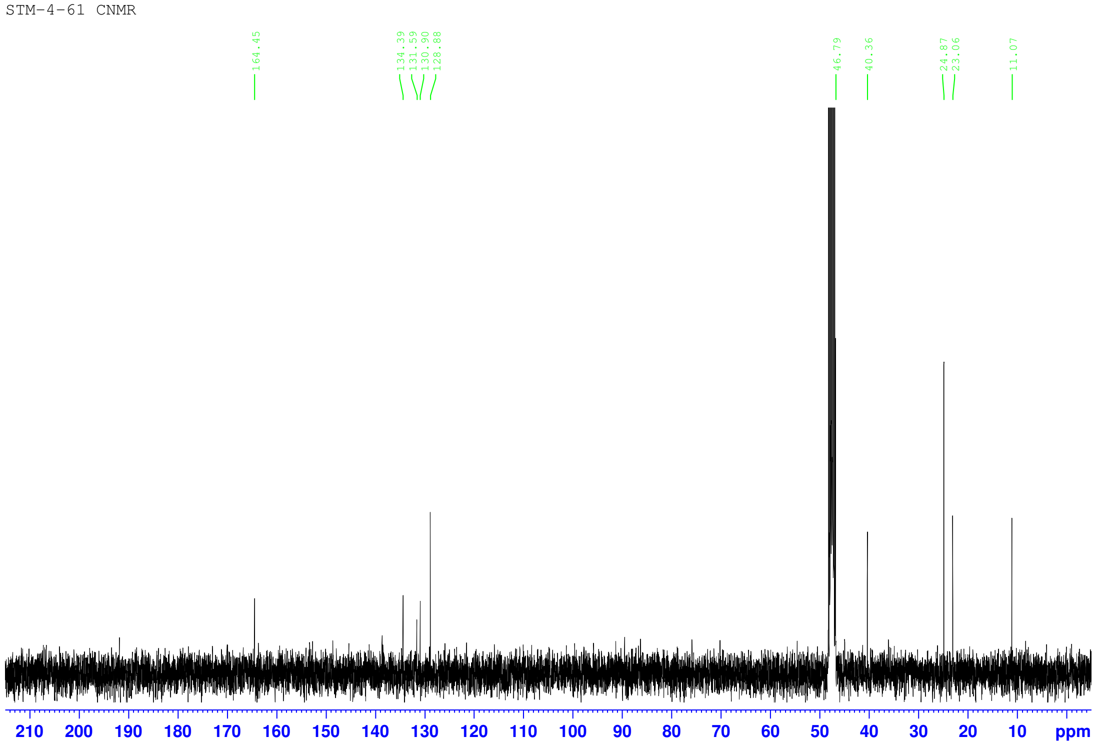
STM-4-61 CNMR
164.45
134.39
131.59
130.90
128.88
46.79
40.36
24.87
23.06
11.07
210
200
190
180
170
160
150
140
130
120
110
100
90
80
70
60
50
40
30
20
10
ppm

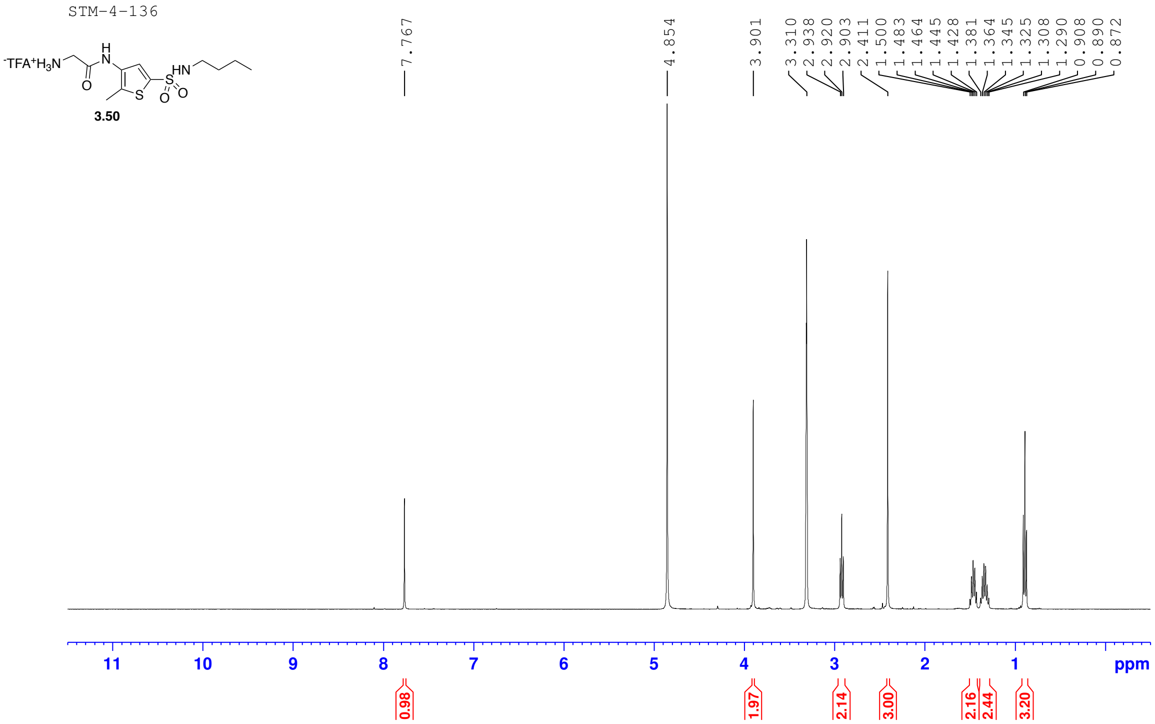
STM-4-136
-TFA+H3N
H
N
O
S
HN
S
O
O
3.50
7.767
4.854
3.901
3.310
2.938
2.920
2.903
2.411
1.500
1.483
1.464
1.445
1.428
1.381
1.364
1.345
1.325
1.308
1.290
0.908
0.890
0.872
11
10
9
8
7
6
5
4
3
2
1
ppm
0.98
1.97
2.14
3.00
2.16
2.44
3.20

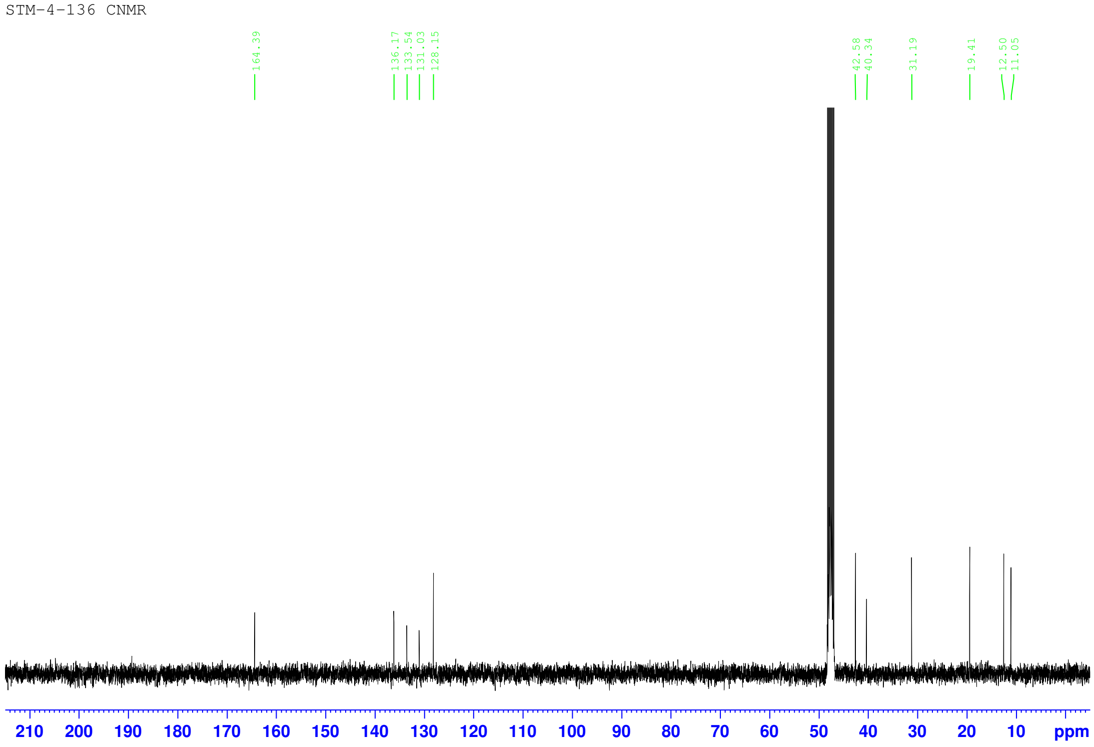
STM-4-136 CNMR
164.39
136.17
133.54
131.03
128.15
42.58
40.34
31.19
19.41
12.50
11.05
210
200
190
180
170
160
150
140
130
120
110
100
90
80
70
60
50
40
30
20
10
ppm

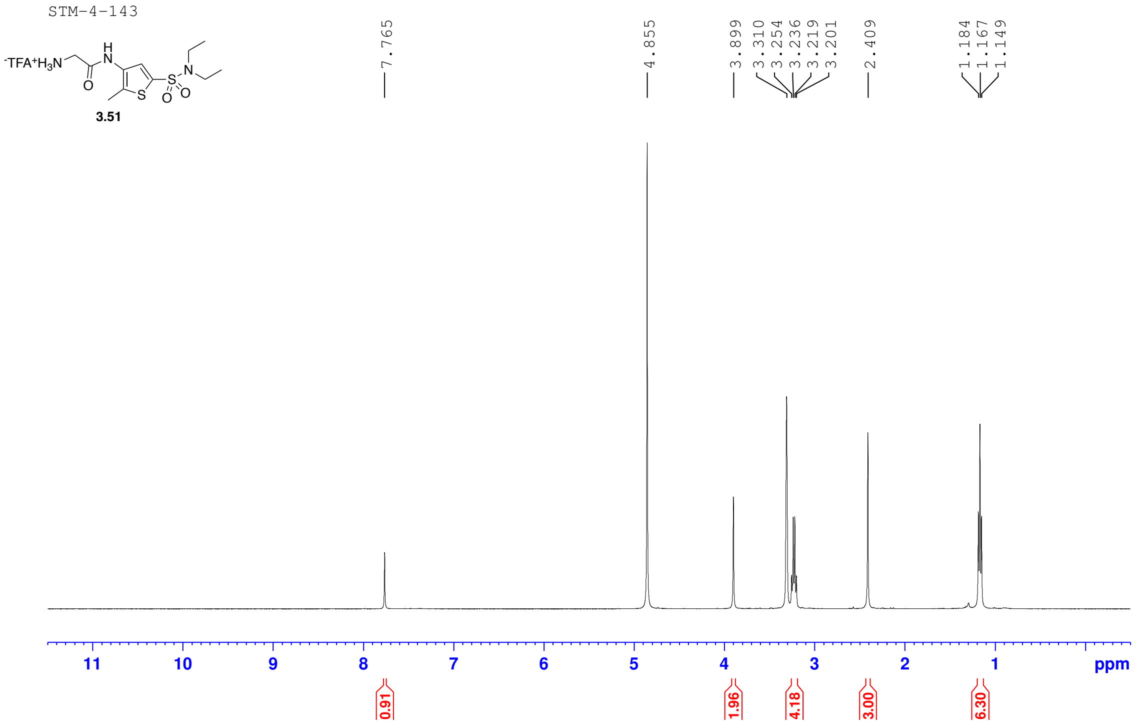
STM-4-143
-TFA+H3N
H
N
O
S
S
O
O
N
3.51
7.765
4.855
3.899
3.310
3.254
3.236
3.219
3.201
2.409
1.184
1.167
1.149
11
10
9
8
7
6
5
4
3
2
1
ppm
0.91
1.96
4.18
3.00
6.30

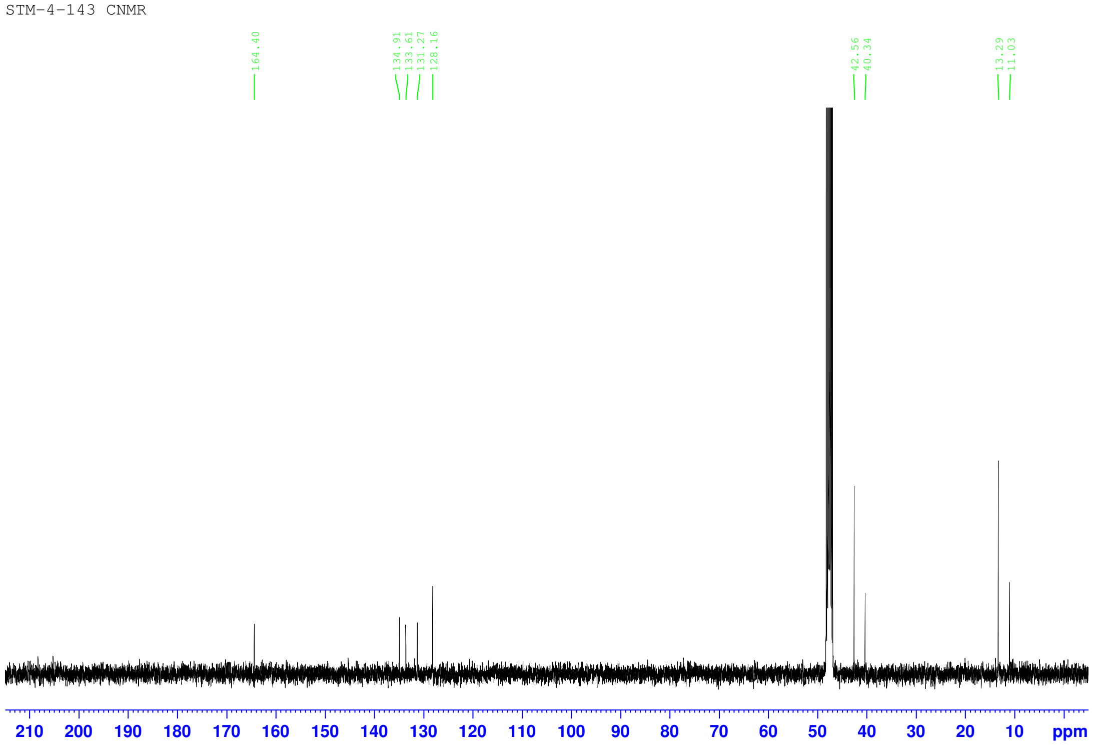
STM-4-143 CNMR
164.40
134.91
133.61
131.27
128.16
42.56
40.34
13.29
11.03
210
200
190
180
170
160
150
140
130
120
110
100
90
80
70
60
50
40
30
20
10
ppm

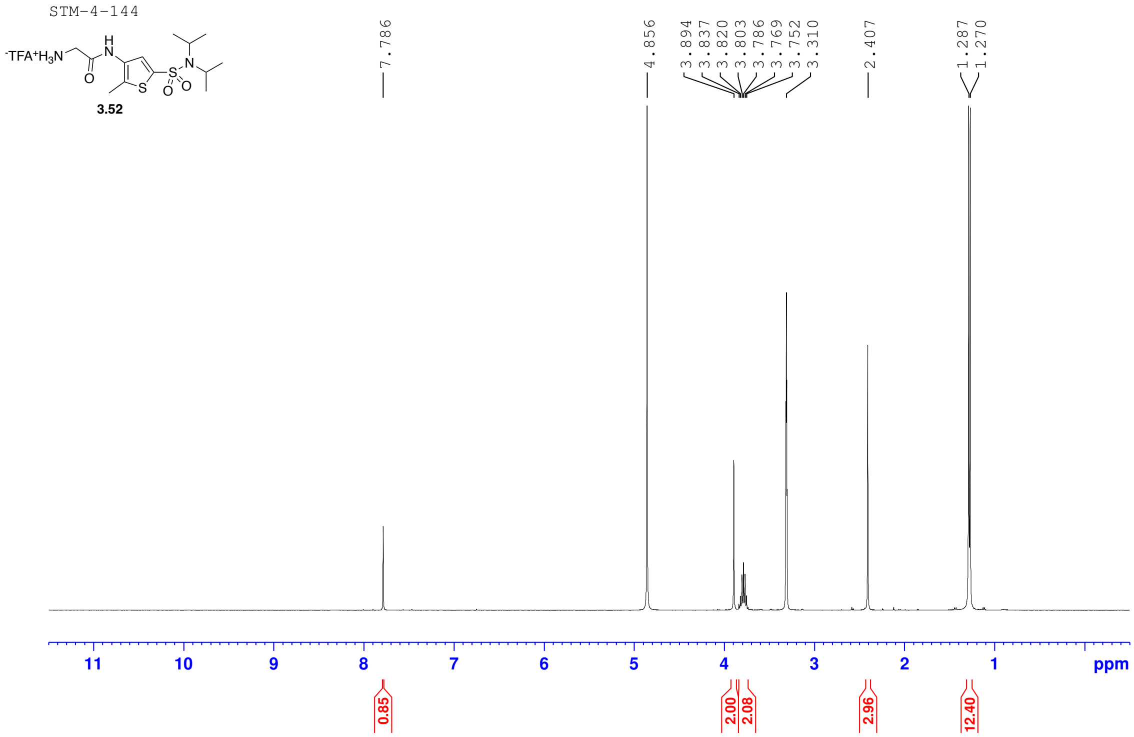
STM-4-144
⁻TFA⁺H₃N
H
N
O
S
S
O
O
N
3.52
7.786
4.856
3.894
3.837
3.820
3.803
3.786
3.769
3.752
3.310
2.407
1.287
1.270
11
10
9
8
7
6
5
4
3
2
1
ppm
0.85
2.00
2.08
2.96
12.40

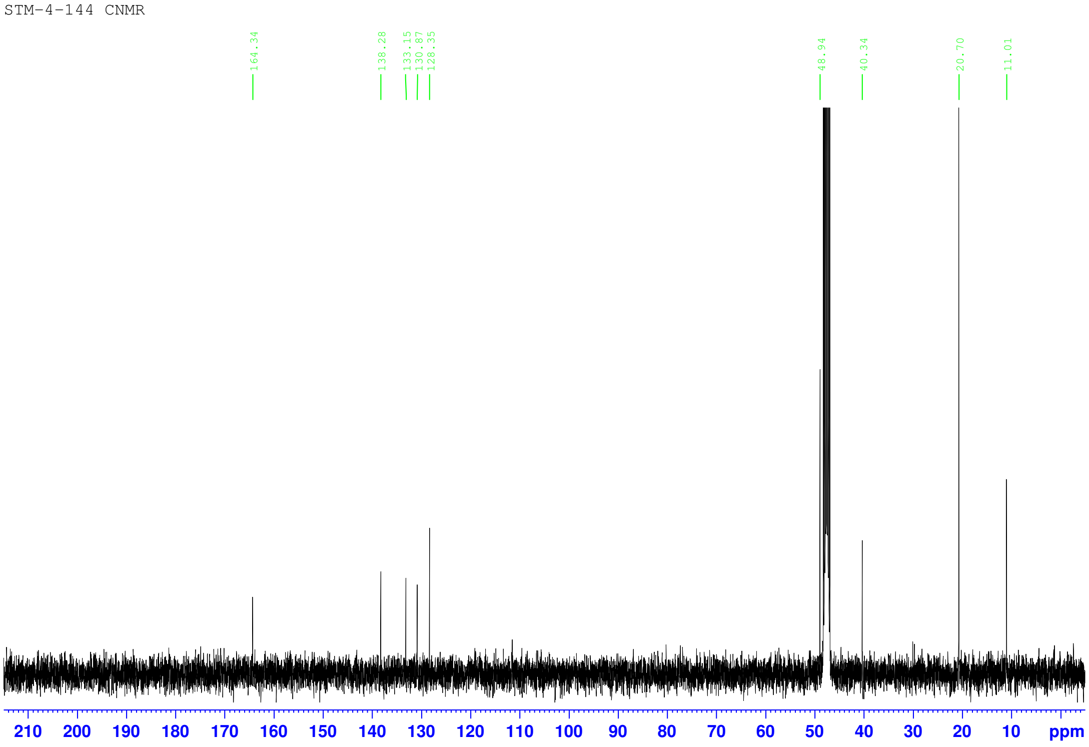
STM-4-144 CNMR
164.34
138.28
133.15
130.87
128.35
48.94
40.34
20.70
11.01
210
200
190
180
170
160
150
140
130
120
110
100
90
80
70
60
50
40
30
20
10
ppm

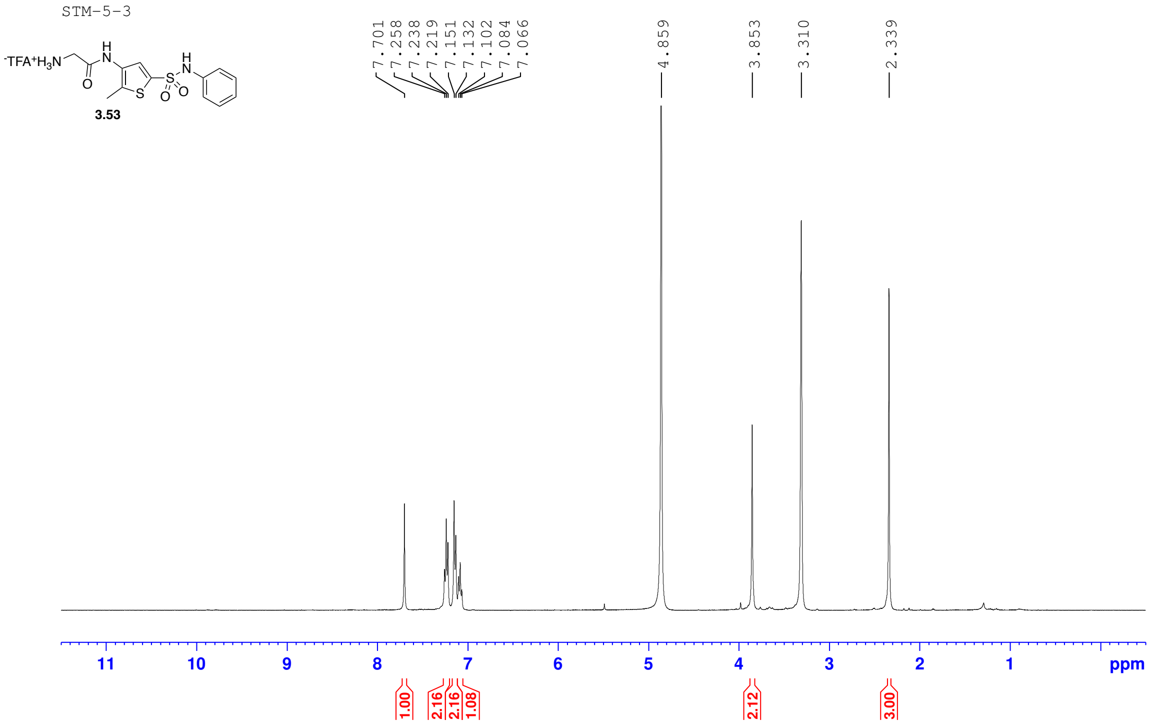
STM-5-3
-TFA+H3N
H
N
O
S
S
O
O
H
N
3.53
7.701
7.258
7.238
7.219
7.151
7.132
7.102
7.084
7.066
4.859
3.853
3.310
2.339
11
10
9
8
7
6
5
4
3
2
1
ppm
1.00
2.16
2.16
1.08
2.12
3.00

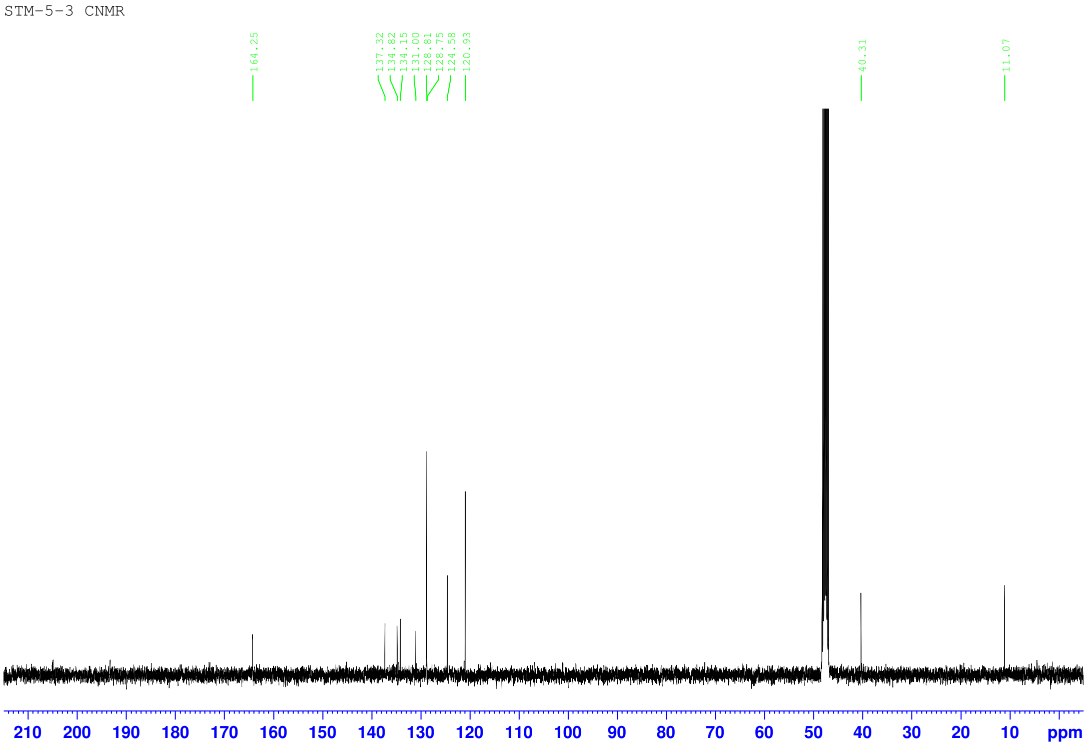
STM-5-3 CNMR
164.25
137.32
134.82
134.15
131.00
128.81
128.75
124.58
120.93
40.31
11.07
210
200
190
180
170
160
150
140
130
120
110
100
90
80
70
60
50
40
30
20
10
ppm

STM-5-28

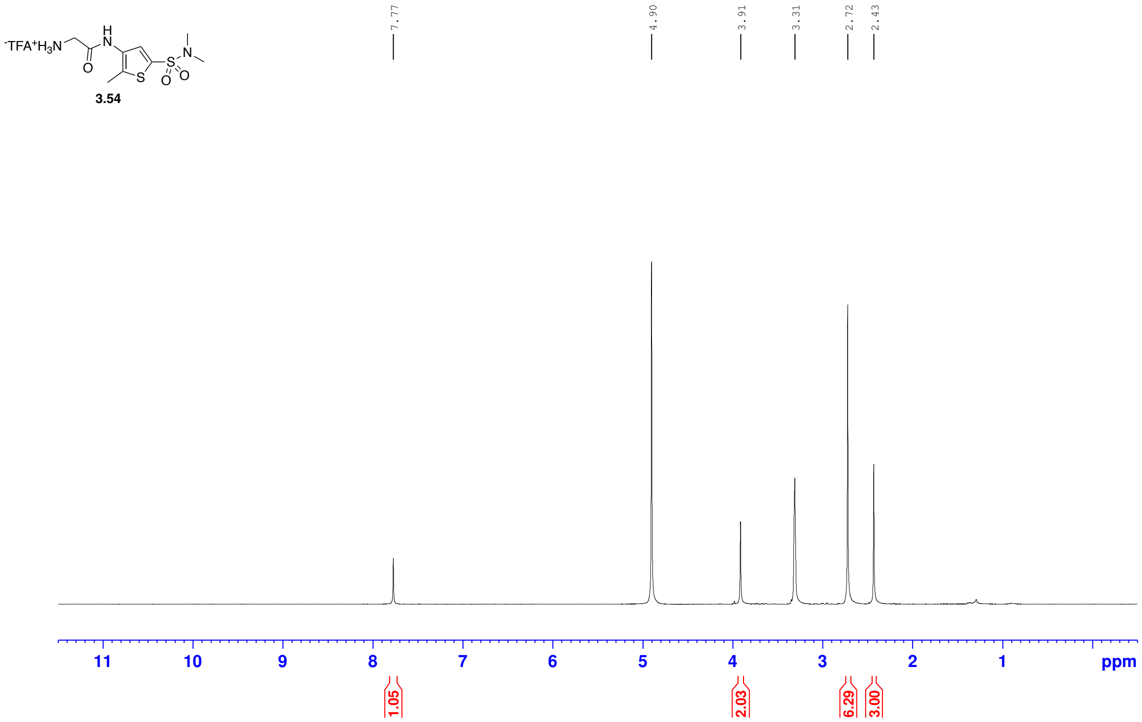

3.54

STM-5-28 CNMR

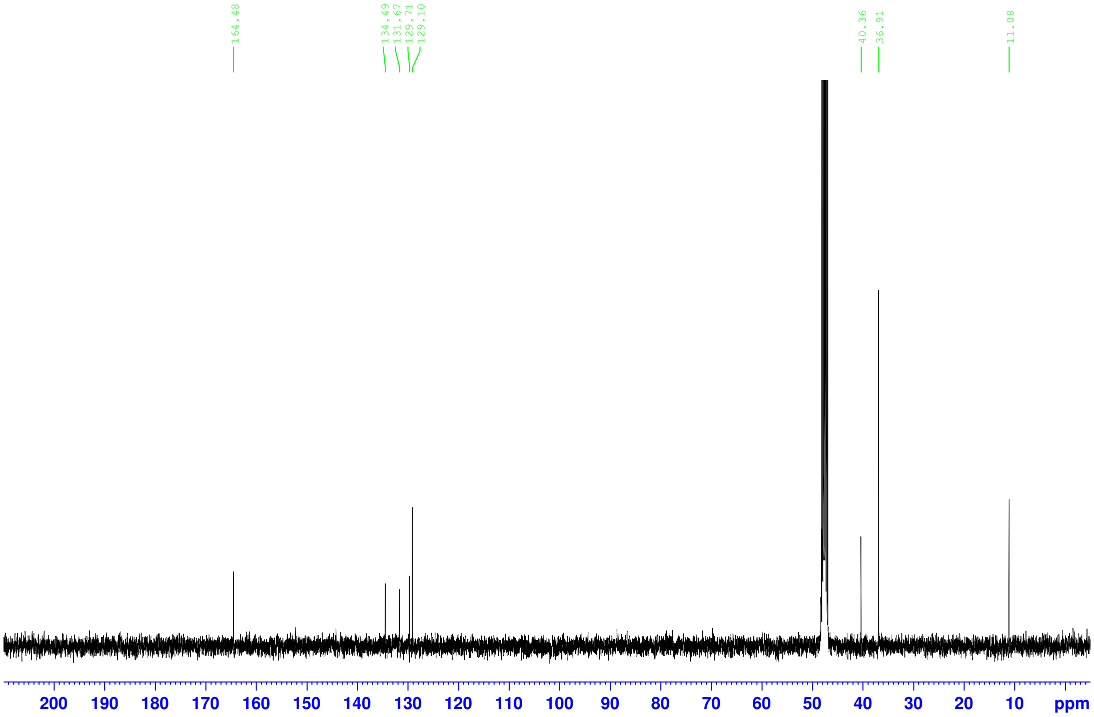

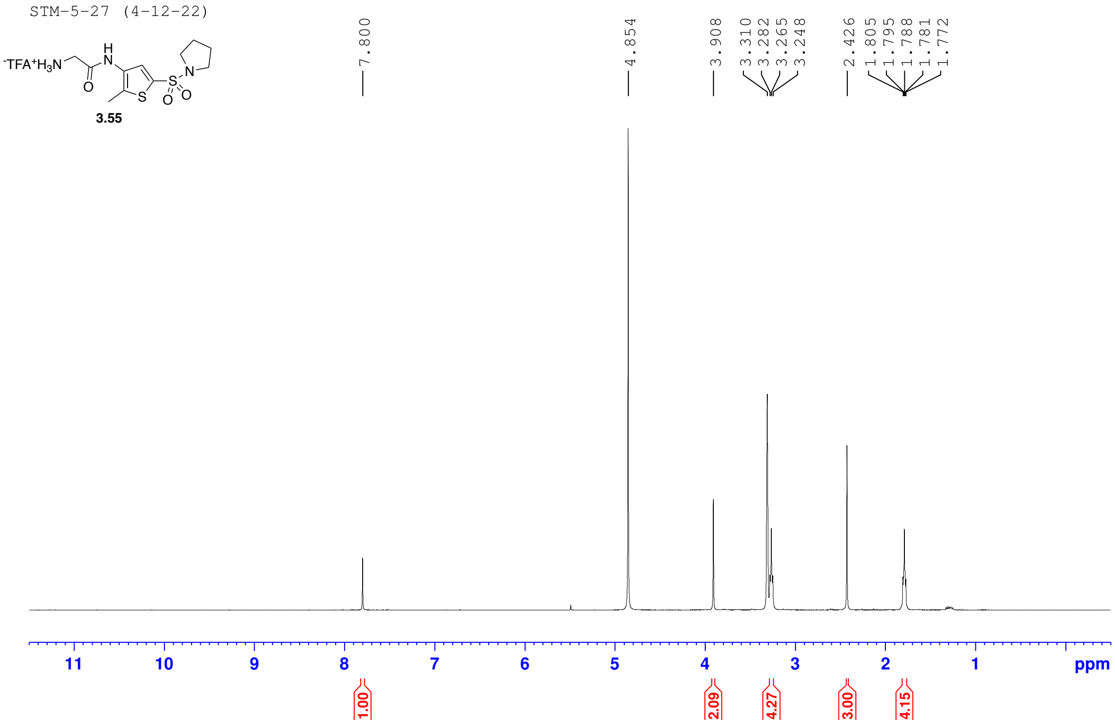
STM-5-27 (4-12-22)
⁻TFA⁺H₃N
H
N
O
S
S
N
O
O
3.55
7.800
4.854
3.908
3.310
3.282
3.265
3.248
2.426
1.805
1.795
1.788
1.781
1.772
11
10
9
8
7
6
5
4
3
2
1
ppm
1.00
2.09
4.27
3.00
4.15

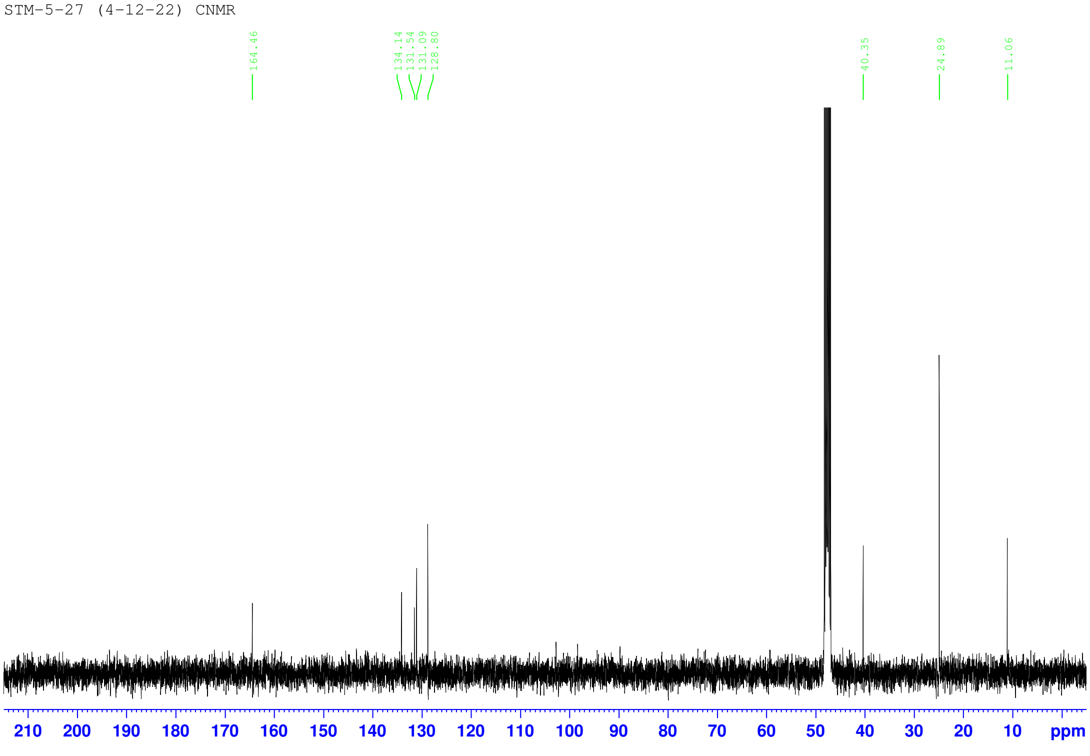
STM-5-27 (4-12-22) CNMR
164.46
134.14
131.54
131.09
128.80
40.35
24.89
11.06
210
200
190
180
170
160
150
140
130
120
110
100
90
80
70
60
50
40
30
20
10
ppm

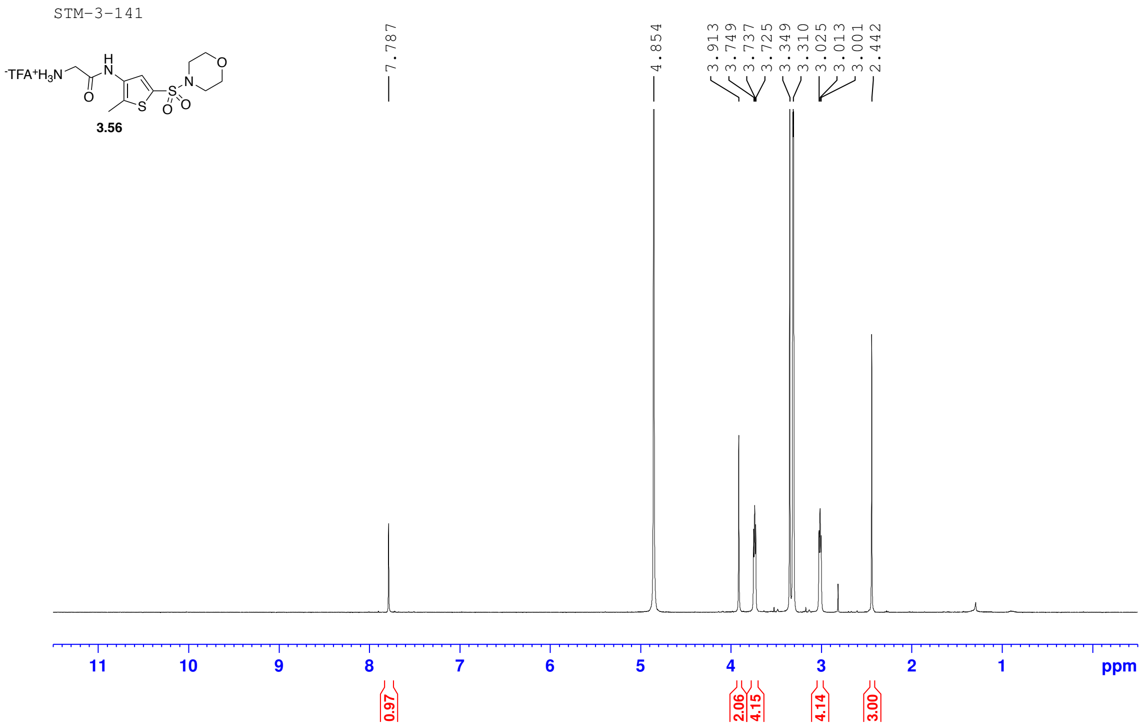
STM-3-141
-TFA+H3N
H
N
O
S
O
O
N
O
3.56
7.787
4.854
3.913
3.749
3.737
3.725
3.349
3.310
3.025
3.013
3.001
2.442
11
10
9
8
7
6
5
4
3
2
1
ppm
0.97
2.06
4.15
4.14
3.00

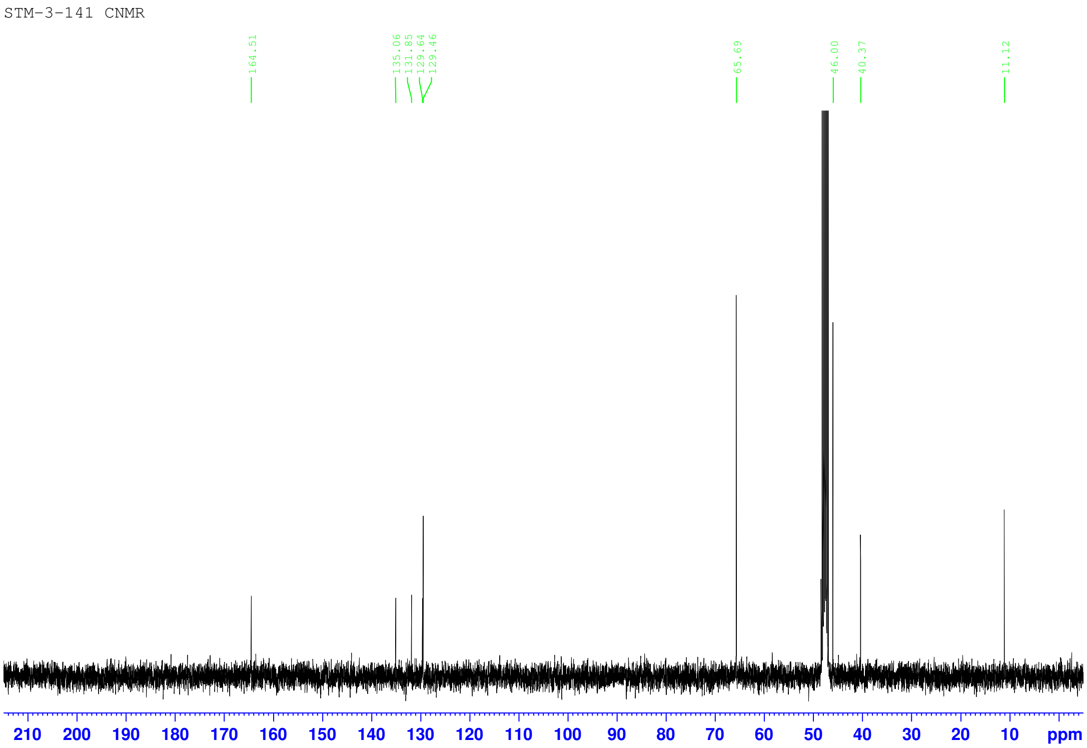
STM-3-141 CNMR
164.51
135.06
131.85
129.64
129.46
65.69
46.00
40.37
11.12
210
200
190
180
170
160
150
140
130
120
110
100
90
80
70
60
50
40
30
20
10
ppm

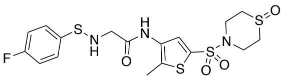
F
S
N
H
O
H
N
S
S
O
O
N
S
O

3.57

STM-4-101 DMSO

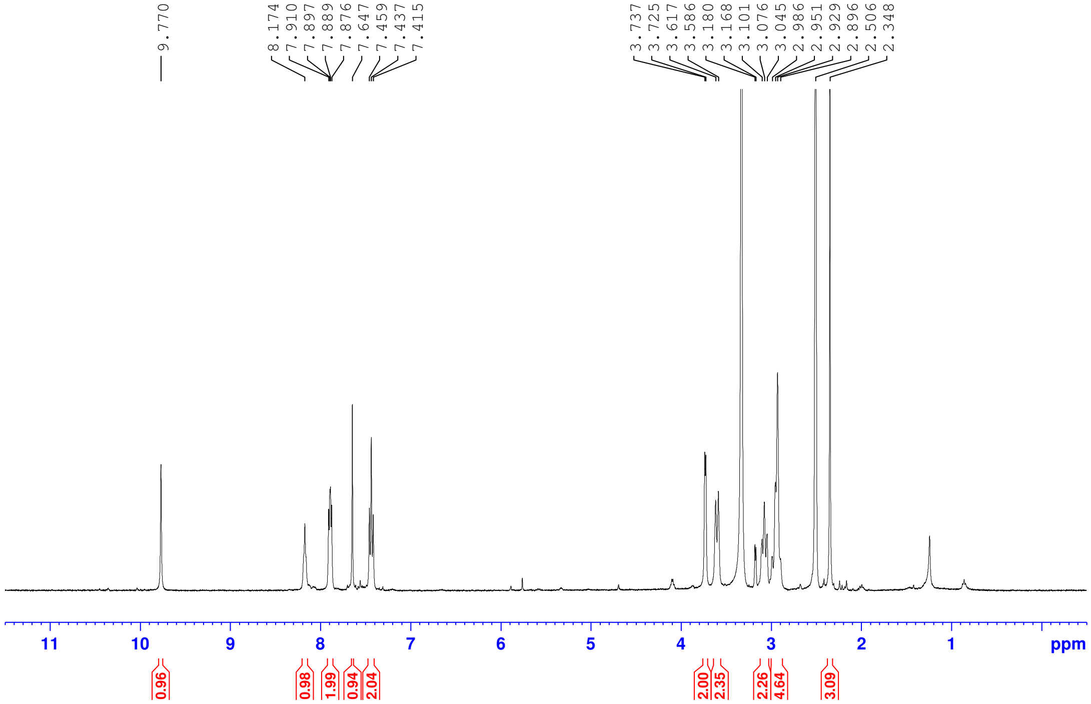

STM-4-101 DMSO CNMR

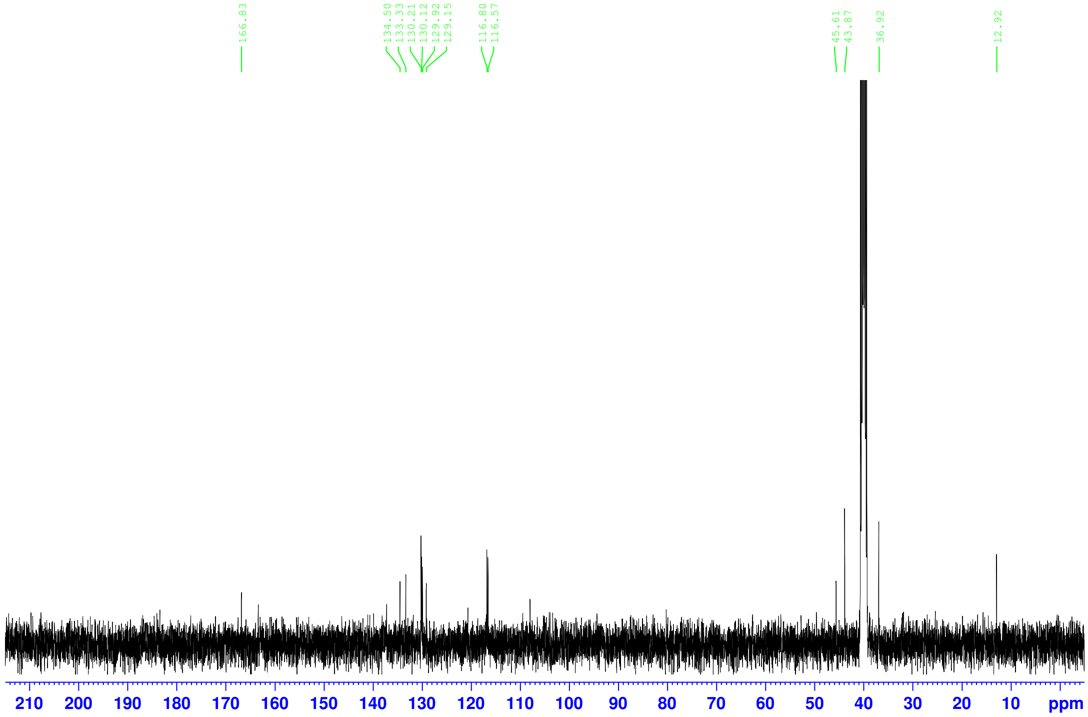

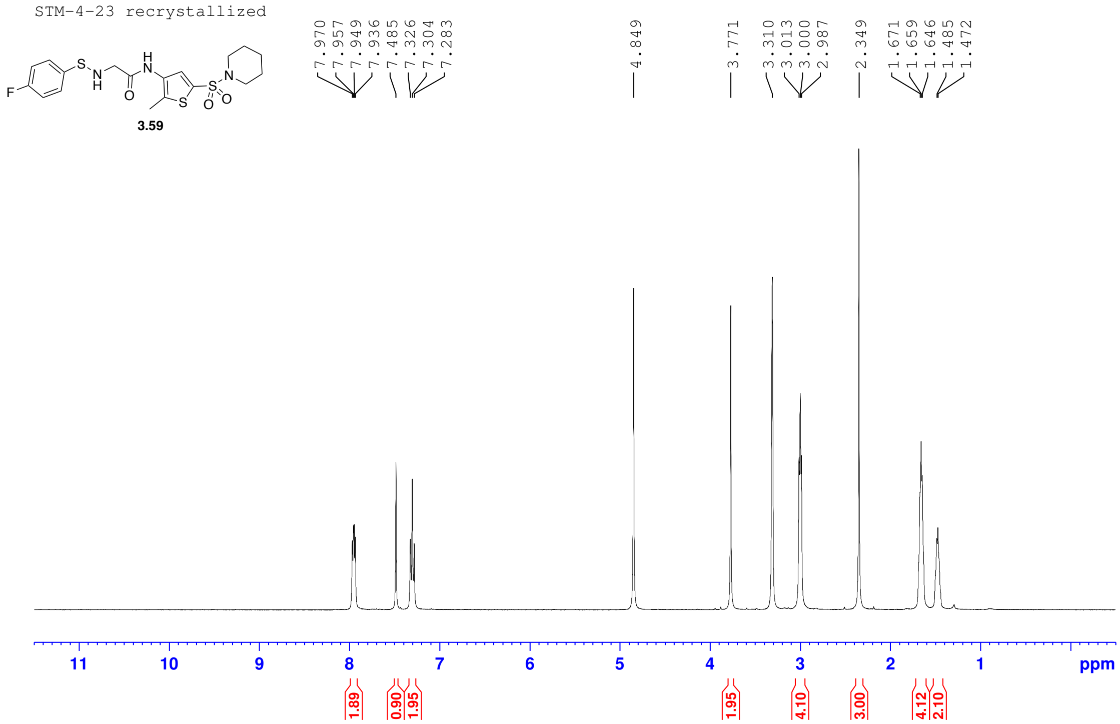
STM-4-23 recrystallized
F
S
N
H
O
H
N
S
O
O
N
S
3.59
7.970
7.957
7.949
7.936
7.485
7.326
7.304
7.283
4.849
3.771
3.310
3.013
3.000
2.987
2.349
1.671
1.659
1.646
1.485
1.472
11
10
9
8
7
6
5
4
3
2
1
ppm
1.89
0.90
1.95
1.95
4.10
3.00
4.12
2.10

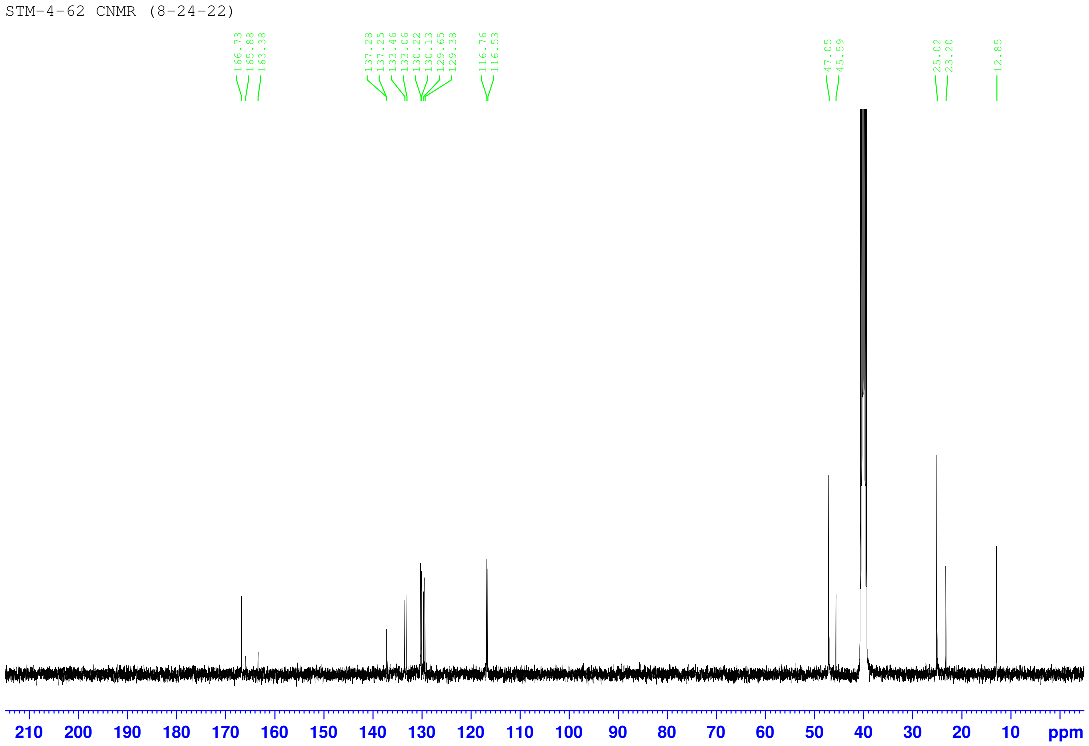
STM-4-62 CNMR (8-24-22)
166.73
165.88
163.38
137.28
137.25
133.46
133.06
130.22
130.13
129.65
129.38
116.76
116.53
47.05
45.59
25.02
23.20
12.85
210
200
190
180
170
160
150
140
130
120
110
100
90
80
70
60
50
40
30
20
10
ppm

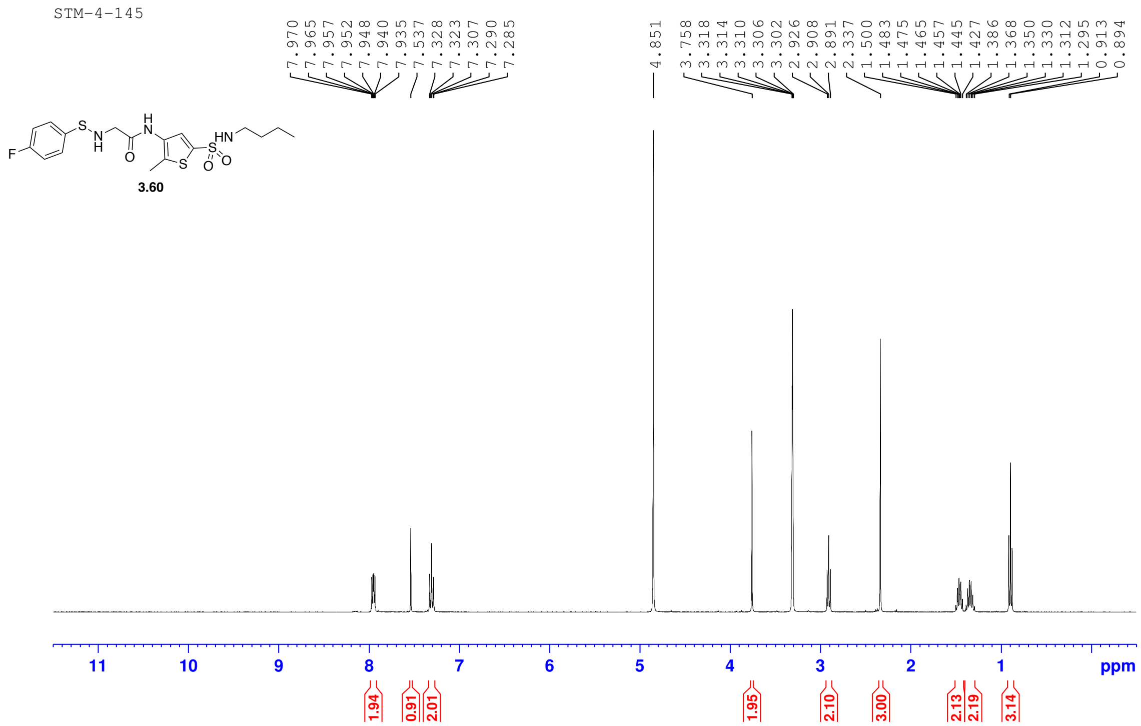
STM-4-145
7.970
7.965
7.957
7.952
7.948
7.940
7.935
7.537
7.328
7.323
7.307
7.290
7.285
4.851
3.758
3.318
3.314
3.310
3.306
3.302
2.926
2.908
2.891
2.337
1.500
1.483
1.475
1.465
1.457
1.445
1.427
1.386
1.368
1.350
1.330
1.312
1.295
0.913
0.894
F
S
N
H
O
H
N
S
S
O
O
HN
11
10
9
8
7
6
5
4
3
2
1
ppm
1.94
0.91
2.01
1.95
2.10
3.00
2.13
2.19
3.14

3.60

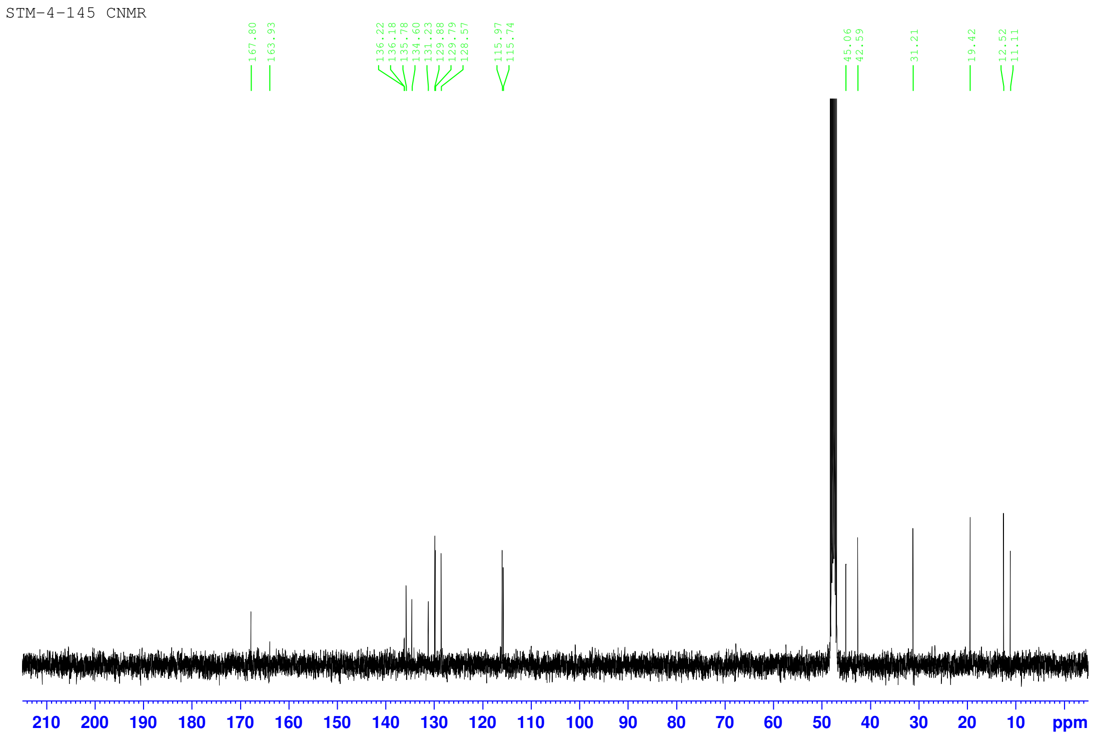
STM-4-145 CNMR
167.80
163.93
136.22
136.18
135.78
134.60
131.23
129.88
129.79
128.57
115.97
115.74
45.06
42.59
31.21
19.42
12.52
11.11
210
200
190
180
170
160
150
140
130
120
110
100
90
80
70
60
50
40
30
20
10
ppm

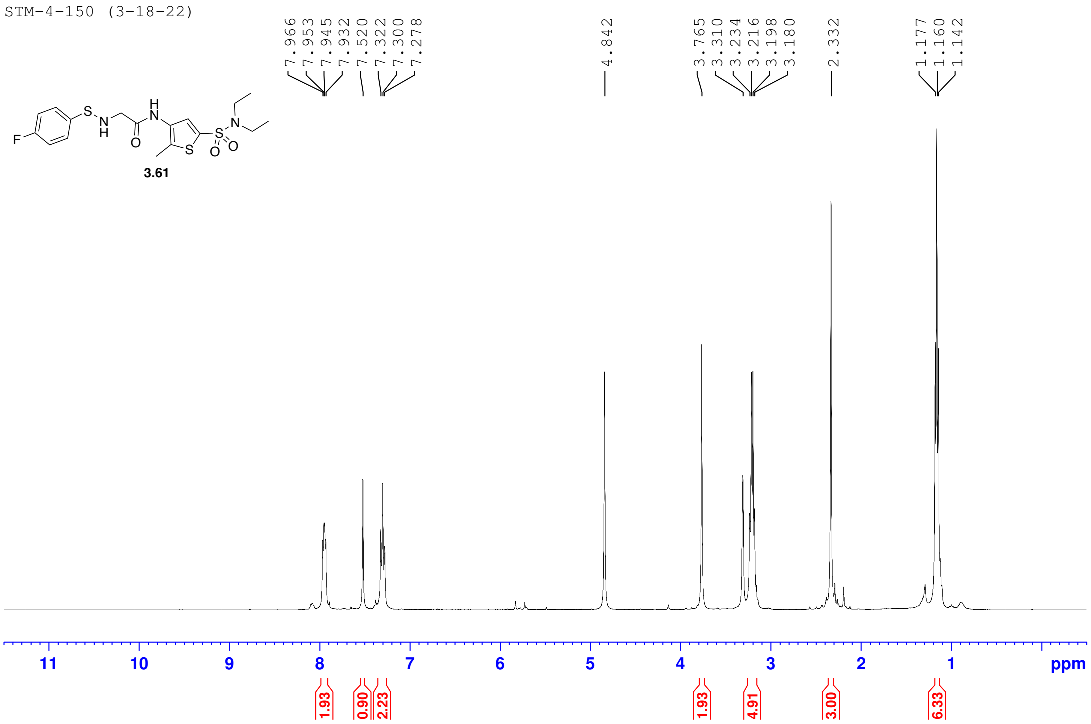
STM-4-150 (3-18-22)
3.61
7.966
7.953
7.945
7.932
7.520
7.322
7.300
7.278
4.842
3.765
3.310
3.234
3.216
3.198
3.180
2.332
1.177
1.160
1.142
11
10
9
8
7
6
5
4
3
2
1
ppm
1.93
0.90
2.23
1.93
4.91
3.00
6.33

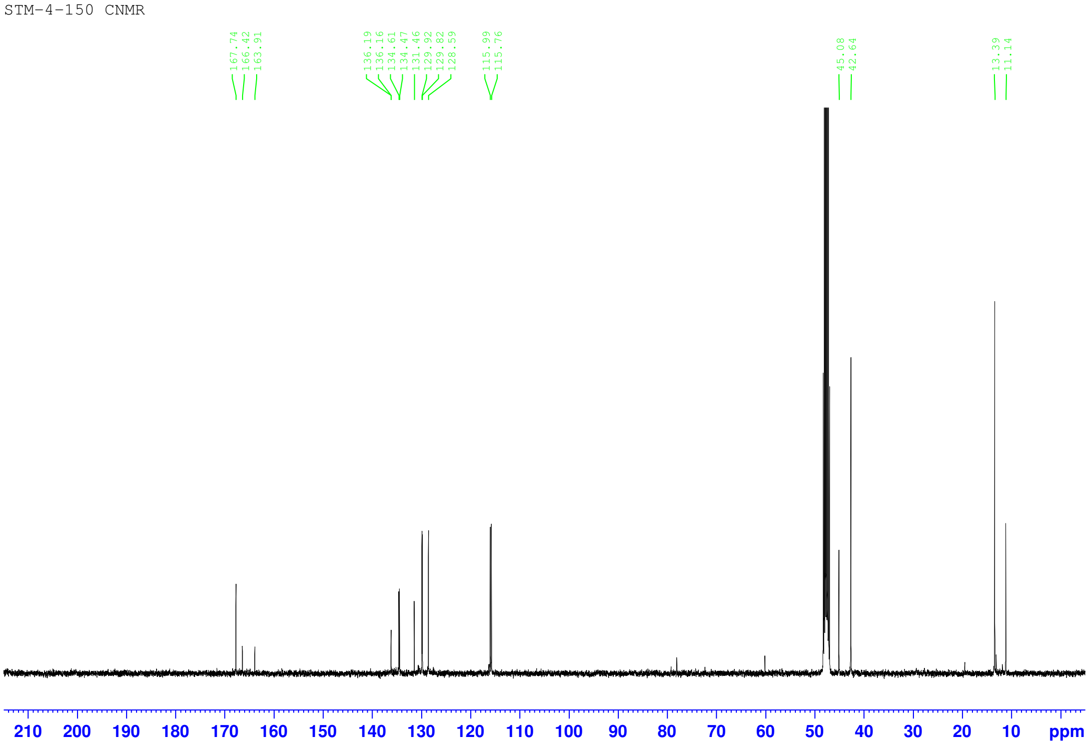
STM-4-150 CNMR
167.74
166.42
163.91
136.19
136.16
134.61
134.47
131.46
129.92
129.82
128.59
115.99
115.76
45.08
42.64
13.39
11.14
210
200
190
180
170
160
150
140
130
120
110
100
90
80
70
60
50
40
30
20
10
ppm

STM-4-151 (3-18-22)

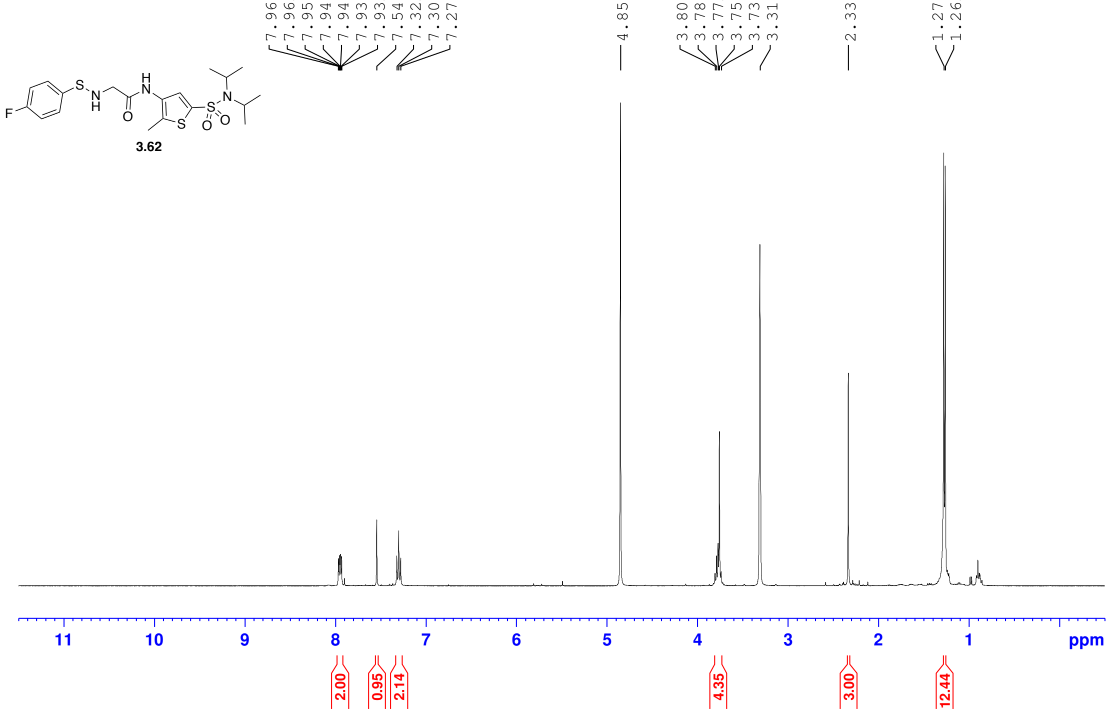

3.62

STM-4-151 CNMR (3-22-22)

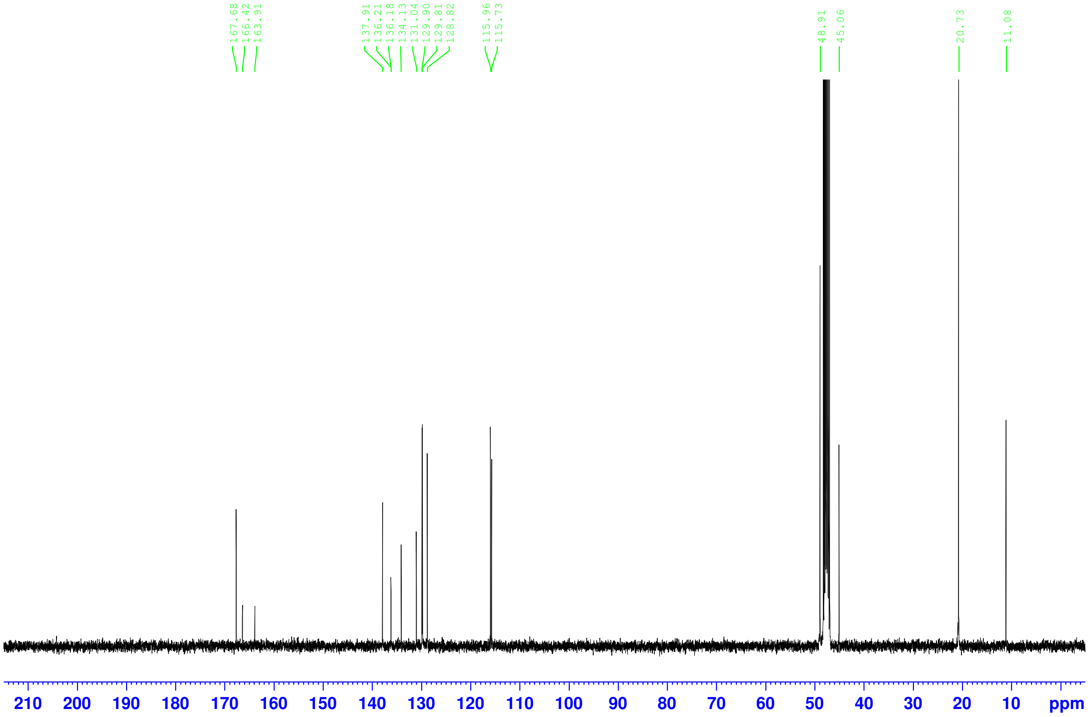

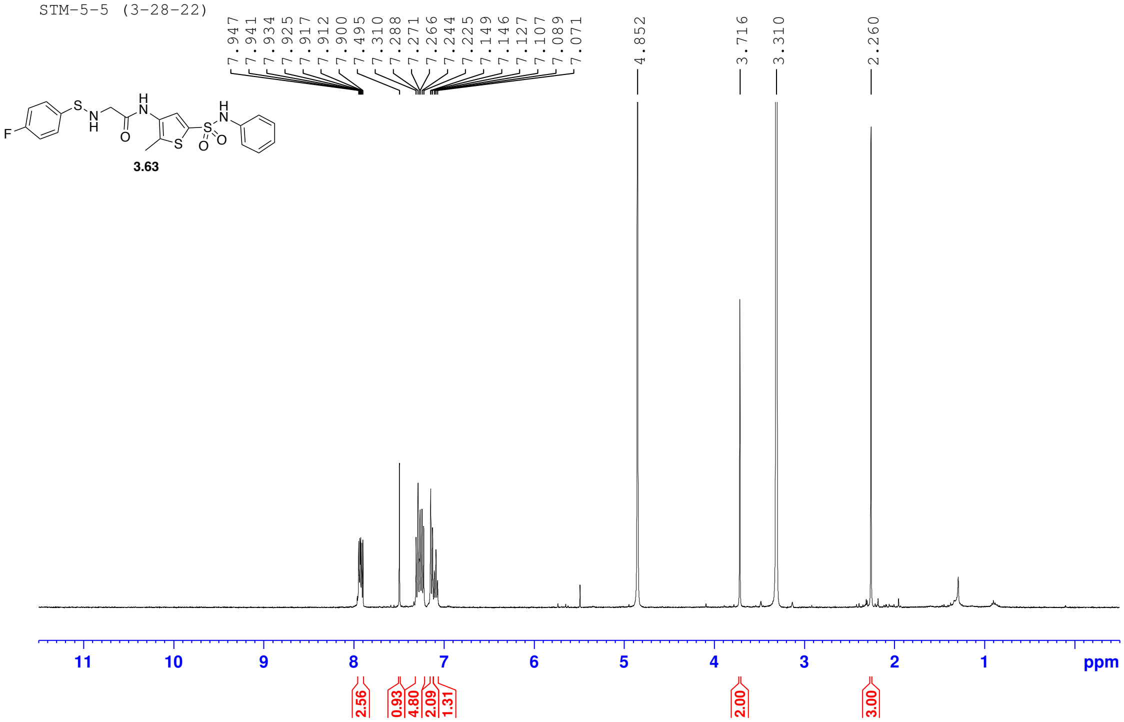
STM-5-5 (3-28-22)
7.947
7.941
7.934
7.925
7.917
7.912
7.900
7.495
7.310
7.288
7.271
7.266
7.244
7.225
7.149
7.146
7.127
7.107
7.089
7.071
4.852
3.716
3.310
2.260
F
S
N
H
O
H
N
S
S
O
O
H
N
3.63
11
10
9
8
7
6
5
4
3
2
1
ppm
2.56
0.93
4.80
2.09
1.31
2.00
3.00

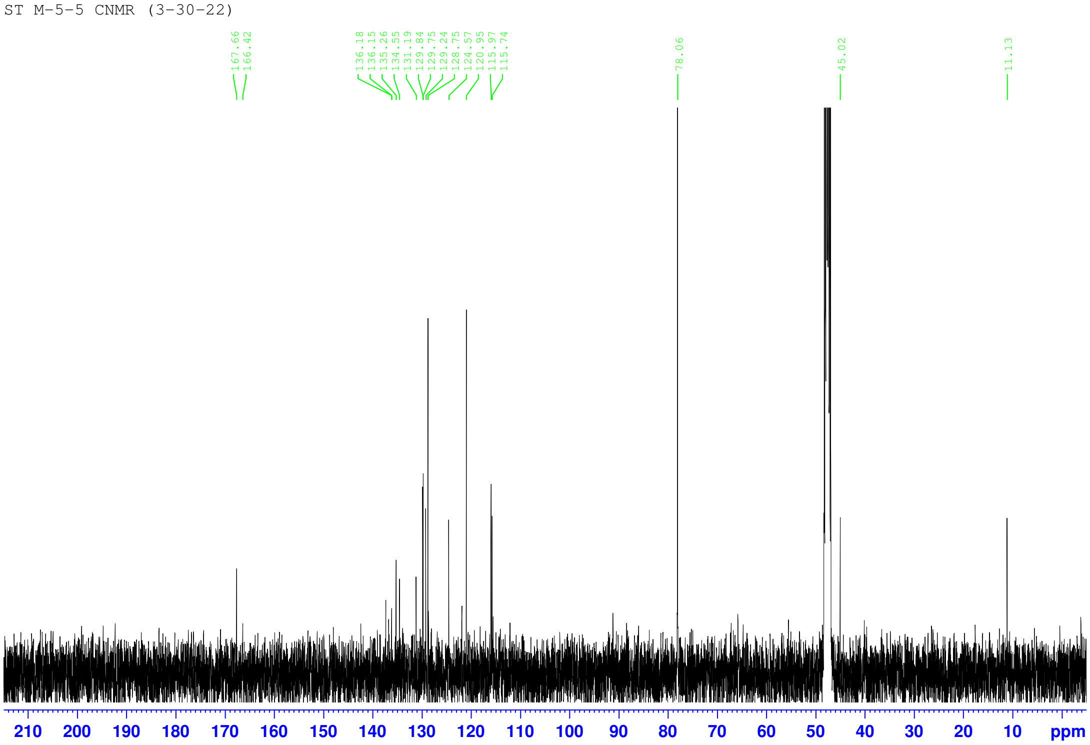
ST M-5-5 CNMR (3-30-22)
167.66
166.42
136.18
136.15
135.26
134.55
131.19
129.84
129.75
129.24
128.75
124.57
120.95
115.97
115.74
78.06
45.02
11.13
210
200
190
180
170
160
150
140
130
120
110
100
90
80
70
60
50
40
30
20
10
ppm

STM-5-30 (4-18-22)

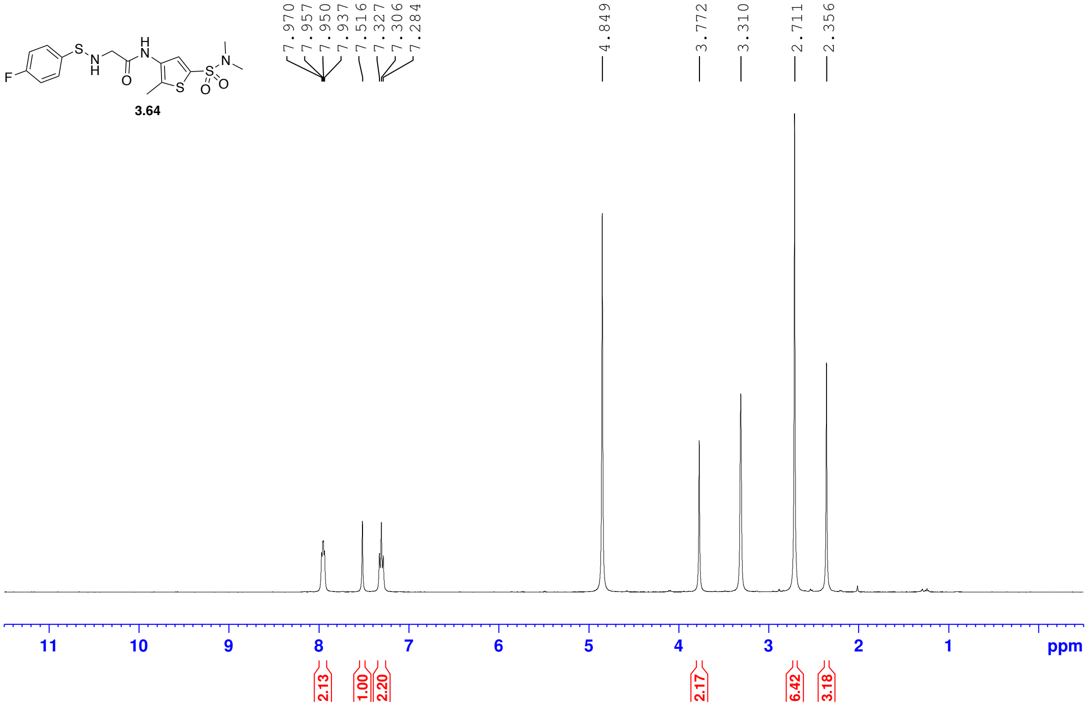

STM-5-30 CNMR

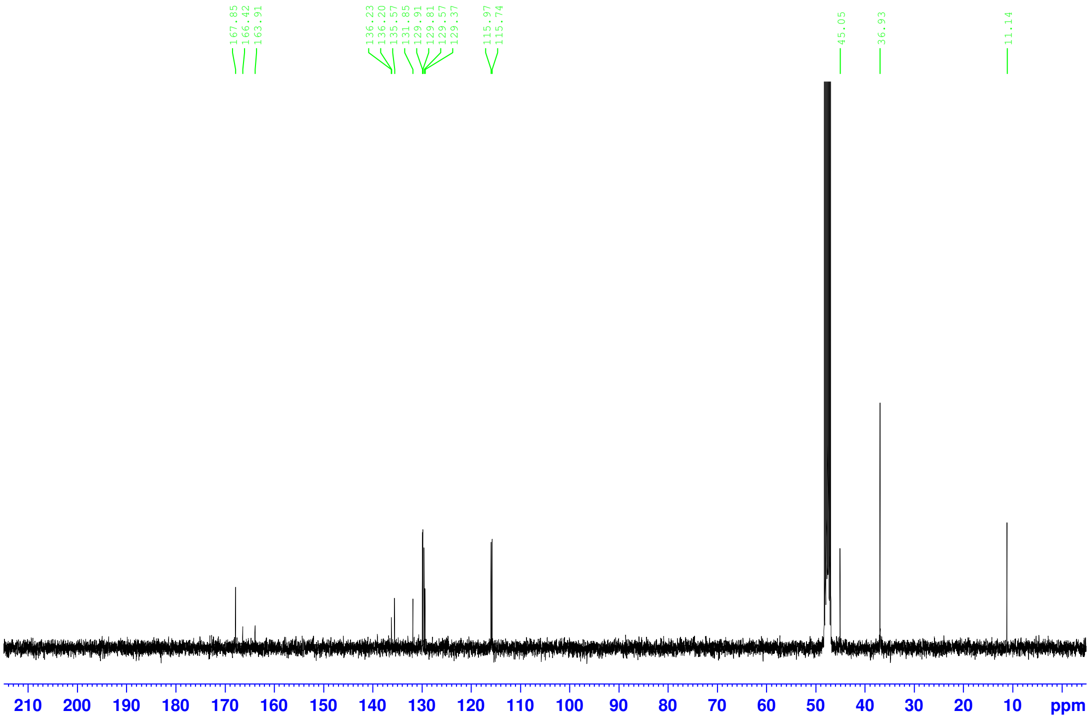

STM-5-29 (4-15-22)

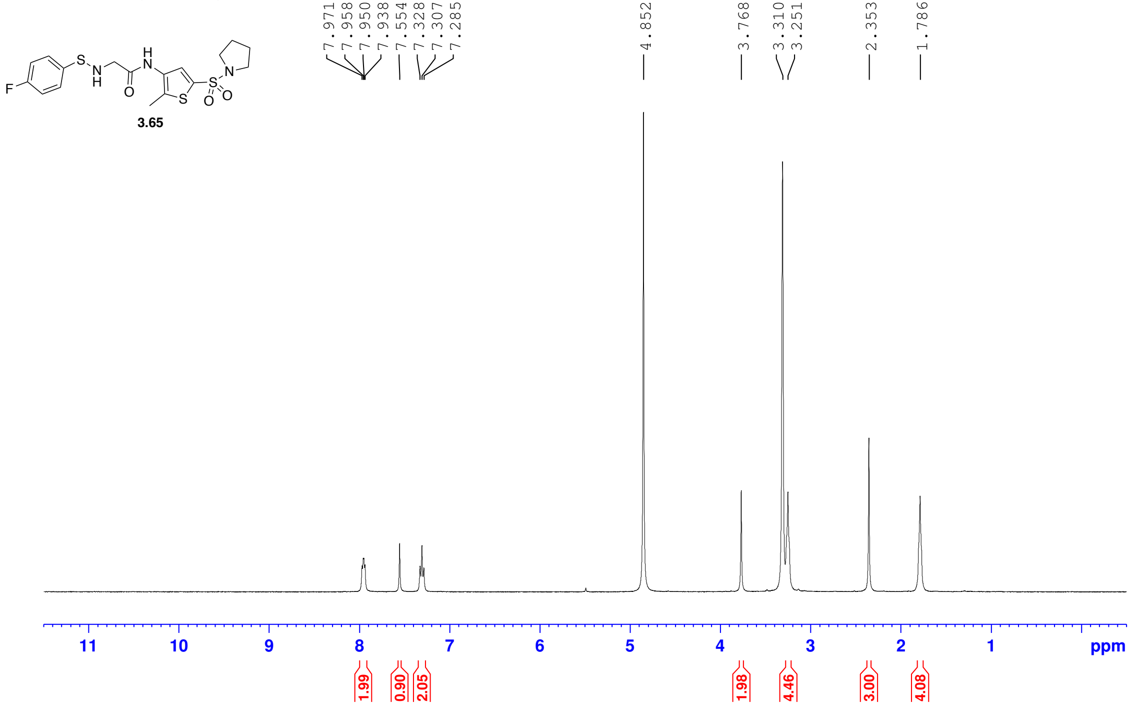

3.65

STM-5-29 (4-15-22) CNMR

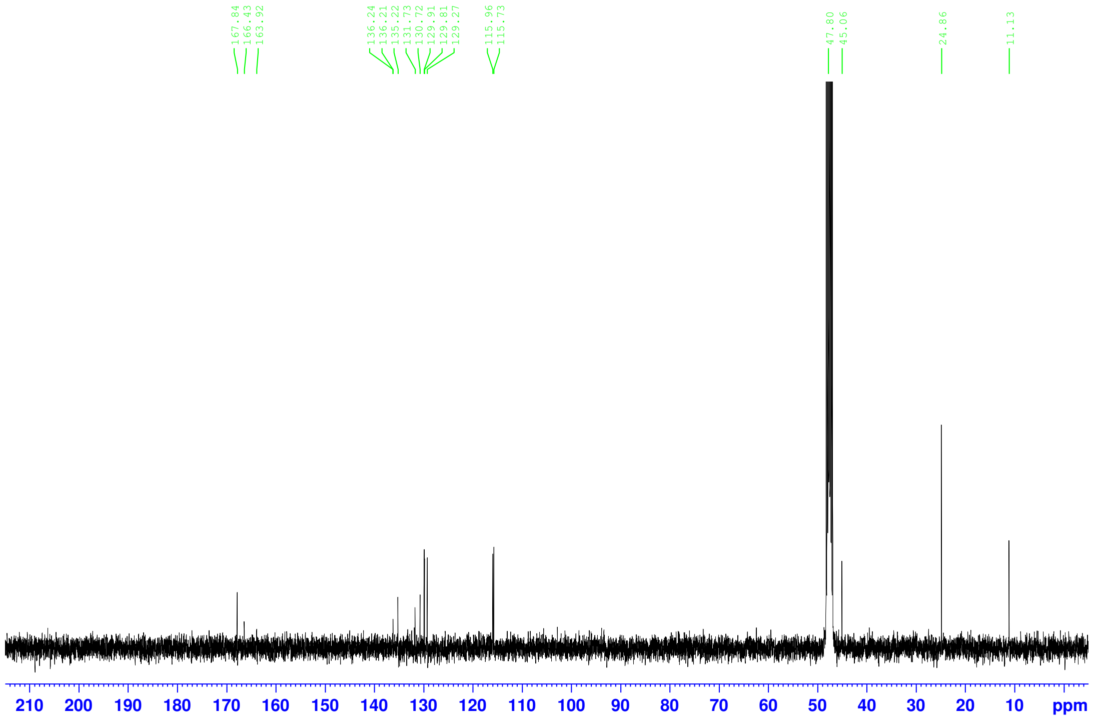

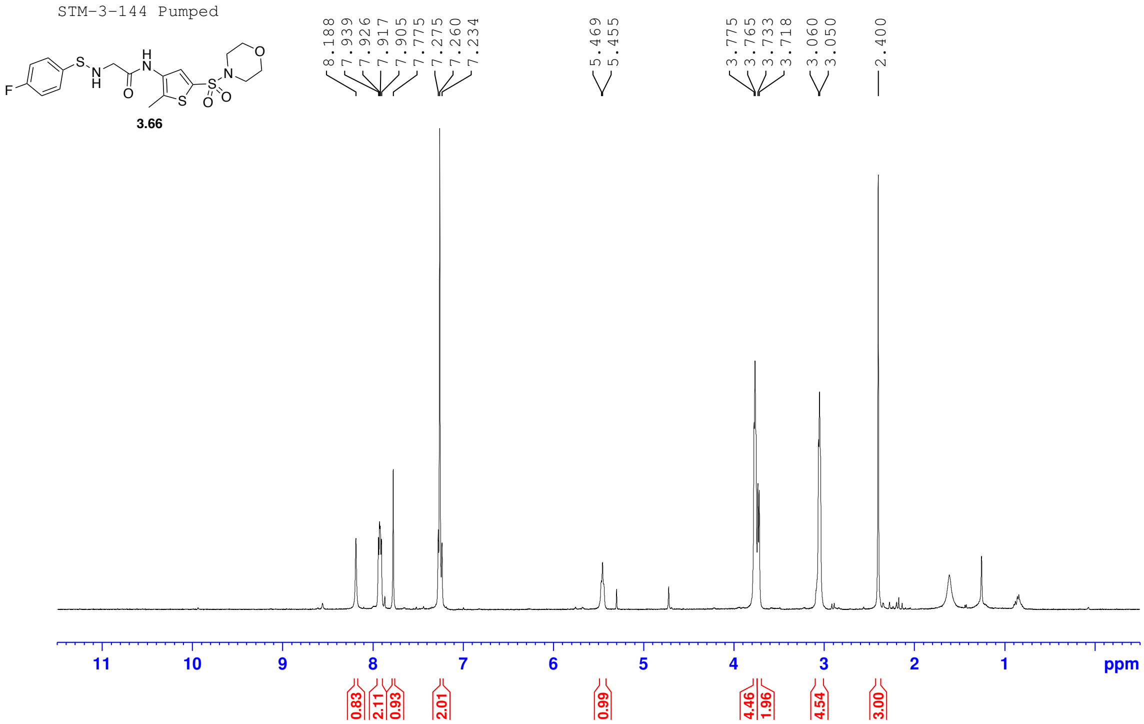
STM-3-144 Pumped
F
S
N
H
O
H
N
S
S
O
O
N
O
3.66
8.188
7.939
7.926
7.917
7.905
7.775
7.275
7.260
7.234
5.469
5.455
3.775
3.765
3.733
3.718
3.060
3.050
2.400
11
10
9
8
7
6
5
4
3
2
1
ppm
0.83
2.11
0.93
2.01
0.99
4.46
1.96
4.54
3.00

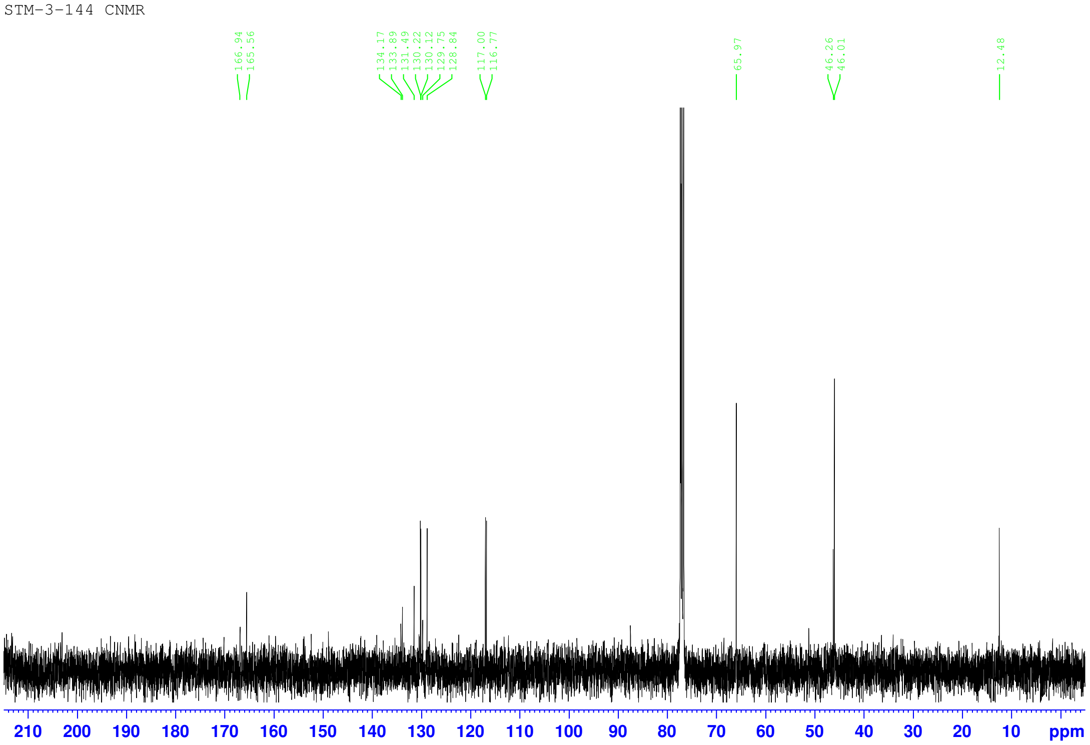
STM-3-144 CNMR
166.94
165.56
134.17
133.89
131.49
130.22
130.12
129.75
128.84
117.00
116.77
65.97
46.26
46.01
12.48
210
200
190
180
170
160
150
140
130
120
110
100
90
80
70
60
50
40
30
20
10
ppm

STM-4-75 (8-16-22)

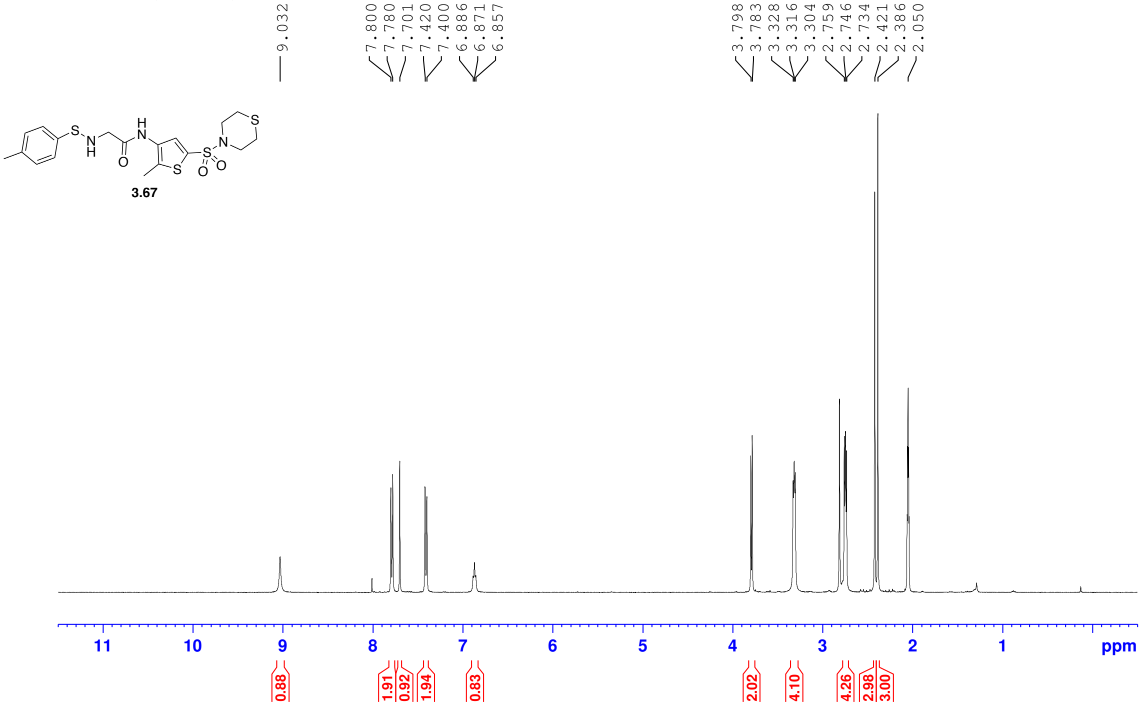

STM-4-75 CNMR (8-16-22)

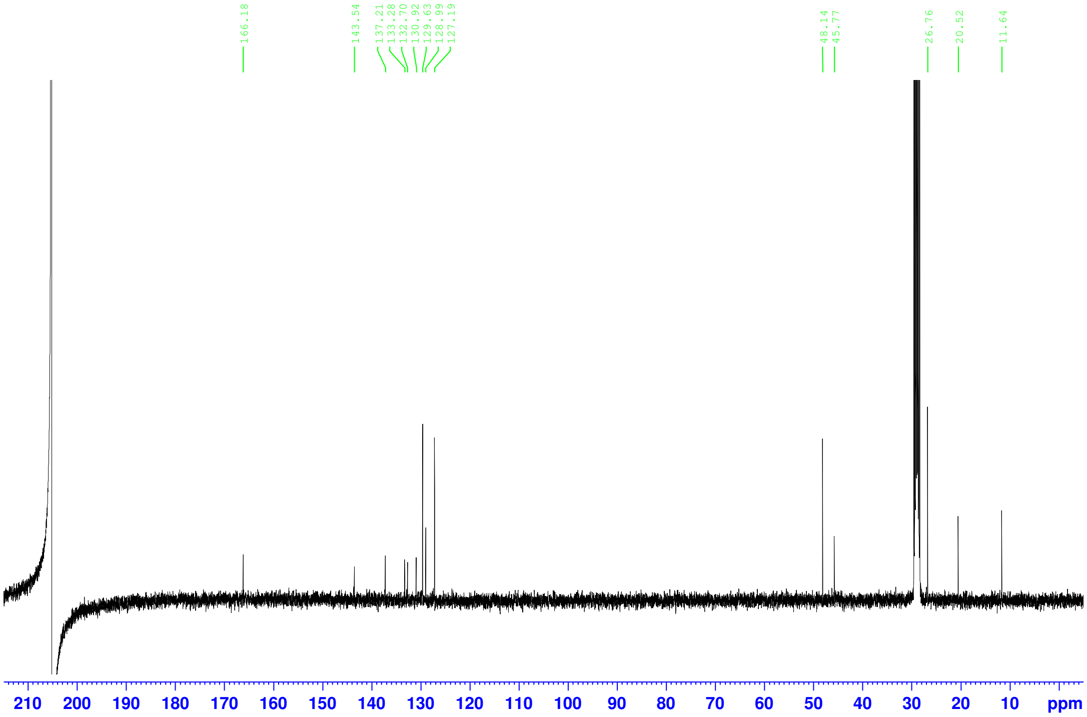

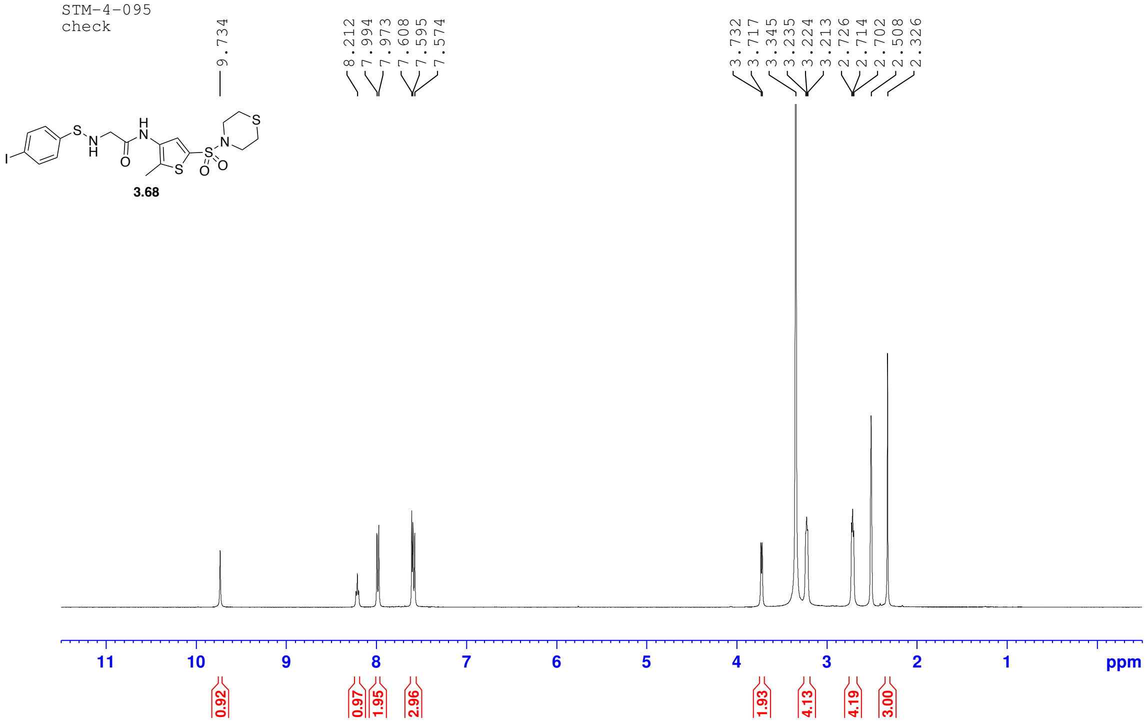
STM-4-095
check
9.734
8.212
7.994
7.973
7.608
7.595
7.574
3.732
3.717
3.345
3.235
3.224
3.213
2.726
2.714
2.702
2.508
2.326
I
S
N
H
O
H
N
S
S
O
O
N
S
3.68
11
10
9
8
7
6
5
4
3
2
1
ppm
0.92
0.97
1.95
2.96
1.93
4.13
4.19
3.00

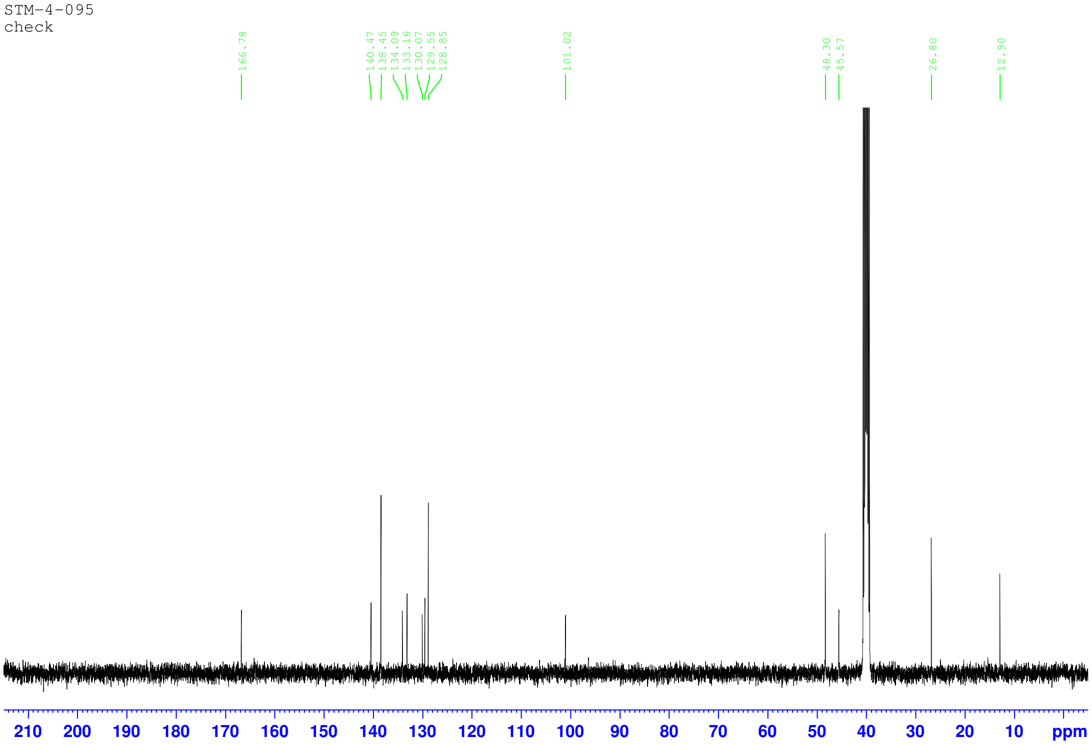
STM-4-095
check
166.78
140.47
138.45
134.09
133.16
130.07
129.55
128.85
101.02
48.30
45.57
26.80
12.90
210
200
190
180
170
160
150
140
130
120
110
100
90
80
70
60
50
40
30
20
10
ppm

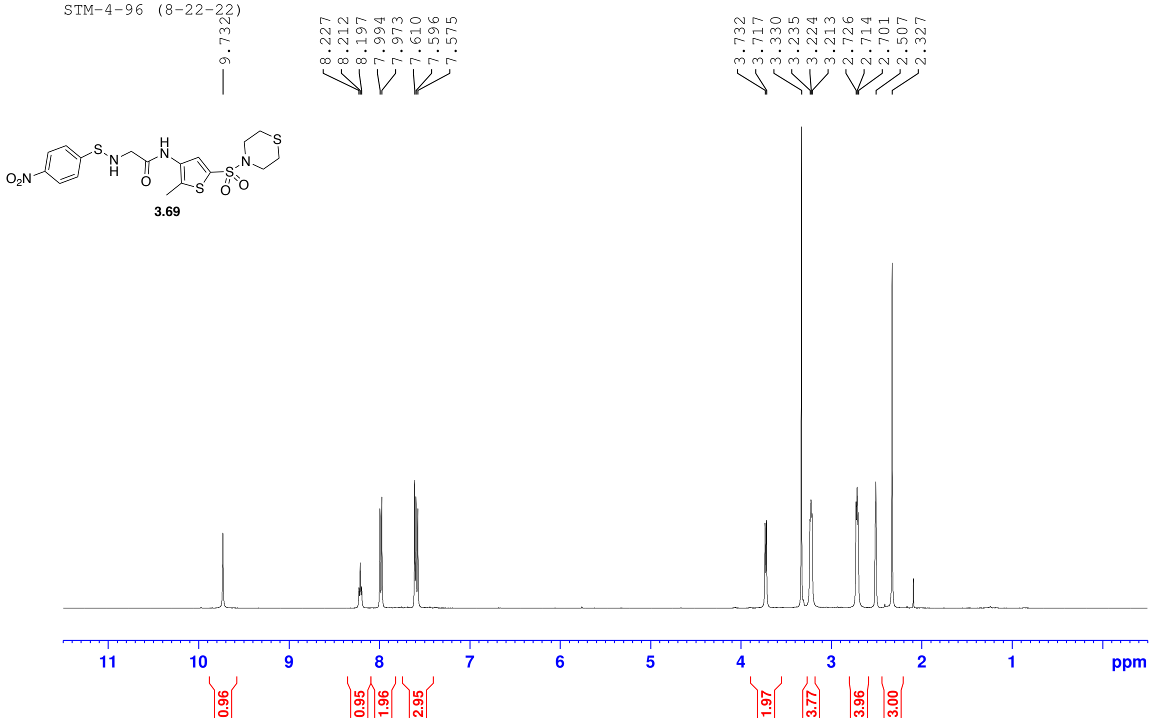
STM-4-96 (8-22-22)
9.732
8.227
8.212
8.197
7.994
7.973
7.610
7.596
7.575
3.732
3.717
3.330
3.235
3.224
3.213
2.726
2.714
2.701
2.507
2.327
O_2N
S
N
H
H
N
O
S
S
O
O
N
S
3.69
11
10
9
8
7
6
5
4
3
2
1
ppm
0.96
0.95
1.96
2.95
1.97
3.77
3.96
3.00

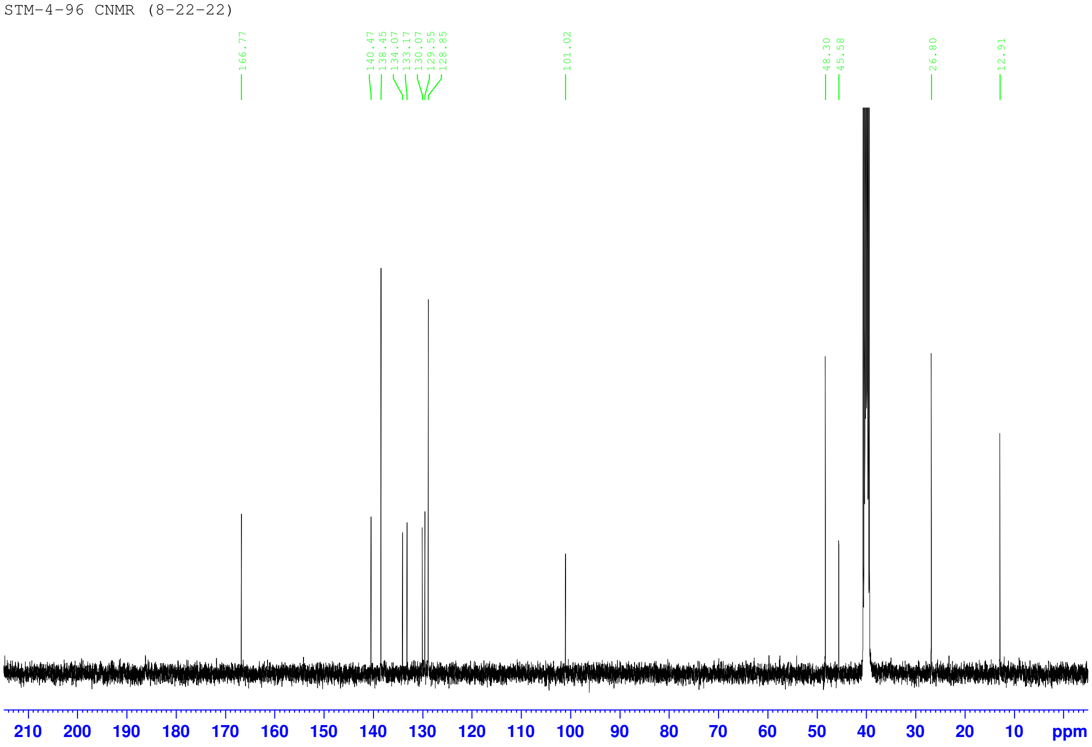
STM-4-96 CNMR (8-22-22)
166.77
140.47
138.45
134.07
133.17
130.07
129.55
128.85
101.02
48.30
45.58
26.80
12.91
210
200
190
180
170
160
150
140
130
120
110
100
90
80
70
60
50
40
30
20
10
ppm

STM-5-35 (5-21-22)

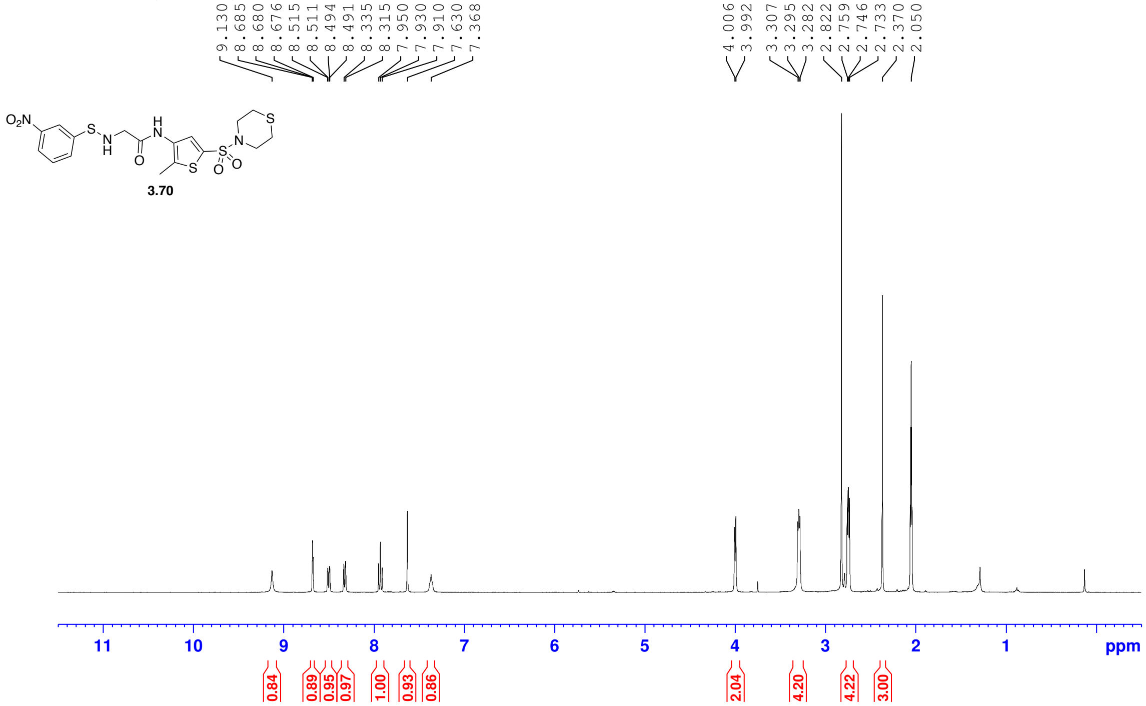

3.70

STM-5-35 CNMR (5-22-22)

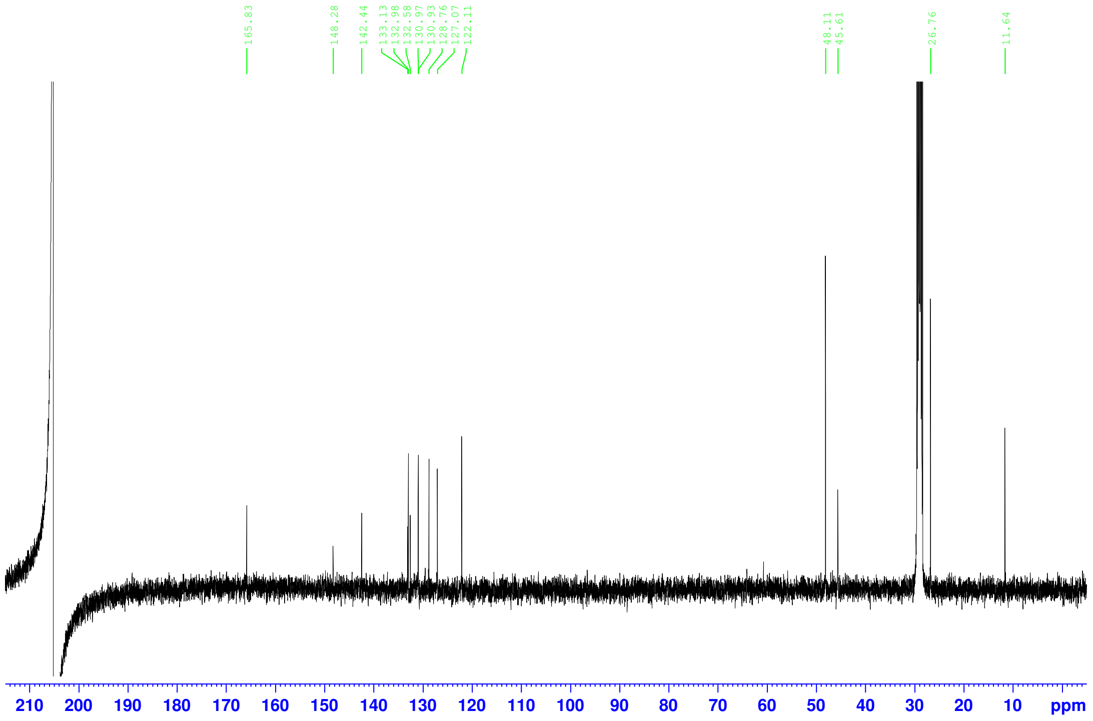

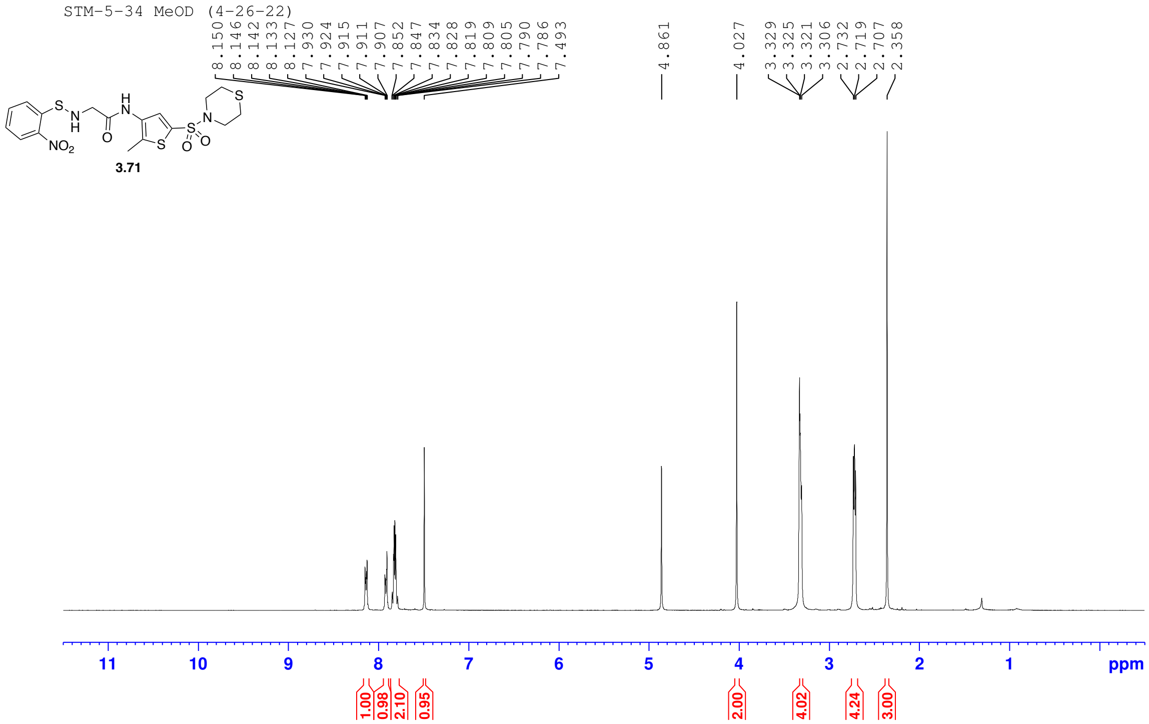

3.71

STM-5-34 MeOD (4-26-22)
8.150
8.146
8.142
8.133
8.127
7.930
7.924
7.915
7.911
7.907
7.852
7.847
7.834
7.828
7.819
7.809
7.805
7.790
7.786
7.493
4.861
4.027
3.329
3.325
3.321
3.306
2.732
2.719
2.707
2.358
S
N
H
O
NO2
H
N
S
O
S
O
N
S
11
10
9
8
7
6
5
4
3
2
1
ppm
1.00
0.98
2.10
0.95
2.00
4.02
4.24
3.00

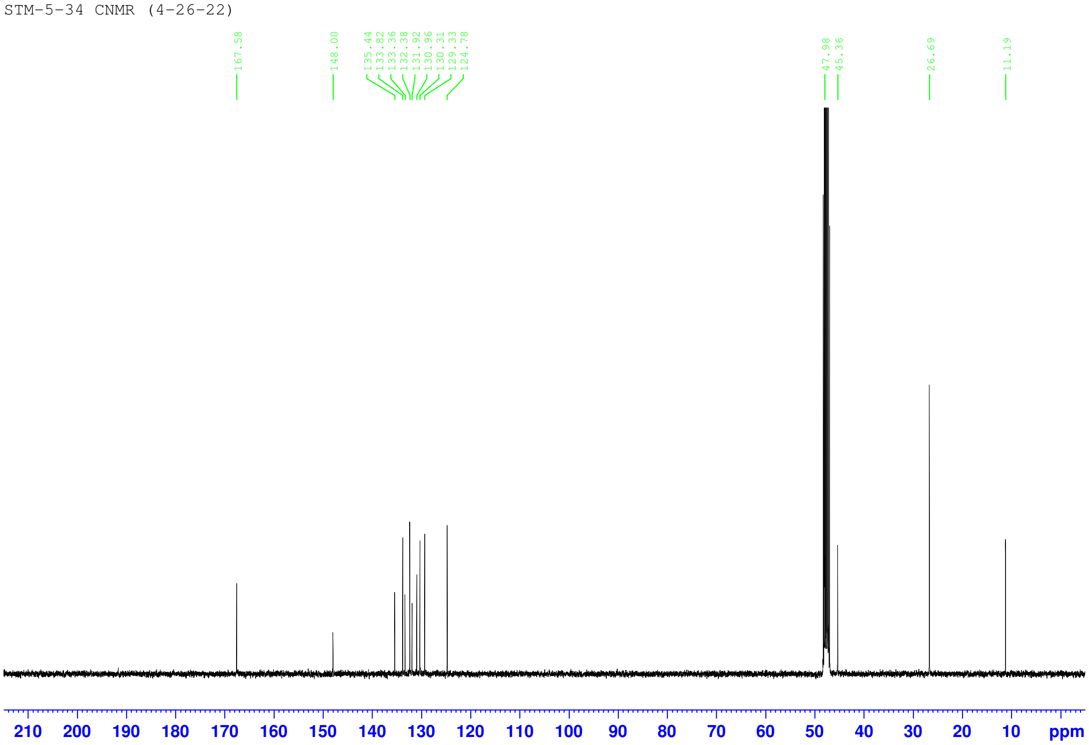

STM-5-34 CNMR (4-26-22)
167.58
148.00
135.44
133.82
133.36
132.38
131.92
130.96
130.31
129.33
124.78
47.98
45.36
26.69
11.19
210
200
190
180
170
160
150
140
130
120
110
100
90
80
70
60
50
40
30
20
10
ppm

STM-4-97 (8-19-22)

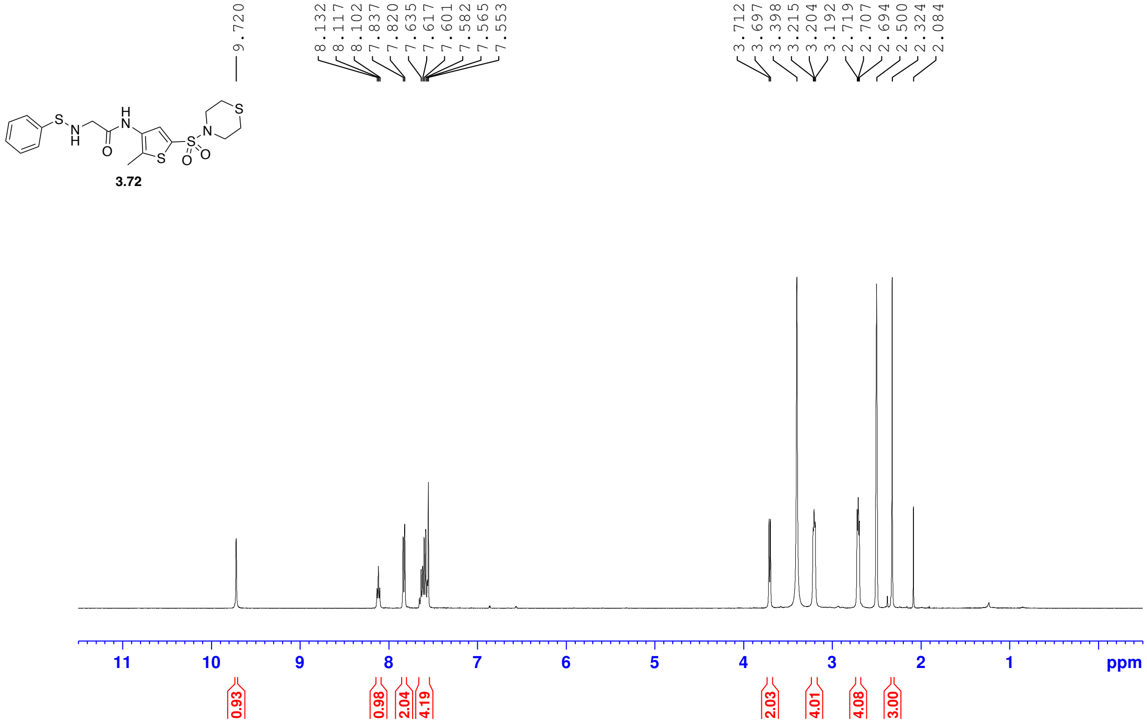

3.72

STM-4-97 CNMR (8-19-22)

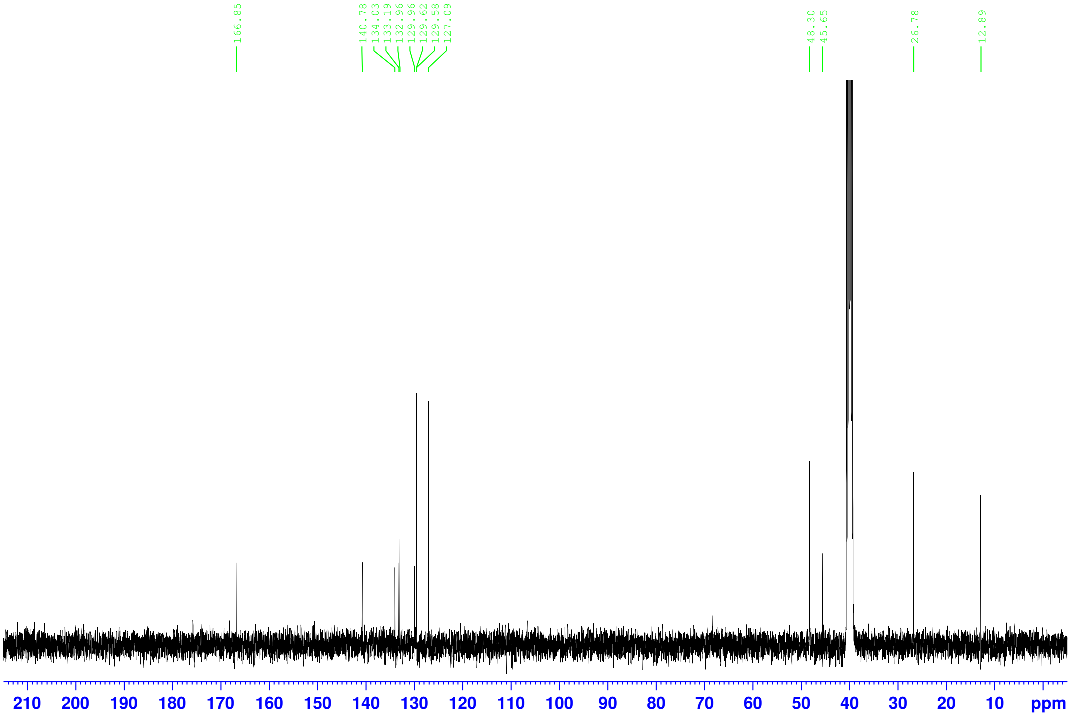

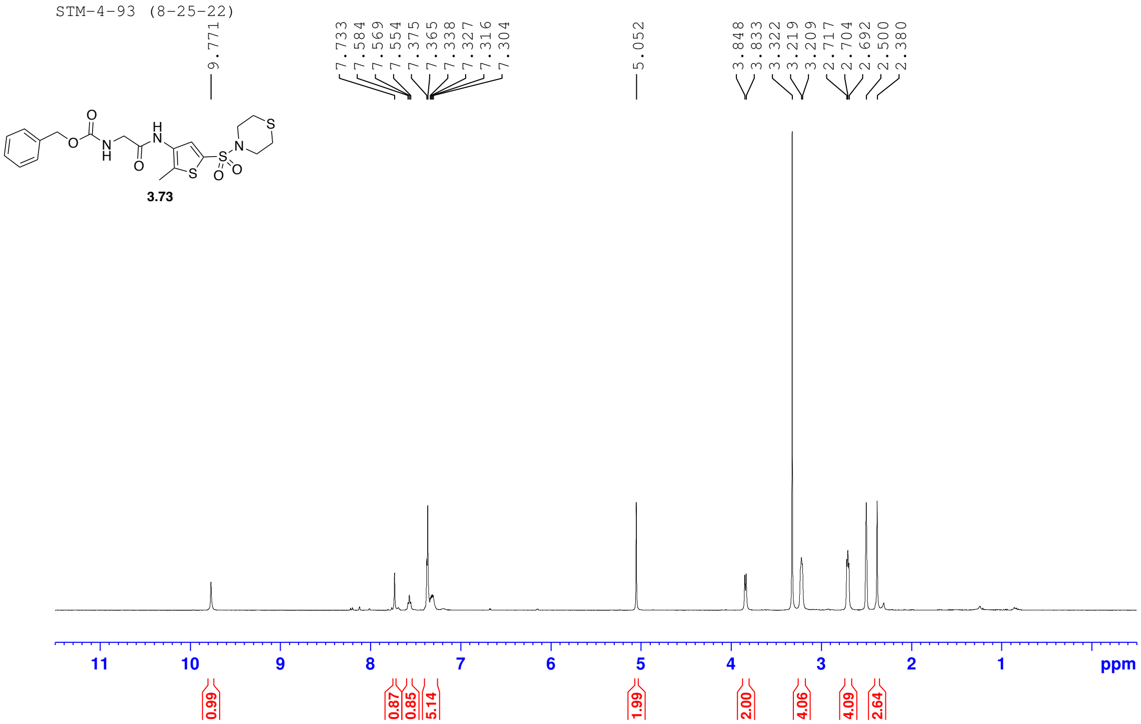
STM-4-93 (8-25-22)
9.771
7.733
7.584
7.569
7.554
7.375
7.365
7.338
7.327
7.316
7.304
5.052
3.848
3.833
3.322
3.219
3.209
2.717
2.704
2.692
2.500
2.380
3.73
11
10
9
8
7
6
5
4
3
2
1
ppm
0.99
0.87
0.85
5.14
1.99
2.00
4.06
4.09
2.64

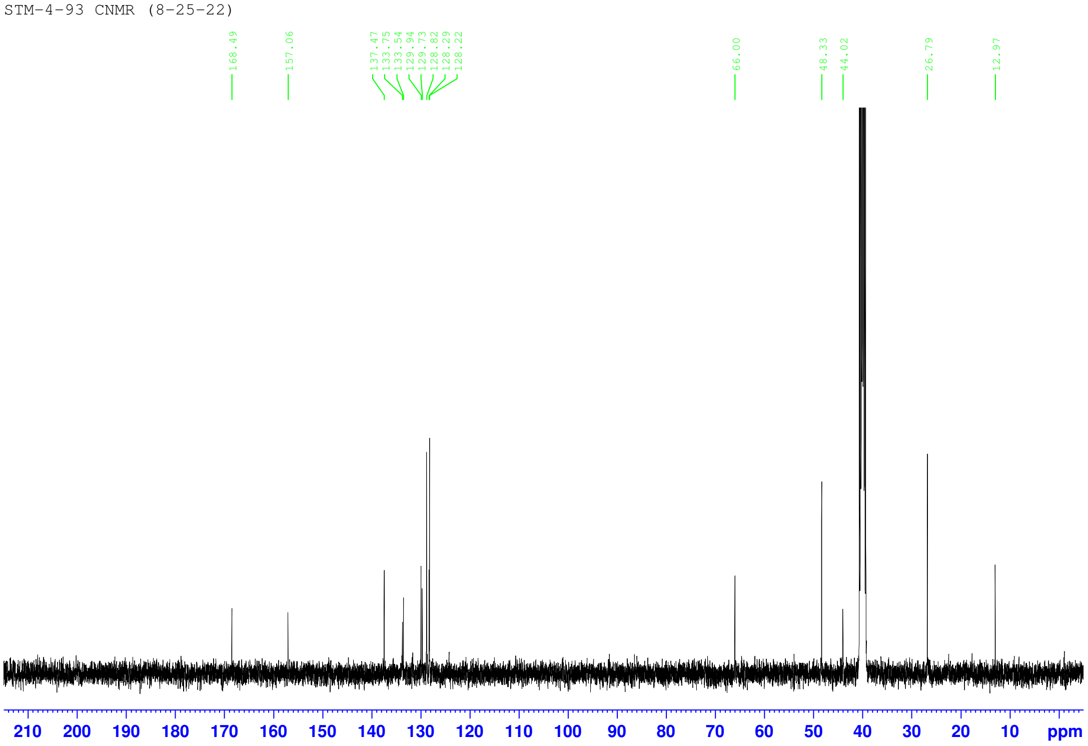
STM-4-93 CNMR (8-25-22)
168.49
157.06
137.47
133.75
133.54
129.94
129.73
128.82
128.29
128.22
66.00
48.33
44.02
26.79
12.97
210
200
190
180
170
160
150
140
130
120
110
100
90
80
70
60
50
40
30
20
10
ppm

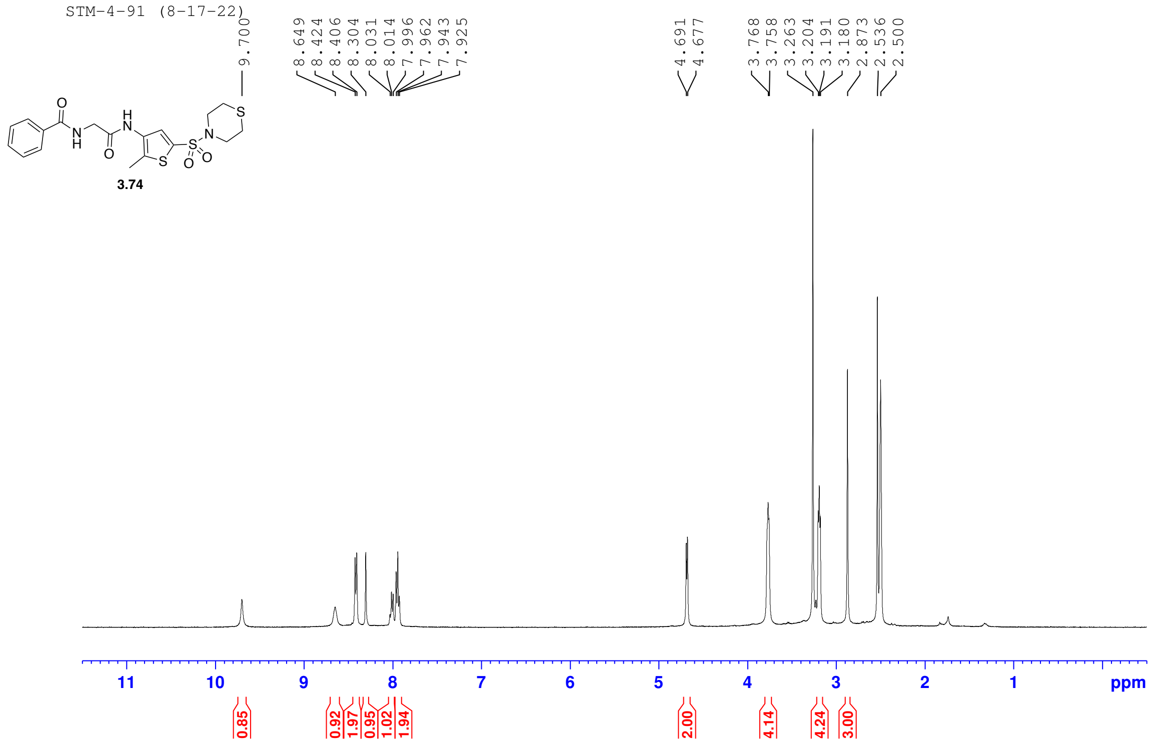
STM-4-91 (8-17-22)
3.74
9.700
8.649
8.424
8.406
8.304
8.031
8.014
7.996
7.962
7.943
7.925
4.691
4.677
3.768
3.758
3.263
3.204
3.191
3.180
2.873
2.536
2.500
11
10
9
8
7
6
5
4
3
2
1
ppm
0.85
0.92
1.97
0.95
1.02
1.94
2.00
4.14
4.24
3.00

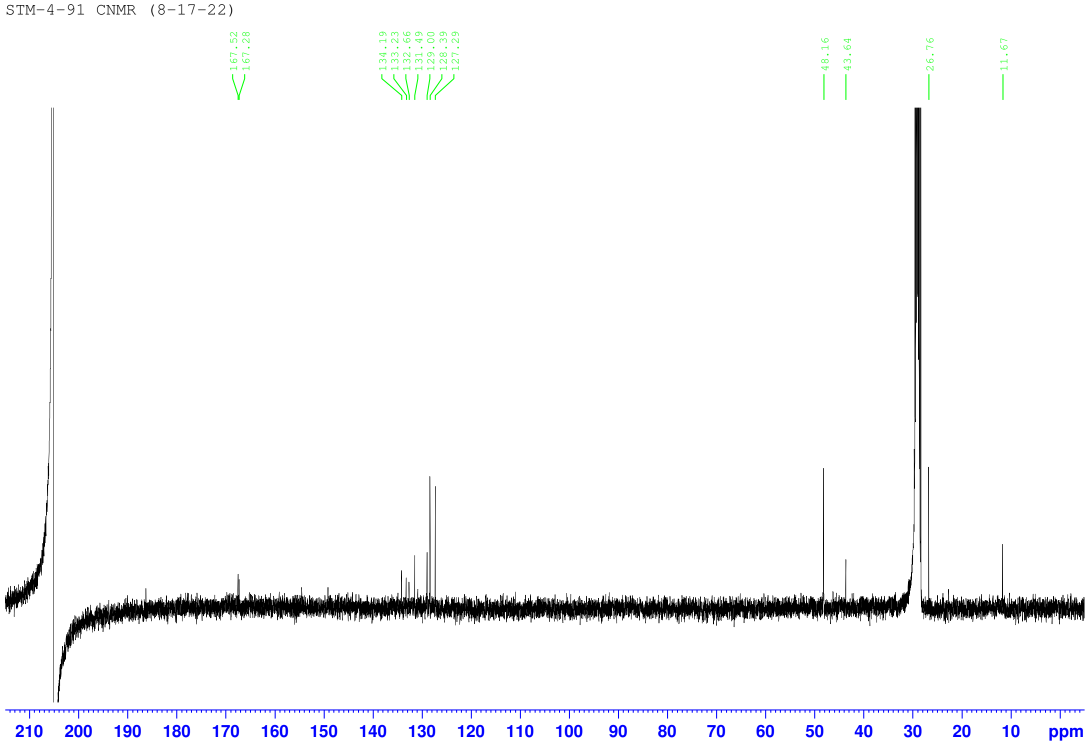
STM-4-91 CNMR (8-17-22)
167.52
167.28
134.19
133.23
132.66
131.49
129.00
128.39
127.29
48.16
43.64
26.76
11.67
210
200
190
180
170
160
150
140
130
120
110
100
90
80
70
60
50
40
30
20
10
ppm

STM-4-92 (8-17-22)

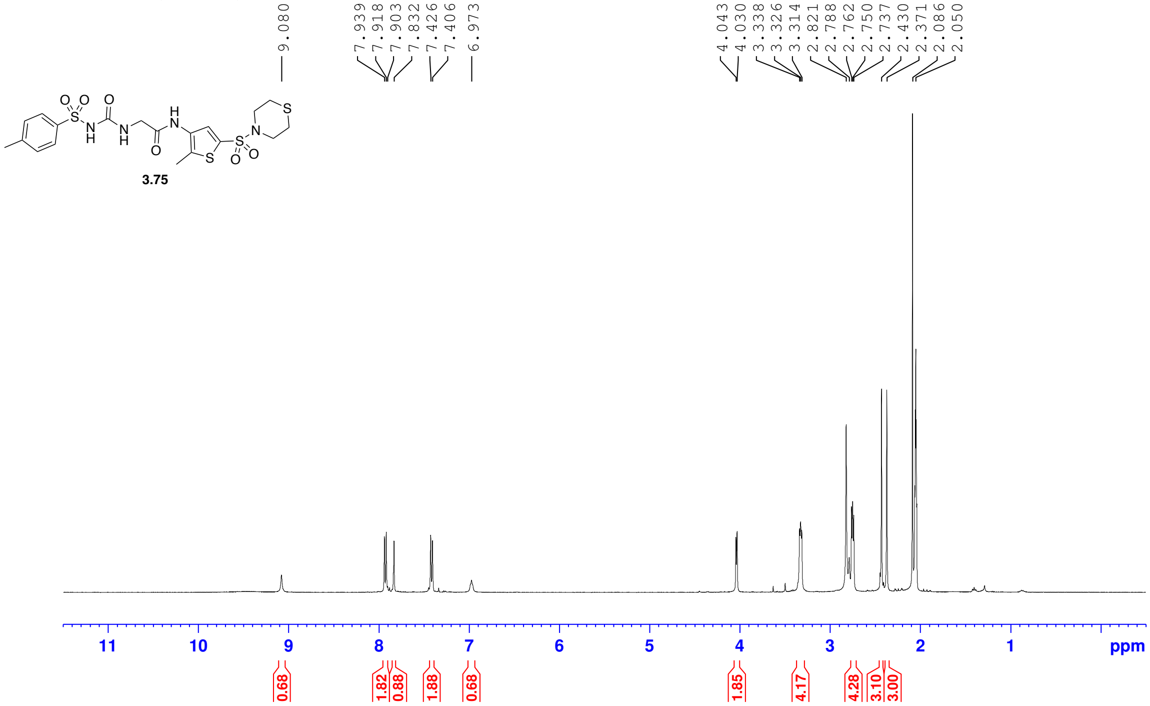

STM-4-92 CNMR (8-17-22)

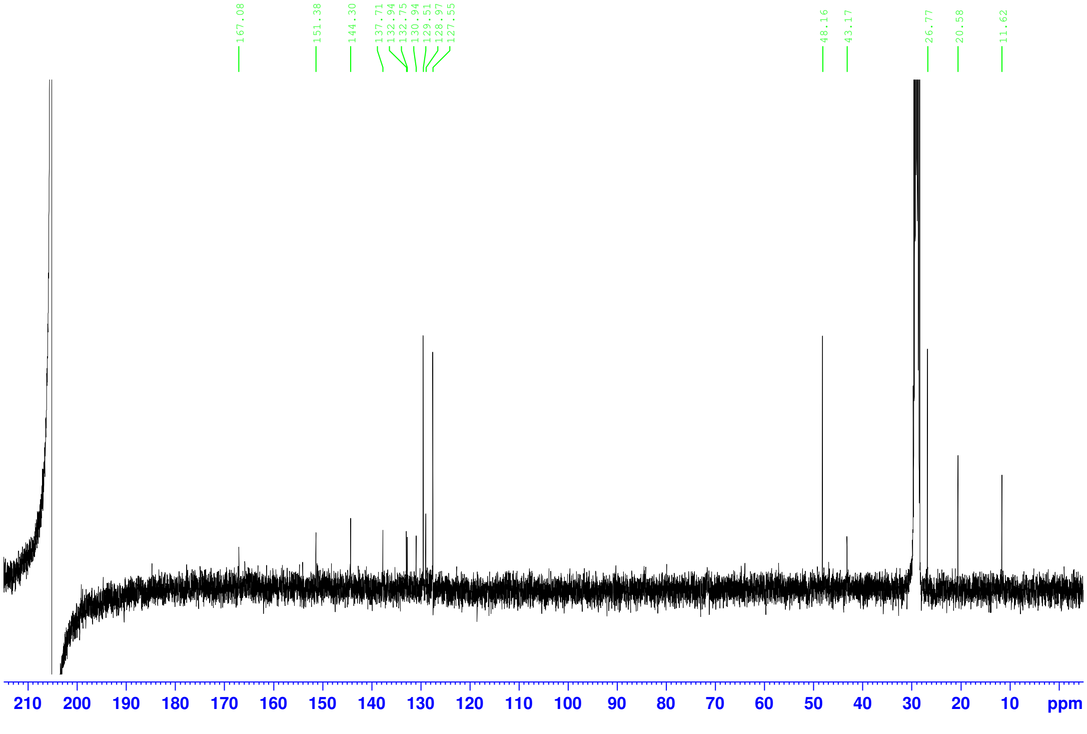

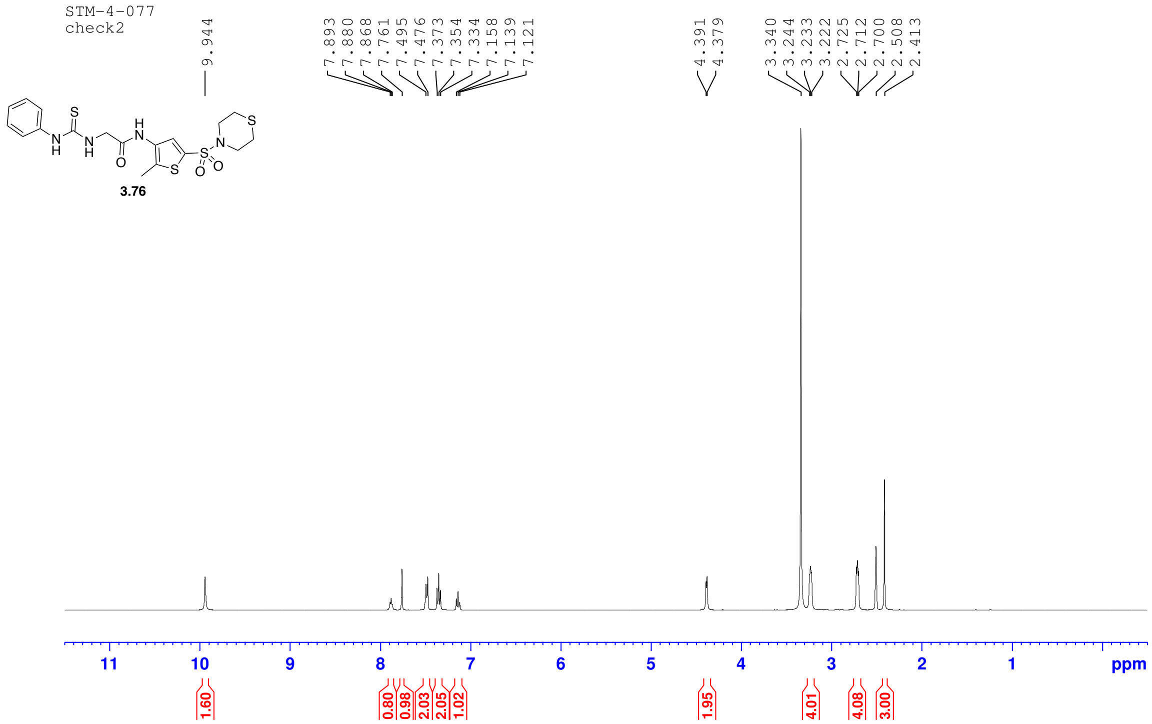

3.76

STM-4-077
check2
9.944
7.893
7.880
7.868
7.761
7.495
7.476
7.373
7.354
7.334
7.158
7.139
7.121
4.391
4.379
3.340
3.244
3.233
3.222
2.725
2.712
2.700
2.508
2.413
11
10
9
8
7
6
5
4
3
2
1
ppm
1.60
0.80
0.98
2.03
2.05
1.02
1.95
4.01
4.08
3.00

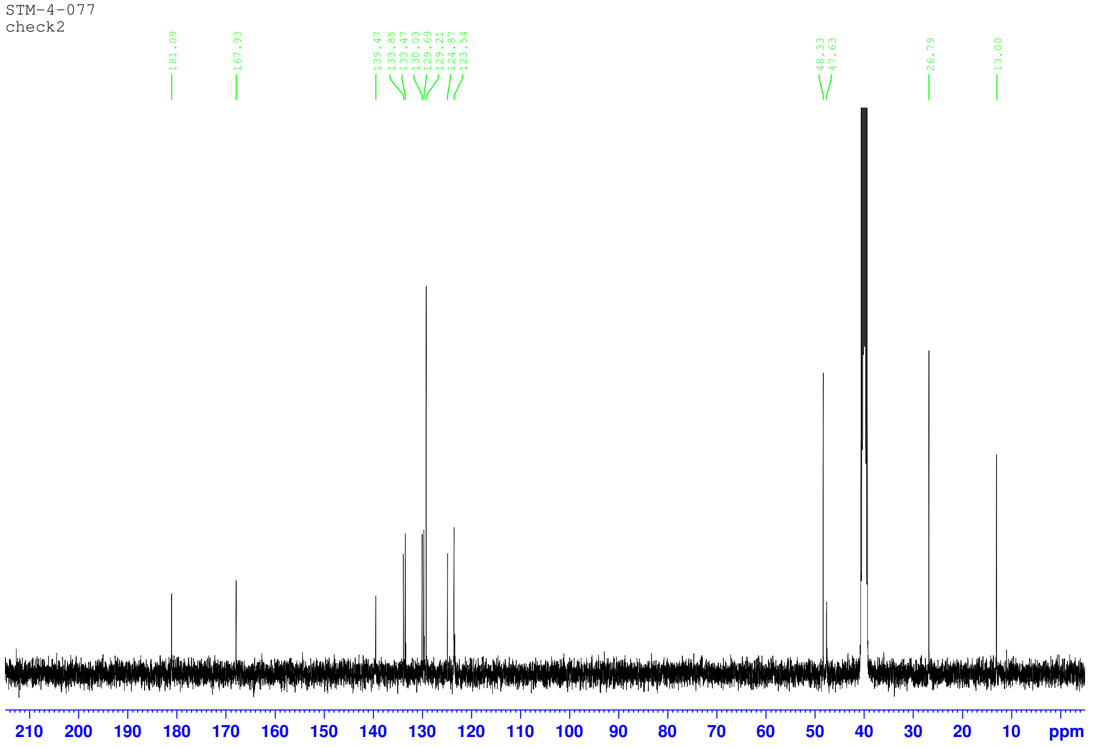

STM-4-077
check2
181.09
167.93
139.47
133.85
133.47
130.03
129.69
129.21
124.87
123.54
48.33
47.63
26.79
13.00
210
200
190
180
170
160
150
140
130
120
110
100
90
80
70
60
50
40
30
20
10
ppm

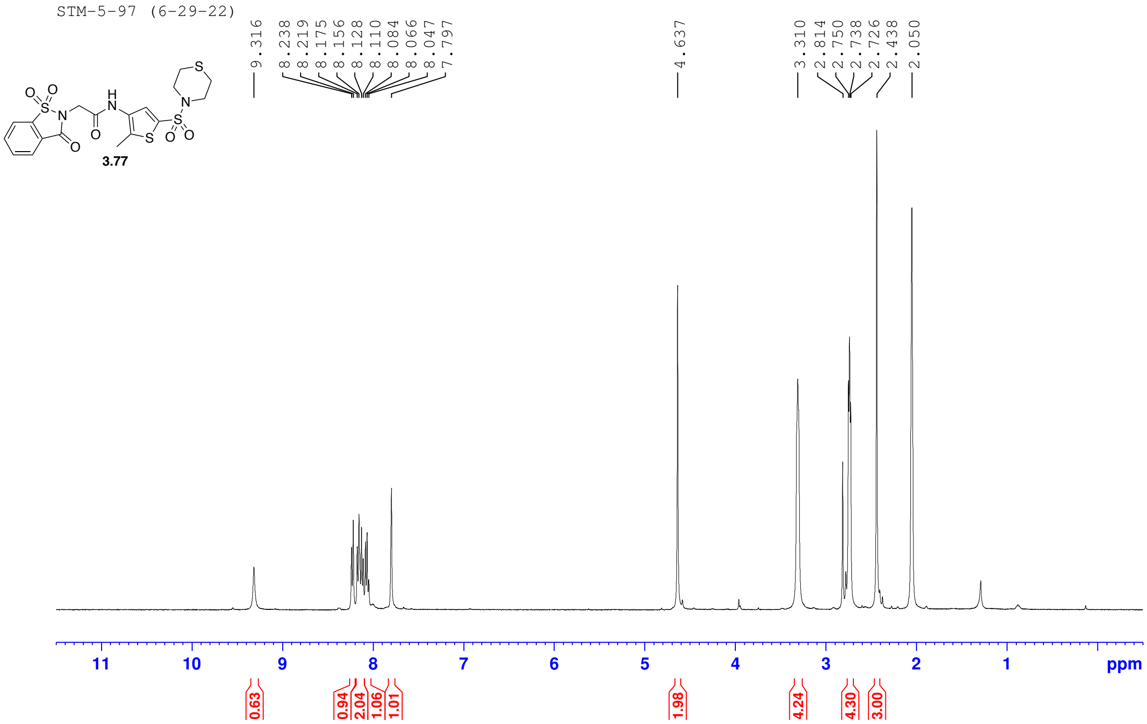
STM-5-97 (6-29-22)
3.77
9.316
8.238
8.219
8.175
8.156
8.128
8.110
8.084
8.066
8.047
7.797
4.637
3.310
2.814
2.750
2.738
2.726
2.438
2.050
11
10
9
8
7
6
5
4
3
2
1
ppm
0.63
0.94
2.04
1.06
1.01
1.98
4.24
4.30
3.00

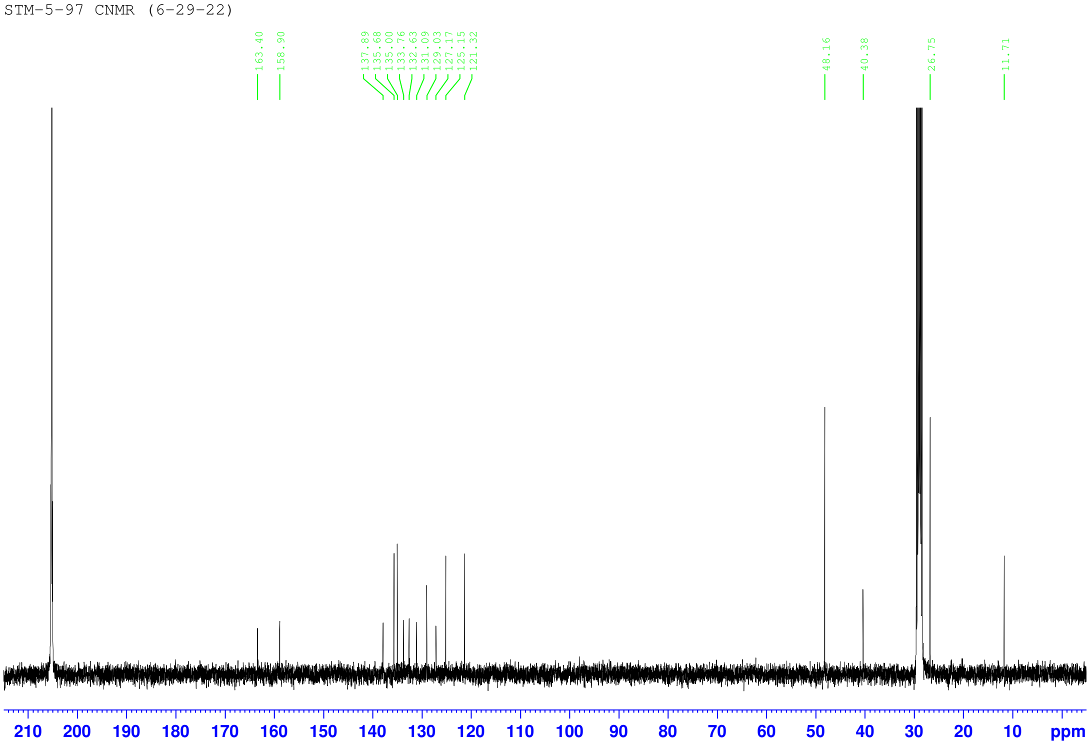
STM-5-97 CNMR (6-29-22)
163.40
158.90
137.89
135.68
135.00
133.76
132.63
131.09
129.03
127.17
125.15
121.32
48.16
40.38
26.75
11.71
210
200
190
180
170
160
150
140
130
120
110
100
90
80
70
60
50
40
30
20
10
ppm

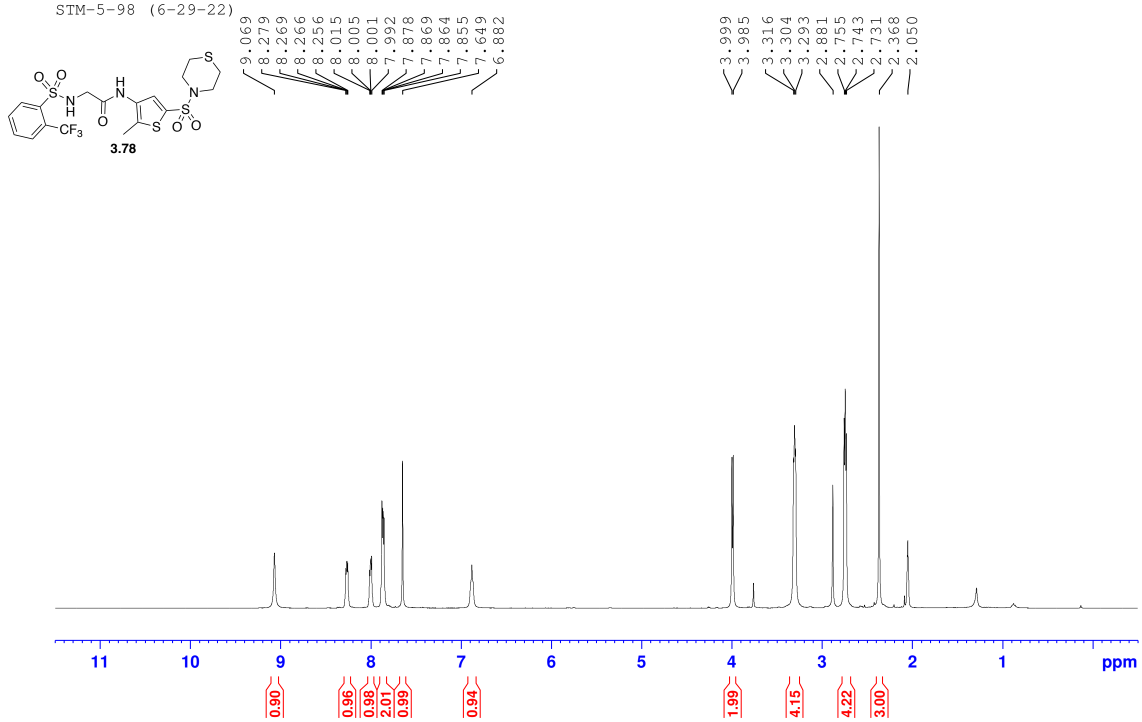
STM-5-98 (6-29-22)
O
O
S
N
H
H
N
O
CF$_3$
S
N
S
O
O
S
9.069
8.279
8.269
8.266
8.256
8.015
8.005
8.001
7.992
7.878
7.869
7.864
7.855
7.649
6.882
3.999
3.985
3.316
3.304
3.293
2.881
2.755
2.743
2.731
2.368
2.050
11
10
9
8
7
6
5
4
3
2
1
ppm
0.90
0.96
0.98
2.01
0.99
0.94
1.99
4.15
4.22
3.00

3.78

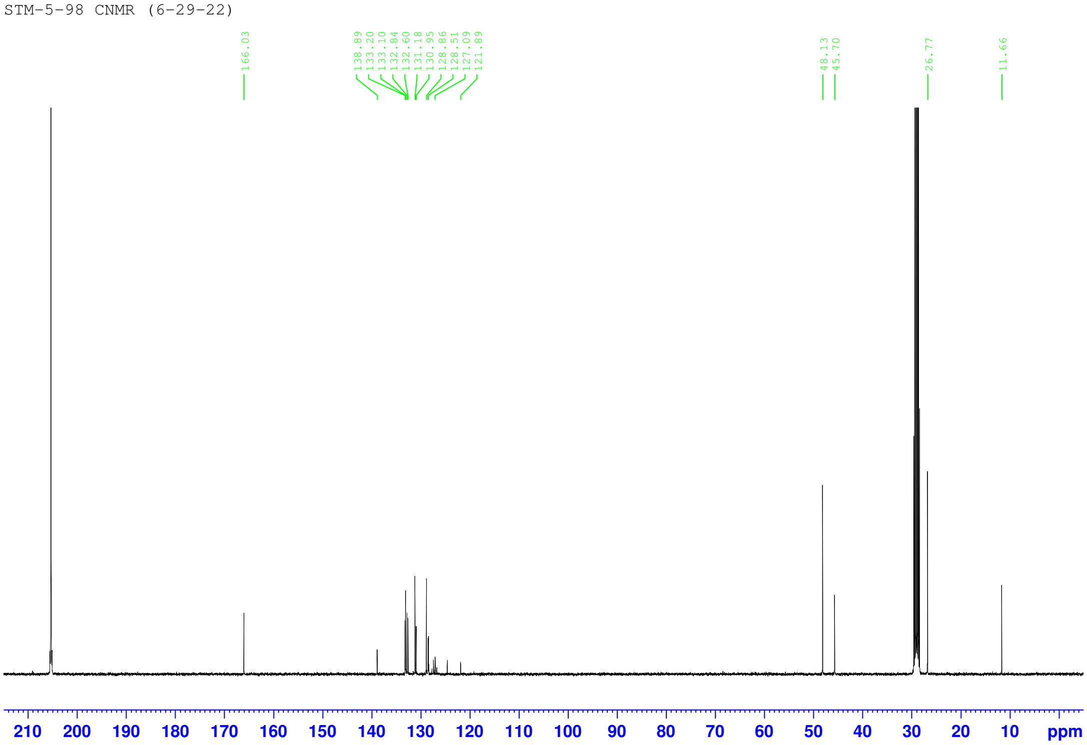
STM-5-98 CNMR (6-29-22)
166.03
138.89
133.20
133.10
132.84
132.60
131.18
130.95
128.86
128.51
127.09
121.89
48.13
45.70
26.77
11.66
210
200
190
180
170
160
150
140
130
120
110
100
90
80
70
60
50
40
30
20
10
ppm

STM-5-79 (7-8-22)

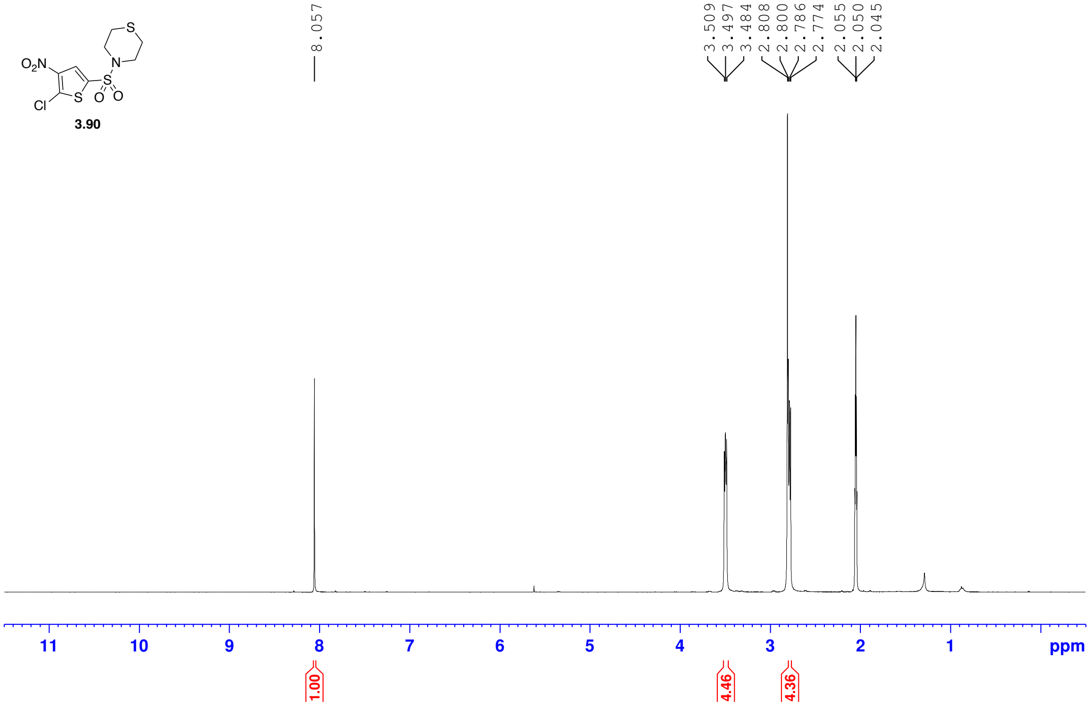

STM-5-79 CNMR DMSO

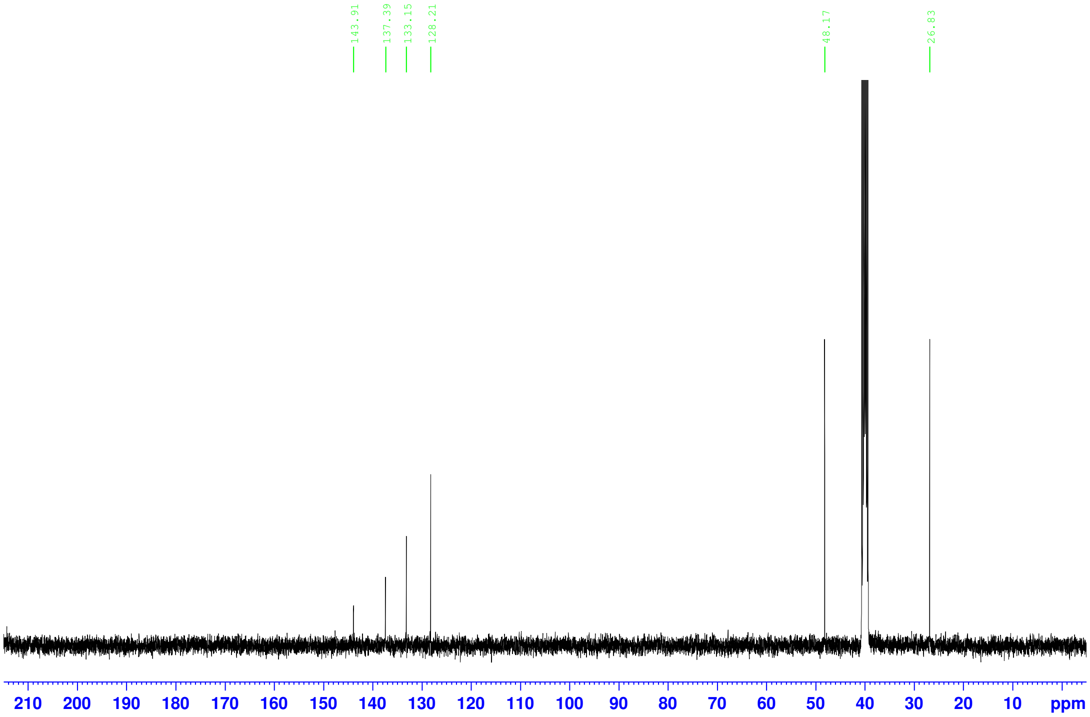

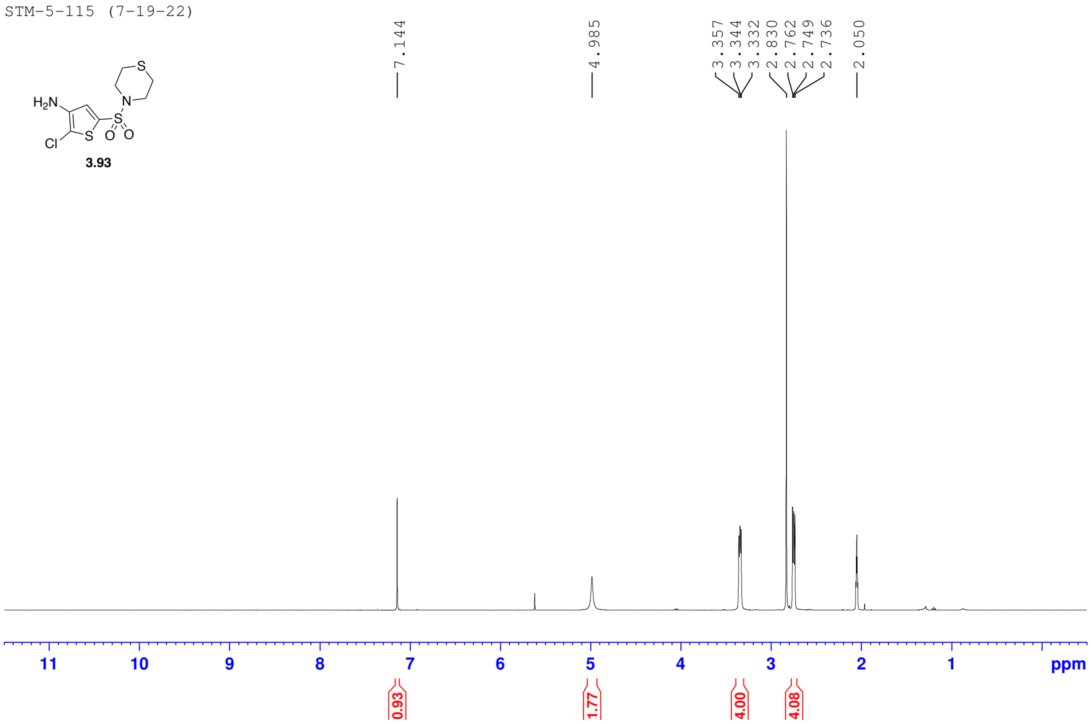
STM-5-115 (7-19-22)
H2N
Cl
S
N
S
O
O
S
3.93
7.144
4.985
3.357
3.344
3.332
2.830
2.762
2.749
2.736
2.050
11
10
9
8
7
6
5
4
3
2
1
ppm
0.93
1.77
4.00
4.08

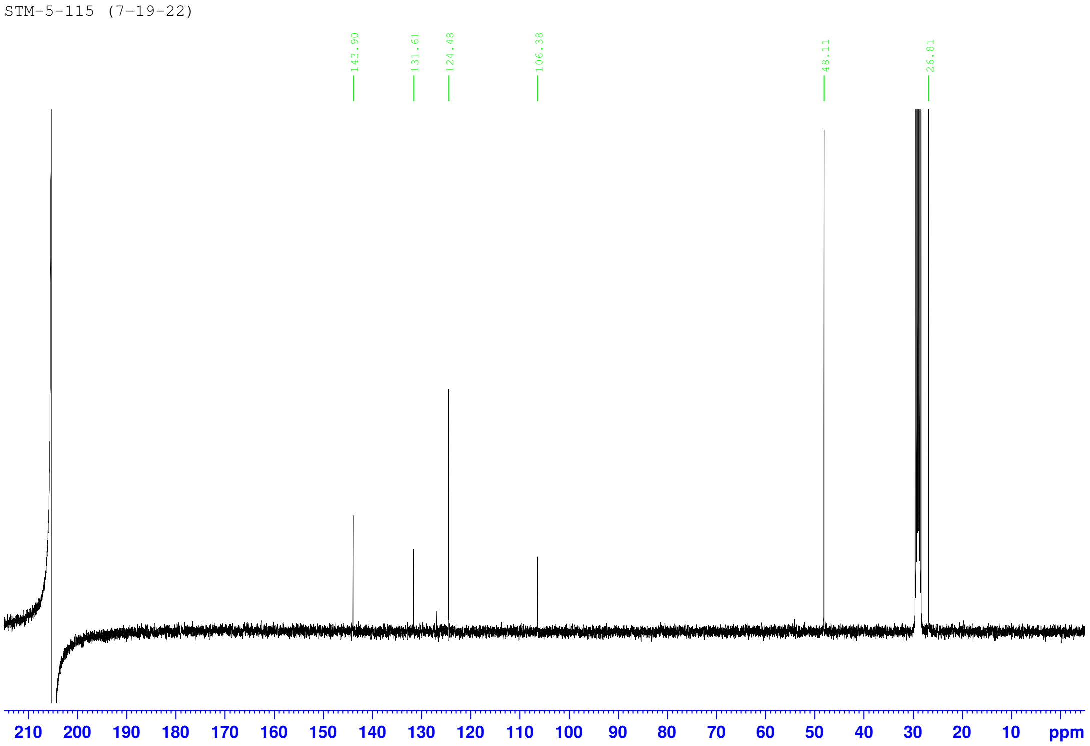
STM-5-115 (7-19-22)
143.90
131.61
124.48
106.38
48.11
26.81
210
200
190
180
170
160
150
140
130
120
110
100
90
80
70
60
50
40
30
20
10
ppm

STM-5-116 (8-24-22)

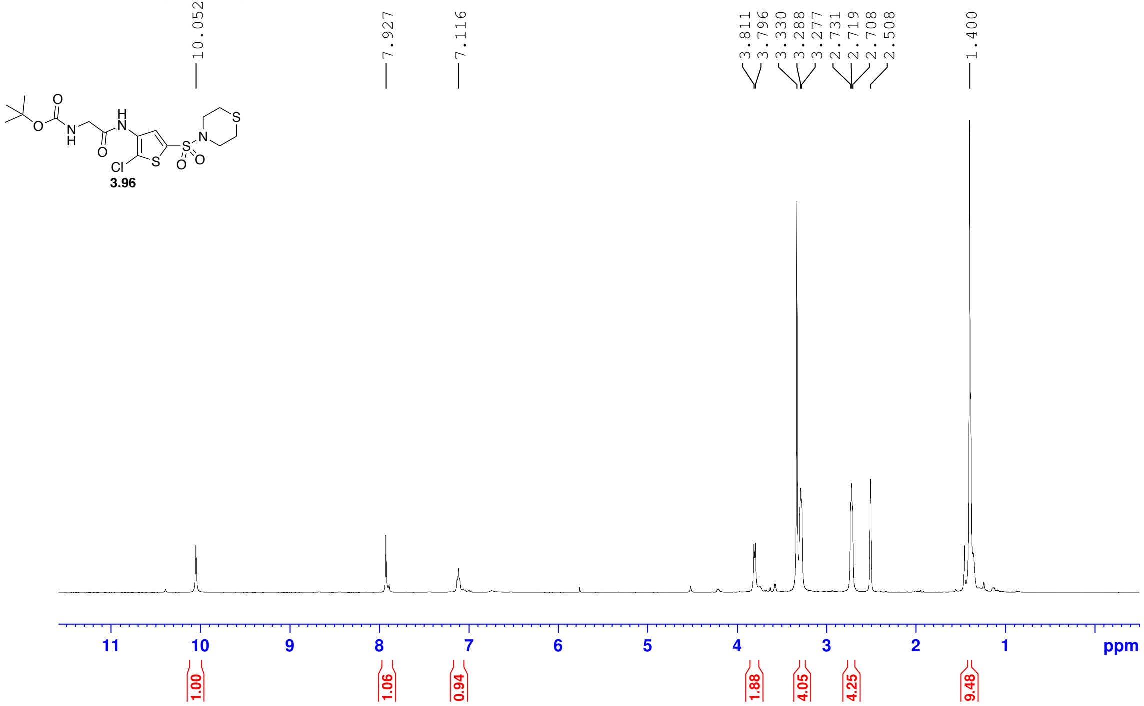

3.96

STM-5-116 CNMR (8-25-22)

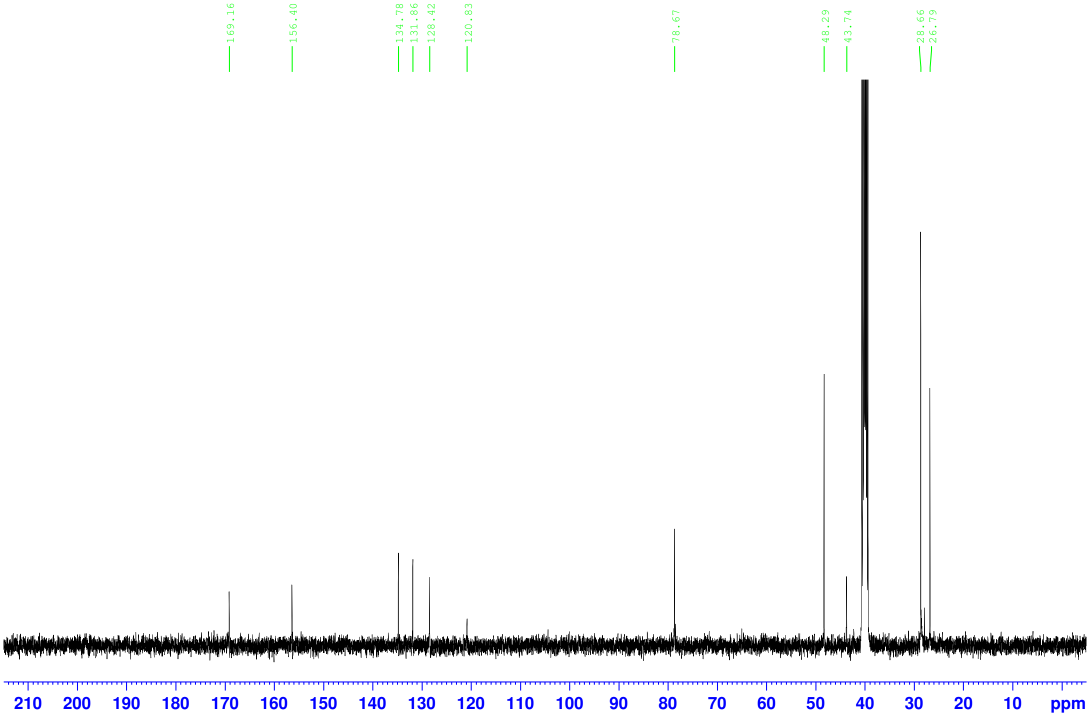

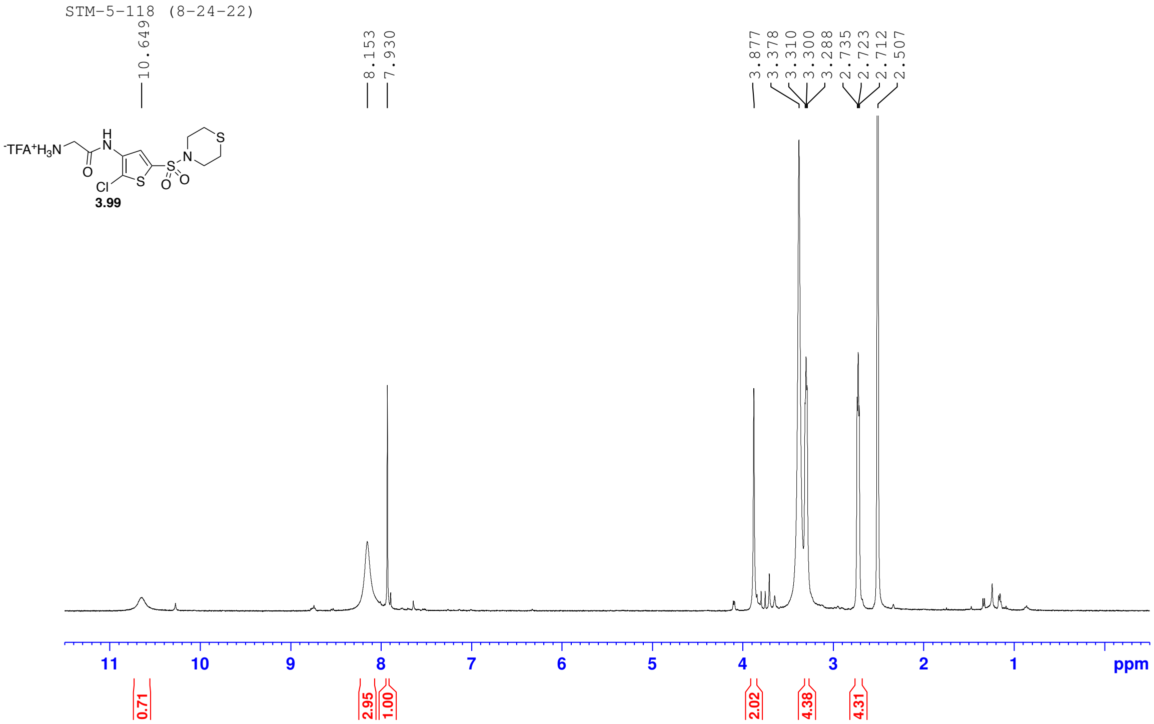
STM-5-118 (8-24-22)

3.99

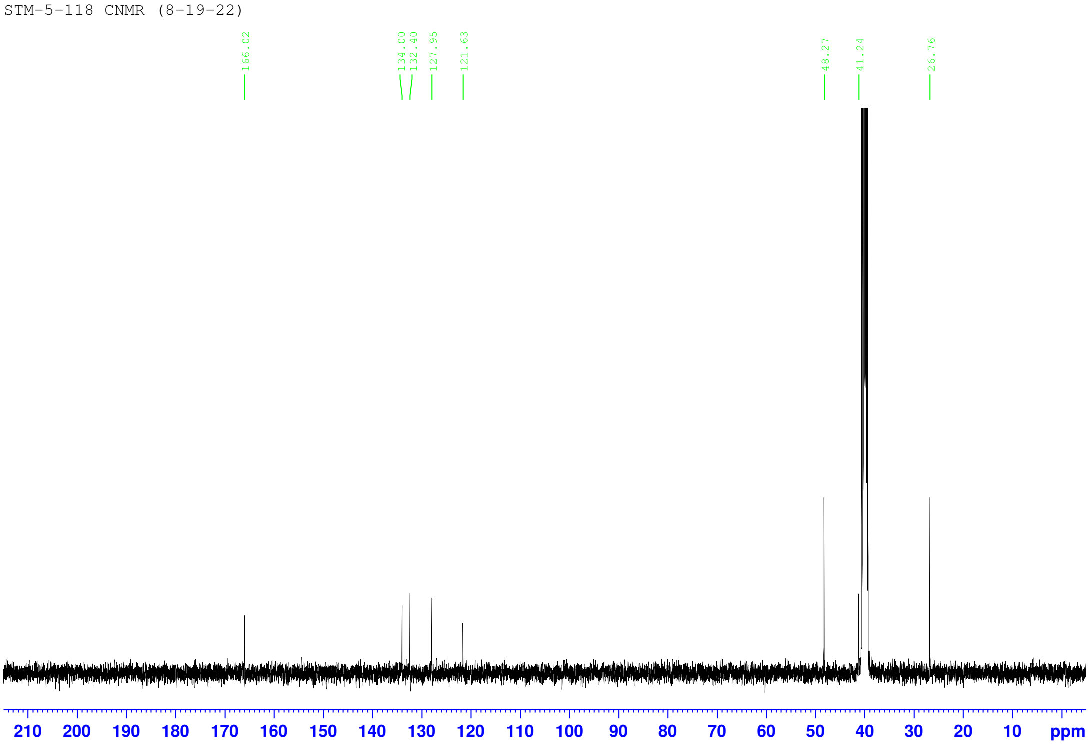
STM-5-118 CNMR (8-19-22)

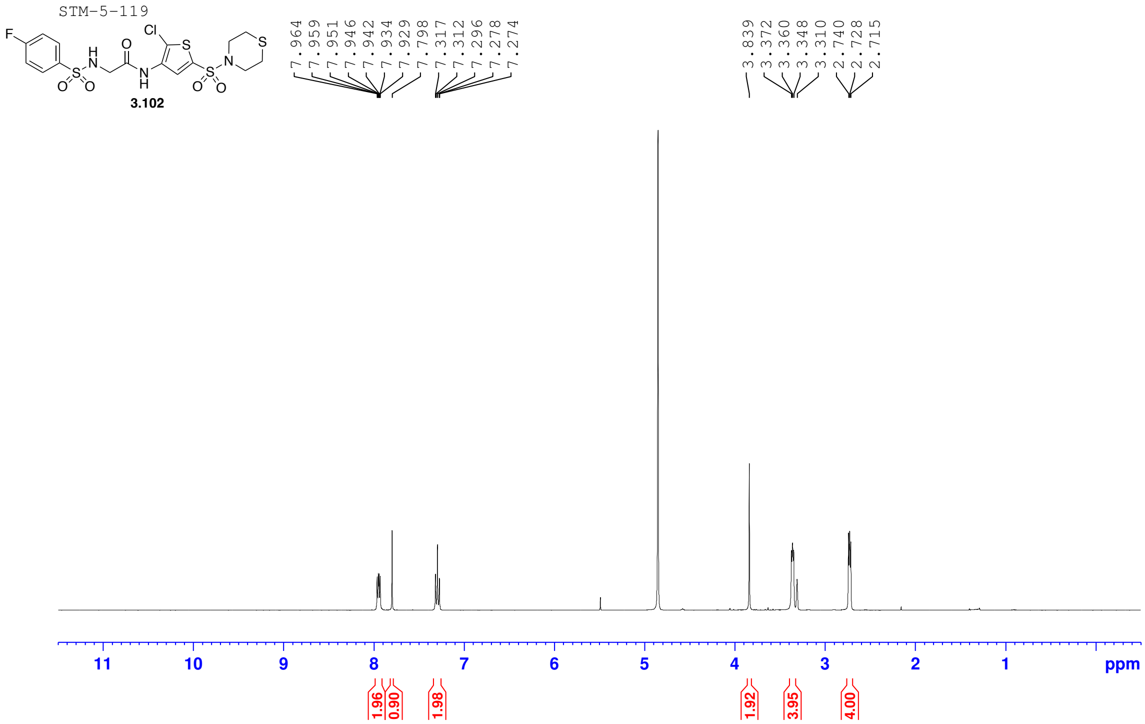
STM-5-119
F
Cl
S
S
H
N
O
N
H
O
S
O
O
S
N
O
3.102
7.964
7.959
7.951
7.946
7.942
7.934
7.929
7.798
7.317
7.312
7.296
7.278
7.274
3.839
3.372
3.360
3.348
3.310
2.740
2.728
2.715
11
10
9
8
7
6
5
4
3
2
1
ppm
1.96
0.90
1.98
1.92
3.95
4.00

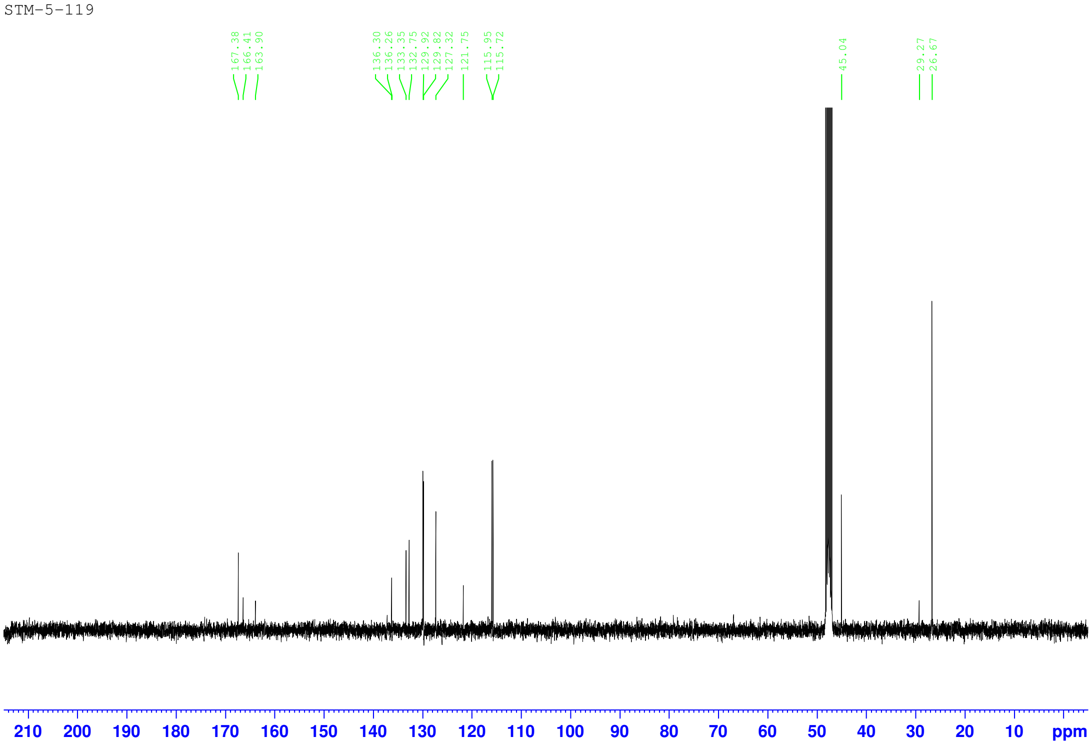
STM-5-119
167.38
166.41
163.90
136.30
136.26
133.35
132.75
129.92
129.82
127.32
121.75
115.95
115.72
45.04
29.27
26.67
210
200
190
180
170
160
150
140
130
120
110
100
90
80
70
60
50
40
30
20
10
ppm

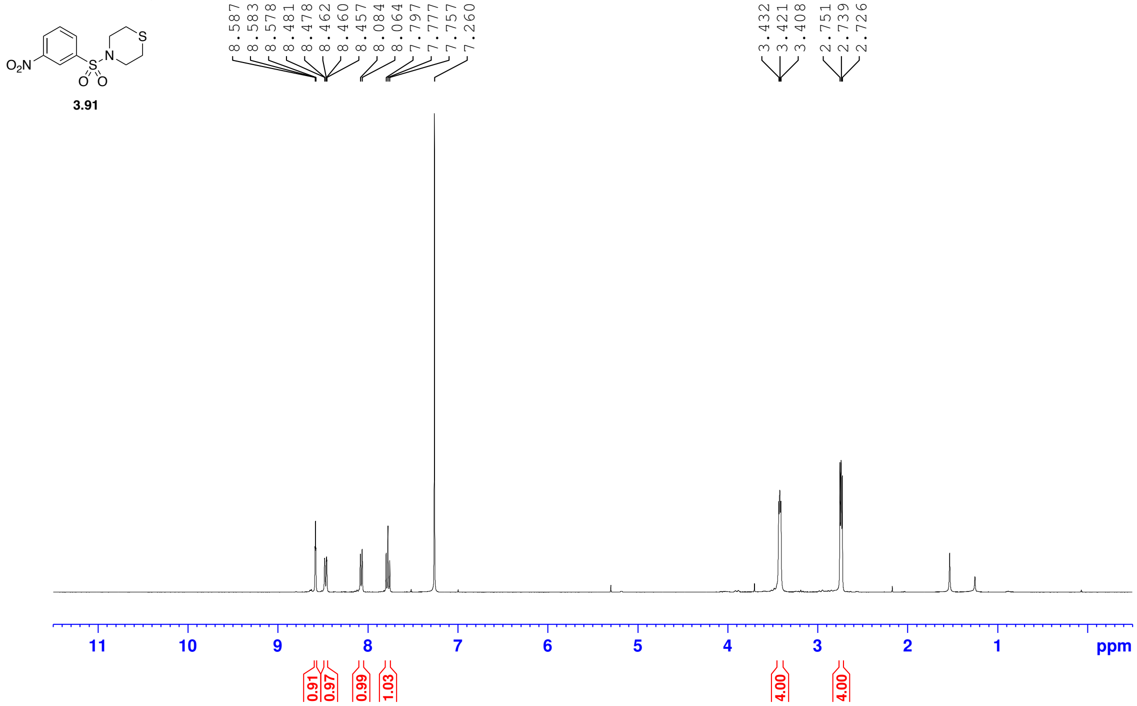

STM-5-33 (4-20-22)

3.91

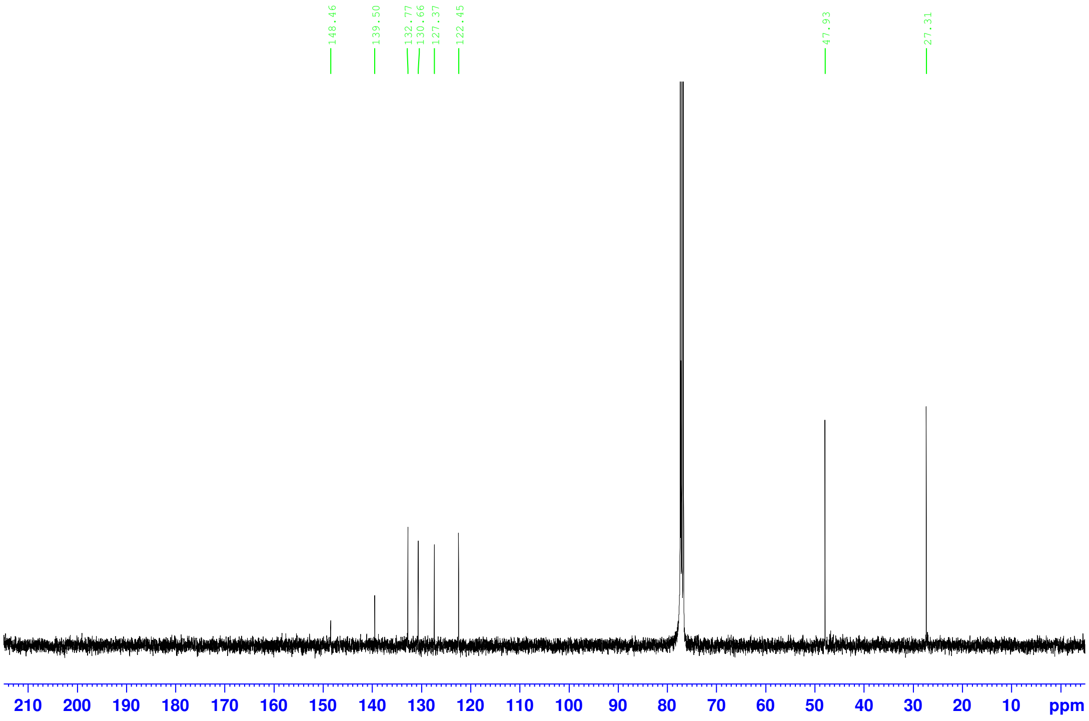

STM-5-33 CNMR (4-25-22)

STM-5-41 DMSO (7-18-22)

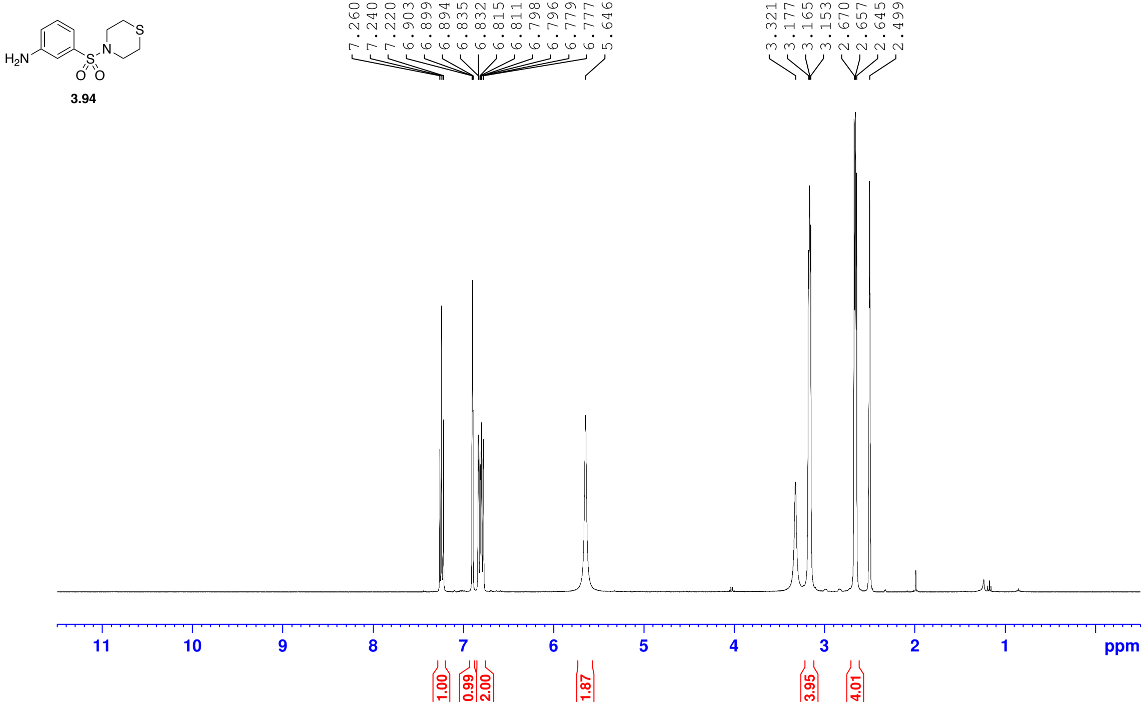

3.94

STM-5-41 DMSO CNMR (7-18-22)

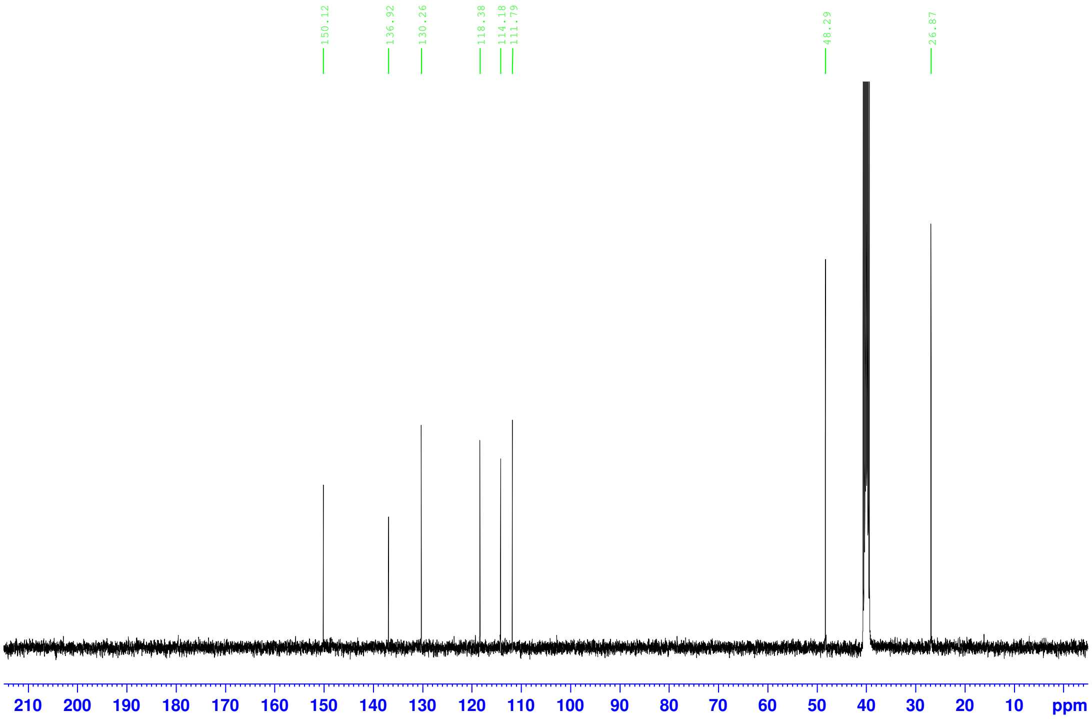

STM-5-47 (5-3-22)

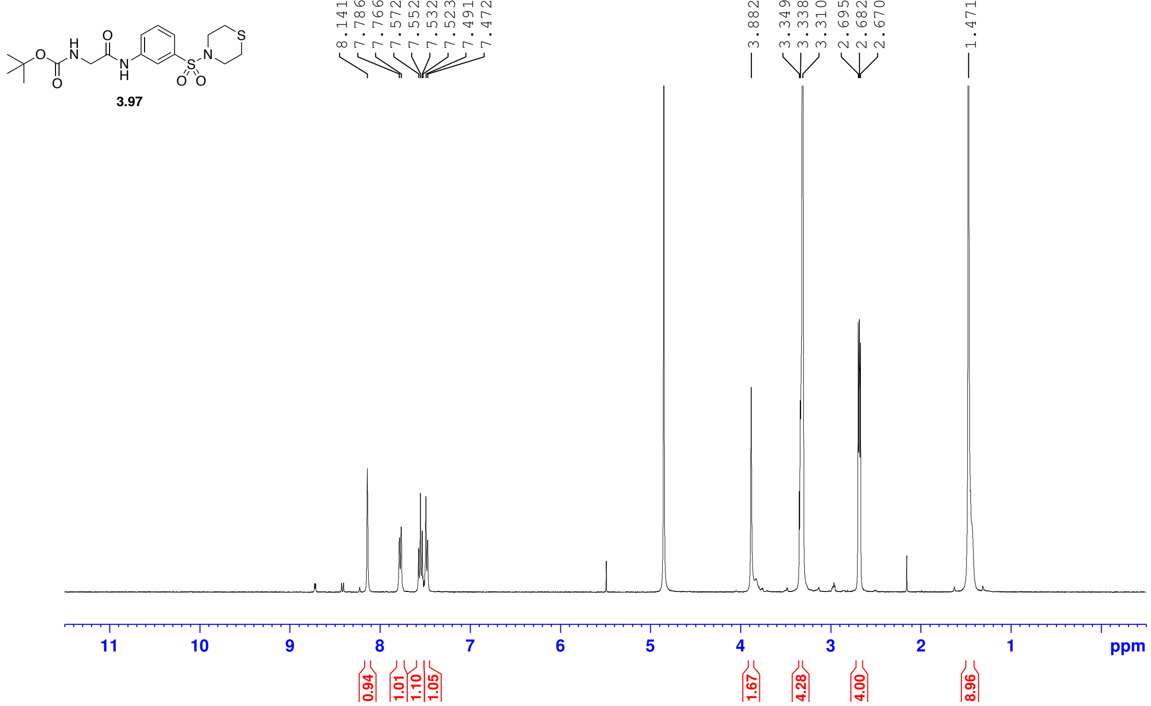

3.97

STM-5-47 CNMR (5-9-22)

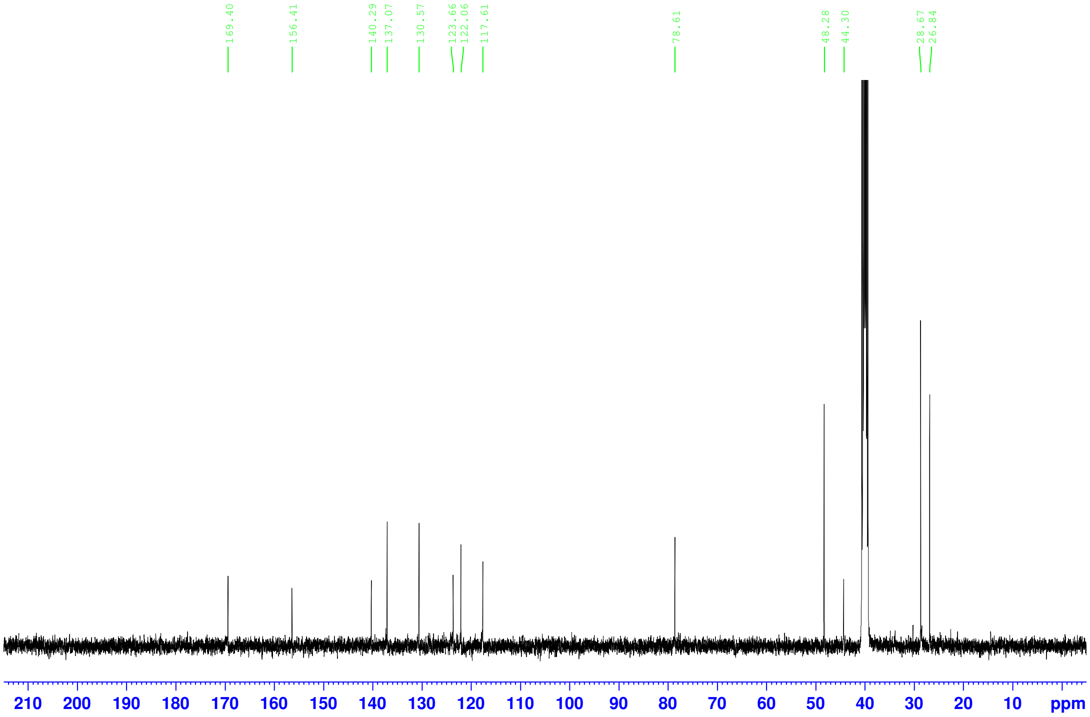

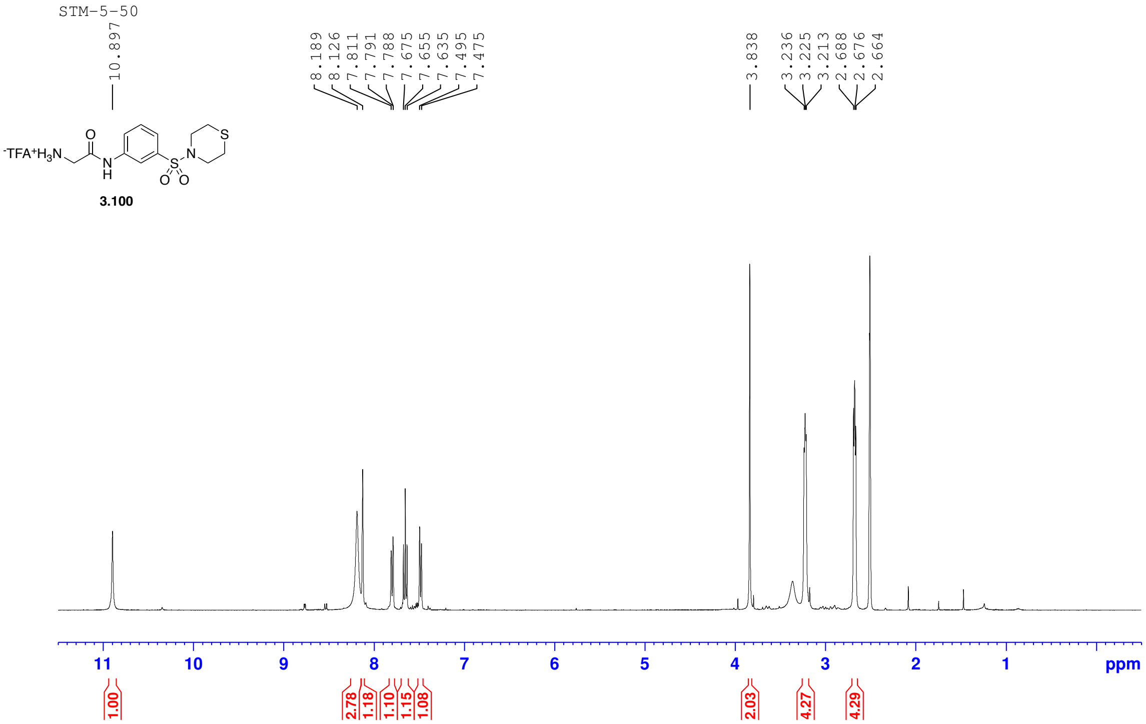
STM-5-50
10.897
8.189
8.126
7.811
7.791
7.788
7.675
7.655
7.635
7.495
7.475
3.838
3.236
3.225
3.213
2.688
2.676
2.664
⁻TFA⁺H₃N
O
N
H
S
O
O
N
S
11
10
9
8
7
6
5
4
3
2
1
ppm
1.00
2.78
1.18
1.10
1.15
1.08
2.03
4.27
4.29

3.100

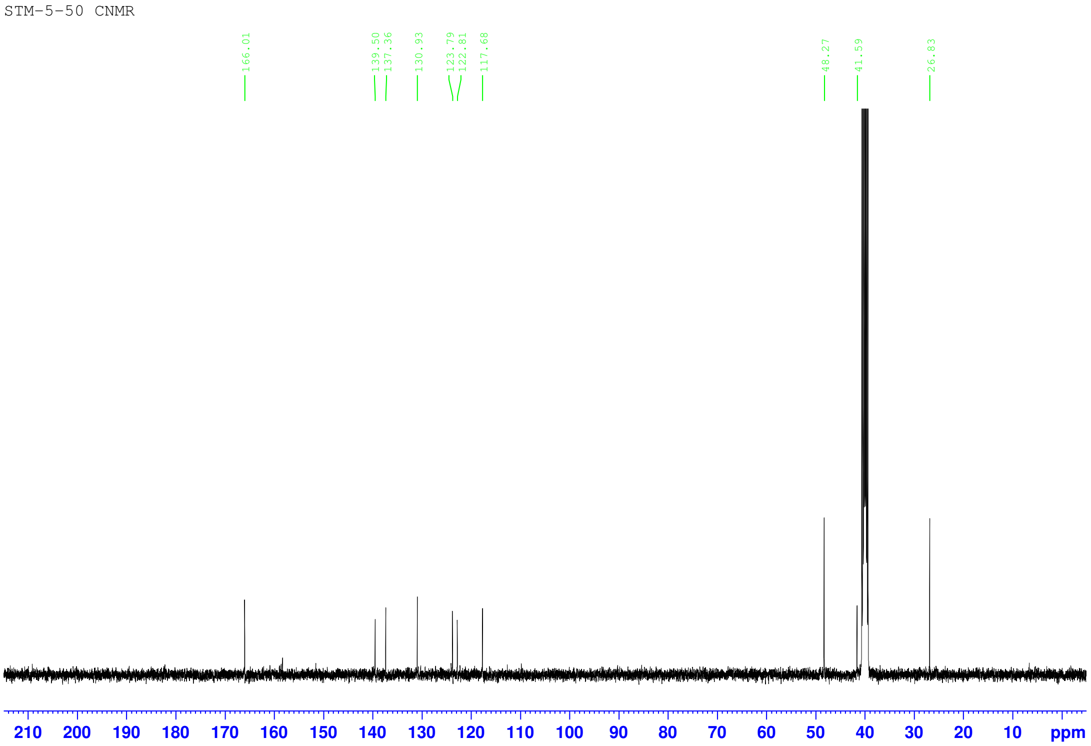
STM-5-50 CNMR
166.01
139.50
137.36
130.93
123.79
122.81
117.68
48.27
41.59
26.83
210
200
190
180
170
160
150
140
130
120
110
100
90
80
70
60
50
40
30
20
10
ppm

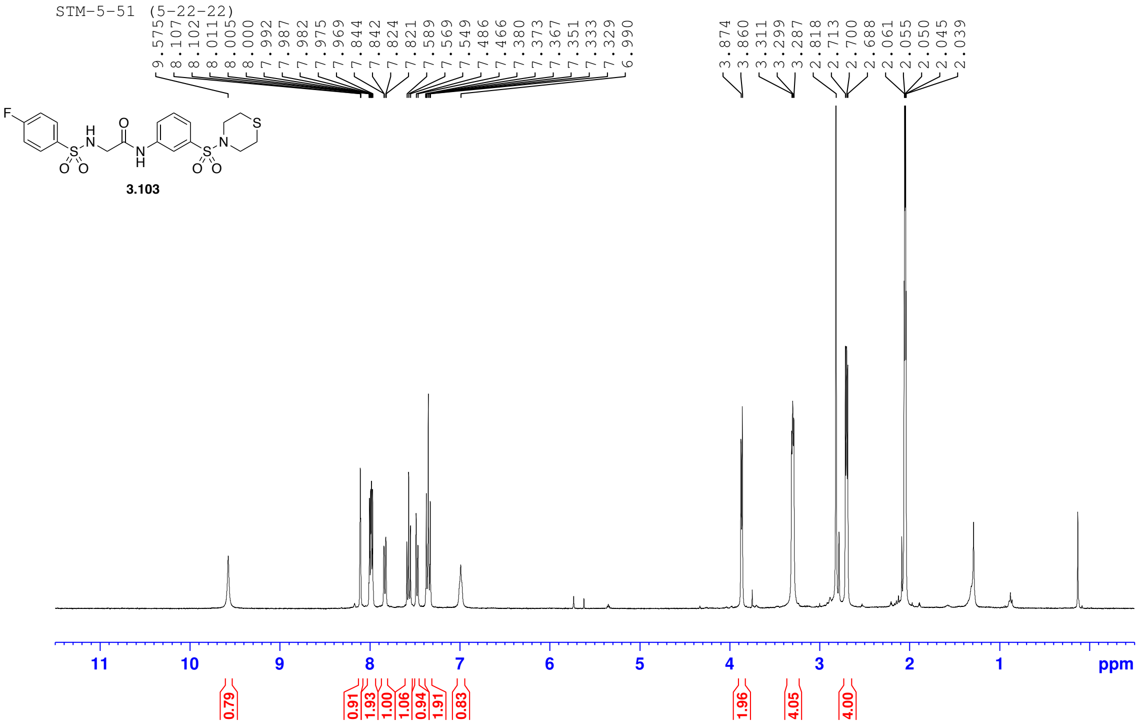
STM-5-51 (5-22-22)
9.575
8.107
8.102
8.011
8.005
8.000
7.992
7.987
7.982
7.975
7.969
7.844
7.842
7.824
7.821
7.589
7.569
7.549
7.486
7.466
7.380
7.373
7.367
7.351
7.333
7.329
6.990
3.874
3.860
3.311
3.299
3.287
2.818
2.713
2.700
2.688
2.061
2.055
2.050
2.045
2.039
F
H
N
O
N
H
S
O O
S
O O
N
S
3.103
11
10
9
8
7
6
5
4
3
2
1
ppm
0.79
0.91
1.93
1.00
1.06
0.94
1.91
0.83
1.96
4.05
4.00

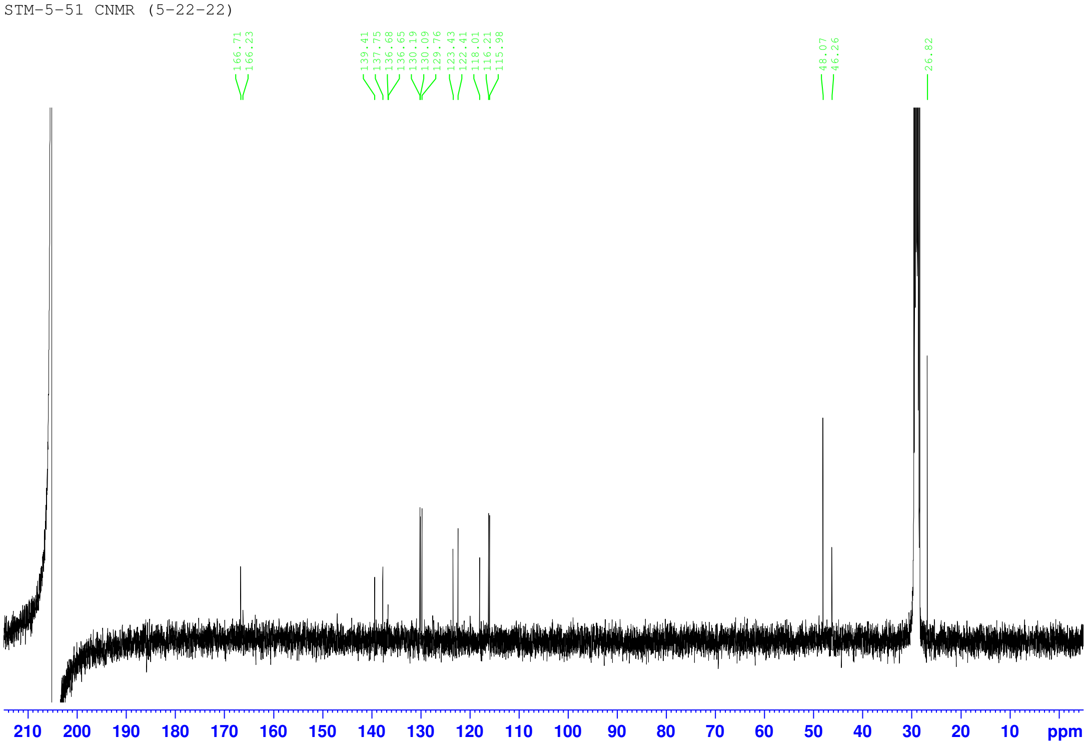
STM-5-51 CNMR (5-22-22)
166.71
166.23
139.41
137.75
136.68
136.65
130.19
130.09
129.76
123.43
122.41
118.01
116.21
115.98
48.07
46.26
26.82
210
200
190
180
170
160
150
140
130
120
110
100
90
80
70
60
50
40
30
20
10
ppm

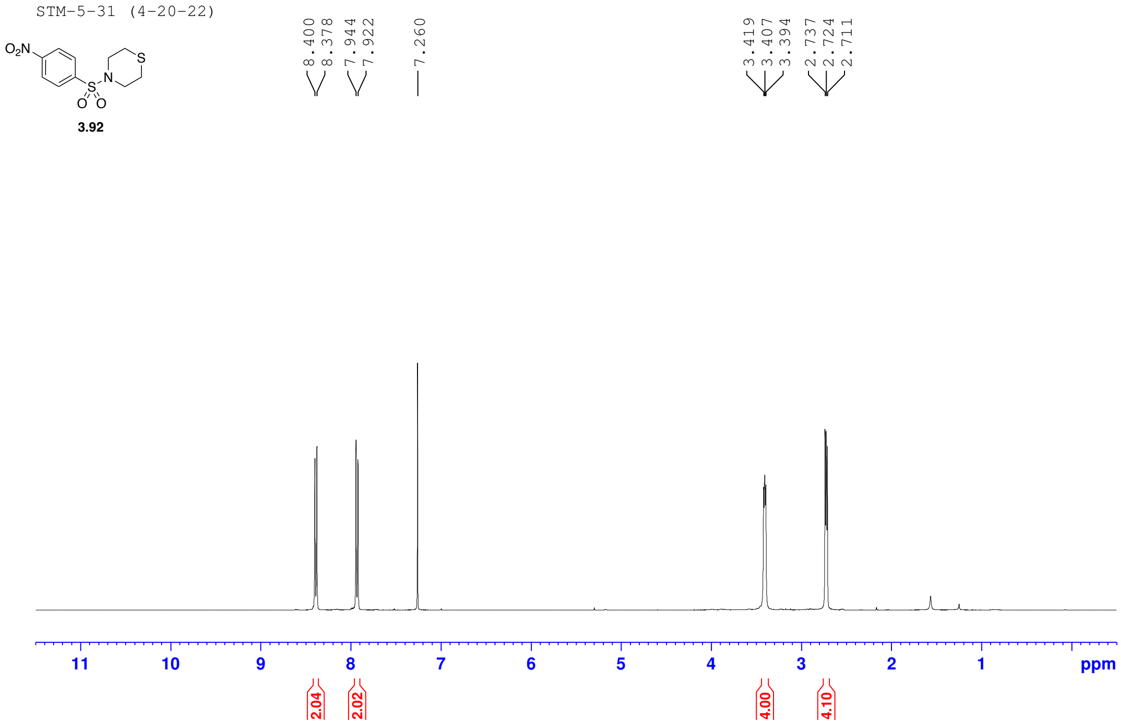
STM-5-31 (4-20-22)
O_2N
S
N
O
O
3.92
8.400
8.378
7.944
7.922
7.260
3.419
3.407
3.394
2.737
2.724
2.711
11
10
9
8
7
6
5
4
3
2
1
ppm
2.04
2.02
4.00
4.10

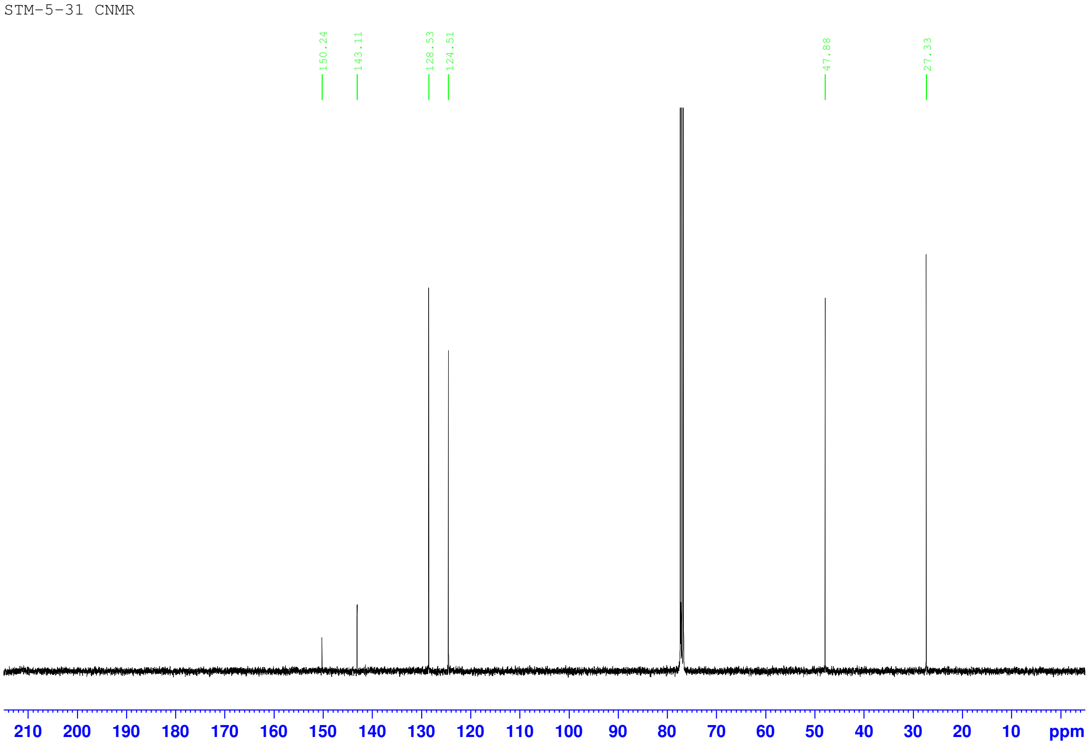
STM-5-31 CNMR
150.24
143.11
128.53
124.51
47.88
27.33
210
200
190
180
170
160
150
140
130
120
110
100
90
80
70
60
50
40
30
20
10
ppm

STM-5-39 (6-21-22)

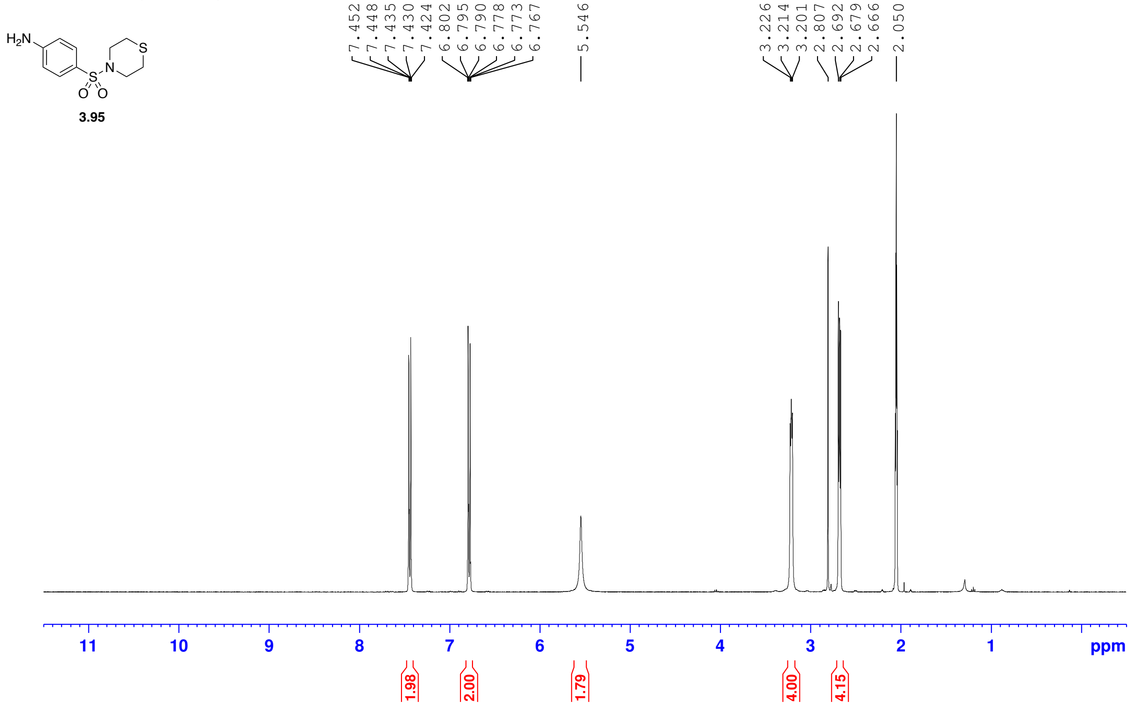

STM-5-39 CNMR (6-21-22)

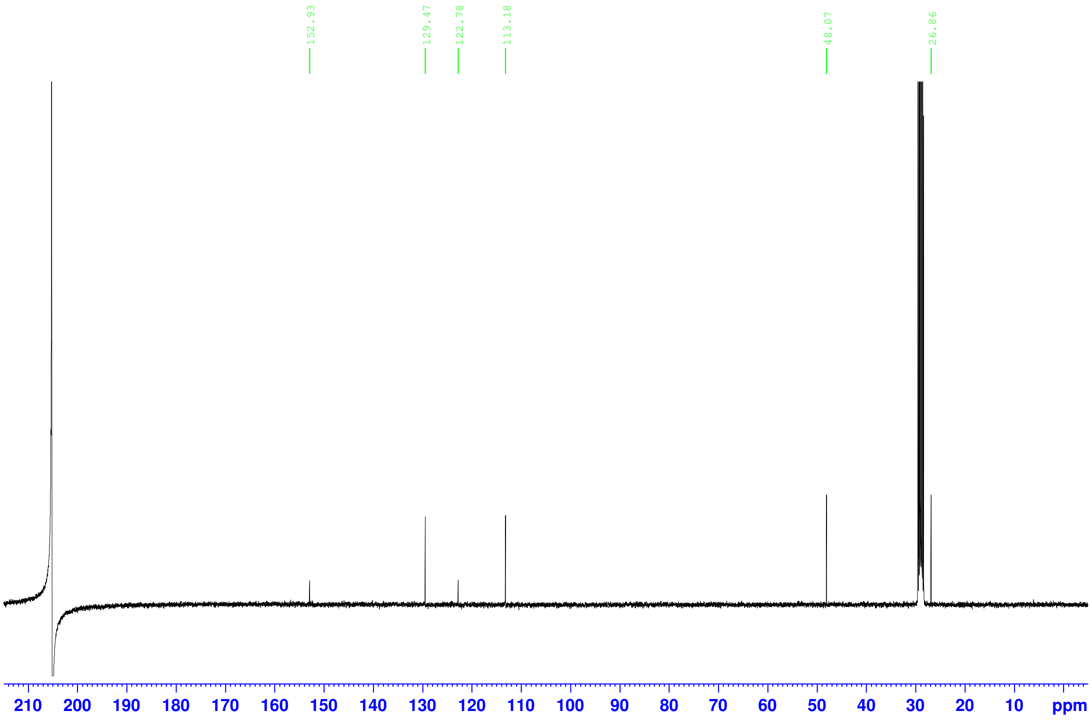

STM-5-46 (5-3-22)

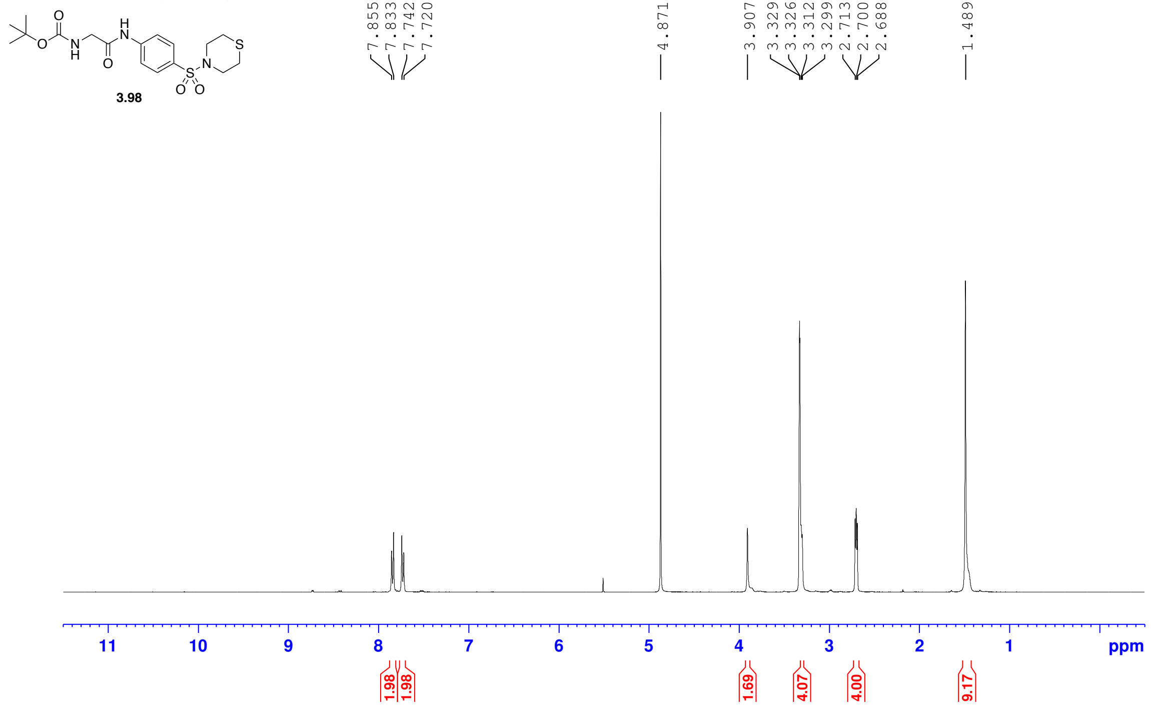

3.98

STM-5-46 CNMR (5-11-22)

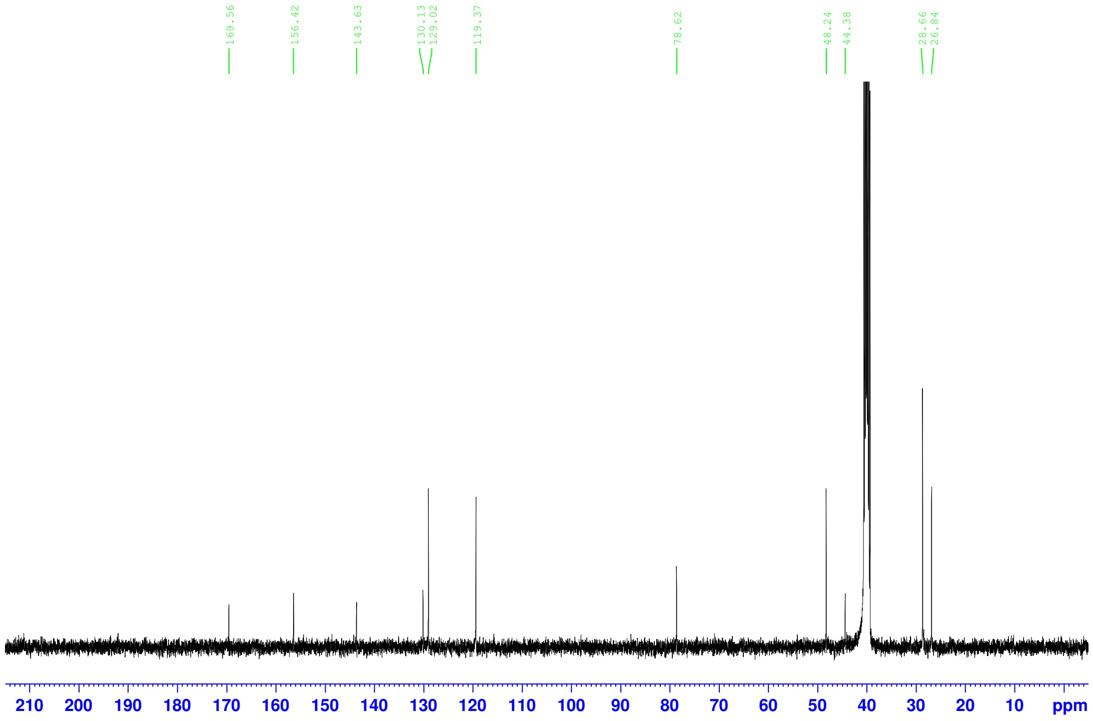

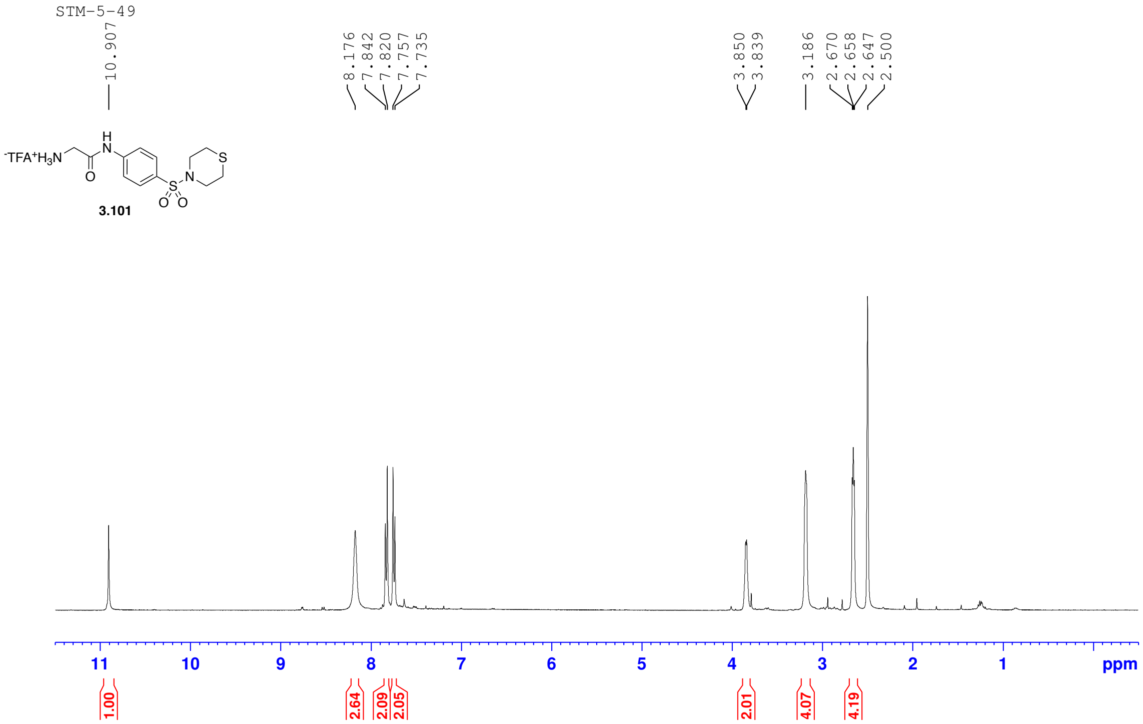
STM-5-49
10.907
8.176
7.842
7.820
7.757
7.735
3.850
3.839
3.186
2.670
2.658
2.647
2.500
-TFA+H3N
H
N
O
S
N
O
O
3.101
11
10
9
8
7
6
5
4
3
2
1
ppm
1.00
2.64
2.09
2.05
2.01
4.07
4.19

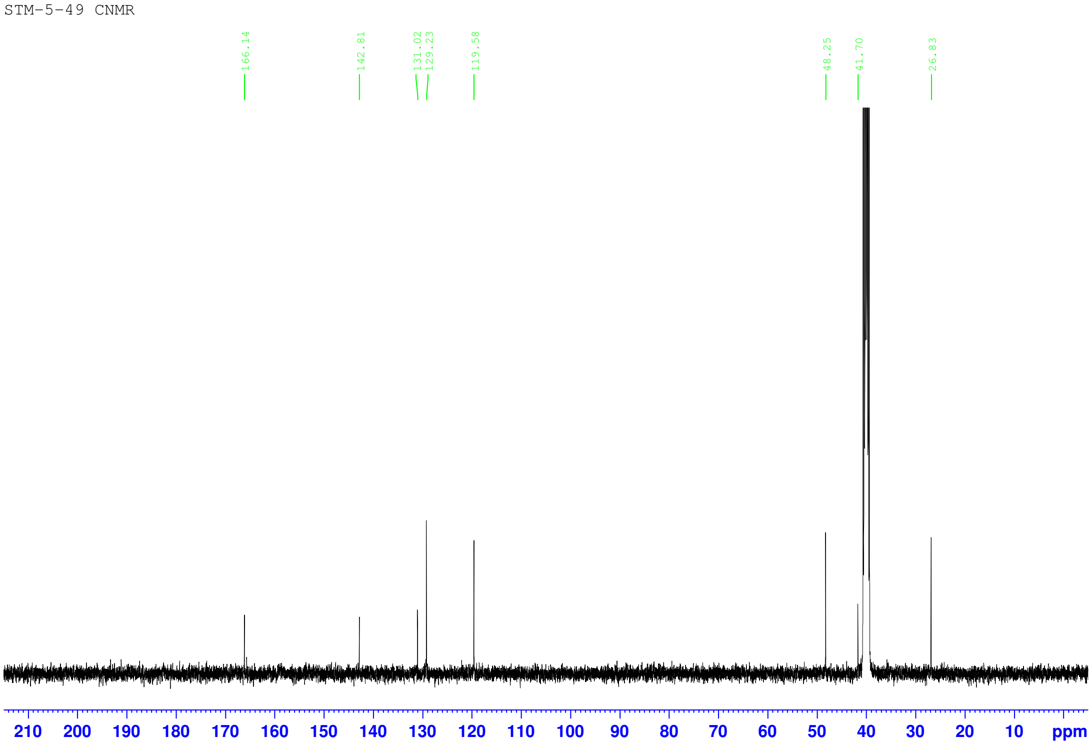
STM-5-49 CNMR
166.14
142.81
131.02
129.23
119.58
48.25
41.70
26.83
210
200
190
180
170
160
150
140
130
120
110
100
90
80
70
60
50
40
30
20
10
ppm

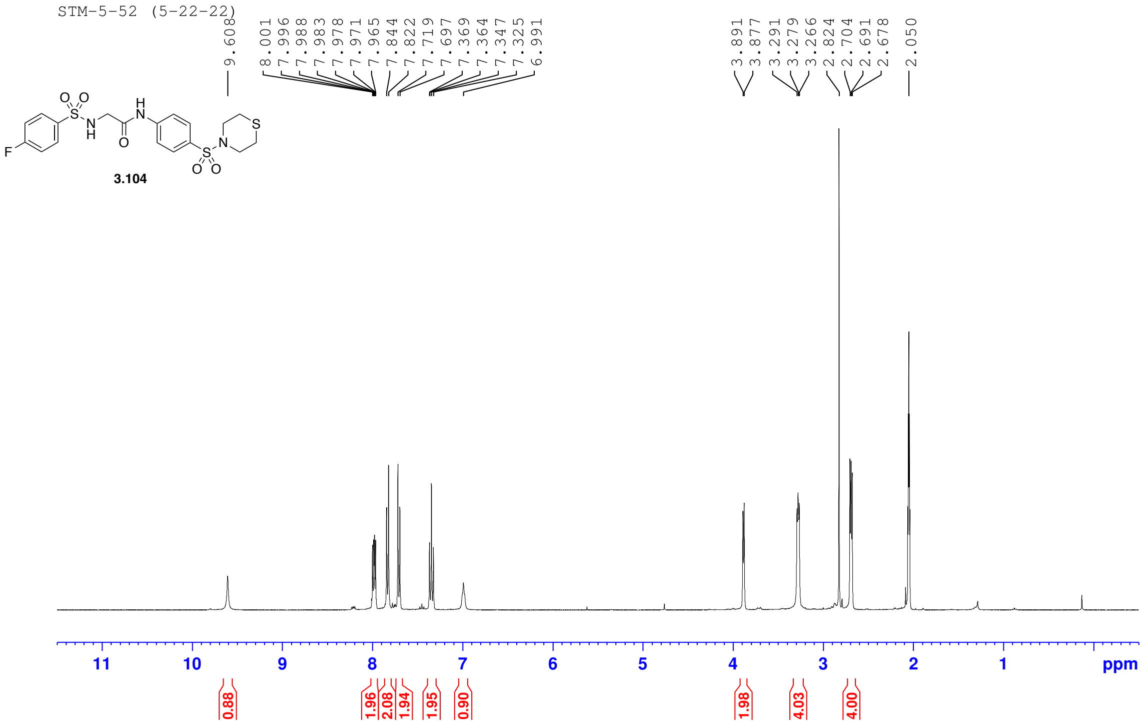
3.104
STM-5-52 (5-22-22)
9.608
8.001
7.996
7.988
7.983
7.978
7.971
7.965
7.844
7.822
7.719
7.697
7.369
7.364
7.347
7.325
6.991
3.891
3.877
3.291
3.279
3.266
2.824
2.704
2.691
2.678
2.050
F
O
S
N
H
O
N
H
O
S
N
S
O
O
11
10
9
8
7
6
5
4
3
2
1
ppm
0.88
1.96
2.08
1.94
1.95
0.90
1.98
4.03
4.00

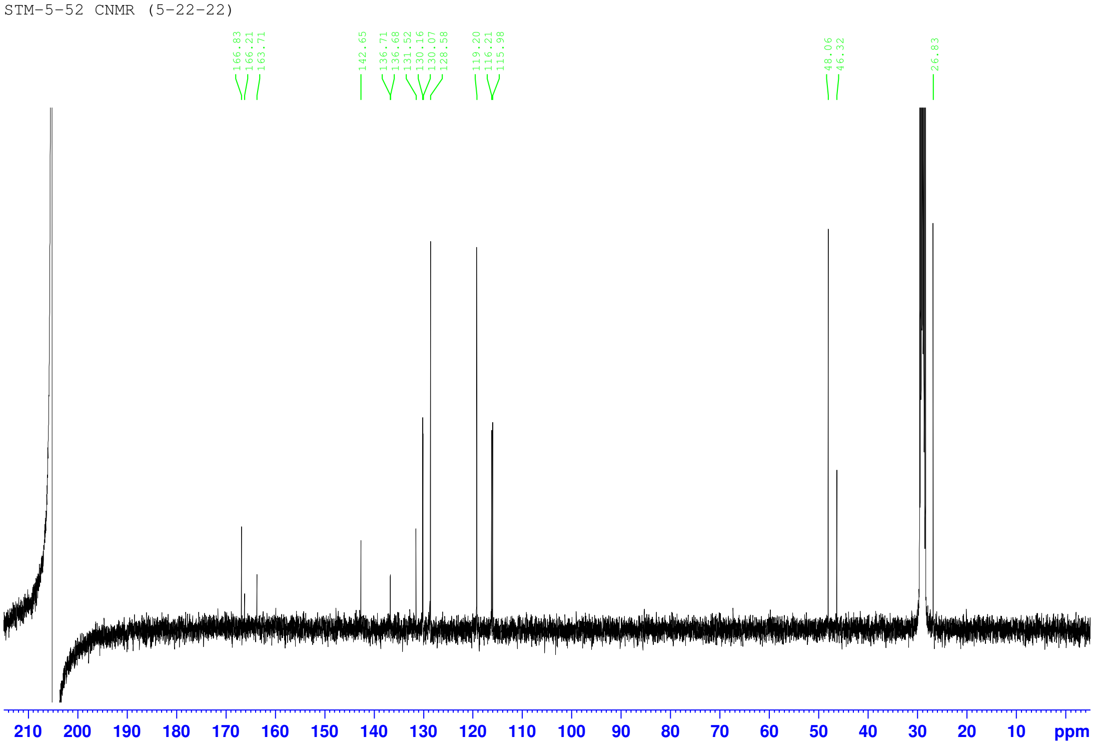
STM-5-52 CNMR (5-22-22)
166.83
166.21
163.71
142.65
136.71
136.68
131.52
130.16
130.07
128.58
119.20
116.21
115.98
48.06
46.32
26.83
210
200
190
180
170
160
150
140
130
120
110
100
90
80
70
60
50
40
30
20
10
ppm

STM-5-45

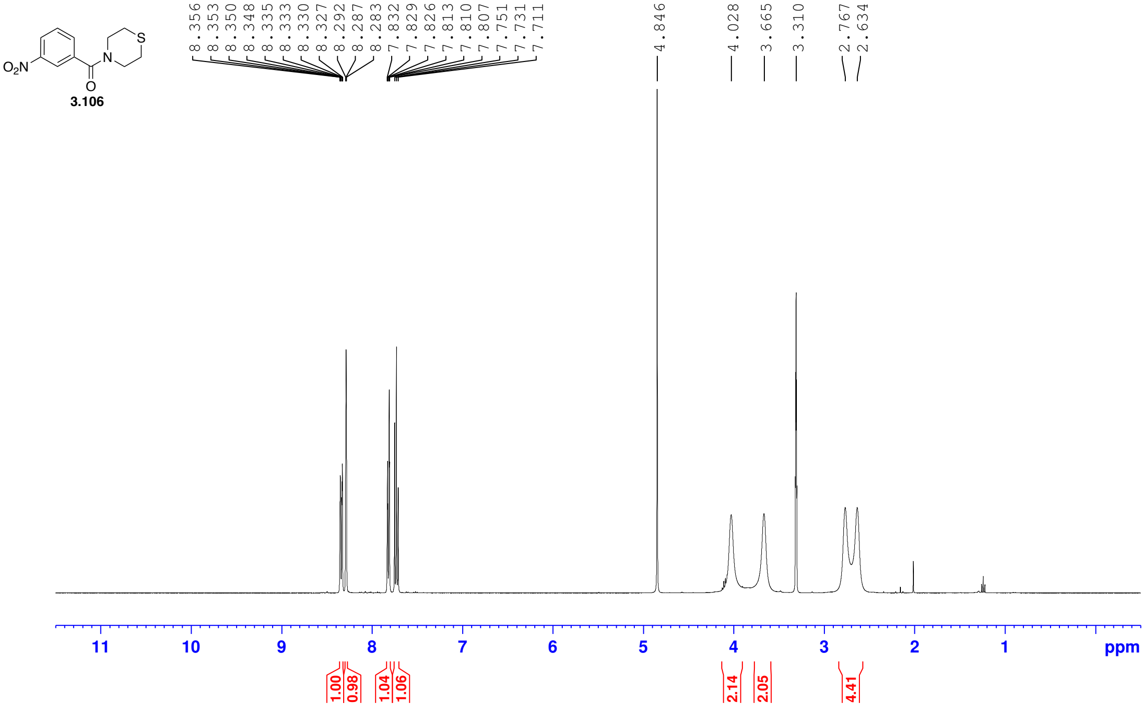

3.106

STM-5-45 CNMR

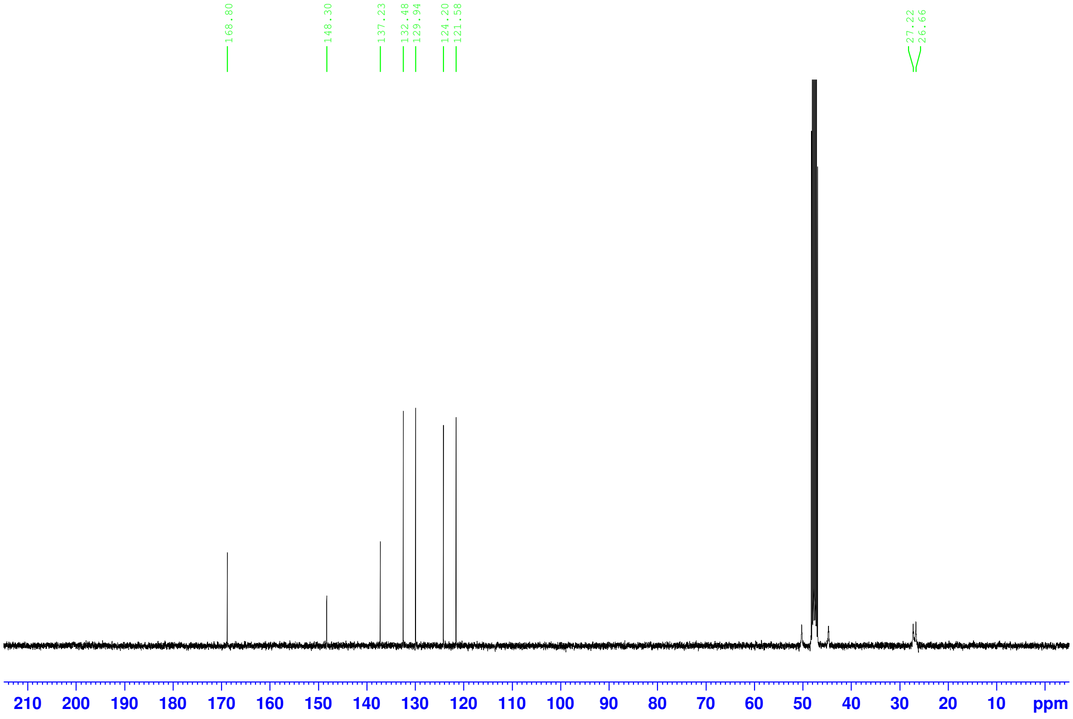

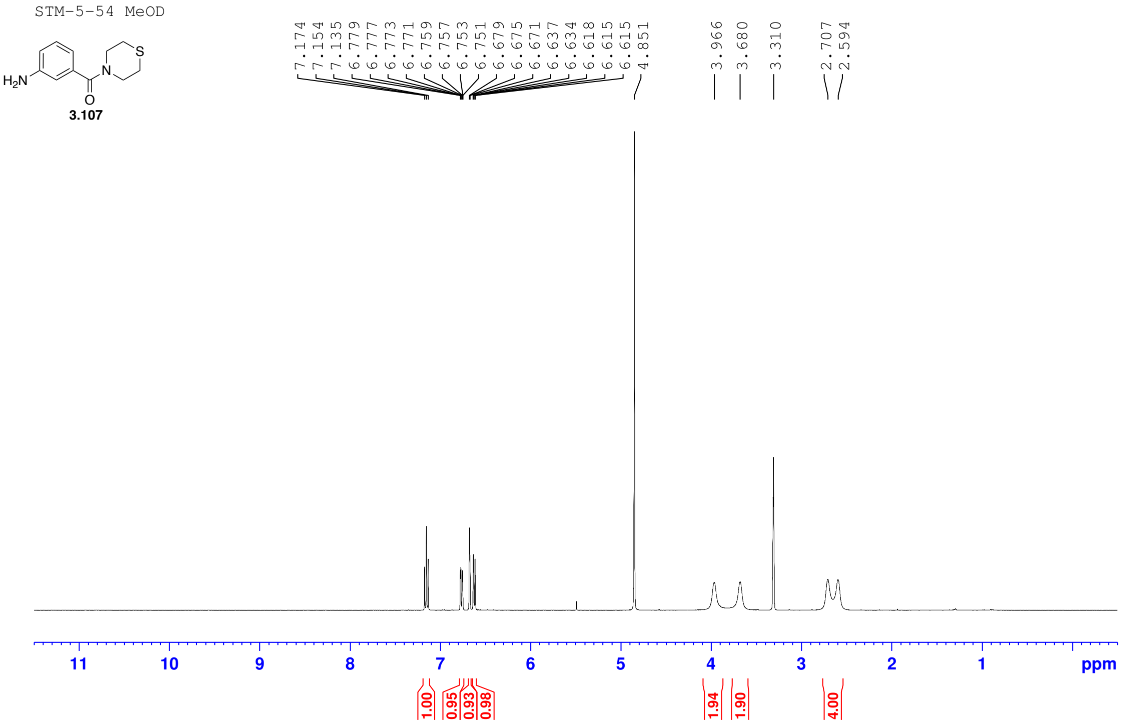
3.107
STM-5-54 MeOD
H2N
N
S
O
7.174
7.154
7.135
6.779
6.777
6.773
6.771
6.759
6.757
6.753
6.751
6.679
6.675
6.671
6.637
6.634
6.618
6.615
6.615
4.851
3.966
3.680
3.310
2.707
2.594
11
10
9
8
7
6
5
4
3
2
1
ppm
1.00
0.95
0.93
0.98
1.94
1.90
4.00

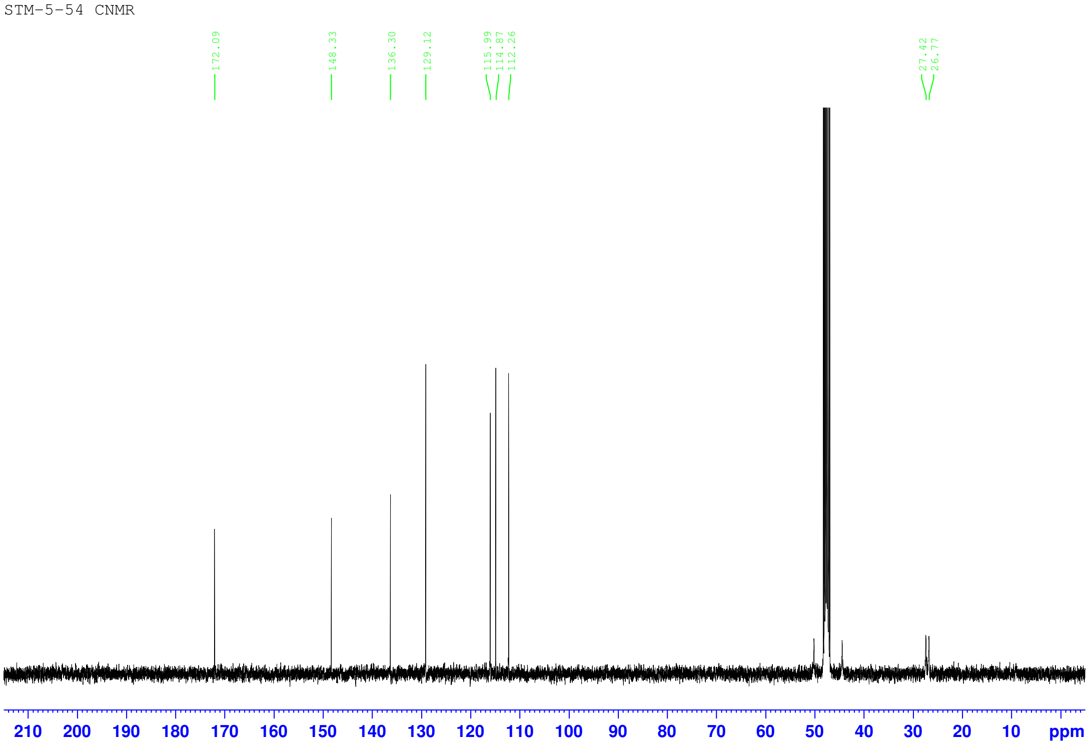
STM-5-54 CNMR
172.09
148.33
136.30
129.12
115.99
114.87
112.26
27.42
26.77
210
200
190
180
170
160
150
140
130
120
110
100
90
80
70
60
50
40
30
20
10
ppm

STM-5-58 (6-29-22)

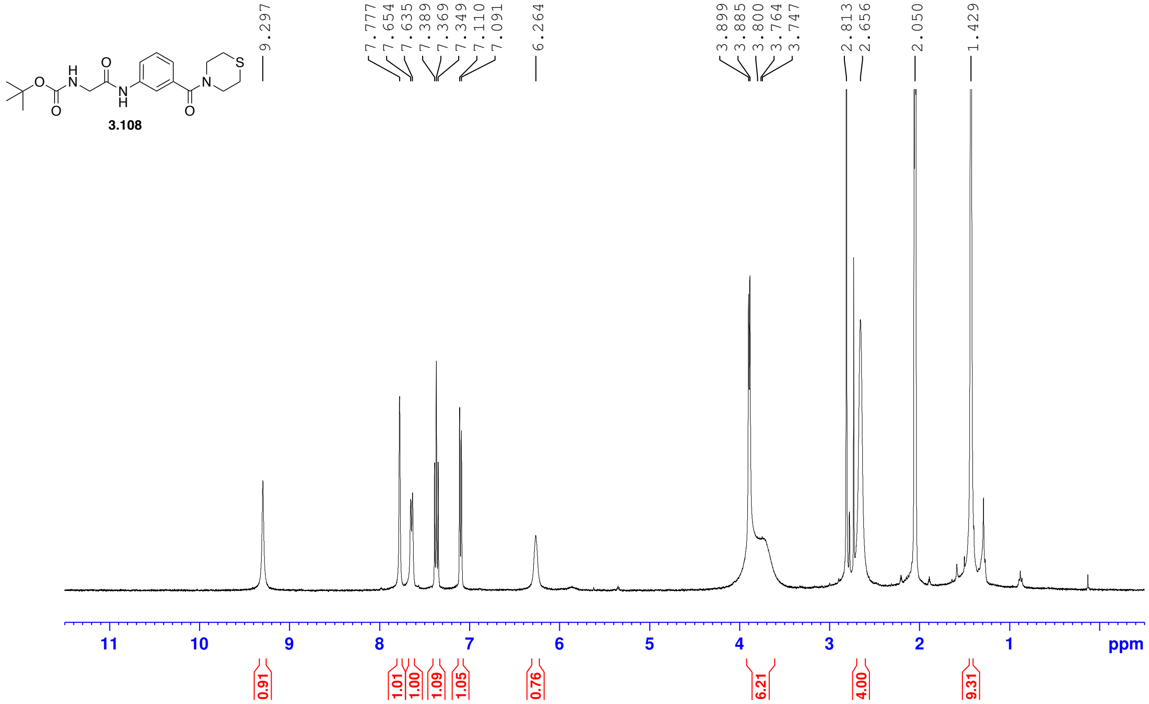

3.108

STM-5-58 (5-18-22)

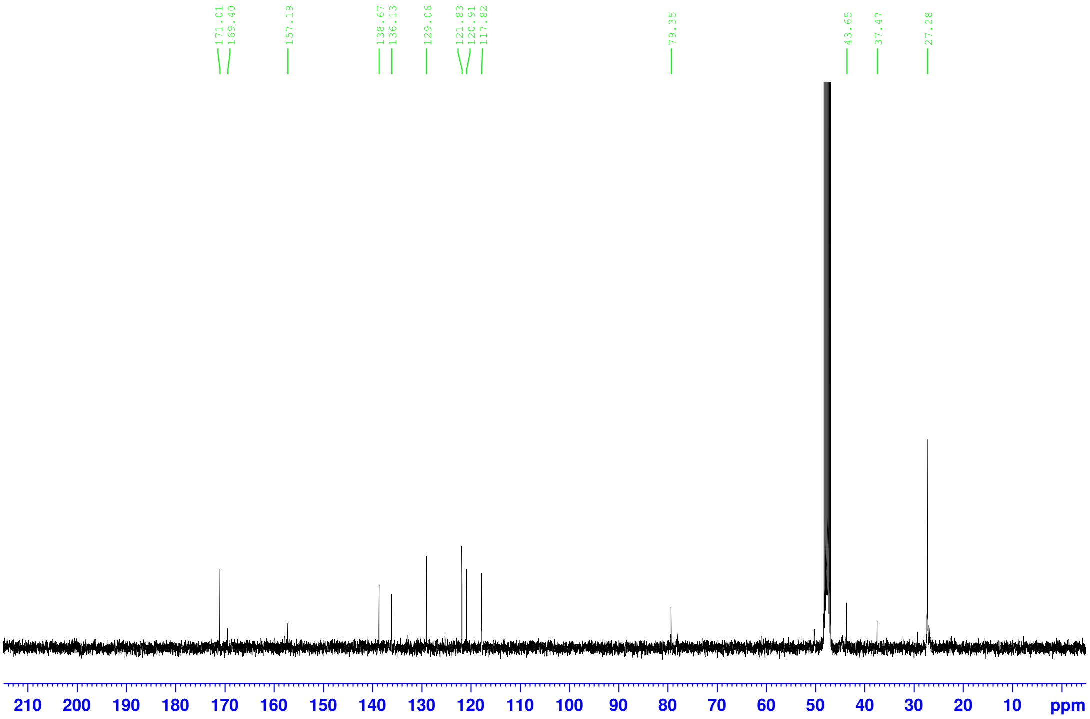

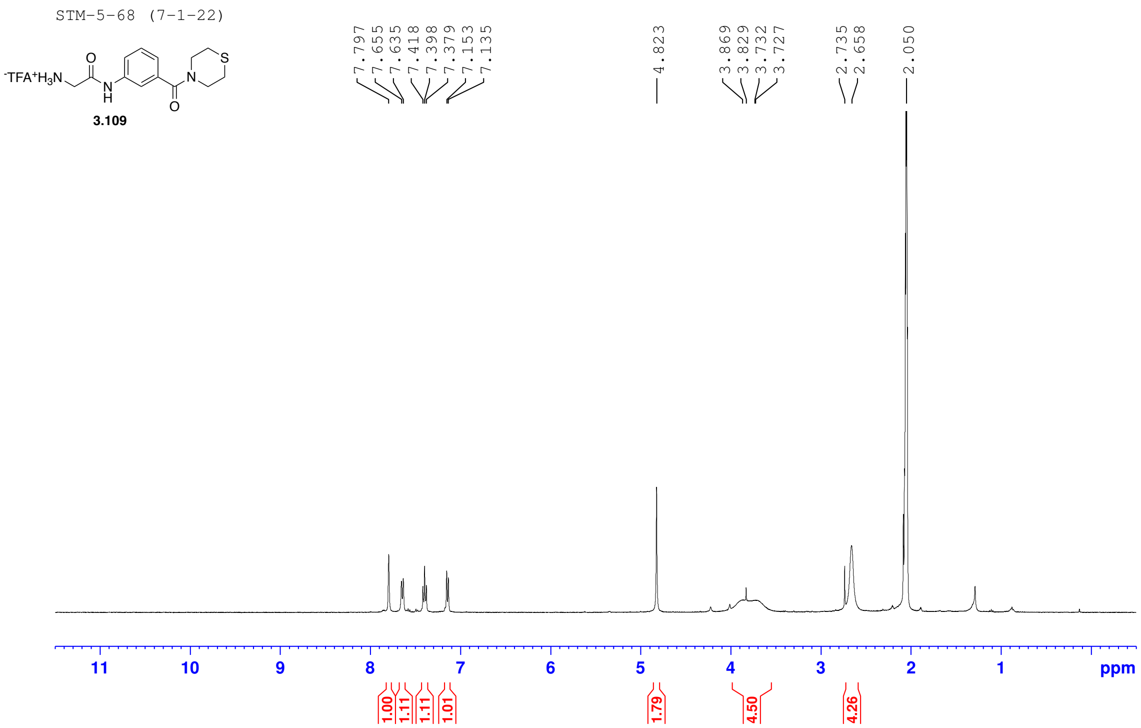
STM-5-68 (7-1-22)
-TFA+H3N
O
N
H
S
N
O
3.109
7.797
7.655
7.635
7.418
7.398
7.379
7.153
7.135
4.823
3.869
3.829
3.732
3.727
2.735
2.658
2.050
11
10
9
8
7
6
5
4
3
2
1
ppm
1.00
1.11
1.11
1.01
1.79
4.50
4.26

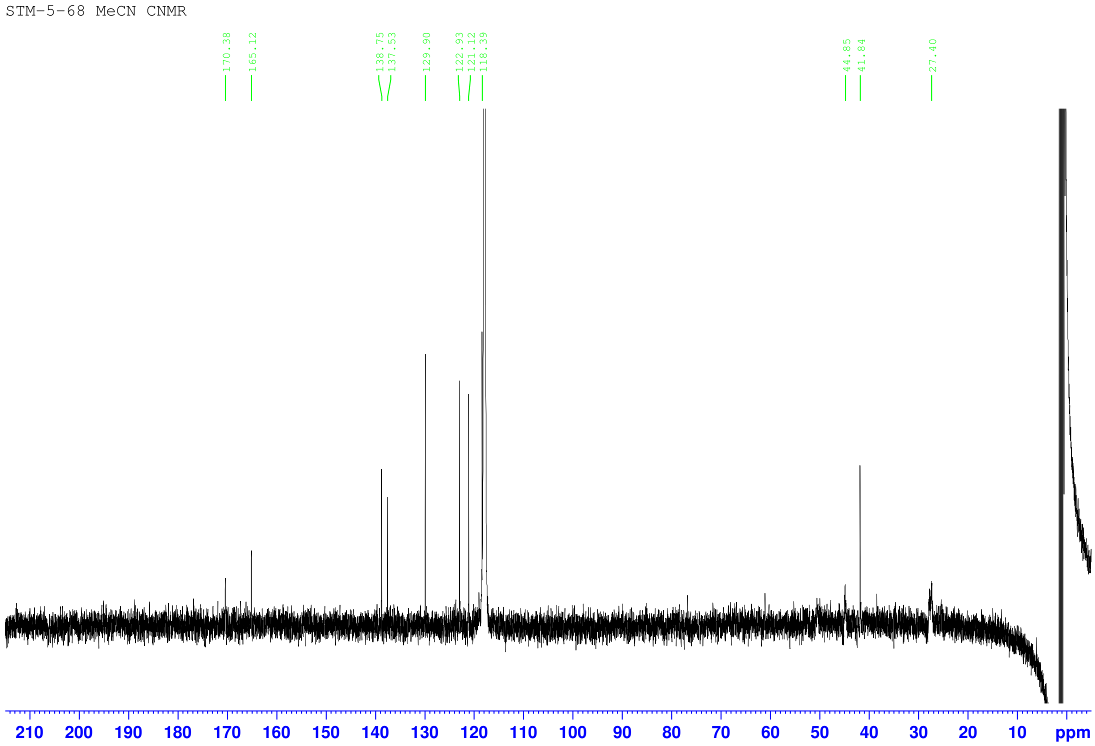
STM-5-68 MeCN CNMR
170.38
165.12
138.75
137.53
129.90
122.93
121.12
118.39
44.85
41.84
27.40
210
200
190
180
170
160
150
140
130
120
110
100
90
80
70
60
50
40
30
20
10
ppm

STM-5-74 (6-21-22)

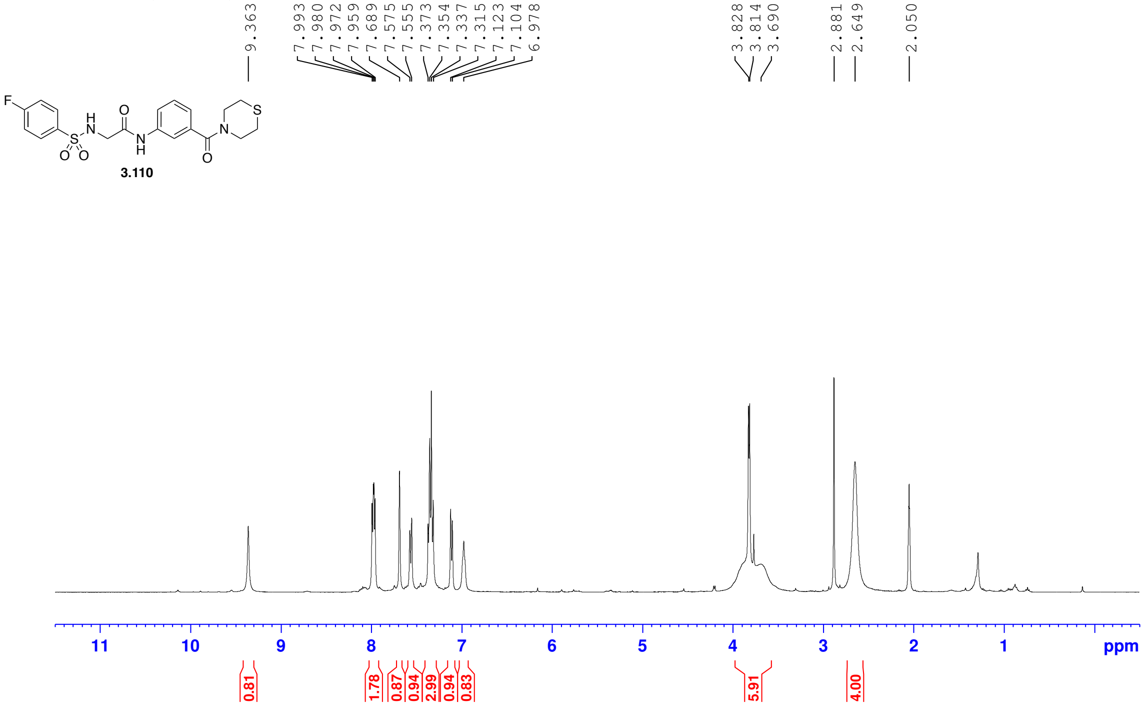

3.110

STM-5-74 CNMR (6-21-22)

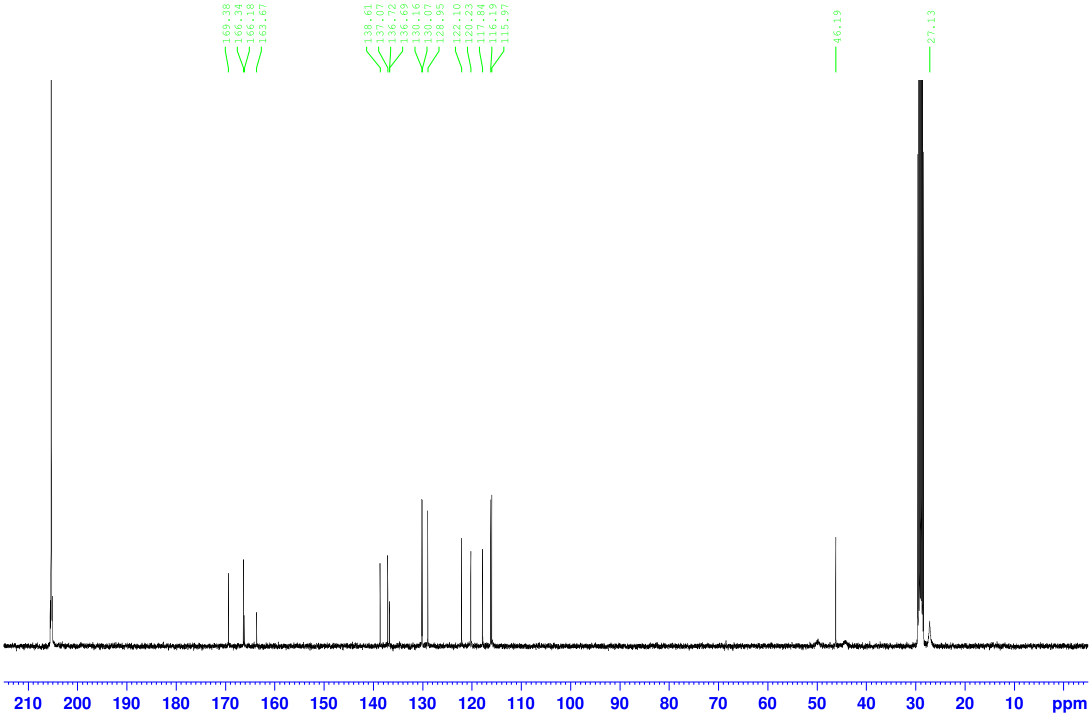

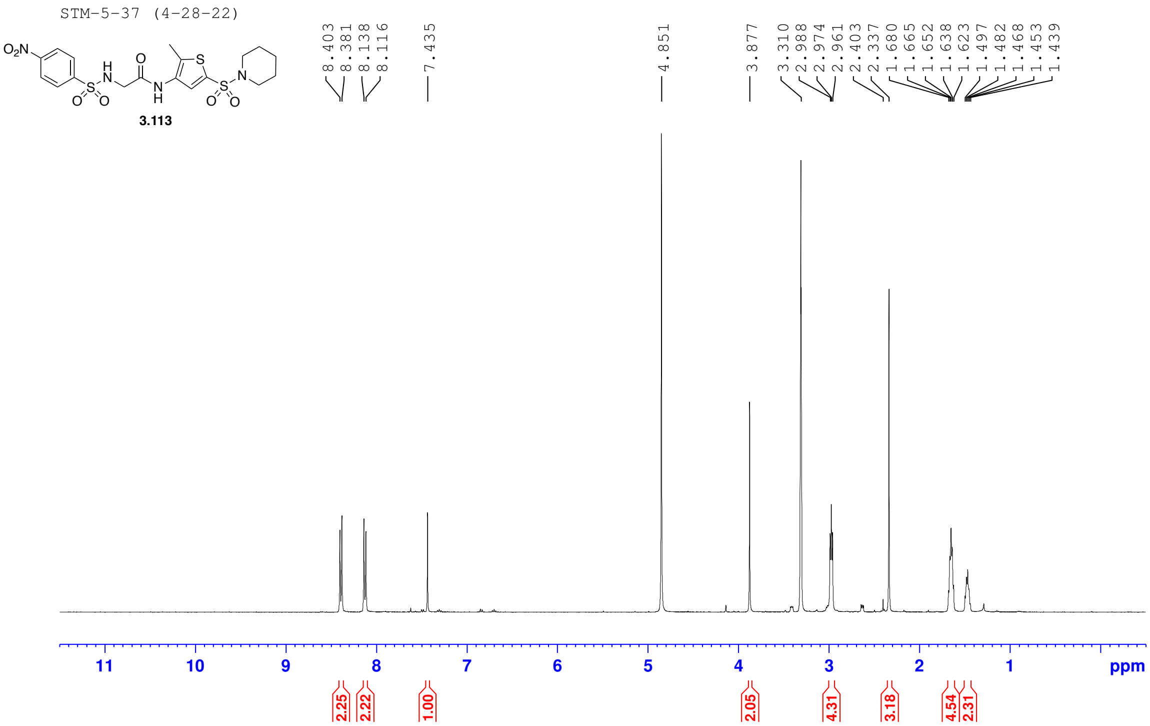
STM-5-37 (4-28-22)
3.113
8.403
8.381
8.138
8.116
7.435
4.851
3.877
3.310
2.988
2.974
2.961
2.403
2.337
1.680
1.665
1.652
1.638
1.623
1.497
1.482
1.468
1.453
1.439
11
10
9
8
7
6
5
4
3
2
1
ppm
2.25
2.22
1.00
2.05
4.31
3.18
4.54
2.31

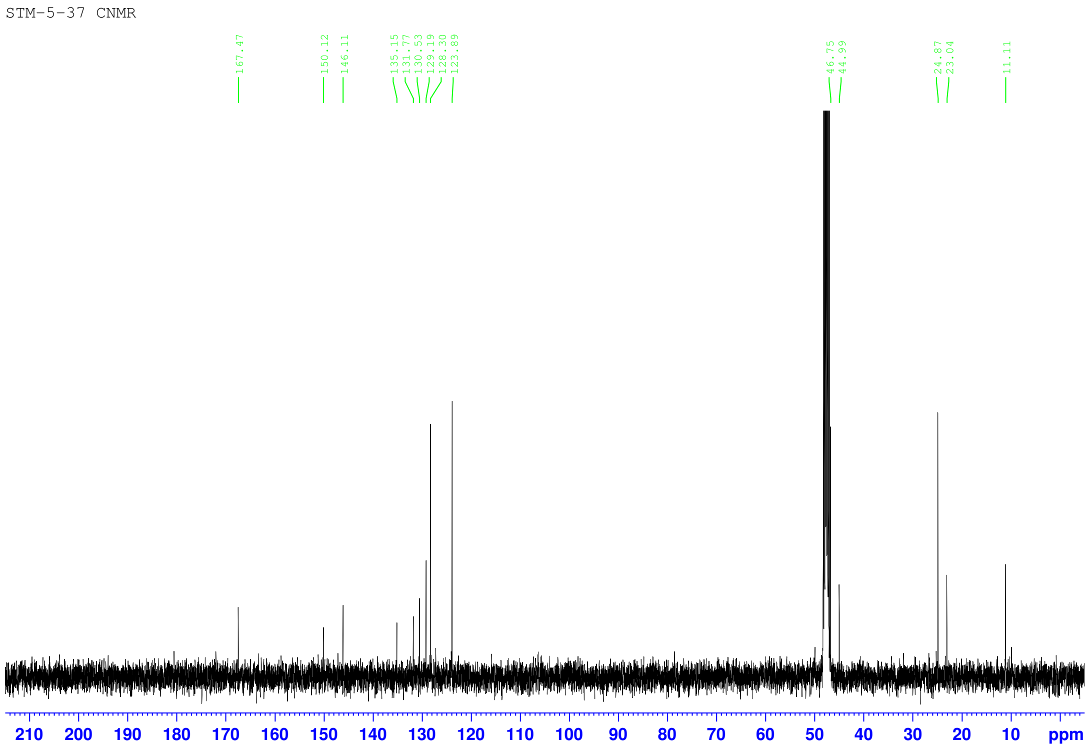
STM-5-37 CNMR
167.47
150.12
146.11
135.15
131.77
130.53
129.19
128.30
123.89
46.75
44.99
24.87
23.04
11.11
210
200
190
180
170
160
150
140
130
120
110
100
90
80
70
60
50
40
30
20
10
ppm

Shea T. Meyer

1003 Windfall Road, St. Marys, PA 15857
814-389-6979, meyershea@yahoo.com

EDUCATION:

Syracuse University (August 2017-November 2022)

- Doctor of Philosophy in Chemistry, November 2022
- Master of Philosophy in Chemistry, May 2019

The Pennsylvania State University, University Park, PA (2013-2017)

- B.S. in Chemistry, Synthetic Option, May 2017

RESEARCH EXPERIENCE:

Graduate Research Assistant, Syracuse University (August 2017-Present):

- Synthesis of the newly discovered SHIP1 agonist: 2-(4-fluorobenzenesulfonamido)-N-[2-methyl-5-(thiomorpholine-4-sulfonyl)thiophene-3-yl]acetamide
- Design and synthesis of bis-sulfonamide agonist analogs for structure activity relationship testing
- Design and synthesis of tryptamine-based SHIP inhibitors
- Development of a β-(trimethylsilyl)ethyl imidate protecting group under thermal conditions, without the need for exogenous catalyst or promoter

Amphenol Sensors - St. Marys, PA - Chemical Intern (May 2017-August 2017)

- Studied effects of epoxy coatings on composite sintered metals
- Performed heat induced age tests of sintered metals
- Analyzed epoxy-metal interactions via SEM and XRD

Undergraduate Research Assistant, The Pennsylvania State University (Jan. 2016 – May 2017):

- Synthesized single and mixed-substituent polymers through the use of organic and organometallic nucleophiles
- Analyzed new reactions for potential high polymer synthesis

TEACHING EXPERIENCE:

Syracuse University

- Organic Chemistry Laboratory Teaching Assistant (CHE 276 & 326) – Fall 2017 – Spring 2022

The Pennsylvania State University

- Organic Chemistry Learning Assistant (CHEM 203) – Spring 2016 – Spring 2017

PUBLICATIONS:

- **Meyer, S. T.**; Fernandes, S.; Anderson, R.E.; Pacherille, A.; Kerr, W. G.; Chisholm, J. D. Structure Activity Studies on Bis-Sulfonamide SHIP1 Agonists. *In Preparation.*

- Fernandes, S.; **Meyer, S. T.**; Shah, J. P.; Adhikari, A. A.; Kerr, W. G.; Chisholm, J. D. N1-Benzyl Tryptamine Pan-SHIP1/2 Inhibitors: Synthesis and Preliminary Biological Evaluation as Anti-Tumor Agents. *Molecules* **2022**, *27* (23), 8451.

- Sudan, R.; Fernandes, S.; Srivastava, N.; Pedicone, C.; **Meyer, S. T.**; Chisholm, J. D.; Engelman, R. W.; Kerr, W. G. LRBA Deficiency Can Lead to Lethal Colitis That Is Diminished by SHIP1 Agonism. *Front. Immunol.* **2022**, *13*, 830961.

- Kerr, W.; Fernandes, S.; Srivastava, N.; Pedicone, C.; Sudan, R.; Luke, E.; Dungan, O. M.; Pacherille, A.; **Meyer, S. T**.; Dormann, S.; Chisholm, J. D. Obesity control by SHIP inhibition requires pan-paralog inhibition and an intact eosinophil compartment. *Submitted. bioRxiv* DOI:10.1101/2020.09.15.299073

- Pedicone, C.; Fernandes, S.; Matera, A.; **Meyer, S. T.**; Loh, S.; Ha, J.-H.; Bernard, D.; Chisholm, J. D.; Paolicelli, R. C.; Kerr, W. G. Discovery of a Novel SHIP1 Agonist That Promotes Degradation of Lipid-Laden Phagocytic Cargo by Microglia. *iScience* **2022**, 104170.

- Pedicone, C.; **Meyer, S.T.**; Chisholm, J.D.; Kerr, W.G. Targeting SHIP1 and SHIP2 in Cancer. *Cancers* **2021**, *13*, 890.

- Lin, W.; **Meyer, S.T.**; Dormann, S.; Chisholm, J.D. Esterifications with 2-(Trimethylsilyl)ethyl 2,2,2-Trichloroacetimidate. *Organics* **2021**, *2*, 17.
  Selected as cover article of *Organics*, Volume 2, Issue 1 (March 2021)

PRESENTATIONS:

- "Structure Activity Studies on Bis-Sulfonamide SHIP1 Agonists," Syracuse University BioInspired Symposium, Syracuse University, Syracuse, NY October 2022, Poster Presentation

TECHNICAL SKILLS:

- Multi-step synthesis of organic compounds
- Characterization of small organic compounds by ^{1}H NMR, ^{13}C NMR, 2D NMR, IR, mass spectroscopy, HPLC and combustion analysis
- Strong verbal and written communication